TIME DEPENDENT QUANTUM MECHANICS AND SPECTROSCOPY 2025E



Andrei Tokmakoff
University of Chicago

LibreTexts™

Info Page

This text is disseminated via the Open Education Resource (OER) LibreTexts Project (https://LibreTexts.org) and like the thousands of other texts available within this powerful platform, it is freely available for reading, printing, and "consuming."

The LibreTexts mission is to bring together students, faculty, and scholars in a collaborative effort to provide an accessible, and comprehensive platform that empowers our community to develop, curate, adapt, and adopt openly licensed resources and technologies; through these efforts we can reduce the financial burden born from traditional educational resource costs, ensuring education is more accessible for students and communities worldwide.

Most, but not all, pages in the library have licenses that may allow individuals to make changes, save, and print this book. Carefully consult the applicable license(s) before pursuing such effects. Instructors can adopt existing LibreTexts texts or Remix them to quickly build course-specific resources to meet the needs of their students. Unlike traditional textbooks, LibreTexts' web based origins allow powerful integration of advanced features and new technologies to support learning.



LibreTexts is the adaptable, user-friendly non-profit open education resource platform that educators trust for creating, customizing, and sharing accessible, interactive textbooks, adaptive homework, and ancillary materials. We collaborate with individuals and organizations to champion open education initiatives, support institutional publishing programs, drive curriculum development projects, and more.

The LibreTexts libraries are Powered by NICE CXone Expert and was supported by the Department of Education Open Textbook Pilot Project, the California Education Learning Lab, the UC Davis Office of the Provost, the UC Davis Library, the California State University Affordable Learning Solutions Program, and Merlot. This material is based upon work supported by the National Science Foundation under Grant No. 1246120, 1525057, and 1413739.

Any opinions, findings, and conclusions or recommendations expressed in this material are those of the author(s) and do not necessarily reflect the views of the National Science Foundation nor the US Department of Education.

Have questions or comments? For information about adoptions or adaptions contact info@LibreTexts.org or visit our main website at https://LibreTexts.org.

The LibreTexts name, logo, and book covers are trademarked by LibreTexts, Inc. (a 501(c)(3) not-for-profit organization) and protected against unauthorized use.

This text was compiled on 08/26/2026

This page titled Info Page is shared under a CC BY-NC-SA 4.0 license and was authored, remixed, and/or curated by Andrei Tokmakoff via source content that was edited to the style and standards of the LibreTexts platform.

TABLE OF CONTENTS

Title Page

Info Page

Licensing

Preface

1: Overview of Time-Independent Quantum Mechanics

1.1: Introduction

1.2: Describing a System Quantum Mechanically

1.3: Dirac Notation and Matrix Mechanics

1.4: Basic Quantum Models

1.5: Raising and Lowering Operators

1.6: Angular Momentum

1.7: Exponential Operators

1.8: Readings

2: The Schrödinger Equation and Time-Propagator

2.1: Dynamics with a Time-Independent Hamiltonian

2.2: Time-Evolution Operator

2.3: Two-Level System

2.4: Equation of Motion for the Time-Evolution Operator

2.5: Dynamics with a Time-Dependent Hamiltonian

2.6: Schrödinger and Heisenberg Representations

2.7: Readings

3: Solving the Time-Dependent Schrödinger Equation

3.1: Introduction

3.2: Integrating the TDSE Directly

3.3: Transitions Induced by a Time-Dependent Potential

3.4: Resonant Driving of a Two-Level System

3.5: The Interaction Picture

3.6: Time-Dependent Perturbation Theory

3.7: The Golden Rule

3.8: Readings

4: Wavepacket Dynamics

4.1: Position and Momentum Representation

4.2: Free-Particle Eigenstates

4.3: Free-Particle Wavepacket

4.4: Readings

5: Adiabatic Approximation

5.1: Adiabatic Processes

5.2: Born–Oppenheimer Approximation

5.3: Nonadiabatic Coupling

5.4: Diabatic and Adiabatic States

5.5: Landau–Zener Transition Probability

5.6: Adiabaticity criterion

5.7: Readings

6: Classical Description of Spectroscopy

6.1: Introduction

6.2: Absorption by a Driven Oscillator

6.3: Complex formulation of the driven dipole oscillator

6.4: Response of an Impulsively Driven Oscillator

6.5: Polarizability

6.6: Appendix- Laplace Transform Solution for the Driven Damped Oscillator

6.7: Readings

7: Interaction of Light and Matter

7.1: Introduction

7.2: Electromagnetic Plane Waves

7.3: Classical Light–Matter Interactions

7.4: Electric Dipole Hamiltonian

7.5: The Dipole Operator and Transition Dipole Matrix Elements

7.6: Absorption Cross Section

7.7: Quantitative Examples of Light-Matter Interactions

7.8: Appendix- Electromagnetic Fields and Potentials

7.9: Appendix- Magnetic Dipole and Electric Quadrupole Transitions

7.10: Readings

8: Emission of Radiation

8.1: Classical rate of light emission

8.2: Radiation from an Oscillating Dipole

8.3: Appendix- Wave equation with a source

8.4: Readings

9: Quantum Electromagnetic Field

9.1: Introduction

9.2: Hamiltonian for quantized electromagnetic field

9.3: Electromagnetic field

9.4: Light-Matter Interactions and Spontaneous Emission

9.5: Coherent States

9.6: Readings

10: Transition Dipole Moment and Selection Rules

10.1: The Molecular Transition Dipole Moment

10.2: Selection Rules in the Electric Dipole Approximation

10.3: Molecular Electronic Spectroscopy and Franck Condon Factors

10.4: Appendix - Rotational Transition Matrix Elements

10.5: Readings

11: Irreversible Relaxation

11.1: Introduction

11.2: Coupling to a continuum

11.3: Spontaneous Emission

11.4: Relaxation and Line-broadening

11.5: Readings

12: Quantum Statistical Mechanics For Condensed Matter

12.1: Concepts for Condensed Matter

12.2: Statistics of Ensembles

12.3: Equilibrium Systems

12.4: Mixed States

12.5: The Density Matrix

12.6: Time-Dependence of the Density Matrix

12.7: Readings

13: Correlation Functions

13.1: Classical Time-Correlation Functions

13.2: Examples of Classical Time-Correlation Functions

13.3: Calculating the Correlation Function from a Discrete Trajectory

13.4: Quantum Time-Correlation Functions

13.5: Transition Rates from Time Correlation Functions

13.6: Appendix- Weiner-Khinchin Theorem and the Power Spectrum

13.7: Readings

14: Linear Response Theory

14.1: Classical Linear Response Theory

14.2: Example- Response of a damped harmonic oscillator

14.3: The Response Function and Energy Absorption

14.4: Quantum Linear Response Functions

14.5: Nonlinear response functions

14.6: Relaxation of a Prepared State

14.7: Example- Response of an abruptly shifted oscillator

14.8: Readings

15: Time-Domain Spectroscopy

15.1: Absorption Spectra from Time-Correlation Functions

15.2: Describing Diverse Spectroscopies with the Dipole Correlation Function
15.3: Vibrational and Rotational Spectroscopy
15.4: Line Broadening Mechanisms
15.5: Readings

16: Coupling of Electronic and Nuclear Motion
16.1: The Displaced Harmonic Oscillator Model
16.2: Coupling to a Harmonic Bath
16.3: Semiclassical Approximation to the Dipole Correlation Function
16.4: Readings

17: Fluctuations and Dephasing
17.1: Line-broadening, dephasing, and spectral diffusion
17.2: Gaussian-Stochastic Model for Spectral Diffusion
17.3: The Energy Gap Hamiltonian
17.4: Spectral Density for Condensed Phase Spectroscopy
17.5: The Harmonic Bath's Relation to the Langevin Equation
17.6: Readings

18: Quantum Relaxation Processes
18.1: Vibrational Relaxation
18.2: Golden Rule Vibrational Relaxation Rates
18.3: Multiquantum relaxation of polyatomic molecules
18.4: Redfield Theory and Master Equation
18.5: Readings

19: Energy and Charge Transfer
19.1: Intermolecular Electronic Interactions
19.2: Resonance Energy Transfer and Transition Dipole Coupling
19.3: Förster Resonance Energy Transfer
19.4: Marcus Theory for Electron Transfer
19.5: Readings

20: Excitons
20.1: What are excitons?
20.2: Frenkel excitons in molecular aggregates
20.3: Absorption spectrum of a dimer
20.4: Absorption spectra of J aggregates
20.5: Frenkel exciton transport
20.6: Tight-binding model
20.7: Readings

21: Appendices
21.1: Math and Physics Reference Material
21.1.1: Atomic Units

21.1.2: Dirac Delta Function
21.1.3: Gaussian Integrals and Error Function

21.2: Quantum Mechanics- Extra Topics
21.2.1: Numerically Solving the Schrödinger Equation
21.2.2: Separation of Subsystems
21.2.3: Morse Oscillator

Notation and variables used

Index

Glossary

Detailed Licensing

This page titled Time-Dependent Quantum Mechanics and Spectroscopy 2025e (Tokmakoff) is shared under a CC BY-NC-SA 4.0 license and was authored, remixed, and/or curated by Andrei Tokmakoff via source content that was edited to the style and standards of the LibreTexts platform.

Licensing

Copyright © 2025 Andrei Tokmakoff

Virtually all of this book can be used under a Creative Commons Attribution-NonCommercial-ShareAlike 4.0 International license (CC BY-NC-SA 4.0). This means that it is freely available for non-commercial purposes with a limited number of conditions. Please read the license to understand the appropriate reuse of the material. One key requirement of reuse is *appropriate credit*: You must provide the name of the creator, a copyright notice, a license notice, and a link to the material. See the detailed licensing section for complete information.

Download a PDF of the entire book.

The non-profit nature of higher education means that citation of this material is the principal way of establishing the value of the content. Please cite this electronic book in the following manner:

> Andrei Tokmakoff, *Time-Dependent Quantum Mechanics and Spectroscopy*, 2025 ed., University of Chicago, 2025. DOI:10.6082/uchicago.16831.

Download this reference to your citation manager: RIS (Mendeley, Zotero), ENW (Endnote), Bibtex, TXT (Refworks)

Commercial use for the purpose of training large language models and other AI tools and systems is prohibited for any paid or revenue-generating workstreams or any monetized downstream application without obtaining a separate license explicitly permitting commercial use. Use for strictly non-commercial applications in datasets, training, and model deployment still require clear attribution to the original creators and licenses.

A detailed breakdown of this resource's licensing can be found in ***Back Matter/Detailed Licensing***.

This page titled Licensing is shared under a CC BY-NC-SA 4.0 license and was authored, remixed, and/or curated by Andrei Tokmakoff.

Preface

This book is designed to be a resource for those studying time-dependent quantum mechanics, dynamics, and spectroscopy of molecular systems. This text is largely for chemists: people whose view of the world is formed in the language of atoms and molecules. It is for chemistry students who are starting—like I did—without a deep knowledge of physics and math, but who find it important to understand the concepts and tools that lie outside of the traditional chemistry curriculum. However, I also hope this may be a useful reference for practitioners in the field, including those who are familiar with the content but haven't trained with a molecular perspective. Writing for these different audiences means that the material varies between basic qualitative concepts and advanced formalism.

This is not a textbook or lecture notes or a handbook but all of these at the same time. The online format provides an opportunity to do things differently: There are no stringent constraints on length, which allows a self-contained presentation of material that doesn't hesitate to be repetitive and permits more detail in derivations, lengthy examples, math notes, and appendices. We can incorporate video and readily link to content within the book and externally. These digital features are still somewhat limited but will grow with time.

Perhaps most importantly, this is not a static document but is regularly corrected and expanded. Since the first public release of this content as simple lecture notes on MIT's OpenCourseWare in 2003, there have been periodic releases of new content and updates to transform what were lecture notes into a book's narrative form. 2025 brings the first substantial release of new material since the 2014 edition, along with extensive editing of all earlier material.

In some sense, the content here draws from and curates material originating from many sources. In part these sources are recorded in the references to books, papers, and notes given throughout the text. However, the structure and scope of the content was strongly shaped by lecture notes and co-teaching with colleagues and instructors, including Bob Field, Graham Fleming, Keith Nelson, Troy Van Voorhis, and John Ross. Bob Silbey deserves a special acknowledgement, not only for giving me material when I started teaching, but for shaping my whole approach to quantum mechanics, such as his mantra: *First write down the Hamiltonian*... In more recent years, numerous people have offered feedback and found errors, but Sukhbir Mahajan, Ruoyu Xu, and Samuel Knight were particularly helpful. Special thanks to the many students, postdocs, and faculty who have reached out to tell me how helpful my notes were for them or point out errors; I continue this work in hopes that it may continue to be a useful resource for its readers.

Finally, I want to thank Artemie Chang, Peter Giunta, Anne Hudson, and Tanya Shpigel, for their assistance over the years with transcribing and editing the material and with preparing it for electronic distribution, MIT and UChicago for administrative support, the Department of Energy and National Science Foundation for their support of my research in this area, and my wife Karen for her enduring support and patience with my project.

Andrei Tokmakoff

December 2025

This page titled Preface is shared under a CC BY-NC-SA 4.0 license and was authored, remixed, and/or curated by Andrei Tokmakoff via source content that was edited to the style and standards of the LibreTexts platform.

1: OVERVIEW OF TIME-INDEPENDENT QUANTUM MECHANICS

1.1: Introduction

1.2: Describing a System Quantum Mechanically

1.3: Dirac Notation and Matrix Mechanics

1.4: Basic Quantum Models

1.5: Raising and Lowering Operators

1.6: Angular Momentum

1.7: Exponential Operators

1.8: Readings

This page titled 1: Overview of Time-Independent Quantum Mechanics is shared under a CC BY-NC-SA 4.0 license and was authored, remixed, and/or curated by Andrei Tokmakoff via source content that was edited to the style and standards of the LibreTexts platform.

1.1: Introduction

Quantum mechanics describes the physical properties of matter on the scale of atoms and molecules. We use it to represent the interactions between atoms, nuclei, electrons and molecules; how external fields influence these particles; and their resulting behavior. As chemists, we are interested in the molecular structures that emerge from atomic building blocks, as well as the processes by which these structures change. Beyond this microscopic description, we seek to understand how these properties manifest themselves in the macroscopic world.

Quantum mechanics has been part of chemistry studies for a century, and the fundamentals are very well established. During this first century, the dominant application of quantum mechanics in chemistry has been molecular structure. The chemistry curriculum during this period implicitly conveyed a rigid and immovable quantum mechanical world, where any dynamics occurred in a deterministic and stepwise manner between well-defined structures.

In most cases, though, the quantum world is made up of wiggly, jiggly, constantly evolving molecular structures. Condensed systems, such as liquids and solids near room temperature, are of particular interest to us. They involve strongly interacting molecules, with structures that are often disordered or dynamically evolving or maybe even unknown in a detailed manner. Over the past three decades, the molecular dynamics of quantum systems has increasingly been addressed in a realistic manner, and we have become more adept at describing condensed matter systems at finite temperatures. The key phenomenon that emerges is irreversibility: real quantum systems have an arrow of time attached to them that is not apparent from the Schrödinger equation. Irreversibility, relaxation, dissipation, random fluctuations, and dephasing are hallmark properties of condensed matter dynamics, so we need to understand the origins of these processes. For this purpose, it is crucial that we closely integrate the tools of statistical mechanics to model realistic quantum mechanical systems that are not deterministic.

To study molecules and nanometer-scale matter, you need to interact with it in some way, and the most common way of studying matter is through light—electromagnetic radiation. There are numerous possible outcomes to light encountering a molecule, and there is an extensive spectroscopic toolbox to investigate the resulting changes to the light and the molecule. To deeply understand spectroscopic research, one must have a deep understanding of the molecular and optical physics governing spectroscopy, starting with the fundamentals of light-matter interactions. Therefore, spectroscopy is the second major theme of the book, and the main source of its examples. Given the importance of time to the dynamical behavior of real quantum systems, we are particularly interested in studying the time-dependent formalism for spectroscopy.

These goals and observations motivate the organization of the book. The assumption going forward is that the reader has already been exposed to the basic concepts of quantum mechanics for chemistry at the level of an introductory graduate level class. The first five chapters will concentrate on describing the time-dependent quantum mechanics of systems in isolation, and the subsequent five chapters will cover the spectroscopy of those systems. Then our focus will switch to condensed matter topics. Four chapters will cover the basic tools for describing condensed matter and irreversibility, and the following three chapters will describe how these dynamic processes influence spectroscopy. Finally, the three concluding chapters will cover application of the tools we have developed to relaxation, energy, and charge transport.

This page titled 1.1: Introduction is shared under a CC BY-NC-SA 4.0 license and was authored, remixed, and/or curated by Andrei Tokmakoff via source content that was edited to the style and standards of the LibreTexts platform.

1.2: Describing a System Quantum Mechanically

As a starting point it is useful to review the postulates of quantum mechanics and use this as an opportunity to elaborate on some additional definitions and properties of quantum systems.

The Wavefunction

Quantum mechanical matter exhibits wave-particle duality in which the particle properties emphasize classical aspects of the object's position, mass, and momentum, and the wave properties reflect its spatial delocalization and ability to interfere constructively or destructively with other particles or waves. As a result, in quantum mechanics the physical properties of the system are described by the wavefunction Ψ. The wavefunction is a complex function of real variables and cannot be observed itself, but through it we can describe the time-dependent properties of the system's particles and fields. Depending on the context, *particle* is a term that will refer to a variety of objects—such as electrons, nucleons, and atoms—that fill space and have mass, but also retain wavelike properties. *Fields* refer to a variety of physical quantities that are continuous in time and space, which have energy and influence the behavior of particles.

In the general sense, the wavefunction, or *state*, does not refer to a three-dimensional physical space in which quantum particles exist, but rather an abstract linear vector space, or *Hilbert space*, that accounts for all possible observable properties of the system. We can represent the wavefunction in physical space, $\Psi(\mathbf{r})$, by carrying out a projection onto the desired spatial coordinates. As a probability amplitude function, the wavefunction describes the statistical probability of locating particles or fields in space and time. Specifically, we claim that the square of the wavefunction is proportional to a probability density (probability per unit volume). In one dimension, the probability of finding a particle in a space between x and $x + dx$ at a particular time t is

$$P(\mathbf{x}, t)\, d\mathbf{x} = \Psi^*(\mathbf{x}, t)\Psi(\mathbf{x}, t)\, d\mathbf{x} \tag{1.2.1}$$

$P(\mathbf{x}, t)$ is known as a probability density. We will always assume that the wavefunctions for a particle are properly normalized, so that $\int d\tau\ \Psi^*\Psi = 1$ where the integration is over Hilbert space.

Operators

Quantum mechanics parallels Hamilton's formulation of classical mechanics, in which the properties of particles and fields are described in terms of their position and momenta. Each particle described by the wavefunction will have associated with it one or more *degrees of freedom* that are defined by the dimensionality of the problem. For each degree of freedom, particles which are described classically by a position x and momentum p_x, will have associated with it a quantum mechanical operator $\hat{x}$ or $\hat{p}_x$, which will be used to describe physical properties and experimental observables in space and time. Operators correspond to dynamical variables, whereas static variables, such as mass, do not have operators associated with them. In practice there is a quantum/classical correspondence which implies that the quantum mechanical behavior can often be deduced from the classical dynamical equations by substituting the quantum mechanical operator for the corresponding classical variables. In the case of position and momenta, these operators are $x \rightarrow \hat{x}$ and $\hat{p}_x = -\mathrm{i}\hbar(\partial/\partial x)$.

Table 1.2.1. Operators in the position representation corresponding to observable classical dynamical variables in one and three dimensions

Classical Variable			Operator
Position	(1D)	x	$\hat{x}$
	(3D)	$\mathbf{r} = (x, y, z)$	$\hat{\mathbf{r}} = (\hat{x}, \hat{y}, \hat{z})$
Linear momentum	(1D)	p_x	$\hat{p}_x = -\mathrm{i}\hbar(\partial/\partial x)$
	(3D)	$\mathbf{p}$	$\hat{\mathbf{p}} = -\mathrm{i}\hbar\bar{\nabla}$
Function of position and momentum	(1D)	$f(x, p_x)$	$f(\hat{x}, \hat{p}_x)$

Classical Variable			Operator
Kinetic energy of a particle with mass m	(1D)	$T = \frac{p_x^2}{2m}$	$\hat{T} = -\frac{\hbar^2}{2m}\frac{\partial^2}{\partial x^2}$
Potential energy		V	$\hat{V}$
Orbital angular momentum	(3D)	$\mathbf{L} = \mathbf{r} \times \mathbf{p}$	$\hat{\mathbf{L}} = -\mathrm{i}\hbar\hat{\mathbf{r}} \times \nabla$
z-component of orbital angular momentum			$\hat{L}_z = -\mathrm{i}\hbar(\partial/\partial\phi)$

Table (1.2.1) lists some important operators. Note that time does not have an operator associated with it, and for our purposes is considered an immutable variable that applies uniformly to the entire system.

What do operators do? Operators map one state of the system to another—also known as acting on the wavefunction. They represent a mathematical operation on the wavefunction that changes it, for instance moving in time and space:

$$\hat{A}\Psi_0 = \Psi_A \tag{1.2.2}$$

Here Ψ_0 is the initial wavefunction and Ψ_A refers to the wavefunction after the action of the operator $\hat{A}$. The operator is understood to be acting on a wavefunction to the right. For instance, the operator $\hat{p}_x$ implies that one expresses $\hat{p}$ in the x basis, differentiates the wavefunction to its right with respect to x, and then multiplies the result by $-\mathrm{i}\hbar$.

Operators may be simply multiplicative, as with the operator $\hat{x}$, or they may take differential or integral forms. The gradient $\bar{\nabla}$, divergence $\nabla\cdot$, and curl $\nabla\times$ are examples of differential operators, whereas Fourier and Laplace transforms are integral operators. Since operators generally do not commute, a series of operators must be applied in the prescribed right-to-left order. We can write this series of operations as:

$$\hat{B}\hat{A}\Psi_0 = \hat{B}\Psi_A = \Psi_{B,A} \tag{1.2.3}$$

Of particular interest is the Hamiltonian, $\hat{H}$, an operator corresponding to the total energy of the system. The Hamiltonian operator describes all interactions between particles and fields, and thereby determines the state of the system. The Hamiltonian is a sum of the total kinetic and potential energy for the system of interest, $\hat{H} = \hat{T} + \hat{V}$, and is obtained by substituting the position and momentum operators into the classical Hamiltonian. For a particle in one dimension under the influence of a potential,

$$\hat{H} = -\frac{\hbar^2}{2m}\frac{\partial^2}{\partial x^2} + V(\hat{x}, t) \tag{1.2.4}$$

Note

In the following chapters, we will denote operators with a circumflex only when we are trying to explicitly note its role as an operator, but otherwise we take the distinction between variables and operators to be understood.

Eigenvalues and Eigenfunctions

The properties of a system described by mapping with the operator $\hat{A}$ can only take on the values λ that satisfy an eigenvalue equation

$$\hat{A}\Psi = \lambda\Psi \tag{1.2.5}$$

For instance, if the state of the system is $\Psi(x) = e^{\mathrm{i}px/h}$, the momentum operator $\hat{p}_x = -\mathrm{i}\hbar(\partial/\partial x)$ returns the eigenvalue p (a scalar) times the original wavefunction. Then $\Psi(x)$ is said to be an eigenfunction of $\hat{p}_x$. For the Hamiltonian, the solutions to the eigenvalue equation

$$\hat{H}\Psi = E\Psi \tag{1.2.6}$$

yield possible energy eigenvalues of the system, E. The set of all possible eigenvectors are also known as the eigenstates ψ_1.

Equation (1.2.6) is the time-independent Schrödinger equation (TISE).

Linear Superposition

The eigenstates of an operator $\hat{A}$ form a complete orthonormal *basis set* $\{\psi_i\}$ which can be used to describe the wavefunction's properties.

$$\int_{-\infty}^{+\infty} d\tau\, \psi_i^* \psi_j = \delta_{ij} \tag{1.2.7}$$

The wavefunction is expressed as a linear combination, or superposition, of basis functions

$$\Psi = \sum_{i=0}^{\infty} c_i \psi_i \tag{1.2.8}$$

where c_i are complex coefficients (numbers), and the index i is an index often called a quantum number. The probability that a particle occupies an eigenstate ψ_i, the probability amplitude, is obtained from

$$P_i = |c_i|^2 = c_i^* c_i \tag{1.2.9}$$

where conserved probability (completeness) dictates that

$$\sum_{i=0}^{\infty} |c_i|^2 = 1 \tag{1.2.10}$$

The choice of basis set by which to represent the system is not unique. The change of basis set is effectively a transformation that rotates the wavefunction in Hilbert space. Eigenfunctions that have the same eigenvalue are known as degenerate. Linear combinations of degenerate eigenfunctions can be formed that will be orthogonal.

Time Dependence

The wavefunction evolves in time as described by the time-dependent Schrödinger equation (TDSE):

$$-\mathrm{i}\hbar \frac{\partial \Psi}{\partial t} = \hat{H}\Psi \tag{1.2.11}$$

The dynamics described by the TDSE are the primary topic of this book. In the following chapter, we will see the reasoning that results in this equation.

Expectation Values

The outcome of a quantum measurement cannot be known with arbitrary accuracy; however, we can statistically describe the probability of measuring a certain value. The measurement of a value associated with the operator is obtained by calculating the expectation value of the operator

$$\langle A \rangle = \int d\tau\, \Psi^* \hat{A} \Psi \tag{1.2.12}$$

The brackets $\langle \ldots \rangle$ refer to an average value that will emerge from a large series of measurements on identically prepared systems. Comparing this expression with the TISE shows that the expectation value for the Hamiltonian is the total energy of the system, $\langle \hat{H} \rangle = E$. Whereas $\langle A \rangle$ is the mean value, the variance in a distribution of values measured can be calculated from $\Delta A = \langle A^2 \rangle - \langle A \rangle^2$.

One special characteristic of operators that we will look for is whether operators are Hermitian, that is operators which obey the equality $\hat{A} = \hat{A}^*$. Since an observable must be real-valued, the quantum mechanical operators corresponding to physical observables are Hermitian:

$$\int d\tau\, \Psi^* \hat{A} \Psi = \int d\tau\, \hat{A}^* \Psi^* \Psi \tag{1.2.13}$$

a Hermitian operator must have real eigenvalues and orthogonal eigenfunctions.

Commutators

Operators are associative but not necessarily commutative. Commutators determine whether two operators commute. The commutator of two operators $\hat{A}$ and $\hat{B}$ is defined as

$$[\hat{A}, \hat{B}] = \hat{A}\hat{B} - \hat{B}\hat{A} \tag{1.2.14}$$

If we first make an observation of an eigenvalue a for $\hat{A}$, one cannot be assured of determining a unique eigenvalue b for a second operator $\hat{B}$. This is only possible if the system is an eigenstate of both $\hat{A}$ and $\hat{B}$. This would allow one to state that $\hat{A}\hat{B}\psi = \hat{B}\hat{A}\psi$ or alternatively $[\hat{A}, \hat{B}]\psi = 0$. If the operators commute, the commutator is zero, and $\hat{A}$ and $\hat{B}$ have simultaneous eigenfunctions. If the operators do not commute, one cannot specify a and b exactly, however, the variance in their uncertainties can be expressed as $\Delta A^2 \Delta B^2 \geq \left\langle \frac{1}{2}[\hat{A}, \hat{B}] \right\rangle^2$. As an example, we see that $\hat{p}_x$ and $\hat{p}_y$ commute, but $\hat{x}$ and $\hat{p}_x$ do not. Thus we can specify the momentum of a particle in the x and y coordinates precisely, but cannot specify both the momentum and position of a particle in the x dimension to arbitrary resolution. We find that $[\hat{x}, \hat{p}_x] = \mathrm{i}\hbar$ and $\Delta x \Delta p_x \geq \hbar/2$.

Note that for the case that the Hamiltonian can be written as a sum of commuting terms, as is the case for a set of independent or separable coordinates or momenta, then the total energy is additive in eigenvalues for each term, and the total eigenfunction can be written as product states in the eigenfunctions for each term.

Exchange Symmetry

Quantum mechanical particles also have the property of spin, or intrinsic angular momentum, and are classified by their spin either as Fermions with half-integer spin $(1/2, 3/2 \ldots)$ or Bosons with integer spin $(0, 1, 2, \ldots)$ For Fermions (such as electrons), the total wavefunction must be antisymmetric with respect to exchange of two Fermions, $\Psi(r_1, r_2) = -\Psi(r_2, r_1)$. This implies that $r_2 \neq r_1$, implying that two Fermions cannot occupy the same state, i.e. the Pauli Exclusion Principle. Bosons (such as photons and phonons) are symmetric to exchange of particles, $\Psi(r_1, r_2) = \Psi(r_2, r_1)$. They do not obey the Pauli principle, and multiple bosons can occupy the same quantum state. In the product basis, we can construct the wavefunctions for particles a and b as

$$\Psi_{\pm}(r_1, r_2) = 2^{-1/2} \left[\psi_a(r_1)\psi_b(r_2) \pm \psi_b(r_1)\psi_a(r_2)\right] \tag{1.2.15}$$

where "+" refers to symmetric and "−" to antisymmetric states.

This page titled 1.2: Describing a System Quantum Mechanically is shared under a CC BY-NC-SA 4.0 license and was authored, remixed, and/or curated by Andrei Tokmakoff via source content that was edited to the style and standards of the LibreTexts platform.

1.3: Dirac Notation and Matrix Mechanics

Most of our work will make use of Dirac notation and the matrix formulation of quantum mechanics, for which the wavefunction is written as $|\Psi\rangle$ and referred to as a *ket* vector and the Hermitian conjugate (complex conjugate transpose) $\Psi^* = \langle\Psi|$ is a *bra* vector. Dirac notation has the advantage of brevity, often shortening the wavefunction to a simple abbreviated notation and can lead to considerable simplifications if a real space description is not necessary. For instance, we can write eq. (1.1.8) as

$$|\Psi\rangle = \sum_i c_i |i\rangle \tag{1.3.1}$$

where the sum is over all eigenstates and the i^{th} eigenstate $|i\rangle = \psi_i$. Implicit in this equation is that the expansion coefficient for the i^{th} eigenstate is $c_i = \langle i|\Psi\rangle$. With this brevity comes the tendency to hide some of the variables important to the description of the wavefunction. One must be aware of this, and although we will use Dirac notation for most of our work, where detail is required, Schrödinger notation will be used.

In the matrix representation, $|\Psi\rangle$ is represented as a column vector for the expansion coefficients c_i in a particular basis set $\{\psi_i\} = \{|i\rangle\}$.

$$|\Psi\rangle = \begin{pmatrix} \langle\psi_1|\Psi\rangle \\ \langle\psi_2|\Psi\rangle \\ \langle\psi_3|\Psi\rangle \\ \vdots \end{pmatrix} = \begin{pmatrix} c_1 \\ c_2 \\ c_3 \\ \vdots \end{pmatrix} \tag{1.3.2}$$

The bra vector $\langle\Psi|$ is a row vector of the conjugate expansion coefficients c_i^* obtained from the conjugate transpose of the ket $|\Psi\rangle$. The product of a bra and ket vector, $\langle\Phi|\Psi\rangle$, is therefore an inner product (a scalar) whereas the product of a ket and bra $|\Phi\rangle\langle\Psi|$ is an outer product (a matrix). The inner product of two wavefunctions is

$$\langle\Phi|\Psi\rangle = \sum_i^{\infty} c_i^* d_i \tag{1.3.3}$$

Where c_i and d_i are the respective expansion coefficients for the Φ and Ψ wavefunctions in the eigen basis. Since wavefunctions are normalized, $\langle\Psi|\Psi\rangle = 1$, which is a restatement of eq. (1.1.10) . The orthogonality of eigenfunctions in eq. (1.3.1) can be summarized as $\langle i|j\rangle = \delta_{ij}$.

The outer product $|i\rangle\langle i|$ is known as a projection operator because it can be used to project the wavefunction of the system onto the i^{th} eigenstate of the system as $|i\rangle\langle i|\Psi\rangle = c_i|i\rangle$. If we sum projections over the complete basis set, we obtain the projection identity operator

$$\hat{P} = \sum_i |i\rangle\langle i| = 1 \tag{1.3.4}$$

This a statement of the completeness of a basis set. Applying a projection operator to a wavefunction $\hat{P}|\Psi\rangle$ results in eq. (1.3.1).

The operator $\hat{A}$ is represented by a square matrix that changes a vector wavefunction from one state or representation into another: $|\Psi_A\rangle = \hat{A}\,|\Psi_0\rangle$. The matrix is composed of matrix elements A_{ij} in the basis set $\{|i\rangle\}$:

$$A_{ij} = \langle i|A|j\rangle \tag{1.3.5}$$

The operator can equivalently be written in Dirac notation as

$$\hat{A} = \sum_{i,j} |i\rangle A_{ij} \langle j| \tag{1.3.6}$$

The expectation value of the operator, a restatement of eq. (1.1.12), is written

$$\langle A\rangle = \langle\Psi|\hat{A}|\Psi\rangle \tag{1.3.7}$$

or from eq. (1.3.1)

$$\langle A \rangle = \sum_i \sum_j c_i^* c_j A_{ij} \tag{1.3.8}$$

The *Hermitian conjugate*, or adjoint, of an operator $\hat{A}$, written $\hat{A}^\dagger$, is used to designate conjugate operators, wavefunctions and expectation values. $\hat{A}^\dagger$ is defined by

$$\left\langle \hat{A}^\dagger \psi | \phi \right\rangle = \left\langle \psi | \hat{A} \phi \right\rangle \tag{1.3.9}$$

To obtain a Hermitian conjugate an expression we must invert the sequence of operators or wavefunctions, replace constants with their complex conjugates, $c^\dagger = c^*$, replace kets with their corresponding bras (and vice versa), and replace operators with their adjoints. Thus $|\Psi\rangle^\dagger = \langle\Psi|$, $(\hat{A}\hat{B})^\dagger = \hat{B}^\dagger \hat{A}^\dagger$, and $(c\hat{A}|\Psi\rangle)^\dagger = c^* \langle\Psi|\hat{A}^\dagger$. Since their expectation values are real, a Hermitian operator is one that is self-adjoint, i.e., $\hat{A}^\dagger = \hat{A}$.

The eigenvalue equation, eq. (1.1.5), can be expressed in matrix form as

$$\hat{\mathbf{A}}|\Psi\rangle = \Lambda|\Psi\rangle \tag{1.3.10}$$

where $|\Psi\rangle$ are the eigenvectors and Λ is a diagonal matrix composed of the eigenvalues. The time-independent Schrödinger equation, eq. (1.1.6), is

$$\hat{H}|\Psi\rangle = E|\Psi\rangle \tag{1.3.11}$$

E are the energy eigenvalues which can be obtained by solving the characteristic equation

$$\det(H - E\mathbf{I}) = 0 \tag{1.3.12}$$

where $\mathbf{I}$ is the identity matrix. From eq. (1.3.11), we see that the expectation value of the Hamiltonian is the energy of the system,

$$E = \langle\Psi|H|\Psi\rangle \tag{1.3.13}$$

Each basis set provides a different route to representing the same physical system, and a similarity transformation S transforms a matrix from one basis to another. A transformation from the state $|\Psi\rangle$ to the state $|\Theta\rangle$ can be expressed as

$$|\Theta\rangle = S|\Psi\rangle \tag{1.3.14}$$

where the elements of the matrix are $S_{ij} = \langle\theta_i|\psi_j\rangle$. Then the reverse transformation is

$$|\Psi\rangle = S^{-1}|\Theta\rangle \tag{1.3.15}$$

If $S^{-1} = S^\dagger, S^\dagger S = 1$ and the transformation is said to be unitary. A *unitary transformation* refers to a similarity transformation in Hilbert space that preserves the scalar product, i.e., the length of the vector. Hermitian operators will always have a unitary transformation that puts the matrix A in diagonal form.

$$\Lambda = \mathbf{S}^{-1}\mathbf{A}\mathbf{S} \tag{1.3.16}$$

This is referred to as *diagonalizing* the matrix and is equivalent to solving the characteristic eigenvalue equation.

Properties of Operators

1. The inverse of $\hat{A}$ (written $\hat{A}^{-1}$) is defined by

$$\hat{A}^{-1}\hat{A} = \hat{A}\hat{A}^{-1} = 1 \tag{1.3.17}$$

2. The transpose of $\hat{A}$ (written A^T) is

$$A^T_{nq} = A_{qn} \tag{1.3.18}$$

If $A^T = -A$, then the matrix is antisymmetric.

3. If the product of two matrices is $\hat{P} = \hat{A}\hat{B}$, then the matrix elements of $\hat{P}$ are

$$\hat{P}_{nq} = \sum_k \hat{A}_{nk}\hat{B}_{kq} \tag{1.3.19}$$

4. The trace of $\hat{A}$ is defined as

$$\mathrm{Tr}(\hat{A}) = \sum_q A_{qq} \tag{1.3.20}$$

The trace of a matrix is invariant to a similarity transformation.

5. The Hermitian adjoint of $\hat{A}$ (written $\hat{A}^\dagger$) is

$$\hat{A}^\dagger = \left(\hat{A}^T\right)^* \tag{1.3.21}$$

$$\left(\hat{A}^\dagger\right)_{nq} = \left(\hat{A}_{qn}\right)^* \tag{1.3.22}$$

The Hermitian adjoint of a product of operators is the product of individual adjoints in the reverse order:

$$(\hat{A}\hat{B}\hat{C})^\dagger = \hat{C}^\dagger\hat{B}^\dagger\hat{A}^\dagger \tag{1.3.23}$$

6. $\hat{A}$ is a Hermitian operator if

$$\hat{A}^\dagger = \hat{A} \tag{1.3.24}$$

$$\left(\hat{A}^T\right)^* = \hat{A} \tag{1.3.25}$$

If $\hat{A}$ is Hermitian, then $\hat{A}^n$ is Hermitian and $e^{\hat{A}}$ is Hermitian. For a Hermitian operator, $\langle\psi|\hat{A}\varphi\rangle = \langle\psi\hat{A}|\varphi\rangle$

7. $\hat{A}$ is a unitary operator if its adjoint is also its inverse:

$$\hat{A}^\dagger = \hat{A}^{-1} \tag{1.3.26}$$

$$\left(\hat{A}^T\right)^* = \hat{A}^{-1} \tag{1.3.27}$$

$$\hat{A}\hat{A}^\dagger = 1 \implies \left(\hat{A}\hat{A}^\dagger\right)_{nq} = \delta_{nq} \tag{1.3.28}$$

If $\hat{A}$ and $\hat{B}$ are unitary then $\hat{A}\hat{B}$ is unitary.

Properties of Commutators

From the definition of a commutator:

$$[\hat{A}, \hat{B}] = \hat{A}\hat{B} - \hat{B}\hat{A} \tag{1.3.29}$$

we find it is antisymmetric to exchange:

$$[\hat{A}, \hat{B}] = -[\hat{B}, \hat{A}] \tag{1.3.30}$$

and distributive:

$$[\hat{A}, \hat{B} + \hat{C}] = [\hat{A}, \hat{B}] + [\hat{B}, \hat{C}] \tag{1.3.31}$$

These properties lead to a number of useful identities:

$$\left[\hat{A}, \hat{B}^n\right] = n\hat{B}^{n-1}[\hat{A}, \hat{B}] \tag{1.3.32}$$

$$[\hat{A}n, \hat{B}] = n\hat{A}^{n-1}[\hat{A}, \hat{B}] \tag{1.3.33}$$

$$[\hat{A}, \hat{B}\hat{C}] = [\hat{A}, \hat{B}]\hat{C} + \hat{B}[\hat{A}, \hat{C}] \tag{1.3.34}$$

$$[[\hat{C}, \hat{B}], \hat{A}] = [[\hat{A}, \hat{B}], \hat{C}] \tag{1.3.35}$$

$$[\hat{A}, [\hat{B}, \hat{C}]] + [\hat{B}, [\hat{C}, \hat{A}]] + [\hat{C}, [\hat{A}, \hat{B}]] = 0 \tag{1.3.36}$$

The Hermitian conjugate of a commutator is

$$[\hat{A}, \hat{B}]^\dagger = \left[\hat{B}^\dagger, \hat{A}^\dagger\right] \tag{1.3.37}$$

Also, the commutator of two Hermitian operators is also Hermitian.

The anticommutator is defined as

$$[\hat{A}, \hat{B}]_+ = \hat{A}\hat{B} + \hat{B}\hat{A} \tag{1.3.38}$$

and is symmetric to exchange.

For two Hermitian operators, their product can be written in terms of the commutator and anticommutator as

$$\hat{A}\hat{B} = \frac{1}{2}[\hat{A}, \hat{B}] + \frac{1}{2}[\hat{A}, \hat{B}]_+ \tag{1.3.39}$$

The anticommutator is the real part of the product of two operators, whereas the commutator is the imaginary part.

This page titled 1.3: Dirac Notation and Matrix Mechanics is shared under a CC BY-NC-SA 4.0 license and was authored, remixed, and/or curated by Andrei Tokmakoff via source content that was edited to the style and standards of the LibreTexts platform.

1.4: Basic Quantum Models

The first step in solving a quantum mechanical problem is to write a Hamiltonian describing the particles and interactions that give rise to the molecular properties of interest. Formulating a Hamiltonian in a simple but effective manner is a valuable skill and can be built on an understanding of simpler model problems. This section summarizes the time-independent Hamiltonians and wavefunctions that emerge for common models for quantum mechanical objects. These models form the starting point for describing the motion of electrons and the translational, rotational, and vibrational motions of molecules and are the basis for models we will explore further. Understanding them is key in developing intuition about more complex problems.

Waves and free particles

Waves form the basis for our quantum mechanical description of matter. Waves describe the oscillatory amplitude of matter and fields in time and space, taking a number of forms. The simplest form we will use is plane waves, which can be written as

$$\psi(\mathbf{r},t) = \mathbf{A}\exp[\mathrm{i}\mathbf{k}\cdot\mathbf{r} - \mathrm{i}\omega t] \tag{1.4.1}$$

The angular frequency ω describes the oscillations in time and is related to the number of cycles per second through $\nu = \omega/2\pi$. The wave amplitude also varies in space as determined by the wavevector $\mathbf{k}$, where the number of cycles per unit distance (wavelength) is $\lambda = \omega/k$. Thus, the wave propagates in time and space along a direction $\mathbf{k}$ with a vector amplitude $\mathbf{A}$ and a phase velocity $v_\phi = v\lambda$

For a free particle of mass m in one dimension, the Hamiltonian only reflects the kinetic energy of the particle energy

$$\hat{H} = \hat{T} = \frac{\hat{p}_x^2}{2m} = -\frac{\hbar^2}{2m}\frac{\partial^2}{\partial x^2} \tag{1.4.2}$$

Solving the time-independent Schrödinger equation leads to plane-wave eigenstates of the form:

$$\psi_k(x) = \frac{1}{\sqrt{2\pi\hbar}}\exp\left(\frac{\pm\mathrm{i}px}{\hbar}\right) = \frac{1}{\sqrt{2\pi}}\exp(\pm\mathrm{i}kx) \tag{1.4.3}$$

where $k = p/\hbar$. Inserting this expression into the TISE, $\hat{H}\Psi = E\Psi$, we find that k, the wavenumber, is given by

$$k = \sqrt{\frac{2mE}{\hbar^2}} \tag{1.4.4}$$

The energy eigenvalues are given by

$$E_k = \frac{\hbar^2 k^2}{2m} \tag{1.4.5}$$

We added a subscript k to the expressions for the eigenfunctions and eigenenergies to emphasize that k is used as a label or index for an eigenstate in the position basis in addition to being a real number.

Free particle plane waves $\psi_k(x)$ are the eigenstates describing a free particle or a particle under the influence of a constant potential, but they form a complete and continuous basis set with which to describe the spatial characteristics of any wavefunction. Note that the eigenfunctions, eq. (1.4.3), are oscillatory over all space. Thus, describing a plane wave allows one to exactly specify the wavevector or momentum of the particle, but one cannot localize it to any point in space. In this form, the free particle is not observable because its wavefunction extends infinitely and cannot be normalized. An observation, however, taking an expectation value of a Hermitian operator will collapse this wavefunction to yield an average momentum of the particle with a corresponding uncertainty relationship to its position.

Particle-in-a-Box

The minimal model for translational motion of a particle that is confined in space is given by the particle-in-a-box. For the case of a particle confined in one dimension in a box of length L with impenetrable walls, we define the Hamiltonian as

\[\begin{align} \hat{H} &=\frac{\hat{p}^{2}}{2 m}+V(x) \[3pt] V(x) &= \begin{cases} 0 \ & 0

The boundary conditions require that the particle cannot have any probability of being within the wall, so the wavefunction should vanish at $x = 0$ and L_x, as with standing waves. Solutions to the Schrödinger equation with these boundary conditions lead to normalized eigenfunctions of the form

$$\psi_n = \sqrt{\frac{2}{L}} \sin \frac{n\pi x}{L} \qquad n = 1, 2, 3 \ldots \tag{1.4.6}$$

Here values of n are the integer quantum numbers that describe the harmonics of the fundamental frequency π/L whose oscillations will fit into the box while obeying the boundary conditions. We see that any state of the particle-in-a-box can be expressed in a Fourier series. On inserting eq. (1.4.8) into the time-independent Schrödinger equation (TISE) we find the energy eigenvalues

$$E_n = \frac{n^2 \pi^2 \hbar^2}{2mL^2} \tag{1.4.7}$$

Recognizing that the wavevector of these waves is $k_n = (n\pi/L)$, we see that the energies correspond to free-particle energies $E_n = \hbar^2 k_n^2/2m$, although now with limits on what values k can assume. Note that the spacing between adjacent energy levels grows as $n(n + 1)$.

This model is readily extended to a three-dimensional box by separating the box into x, y, and z coordinates. Then

$$\hat{H} = \hat{H}_x + \hat{H}_y + \hat{H}_z \tag{1.4.8}$$

in which each term is specified as eq. (1.4.6). Since $\hat{H}_x, \hat{H}_y$, and $\hat{H}_z$ commute, each dimension is separable from the others. Then we find

$$\psi(x, y, z) = \psi_x \psi_y \psi_z \tag{1.4.9}$$

$$E_{x,y,z} = E_x + E_y + E_z \tag{1.4.10}$$

which follow the definitions given in eq. (1.4.8) and eq. (1.4.9) above. The state of the system is now specified by three quantum numbers with positive integer values: $n_x, n_y, n_z = 1, 2, 3 \ldots$.

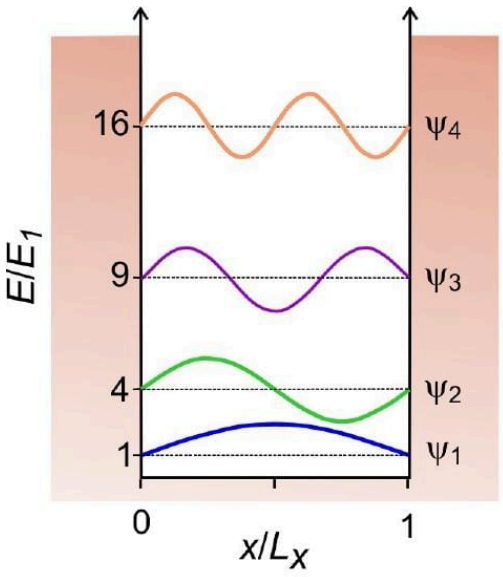


Figure 1.4.1. Particle-in-a-box potential wavefunctions that are plotted superimposed on their corresponding energy levels.

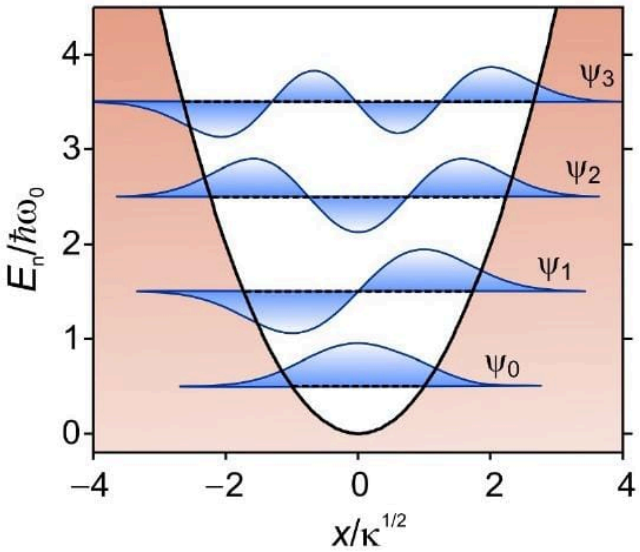


Figure 1.4.2. Harmonic oscillator potential showing wavefunctions that are superimposed on their corresponding energy levels.

Harmonic Oscillator

The harmonic oscillator Hamiltonian refers to a particle confined to a parabolic, or harmonic, potential. We will use it to represent vibrational motion in molecules, but it also becomes a general framework for understanding all bosons. For a classical particle bound in a one-dimensional potential, the potential near the minimum x_0 can be expanded as

$$V(x) = V(x_0) + \left(\frac{\partial V}{\partial x}\right)_{x=x_0}(x - x_0) + \frac{1}{2}\left(\frac{\partial V^2}{\partial x^2}\right)_{x=x_0}(x - x_0)^2 + \cdots \tag{1.4.11}$$

Setting x_0 to 0 , the leading term with a dependence on x is the second-order (harmonic) term $V = -\kappa x^2/2$, where the force constant $\kappa = -\left(\partial^2 V/\partial x^2\right)_{x=0}$. The classical Hamiltonian for a particle of mass m confined to this potential is

$$H = \frac{p^2}{2m} + \frac{1}{2}\kappa x^2 \tag{1.4.12}$$

Noting that the force constant and frequency of oscillation for a harmonic oscillator are related by $\kappa = m\omega_0^2$, we can substitute operators for p and x in eq. (1.4.14) to obtain the quantum Hamiltonian

$$\hat{H} = -\frac{1}{2}\frac{\hbar^2}{m}\frac{\partial^2}{\partial x^2} + \frac{1}{2}m\omega_0^2\hat{x}^2 \tag{1.4.13}$$

We will also make use of reduced, or mass-weighted, coordinates defined as

$$\begin{aligned} \underset{\sim}{p} &= \sqrt{\frac{1}{m\hbar\omega_0}}\hat{p} \\ \underset{\sim}{x} &= \sqrt{\frac{m\omega_0}{\hbar}}\hat{x} \end{aligned} \tag{1.4.14}$$

for which the Hamiltonian can be written as

$$\hat{H} = \frac{1}{2}\hbar\omega_0\left(\underset{\sim}{p}^2 + \underset{\sim}{x}^2\right) \tag{1.4.15}$$

In this form, one can readily see that the energy—the expectation value of the Hamiltonian—is equally split between the kinetic and potential energy.

The energy eigenvalues for the harmonic oscillator Hamiltonian are discrete equally spaced in units of the vibrational quantum $\hbar\omega_0$ above the zero-point energy $\hbar\omega_0/2$.

$$E_n = \hbar\omega_0\left(n + \frac{1}{2}\right) \quad n = 0, 1, 2\ldots \tag{1.4.16}$$

where n is the vibrational quantum number. The corresponding eigenstates in the position representation are expressed in terms of Hermite polynomials, $\mathcal{H}_n(x)$,

$$\psi_n(x) = \sqrt{\frac{\alpha}{2^n\sqrt{\pi}n!}} e^{-\alpha^2 x^2/2}\, \mathcal{H}_n(\alpha x) \qquad n = 0, 1, 2 \ldots \tag{1.4.17}$$

where $\alpha = \sqrt{m\omega_0/\hbar}$ and the Hermite polynomials are obtained from

$$\mathcal{H}_n(x) = (-1)^n e^{x^2} \frac{d^n}{dx^n} e^{-x^2} \tag{1.4.18}$$

The ground state wavefunction is a Gaussian function: $\psi_0(x) = (m\omega_0/\pi\hbar)^{1/4} \exp\left(-m\omega_0 x^2/2\hbar\right)$.

This page titled 1.4: Basic Quantum Models is shared under a CC BY-NC-SA 4.0 license and was authored, remixed, and/or curated by Andrei Tokmakoff via source content that was edited to the style and standards of the LibreTexts platform.

1.5: Raising and Lowering Operators

From a practical point of view, often it will be useful for us to bypass the position representation and work problems involving harmonic oscillators in terms of raising and lower operators, also known as *creation and annihilation operators*, or ladder operators. We define these as:

$$\hat{a} = \sqrt{\frac{m\omega_0}{2\hbar}}\left(\hat{x} + \frac{\mathrm{i}}{m\omega_0}\hat{p}\right) \tag{1.5.1}$$

$$\hat{a}^\dagger = \sqrt{\frac{m\omega_0}{2\hbar}}\left(\hat{x} - \frac{\mathrm{i}}{m\omega_0}\hat{p}\right) \tag{1.5.2}$$

This definition is motivated by the fact that the classical expression $\underset{\sim}{p}^2 + \underset{\sim}{x}^2$ that we see in the Hamiltonian can be factored as $(\underset{\sim}{x} + \mathrm{i}\underset{\sim}{p})(\underset{\sim}{x} - \mathrm{i}\underset{\sim}{p})$, although for the quantum case one has to consider that $\hat{x}$ and $\hat{p}$ do not commute. The $\hat{a}$ and $\hat{a}^\dagger$ operators are Hermitian conjugates of one another, but they are not Hermitian operators (self-adjoint). These operators get their name from their action, which is to lower or raise the state of the system:

$$\hat{a}|n\rangle = \sqrt{n}\,|n-1\rangle \tag{1.5.3}$$

$$\hat{a}^\dagger|n\rangle = \sqrt{n+1}\,|n+1\rangle \tag{1.5.4}$$

Then we find that the position and momentum operators are

$$\hat{x} = \sqrt{\frac{\hbar}{2m\omega_0}}\left(\hat{a}^\dagger + \hat{a}\right) \tag{1.5.5}$$

$$\hat{p} = \mathrm{i}\sqrt{\frac{m\hbar\omega_0}{2}}\left(\hat{a}^\dagger - \hat{a}\right) \tag{1.5.6}$$

When we substitute these ladder operators for the position and momentum operators-known as second quantization - the Hamiltonian becomes

$$\hat{H} = \hbar\omega_0\left(\hat{n} + \frac{1}{2}\right) \tag{1.5.7}$$

The number operator is defined as $\hat{n} = \hat{a}^\dagger\hat{a}$ and returns a count of the quantum number for the state of the system: $\hat{n}\,|n\rangle = n\,|n\rangle$. (Note here n is playing the role of an operator, an eigenstate index, and an integer number). The energy eigenvalues satisfying $\hat{H}\,|n\rangle = E_n\,|n\rangle$ are given by eq. (1.4.18). Since the quantum numbers cannot be negative, we assert a boundary condition $a|0\rangle = 0$, where $\mathbb{0}$ refers to the null vector.

This is an example of second quantization, in which the operators that we originally replaced the classical position and momentum with, are themselves replaced by the raising and lowering operators in the energy representation of the system. In fact the Hamiltonian, eq. (1.5.7), is often expressed directly as $\hat{H} = \hbar\omega_0\hat{a}^\dagger\hat{a}$, where dropping the constant factor $\hbar\omega_0/2$ merely changes the reference point for the zero of energy. The harmonic oscillator Hamiltonian expressed in raising and lowering operators, together with its commutation relationship

$$\left[\hat{a}, \hat{a}^\dagger\right] = 1 \tag{1.5.8}$$

is used as a general representation of all bosons, which for our purposes includes vibrations, phonons, and photons.

Properties of Raising and Lowering Operators

$$\left[\hat{a}, \hat{a}^\dagger\right] = 1 \tag{1.5.9}$$

$$\left[\hat{n}, \hat{a}\right] = -\hat{a} \qquad \left[\hat{n}, \hat{a}^\dagger\right] = \hat{a}^\dagger \tag{1.5.10}$$

$$\left[\hat{a}, \hat{a}\right] = 0 \qquad \left[\hat{a}^\dagger, \hat{a}^\dagger\right] = 0 \tag{1.5.11}$$

$$\left[\hat{a}, (\hat{a}^\dagger)^n\right] = n(\hat{a}^\dagger)^{n-1} \tag{1.5.12}$$

$$\left[\hat{a}^\dagger, \hat{a}^n\right] = -n\hat{a}^{n-1} \tag{1.5.13}$$

$$|n\rangle = \frac{1}{\sqrt{n!}}(\hat{a}^\dagger)^n|0\rangle \tag{1.5.14}$$

$$\hat{a}|n\rangle = \sqrt{n}\,|n-1\rangle \qquad \hat{a}^\dagger|n\rangle = \sqrt{n+1}\,|n+1\rangle \tag{1.5.15}$$

$$\langle n|\hat{a} = \sqrt{n+1}\,\langle n+1| \qquad \langle n|\hat{a}^\dagger = \sqrt{n}\,\langle n-1| \tag{1.5.16}$$

This page titled 1.5: Raising and Lowering Operators is shared under a CC BY-NC-SA 4.0 license and was authored, remixed, and/or curated by Andrei Tokmakoff via source content that was edited to the style and standards of the LibreTexts platform.

1.6: Angular Momentum

Angular momentum operators

To describe quantum mechanical rotation or orbital motion, one must quantize angular momentum. The orbital angular momentum operator is defined as

$$\hat{L} = \hat{r} \times \hat{p} = \mathrm{i}\hbar(\hat{r} \times \nabla) \tag{1.6.1}$$

It has three components $(\hat{L}_x, \hat{L}_y, \hat{L}_z)$ that generate rotation about the x, y, or z axis, and whose magnitude is given by $\hat{L}^2 = \hat{L}_x^2 + \hat{L}_y^2 + \hat{L}_z^2$. The angular momentum operators follow the commutation relationships

$$\left[H, L^2\right] = 0 \tag{1.6.2}$$

$$\left[L^2, L_z\right] = 0 \tag{1.6.3}$$

$$[L_x, L_y] = \mathrm{i}\hbar L_z \tag{1.6.4}$$

Note that in eq. (1.6.4) the x, y, and z indices can be cyclically permuted. There is an eigenbasis common to H and L^2 and one of the three L_i, which is L_z by convention. The eigenvalues for the orbital angular momentum operator L and z-projection of the angular momentum L_z are

$$L^2 |\ell m\rangle = \hbar^2 \ell(\ell+1) |\ell m\rangle \qquad \ell = 0, 1, 2 \ldots \tag{1.6.5}$$

$$L_z |\ell m\rangle = \hbar m |\ell m\rangle \qquad m = 0, \pm 1, \pm 2 \ldots \pm \ell \tag{1.6.6}$$

where the eigenstates $|\ell m\rangle$ are labeled by the orbital angular momentum quantum number ℓ, and the magnetic quantum number m. The eigenstates are found to be spherical harmonics $|\ell m\rangle = Y_\ell^m(\theta, \phi)$ as discussed below.

Similar to the strategy used for the harmonic oscillator, we can also define raising and lowering operators for the total angular momentum,

$$\hat{L}_\pm = \hat{L}_i \pm \mathrm{i}\hat{L}_y \tag{1.6.7}$$

which follow the commutation relations $[\hat{L}^2, \hat{L}_\pm] = 0$ and $[\hat{L}_z, \hat{L}_\pm] = \pm\ \hbar\hat{L}_\pm$, and satisfy the eigenvalue equation

$$\hat{L}_\pm |\ell m\rangle = C_{\ell,m}^\pm |\ell(m \pm 1)\rangle \tag{1.6.8}$$

$$C_{\ell,m}^\pm = \hbar[\ell(\ell+1) - m(m \pm 1)]^{1/2} \tag{1.6.9}$$

Thus, $\hat{L}_+$ and $\hat{L}_-$ respectively raise and lower the magnetic quantum number by 1, changing the projection of the angular momentum on z by $\pm\hbar$.

Spherically Symmetric Potential

Let's examine the role of angular momentum for the case of a particle experiencing a spherically symmetric potential $V(r)$ such as the hydrogen atom and a 3D isotropic harmonic oscillator.(1) For a particle with mass m_R, the Hamiltonian is

$$\hat{H} = -\frac{\hbar^2}{2m_R}\nabla^2 + V(r) \tag{1.6.10}$$

Writing the kinetic energy operator in spherical coordinates,

$$-\frac{\hbar^2}{2m_R}\nabla^2 = -\frac{\hbar^2}{2m_R}\left(\frac{1}{r^2}\frac{\partial}{\partial r}r^2\frac{\partial}{\partial r} - \frac{1}{r^2}L^2\right) \tag{1.6.11}$$

where the square of the total angular momentum is

$$L^2 = -\frac{1}{\sin\theta}\left(\frac{1}{\sin\theta}\frac{\partial^2}{\partial\phi^2} + \frac{\partial}{\partial\theta}\sin\theta\frac{\partial}{\partial\theta}\right) \tag{1.6.12}$$

We note that this representation separates the radial dependence in the Hamiltonian from the angular part. We therefore expect that the overall wavefunction can be written as a product of a radial and an angular part in the form

$$\psi(r,\theta,\phi) = R(r)Y(\theta,\phi) \tag{1.6.13}$$

Substituting eq. (1.6.13) into the TISE, we find that we solve for the orientational and radial wavefunctions separately. Considering solutions first to the angular part, we note that the potential is only a function of r, and only need to consider the angular momentum. This leads to the identities in eq. (1.6.5) and eq. (1.6.6), revealing that the $|\ell m\rangle$ wavefunctions projected onto spherical coordinates are represented by the spherical harmonics:

$$Y_\ell^m(\theta,\phi) = N_{\ell m}^{(Y)} P_\ell^{|m|}(\cos\theta)\mathrm{e}^{\mathrm{i}m\phi} \tag{1.6.14}$$

where $\ell = 0, 1, 2 \ldots$ and $m = 0, \pm 1, \pm 2 \ldots$ P_ℓ^m are the associated Legendre polynomials, and the normalization factor is

$$N_{\ell m}^{(Y)} = (-1)^{(m+|m|)/2}(\mathrm{i})^\ell \left[\frac{2\ell+1}{4\pi}\frac{(\ell-|m|)!}{(\ell+|m|)!}\right]^{1/2} \tag{1.6.15}$$

The angular components of the wavefunction are common to all eigenstates of spherically symmetric potentials. In chemistry, it is common to use real angular wavefunctions instead of the complex form in eq. (1.6.14). These are constructed from the linear combinations $Y_{\ell,m} \pm Y_{\ell,-m}$.

Substituting eq. (1.6.11) and eq. (1.6.5) into eq. (1.6.10) leads to a new Hamiltonian that can be inserted into the Schrödinger equation. This can be solved as a purely radial problem for a given

$$\left(-\frac{\hbar^2}{2m_R}\frac{\partial^2}{\partial r^2} + U(r,\ell)\right)\chi = E\chi \tag{1.6.16}$$

U plays the role of an effective potential:

$$U(r,\ell) = V(r) + \frac{\hbar^2}{2m_R r^2}\ell(\ell+1) \tag{1.6.17}$$

Equation (1.6.16) is known as the radial wave equation. It looks like the TISE for a one-dimensional problem in r, where we could solve this equation for each value of ℓ. Note U has a repulsive wall as $r \to 0$ due to the centrifugal kinetic energy that scales as r^{-2} for $\ell > 0$.

The wavefunctions defined in eq. (1.6.13) are normalized such that

$$\int |\psi|^2 d\Omega = 1 \tag{1.6.18}$$

where

$$\int d\Omega \equiv \int_0^\infty r^2\, dr \int_0^\pi \sin\theta\, d\theta \int_0^{2\pi} d\phi \tag{1.6.19}$$

If we restrict the integration to be over all angles, we find that the probability of finding a particle between a distance r and $r + dr$ is $P(r) = 4\pi r^2 |R(r)|^2 = 4\pi|\chi(r)|^2$.

To this point the treatment of orbital angular momentum is identical for any spherically symmetric potential. Now we must consider the specific form of the potential. For instance, in the case of the isotropic harmonic oscillator, $U(r) = \frac{1}{2}\kappa r^2$. In the case of a free particle, we substitute $V(r) = 0$ in eq. (1.6.17) and find that the radial solutions can be written in terms of spherical Bessel functions, j_ℓ. Then the solutions to the full wavefunction for the free particle can be expanded in the product states:

$$\Psi_{\ell,m}(r,\theta,\phi) = j_\ell(kr)Y_\ell^m(\theta,\phi) \tag{1.6.20}$$

where the wavevector k is defined as in eq. (1.4.4). Of course, these spherical waves form a poor substitute for describing linear motion of a particle with a plane wave basis set.

Hydrogen Atom

For a hydrogen-like atom, a single electron of charge e and rest mass m_e interacts with a nucleus of charge Ze under the influence of a Coulomb potential

$$V_H(r) = -\frac{Ze^2}{4\pi\dot{o}_0}\frac{1}{r} \tag{1.6.21}$$

We can simplify the expression by defining atomic units for distance and energy. The Bohr radius is defined as

$$a_0 = 4\pi\varepsilon_0\frac{\hbar^2}{m_e e^2} = 5.2918 \times 10^{-11}\,\mathrm{m} \tag{1.6.22}$$

and the Hartree is

$$\mathcal{E}_H = \frac{1}{4\pi\varepsilon_0}\frac{e^2}{a_0} = 4.3598 \times 10^{-18}\ \mathrm{J} = 27.2\,\mathrm{eV} \tag{1.6.23}$$

Written in terms of atomic units, we can see from eq. (1.6.23) that eq. (1.6.21) becomes $(V/\mathcal{E}_H) = -Z/(r/a_0)$. Thus, the conversion effectively sets the SI variables $m_\mathrm{e} = e = (4\pi\varepsilon_0)^{-1} = \hbar = 1$. Then the radial wave equation is

$$\frac{\partial^2\chi}{\partial r^2} + \left(\frac{2Z}{r} - \frac{\ell(\ell+1)}{r^2}\right)\chi = 2E\chi \tag{1.6.24}$$

The effective potential within the parentheses in eq. (1.6.24) is shown in Figure 1.6.1 for varying ℓ. Solutions to the radial wavefunction for the hydrogen atom take the form

$$R_{n\ell}(r) = N_{n\ell}^{(H)}\rho^\ell\mathcal{L}_{n+\ell}^{2\ell+1}(\rho)e^{-\rho/2} \tag{1.6.25}$$

where the reduced radius $\rho = 2r/na_0$ and $\mathcal{L}_k^\alpha(z)$ are the associated Laguerre polynomials. The primary quantum number takes on integer values $n = 1, 2, 3\ldots$, and ℓ is constrained such that $\ell = 0, 1, 2\ldots n-1$. The radial normalization factor in eq. (1.6.25) is

$$N_{n\ell}^{(H)} = -\frac{2}{n^3 a_0^{3/2}}\left[\frac{(n-\ell-1)!}{[(n+1)!]^3}\right]^{1/2} \tag{1.6.26}$$

The energy eigenvalues are

$$E_n = -\frac{Z^2}{2n^2}\mathcal{E}_H \tag{1.6.27}$$

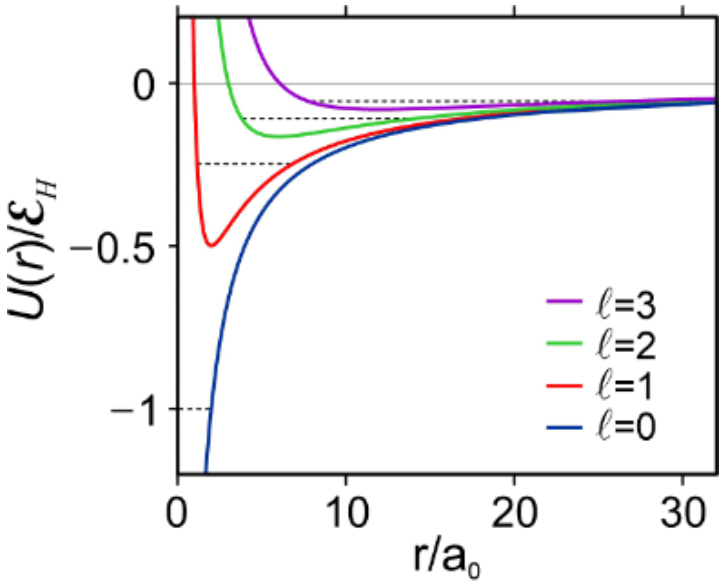


Figure 1.6.1. The radial effective potential for the hydrogen atom, $U_{\mathrm{eff}}(\rho)$.

Electron Spin

In describing electronic wavefunctions, we also include the contribution from electron spin. The electron spin angular momentum S and its z-projection are quantized as

$$S^2 |sm_s\rangle = \hbar^2 s(s+1) |sm_s\rangle \qquad s = 0, \tfrac{1}{2}, 1, \tfrac{3}{2}, 2 \ldots \tag{1.6.28}$$

$$S_z |sm_s\rangle = \hbar m_s |sm_s\rangle \qquad m_s = -s, -s+1, \ldots, s \tag{1.6.29}$$

where the electron spin eigenstates $|sm_s\rangle$, are labeled by the electron spin angular momentum quantum number s, and the spin magnetic quantum number m_s. The number of values of S_z is $2s+1$ and is referred to as the spin multiplicity. As fermions, electrons have half-integer spin, and each unpaired electron contributes $\frac{1}{2}$ to the electron spin quantum number s. A single unpaired electron has $s = \frac{1}{2}$, for which $m_s = \pm\frac{1}{2}$ corresponding to spin-up and spin-down configurations. For multielectron systems, the spin is calculated as the vector sum of spins, essentially $\frac{1}{2}$ times the number of unpaired electrons.

The resulting total angular momentum for an electron is $J = L + S$. J has associated with it the total angular momentum quantum number j, which takes on values of $j = |\ell - s|, |\ell - s| + 1, \ldots, \ell + s$. The additive nature of the orbital and spin contributions to the angular momentum leads to a total electronic wavefunction that is a product of spatial and spin wavefunctions.

$$\Psi_{\text{tot}} = \Psi(r, \theta, \phi) |sm_s\rangle \tag{1.6.30}$$

Thus, the state of an electron can be specified by four quantum numbers $\Psi_{\text{tot}} = |n\ell m_\ell m_s\rangle$.

Rigid Rotor

In the case of an isolated molecule spinning freely about its center of mass, the total angular momentum J is obtained from the sum of the orbital angular momentum L and spin angular momentum S for the molecular constituents: $J = L + S$, where $L = \sum_i L_i$ and $S = \sum_i S_i$. The case of the rigid rotor refers to the minimal model for the rotational quantum states of a freely spinning object with one principle axis of rotation (cylindrical symmetry) and no magnetic spin. Then, the Hamiltonian is given by the rotational kinetic energy

$$H_{\text{rot}} = \frac{\hat{J}^2}{2I} \tag{1.6.31}$$

I is the moment of inertia about the principle axis of rotation. The eigenfunctions for this Hamiltonian $|JM\rangle$ can be expressed as the spherical harmonics $Y_{J,M}(\theta, \phi)$ in eq. (1.6.14)

$$\hat{J}^2 |JM\rangle = \hbar^2 J(J+1) |JM\rangle \qquad J = 0, 1, 2 \ldots \tag{1.6.32}$$

$$\hat{J}_z |JM\rangle = M\hbar |JM\rangle \qquad M = -J, -J+1, \ldots, J \tag{1.6.33}$$

J is the rotational quantum number. M is its projection onto the z axis. The energy eigenvalues for H_{rot} are

$$E_{J,M} = \bar{B} J(J+1) \tag{1.6.34}$$

where the rotational constant $\bar{B}$ is

$$\bar{B} = \frac{\hbar^2}{2I} \tag{1.6.35}$$

More commonly, $\bar{B}$ is given in spectroscopic units of cm^{-1} using $\bar{B} = h/8\pi^2 Ic$.

References

(1) Zettili, N. *Quantum Mechanics: Concepts and Applications*, 2nd ed.; Wiley, 2009.

This page titled 1.6: Angular Momentum is shared under a CC BY-NC-SA 4.0 license and was authored, remixed, and/or curated by Andrei Tokmakoff via source content that was edited to the style and standards of the LibreTexts platform.

1.7: Exponential Operators

Throughout our work, we will make use of exponential operators of the form

$$\hat{T} = e^{-\mathrm{i}\hat{A}} \tag{1.7.1}$$

These appear commonly as unitary transformations, although generally $\hat{A}$ need not be Hermitian. We will see that these exponential operators act on a wavefunction to move it in time and space and are therefore also referred to as propagators. Of particular interest to us is the time-evolution operator $\hat{U} = e^{-\mathrm{i}\hat{H}t/\hbar}$, which propagates the wavefunction in time. Note that $\hat{T}$ is a function of an operator, $f(\hat{A})$. A function of an operator is defined through its expansion in a Taylor series, for instance

$$\hat{T} = e^{\mathrm{i}\hat{A}} = \sum_{n=0}^{\infty} \frac{(\mathrm{i}\hat{A})^n}{n!} = 1 + \mathrm{i}\hat{A} - \frac{\hat{A}\hat{A}}{2} - \cdots \tag{1.7.2}$$

Since we use them so frequently, let's review the properties of exponential operators that can be established with eq. (1.7.2). If the operator $\hat{A}$ is Hermitian, then $\hat{T} = e^{\mathrm{i}\hat{A}}$ is unitary, and we call $\hat{T}$ a unitary transformation. Then $\hat{T}^\dagger = \hat{T}^{-1}$, and the Hermitian conjugate of $\hat{T}$ reverses the action of $\hat{T}$. For the time-propagator $\hat{U}$, the Hermitian conjugate $\hat{U}^\dagger$ is often referred to as the time-reversal operator.

The eigenstates of the operator $\hat{A}$ also are also eigenstates of $f(\hat{A})$, and eigenvalues are functions of the eigenvalues of $\hat{A}$. Namely, if we know the eigenvalues and eigenvectors of $\hat{A}$, i.e., $\hat{A}\varphi_n = a_n\varphi_n$, we can show by expanding the function that

$$f(\hat{A})\varphi_n = f(a_n)\varphi_n \tag{1.7.3}$$

Our most common application of this property will be in exponential operators involving time-propagation with the Hamiltonian. Given the eigenstates φ_n, then $\hat{H}\left|\varphi_n\right\rangle = E_n\left|\varphi_n\right\rangle$ implies

$$e^{-\mathrm{i}\hat{H}t/\hbar}\left|\varphi_n\right\rangle = e^{-\mathrm{i}E_n t/\hbar}\left|\varphi_n\right\rangle \tag{1.7.4}$$

This is the expression for a time-independent operator, the Hamiltonian. We will discuss the nuances of how this expression changes for a time-dependent operator in the next chapter.

Just as $\hat{U} = e^{-\mathrm{i}\hat{H}t/\hbar}$ is the time-evolution operator that displaces the wavefunction in time, $\hat{D}_x = e^{-\mathrm{i}\hat{p}_x x/\hbar}$ is the spatial displacement operator that moves ψ along the x coordinate. If we define $\hat{D}_x(\lambda) = e^{-\mathrm{i}\hat{p}_x\lambda/\hbar}$, then the action is to displace the wavefunction by an amount λ.

$$\left|\psi(x-\lambda)\right\rangle = \hat{D}_x(\lambda)\left|\psi(x)\right\rangle \tag{1.7.5}$$

Also, applying $\hat{D}_x(\lambda)$ to a position operator shifts the operator by λ:

$$\hat{D}_x^\dagger \hat{x} \hat{D}_x = x + \lambda \tag{1.7.6}$$

Thus $e^{-\mathrm{i}\hat{p}_x\lambda/\hbar}\left|x\right\rangle$ is an eigenvector of $\hat{x}$ with eigenvalue $x + \lambda$ instead of x. The operator $\hat{D}_x = e^{-\mathrm{i}\hat{p}_x\lambda/\hbar}$ is a displacement operator for x position coordinates. Similarly, $\hat{D}_y = e^{-\mathrm{i}\hat{p}_y\lambda/\hbar}$ generates displacements in y and $\hat{D}_z$ in z. The displacement operator $\hat{D}$ must be unitary, since the action of $\hat{D}^\dagger\hat{D}$ must leave the system unchanged. That is if $\hat{D}_x$ shifts the system to x from x_0, then $\hat{D}_x^\dagger$ shifts the system from x back to x_0.

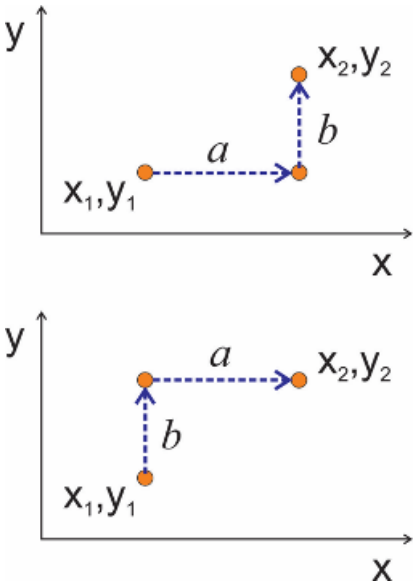


Figure 1.7.1: (Top) Displacement first along y by an amount a, then along y by b. (Bottom) Displacement in the reverse order yields the same state.

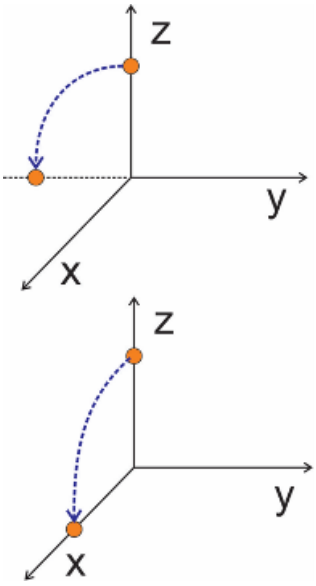


Figure 1.7.2: (Top) Rotation first about x by $\pi/2$, then about y by $\pi/2$, leaves the particle on the $-y$ axis. (Bottom) Changing order by first rotating about y, then about x, leads to particle along the $+x$ axis.

We know intuitively that linear displacements commute. For example, if we wish to shift a particle in two dimensions, x and y, the order of displacement does not matter. We end up at the same position, whether we move along x first or along y, as illustrated in Figure 1.7.1 In terms of displacement operators, we can write

$$\begin{aligned} |x_2, y_2\rangle &= e^{-ibp_y/\hbar} e^{-iap_x/\hbar} |x_1, y_1\rangle \\ &= e^{-iap_x/\hbar} e^{-ibp_y/\hbar} |x_1, y_1\rangle \end{aligned} \tag{1.7.7}$$

These displacement operators commute, as expected from $[p_x, p_y] = 0$.

Like the displacement operator, we can define rotation operators that depend on the angular momentum operators, L_x, L_y, and L_z. For instance, $\hat{R}_x(\phi) = e^{-i\phi L_x/\hbar}$ gives a rotation by angle ϕ about the x axis. Unlike linear displacement, rotations about different axes do not commute. For example, consider a state representing a particle displaced along the z axis, $|z_0\rangle$. Now the action of two rotations $\hat{R}_x$ and $\hat{R}_y$ by an angle of $\phi = \pi/2$ on this particle differs depending on the order of operation, as illustrated in Figure 1.7.2. If we rotate first about x, the operation

$$e^{-i\frac{\pi}{2}L_y/\hbar} e^{-i\frac{\pi}{2}L_x/\hbar} |z_0\rangle \rightarrow |-y\rangle \tag{1.7.8}$$

leads to the particle on the $-y$ axis, whereas the reverse order

$$e^{-i\frac{\pi}{2}L_x/\hbar}e^{-i\frac{\pi}{2}L_y/\hbar}|z_0\rangle \rightarrow |+x\rangle \tag{1.7.9}$$

leads to the particle on the $+x$ axis. The final state of these two rotations taken in opposite order differ by a rotation about the z axis. Since rotations about different axes do not commute, we expect the angular momentum operators not to commute. Indeed, we know that $[L_x, L_y] = i\hbar L_z$, where the commutator of rotations about the x and y axes is related by a z-axis rotation. As with rotation operators, we will need to be careful with time-propagators to determine whether the order of time-propagation matters. This, in turn, will depend on whether the Hamiltonians at two points in time commute.

Properties of Exponential Operators

1. If $\hat{A}$ and $\hat{B}$ do not commute, but $[\hat{A}, \hat{B}]$ commutes with $\hat{A}$ and $\hat{B}$, then

$$e^{\hat{A}+\hat{B}} = e^{\hat{A}}e^{\hat{B}}e^{-\frac{1}{2}[\hat{A},\hat{B}]} \tag{1.7.10}$$

$$e^{\hat{A}}e^{\hat{B}} = e^{\hat{B}}e^{\hat{A}}e^{-[\hat{B},\hat{A}]} \tag{1.7.11}$$

2. More generally, if $\hat{A}$ and $\hat{B}$ do not commute,

$$e^{\hat{A}}e^{\hat{B}} = \exp\left[\hat{A}+\hat{B}+\frac{1}{2}[\hat{A},\hat{B}]+\frac{1}{12}([\hat{A},[\hat{A},\hat{B}]]+[\hat{A},[\hat{B},\hat{B}]])+\cdots\right] \tag{1.7.12}$$

3. The Baker-Campbell-Hausdorff formula for non-commuting operators:

$$e^{i\hat{B}\lambda}\hat{A}e^{-i\hat{B}\lambda} = \hat{A}+i\lambda[\hat{B},\hat{A}]+\left(\frac{i^2\lambda^2}{2!}\right)[\hat{B},[\hat{B},\hat{A}]]+\ldots \tag{1.7.13}$$
$$+\left(\frac{i^n\lambda^n}{n!}\right)[\hat{B},[\hat{B}\ldots[\hat{B},\hat{A}]]\ldots]+\ldots$$

where λ is a number.

4. In the matrix representation, the exponential operator is defined through an expansion of products of matrices, as in eq. (1.7.2). The exponential of a diagonal matrix is obtained just by exponentiating the diagonal elements. Thus, if the matrix $\hat{A}$ is diagonalizable as $\hat{\Lambda} = S^{-1}\hat{A}S$ then $e^{\hat{A}} = Se^{\hat{\Lambda}}S^{-1}$. Also, the determinant of $\hat{A}$, $\det(e^{\hat{A}}) = e^{\mathrm{Tr}(\hat{A})}$.
5. The Lie-Trotter product formula can be used to discretize an operator into small steps:

$$e^{\hat{A}+\hat{B}} = \lim_{n\to\infty}\left(e^{\hat{A}/n}e^{\hat{B}/n}\right)^n \tag{1.7.14}$$

6. For functions of operators: if $\hat{A}$ commutes with $\hat{B}$, then $\hat{B}$ commutes with $f(\hat{A})$. For functions of x and p,

$$[f(\hat{x}),\hat{p}] = i\hbar\frac{\partial f(x)}{\partial x} \tag{1.7.15}$$

7. The adjoint of $f(\hat{A})$ is $[f(\hat{A})]^\dagger = f^*(\hat{A}^\dagger)$

This page titled 1.7: Exponential Operators is shared under a CC BY-NC-SA 4.0 license and was authored, remixed, and/or curated by Andrei Tokmakoff via source content that was edited to the style and standards of the LibreTexts platform.

1.8: Readings

Useful texts that are good to review introductory concepts and which we will refer to

1. Atkins, P. W.; Friedman, R. *Molecular Quantum Mechanics*, 4th ed.; Oxford University Press, 2005.
2. Baym, G. *Lectures on Quantum Mechanics*; W.A. Benjamin, 1969. DOI: 10.1201/9780429499265
3. Cohen-Tannoudji, C.; Diu, B.; Laloë, F. *Quantum Mechanics*; Wiley, 1977.
4. Griffiths, D. J. *Introduction to Quantum Mechanics*, 2nd ed.; Pearson Prentice Hall, 2005.
5. Merzbacher, E. *Quantum Mechanics*, 3rd ed.; Wiley, 1998.
6. Messiah, A. *Quantum Mechanics*; Dover Publications, 1999.
7. Sakurai, J. J. *Modern Quantum Mechanics*, Rev. ed.; Addison-Wesley, 1994.

The classic paper that introduced bra-ket notation

1. Dirac, P. A. M. A new notation for quantum mechanics. *Mathematical Proceedings of the Cambridge Philosophical Society* **1939**, *35* (3), 416-418. DOI: 10.1017/S0305004100021162

This page titled 1.8: Readings is shared under a CC BY-NC-SA 4.0 license and was authored, remixed, and/or curated by LibreTexts.

2: THE SCHRÖDINGER EQUATION AND TIME-PROPAGATOR

2.1: Dynamics with a Time-Independent Hamiltonian

2.2: Time-Evolution Operator

2.3: Two-Level System

2.4: Equation of Motion for the Time-Evolution Operator

2.5: Dynamics with a Time-Dependent Hamiltonian

2.6: Schrödinger and Heisenberg Representations

2.7: Readings

This page titled 2: The Schrödinger Equation and Time-Propagator is shared under a CC BY-NC-SA 4.0 license and was authored, remixed, and/or curated by Andrei Tokmakoff via source content that was edited to the style and standards of the LibreTexts platform.

2.1: Dynamics with a Time-Independent Hamiltonian

This book concerns itself primarily with describing time-dependent properties of a molecular quantum system, with an emphasis on dynamics. *Dynamics* refers to a unified description of the particles and fields of a system as a function of time and position, which we can express in terms of the time-dependent state of the system $|\Psi(\mathbf{r},t)\rangle$. The time evolution of $|\Psi(\mathbf{r},t)\rangle$ is described by the time-dependent Schrödinger equation (TDSE):

$$\mathrm{i}\hbar\frac{\partial}{\partial t}\psi(\mathbf{r},t)=\hat{H}(\mathbf{r},t)\psi(\mathbf{r},t) \tag{2.1.1}$$

In this differential equation, the Hamiltonian $\hat{H}$, which describes all interactions between particles and fields, is the quantity that determines how the state of the system evolves in time and space. For many interacting nuclei and electrons and possibly time-varying external potentials, this is a daunting equation to solve, and we will approach this with different strategies.

We start by summarizing the case in which the Hamiltonian $\hat{H}$ is assumed to be independent of time: $\hat{H}=\hat{H}(\mathbf{r})$. We then assume a solution that is a simple product of two functions, one of which is a function of time, and the other of space:

$$\Psi(\mathbf{r},t)=\varphi(\mathbf{r})T(t) \tag{2.1.2}$$

Inserting this into eq. (2.1.1) allows us to rewrite the TDSE as

$$\mathrm{i}\hbar\frac{1}{T(t)}\frac{\partial}{\partial t}T(t)=\frac{\hat{H}(\mathbf{r})\varphi(\mathbf{r})}{\varphi(\mathbf{r})} \tag{2.1.3}$$

Here we have separated variables leaving the left-hand side as a function only of time, and the right-hand side as a function only of space. Equation (2.1.3) can only be satisfied if both sides are equal to the same constant, E. Taking the right-hand side, we obtain,

$$\hat{H}(\mathbf{r})\varphi(\mathbf{r})=E\varphi(\mathbf{r}) \tag{2.1.4}$$

This is the time-independent Schrödinger equation (TISE), an eigenvalue equation, for which $\varphi(\mathbf{r})$ are the eigenstates and E are the eigenvalues. Here we note that $\langle\hat{H}\rangle=\langle\psi|\hat{H}|\psi\rangle=E$, so $\hat{H}$ is the operator corresponding to E and drawing on classical mechanics we associate $\langle\hat{H}\rangle$ with the expectation value of the energy of the system.

Now taking the left-hand side of eq. (2.1.3) we find,

$$\mathrm{i}\hbar\frac{1}{T(t)}\frac{\partial T}{\partial t}=E \tag{2.1.5}$$

Integrating over time t we have,

$$T(t)=\exp(-\mathrm{i}Et/\hbar) \tag{2.1.6}$$

Considering the set of eigenfunctions $\varphi_n(\mathbf{r})$ with corresponding energy eigenvalues E_n obtained from solving the TISE, we obtain a set of corresponding solutions to the TDSE.

$$\psi_n(\mathbf{r},t)=\varphi_n(\mathbf{r})\exp\left(-\mathrm{i}E_nt/\hbar\right) \tag{2.1.7}$$

The time-dependence of the system is complex and oscillatory with a frequency dictated by the energy of the system. Since the probability density for the eigenstate $|\psi_n(\mathbf{r},t)|^2\,d\mathbf{r}$ is independent of time, the eigenstates are called *stationary states*. More generally, a system may exist as a linear superposition of eigenstates:

$$\Psi(\mathbf{r},t)=\sum_n c_n\psi_n(\mathbf{r},t)=\sum_n c_ne^{-\mathrm{i}E_nt/\hbar}\varphi_n(\mathbf{r}) \tag{2.1.8}$$

where the coefficients c_n are complex numbers satisfying the normalization condition $\sum_n|c_n|^2=1$. In this case, the probability density will oscillate with time. As an example, consider a linear combination of two eigenstates:

$$\Psi(\mathbf{r},t) = \psi_1 + \psi_2 = c_1\varphi_1(\mathbf{r})e^{-\mathrm{i}E_1t/\hbar} + c_2\varphi_2(\mathbf{r})e^{-\mathrm{i}E_2t/\hbar} \tag{2.1.9}$$

For this state the probability density oscillates in time at a frequency dictated by the energy difference between states:

$$\begin{aligned} P(t) &= |\Psi|^2 = |\psi_1 + \psi_2|^2 \\ &= |c_1\varphi_1|^2 + |c_2\varphi_2|^2 + c_1^*c_2\varphi_1^*\varphi_2 e^{-\mathrm{i}(E_2-E_1)t/\hbar} + c_2^*c_1\varphi_2^*\varphi_1 e^{+\mathrm{i}(E_2-E_1)t/\hbar} \\ &= |\psi_1|^2 + |\psi_2|^2 + 2\,|\psi_1\psi_2|\cos(\omega_{21}t) \end{aligned} \tag{2.1.10}$$

where the last line uses the following definition:

$$\omega_{mn} = \frac{E_m - E_n}{\hbar} \tag{2.1.11}$$

We refer to the state of the system that gives rise to this time-dependent oscillation in probability density as a coherent superposition state, or *coherence*. More generally, the oscillation term in eq. (2.1.10) may also include a time-independent phase factor ϕ that arises from the complex nature of the expansion coefficients c_i.

As an example, consider the superposition of the ground and first excited states of the quantum harmonic oscillator. The basis wavefunctions, $\psi_0(x)$ and $\psi_1(x)$, and their stationary probability densities $P_i = \langle\psi_i(x)|\psi_i(x)\rangle$ are shown in Figures 2.1.1 a and b. If we create a superposition of these states with eq. (2.1.9), here with $c_0 = c_1 = \sqrt{2}$, the time-dependent probability density oscillates, with $\langle x(t)\rangle$ tracking the classical motion, as shown in Figure 2.1.1c and the accompanying video.

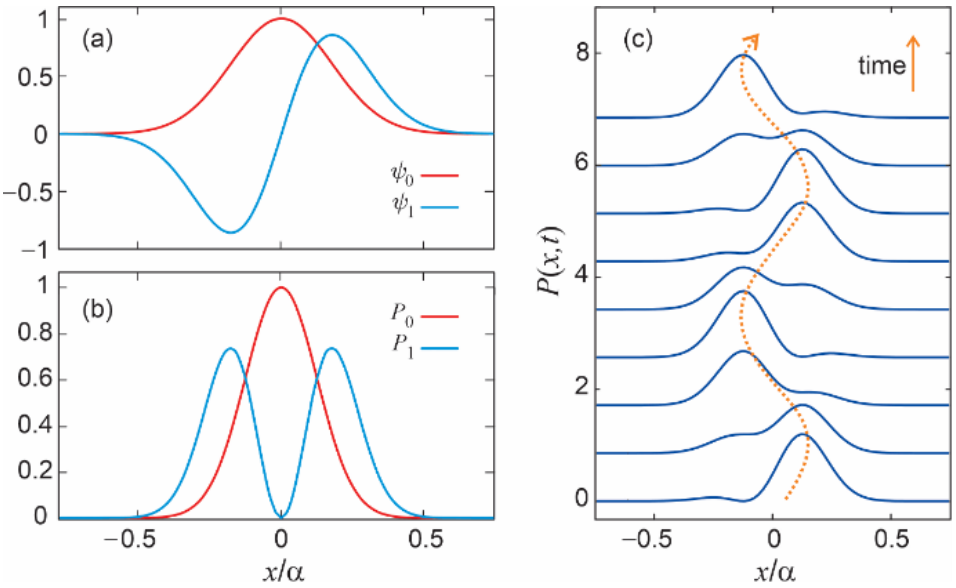


Figure 2.1.1: (a) Real part of wavefunction for the ground (red) and first excited state (blue) of the harmonic oscillator. (b) Probability densities corresponding to (a). (c) Time-dependent superposition of the ground and first excited states of the harmonic oscillator for $c_0 = c_1 = 0.707$. Curves are offset and separated in time in increments of $2\pi/7\omega$. Here $\alpha^2 = 2\hbar/m\omega$ for the harmonic oscillator.

Video

This interactive element is not available in this format. Visit the link or scan the QR code to access it online.

View this Video online

Figure 2.1.2

This page titled 2.1: Dynamics with a Time-Independent Hamiltonian is shared under a CC BY-NC-SA 4.0 license and was authored, remixed, and/or curated by Andrei Tokmakoff via source content that was edited to the style and standards of the LibreTexts platform.

2.2: Time-Evolution Operator

To understand how the wavefunction evolves with time, the TDSE can be solved by integrating coupled differential equations for the different degrees of freedom to be described, but there is an alternate representation of quantum dynamics we commonly employ. Since the TDSE is a deterministic equation of motion that allow us to compute the continuous evolution of the state of a system forward or backward in time, we can define an operator that describes the dynamics of the wavefunction:

$$\Psi(t) = \hat{U}(t, t_0)\Psi(t_0) \tag{2.2.1}$$

$\hat{U}$ is the time-evolution operator, or time-propagator, which describes the evolution of the quantum system from an initial time point t_0 to to a final time t. In essence, eq. (2.2.1) is the integral solution to the TDSE obtained by integrating over these time limits.

To investigate the form of $\hat{U}$, we again consider the TDSE for a time-independent Hamiltonian:

$$\frac{\partial}{\partial t}\Psi(t) + \frac{\mathrm{i}}{\hbar}\hat{H}\Psi(t) = 0 \tag{2.2.2}$$

If $\hat{H}$ were a constant rather than an operator, we see that the solution to this equation would take an exponential form with $\Psi(t) \sim \exp(-\mathrm{i}Ht/\hbar)$, but since it is an operator lets proceed more cautiously. We define an exponential operator of the form

$$\hat{T} = \exp(-\mathrm{i}\hat{H}t/\hbar) = 1 - \frac{\mathrm{i}\hat{H}t}{\hbar} + \frac{1}{2!}\left(\frac{\mathrm{i}\hat{H}t}{\hbar}\right)^2 - \cdots \tag{2.2.3}$$

We can confirm from the expansion that $\hat{T}^{-1} = \exp(\mathrm{i}\hat{H}t/\hbar)$, noting that $\hat{H}$ is Hermitian and $\hat{H}$ commutes with $\hat{T}$. Multiplying eq. (2.2.2) from the left by $\hat{T}^{-1}$, we can write

$$\frac{\partial}{\partial t}\left[\exp\left(\frac{\mathrm{i}}{\hbar}\hat{H}t\right)\Psi(t)\right] = 0 \tag{2.2.4}$$

Integrating from t_0 to t, we obtain

$$\Psi(t) = \exp\left(-\frac{\mathrm{i}}{\hbar}\hat{H}(t - t_0)\right)\Psi(t_0) \tag{2.2.5}$$

Comparing eq. (2.2.1) and eq. (2.2.5), we see that the time-propagator is

$$\hat{U}(t, t_0) = \exp\left(-\mathrm{i}\frac{\hat{H}}{\hbar}(t - t_0)\right) \tag{2.2.6}$$

Given the eigenstates φ_n and eigenvalues E_n of a time-independent Hamiltonian, we can insert this operator into eq. (2.2.1) and evaluate it to yield a practical form. Remembering that the eigenvalues and eigenvectors of an operator $\hat{A}$ ($\hat{A}\psi_n = a_n\psi_n$) can be used to evaluate functions of operators as $f(\hat{A})\psi_n = f(a_n)\psi_n$, we see that

$$e^{-\mathrm{i}\hat{H}t/\hbar}\,|\psi_n\rangle = e^{-\mathrm{i}E_n t/\hbar}\,|\psi_n\rangle \tag{2.2.7}$$

and therefore

$$\psi_n(t) = e^{-\mathrm{i}E_n(t-t_0)/\hbar}\psi_n(t_0) \tag{2.2.8}$$

Alternatively, we can reach this result, now written in Dirac notation with $\psi_n = |n\rangle$, by substituting the identity relationship $\sum_n |n\rangle\langle n| = 1$ into the right side of eq. (2.2.6), to yield

$$\hat{U}(t, t_0) = \sum_n e^{-\mathrm{i}E_n(t-t_0)/\hbar}|n\rangle\langle n| \tag{2.2.9}$$

Then the time-development of the wavefunction from eq. (2.2.1) is

$$|\Psi(t)\rangle = \sum_n c_n(t)|n\rangle \tag{2.2.10}$$

where

$$c_n(t) = e^{-\mathrm{i}E_n(t-t_0)/\hbar}c_n(t_0) \tag{2.2.11}$$

This leads us back to the expression we deduced before in eq. (2.1.7).

As written in eq. (2.2.1), we see that the time-propagator $\hat{U}(t,t_0)$ acts to the right (on *kets*) to evolve the system in time. The evolution of the conjugate wavefunctions (*bras*) is under the Hermitian conjugate of $\hat{U}(t,t_0)$ acting to the left:

$$\langle\psi(t)| = \langle\psi(t_0)|\,\hat{U}^\dagger(t,t_0) \tag{2.2.12}$$

From its definition as an expansion and recognizing $\hat{H}$ as Hermitian, we see that

$$\hat{U}^\dagger(t,t_0) = \exp\left[\frac{\mathrm{i}}{\hbar}\hat{H}(t-t_0)\right] \tag{2.2.13}$$

Noting that $\hat{U}$ is unitary, $\hat{U}^\dagger = \hat{U}^{-1}$, we sometimes refer to $\hat{U}^\dagger$ as the time reversal operator.

Now that we know the time-evolution operator, it is possible to calculate the time-dependence to expectation values for a dynamical operator:

$$\langle\hat{A}(t)\rangle = \langle\Psi(t)|\hat{A}|\Psi(t)\rangle \tag{2.2.14}$$

$$= \langle\Psi(0)|\,\hat{U}^\dagger\hat{A}\hat{U}\,|\Psi(0)\rangle \tag{2.2.15}$$

For an arbitrary initial state, $|\Psi(0)\rangle = \sum_n c_n|n\rangle$

$$\langle\hat{A}(t)\rangle = \sum_{m,n} c_n c_m^* e^{-\mathrm{i}(E_n-E_m)t/\hbar}\,\langle m|\hat{A}|n\rangle \tag{2.2.16}$$

$$= \sum_{m,n} c_n c_m^* e^{-\mathrm{i}\omega_{nm}t}A_{mn} \tag{2.2.17}$$

where

$$\omega_{nm} = \frac{E_n - E_m}{\hbar} \tag{2.2.18}$$

Note that for a Hermitian operator, eq. (2.2.16) is real. In this equation, the matrix of complex amplitude coefficients correspond to density matrix elements $\rho_{nm} = c_n c_m^*$, which will be further discussed in Section 12.5.

This page titled 2.2: Time-Evolution Operator is shared under a CC BY-NC-SA 4.0 license and was authored, remixed, and/or curated by Andrei Tokmakoff via source content that was edited to the style and standards of the LibreTexts platform.

2.3: Two-Level System

Let us use the time-propagator in a model calculation that we will refer to often. It is common to reduce or map quantum problems onto a two-level (or two-state) system. We will pick the most important states for our problem and find strategies for discarding or simplifying the influence of the remaining degrees of freedom. The two-level system is particularly common for spectroscopy in which light acts to drive transitions between a ground and excited state, and in the magnetic resonance spectroscopy for the $\pm$ states of a spin $\frac{1}{2}$ system. It is often used in describing an experimentally observed sub-system immersed in a continuum representative of condensed phases.

The two-level system consists of two unperturbed or "zero-order" states, $|\varphi_a\rangle$ and $|\varphi_b\rangle$, with energies ε_a and ε_b, which are described by a zero-order Hamiltonian H_0:

$$\begin{aligned}\hat{H}_0 &= |\varphi_a\rangle\,\varepsilon_a\,\langle\varphi_a| + |\varphi_b\rangle\,\varepsilon_b\,\langle\varphi_b| \\ &= \begin{pmatrix} \varepsilon_a & 0 \\ 0 & \varepsilon_b \end{pmatrix}\end{aligned} \tag{2.3.1}$$

These states interact through a potential or coupling V of the form

$$\begin{aligned}\hat{V} &= |\varphi_a\rangle\,V_{ab}\,\langle\varphi_b| + |\varphi_b\rangle\,V_{ba}\,\langle\varphi_a| \\ &= \begin{pmatrix} 0 & V_{ab} \\ V_{ba} & 0 \end{pmatrix}\end{aligned} \tag{2.3.2}$$

The full Hamiltonian for the two coupled states is

$$\begin{aligned}\hat{H} &= \hat{H}_0 + \hat{V} \\ &= \begin{pmatrix} \varepsilon_a & V_{ab} \\ V_{ba} & \varepsilon_b \end{pmatrix}\end{aligned} \tag{2.3.3}$$

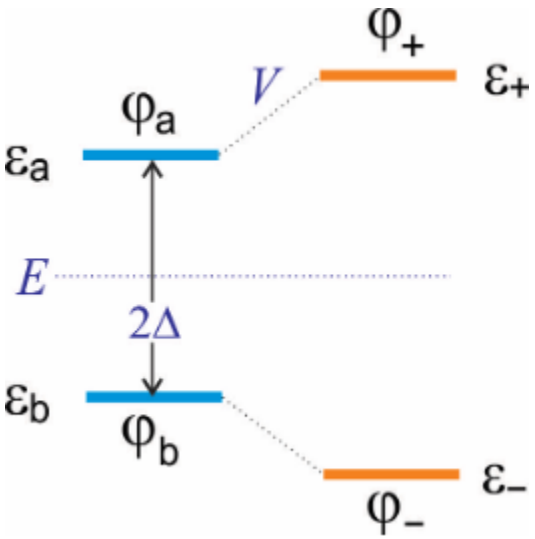


Figure 2.3.1: Energy level diagram illustrating the zero-order states φ_a and φ_b and the energy eigenvalues that result from coupling these states by V.

Since the Hamiltonian is Hermitian, we can also express the coupling matrix elements as

$$V_{ab} = V_{ba}^{*} = Ve^{-\mathrm{i}\phi} \tag{2.3.4}$$

$$\hat{H} = \begin{pmatrix} \varepsilon_a & Ve^{-\mathrm{i}\phi} \\ Ve^{+\mathrm{i}\phi} & \varepsilon_b \end{pmatrix} \tag{2.3.5}$$

This Hamiltonian could be used to describe a variety of problems involving two interacting quantum states, such as a dipole-dipole interaction between molecules, a mechanical interaction (or anharmonic coupling) between bond vibrations in a molecule, the action of an external light field to couple to quantum states, or the influence of the surroundings on the energy levels of a molecule.(1) For intermolecular interactions, this form of the Hamiltonian is sometimes referred to as the site basis to indicate that there are two particles or quantum states, the sites, interacting with one another via V.

We now ask: If we prepare the system in state $|\varphi_a\rangle$, what is the time-dependent probability of observing it in $|\varphi_b\rangle$? The coupling mixes the zero-order states, resulting in two eigenstates of $\hat{H}, |\varphi_+\rangle$and $|\varphi_-\rangle$, with corresponding energy eigenvalues $\varepsilon_+$and ε_-. Since $|\varphi_a\rangle$ and $|\varphi_b\rangle$ are not eigenstates of $\hat{H}$, a system prepared in one of these zero-order states will exchange population (the probability density) with the other. To describe this, our time-propagation will be performed in the eigenbasis using eq. (2.2.9), and we will need to find the transformation between these basis sets.

We start by searching for the eigenvalues of the Hamiltonian. To help simplify our notation, we define the mean energy and energy splitting between the uncoupled states as

$$E = \frac{\varepsilon_a + \varepsilon_b}{2} \tag{2.3.6}$$

$$\Delta = \frac{\varepsilon_a - \varepsilon_b}{2} \tag{2.3.7}$$

We can then obtain the eigenvalues of the coupled system by solving the secular equation

$$\det(H - \lambda I) = 0 \tag{2.3.8}$$

giving

$$\varepsilon_\pm = E \pm \Omega \tag{2.3.9}$$

with

$$\Omega = \sqrt{\Delta^2 + V^2} \tag{2.3.10}$$

To summarize, the explicit form of the energy eigenvalues of a coupled two-level system in terms of the zero-order energies and coupling is

$$\varepsilon_\pm = \frac{\varepsilon_a + \varepsilon_b}{2} \pm \frac{1}{2}\sqrt{(\varepsilon_a - \varepsilon_b)^2 + 4\,|V_{ab}|^2} \tag{2.3.11}$$

This is a common equation that will repeatedly arise in discussing quantum interactions.

To determine the eigenvectors of the coupled system $|\varphi_\pm\rangle$, it proves to be a great simplification to define a mixing angle θ that describes the relative magnitude of the coupling relative to the zero-order energy splitting through

$$\tan 2\theta = \frac{V}{\Delta} \tag{2.3.12}$$

We see that the mixing angle adopts values such that $0 \leq \theta \leq \frac{\pi}{4}$. Also, we note that

$$\sin 2\theta = V/\Omega \tag{2.3.13}$$

$$\cos 2\theta = \Delta/\Omega \tag{2.3.14}$$

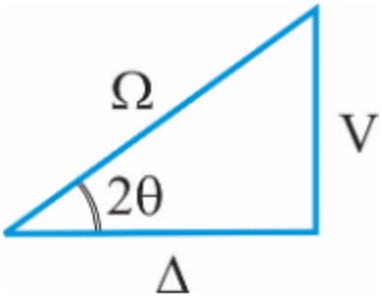


Figure 2.3.2 : Trigonometric relationships for the mixing angle θ in terms of the coupling V and energy splitting of the zero order states, 2Δ

In this representation the Hamiltonian eq. (2.3.5) becomes

$$\hat{H} = E\mathbf{I} + \Delta \begin{pmatrix} 1 & \tan(2\theta)e^{-\mathrm{i}\phi} \\ \tan(2\theta)e^{+\mathrm{i}\phi} & -1 \end{pmatrix} \tag{2.3.15}$$

and we can express the eigenvalues as

$$\varepsilon_{\pm} = E \pm \Delta \sec 2\theta \tag{2.3.16}$$

Next, we want to find S, the transformation matrix that diagonalizes the Hamiltonian (i.e. $S^{-1}\hat{H}S$) and transforms the coefficients of the wavefunction from the zero-order basis to the eigenbasis. The eigenstates can be expanded in the zero-order basis in the form

$$|\varphi_{\pm}\rangle = c_a |\varphi_a\rangle + c_b |\varphi_b\rangle \tag{2.3.17}$$

So that the transformation can be expressed in matrix form as

$$\begin{pmatrix} \varphi_+ \\ \varphi_- \end{pmatrix} = S \begin{pmatrix} \varphi_a \\ \varphi_b \end{pmatrix} \tag{2.3.18}$$

To find S, we substitute eq. (2.3.17) into the Schrödinger equation $\hat{H}|\varphi_{\pm}\rangle = \varepsilon_{\pm}|\varphi_{\pm}\rangle$ to find

$$S = \begin{pmatrix} \cos\theta\ e^{-\mathrm{i}\phi/2} & \sin\theta\ e^{\mathrm{i}\phi/2} \\ -\sin\theta\ e^{-\mathrm{i}\phi/2} & \cos\theta\ e^{\mathrm{i}\phi/2} \end{pmatrix} \tag{2.3.19}$$

Note that S is unitary since $S^{\dagger} = S^{-1}$ and $(S^T)^* = S^{-1}$. Note also that S takes the form of a rotation matrix in Hilbert-space, and S^{-1} reverses the rotation of S. The rotation is determined by the mixing angle, which encodes the projection of the eigenbasis and zero-order basis on one another.

Now, let's examine the eigenstates and eigenvalues of the two-level system in two limits:

1. Weak coupling refers to the case $|\mathrm{V}/\Delta| \ll 1$, or $\theta \approx 0$. The eigenstate $|\varphi_+\rangle$ corresponds to $|\varphi_a\rangle$ weakly perturbed by the V_{ab} interaction. Similarly, $|\varphi_-\rangle$ corresponds closely to $|\varphi_b\rangle$. Stated another way, one finds that as $\theta \to 0$, the character of $|\varphi_+\rangle \to |\varphi_a\rangle$ and $|\varphi_-\rangle \to |\varphi_b\rangle$. Expanding the square root in eq. (2.3.10), we find—not surprisingly—that the eigenstate energies are those we calculate from first-order perturbation theory:

$$\varepsilon_{\pm} = \varepsilon_a + \frac{|V_{ab}|^2}{\varepsilon_a - \varepsilon_b} \quad \text{and} \quad \varepsilon_b - \frac{|V_{ab}|^2}{\varepsilon_a - \varepsilon_b} \tag{2.3.20}$$

2. Strong coupling. When $|V/\Delta| \gg 1$, the mixing angle $\theta = \pi/4$. In this case, the original (a, b) basis states have become so strongly mixed that they are indistinguishable. The eigenstates are symmetric and antisymmetric combinations:

$$|\varphi_{\pm}\rangle = \frac{1}{\sqrt{2}}\left(|\varphi_b\rangle \pm |\varphi_a\rangle\right) \tag{2.3.21}$$

Note from eq. (2.3.19) that the sign of V dictates whether $|\varphi_+\rangle$ or $|\varphi_-\rangle$ corresponds to the symmetric or antisymmetric eigenstate. For negative couplings such that $-V \gg \Delta$, the correspondence in eq (2.3.21) is inverted to $\mp$, and $\theta = -\pi/4$. For the energy eigenvalues in the strong coupling limit, we find a quadratic dependence on splitting: $\varepsilon_{\pm} \approx E \pm (V + \Delta^2/2V)$.

We can schematically represent the full range of energy eigenvalues with the diagram in Figure 2.3.3. Here we plot $\varepsilon_{\pm}$as a function of the splitting Δ for a fixed coupling V.

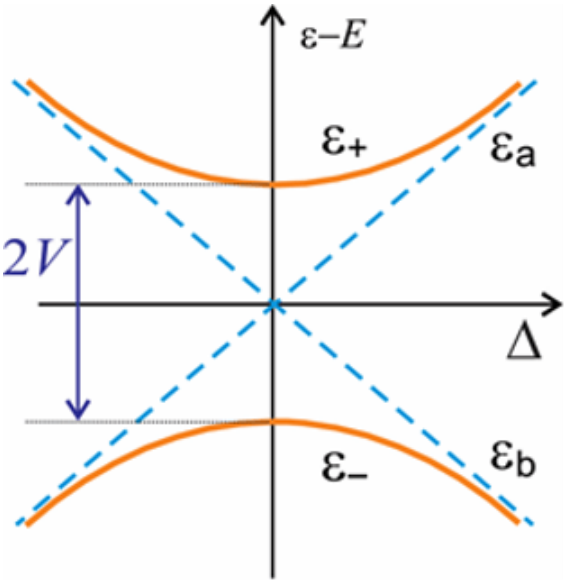


Figure $2.3.3$: Illustration of how the mixing of zero-order states depends on the relative magnitude of the coupling (V) and the zero-order splitting (2Δ).

This diagram illustrates an avoided crossing effect. The strong coupling limit is equivalent to a degeneracy point ($\Delta \approx 0$) between the states $|\varphi_a\rangle$ and $|\varphi_b\rangle$. The eigenstates completely mix the unperturbed states yet remain split by the strength of interaction $2V$. Of course, this is not a real space representation. We will return to the discussion of avoided crossings when we describe potential energy surfaces and the adiabatic approximation, where the dependence of V and Δ on position must be considered.

Now we can turn to describing the dynamics of the two-level system when we prepare the system initially in $|\varphi_a\rangle$.

$$|\psi(0)\rangle = |\varphi_a\rangle \tag{2.3.22}$$

The time-propagator can be evaluated in the eigenbasis using eq. (2.2.9)

$$U(t) \;=\; |\varphi_+\rangle e^{-\mathrm{i}\varepsilon_+ t/\hbar}\langle\varphi_+| + |\varphi_-\rangle e^{-\mathrm{i}\varepsilon_- t/\hbar}\langle\varphi_-| \tag{2.3.23}$$

Since φ_a and φ_b are not eigenstates, preparing the system in state φ_a creates a superposition of $|\varphi_+\rangle$and $|\varphi_-\rangle$, which will lead to time evolution. With the help of the matrix elements of S in eq. (2.3.19) that transform the wavefunction from the zero-order (a, b) basis to the eigenbasis $(\pm)$, we can use eq. (2.3.23) to evaluate the time-dependent amplitudes of initial and final states

$$\begin{aligned} c_a(t) &= \langle\varphi_a|U(t)|\varphi_a\rangle \\ &= e^{-\mathrm{i}Et/\hbar}[\cos(\Omega t/\hbar) - \mathrm{i}\cos(2\theta)\sin(\Omega t/\hbar)] \end{aligned} \tag{2.3.24}$$

$$\begin{aligned} c_b(t) &= \langle\varphi_b|U(t)|\varphi_a\rangle \\ &= \mathrm{i}\sin(2\theta)e^{-\mathrm{i}Et/\hbar}\sin(\Omega t/\hbar) \end{aligned} \tag{2.3.25}$$

So, what is the probability that it is found in state $|\varphi_b\rangle$ at time t? With the help of eq. (2.3.13), we obtain

$$\begin{aligned} P_{ba}(t) &= |c_b(t)|^2 \\ &= \frac{V^2}{V^2+\Delta^2}\sin^2\Omega_R t \end{aligned} \tag{2.3.26}$$

where

$$\Omega_R = \frac{1}{\hbar}\sqrt{\Delta^2 + V^2} \tag{2.3.27}$$

The probability amplitude P_{ab}, or population, oscillates between the φ_a and φ_b states, on a timescale given by the Rabi Frequency,

Ω_R, as seen in Figure 2.3.4. Both the maximum value of P_{ba} and Ω_R depend on the strength of coupling. Notice for the weak coupling limit the eigenstates resemble the zero-order states, and the time-dependence disappears. In the strong coupling limit $(V \gg \Delta)$, amplitude is exchanged completely between the zero-order states at a rate given by the coupling: $\Omega_R \rightarrow V/\hbar$. Even in this limit it takes a finite amount of time for amplitude to move between states. To get $P_{ba} = 1$ requires a time $t = \frac{\pi}{2\Omega_R} = \frac{\hbar\pi}{2V}$. We can determine the probability that the system is still found in $|a\rangle$ after time t is P_{aa}, in much the same manner; however, with the expression for P_{ab} in hand, it is easiest to recognize that it can be quickly determined from $P_{aa} = 1 - P_{ab}$

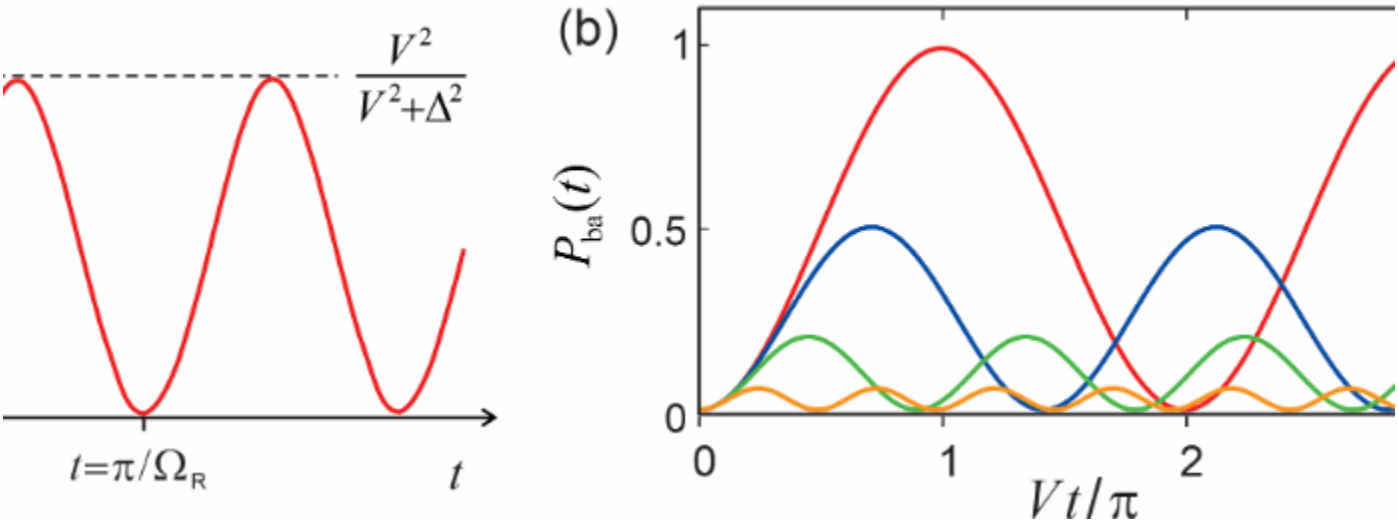


Figure 2.3.4 : The probability of observing the system in state b if it is prepared in a. (a) General properties of eq. (2.3.26) (b) Comparison of the Rabi frequency and probability amplitude as a function of the strength of coupling V.

Note that as an operator, $\hat{U}$ can be expressed as a matrix, and eq. (2.3.24) and eq. (2.3.25) are matrix elements of the time-evolution operator in the zero-order basis, $\hat{\mathbf{U}}_{a,b}$. We obtain $\hat{\mathbf{U}}_{a,b}$ using a transformation from the eigenbasis:

$$\hat{\mathbf{U}}_{a,b} = \mathbf{S}^{-1}\hat{\mathbf{U}}\mathbf{S} \tag{2.3.28}$$

The full time-propagator for the two-level system in the matrix representation is

$$\hat{\mathbf{U}}_{a,b}(t) = e^{-\mathrm{i}Et/\hbar}\begin{pmatrix} \cos\Omega_R t - \mathrm{i}(\frac{\Delta}{\Omega})\sin\Omega_R t & -\mathrm{i}(\frac{V}{\Omega})\sin\Omega_R t \\ -\mathrm{i}(\frac{V}{\Omega})\sin\Omega_R t & \cos\Omega_R t + \mathrm{i}(\frac{\Delta}{\Omega})\sin\Omega_R t \end{pmatrix} \tag{2.3.29}$$

and the time-evolution of the wavefunctions are calculated from

$$\mathbf{\Psi}(t) = \hat{\mathbf{U}}_{a,b}\mathbf{\Psi}(0) \qquad \text{with } \mathbf{\Psi}(0) = \begin{pmatrix} c_a \\ c_b \end{pmatrix} \tag{2.3.30}$$

More generally, in the matrix representation the time propagator is an exponential operator $\hat{\mathbf{U}} = \exp(-\mathrm{i}\hat{\mathbf{H}}t/\hbar)$, defined through its series expansion in products of Hamiltonian matrices. Evaluating the time-dependence in the eigenbasis, although not required, is far easier than the zero-order basis. The exponential of a diagonal matrix is readily obtained by exponentiating the elements, so if the Hamiltonian can be diagonalized as $\hat{\Lambda} = S^{-1}\hat{H}S$ then $e^{\hat{H}} = Se^{\hat{\Lambda}}S^{-1}$.

References

When used in magnetic resonance, quantum optics, and atomic spectroscopy it is common to represent the Energies and interactions in spin $1/2$ systems using the Pauli matrices[1]

$$\sigma_x = \begin{pmatrix} 0 & 1 \\ 1 & 0 \end{pmatrix} \quad \sigma_y = \begin{pmatrix} 0 & -\mathrm{i} \\ \mathrm{i} & 0 \end{pmatrix} \quad \sigma_z = \begin{pmatrix} 1 & 0 \\ 0 & -1 \end{pmatrix}$$

For which our two-level system Hamiltonian is written $\hat{H} = E\bar{I} + \Delta\sigma_z + V\sigma_x$.

This page titled 2.3: Two-Level System is shared under a CC BY-NC-SA 4.0 license and was authored, remixed, and/or curated by Andrei Tokmakoff via source content that was edited to the style and standards of the LibreTexts platform.

2.4: Equation of Motion for the Time-Evolution Operator

Our primary interest is with dynamical processes, and for this we need to work with a time-dependent Hamiltonian. Let's start at the beginning by obtaining the equation of motion that describes the wavefunction and its time evolution through the time propagator. We are seeking equations of motion for quantum systems equivalent to Newton's—or more accurately Hamilton's—equations for classical systems. The question is, if we know the wavefunction at time t_0 is $|\psi(\mathbf{r},t_0)\rangle$, how does it change with time? How do we determine $|\psi(\mathbf{r},t_0)\rangle$ for some later time $t > t_0$? We will use our intuition here, relying heavily on correspondence to classical mechanics. To simplify notation, in the following discussion we will not explicitly show the spatial dependence $(\mathbf{r})$ of the wavefunction.

To derive a deterministic equation of motion, we start by asserting *causality*—that $|\psi(t_0)\rangle$ precedes and determines $|\psi(t)\rangle$. As above, we define a "time-evolution operator" or "propagator" $\hat{U}$ that acts on the wavefunction to the right to propagate the system forward in time from t_0 to t:

$$|\psi(t)\rangle = \hat{U}(t,t_0)\,|\psi(t_0)\rangle \tag{2.4.1}$$

Additionally, the wavefunction must be continuously differentiable in time, and therefore the state is unchanged when the initial and final time-points are the same

$$\hat{U}(t,t) = 1 \tag{2.4.2}$$

If we take the system to be deterministic, then it stands to reason that we should get the same wavefunction whether we evolve to a target time in one step $(t_0 \to t_2)$ or multiple steps $(t_0 \to t_1 \to t_2)$. Therefore, we can write the composition property

$$\hat{U}(t_2,t_0) = \hat{U}(t_2,t_1)\hat{U}(t_1,t_0) \tag{2.4.3}$$

Note that since $\hat{U}$ acts to the right, order matters:

$$\begin{aligned} |\psi(t_2)\rangle &= \hat{U}(t_2,t_1)\hat{U}(t_1,t_0)\,|\psi(t_0)\rangle \\ &= \hat{U}(t_2,t_0)\,|\psi(t_1)\rangle \end{aligned} \tag{2.4.4}$$

Equation (2.4.4) is already very suggestive of an exponential form for $\hat{U}$. Furthermore, since time is continuous and the operator is linear, it also suggests that the time propagator is only dependent on a time interval rather than the absolute initial and final time points:

$$\hat{U}(t_1,t_0) = \hat{U}(t_1 - t_0) \tag{2.4.5}$$

As a result of the linearity and the principle of superposition, $\hat{U}$ is distributive. If we express the state of a system as the superposition

$$|\psi(t_0)\rangle = c_1|\varphi_1(t_0)\rangle + c_2|\varphi_2(t_0)\rangle \tag{2.4.6}$$

then

$$\begin{aligned} |\psi(t)\rangle &= \hat{U}(t,t_0)\,|\psi(t_0)\rangle \\ &= \hat{U}(t,t_0)c_1|\varphi_1(t_0)\rangle + \hat{U}(t,t_0)c_2|\varphi_2(t_0)\rangle \\ &= c_1(t)\,|\varphi_1\rangle + c_2(t)\,|\varphi_2\rangle \end{aligned} \tag{2.4.7}$$

While the coefficients $c_i(t)$ evolve with time, the total population of the system must be conserved, and therefore

$$\sum_n |c_n(t)|^2 = \sum_n |c_n(t_0)|^2 \tag{2.4.8}$$

Thus $\hat{U}$ is not dependent on $|\psi\rangle$, and the differential equation of motion for $\hat{U}$ is linear in time. Note that eq. (2.4.8) implies that $\hat{U}$ must be unitary.

$$P = \langle\psi(t)|\psi(t)\rangle = \langle\psi(t_0)|\,\hat{U}^\dagger\hat{U}\,|\psi(t_0)\rangle \tag{2.4.9}$$

which holds if $U^\dagger = U^{-1}$. Also, the inverse of the time-propagator is the time reversal operator. From eq. (2.4.3):

$$\hat{U}(t,t_0)\hat{U}(t_0,t) = 1 \tag{2.4.10}$$

$$\therefore \hat{U}^{-1}(t,t_0) = \hat{U}(t_0,t) \tag{2.4.11}$$

Now we are able to find an equation of motion that describes the time-evolution operator using the change of the system for an *infinitesimal* time-step, $\delta t : \hat{U}(t+\delta t, t)$. Since

$$\lim_{\delta t \to 0} \hat{U}(t+\delta t, t) = 1 \tag{2.4.12}$$

we expect that for small enough $\delta t, \hat{U}$ will change linearly with δt. This is based on analogy to thinking of deterministic motion in classical systems. Setting t_0 to 0, so that $\hat{U}(t,t_0) = \hat{U}(t)$, we can write

$$\hat{U}(t+\delta t) = \hat{U}(t) - \mathrm{i}\hat{\Omega}(t)\delta t \tag{2.4.13}$$

$\hat{\Omega}$ is a time-dependent Hermitian operator, which is required for $\hat{U}$ to be unitary. We can now write a differential equation for the time-development of $\hat{U}$ starting with

$$\frac{d\hat{U}(t)}{dt} = \lim_{\delta t \to 0} \frac{\hat{U}(t+\delta t) - \hat{U}(t)}{\delta t} \tag{2.4.14}$$

So from eq. (2.4.13) we have

$$\frac{\partial \hat{U}(t,t_0)}{\partial t} = -\mathrm{i}\hat{\Omega}\hat{U}(t,t_0) \tag{2.4.15}$$

We can now see that the operator needed a complex argument. Otherwise, probability density would not be conserved; it would rise or decay. Rather it oscillates through different states of the system.

We note that $\hat{\Omega}$ has units of frequency. Since quantum mechanics fundamentally associates frequency and energy as $E = \hbar\omega$, and since the Hamiltonian is the operator corresponding to the energy, and responsible for time evolution in classical Hamiltonian mechanics, we write

$$\hat{\Omega} = \frac{\hat{H}}{\hbar} \tag{2.4.16}$$

With that substitution we have an equation of motion for $\hat{U}$:

$$\mathrm{i}\hbar\frac{\partial}{\partial t}\hat{U}(t,t_0) = \hat{H}\hat{U}(t,t_0) \tag{2.4.17}$$

Multiplying from the right by $|\psi(t_0)\rangle$ gives the TDSE:

$$\mathrm{i}\hbar\frac{\partial}{\partial t}|\psi\rangle = \hat{H}|\psi\rangle \tag{2.4.18}$$

If we use the Hamiltonian for a free particle, $-(\hbar^2/2m)(\partial^2/\partial x^2)$, we will notice it looks similar to a classical wave equation except that it's linear in time. Rather, eq. (2.4.18) looks like a diffusion equation with an imaginary diffusion constant.

We are also interested in the equation of motion for $\hat{U}^\dagger$ which describes the time evolution of the conjugate wavefunctions. If we follow the same approach, recognizing that $\hat{U}^\dagger$ acts to the left:

$$\langle\psi(t)| = \langle\psi(t_0)|\hat{U}^\dagger(t,t_0) \tag{2.4.19}$$

we get

$$-\mathrm{i}\hbar\frac{\partial}{\partial t}\hat{U}^\dagger(t,t_0) = \hat{U}^\dagger(t,t_0)\hat{H} \tag{2.4.20}$$

This page titled 2.4: Equation of Motion for the Time-Evolution Operator is shared under a CC BY-NC-SA 4.0 license and was authored, remixed, and/or curated by Andrei Tokmakoff via source content that was edited to the style and standards of the LibreTexts platform.

2.5: Dynamics with a Time-Dependent Hamiltonian

We now turn to finding a more useful form of the time-evolution operator. At first glance it may seem straightforward to integrate eq. (2.4.17). If $\hat{H}$ is merely a function of time, then

$$\hat{U}(t,t_0) = \exp\left[-\frac{\mathrm{i}}{\hbar}\int_{t_0}^{t}\hat{H}(\tau)\,d\tau\right] \tag{2.5.1}$$

If we followed our earlier definition of the time-propagator, this exponential would be cast as a series expansion:

$$\begin{aligned}\hat{U}(t,t_0) \stackrel{?}{=} 1 &- \frac{\mathrm{i}}{\hbar}\int_{t_0}^{t}\hat{H}(\tau)\,d\tau \\ &+ \frac{1}{2!}\left(\frac{-\mathrm{i}}{\hbar}\right)^2\int_{t_0}^{t}\int_{t_0}^{t}d\tau\,d\tau'\hat{H}(\tau)\hat{H}(\tau') \\ &+ \ldots\end{aligned} \tag{2.5.2}$$

But we must be careful here, since this expression is not properly addressing the time-dependence of the operator $\hat{H}$. Looking at the second term in eq. (2.5.2), we see that this expression integrates over both possible time-orderings of the two Hamiltonian operations, those with $\tau > \tau'$ and those with $\tau < \tau'$. This would only be proper if the Hamiltonians at different times commute, allowing us to reverse their order to assure that their action on the wavefunctions, $\hat{H}(\tau)\hat{H}(\tau')\,|\psi\rangle$, could be evaluated consistently with the proper time-ordering.

Although it doesn't generally occur, what happens when the Hamiltonian commutes over the time-period of interest? When two operators commute one can construct a basis of eigenfunctions common to those operators. In other words, a set of time-dependent eigenstates $H(t)\,|\alpha\rangle = E_\alpha(t)\,|\alpha\rangle$ exists that remain orthogonal over the entire time interval, allowing us to propagate our wavefunction as a superposition in this basis set. If we apply the projection operator $\sum_\alpha |\alpha\rangle\langle\alpha| = 1$ to eq. (2.5.1) then we find we can express the time-propagator in the eigenbasis as

$$\hat{U}(t,t_0) = \sum_\alpha |\alpha\rangle\langle\alpha| \exp\left[-\frac{\mathrm{i}}{\hbar}\int_{t_0}^{t}E_\alpha(\tau)\,d\tau\right] \tag{2.5.3}$$

and the time-dependent wavefunction is

$$|\Psi(t,t_0)\rangle = \sum_\alpha c_\alpha|\alpha\rangle \exp\left[-\frac{\mathrm{i}}{\hbar}\int_{t_0}^{t}E_\alpha(\tau)\,d\tau\right] \tag{2.5.4}$$

These expressions closely mirror those we derived for a time-independent Hamiltonian, although now with time-dependent eigenvalues.

When can we expect $[\hat{H}(\tau),\hat{H}(\tau')] = 0$? Clearly it applies to all Hamiltonians when $\tau = \tau'$, so one can expect that the timescale of the dynamics will matter. Generally, we will need the system to evolve slowly enough that the distribution of population amongst eigenstates is preserved. This is the limit of adiabatic dynamics, which we will address more carefully below. Now, let's proceed a bit more carefully assuming the Hamiltonians at different times do not commute. Integrating equation (2.4.17) directly from t_0 to t gives

$$\hat{U}(t,t_0) = 1 - \frac{\mathrm{i}}{\hbar}\int_{t_0}^{t}d\tau\,\hat{H}(\tau)\hat{U}(\tau,t_0) \tag{2.5.5}$$

This is the solution; however, it is not very practical since $\hat{U}(t,t_0)$ is a function of itself. But we can make an iterative expansion by repetitive substitution of $\hat{U}$ into itself. The first step in this process is as follows:

$$\begin{aligned}\hat{U}(t,t_0) &= 1-\frac{\mathrm{i}}{\hbar}\int_{t_0}^{t} d\tau \hat{H}(\tau)\left[1-\frac{\mathrm{i}}{\hbar}\int_{t_0}^{\tau} d\tau' \hat{H}(\tau')\hat{U}(\tau',t_0)\right] \\ &= 1+\left(\frac{-\mathrm{i}}{\hbar}\right)\int_{t_0}^{t} d\tau\, \hat{H}(\tau) \\ &\quad +\left(\frac{-\mathrm{i}}{\hbar}\right)^2\int_{t_0}^{t} d\tau \int_{t_0}^{\tau} d\tau' \hat{H}(\tau)\hat{H}(\tau')\hat{U}(\tau',t_0)\end{aligned} \tag{2.5.6}$$

Note in the last term of this equation, the integration limits enforce a time-ordering; that is, the first integration variable τ' covers all time points up to the second τ. The integration region when calculating the time evolution is from t_0 to t is illustrated in Figure 2.5.1.

The next substitution step gives

$$\begin{aligned}U(t,t_0) &= 1+\left(\frac{-\mathrm{i}}{\hbar}\right)\int_{t_0}^{t} d\tau\, H(\tau) \\ &\quad +\left(\frac{-\mathrm{i}}{\hbar}\right)^2\int_{t_0}^{t} d\tau \int_{t_0}^{\tau} d\tau' H(\tau)H(\tau') \\ &\quad +\left(\frac{-\mathrm{i}}{\hbar}\right)^3\int_{t_0}^{t} d\tau \int_{t_0}^{\tau} d\tau' \int_{t_0}^{\tau'} d\tau'' H(\tau)H(\tau')H(\tau'')U(\tau'',t_0)\end{aligned} \tag{2.5.7}$$

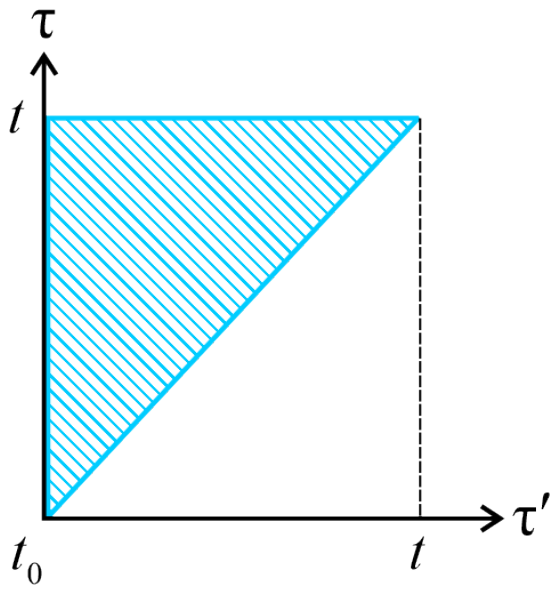


Figure 2.5.1: Integration region for the time evolution from t_0 to t.

From this expansion, we should be aware that there is a time-ordering to the interactions. For the third term, τ'' acts before τ', which acts before τ: $t_0 \le \tau'' \le \tau' \le \tau \le t$.

What does this expression represent? Imagine we are starting in state $|\psi_0\rangle = |\ell\rangle$ and we want to describe how one evolves toward a target state $|\psi\rangle = |k\rangle$. The possible paths by which one can shift amplitude and evolve the phase, pictured in terms of these time variables are represented in Figure 2.5.2.

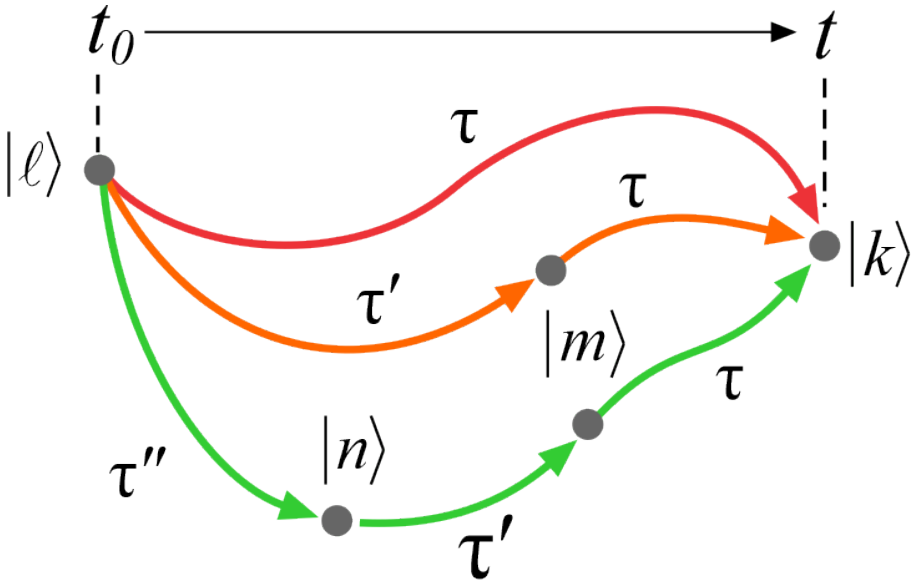


Figure 2.5.2: Illustration of direct and indirect transition paths initiating in a starting state $|\psi_0\rangle = |\ell\rangle$ at time to and ending in a target state $|\psi\rangle = |k\rangle$ at time t, including possible intermediate states $|m\rangle$ and $|n\rangle$.

The first term in eq. (2.5.7) represents all actions of the Hamiltonian that act to directly couple $|\ell\rangle$ and $|k\rangle$. The second term described possible transitions from $|\ell\rangle$ to $|k\rangle$ via an intermediate state $|m\rangle$. The expression for $\hat{U}$ describes all possible paths between the initial and final state. Each of these paths interferes in ways dictated by the acquired phase of our eigenstates under the timedependent Hamiltonian.

The solution for $\hat{U}$ obtained from this iterative substitution is known as a positive timeordered exponential

$$\begin{aligned}\hat{U}(t,t_0) &\equiv \exp_+\left[\frac{-\mathrm{i}}{\hbar}\int_{t_0}^{t} d\tau\, \hat{H}(\tau)\right] \\ &= 1+\sum_{n=1}^{\infty}\left(\frac{-\mathrm{i}}{\hbar}\right)^n \int_{t_0}^{t} d\tau_n \int_{t_0}^{\tau_n} d\tau_{n-1} \ldots \int_{t_0}^{\tau_2} d\tau_1\ \hat{H}(\tau_n)\hat{H}(\tau_{n-1})\ldots\hat{H}(\tau_1)\end{aligned} \tag{2.5.8}$$

and this expansion is known as the Dyson series. In this expression the time-ordering of variables can be summarized as

$$\begin{aligned} &t_0 \to \tau_1 \to \tau_2 \to \tau_3 \ldots \tau_n \to t \\ &t_0 \to \ldots\ \ \tau''' \to \tau'' \to \tau' \to \tau \end{aligned} \tag{2.5.9}$$

Equation (2.5.8) tells us how a quantum system evolves over a given time interval. It allows for any possible trajectory from an initial state to a final state through any number of intermediate states. Each term in the expansion accounts for more possible transitions between different intermediate quantum states during this trajectory.

Now we compare the time-ordered exponential with the traditional expansion of an exponential:

$$1+\sum_{n=1}^{\infty}\frac{1}{n!}\left(\frac{-\mathrm{i}}{\hbar}\right)^n \int_{t_0}^{t} d\tau_n \ldots \int_{t_0}^{t} d\tau_1 H(\tau_n)H(\tau_{n-1})\ldots H(\tau_1) \tag{2.5.10}$$

Here the time integration variables assume all values between t_0 and t, and therefore, proper and improper orderings for $H(\tau_i)$ are included. As illustrated for the second-order case ($n = 2$) in Figure 2.5.2, by discarding the improper terms, the time-ordered integration covers only half of this time-variable region. For the n^{th} expansion term in this series, there are $n!$ possible time-orderings of the τ_n time intervals, which is accounted for by the $n!$ factor in eq. (2.5.10).

We are also interested in the Hermitian conjugate of $\hat{U}$, describes motion in eq. (2.4.20). If we repeat the method above, remembering that $\hat{U}^{\dagger}(t,t_0)$ acts to the left, then we obtain

$$\hat{U}^{\dagger}(t,t_0) = 1+\frac{\mathrm{i}}{\hbar}\int_{t_0}^{t} d\tau\, \hat{U}^{\dagger}(t,\tau)\hat{H}(\tau) \tag{2.5.11}$$

Performing iterative substitution leads to a negative-time-ordered exponential:

$$\begin{aligned}\hat{U}^{\dagger}(t,t_0) &= \exp_{-}\left[\frac{\mathrm{i}}{\hbar}\int_{t_0}^{t} d\tau\, \hat{H}(\tau)\right] \\ &= 1+\sum_{n=1}^{\infty}\left(\frac{\mathrm{i}}{\hbar}\right)^{n}\int_{t_0}^{t} d\tau_n \int_{t_0}^{\tau_n} d\tau_{n-1} \ldots \int_{t_0}^{\tau_2} d\tau_1\, \hat{H}(\tau_1)\hat{H}(\tau_2)\ldots\hat{H}(\tau_n)\end{aligned} \tag{2.5.12}$$

Here $\hat{H}(\tau_i)$ acts to the left.

This page titled 2.5: Dynamics with a Time-Dependent Hamiltonian is shared under a CC BY-NC-SA 4.0 license and was authored, remixed, and/or curated by Andrei Tokmakoff via source content that was edited to the style and standards of the LibreTexts platform.

2.6: Schrödinger and Heisenberg Representations

The mathematical formulation of quantum dynamics that has been presented is not unique. So far, we have described the dynamics by propagating the wavefunction, which encodes probability densities. Ultimately, since we cannot measure a wavefunction, we are interested in observables, which are probability amplitudes associated with Hermitian operators. Since operators and wavefunctions can be both be time-dependent, there are different representations of quantum dynamics that emerge. Consider the time-dependent expectation value for an operator $\hat{A}$ applied to a wavefunction beginning in the initial state ψ_0:

$$\begin{aligned} \left\langle \hat{A}(t) \right\rangle &= \langle \psi_0 | \, \hat{U}^\dagger \hat{A} \hat{U} \, | \psi_0 \rangle \\ &= \left(\langle \psi_0 | \hat{U}^\dagger \right) \hat{A} \left(\hat{U} | \psi_0 \rangle \right) \quad \longrightarrow \quad \langle \psi(t) | \hat{A} | \psi(t) \rangle \quad \text{Schrödinger} \\ &= \langle \psi_0 | \left(\hat{U}^\dagger \hat{A} \hat{U} \right) | \psi_0 \rangle \quad \longrightarrow \quad \langle \psi_0 | \hat{A}(t) | \psi_0 \rangle \quad \text{Heisenberg} \end{aligned} \tag{2.6.1}$$

The last two expressions are written to emphasize alternate representations of the dynamics. The first, known as the Schrödinger picture, refers to everything we have done so far. Here we propagate the wavefunction in time as $\hat{U} \, | \psi \rangle$ and use the time-dependent wavefunction $\psi(t)$ to obtain the expectation value. Operators are unchanged because they carry no time-dependence. Alternatively, we can work in the Heisenberg picture. This uses the unitary property of $\hat{U}$ to time-propagate the operators as $\hat{A}(t) = \hat{U}^\dagger \hat{A} \hat{U}$, but the wavefunction is now stationary. The Heisenberg picture has an appealing physical picture behind it because it carries a classical correspondence to the motion of particles. That is, there is a time-dependence to position and momentum.

To compare these representations, we can start by defining operators and wavefunctions in the Schrödinger and Heisenberg pictures using eq. (2.6.1),

$$\left\langle \hat{A}(t) \right\rangle = \left\langle \psi(t) \left| \hat{A} \right| \psi(t) \right\rangle_S = \left\langle \psi \left| \hat{A}(t) \right| \psi \right\rangle_H \tag{2.6.2}$$

Here the Heisenberg operator $\hat{A}_H$ is related to the Schrödinger picture operator $\hat{A}_S$ by

$$\begin{aligned} \hat{A}_H(t) &= \hat{U}^\dagger(t, t_0) \hat{A}_S \hat{U}(t, t_0) \\ \hat{A}_H(t_0) &= \hat{A}_S \end{aligned} \tag{2.6.3}$$

Note, the pictures have the same wavefunction at the reference time point t_0. Since the wavefunction in the Heisenberg picture is time-independent, we can relate the Schrödinger and Heisenberg wavefunctions as

$$| \psi_S(t) \rangle = \hat{U}(t, t_0) \, | \psi_H \rangle \tag{2.6.4}$$

So,

$$| \psi_H \rangle = \hat{U}^\dagger(t, t_0) \, | \psi_S(t) \rangle = | \psi_S(t_0) \rangle \tag{2.6.5}$$

As expected for a unitary transformation, in either picture the eigenvalues are preserved:

$$\begin{aligned} \hat{A} \, | \varphi_i \rangle_S &= a_i | \varphi_i \rangle_S \\ \hat{A}_H \, | \varphi_i \rangle_H &= a_i | \varphi_i \rangle_H \end{aligned} \tag{2.6.6}$$

The time evolution of the operators in the Heisenberg picture is:

$$\begin{aligned}\frac{\partial \hat{A}_H}{\partial t} &= \frac{\partial}{\partial t}\left(\hat{U}^\dagger \hat{A}_S \hat{U}\right) = \frac{\partial \hat{U}^\dagger}{\partial t}\hat{A}_S\hat{U} + \hat{U}^\dagger\hat{A}_S\frac{\partial \hat{U}}{\partial t} + \hat{U}^\dagger \cancel{\frac{\partial \hat{A}_S}{\partial t}}\hat{U} \\ &= \frac{\mathrm{i}}{\hbar}\hat{U}^\dagger H\hat{A}_S\hat{U} - \frac{\mathrm{i}}{\hbar}\hat{U}^\dagger\hat{A}_S H\hat{U} \\ &= \frac{\mathrm{i}}{\hbar}H\hat{A}_H - \frac{\mathrm{i}}{\hbar}\hat{A}_H H \\ &= -\frac{\mathrm{i}}{\hbar}\left[\hat{A}_H, H\right]\end{aligned} \tag{2.6.7}$$

Here we dropped the last term in eq. (2.6.7), with the understanding that $\hat{A}_S$ is independent of time. If it is time-independent H commutes with U, and the Hamiltonian will take the same form in the Schrödinger or Heisenberg picture, so the label has been dropped for H.

The result

$$\mathrm{i}\hbar\frac{\partial}{\partial t}\hat{A}_H = \left[\hat{A}_H, H\right] \tag{2.6.8}$$

is known as the Heisenberg equation of motion. In practice, it is not typical to keep the "H" subscript in designating the operator; it is just understood that a time-dependent operator is obtained in the Heisenberg representation.

Let's see how this works. Consider a particle with an arbitrary one-dimensional potential

$$\hat{H} = \frac{\hat{p}^2}{2m} + \hat{V}(x) \tag{2.6.9}$$

For this Hamiltonian, the Heisenberg equation gives the time-dependence of the momentum and position as

$$\frac{\partial \hat{p}}{\partial t} = -\frac{\partial V}{\partial x} \tag{2.6.10}$$

$$\frac{\partial \hat{x}}{\partial t} = \frac{\hat{p}}{m} \tag{2.6.11}$$

These expressions are helpful in evaluating the commutator:

$$\left[\hat{x}^n, \hat{p}\right] = \mathrm{i}\hbar n\hat{x}^{n-1} \tag{2.6.12}$$

$$\left[\hat{x}, \hat{p}^n\right] = \mathrm{i}\hbar n\hat{p}^{n-1} \tag{2.6.13}$$

Curiously, the factors of $\hbar$ have vanished in equations (2.6.10) and (2.6.11). Instead, these equations indicate that the position and momentum operators follow the same equations of motion as Hamilton's equations for the classical variables.

Let's look at how this plays out for the harmonic oscillator. We use $H = \frac{\hat{p}^2}{2m} + \frac{1}{2}m\omega_0^2\hat{x}^2$, where $m\omega_0^2$ is the force constant and ω_0 is the oscillator frequency. The Heisenberg equation gives

$$\frac{\partial \hat{p}}{\partial t} = -m\omega_0\hat{x} \tag{2.6.14}$$

$$\frac{\partial \hat{x}}{\partial t} = \frac{\hat{p}}{m} \tag{2.6.15}$$

and the equations look like Hamilton's classical coupled equations for the position and momentum of the harmonic oscillator. Since we use these expressions a lot, we will quote the solutions. We get the equation of motion for $\hat{x}$ by differentiating eq. (2.6.15) and substituting into (2.6.14) to get $\ddot{\hat{x}} + \omega_0^2\hat{x} = 0$. We get the equation of motion for $\hat{p}$ in a similar way: $\ddot{\hat{p}} + \omega_0^2\hat{p} = 0$. These equations have sinusoidal solutions, and by specifying the initial values of the position and momentum $x(0)$ and $p(0)$, we can find the general solution:

$$\hat{x}(t) = \hat{x}(0)\cos\omega_0 t + \frac{\hat{p}(0)}{m\omega_0}\sin\omega_0 t \tag{2.6.16}$$

$$\hat{p}(t) = \hat{p}(0)\cos\omega_0 t + m\omega_0\hat{x}(0)\sin\omega_0 t \tag{2.6.17}$$

Again, these equations show the exact form of the classical equations with no explicit indication that this is describing the

quantum mechanical operators.

A similar equation of motion for the expectation value of an operator, rather than the operator itself, can be obtained in the Schrödinger picture. Differentiating $\langle A(t)\rangle = \langle\psi|\hat{A}\,|\psi\rangle$ with respect to time and following the same strategy as eq. (2.6.7), we obtain

$$\begin{aligned} \mathrm{i}\hbar\frac{\partial}{\partial t}\left\langle \hat{A}_S(t)\right\rangle &= \mathrm{i}\hbar\left[\left\langle\psi\left|\hat{A}_S\right|\frac{\partial\psi}{\partial t}\right\rangle + \left\langle\frac{\partial\psi}{\partial t}\left|\hat{A}_S\right|\psi\right\rangle + \left\langle\psi\left|\cancel{\frac{\partial\hat{A}_S}{\partial t}}\right|\psi\right\rangle\right] \\ &= \left\langle\psi\left|\hat{A}_S H\right|\psi\right\rangle - \left\langle\psi\left|H\hat{A}_S\right|\psi\right\rangle \\ &= \left\langle\left[\hat{A},H\right]\right\rangle \end{aligned} \tag{2.6.18}$$

If $\hat{A}$ is independent of time, as we expect in the Schrödinger picture, then $\partial\hat{A}_S/\partial t = 0$. If $\hat{A}$ commutes with H, its expectation value does not change with time, $\frac{d}{dt}\left\langle\hat{A}_S(t)\right\rangle = 0$, and it is referred to as a constant of motion.

Returning to the Hamiltonian for a bound particle, eq. (2.6.9), we can use eq. (2.6.18) to find that the time-dependent expectation value for the particles position depends on the expectation value for its momentum as

$$\frac{\partial\langle\hat{x}\rangle}{\partial t} = \frac{\langle\hat{p}\rangle}{m} \tag{2.6.19}$$

If we integrate this over a time period t with constant p, we find that the expectation value for the position of the particle follows the classical motion, i.e. $x = x_0 + vt$:

$$\langle x(t)\rangle = \langle x(0)\rangle + \frac{\langle p\rangle\, t}{m} \tag{2.6.20}$$

We can also use the time derivative of eq. (2.6.19) with (2.6.10) to obtain an equation that mirrors Newton's second law of motion, $F = ma$:

$$-\left\langle\frac{\partial V}{\partial x}\right\rangle = m\frac{\partial^2\langle x\rangle}{\partial t^2} \tag{2.6.21}$$

The observations made in eqs. (2.6.19) and (2.6.21) underlie Ehrenfest's classical correspondence principle, which states that the expectation values for the position and momentum operators will follow the classical equations of motion. Equation (2.6.21) is a bit different than one would expect for a classical force on a particle, with an expression for the expectation value of the force $-\langle\partial V/\partial x\rangle$ replacing the force at the expectation value of the particle position $-\partial V(\langle x\rangle)/\partial x$.

Example

The Heisenberg equation of motion can also be applied to non-Hermitian operators, such as the raising (creation) and lowering (annihilation) operators, $a^\dagger$ and a. Turning again to the harmonic oscillator, we can use the Hamiltonian in the form $H = \hbar\omega_0\left(a^\dagger a + 1/2\right)$ to calculate the time dependence of the lowering operator from eq. (2.6.8)

$$\begin{aligned} \frac{d\hat{a}}{dt} &= \frac{\mathrm{i}}{\hbar}\left[\hat{H},\hat{a}\right] \\ &= \mathrm{i}\omega_0\left[\hat{a}^\dagger\hat{a},\hat{a}\right] \\ &= -\mathrm{i}\omega_0\hat{a} \end{aligned} \tag{2.6.22}$$

This can be integrated over time to obtain

$$\hat{a}(t) = \hat{a}e^{-\mathrm{i}\omega_0 t} \tag{2.6.23}$$

The time dependence of the raising operator is obtained in a similar manner from the equation of motion $d\hat{a}^\dagger/dt = \mathrm{i}\omega_0\hat{a}^\dagger$ giving

$$\hat{a}^\dagger(t) = \hat{a}^\dagger e^{\mathrm{i}\omega_0 t} \tag{2.6.24}$$

Using the expressions for the position and momentum of the harmonic oscillator in terms of $a^\dagger$ and a, we can express their time-dependence as

$$x(t) = \sqrt{\frac{\hbar}{2m\omega_0}}\left(a^\dagger e^{\mathrm{i}\omega_0 t} + a e^{-\mathrm{i}\omega_0 t}\right) \tag{2.6.25}$$

$$p(t) = \mathrm{i}\sqrt{\frac{m\hbar\omega_0}{2}}\left(a^\dagger e^{\mathrm{i}\omega_0 t} - a e^{-\mathrm{i}\omega_0 t}\right) \tag{2.6.26}$$

These equations are equivalent to eqs. (2.6.16) and (2.6.17), but have practical advantages in problem solving.

This page titled 2.6: Schrödinger and Heisenberg Representations is shared under a CC BY-NC-SA 4.0 license and was authored, remixed, and/or curated by Andrei Tokmakoff via source content that was edited to the style and standards of the LibreTexts platform.

2.7: Readings

Dynamics with a Time-Independent Hamiltonian

1. Cohen-Tannoudji, C.; Diu, B.; Laloë, F. *Quantum Mechanics*; Wiley, 1977; pp 405.
2. Nitzan, A. *Chemical dynamics in condensed phases: Relaxation, transfer and reactions in condensed molecular systems*; Oxford University Press, 2006; Ch 1. DOI: 10.1093/oso/9780198529798.001.0001
3. Schatz, G. C.; Ratner, M. A. *Quantum Mechanics in Chemistry*; Dover Publications, 2002; Ch 2.

Two-Level System

1. Cohen-Tannoudji, C.; Diu, B.; Laloë, F. *Quantum Mechanics*; Wiley, 1977; pp 405-420.
2. Liboff, R. L. Introductory Quantum Mechanics; Addison-Wesley, 1980; p 77.
3. Mukamel, S. *Principles of Nonlinear Optical Spectroscopy*; Oxford University Press, 1995; Ch 2.
4. Sakurai, J. J. *Modern Quantum Mechanics*, rev. ed.; Addison-Wesley, 1994.

Dynamics with a Time-Dependent Hamiltonian

1. Cohen-Tannoudji, C.; Diu, B.; Laloë, F. *Quantum Mechanics*; Wiley, 1977; p 1340.
2. Merzbacher, E. *Quantum Mechanics*, 3rd ed.; Wiley, 1998; Ch 14.
3. Mukamel, S. *Principles of Nonlinear Optical Spectroscopy*; Oxford University Press, 1995; Ch 2.
4. Sakurai, J. J. *Modern Quantum Mechanics*, rev. ed.; Addison-Wesley, 1994; Ch 2.

Schrödinger and Heisenberg Representations

1. Cohen-Tannoudji, C.; Diu, B.; Laloë, F. *Quantum Mechanics*; Wiley, 1977; p 312.
2. Mukamel, S. *Principles of Nonlinear Optical Spectroscopy*; Oxford University Press, 1995.
3. Nitzan, A. *Chemical dynamics in condensed phases: Relaxation, transfer and reactions in condensed molecular systems*; Oxford University Press, 2006; Ch 4. DOI: 10.1093/oso/9780198529798.001.0001
4. Sakurai, J. J. *Modern Quantum Mechanics*, rev. ed.; Addison-Wesley, 1994; Ch 2.

This page titled 2.7: Readings is shared under a CC BY-NC-SA 4.0 license and was authored, remixed, and/or curated by Andrei Tokmakoff.

3: SOLVING THE TIME-DEPENDENT SCHRÖDINGER EQUATION

3.1: Introduction

3.2: Integrating the TDSE Directly

3.3: Transitions Induced by a Time-Dependent Potential

3.4: Resonant Driving of a Two-Level System

3.5: The Interaction Picture

3.6: Time-Dependent Perturbation Theory

3.7: The Golden Rule

3.8: Readings

This page titled 3: Solving the Time-Dependent Schrödinger Equation is shared under a CC BY-NC-SA 4.0 license and was authored, remixed, and/or curated by Andrei Tokmakoff via source content that was edited to the style and standards of the LibreTexts platform.

3.1: Introduction

We have described the high-level formalism for quantum dynamics, so how do we go about applying it? There are countless ways of dealing with such problems, and the selection of strategies depends very much on the specific details of what we are trying to learn. Gaining insight into the evolution of molecular structure with time will be very different from describing how energy flows within a molecule. In the former case, one is interested in describing the wavefunction in real space and how it evolves with time $|\psi(r,t)\rangle$, whereas in the latter one examines a state's probability amplitude $c(t)$ or population $P(t) = |c(t)|^2$ and how it flows among quantum states of the system (state space). However, our strategies are also limited by computational power.

In the case of an evolving wavefunction in real space, the time-dependent Schrödinger equation can, in principle, be directly integrated with an appropriate basis set. Using a potential energy surface, one can propagate the system forward in small time-steps and follow the evolution of the complex amplitudes through the basis states. In practice, even this is impossible for more than a handful of atoms when treating all degrees of freedom quantum mechanically. The mathematical complexity of solving the time-dependent Schrödinger equation in real space for most molecular systems makes it impossible to obtain exact analytical solutions. We are thus typically forced to seek numerical solutions or simpler models based on approximation methods that will reduce the complexity, very often confining ourselves to calculating the probability amplitudes. Among these methods, time-dependent perturbation theory is the most widely used approach for calculations in spectroscopy, relaxation, and other rate processes. In this chapter, we will briefly outline the strategies for directly integrating the Schrödinger equation, describe approximation methods for studying how a molecular system is influenced by an external potential, and work through the details of time-dependent perturbation theory.

This page titled 3.1: Introduction is shared under a CC BY-NC-SA 4.0 license and was authored, remixed, and/or curated by Andrei Tokmakoff via source content that was edited to the style and standards of the LibreTexts platform.

3.2: Integrating the TDSE Directly

How do we realistically evaluate the time-propagator and obtain a time-dependent trajectory for a quantum system? Expressions such as the time-ordered exponential are daunting, and there are no simple ways to handle them. We can't truncate the exponential because, usually, this expansion is not a rapidly converging series. Also, the solutions oscillate rapidly due to the phase acquired at the energy splitting of the states involved. This leads to a formidable integration problem. Rapid oscillations require small time-steps, while the time scales we are interested in describing are typically orders of magnitude longer. For instance, in a molecular dynamics problem, the highest frequency oscillations may be a result of electronic energy splittings with periods of 1–2 femtoseconds, and the nuclear dynamics that we hope to describe may occur on multi-picosecond time scales. Rather than one general approach to solving the TDSE, there exists an arsenal of different strategies, each suited to a particular range of problems. The choice of how to proceed is generally dictated by the details of the problem and is often an art form. Considerable effort is needed to even formulate the problem, particularly in choosing an appropriate basis. In this section, it is our goal to gain some insight into the types of strategies available, working mainly with the principles rather than the specifics of how they are implemented.

Let's begin by discussing the most general method: the brute force approach of numerical integration. With adequate computational resources, numerical integration is possible. We start by choosing a basis set and defining the initial state ψ_0. We can the numerically evaluate the time-dependence of the wavefunction over a period t by discretizing time into n small intervals of width $\delta t = t/n$, a short enough time that each change of the system is small.

While a variety of strategies can be pursued in practice, one possibility is to expand our wavefunction in the basis set of our choice,

$$|\psi(t)\rangle = \sum_n c_n(t)\,|\varphi_n\rangle \tag{3.2.1}$$

and solve for the time-dependence of the probability amplitude expansion coefficients. Substituting into the right side of the TDSE,

$$\mathrm{i}\hbar\frac{\partial}{\partial t}\,|\psi\rangle = \hat{H}\,|\psi\rangle \tag{3.2.2}$$

and then acting from the left by $\langle k|$ on both sides leads to an equation that describes their time-dependence:

$$\mathrm{i}\hbar\frac{\partial c_k(t)}{\partial t} = \sum_n H_{kn}(t)c_n(t) \tag{3.2.3}$$

or in matrix form $\mathrm{i}\hbar\dot{\mathbf{c}} = \mathbf{H}\mathbf{c}$. This represents a set of coupled first-order differential equations, in which probability amplitude flows between different basis states at rates determined by the matrix elements of the time-dependent Hamiltonian. Such equations are straightforward to integrate numerically. We recognize that we can integrate on a grid if the forward time-step (δt) is small enough that the Hamiltonian is essentially constant. Then eq. (3.2.3) becomes

$$\mathrm{i}\hbar\,\delta c_k(t) = \sum_n H_{kn}(t)c_n(t)\,\delta t \tag{3.2.4}$$

and the system is propagated from time t to $t+\delta t$ as

$$c_k(t+\delta t) = c_k(t) + \delta c_k(t) \tag{3.2.5}$$

The downside of such a calculation is the unusually small time-steps and significant computational cost required.

Similarly, we can use a grid with short time steps to simplify our time-propagator. For a short time interval δt, for which the Hamiltonian is essentially constant, the time propagator can be expressed as

$$\hat{U}(t+\delta t, t) = \exp\left[-\frac{\mathrm{i}}{\hbar}\int_t^{t+\delta t} dt'\,\hat{H}\,(t')\right] \approx \exp\left[-\frac{\mathrm{i}}{\hbar}\,\delta t\,\hat{H}(t)\right] \tag{3.2.6}$$

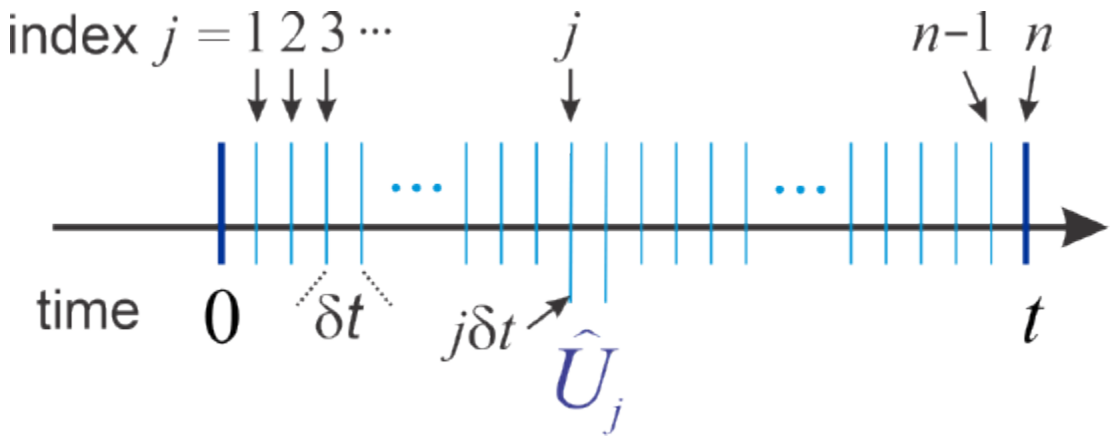


Figure 3.2.1: Illustration of notation for time discretization.

As illustrated in Figure 3.2.1, the time propagator over the full period 0 to t can be written as a product of n propagators over these small intervals,

$$\begin{aligned}\hat{U}(t) &= \lim_{\delta t \to 0} \left[\hat{U}_n \hat{U}_{n-1} \cdots \hat{U}_2 \hat{U}_1\right] \\ &= \lim_{n\to\infty} \prod_{j=0}^{n-1}{}_{+} \hat{U}_j\end{aligned} \tag{3.2.7}$$

where the time-propagation over the j^{th} small time step is

$$\hat{U}_j = \exp\left[-\frac{\mathrm{i}}{\hbar}\,\delta t\,\hat{H}_j\right] \tag{3.2.8}$$

and the Hamiltonian $\hat{H}_j = \hat{H}(j\,\delta t)$ is evaluated at the time point $t_j = j\ \delta t$.

Note that the expressions in eq. are operators, time ordered from right to left, denoted with the "+" subscript. Although the value of $U(t)$ in eq. (3.2.7) is exact in the limit $\delta t \to 0$, when $n \to \infty$, we can choose a finite number for n such that $H(t)$ does not change much over the time δt. With a finite n, the elements of the time propagator does not change much, and it can be approximated by the short-time expansion:

$$\hat{U}_j \approx 1 - \frac{\mathrm{i}}{\hbar}\,\delta t\,\hat{H}_j \tag{3.2.9}$$

In a general sense, this approach is not very practical since the time step is determined by $\delta t \ll \hbar/|H|$, which is typically very small in comparison to the dynamics of interest.

Another complication arises when the potential and kinetic energy operators in the Hamiltonian do not commute. Taking the time-dependent Hamiltonian to be $\hat{H}(t) = \hat{T}(t) + \hat{V}(t)$,

$$\begin{aligned}\exp\left[-\mathrm{i}\frac{\hat{H}(t)}{\hbar}\,\delta t\right] &= \exp\left[-\mathrm{i}\frac{(\hat{T}(t)+\hat{V}(t))}{\hbar}\,\delta t\right] \\ &\approx \exp\left[-\frac{\mathrm{i}\hat{T}(t)}{\hbar}\,\delta t\right]\exp\left[-\frac{\mathrm{i}\hat{V}(t)}{\hbar}\,\delta t\right]\end{aligned} \tag{3.2.10}$$

The second line makes the Split Operator approximation, which states that the time propagator over a short enough period can be approximated as a product of two independent propagators evolving the system, first with the potential energy operator and then with the kinetic energy operator. The validity of this approximation depends on the time-step and how well these operators commute. The error in this approximation scales as $\frac{1}{2}[\hat{T}(t), \hat{V}(t)](\delta t/\hbar)^2$, so to counteract this effect we should use a time step δt such that $\delta t < \{2\hbar^2/[\hat{T}(t), \hat{V}(t)]\}^{1/2}$.(1) The approximation can be improved by symmetrizing the split operator as

$$\exp\left[-\frac{\mathrm{i}\hat{H}(t)}{\hbar}\,\delta t\right] \approx \exp\left[-\frac{\mathrm{i}\hat{V}(t)}{\hbar}\,\frac{\delta t}{2}\right]\exp\left[-\frac{\mathrm{i}\hat{T}(t)}{\hbar}\,\delta t\right]\exp\left[-\frac{\mathrm{i}\hat{V}(t)}{\hbar}\,\frac{\delta t}{2}\right] \tag{3.2.11}$$

Here the error scales as $\frac{1}{12}(\delta t/\hbar)^3\{[\hat{T},[\hat{T},\hat{V}]]+\frac{1}{2}[\hat{V},[\hat{V},\hat{T}]]\}$. There is no significant increase in computational effort since half of the operations can be combined as

$$\exp\left[-\frac{\mathrm{i}\hat{V}}{\hbar}\,\frac{(j+1)\,\delta t}{2}\right]\exp\left[-\frac{\mathrm{i}\hat{V}}{\hbar}\,\frac{j\,\delta t}{2}\right] \approx \exp\left[-\frac{\mathrm{i}\hat{V}\,j\,\delta t}{\hbar}\right] \tag{3.2.12}$$

to give

$$U(t) \approx \exp\left[-\frac{\mathrm{i}\hat{V}n\,\delta t}{\hbar}\right]\left[\prod_{j=1}^{n}{}_{+}\exp\left[-\frac{\mathrm{i}\hat{V}j\,\delta t}{\hbar}\right]\exp\left[-\frac{\mathrm{i}\hat{T}j\,\delta t}{\hbar}\right]\right]\exp\left[-\frac{\mathrm{i}\hat{V}\,\delta t}{\hbar}\right] \tag{3.2.13}$$

References

(1) Tannor, D. J. *Introduction to Quantum Mechanics: A Time-Dependent Perspective*; University Science Books, 2007.

This page titled 3.2: Integrating the TDSE Directly is shared under a CC BY-NC-SA 4.0 license and was authored, remixed, and/or curated by Andrei Tokmakoff via source content that was edited to the style and standards of the LibreTexts platform.

3.3: Transitions Induced by a Time-Dependent Potential

For many of the time-dependent problems we encounter, most notably in spectroscopy, we can often partition the problem so that the time-dependent Hamiltonian comprises a time-independent system Hamiltonian H_0, which we can describe exactly, and a time-dependent potential $V(t)$:

$$H = H_0 + V(t) \tag{3.3.1}$$

We don't explicitly treat what happens to any other degrees of freedom—for instance, an electromagnetic field or other molecules. They only enter in the sense that they give rise to the interaction potential H_0, for instance through an electrostatic or mechanical interaction. This partitioning is only possible if the influence of the potential on the system is weak enough that it doesn't alter H_0.

If the Hamiltonian can be cast in the form of eq. (3.3.1), then the eigenstates of H_0 form a complete basis set for describing the state of the system, and we can describe the time-evolving wavefunction for the system $|\psi(t)\rangle$ in terms of an expansion in eigenstates $|n\rangle$. To begin, we obtain the eigenstates and energy eigenvalues for H_0 from the time-independent Schrödinger equation.

$$H_0 |n\rangle = E_n |n\rangle \tag{3.3.2}$$

The state of the system can then be expressed as a superposition of these eigenstates in terms of time-dependent probability amplitudes $c_n(t)$

$$|\psi(t)\rangle = \sum_n c_n(t) |n\rangle \tag{3.3.3}$$

Let's find an equation of motion for the eigenstate coefficients of a specific target state $|k\rangle$

$$c_k(t) = \langle k|\psi(t)\rangle \tag{3.3.4}$$

From this expression and the TDSE

$$\frac{\partial |\psi\rangle}{\partial t} = -\frac{\mathrm{i}}{\hbar} H |\psi\rangle \tag{3.3.5}$$

we can express the time-dependence of c_k as

$$\frac{\partial c_k(t)}{\partial t} = -\frac{\mathrm{i}}{\hbar} \langle k | H | \psi(t)\rangle \tag{3.3.6}$$

Inserting the identity $1 = \sum_n |n\rangle\langle n|$, we obtain

$$\frac{\partial c_k(t)}{\partial t} = -\frac{\mathrm{i}}{\hbar} \sum_n \langle k | H | n\rangle \, c_n(t) \tag{3.3.7}$$

Already we see that the time evolution amounts to solving a set of coupled linear ordinary differential equations. These are rate equations with complex rate constants. They describe the feeding of amplitude from one state into another. Substituting eq. (3.3.1), we have:

$$\begin{aligned} \frac{\partial c_k(t)}{\partial t} &= -\frac{\mathrm{i}}{\hbar} \sum_n \langle k | (H_0 + V(t)) | n\rangle \, c_n(t) \\ &= -\frac{\mathrm{i}}{\hbar} \sum_n \left[E_n \, \delta_{kn} + V_{kn}(t)\right] c_n(t) \end{aligned} \tag{3.3.8}$$

or,

$$\frac{\partial c_k(t)}{\partial t} + \frac{\mathrm{i}}{\hbar} E_k c_k(t) = -\frac{\mathrm{i}}{\hbar} \sum_n V_{kn}(t) c_n(t) \tag{3.3.9}$$

Next, we define an alternate eigenstate coefficient

$$c_m(t) = e^{-\mathrm{i}E_m t/\hbar}\, b_m(t) \tag{3.3.10}$$

which implies a definition for the wavefunction as

$$|\psi(t)\rangle = \sum_n b_n(t) e^{-\mathrm{i}E_n t/\hbar}\ |n\rangle \tag{3.3.11}$$

This introduces a slightly different complex amplitude, allowing us to simplify things considerably. Notice that $|b_k(t)|^2 = |c_k(t)|^2$. Also, $b_k(0) = c_k(0)$. In practice what we are doing is pulling out the "trivial" part of the time evolution--that is, the time-evolving phase factor, which typically oscillates much faster than the changes to the amplitude of b or c.

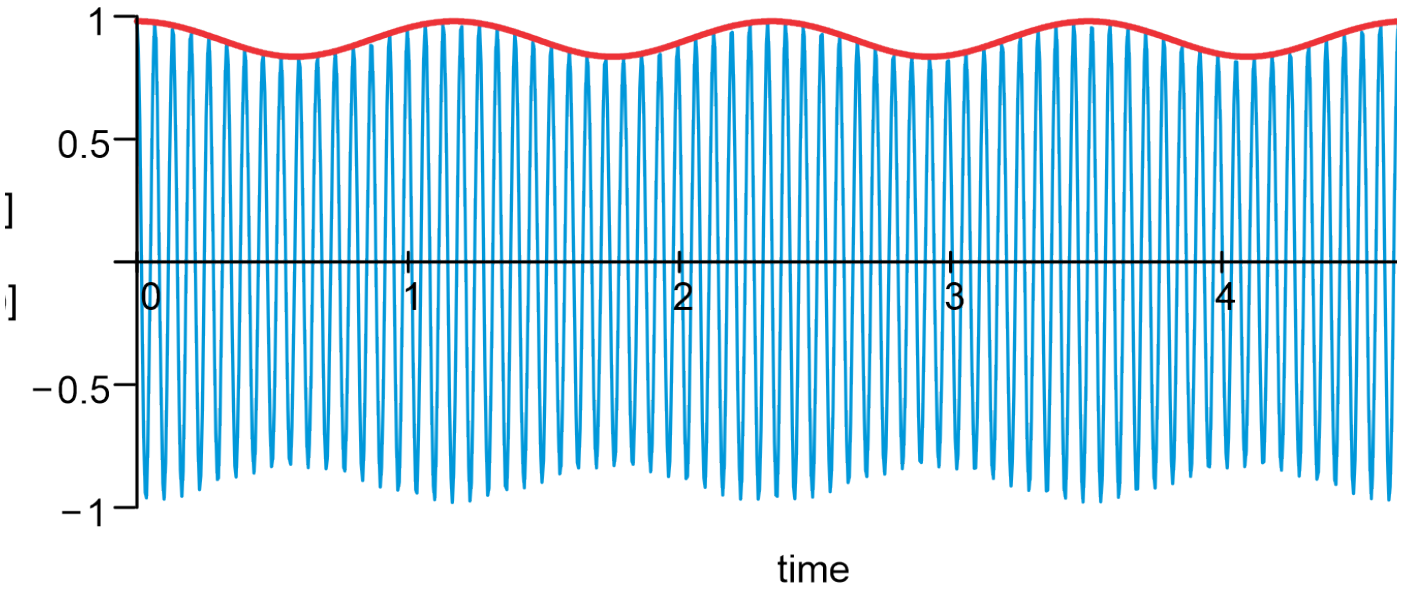


Figure 3.3.1: Comparison of the time dependent amplitudes $c(t)$ and $b(t)$ of a weakly coupled two-level system, illustrating their fast and slow oscillations, respectively. The mixing angle for this calculation is $\theta = \pi/16$ and the magnitude of the coupling is $V_{k\ell}/H_0 = 10^{-4}$.

We will come back to this strategy when we discuss the interaction picture.

Now, substituting eq. (3.3.10) for c_k and c_n in eq. (3.3.9), we obtain

$$e^{-\mathrm{i}E_k t/\hbar}\frac{\partial b_k}{\partial t} = -\frac{\mathrm{i}}{\hbar}\sum_n V_{kn}(t)\ \ e^{-\mathrm{i}E_n t/\hbar} b_n(t) \tag{3.3.12}$$

or

$$\mathrm{i}\hbar\frac{\partial b_k}{\partial t} = \sum_n V_{kn}(t) e^{-\mathrm{i}\omega_{nk}t} b_n(t) \tag{3.3.13}$$

This equation is an exact solution. It is a set of coupled differential equations that describes how probability amplitude moves through eigenstates due to a time-dependent potential. In matrix notation we write eq. (3.3.13) as

$$\mathrm{i}\hbar\dot{\mathbf{b}} = \mathbf{V}_\mathrm{I}\mathbf{b} \tag{3.3.14}$$

where the matrix elements of $\mathbf{V}_\mathrm{I}$ (the interaction picture Hamiltonian) are

$$[\mathbf{V}_\mathrm{I}]_{kn} = V_{kn}(t) e^{\mathrm{i}\omega_{kn}t} \tag{3.3.15}$$

Except in simple cases, these equations cannot be solved analytically, but it is often straightforward to integrate numerically, for instance using Runga-Kutta methods.

In a different approach, we can start with taking the integral of eq. (3.3.14)

$$\mathbf{b} = \mathbf{b}_0 - \frac{\mathrm{i}}{\hbar}\int_0^t d\tau\, \mathbf{V}_\mathrm{I}(\tau)\mathbf{b}(\tau) \tag{3.3.16}$$

For numerical evaluation, we can again discretize time into n small intervals δt of length

$$\begin{aligned}\mathbf{b}(t) &= \mathbf{b}\left(t_0\right) - \frac{\mathrm{i}}{\hbar}\sum_{j=1}^{N}\mathbf{V}_\mathrm{I}\left(t_{j-1}\right)\mathbf{b}\left(t_{j-1}\right)\delta t \\ &= \mathbf{b}(t_0) - \sum_{j=1}^{N}\delta\mathbf{b}(t_j)\end{aligned} \tag{3.3.17}$$

Here t_j is the time at the j^{th} time interval, $t_j = j\ \delta t$. We calculate the expansion coefficients through iterative corrections $\delta\mathbf{b}$ to the value of the b over subsequent time intervals. At any point in time point t_j, corrections are evaluated using the values of V_I and b at the previous time interval t_{j-1}. Equation (3.3.17) implies a recursion relationship relating ($\mathbf{b}t_j$) to its value at the previous time interval ($\mathbf{b}\,t_{j-1}$):

$$\mathbf{b}(t_j) = \mathbf{b}(t_{j-1})\left(1 - \frac{\mathrm{i}}{\hbar}\mathbf{V}_\mathrm{I}\left(t_{j-1}\right)\delta t\right) \tag{3.3.18}$$

In practice this can be evaluated by sequential matrix multiplication and addition, and the value of δt shortened until probability amplitude is conserved over the course of the calculation. Although this is in essence the method discussed in the previous section, it is a bit more practical in the interactions picture since the integration time step can be much longer for weak external potentials.

When can we use these approaches? Consider partitioning the full Hamiltonian into two components, one that we want to study, H_0 and the remaining degrees of freedom, H_1. For each part, we have knowledge of the complete eigenstates and eigenvalues of the Hamiltonian: $H_i|\psi_{i,n}\rangle = E_{i,n}|\psi_{i,n}\rangle$. These subsystems will interact with one another through a Hamiltonian of interaction, H_{int} . If we are careful to partition this in such a way that H_{int} is small compared H_0 and H_1, then it should be possible to properly describe the state of the full system as product states in the sub-systems: $|\psi\rangle = |\psi_0\psi_1\rangle$. Further, we can write a time-dependent Schrödinger equation for the motion of each subsystem as

$$\mathrm{i}\hbar\frac{\partial\left|\psi_1\right\rangle}{\partial t} = H_1\left|\psi_1\right\rangle \tag{3.3.19}$$

Within these assumptions, we can write the complete time-dependent Schrödinger equation in terms of the two sub-states:

$$\mathrm{i}\hbar\left|\psi_0\right\rangle\frac{\partial\left|\psi_1\right\rangle}{\partial t} + \mathrm{i}\hbar\left|\psi_1\right\rangle\frac{\partial\left|\psi_0\right\rangle}{\partial t} = \left|\psi_0\right\rangle H_1\left|\psi_1\right\rangle + \left|\psi_1\right\rangle H_0\left|\psi_0\right\rangle + H_{\text{int}}\left|\psi_0\right\rangle\left|\psi_1\right\rangle \tag{3.3.20}$$

Then making use of eq. (3.3.19) and left operating by $\langle\psi_1|$, we can write

$$\mathrm{i}\hbar\frac{\partial\left|\psi_0\right\rangle}{\partial t} = \left[H_0 + \left\langle\psi_1\right| H_{\text{int}}\left|\psi_1\right\rangle\right]\left|\psi_0\right\rangle \tag{3.3.21}$$

This is equivalent to the TDSE for a Hamiltonian of form (3.3.1) where the external interaction $V(t) = \langle\psi_1| H_{\text{int}}(t)\left|\psi_1\right\rangle$ comes from integrating the 1–2 interaction over the sub-space of $|\psi_1\rangle$. This represents a time-dependent mean field method.

Example 3.3.1: Vibrational Excitation by Chirped IR Pulses

To illustrate how eq. (3.3.14) is applied to directly, numerically calculate transitions induced by a time-dependent potential, we will examine the use of pulsed infrared light fields to drive anharmonic vibrations from the ground vibrational state $n = 0$ to high levels of vibrational excitation. Our focus will be on the process of sequential excitation, a series of multiple $n \rightarrow n + 1$ transitions up the "vibrational ladder," rather than direct excitation from $n = 0$ to a high vibrational level. For anharmonic potentials, the frequency of each successive one-quantum transition is progressively lower. This suggests that an efficient way of driving the system to high vibrational excitation with pulsed infrared light would be to frequency sweep (or "chirp") the infrared field in such a way that the frequency changes as one progresses to higher levels of excitation to match the $n \rightarrow n + 1$ transition frequency .

We use a partitioned Hamiltonian of the form eq. (3.3.1), in which the vibration characterized by H_0 will be treated using a Morse oscillator, and the time-dependent potential takes the form of a electric dipole Hamiltonian $V(t) = -\mu \cdot E(t)$. The dipole moment μ is defined as the charge of the bound particle q times the displacement of the oscillator x, which makes $\mu = qx$. The electric field of the chirped pulse is given by

$$E(t) = E_0\, G(t) \cos\left(\Omega_0 t + \beta t^2\right) \tag{3.3.22}$$

E_0 and Ω_0 are the magnitude and frequency of the field, $G(t)$ is the pulse field envelope (which we take to have a Gaussian form), and β is the pulse chirp parameter which describes the time-variance of the frequency. We expect to be able to transfer probability amplitude to high vibrational levels by varying the frequency so that the "instantaneous frequency" $\omega = \Omega_0 + (\partial\omega/\partial t)t = \Omega_0 + 2\beta t$ matches progressively higher vibrational transitions.

To calculate the dynamics using eq. (3.3.13) we require the energy eigenvalues for the potential, and the matrix elements in the time-dependent potential. Using a Morse potential with parameters $D_e = 38220\ \text{cm}^{-1}$, $R_e = 0.741\ \text{Å}$, and $\alpha = 1.945$, the energy eigenvalues for the first six vibrational levels ($n = 0 - 5$) are 2170, 6320, 10216, 13860, 17251, and $20388\ \text{cm}^{-1}$. These determine all energy splittings, ω_{nk}. The time-dependent matrix elements can be partitioned into three parts—(1) an as-yet-unknown electric field amplitude, (2) a matrix element in the vibrational coordinate, and (3) a time-dependent function which characterizes the field: $V_{kn}(t) = qE_0\langle k|x|n\rangle f(t)$. The matrix elements $\langle k|x|n\rangle$ are calculated for all pairs of states by numerically calculating the overlap integral over the product, $\int dx\ \varphi_k^*(x) x \varphi_n(x)$, or from analytical formulas.

These values allow us to estimate the pulse parameters. We estimate that the pulse frequency should be approximately equal to the $0 - 1$ transition frequency: $\Omega_0 \approx (E_1 - E - 0)/\hbar = 4150\ \text{cm}^{-1}$ or $0.767\ \text{fs}^{-1}$. From ω_{nk} we find that the average shift in transition frequency between adjacent states up the anharmonic vibrational ladder is $-21.4\ \text{cm}^{-1}$/level. To estimate an effective chirp rate we assume that the instantaneous frequency shifts $-x_e = -21.4\ \text{cm}^{-1}$ per 8 fs vibrational period, which results in $\beta = -x_e/\Omega_0 = -3.18 \times 10^{-3}\ \text{fs}^{-2}$.

We are now able to determine how good this estimate is by exploring the pulse widths and amplitude that can be used to selectively drive the system from $n = 0$ to $n = 5$. The functional form of the time-dependent potential introduced by the pulse, the initial occupation of the levels, and the time-integration range are input into a Runga-Kutta algorithm. Using our estimated parameters, a pulse width of $\sigma = 25$ fs, and an amplitude of $qE_0 = 5 \times 10^{11}\ \text{J/m}$, we see in Figure 3.3.2 that we are able to drive 90% of the population initially in $n = 0$ into $n = 5$. Changing only the sign of the chirp parameter from negative to positive results in 70% of the population being distributed in $n = 2$ and $n = 3$. Although this is an idealized model, it illustrates how a calculation of this sort can be used to calculate optimal waveforms for creating targeted optical excitations in matter.

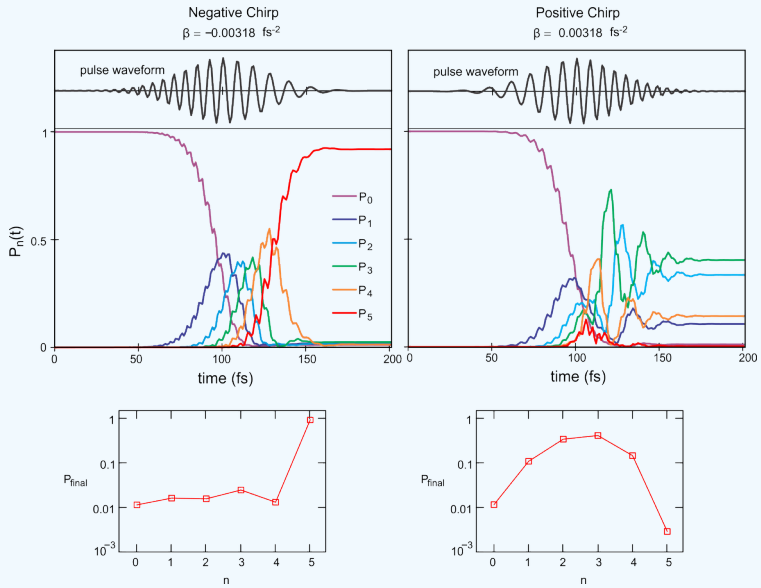


Figure 3.3.2: Time-dependent populations of the six lowest energy levels of the Morse oscillator being driven by a chirped femtosecond pulse. (Left) Outcome for negative chirp matched to vibrational energy spacing, and (right) flipping the chirp to positive while all other parameters remain the same.

This page titled 3.3: Transitions Induced by a Time-Dependent Potential is shared under a CC BY-NC-SA 4.0 license and was authored, remixed, and/or curated by Andrei Tokmakoff via source content that was edited to the style and standards of the LibreTexts platform.

3.4: Resonant Driving of a Two-Level System

As an example of how we can describe the transitions induced by a time-dependent potential, let's examine a two-level system under the influence of an external oscillating potential. This important example is one we can solve exactly, and it establishes a basis for understanding the resonant transitions induced by electromagnetic fields in spectroscopy. We consider a two-state system shown in Figure 3.4.1, with a ground state $|g\rangle$ and an excited state $|e\rangle$.

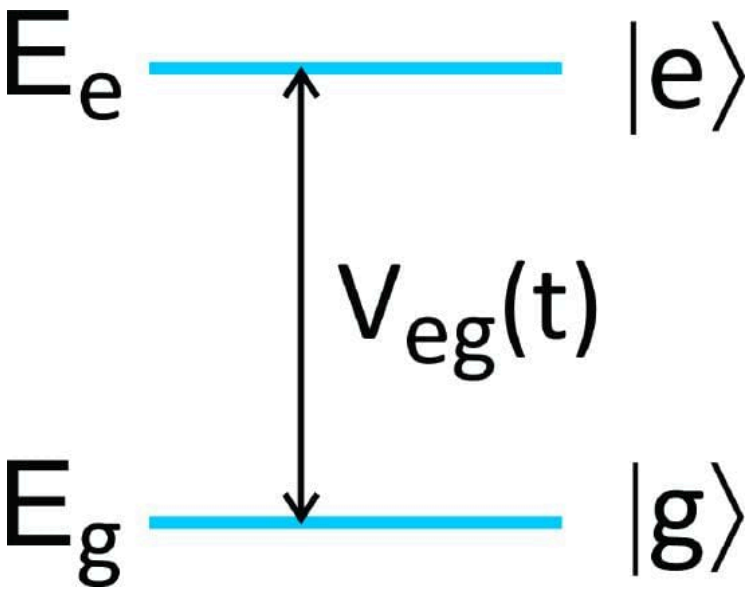


Figure 3.4.1: Energy level diagram for the harmonically driven two-level system.

The energy of the states is ordered such that $E_e > E_g$. These are eigenstates of the system Hamiltonian H_0. To this system, we apply a potential that sinusoidally oscillates at frequency ω

$$V(t) = V\cos\omega t \tag{3.4.1}$$

$$V_{eg}(t) = V_{eg}\cos\omega t \tag{3.4.2}$$

Let's ask, if the system starts in the ground state $|g\rangle$, what is the probability of finding it in the excited state $|e\rangle$ at time t? This potential is of the form that we expect for an electromagnetic field interacting with charged particles, which we will describe in Sec. 7.4. We will find then that the electric field is $\mathcal{E}(t) = \mathcal{E}_0\cos\omega t$ and the interaction potential can be written as $V(t) = -\mu\cdot\mathcal{E}(t)$, where μ represents the dipole operator.

From eq. (3.3.13), the system of differential equations for states e and g that describes this problem is:

$$\mathrm{i}\hbar\frac{\partial}{\partial t}b_k(t) = \sum_{n=e,g} b_n(t)V_{kn}(t)e^{-\mathrm{i}\omega_{nk}t} \qquad k = e,g \tag{3.4.3}$$

Inserting eq. (3.4.2) and expressing $\cos\omega t$ in its complex form:

$$\mathrm{i}\hbar\frac{\partial}{\partial t}b_k(t) = \sum_{n=e,g} b_n(t)V_{kn}e^{-\mathrm{i}\omega_{nk}t}\cdot\frac{1}{2}\left(e^{-\mathrm{i}\omega t} + e^{\mathrm{i}\omega t}\right) \qquad k = e,g \tag{3.4.4}$$

Writing this explicitly for states e and g, we get

$$\mathrm{i}\hbar\dot{b}_e = \frac{1}{2}b_gV_{eg}\left(e^{\mathrm{i}(\omega_{eg}-\omega)t} + e^{\mathrm{i}(\omega_{eg}+\omega)t}\right) + \frac{1}{2}b_e\cancel{V_{ee}}\left(e^{\mathrm{i}\omega t} + e^{-\mathrm{i}\omega t}\right) \tag{3.4.5}$$

$$\mathrm{i}\hbar\dot{b}_g = \frac{1}{2}b_g\cancel{V_{gg}}\left(e^{\mathrm{i}\omega t} + e^{-\mathrm{i}\omega t}\right) + \frac{1}{2}b_eV_{ge}\left(e^{-\mathrm{i}(\omega_{eg}+\omega)t} + e^{-\mathrm{i}(\omega_{eg}-\omega)t}\right) \tag{3.4.6}$$

Note that the expressions in the last term of eq. (3.4.6) have been rewritten in terms of the positive frequency, $\omega_{eg} = -\omega_{ge}$. As shown, two of the terms in these equations are dropped, since we take the diagonal matrix elements to be zero, $V_{ii} = 0$. We also make the secular approximation (or rotating wave approximation) in which the non-resonant terms are dropped. When $\omega_{ba} \approx \omega$, terms of the form $\exp\left[\pm \mathrm{i}\omega t\right]$ or $\exp\left[\pm \mathrm{i}\left(\omega_{eg} + \omega\right) t\right]$ oscillate rapidly relative to $|V_{eg}|^{-1}$ and thus do not contribute much to the changes of b_n in comparison to resonant terms of the form $\exp\left[\pm \mathrm{i}\left(\omega_{eg} - \omega\right) t\right]$.

The detuning from resonance, the mismatch in the frequencies of the energy gap between states, and the frequency of the sinusoidal driving potential are the criteria for efficient coupling. We define it as

$$\Delta\omega = \omega_{eg} - \omega \tag{3.4.7}$$

With this expression and the simplifications made, equations (3.4.5) and (3.4.6) become

$$\dot{b}_e = -\frac{\mathrm{i}}{2\hbar} b_g V_{eg} e^{\mathrm{i}\Delta\omega t} \tag{3.4.8}$$

$$\dot{b}_g = -\frac{\mathrm{i}}{2\hbar} b_e V_{ge} e^{-\mathrm{i}\Delta\omega t} \tag{3.4.9}$$

Note that the coefficients are oscillating at the same frequency, but the opposite sign of the exponential argument means that they are oscillating out-of-phase with one another.

Now to solve this pair of equations, we begin by differentiating eq. (3.4.8) with respect to time

$$\ddot{b}_e = -\frac{\mathrm{i}}{2\hbar}\left[\dot{b}_g V_{eg} e^{\mathrm{i}\Delta\omega t} + \mathrm{i}\Delta\omega\, b_g V_{eg} e^{\mathrm{i}\Delta\omega t}\right] \tag{3.4.10}$$

We also rewrite eq. (3.4.8) as

$$b_g = \frac{2\mathrm{i}\hbar}{V_{eg}} \dot{b}_e e^{-\mathrm{i}\Delta\omega t} \tag{3.4.11}$$

and substitute eq. (3.4.9) and eq. (3.4.11) into eq. (3.4.10), to give an equation for b_e:

$$\ddot{b}_e - \mathrm{i}\Delta\omega \dot{b}_e + \frac{|V_{eg}|^2}{4\hbar^2} b_e = 0 \tag{3.4.12}$$

We might notice that this looks the same as the equation for the damped harmonic oscillator, though with an imaginary damping coefficient. This is a homogeneous second-order differential equation of the form

$$a\ddot{x} + b\dot{x} + cx = 0 \tag{3.4.13}$$

Which has the solution

$$\begin{aligned} x &= e^{-(b/2a)t}\left(A\cos\mu t + B\sin\mu t\right) \\ \mu &= \frac{1}{2a}\sqrt{4ac - b^2} \end{aligned} \tag{3.4.14}$$

Then we find that the probability amplitude for state e is

$$b_e = e^{-\mathrm{i}\Delta\omega t/2}\left[A\cos\left(\frac{1}{2}\Omega_R t\right) + B\sin\left(\frac{1}{2}\Omega_R t\right)\right] \tag{3.4.15}$$

where A and B are constants, and we have defined the Rabi Frequency as

$$\Omega_R = \frac{1}{\hbar}\sqrt{|V_{eg}|^2 + \hbar^2(\Delta\omega)^2} \tag{3.4.16}$$

If the system starts in state g, the initial conditions are $b_e(0) = 0$, $b_g(0) = 1$, and $A = 0$. To find B, we use a similar approach to finding an expression for b_g, which we substitute with the time derivative of eq. (3.4.15) into eq. (3.4.8). This allows us to arrive at our final expressions for the probability amplitudes in both states:

$$b_e = -\mathrm{i}\frac{V_{eg}}{\hbar\Omega_R}e^{-\mathrm{i}\Delta\omega t/2}\sin\frac{1}{2}\Omega_R t \tag{3.4.17}$$

$$b_g = e^{\mathrm{i}\Delta\omega t/2}\left[\cos\left(\frac{1}{2}\Omega_R t\right) - \mathrm{i}\frac{\Delta\omega}{\Omega_R}\sin\left(\frac{1}{2}\Omega_R t\right)\right] \tag{3.4.18}$$

Then, with eq. (3.4.17) we find that the probability of observing the system in the excited state is

$$P_e(t) = |b_e(t)|^2 = P_{\max}\sin^2\left(\frac{1}{2}\Omega_R t\right) \tag{3.4.19}$$

where

$$P_{\max} = \frac{|V_{eg}|^2}{|V_{eg}|^2 + \hbar^2(\Delta\omega)^2} \tag{3.4.20}$$

The probability of observing the system in the ground state is

$$P_g = 1 - P_e \tag{3.4.21}$$

Equation (3.4.19) shows that once the time-dependent potential is applied, the probability of observing the system in the excited state grows, and the probability amplitude oscillates back and forth between the two states at the Rabi frequency Ω_R, which is dependent on the coupling between the states and the detuning from resonance. This is an important observation that we will return to later: electromagnetic fields couple quantum states of matter, creating time-evolving coherences. As illustrated in Figure 3.4.2a, the probability of observing the system in the excited state reaches a maximum value $P_{\max}$ after a time $\tau_{\max} = \pi/\Omega_R$ and returns to zero after $2\tau_{\max}$. $P_{\max}$ reflects how efficiently probability amplitude is exchanged between states g and e, and is also dependent on the coupling and the detuning. As a result, the amplitude and frequency of the oscillations in P_e are dependent both on Ω_R and $P_{\max}$, as illustrated in Figure 3.4.2b.

Another observation is the importance of resonance between the driving potential and the energy splitting between states. Transfer of amplitude from g to e is maximized when the driving field is at the same frequency as the energy splitting between the two states--that is, when the detuning is zero. On resonance, the probability amplitude is driven entirely from one state to another with a Rabi frequency $\Omega_R = |V_{ba}|/\hbar$. The efficiency of driving between g and e states, $P_{\max}$, drops off with detuning as shown in Figure 3.4.2c. When the coupling $|V_{ba}|$ matches the detuning $\hbar\Delta\omega$, only 50% of the amplitude of a can be transferred to b.

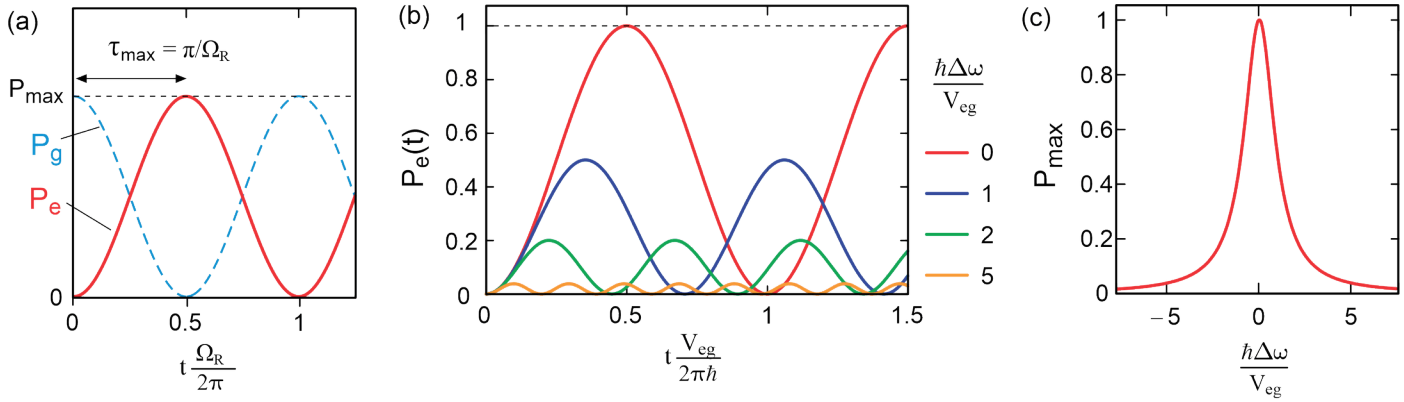


Figure 3.4.2: (a) Sinusoidal oscillations in the population of states e and g induced by harmonic potential. (b) The time-dependent population of state e given that a resonantly driven system started in state g illustrated for various values of the detuning from resonance, $\Delta\omega = (\omega - \omega_{eg})$. (c) The maximum population transferred from state g to state e as a function of detuning from resonance.

This page titled 3.4: Resonant Driving of a Two-Level System is shared under a CC BY-NC-SA 4.0 license and was authored, remixed, and/or curated by Andrei Tokmakoff via source content that was edited to the style and standards of the LibreTexts platform.

3.5: The Interaction Picture

The interaction picture is a representation that is a hybrid of the Schrödinger and Heisenberg representations. It is useful in solving problems in which we can partition the Hamiltonian as

$$\hat{H}(t) = \hat{H}_0 + \hat{V}(t) \tag{3.5.1}$$

where $\hat{H}_0$ is a Hamiltonian for the degrees of freedom we are interested in, which we treat exactly, and can be a function of time (although it usually won't be for us). $\hat{V}(t)$ is a time-dependent potential which can be complicated. In the interaction picture, we will treat each part of the Hamiltonian in a different representation. We will use the eigenstates of $\hat{H}_0$ as a basis set to describe the dynamics induced by $\hat{V}(t)$, assuming $\hat{V}(t)$ is small enough that eigenstates of $\hat{H}_0$ are a useful basis. If $\hat{H}_0$ is not a function of time, then there is a simple time-dependence to this part of the Hamiltonian that we may be able to account for easily.

Setting $\hat{V}$ to $\mathfrak{0}$, we can see that the time evolution of the exact part of the Hamiltonian $\hat{H}_0$ is described by

$$\frac{\partial}{\partial t}\hat{U}_0(t,t_0) = -\frac{\mathrm{i}}{\hbar}\hat{H}_0(t)\hat{U}_0(t,t_0) \tag{3.5.2}$$

where,

$$\hat{U}_0(t,t_0) = \exp_+\left[-\frac{\mathrm{i}}{\hbar}\int_{t_0}^{t} d\tau\, \hat{H}_0(t)\right] \tag{3.5.3}$$

or, for a time-independent $\hat{H}_0$,

$$\hat{U}_0(t,t_0) = e^{-\mathrm{i}\hat{H}_0(t-t_0)/\hbar} \tag{3.5.4}$$

We define a wavefunction in the interaction picture $|\psi_I\rangle$ in terms of the Schrödinger wavefunction through the unitary transformation

$$|\psi_S(t)\rangle \equiv \hat{U}_0(t,t_0)\,|\psi_I(t_0)\rangle \tag{3.5.5}$$

or

$$|\psi_I\rangle = \hat{U}_0^\dagger\,|\psi_S\rangle \tag{3.5.6}$$

Effectively the interaction representation defines wavefunctions such that the phase accumulated under $e^{-i\hat{H}_0 t/\hbar}$ never contributes, in essence removing it from Schrödinger picture. For small $\hat{V}$, these are typically high frequency oscillations relative to the slower amplitude changes induced by $\hat{V}$.

Now we need an equation of motion that describes the time evolution of the interaction picture wavefunctions. We begin by substituting eq. (3.5.5) into the TDSE:

$$\mathrm{i}\hbar\frac{\partial}{\partial t}\,|\psi_S\rangle = \hat{H}\,|\psi_S\rangle \tag{3.5.7}$$

from which we find can express this as an equation of motion for $|\psi_I\rangle$:

$$\therefore \quad \mathrm{i}\hbar\frac{\partial\,|\psi_I\rangle}{\partial t} = \hat{V}_I\,|\psi_I\rangle \tag{3.5.8}$$

where

$$\hat{V}_I(t) = \hat{U}_0^\dagger(t,t_0)\hat{V}(t)\,\hat{U}_0(t,t_0) \tag{3.5.9}$$

We see that $|\psi_I\rangle$ satisfies the Schrödinger equation with a new Hamiltonian in eq. (3.5.9)--the interaction picture Hamiltonian, $\hat{V}_I(t)$. We have performed a unitary transformation of $\hat{V}(t)$ into the frame of reference of $\hat{H}_0$, using $\hat{U}_0$. Note that the matrix elements of $\hat{V}_I$ are $\langle k|\,\hat{V}_I\,|l\rangle = e^{-\mathrm{i}\omega_{lk}t}V_{kl}$ where k and l are eigenstates of $\hat{H}_0$.

We can now define a time-evolution operator in the interaction picture:

$$|\psi_I(t)\rangle = \hat{U}_I(t,t_0)\,|\psi_I(t_0)\rangle \tag{3.5.10}$$

where

$$\hat{U}_I(t,t_0) = \exp_+\left[\frac{-\mathrm{i}}{\hbar}\int_{t_0}^{t} d\tau\,\hat{V}_I(\tau)\right] \tag{3.5.11}$$

Now we see that

$$\begin{aligned} |\psi_S(t)\rangle &= \hat{U}_0(t,t_0)\,|\psi_I(t)\rangle \\ &= \hat{U}_0(t,t_0)\,\hat{U}_I(t,t_0)\,|\psi_I(t_0)\rangle \\ &= \hat{U}_0(t,t_0)\,\hat{U}_I(t,t_0)\,|\psi_S(t_0)\rangle \end{aligned} \tag{3.5.12}$$

$$\therefore \quad \hat{U}(t,t_0) = \hat{U}_0(t,t_0)\hat{U}_I(t,t_0) \tag{3.5.13}$$

Also, the time evolution of conjugate wavefunction in the interaction picture can be written

$$\hat{U}^\dagger(t,t_0) = \hat{U}_I^\dagger(t,t_0)\hat{U}_0^\dagger(t,t_0) = \exp_-\left[\frac{\mathrm{i}}{\hbar}\int_{t_0}^{t} d\tau\,\hat{V}_I(\tau)\right]\exp_-\left[\frac{\mathrm{i}}{\hbar}\int_{t_0}^{t} d\tau\,\hat{H}_0(\tau)\right] \tag{3.5.14}$$

For the last two expressions, the order of these operators certainly matters.

So, what changes about the time-propagation in the interaction representation? Let's start by writing out the time-ordered exponential for $\hat{U}$ in eq. (3.5.13) by using eq. (3.5.11):

$$\begin{aligned} \hat{U}(t,t_0) &= \hat{U}_0(t,t_0) + \left(\frac{-\mathrm{i}}{\hbar}\right)\int_{t_0}^{t} d\tau\,\hat{U}_0(t,\tau)\,\hat{V}(\tau)\,\hat{U}_0(\tau,t_0) + \cdots \\ &= \hat{U}_0(t,t_0) + \sum_{n=1}^{\infty}\left(\frac{-\mathrm{i}}{\hbar}\right)^n \int_{t_0}^{t} d\tau_n \int_{t_0}^{\tau_n} d\tau_{n-1} \ldots \int_{t_0}^{\tau_2} d\tau_1\,\hat{U}_0(t,\tau_n)\,\hat{V}(\tau_n)\,\hat{U}_0(\tau_n,\tau_{n-1})\ldots \\ &\quad \times \hat{U}_0(\tau_2,\tau_1)\,\hat{V}(\tau_1)\,\hat{U}_0(\tau_1,t_0) \end{aligned} \tag{3.5.15}$$

Here we have used the composition property of $\hat{U}(t,t_0)$. The same positive time-ordering applies. Note that the interactions $\hat{V}(\tau_i)$ are not in the interaction representation here. Rather we used the definition in eq. (3.5.9) and collected terms. Now consider how $\hat{U}$ describes the time-dependence if we initiate the system in an eigenstate of $\hat{H}_0\,|\ell\rangle$ and observe the amplitude in a target eigenstate $|k\rangle$. The system evolves in eigenstates of $\hat{H}_0$ during the different time periods, with the time-dependent interactions V driving the transitions between these states. As illustrated in Figure 3.5.1, the first-order term describes direct transitions between $|\ell\rangle$ and $|k\rangle$ induced by $\hat{V}$, integrated over the full time-period. Before the interaction phase is acquired as $e^{-\mathrm{i}E_\ell(\tau-t_0)/\hbar}$, whereas after the interaction phase is acquired as $e^{-\mathrm{i}E_\ell(t-\tau)/\hbar}$. Higher-order terms in the time-ordered exponential account for all possible intermediate pathways.

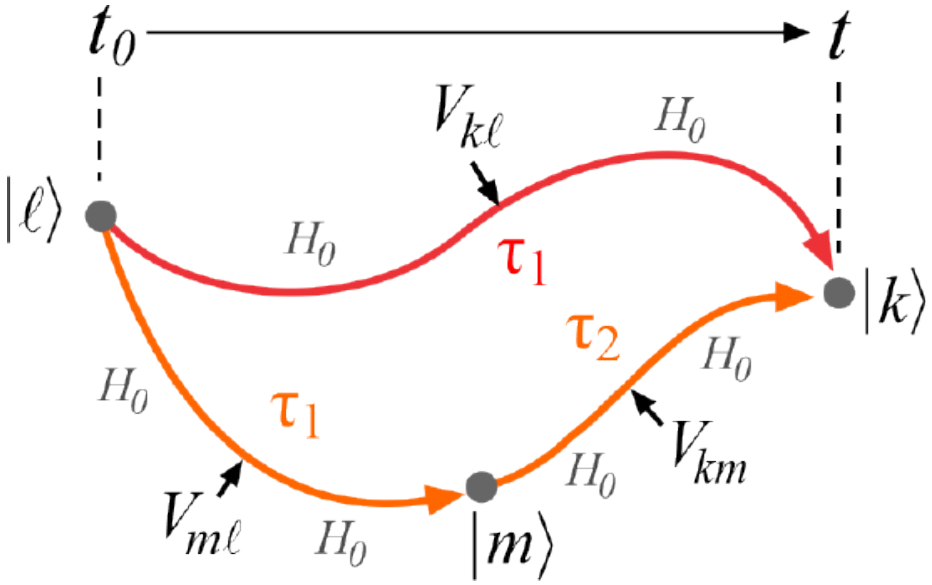


Figure 3.5.1: Illustration of time evolution within the interaction picture expansion of the time-evolution operator. Free evolution under H_0 is interrupted by interactions $V_{k\ell}$ that shift probability amplitude between system eigenstates. These interactions can occur at any time between t_0 and t. The upper (red) curve illustrates the first order term of the expansion, whereas the lower (orange) curve illstrates the second order term.

We now know how the interaction picture wavefunctions evolve in time. What about the operators? First, from examining the expectation value of an operator we see

$$\begin{aligned}\langle \hat{A}(t)\rangle &= \langle\psi(t)|\,\hat{A}\,|\psi(t)\rangle \\ &= \langle\psi(t_0)|\,\hat{U}^\dagger(t,t_0)\,\hat{A}\,\hat{U}(t,t_0)\,|\psi(t_0)\rangle \\ &= \langle\psi(t_0)|\,\hat{U}_I^\dagger\hat{U}_0^\dagger\,\hat{A}\,\hat{U}_0\hat{U}_I\,|\psi(t_0)\rangle \\ &= \langle\psi_I(t)|\,\hat{A}_I\,|\psi_I(t)\rangle\end{aligned} \tag{3.5.16}$$

where

$$\hat{A}_I \equiv \hat{U}_0^\dagger\,\hat{A}_S\,\hat{U}_0 \tag{3.5.17}$$

So, the operators in the interaction picture also evolve in time, but under $\hat{H}_0$. This can be expressed as a Heisenberg equation by differentiating $\hat{A}_I$:

$$\frac{\partial}{\partial t}\hat{A}_I = \frac{\mathrm{i}}{\hbar}\left[\hat{H}_0, \hat{A}_I\right] \tag{3.5.18}$$

We also know

$$\frac{\partial}{\partial t}\,|\psi_I\rangle = \frac{-\mathrm{i}}{\hbar}\hat{V}_I(t)\,|\psi_I\rangle \tag{3.5.19}$$

Notice that the interaction representation is a partition between the Schrödinger and Heisenberg representations. Wavefunctions evolve under $\hat{V}_I$, while operators evolve under $\hat{H}_0$.

$$\text{Schrödinger:}\quad \text{For } \hat{H}_0 = 0, \hat{V}(t) = \hat{H} \quad\Rightarrow\quad \begin{aligned}&\frac{\partial \hat{A}}{\partial t} = 0 \\ &\frac{\partial}{\partial t}\,|\psi_S\rangle = -\frac{\mathrm{i}}{\hbar}\hat{H}\,|\psi_S\rangle\end{aligned} \tag{3.5.20}$$

$$\text{Heisenberg:}\quad \text{For } \hat{H}_0 = \hat{H}, \hat{V}(t) = 0 \quad\Rightarrow\quad \begin{aligned}&\frac{\partial \hat{A}}{\partial t} = \frac{i}{\hbar}\left[\hat{H}, \hat{A}\right] \\ &\frac{\partial \psi}{\partial t} = 0\end{aligned} \tag{3.5.21}$$

To finish our discussion of the interaction picture, let's discuss how interaction picture dynamics relates to our earlier calculation of the probability amplitudes b_n. Earlier we described how time-dependent problems with Hamiltonians of the form $\hat{H} = \hat{H}_0 + \hat{V}(t)$ could be solved in terms of the time-evolving amplitudes in the eigenstates of $\hat{H}_0$. The state of the system is described as a superposition

$$|\psi(t)\rangle = \sum_n c_n(t)\,|n\rangle \tag{3.5.22}$$

where the coefficients, or probability amplitudes, $c_k(t)$ are given by

$$\begin{aligned} c_k(t) &= \langle k|\psi(t)\rangle = \langle k|\,\hat{U}(t,t_0)\,|\psi(t_0)\rangle \\ &= \langle k|\,\hat{U}_0\hat{U}_I\,|\psi(t_0)\rangle \\ &= e^{-\mathrm{i}E_k t/\hbar}\,\langle k|\,\hat{U}_I\,|\psi(t_0)\rangle \end{aligned} \tag{3.5.23}$$

Now, comparing eq. (3.5.23) and eq. (3.3.10) allows us to recognize that our earlier modified probability amplitudes b_n were expansion coefficients for interaction picture wavefunctions

$$b_k(t) = \langle k|\psi_I(t)\rangle = \langle k|\,\hat{U}_I\,|\psi(t_0)\rangle \tag{3.5.24}$$

This page titled 3.5: The Interaction Picture is shared under a CC BY-NC-SA 4.0 license and was authored, remixed, and/or curated by Andrei Tokmakoff via source content that was edited to the style and standards of the LibreTexts platform.

3.6: Time-Dependent Perturbation Theory

Time-dependent perturbation theory refers to calculating the time evolution of a system by truncating the expansion of the interaction picture time-evolution operator after a certain term. In practice, truncating the full time-propagator U is not effective, and only works for times that are short compared to the inverse of the energy splitting between coupled states. The interaction picture applies to Hamiltonians that can be cast as $H(t) = H_0 + V(t)$, which allows us to treat the time evolution under H_0 exactly, but only truncate the influence of $V(t)$. This works well for weak perturbations. Let's look more closely at this.

We know the eigenstates for H_0 from solving the TISE, $H_0 |n\rangle = E_n |n\rangle$, and we can calculate the evolution of the wavefunction that results from $V(t)$:

$$|\psi_I(t)\rangle = \sum_n b_n(t) |n\rangle \tag{3.6.1}$$

For a given state k, we calculate b_k as:

$$b_k(t) = \langle k| U_I(t, t_0) |\psi(t_0)\rangle \tag{3.6.2}$$

where

$$U_I(t, t_0) = \exp_+ \left[\frac{-\mathrm{i}}{\hbar} \int_{t_0}^{t} V_I(\tau)\, d\tau\right] \tag{3.6.3}$$

We can truncate the expansion of U_I after a few terms. This works well for small changes in the probability amplitude of the states involved, $b_k(t) \approx b_k(0)$, and therefore small coupling relative to their energy splittings, $|V| \ll |E_k - E_n|$. As we will see, the results we obtain from perturbation theory are widely used for spectroscopy, condensed phase dynamics, and relaxation.

Let's take the specific case where we have a system prepared in state $|\ell\rangle$, and we want to know the probability density $P_k(t) = |b_k(t)|^2$, the probability of observing the system in $|k\rangle$ at time t due to the external potential. Expanding eq. (3.6.2) we find

$$\begin{aligned} b_k(t) = \langle k|\ell\rangle &- \frac{\mathrm{i}}{\hbar} \int_{t_0}^{t} d\tau\, \langle k| V_I(\tau) |\ell\rangle \\ &+ \left(\frac{-\mathrm{i}}{\hbar}\right)^2 \int_{t_0}^{t} d\tau_2 \int_{t_0}^{\tau_2} d\tau_1\, \langle k| V_I(\tau_2) V_I(\tau_1) |\ell\rangle + \ldots \end{aligned} \tag{3.6.4}$$

Now, we can express the matrix elements in the interaction picture as

$$\langle k |V_I(t)| \ell\rangle = \left\langle k \left| U_0^\dagger V(t) U_0 \right| \ell \right\rangle = e^{-\mathrm{i}\omega_{\ell k} t} V_{k\ell}(t) \tag{3.6.5}$$

and from this we obtain:

$$b_k(t) = \delta_{k\ell} - \frac{\mathrm{i}}{\hbar} \int_{t_0}^{t} d\tau_1\, e^{-\mathrm{i}\omega_{\ell k}\tau_1} V_{k\ell}(\tau_1) \qquad \text{“first-order”} \tag{3.6.6}$$

$$+ \sum_m \left(\frac{-\mathrm{i}}{\hbar}\right)^2 \int_{t_0}^{t} d\tau_2 \int_{t_0}^{\tau_2} d\tau_1\, e^{-\mathrm{i}\omega_{mk}\tau_2} V_{km}(\tau_2) e^{-\mathrm{i}\omega_{\ell m}\tau_1} V_{m\ell}(\tau_1) \qquad \text{“second-order”} \tag{3.6.7}$$

$$+ \ldots$$

The first-order term allows only direct transitions between $|\ell\rangle$ and $|k\rangle$, as allowed by the matrix element in V, whereas the second-order term accounts for transitions occurring through an intermediate state $|m\rangle$. For perturbation theory, the time-ordered integral is truncated at the appropriate order. Including only eq. (3.6.6) is known as first-order perturbation theory, whereas including all terms up to eq. (3.6.7) is second-order perturbation theory. The order of perturbation theory applicable to a particular calculation should be chosen to account for the types of the intermediate pathways that should be allowed between $|\ell\rangle$ and $|k\rangle$, keeping in mind the relative magnitude of the interactions between states.

For first-order perturbation theory, the expression in eq. (3.6.6) is the solution to the differential equation that we get for direct coupling between $|\ell\rangle$ and $|k\rangle$:

$$\frac{\partial}{\partial t} b_k = -\frac{\mathrm{i}}{\hbar} e^{-\mathrm{i}\omega_{\ell k} t} V_{k\ell}(t) b_\ell(0) \tag{3.6.8}$$

The solution will not allow for the feedback between $|\ell\rangle$ and $|k\rangle$, and as a result neglects the changing amplitude in these states. As a result it is only valid in describing the initial rate of transfer out of state $|\ell\rangle$ such that $|b_k(t)|^2 - |b_k(0)|^2 \ll 1$. If the initial state of the system $|\psi_0\rangle$ is not an eigenstate of H_0, we can express it as a superposition of eigenstates, $|\psi_0\rangle = \sum_n b_n(0)\,|\psi_0\rangle$ with

$$b_k(t) = \sum_n b_n(0)\,\langle k|\,U_I\,|n\rangle \tag{3.6.9}$$

Another observation applies to first-order perturbation theory. If the system is initially prepared in a state $|\ell\rangle$, and a time-dependent perturbation is turned on and then turned off over the time interval $t = -\infty$ to $+\infty$, then the complex amplitude $b(t)$ in the target state $|k\rangle$ can be obtained by taking the Fourier transform of $V_{\ell k}(t)$ and evaluating its value at the energy gap $\omega_{\ell k}$.

$$b_k(t) = -\frac{\mathrm{i}}{\hbar} \int_{-\infty}^{+\infty} d\tau\, e^{-\mathrm{i}\omega_{\ell k}\tau}\, V_{k\ell}(\tau) \tag{3.6.10}$$

That is, if the Fourier transform pair is defined in the following manner:

$$\tilde{V}(\omega) \equiv \tilde{\mathcal{F}}\,[V(t)] = \int_{-\infty}^{+\infty} dt\, V(t)\exp(\mathrm{i}\omega t) \tag{3.6.11}$$

$$V(t) \equiv \tilde{\mathcal{F}}^{-1}\left[\tilde{V}(\omega)\right] = \frac{1}{2\pi}\int_{-\infty}^{+\infty} d\omega\, \tilde{V}(\omega)\exp(-\mathrm{i}\omega t) \tag{3.6.12}$$

Then we can substitute (3.6.8) into (3.6.2) and square the result to write the probability of transfer to state k as

$$P_{k\ell} = \frac{2\pi\left|\tilde{V}_{k\ell}(\omega_{k\ell})\right|^2}{\hbar^2} \tag{3.6.13}$$

Example: First-order Perturbation Theory

Let's consider a simple model for vibrational excitation induced by the rapid compression of a harmonic oscillator illustrated in Figure 3.6.1. We will subject a harmonic oscillator initially in its ground state, $|\ell\rangle = |0\rangle$, to a Gaussian compression pulse which increases its force constant κ from κ_0 to $\kappa_0 + \delta\kappa_0$, and determine the probability of population transfer to the other oscillator levels, $|n\rangle$.

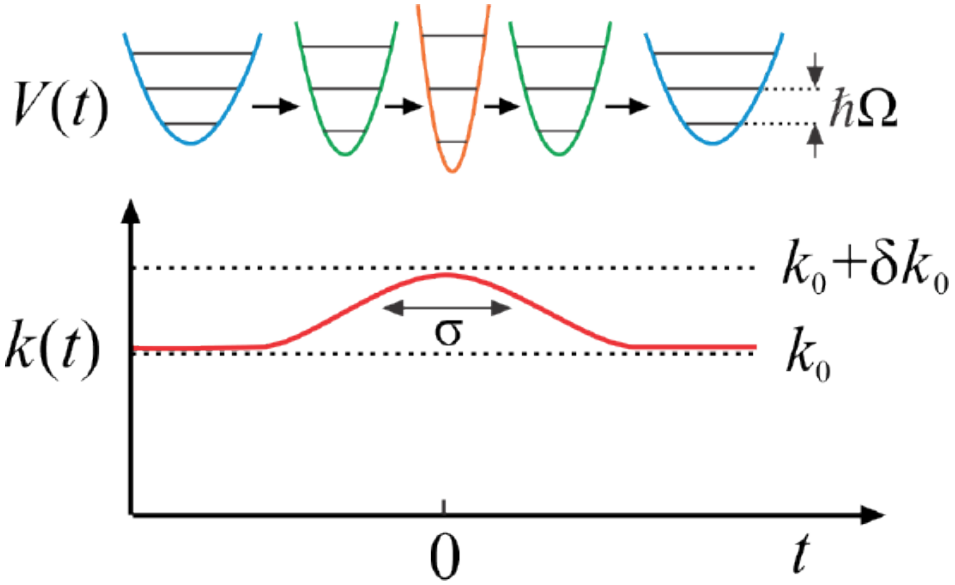


Figure 3.6.1: Illustration of the time-dependence of the force constant and harmonic potential during a compression pulse with standard deviation width σ and amplitude $\delta\kappa_0$.

The complete time-dependent Hamiltonian is:

$$H(t) = T + V(t) = \frac{p^2}{2m} + \frac{1}{2}\kappa(t)x^2 \tag{3.6.14}$$

where

$$\kappa(t) = \kappa_0 + \delta\kappa(t) \tag{3.6.15}$$

$$\delta\kappa(t) = \delta\kappa_0 \, \exp\left(-\frac{(t-t_0)^2}{2\sigma^2}\right) \tag{3.6.16}$$

Here σ is the width in time of the Gaussian perturbation as a standard deviation. Now, we use eq. (3.6.14) to partition the Hamiltonian as $H = H_0 + V(t)$ in such a manner that we can write H_0 as a time-independent harmonic oscillator Hamiltonian.

$$H = \underbrace{\frac{p^2}{2} + \frac{1}{2}\kappa_0 x^2}_{H_0} + \underbrace{\frac{1}{2}\delta\kappa_0 \, x^2 \exp\left(-\frac{(t-t_0)^2}{2\sigma^2}\right)}_{V(t)} \tag{3.6.17}$$

So, we know the eigenstates and eigenvalues of H_0: $H_0 \left|n\right\rangle = E_n \left|n\right\rangle$

$$H_0 = \hbar\Omega\left(a^\dagger a + \frac{1}{2}\right) \tag{3.6.18}$$

$$E_n = \hbar\Omega\left(n + \frac{1}{2}\right) \tag{3.6.19}$$

Now we ask, if the system is in $\left|0\right\rangle$ before applying the perturbation, what is the probability of finding it in state $\left|n\right\rangle$ after the perturbation? For $n \neq 0$:

$$b_n(t) = -\frac{\mathrm{i}}{\hbar}\int_{t_0}^{t} d\tau \, V_{n0}(\tau) e^{\mathrm{i}\omega_{n0}\tau} \tag{3.6.20}$$

Using $\omega_{n0} = \left(E_n - E_0\right)/\hbar = n\Omega$, and recognizing that we can set the limits to $t_0 = -\infty$ and $t = \inf$,

$$b_n = -\frac{\mathrm{i}}{2\hbar}\,\delta\kappa_0 \left\langle n\right| x^2 \left|0\right\rangle \int_{-\infty}^{+\infty} d\tau \, e^{\mathrm{i}n\Omega\tau} e^{-\tau^2/2\sigma^2} \tag{3.6.21}$$

This leads to

$$b_n = -\frac{\mathrm{i}}{2\hbar}\,\delta\kappa_0 \sqrt{2\pi}\sigma \left\langle n\right| x^2 \left|0\right\rangle e^{-n^2\sigma^2\Omega^2/2} \tag{3.6.22}$$

Here we made use of an important identity for Gaussian integrals:

$$\int_{-\infty}^{+\infty} \exp\left(ax^2 + bx + c\right) dx = \sqrt{\frac{-\pi}{a}} \, \exp\left(c - \frac{1}{4}\frac{b^2}{a}\right) \tag{3.6.23}$$

$$\int_{-\infty}^{+\infty} \exp\left(-ax^2 + \mathrm{i}bx\right) dx = \sqrt{\frac{\pi}{a}} \, \exp\left(-\frac{b^2}{4a}\right) \tag{3.6.24}$$

Note that eq. (3.6.21) takes the form of a Fourier transform. By taking the modulus squared of both sides of we have we have illustrated an example of eq. (3.6.13).

Now let's evaluate the matrix element, which we can expand in raising and lowering operators:

$$x^2 = \frac{\hbar}{2m\Omega}\left(a + a^\dagger\right)^2 = \frac{\hbar}{2m\Omega}\left(aa + a^\dagger a + aa^\dagger + a^\dagger a^\dagger\right) \tag{3.6.25}$$

From these we see that first-order perturbation theory will not allow transitions to $n = 1$ from $n = 0$, only $n = 2$. Generally, this would not be realistic because we would certainly expect that excitation to $n = 1$ would dominate over excitation to $n = 2$. A real system would also be anharmonic, in which case, the leading term in the expansion of the potential $V(x)$, that is linear in x, would not vanish as it does for a harmonic oscillator, and this would lead to matrix elements that raise and lower the excitation by one quantum.

However, for the present case, the only matrix element for transfer of amplitude out of $n = 0$ is

$$\langle 2|\, x^2\, |0\rangle = \sqrt{2}\frac{\hbar}{2m\Omega} \tag{3.6.26}$$

So,

$$b_2 = \frac{-\mathrm{i}\sqrt{\pi}\,\delta\kappa_0\,\sigma}{2m\Omega}e^{-4\sigma^2\Omega^2} \tag{3.6.27}$$

Recognizing that $\kappa_0 = m\Omega^2$ allows us to write the probability of occupying the $n = 2$ state after the pulse, i.e. the population of state $|2\rangle$, as

$$P_2 = |b_2|^2 = \frac{\pi}{2}\left(\frac{\delta k_0}{k_0}\right)^2 \Omega^2\sigma^2 e^{-8\sigma^2\Omega^2} \tag{3.6.28}$$

Looking at the exponential argument, we observe that significant transfer of amplitude occurs when the compression pulse width is small compared to the vibrational period.

$$\sigma \ll \frac{1}{\Omega} \tag{3.6.29}$$

In this regime, the potential is changing faster than the atoms can respond to the perturbation. In practice, when considering a solid-state problem, with frequencies matching those of acoustic phonons and unit cell dimensions, we need perturbations that move faster than the speed of sound, i.e., a shock wave. The opposite limit, $\sigma\Omega \gg 1$, is the adiabatic limit. In this case, the perturbation is so slow that the system always remains entirely in $n = 0$, even while it is compressed.

Now, let's consider the range of validity of this first-order treatment. Perturbation theory does not allow for b_n to change much from its initial value, $P_2 \ll 1$, indicating that

$$(\sigma\Omega)\left(\frac{\delta\kappa_0}{\kappa_0}\right) \ll 1 \tag{3.6.30}$$

Generally, the first order result will hold when the magnitude of the perturbation $\delta\kappa_0$ is small compared to κ_0, even if $\sigma \approx \Omega^{-1}$.

One step further

The preceding example was simple and a bit unphysical, but it tracks the general approach to setting up problems that we treat with time-dependent perturbation theory. The approach relies on writing a Hamiltonian that can be cast into a Hamiltonian that we can treat exactly as H_0, and time-dependent perturbations that shift amplitudes between its eigenstates. For this scheme to work well, we need the magnitude of perturbation to be small, which immediately suggests working with a Taylor series expansion of the potential. For instance, take a one-dimensional potential for a bound particle, $V(x)$, which is dependent on the form of an external variable y. We can expand the potential in x about its minimum $x = 0$ as

$$\begin{aligned} V(x) &= \frac{1}{2!}\frac{\partial^2 V}{\partial x^2}\bigg|_{x=0} x^2 + \frac{1}{2!}\frac{\partial^2 V}{\partial x\partial y}\bigg|_{x=0} xy + \frac{1}{3!}\sum_{n=1,2}\frac{\partial^3 V}{\partial x^n\partial y^{3-n}}\bigg|_{x=0} x^n y^{3-n} + \cdots \\ &= \frac{1}{2}kx^2 + V^{(2)}\,xy + \left(V_3^{(3)}x^3 + V_2^{(3)}x^2y + V_1^{(3)}xy^2\right) + \cdots \end{aligned} \tag{3.6.31}$$

The first expansion coefficient is the harmonic force constant for x, and the second term describes a bi-linear coupling whose magnitude $V^{(2)}$ indicates how much a change in the variable y influences the variable x. The remaining $V^{(3)}$ terms are cubic expansion terms. $V_0^{(3)}$ is the cubic anharmonicity of $V(x)$, and the remaining two terms are cubic couplings that describe the dependence of x on y. Introducing a time-dependent potential is equivalent to introducing a time-dependence to the operator y, where the form and strength of the interaction is subsumed into the amplitude V. In the case of the previous example, our formulation of the problem was equivalent to selecting only the $V_2^{(3)}$ term, so that $\delta\kappa_0/2 = V_2^{(3)}$, and giving the value of y a time-dependence described by the Gaussian waveform. If we consider matrix elements in the other cubic terms, we recognize that terms such as $V_2^{(3)}$ in the above example will give rise to single quantum excitations from $|0\rangle$ to $|1\rangle$ not present in our earlier solution. We will take a deeper dive into this type of problem when we study vibrational relaxation processes in Chapter 18.

This page titled 3.6: Time-Dependent Perturbation Theory is shared under a CC BY-NC-SA 4.0 license and was authored, remixed, and/or curated by Andrei Tokmakoff via source content that was edited to the style and standards of the LibreTexts platform.

3.7: The Golden Rule

Several important relationships in quantum mechanics that describe rate processes come from time-dependent perturbation theory. The Golden Rule, typically attributed to Fermi even though Dirac first developed it, refers to a series of expressions from first-order perturbation theory that describe the population transfer rate from one quantum state to another that arise from applying an external potential that couples the two states. Specifically, these expressions apply if the changes in the population of the states is very small, and we only consider direct coupling between the initial and final state. As we will see, there are many ways in which these expressions can be written and applied. The important results are derived from two model problems that we want to work through: (1) time evolution after applying a step perturbation, and (2) time evolution after applying a harmonic or sinusoidal perturbation.

As before, the Hamiltonian for the problem takes the form $H = H_0 + V(t)$, where H_0 is the time-independent Hamiltonian for the system we are observing, and $V(t)$ is an external potential which we apply to the system. Again, we will ask: if we prepare the system in the state $|\ell\rangle$, an eigenstate of H_0, what is the probability of observing the system in state $|k\rangle$ following the perturbation? In both cases, we will abruptly turn on a perturbation at time $t_0 = 0$.

Constant perturbation

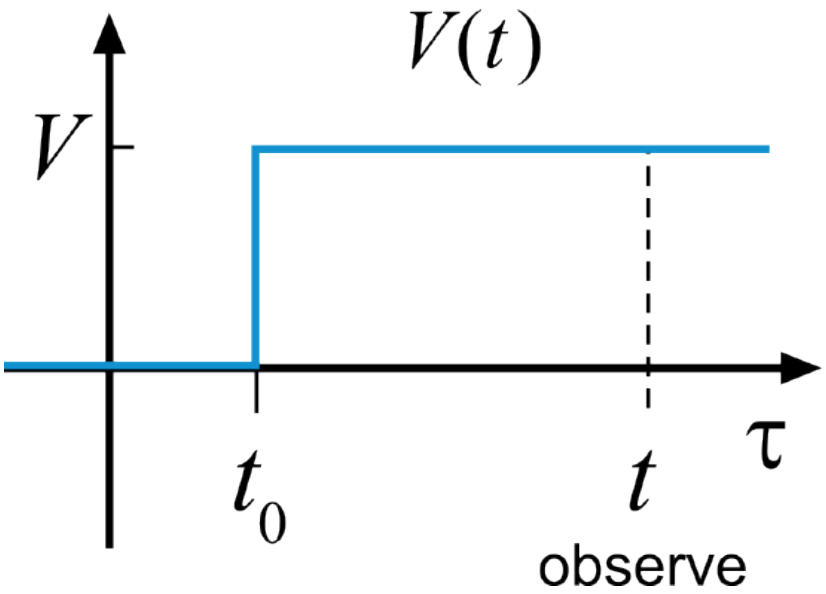


Figure 3.7.1

For the first model calculation, we simply apply a step perturbation, during on a constant potential of amplitude V at time t_0:

$$V(t) = \begin{cases} 0 & t < t_0 \\ V & t \geq t_0 \end{cases} \tag{3.7.1}$$

and evaluate the resulting state amplitude in other states k, with the first order expression, eq. (3.6.6):

$$b_k = -\frac{\mathrm{i}}{\hbar}\int_{t_0}^{t} d\tau\, e^{\mathrm{i}\omega_{k\ell}(\tau - t_0)} V_{k\ell} \tag{3.7.2}$$

The matrix element $V_{k\ell} = \langle k|\, V\, |\ell\rangle$ is independent of time, and the only time-dependence arises from switching on the perturbation. Setting $t_0 = 0$, we can evaluate this expression as

$$\begin{aligned} b_k &= -\frac{\mathrm{i}}{\hbar} V_{k\ell} \int_0^t d\tau\, e^{i\omega_{k\ell}\tau} \\ &= -\frac{V_{k\ell}}{E_k - E_\ell} \left[\exp\left(\mathrm{i}\omega_{k\ell} t\right) - 1\right] \end{aligned} \tag{3.7.3}$$

We now make use of an identity that is helpful to evaluate population changes:

$$e^{i\theta} - 1 = 2ie^{i\theta/2} \sin\left(\frac{\theta}{2}\right) \tag{3.7.4}$$

With this expression, the time-dependent amplitude of state k is

$$b_k = -\frac{2iV_{k\ell}e^{i\omega_{k\ell}t/2}}{E_k - E_\ell} \sin\left(\frac{1}{2}\omega_{k\ell}t\right) \tag{3.7.5}$$

and the corresponding population in state k is obtained from

$$P_k = |b_k|^2 = \frac{4\,|V_{k\ell}|^2}{|E_k - E_\ell|^2} \sin^2\left(\frac{1}{2}\omega_{k\ell}t\right) \tag{3.7.6}$$

We observe that the abrupt application of a constant perturbation induces a sinusoidal transfer of population between states k and ℓ with an amplitude that depends on the magnitude of the purturbation matrix element squared. If we write this using the energy splitting variable we used earlier,

$$\Delta = \frac{E_k - E_\ell}{2} \tag{3.7.7}$$

then

$$P_k = \frac{V^2}{\Delta^2} \sin^2\left(\frac{\Delta}{\hbar}t\right) \tag{3.7.8}$$

We can compare this with the exact result for the two-level problem that we solved in Section 2.3:

$$P_k = \frac{V^2}{V^2 + \Delta^2} \sin^2\left(\frac{\sqrt{\Delta^2 + V^2}}{\hbar}t\right) \tag{3.7.9}$$

As expected, the perturbation theory result works well when the magnitude of the perturbation is small compared to the energy gap, $V \ll \Delta$, which also corresponds to cases where the population change in the system is small, $P_k \ll 1$.

Looking more carefully, in Figure 3.7.2 we examine the time-dependence to P_k and compare the perturbation theory (solid lines) to the exact result (dashed lines) for different values of Δ. The correspondence is poor at $\Delta = 0$, for which P_k grows quadratically and the probability quickly exceeds unity. It's certainly unrealistic, but not surprising, since we don't expect that the expression will hold for the "strong coupling" case: $\Delta \ll V$. One begins to have quantitative accuracy in for the regime $P_k(t) - P_k(0) < 0.1$ or $\Delta < 4V$. Next, let's plot this a little differently in Figure 3.7.2b, scaling the time axis as $2\pi\hbar/\Delta$, focusing on the changes for $t \ll \Delta/\hbar$, and looking at $\sqrt{P_k}$, the magnitude of the expansion coefficient $|b_k|$. Here we see that the first-order perturbation theory result is excellent at describing the initial changes as amplitude flows into the target state $|k\rangle$, particularly for small changes $|b_k(t)|^2 < 0.1$.

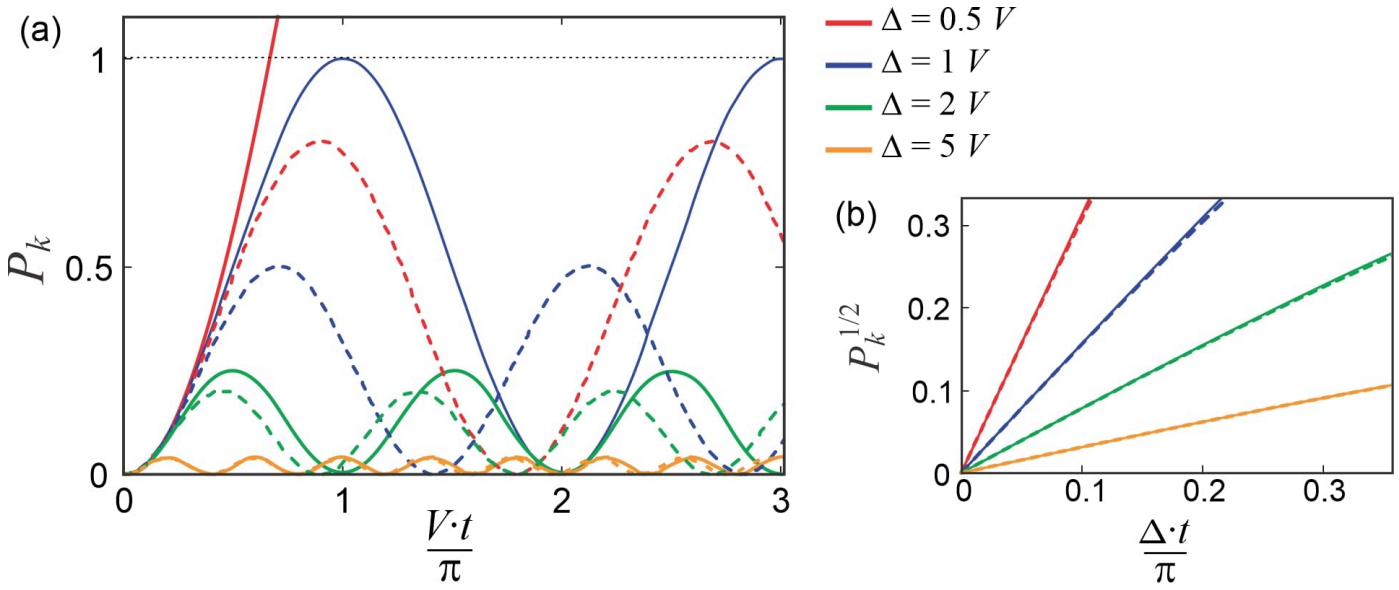


Figure 3.7.2: (a) Comparison of the time-dependent population of target state $|k\rangle$ as a function of time from the exact two-level system result, eq. (3.7.9), in dashed lines with that from first-order perturbation theory, eq. (3.7.8), in solid lines. (b) Changes in the amplitude in b_k the coefficient for the target state for short times illustrating linear growth and good correspondence of first-order perturbation theory with exact result.

Now let's look at how the population transfer to state k depends on both Δ and t. Using $\mathrm{sinc}(x) = \sin(x)/x$, we can rewrite the first-order result in eq. (3.7.8) as

$$P_k = \frac{V^2 t^2}{\hbar^2} \mathrm{sinc}^2 \left(\frac{\Delta}{\hbar} t \right) \tag{3.7.10}$$

A plot of the corresponding population transferred from $|\ell\rangle$ to $|k\rangle$ is shown in Figure 3.7.3 as a function of the detuning Δ. The probability of transfer peaks sharply where the energy of the initial state matches that of the final state, and, over time, efficient transfer requires a narrower energy difference between initial and final states. To examine the time-dependent behavior of P_k, we use $\lim_{x \to 0}\ \mathrm{sinc}(x) = 1$, to show that the probability grows quadratically at short time spans:

$$\lim_{\Delta \to 0} P_k = V^2 t^2 / \hbar^2 \tag{3.7.11}$$

Since P_k will exceed 1, this is clearly non-physical behavior. This serves to illustrate that first-order perturbation theory only applies to small changes in amplitude and for times spans in which feedback of the amplitude back into the initial state is not yet significant.

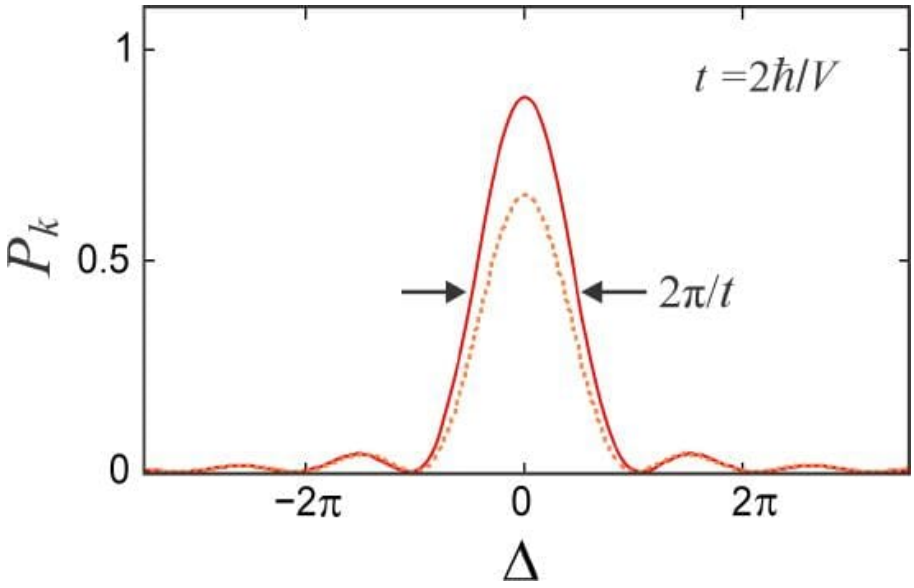


Figure 3.7.3: Illustration of the efficiency of the efficiency of population transfer to the target state $|k\rangle$ as a function of time following the onset of the constant perturbation. The first-order perturbation theory result (solid line) is compared with the exact result (dashed line).

From eq. (3.7.10) we may observe that the spread of final state energies to which transfer remains possible narrows with time at a rate of t^{-1}: $E_k - E_\ell < 2\pi\hbar/t$. If the perturbation continues long enough, the energies of the two states must be equal. This observation is sometimes referred to as a time-energy uncertainty relation, where $\Delta E \cdot \Delta t \geq 2\pi\hbar$. However, remember that this is just an observation of the principles of Fourier transforms. A frequency, and thereby energy, can only be determined as accurately as the length of the time over which we observe oscillations. Since time is not an operator, time and energy do not have a quantum uncertainty relation like $\Delta p \cdot \Delta x \geq 2\pi\hbar$, which derives from the fact that p and x do not commute.

In the long-time limit, the $\mathrm{sinc}^2(x)$ function narrows to a delta function according to

$$\lim_{a\to\infty} \frac{\sin^2(ax/2)}{ax^2} = \frac{\pi}{2}\,\delta(x) \tag{3.7.12}$$

and the population in state k is observed to grow linearly with time:

$$\lim_{t\to\infty} P_k(t) = \frac{2\pi}{\hbar}\,|V_{k\ell}|^2\;\delta(E_k - E_\ell)t \tag{3.7.13}$$

The delta function enforces energy conservation, saying that the energies of the initial and target state must be the same in the long-time limit. Of course, this expression is also unphysical since P_k can exceed 1 on long enough time scales.

What is interesting in eq. (3.7.13) is that a linear growth of population with time indicated that the transfer rate $w_k = \partial P_k/\partial t$ is independent of time, as expected for a rate constant in simple first-order kinetics. This population transfer rate is

$$w_k = \frac{2\pi}{\hbar}|V_{k\ell}|^2\;\delta(E_k - E_\ell) \tag{3.7.14}$$

That is, the rate at which population leaves ℓ and grows into state k is simply related to the square of the matrix element for the perturbation, in addition to requiring that the initial and final states have the same energy. This is one statement of the Golden Rule—the state-to-state form for a constant perturbation—which describes energy transfer and relaxation rates from first-order perturbation theory. In fact we will find that more accurate and complex treatments of the state-to-state transfer rate that properly conserve the probability amplitude of the system still predict the same rate constant as eq. (3.7.14). We will show that this rate properly describes the long time exponential decay observed for irreversible relaxation processes that we would expect from the solution of the rate equation $dP/dt = -wP$.

It is worth noting that the result that we obtained in eq. (3.7.14) is independent of the manner in which the perturbation is switched on. It may seem unphysical to turn on a perturbation instantaneously or that it matters whether the switch happens slowly; however, once we evaluate the $t \to \infty$ limit, the resulting rate expression is independent of the way the perturbation is applied.

Like time-independent perturbation theory, it is possible that the matrix element for first-order transitions $V_{k\ell}$ is zero, and that second-order perturbation theory is needed to describe the primary interactions that couple the initial and final states. This would apply to cases in which an intermediate state $|m\rangle$ mediates the transfer of probability amplitude from $|\ell\rangle$ to $|k\rangle$. Under those circumstances, one can derive a similar Golden Rule expression for the rate of transfer from ℓ to k through m using the strategies described above, and one obtains(1)

$$w_{\ell\to m\to k} = \frac{2\pi}{\hbar}\left|\frac{V_{km}V_{m\ell}}{E_\ell - E_m}\right|^2 \delta(E_k - E_\ell) \tag{3.7.15}$$

If there are multiple intermediate states—either discrete or a continuum—one can sum this expression over the continuum of states that contribute to the transfer using $\sum_m w_{\ell\to\, m\to\, k}$.

Population transfer to a continuum

Since first-order perturbation theory does not allow population feedback between the initial and final states, it turns out to be most useful in cases where we are interested in the rate of leaving an initial state. The Golden Rule is particularly useful for irreversible processes in which an initially prepared state transfers population amplitude continuum of accepting states, which we describe in Section 11.2. Examples include (1) the ionization of atoms in an electric field where the continuum are free particle waves, spontaneous emission of light by electronically excited molecules where the continuum of states are electromagnetic waves of varying frequency, and vibrational energy dissipation to a bath of phonons. Although dynamics of interactions with continua won't come up much until we tackle condensed matter problems, this is a good point to discuss how the Golden Rule rates are expressed for the case of state-to-continuum rate processes.

As in the prior section, we will calculate the transition probability from initial state $|\ell\rangle$ to a continuum of final states, $\{|k\rangle\}$. If P_ℓ is the probability of occupying the initial state, then the probability of occupying any state in the continuum is $\bar{P}_k = 1 - P_\ell$. $\bar{P}_k$ then can be expressed as the sum of probabilities for occupying a particular state within the continuum: $\bar{P} = \sum_k P_k$. The rates of transfer from ℓ to a specific state k' is again obtained from $w_{k'\ell} = \partial P_{k'}/\partial t$. Since first order perturbation theory only concerns itself with the rate of leaving state ℓ, the rate of transfer to all continuum states is merely a sum of the rates to each state:

$$\bar{w}_{k\ell} = \sum_k w_{k\ell} \tag{3.7.16}$$

For a continuum, the sum over discrete states can be replaced by an integral over a density of states $\rho(E_k)$ that describes the number of continuum states per energy interval:

$$\bar{w}_{k\ell} = \int dE_k\, \rho(E_k) w_{k\ell}(E_k) \tag{3.7.17}$$

where $w_{k\ell}$ is given by eq. (3.7.13). One can evaluate this integral if one can make two simplifying assumptions: (1) $\rho\,(E_k)$ varies slowly enough to be a constant and can be removed from the integral. (2) The matrix element $V_{k\ell}$ connecting initial and final states is the same for all states within the continuum. These assumptions are typically reasonable when one is working within the weak coupling requirement of perturbation theory. Then eq. (3.7.17) becomes

$$\bar{w}_{k\ell} = \frac{2\pi}{\hbar}|V_{k\ell}|^2\, \rho(E_\ell) \tag{3.7.18}$$

Thus the rate of transfer of population to the continuum depends only on the matrix element squared for the interaction of state ℓ and continuum states, and the density of accepting continuum states at the energy of the initial state. This is the common state-to-continuum form of the Golden Rule used often in the calculation of chemical and relaxation rate processes.

Harmonic perturbation

The second model calculation is to determine the transfer of population from state ℓ to k after turning on a harmonic or sinusoidal perturbation at time t_0. The results are important for spectroscopy, since they will be used to describe how electromagnetic fields induce transitions between quantum states of the system. In this case, we turn on an external potential that oscillates with an angular frequency ω and the magnitude of the perturbation is governed by V_0.

$$V(t) = V_0 \cos\omega t \qquad t \geq\ t_0 \tag{3.7.19}$$

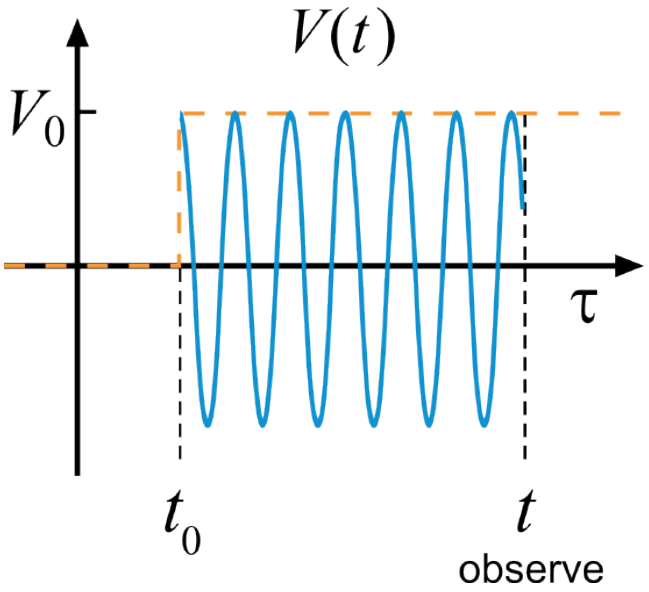


Figure 3.7.4: Illustration of the sudden onset of a sinusoidal perturbation of magnitude V at time t_0.

V_0 can be expressed in terms of operators of the system, so the matrix elements of the interaction potential are given by

$$V_{k\ell}(t) = V_{k\ell}\cos\omega t \tag{3.7.20}$$

where $V_{k\ell} = \langle k|V_0|\ell\rangle$. Note that our results are independent of the phase of this wave, so using a $\sin\omega t$ form will return the same key results.

To calculate resulting probability amplitude in state k we again make use of our first order expression, eq. (3.6.6), and express the cosine in its complex form: $\cos\omega t = \frac{1}{2}\left[e^{-\mathrm{i}\omega t} + e^{\mathrm{i}\omega t}\right]$. Setting $t_0 \to 0$, we obtain:

$$\begin{aligned} b_k &= -\frac{\mathrm{i}}{\hbar}\int_{t_0}^{t} d\tau\, V_{k\ell}(\tau)e^{\mathrm{i}\omega_{k\ell}\tau} \\ &= -\frac{\mathrm{i}V_{k\ell}}{2\hbar}\int_0^t d\tau\,\left[e^{\mathrm{i}(\omega_{k\ell}-\omega)\tau} + e^{\mathrm{i}(\omega_{k\ell}+\omega)\tau}\right] \\ &= -\frac{V_{k\ell}}{2\hbar}\left[\frac{e^{\mathrm{i}(\omega_{k\ell}-\omega)t}-1}{\omega_{k\ell}-\omega} + \frac{e^{\mathrm{i}(\omega_{k\ell}+\omega)t}-1}{\omega_{k\ell}+\omega}\right] \end{aligned} \tag{3.7.21}$$

Then using identity (3.7.4), we get

$$b_k = \frac{\mathrm{i}V_{k\ell}}{\hbar}\left[\frac{e^{\mathrm{i}(\omega_{k\ell}-\omega)t/2}\,\sin\left[\frac{1}{2}\left(\omega_{k\ell}-\omega\right)t\right]}{\omega_{k\ell}-\omega} + \frac{e^{\mathrm{i}(\omega_{k\ell}+\omega)t/2}\,\sin\left[\frac{1}{2}\left(\omega_{k\ell}+\omega\right)t\right]}{\omega_{k\ell}+\omega}\right] \tag{3.7.22}$$

This expression has many omegas, so it is worth reiterating that ω is the frequency of the harmonic perturbation and is positive, whereas $\omega_{k\ell} = \left(E_k - E_\ell\right)/\hbar$ reflects the energy splitting between the initial and final states and can be positive or negative. It is also worth noting that when we set $\omega \to 0$ that we do recover the expected behavior from the constant perturbation in eq. (3.7.5). This observation suggests a mathematical advantage for solving certain time-dependent problems with Fourier transformations over a sinusoidal potential and then applying the $\omega \to 0$ limit at the end.

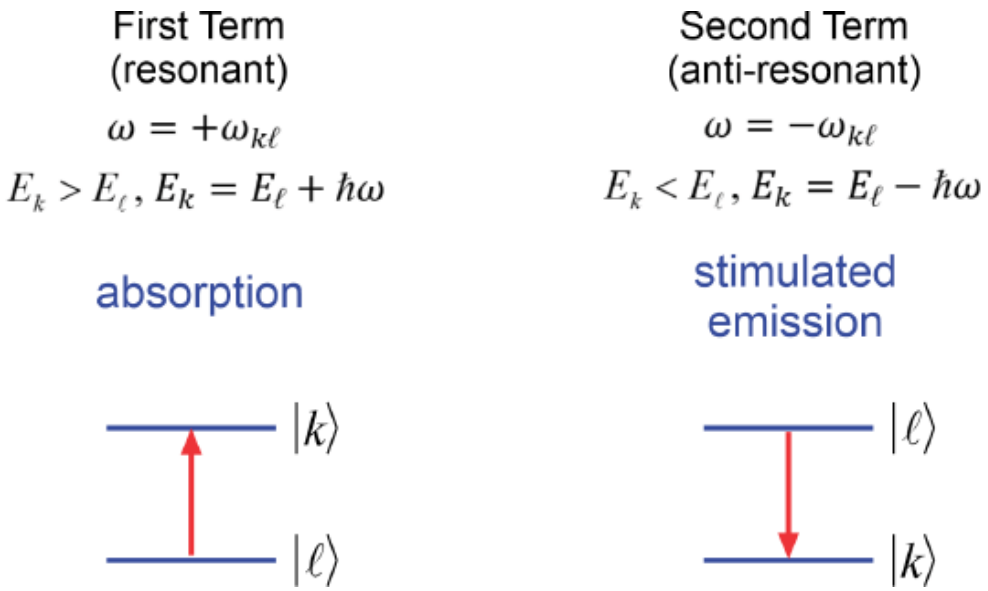


Figure 3.7.5: Energy level diagram illustrating the changes in the system corresponding to the two terms in eq. (3.7.22).

The denominators in eq. (3.7.22) indicate that the two terms only have a significant impact on the system when $\omega \approx |\omega_{k\ell}|$. This condition for efficient transfer is resonance, a matching of the frequency of the harmonic interaction with the energy splitting between quantum states. Consider the resonance conditions that will maximize each of these two terms. The first term in eq. (3.7.22) is maximized when $\omega = \omega_{k\ell}$, which occurs when $E_k > E_\ell$, and thus transfer of population from ℓ to k. requires an input of energy from the external potential by an amount $\hbar\omega$. This term is therefore referred to as absorption. The second term is maximized when $\omega = -\omega_{k\ell}$, which occurs when $E_k < E_\ell$, corresponding to a loss of energy by the system by an amount $\hbar\omega$. This term is often called stimulated emission due to its role in spectroscopy. In a quantum description of spectroscopy, we associate the increase of energy in the system on absorption with a loss of a quantum of energy $\hbar\omega$ in the light field, a photon. Similarly, the loss of energy in the system is related to the creation of a photon with energy $\hbar\omega$ in the light field. Thus, when considering both the light and matter, the total energy is conserved. However, our current first order perturbation theory description of the matter does not concern itself with the state of the light field; the potential is assumed to be unchanged by what happens in the system, so the energy of the system need not be conserved.

If we consider absorption only, we can use the first term in eq. (3.7.22) to calculate the time-dependent probability of occupying state k

$$P_k = |b_k|^2 = \frac{|V_{k\ell}|^2}{\hbar^2 (\omega_{k\ell} - \omega)^2} \sin^2\left[\frac{1}{2}(\omega_{k\ell} - \omega)\, t\right] \tag{3.7.23}$$

This expression is similar to eq. (3.7.6), in that is shows that the onset of the perturbation creates an oscillatory transfer of population between the ℓ and k states with an amplitude that scales as $|V_{k\ell}|^2$, but it also has similar problems. In this case, the important control variable to analyze is the detuning from resonance

$$\Delta\omega = \omega_{k\ell} - \omega \tag{3.7.24}$$

which quantifies how closely matched the frequency of the harmonic perturbation is to the energy splitting between ℓ and k. Rewriting eq. (3.7.23) in terms of $\Delta\omega$ gives:

$$P_k = \frac{|V_{k\ell}|^2}{\hbar^2 \Delta\omega^2} \sin^2\left[\frac{1}{2}\Delta\omega\, t\right] \tag{3.7.25}$$

To assess the validity of the perturbation theory expression, it is helpful for us to compare eq. (3.7.25) with the exact expression that we derived for the driven two-level system, eq. (3.4.19):

$$P_k = \frac{|V_{k\ell}|^2}{\hbar^2 \Delta\omega^2 + |V_{k\ell}|^2} \sin^2\left[\frac{1}{2}\sqrt{\frac{|V_{k\ell}|^2}{\hbar^2} + \Delta\omega^2}\, t\right] \tag{3.7.26}$$

Since perturbation theory requires small changes in population, $P_k \ll 1$, eq. (3.7.25) is valid for perturbations that are small relative to the detuning $|V_{k\ell}| \ll |\hbar\Delta\omega|$. However, the exact solution also shows that we should expect the most efficient population transfer when $\Delta\omega = 0$. As with the constant perturbation, eq. (3.7.25) can be rewritten in sinc function form as

$$P_k = \frac{V_{k\ell}^2 t^2}{4\hbar^2} \operatorname{sinc}\left(\frac{1}{2}\Delta\omega t\right) \tag{3.7.27}$$

In Figure 3.7.6, we plot the population in state k as a function of $\Delta\omega$, showing that P_k is peaked at $\Delta\omega = 0$ and the amplitude grows as t^2. This clearly will not describe long-time behavior since it suggests unlimited growth, but it will hold for small P_k such that

$$t \ll \frac{2\hbar}{V_{k\ell}} \tag{3.7.28}$$

At the same time, we cannot observe the system on too short of a time scale. We need the field to make several oscillations for this to be considered a harmonic perturbation.

$$t > \frac{1}{\omega} \approx \frac{1}{\omega_{k\ell}} \tag{3.7.29}$$

Combining relationships (3.7.28) and (3.7.29) imply that perturbation theory is valid when the magnitude of the external potential's influence is much smaller than the energy splitting between states, or $V_{k\ell} \ll \hbar\omega_{k\ell}$.

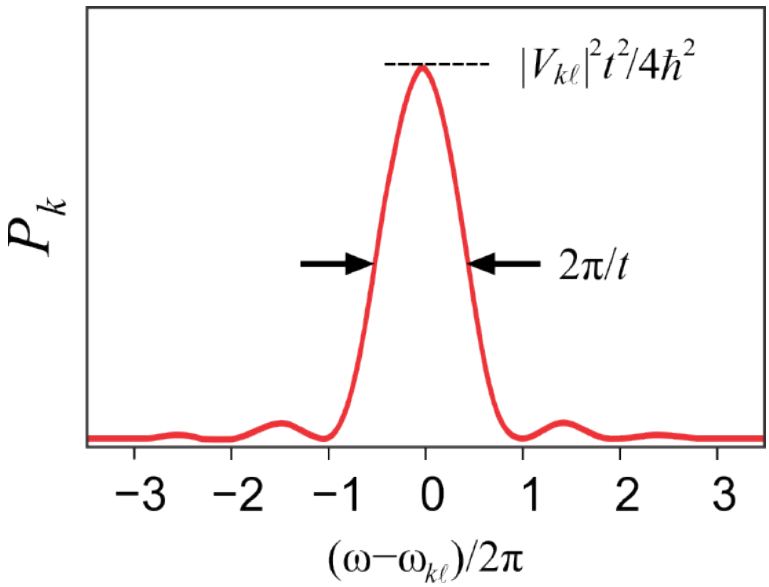


Figure 3.7.6: Time-dependent population of state $|k\rangle$ after applying the harmonic perturbation as a function of detuning from resonance.

Like our description of the constant perturbation, the long-time limit for P_k results in a delta function centered at $\Delta\omega = 0$ and a linear increase with time.

$$\lim_{t\to\infty} P_k = \frac{\pi}{2\hbar^2}|V_{k\ell}|^2\, t\, \delta(\omega_{k\ell} - \omega) \tag{3.7.30}$$

The Golden Rule rate for the rate of absorption from ℓ to k is then calculated by taking the time-derivative: $w_{k\ell} = \partial P_k/\partial t$:

$$w_{k\ell} = \frac{\pi}{2\hbar^2}|V_{k\ell}|^2\, \delta(\omega_{k\ell} - \omega)$$

In this limit, the one can neglect any possible interferences effects between the absorption and stimulated emission terms in eq. (3.7.22). A parallel derivation of rates of stimulated emission from a higher energy state ℓ to a lower energy state k results in the same expression as eq. (3.7.30), except with the delta function $\delta(\omega_{k\ell} + \omega)$. As a result, the total rate of transitions induced by a harmonic perturbation from an initial state ℓ to a final state k independent of which state is higher in energy is

$$w_{k\ell} = \frac{\pi}{2\hbar^2}\,|V_{k\ell}|^2\,[\delta(\omega_{k\ell} - \omega) + \delta(\omega_{k\ell} + \omega)] \tag{3.7.31}$$

This is the state-to-state form of the Golden Rule for a harmonic perturbation, an important result we will use in our description of light-matter interactions and spectroscopy. In practice, state-to-state expressions typically need to be summed over the set of all possible final states $\{|k\rangle\}$ accessible to direct transitions from $|\ell\rangle$. For ensembles, one also needs to sum over the distribution of initial states weighted by their initial population.

Time-domain derivation

Different routes can be taken to obtain the Golden rule, but often it is hard to retain the physical picture that links the characteristics of the time-dependent potential and the rates of population transfer. An alternate approach can be used to obtain a time-domain representation of the state-to-state expressions for the Golden Rule. In this case, we calculate the rate as the time-dependent change of the population in state $|k\rangle$ working directly from

$$w_{k\ell} = \frac{dP_{k\ell}}{dt}$$

Since the population of state k is $P_{k\ell} = |b_k|^2 = b_k^* b_k$, we can expand this equation in the time-derivatives of b_k as

$$w_{k\ell} = \frac{d}{dt}\left(b_k^* b_k\right) = \dot{b}_k^* b_k + b_k^* \dot{b}_k \tag{3.7.32}$$

The first-order expressions for $b_k(t)$ and $\dot{b}_k(t)$ are given by eqs. (3.6.6) and (3.6.7), respectively. Using the fact that our initial state is ℓ and $b_\ell(0) = 1$, we can write the first term in eq. (3.7.32) as

$$\begin{aligned} \dot{b}_k^* b_k &= \frac{\mathrm{i}}{\hbar} V_{k\ell}^\dagger(t) e^{-i\omega_{k\ell}t} \frac{-\mathrm{i}}{\hbar} \int_0^t dt'\, V_{k\ell}(t') e^{i\omega_{k\ell}t'} \\ &= \frac{1}{\hbar^2} \int_0^t dt'\, V_{k\ell}^\dagger(t) V_{k\ell}(t') e^{\mathrm{i}\omega_{k\ell}(t'-t)} \end{aligned} \tag{3.7.33}$$

Since we are investigating the long-time behavior upon application of the perturbation relevant to the Golden Rule, we can set the upper integration limit to $t \to \infty$. Next we substitute the time-interval variable $\tau = t' - t$ and make use of the stationary property of time-propagators

$$\begin{aligned} \dot{b}_k^* b_k &= \frac{1}{\hbar^2} \int_0^t d\tau\, V_{k\ell}^\dagger(t) V_{k\ell}(\tau + t) e^{\mathrm{i}\omega_{k\ell}\tau} \\ &= \frac{1}{\hbar^2} \int_0^t d\tau\, V_{k\ell}^\dagger(0) V_{k\ell}(\tau) e^{\mathrm{i}\omega_{k\ell}\tau} \end{aligned} \tag{3.7.34}$$

Repeating this for the second term in eq. (3.7.32) gives

$$b_k^* \dot{b}_k = \frac{1}{\hbar^2} \int_0^t d\tau\, V_{k\ell}^\dagger(\tau) V_{k\ell}(0) e^{-\mathrm{i}\omega_{k\ell}\tau} \tag{3.7.35}$$

We can observe that the differences between these two similar terms are the arguments of their exponentials and the sequence of the operators over which we integrate. One term is the complex conjugate of the other, as one would expect from $P_{k\ell}$ being real. One can obtain the result directly from taking the real part of either expression, but it is more useful to combine the two integrals. Taking the long-time limit ($t \to \infty$) of the combined integral, we find that the transition rate is

$$w_{k\ell} = \frac{1}{\hbar^2} \int_{-\infty}^{\infty} d\tau\, V_{k\ell}(\tau) V_{\ell k}(0) e^{\mathrm{i}\omega_{k\ell}\tau} \tag{3.7.36}$$

This is a time-domain representation of Fermi's Golden rule which takes the form of a Fourier transform over a correlation function for the time-dependent variation of the coupling matrix elements $V_{k\ell}(t)$. It equates the efficiency of making transitions between two states to the Fourier component at the energy gap between coupled states, $\omega_{k\ell}$. This is an important result that will return to often.

To connect this expression to our prior results, consider the case of a constant perturbation in which the matrix elements are time independent, and we obtain

$$w_{k\ell} = \frac{1}{\hbar^2}|V_{k\ell}|^2 \int_{-\infty}^{\infty} d\tau\, e^{-i\omega_{k\ell}\tau} \tag{3.7.37}$$

The integral in this equation is $2\pi\ \delta(\omega_{k\ell})$. This allows eq. (3.7.37) to be written as eq. (3.7.14). If we instead take the interaction potential to have a harmonic time-dependence, the same procedure results in eq. (3.7.31). The time-domain expression, eq. (3.7.36), will play an increasingly important role in describing how molecular dynamics influence rate processes and spectroscopy as we move forward.

References

(1) Baym, G. *Lectures on Quantum Mechanics*; W.A. Benjamin, 1969; p 257. DOI: 10.1201/9780429499265

This page titled 3.7: The Golden Rule is shared under a CC BY-NC-SA 4.0 license and was authored, remixed, and/or curated by Andrei Tokmakoff via source content that was edited to the style and standards of the LibreTexts platform.

3.8: Readings

Integrating the TDSE Directly

1. Tannor, D. J. *Introduction to Quantum Mechanics: A Time-Dependent Perspective*; University Science Books, 2007.

Transitions Induced by a Time-Dependent Potential

1. Cohen-Tannoudji, C.; Diu, B.; Laloë, F. *Quantum Mechanics*; Wiley, 1977; p 308.
2. Merzbacher, E. *Quantum Mechanics*, 3rd ed.; Wiley, 1998; ch 14.
3. Nitzan, A. *Chemical dynamics in condensed phases: Relaxation, transfer and reactions in condensed molecular systems*; Oxford University Press, 2006; sec 2.3. DOI: 10.1093/oso/9780198529798.001.0001
4. Sakurai, J. J. *Modern Quantum Mechanics*, rev. ed.; Addison-Wesley, 1994; ch 2.

The Interaction Picture

1. Mukamel, S. *Principles of Nonlinear Optical Spectroscopy*; Oxford University Press, 1995.
2. Nitzan, A. *Chemical dynamics in condensed phases: Relaxation, transfer and reactions in condensed molecular systems*; Oxford University Press, 2006; ch 4. DOI: 10.1093/oso/9780198529798.001.0001

Time-Dependent Perturbation Theory

1. Cohen-Tannoudji, C.; Diu, B.; Laloë, F. *Quantum Mechanics*; Wiley, 1977; p 1285.
2. Nitzan, A. *Chemical dynamics in condensed phases: Relaxation, transfer and reactions in condensed molecular systems*; Oxford University Press, 2006; ch 4. DOI: 10.1093/oso/9780198529798.001.0001
3. Sakurai, J. J. *Modern Quantum Mechanics*, rev. ed.; Addison-Wesley, 1994; ch 2.

The Golden Rule

1. Baym, G. *Lectures on Quantum Mechanics*; W. A. Benjamin, 1969; p 257. DOI: 10.1201/9780429499265
2. Cohen-Tannoudji, C.; Diu, B.; Laloë, F. *Quantum Mechanics*; Wiley, 1977; p 1299.
3. McHale, J. L. *Molecular Spectroscopy*, 1st ed.; Prentice-Hall, 1999; ch 4.
4. Sakurai, J. J. *Modern Quantum Mechanics*, rev. ed.; Addison-Wesley, 1994.

This page titled 3.8: Readings is shared under a CC BY-NC-SA 4.0 license and was authored, remixed, and/or curated by Andrei Tokmakoff.

4: WAVEPACKET DYNAMICS

4.1: Position and Momentum Representation
4.2: Free-Particle Eigenstates
4.3: Free-Particle Wavepacket
4.4: Readings

This page titled 4: Wavepacket Dynamics is shared under a CC BY-NC-SA 4.0 license and was authored, remixed, and/or curated by Andrei Tokmakoff via source content that was edited to the style and standards of the LibreTexts platform.

4.1: Position and Momentum Representation

In this chapter, our goal is to describe the dynamics of a quantum mechanical particle in space and time in the language of wavepackets. This topic is closely entwined with the concept of wave/particle duality since this approach requires us to simultaneously account for the particle as a deterministically moving object in space and represent the particle's wavefunction as a constructive superposition of waves with a time-evolving phase characteristics. As a starting point, however, it is a good opportunity to discuss important properties of continuous basis sets and the momentum representation of the wavefunction.

At the most fundamental level, the physical properties of the system in quantum mechanics are formulated in Hilbert space, an abstract linear vector space in which the state of the system can be represented as a complex linear combination of orthonormal basis functions. The choice of which basis set to use depends on the physical information content we wish to obtain or the strategy that is best for solving a particular problem. We have already reviewed several examples. The spatial distribution of probability density for bound particles can be represented by discrete functions such as the Hermite polynomials or spherical harmonics, or they can be continuous, as with free particles and electromagnetic waves. It is the latter case we will now discuss, and which the position and momentum representations refer to. However, as we go forward we will see there are several other representations used in quantum mechanics that ignore the spatial dependence of wavefunctions, such as the matrix representation for describing state populations, the energy representation for describing spectroscopic transitions, and second quantization for many body interactions.

When dealing with the dynamics of particles and fields, we typically work in the position representation, which specifies the evolving state of the system through a wavefunction expressed in terms of position using Cartesian, spherical, or other coordinate system. We obtain this by projecting the wavefunction onto the position basis $\{|x\rangle\}$, where $|x\rangle$ is an eigenstate of the position operator $\hat{x}$ with the eigenvalue x, that is $\hat{x}|x\rangle = x|x\rangle$. The eigenstates of $\hat{x}$ form a continuous orthonormal basis with a continuum of eigenvalues. Whereas we previously expressed the orthogonality and completeness of a discrete basis as $\langle x'|x''\rangle = \delta_{x',x''}$ and $\sum_x |x\rangle\langle x| = 1$, for the continuous basis we replace the Kronecker delta with a Dirac delta function and the sum with an integral

$$\langle x'|x''\rangle = \delta(x' - x'') \tag{4.1.1}$$

$$\int_{-\infty}^{\infty} dx\, |x\rangle\langle x| = 1 \tag{4.1.2}$$

Here x' and x'' refer to specific eigenvalues. Analogous to the expansion of the wavefunction in in a discrete basis $|\psi(x)\rangle = \sum_x c_x|x\rangle$, we use eq. (4.1.2) to express the position dependent wavefunction in terms of a continuous spectrum of expansion coefficients, $c(x)$

$$|\psi(x)\rangle = \int_{-\infty}^{\infty} |x\rangle\langle x|\Psi\rangle\, dx = \int_{-\infty}^{\infty} |x\rangle c(x)\, dx \tag{4.1.3}$$

The coefficient for a specific eigenfunction $c\,(x') = \langle x'|\Psi\rangle$ describes the wavefunction amplitude in the infinitesimal interval between x' and $x' + dx$.

Unlike classical mechanics, we cannot uniquely specify both $\hat{p}$ and $\hat{x}$ for a particle, since the eigenstates of $\hat{x}$ are not eigenstates of $\hat{p}$. It is therefore possible to define a new basis set that describes the wavefunction in the momentum representation $\varphi(p)$. A similar set of identities emerge for the momentum representation. $|p\rangle$ is an eigenvector of the momentum operator $\hat{p}$ with the eigenvalue p:

$$\hat{p}|p\rangle = p|p\rangle \tag{4.1.4}$$

$\{|p\rangle\}$ is also a complete orthonormal basis,

$$\langle p'|p''\rangle = \delta(p' - p'') \tag{4.1.5}$$

$$\int_{-\infty}^{\infty} dp\, |p\rangle\langle p| = 1 \tag{4.1.6}$$

where p' and p'' refer to specific eigenvalues. Analogous to eq. (4.1.3), eq. (4.1.6) allows us to describe the momentum space wavefunction through the momentum distribution

$$|\varphi(p)\rangle = \int_{-\infty}^{\infty} |p\rangle c(p)\, dp \tag{4.1.7}$$

To quantize variables in the coordinate representation, we replace the classical variables x and p with their corresponding operators in the coordinate representation:

$$\begin{aligned} x &\rightarrow \hat{x} \\ p &\rightarrow \hat{p} = -\mathrm{i}\hbar \frac{\partial}{\partial x} \end{aligned} \tag{4.1.8}$$

By operating on eq. (4.1.4) from the left with $\langle x|$ you can see why we quantize position and momentum in the momentum representation by replacing classical variables with

$$\begin{aligned} p &\rightarrow \hat{p} \\ x &\rightarrow \hat{x} = \mathrm{i}\hbar \frac{\partial}{\partial p} \end{aligned} \tag{4.1.9}$$

For instance, we calculate expectation values for that momentum and position of a particle in the momentum representation as

$$\begin{aligned} \langle p \rangle &= \int_{-\infty}^{+\infty} dp\, \varphi^*(p)\, p\, \varphi(p) \\ \langle x \rangle &= \mathrm{i}\hbar \int_{-\infty}^{+\infty} dp\, \varphi^*(p)\, \frac{\partial}{\partial p}\, \varphi(p) \end{aligned} \tag{4.1.10}$$

The unitary transformation between the position and momentum representation in one dimension can be expressed as

$$\langle x'|p'\rangle = \langle p'|x'\rangle^* = \frac{1}{\sqrt{2\pi\hbar}} \exp\left[\mathrm{i}p'x'\hbar\right] \tag{4.1.11}$$

With the completeness expressions, this relationship can be used to relate the wavefunction in the position representation to its momentum representation. Considering first the relationships between expansion coefficients, we can see with eq. (4.1.2) that

$$\begin{aligned} c\left(p'\right) = \langle p'|\psi\rangle &= \frac{1}{\sqrt{2\pi\hbar}} \int_{-\infty}^{+\infty} dx'\, \langle p'|x'\rangle\, \langle x'|\psi\rangle \\ &= \frac{1}{\sqrt{2\pi\hbar}} \int_{-\infty}^{+\infty} dx' e^{-\mathrm{i}p'/\hbar} c(x') \end{aligned} \tag{4.1.12}$$

This can then be inserted in eq. (4.1.7) to describe the full momentum space wavefunction. The result and the result obtained with a similar procedure for the position space function are

$$|\varphi(p)\rangle = \frac{1}{\sqrt{2\pi\hbar}} \int_{-\infty}^{+\infty} dx\, e^{-\mathrm{i}px/\hbar} |\psi(x)\rangle \tag{4.1.13}$$

$$|\psi(x)\rangle = \frac{1}{\sqrt{2\pi\hbar}} \int_{-\infty}^{+\infty} dp\, e^{\mathrm{i}px/\hbar} |\varphi(p)\rangle \tag{4.1.14}$$

Comparing eq. (4.1.13) and eq. (4.1.14) shows us first that x and p are conjugate variables and the two representations are linked by a Fourier transform. The Fourier transform relationship necessitates that real particles have finite dimensions in x space and k space. Since $\psi(x)$ must vanishes as $x \rightarrow \pm\infty$ to be a well behaved wavefunction, $\varphi(p)$ must vanish in the momentum representation as $p \rightarrow \pm\infty$.

The Fourier transform relationship between $\psi(x)$ and $\varphi(p)$ is another manifestation of the uncertainty relationship between x and p. In order to more accurately determine the position of a quantum particle, i.e. localizing the wavefunction in position space, the more information you lose about the momentum of the particle, i.e. broadening the distribution in momentum space. Perhaps the clearest example is the free-particle wavefunction which spans all space $\psi(x) = \exp\left(\mathrm{i}p'x/\hbar\right)$ but has perfectly defined value of the momentum $\varphi_{p'}(p) = (2\pi\hbar)^{1/2}\ \delta(p - p')$. We will address this more in a moment.

In Figure 4.1.1 we compare eigenstates of the particle-in-the-box Hamiltonian in the two representations. The position space wavefunctions $\psi_n(x)$ exhibit $n-1$ nodes and n integer halfwavelengths within the box, which results in a uniformly distributed particle density in the classical limit $(n \rightarrow \infty)$. The corresponding momentum space wavefunction is peaked at $p = \pm n\pi\hbar/L$, with the distribution of allowed momenta narrowing to a precise value as $n \rightarrow \infty$.

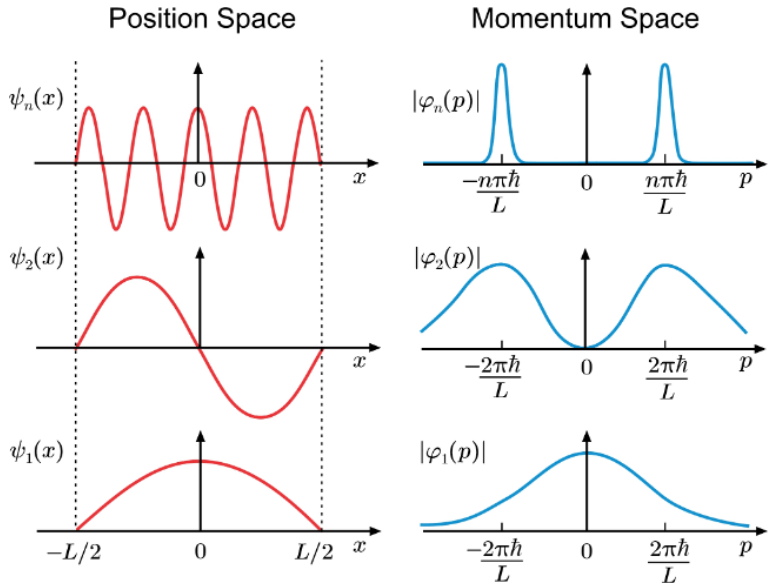


Figure 4.1.1 Illustration of position and momentum space representation of particle-in-a-box wavefunctions ψ_0, ψ_1, and ψ_n for a box of width L centered at $x = 0$. In position space ψ_n has n equally spaced nodes arising from $(n + 1)/2$ sinusoidal cycles within the box.

This example also illustrates how the momentum representation is particularly useful for periodic boundary condition problems. Free particles, electromagnetic waves, and phonons are examples of wavefunctions that are spatially extended in the coordinate representation, or x space, with a well-defined spatial periodicity with a wavelength λ. This leads to a sharp localization of the wavefunction in the momentum representation, which we express in terms of the wavevector

$$k = \frac{p}{\hbar} \quad \text{and} \quad |k| = \frac{2\pi}{\lambda} \tag{4.1.15}$$

In this case we refer to the momentum representation as k space.

Summary of k-space Identities

The orthogonality and completeness expressions are

$$\langle k'|k''\rangle = \delta(k' - k'') \tag{4.1.16}$$

$$\int_{-\infty}^{\infty} dk\, |k\rangle\langle k| = 1 \tag{4.1.17}$$

The transformations between x space and k space in one dimension are

$$\begin{aligned} \psi(x) &= \frac{1}{\sqrt{2\pi}} \int_{-\infty}^{+\infty} \varphi(k) e^{\mathrm{i}kx}\, dk \\ \varphi(k) &= \frac{1}{\sqrt{2\pi}} \int_{-\infty}^{+\infty} \psi(x) e^{-\mathrm{i}kx}\, dx \end{aligned} \tag{4.1.18}$$

and in three dimensions

$$\begin{aligned} \psi(\mathbf{r}) &= \frac{1}{(2\pi)^{3/2}} \int_{-\infty}^{+\infty} \varphi(\mathbf{k}) e^{\mathrm{i}\mathbf{k}\cdot\mathbf{r}}\, d^3k \\ \varphi(\mathbf{k}) &= \frac{1}{(2\pi)^{3/2}} \int_{-\infty}^{+\infty} \psi(\mathbf{r}) e^{\mathrm{i}\mathbf{k}\cdot\mathbf{r}}\, d^3r \end{aligned} \tag{4.1.19}$$

The k-space and momentum space wavefunctions are related by $\varphi(k) = \hbar^{n/2}\varphi(p)$ where n is the dimensionality of the space.

This page titled 4.1: Position and Momentum Representation is shared under a CC BY-NC-SA 4.0 license and was authored, remixed, and/or curated by Andrei Tokmakoff via source content that was edited to the style and standards of the LibreTexts platform.

4.2: Free-Particle Eigenstates

For a free particle in the absence of a potential the Hamiltonian only reflects the kinetic energy of the particle: $\hat{H} = \hat{p}^2/2m = \hbar^2 k^2/2m$. In momentum space we observe that $\hat{H}$ and $\hat{p}$ commute with each other, so each eigenvector of $\hat{p}$ is also an eigenvector of $\hat{H}$, and the eigenvalues of $\hat{p}(\pm\hbar k)$ and $\hat{H}$ are continuous and real. Solving the time-independent Schrödinger equation results in plane wave eigenstates of the form

$$\psi_k(x) = \frac{1}{\sqrt{2\pi}} \exp(\mathrm{i}kx) \equiv |k\rangle \tag{4.2.1}$$

where k is an eigenvalue and the corresponding eigenenergies are

$$E_k = \frac{\hbar^2 k^2}{2m} \tag{4.2.2}$$

We see from this expression that the wavenumber k can take on positive and negative values. Then, the Fourier transform relation in eq. (4.1.18), indicates that the k space eigenstates are

$$\varphi_{k'}(k) = \delta(k - k') \, |k'\rangle \tag{4.2.3}$$

Evaluating the time-evolution operator $\hat{U} = e^{-\mathrm{i}\hat{H}t/\hbar}$ for the free particle wavefunction is straightforward given this is a time-independent Hamiltonian. Using the completeness expression in eq. (4.1.17) , the time-propagator for the free particle in k space is

$$\begin{aligned} \hat{U}(k,t) &= e^{-\mathrm{i}\hat{H}t/\hbar} \int_{-\infty}^{+\infty} |k\rangle\langle k| \, dk \\ &= \int_{-\infty}^{+\infty} |k\rangle \exp\left[-\mathrm{i}E_k t/\hbar\right] \langle k| \, dk \end{aligned} \tag{4.2.4}$$

Applying this time propagator to the eigenstates in eq. (4.2.1) results in the familiar traveling plane wave expression:

$$\psi_k(x,t) = \exp\left[\mathrm{i}(kx - \omega_k t)\right] \tag{4.2.5}$$

where the frequency and wavenumber are related as

$$\omega_k = \frac{E_k}{\hbar} = \frac{\hbar k^2}{2m} \tag{4.2.6}$$

k can take on positive or negative values which correspond to motion to the right (increasing x) or left (decreasing x), respectively. The wave crests move with a phase velocity $v_p = \omega_k/k = p/2m$. Note that this is half of the classical velocity of a particle p/m. Equation (4.2.6) is a dispersion relationship, an expression that describes the dependence of the wave frequency on the wavenumber, $\omega(k)$, which governs the details of wave propagation in a given medium.

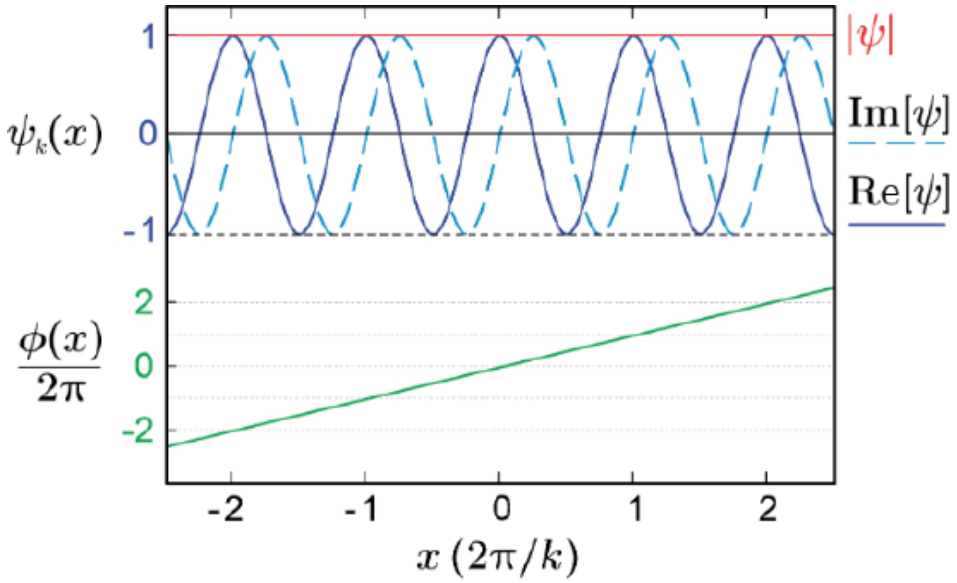


Figure 4.2.1. Properties of ψ_k, the complex plane wave free particle eigenfunctions for wavenumber k, at a fixed time point showing the real and imaginary components, the wave amplitude $|\psi(x)|$, and the phase $\phi(x) = kx$.

Complicating the description of free particles is that the eigenfunctions in eq. (4.2.1) are ill behaved. They extend over all space with a constant probability density $|\psi(x)|^2 = |A|^2$, and therefore cannot be normalized, i.e., $\int |\psi(x)|^2 \ dx = \infty$. Since the wavefunction is extended over all space, it also has a precisely defined momentum. These characteristics are generally unreasonable; we should be able to describe free particles that move in space and time with defined momentum and time-varying position, even if the Heisenberg uncertainty relationship put constraints on how accurately we can determine both x and p. From the Fourier transform relationship, we understand that a more accurate description of the position of a particle comes at the expense of a growing probability density of momenta.

These observations don't mean that plane wave eigenstates aren't useful for our problem—they are a very good basis set to describe free particles. To create a localized wavefunction that will yield useful expectation values for x and p, we can use a superposition of plane waves. As seen in Figure 4.2.2, adding several waves with similar frequencies will produce a superposition that localizes the wave through constructive interference at the position where the wave crests are in phase-a wavepacket.

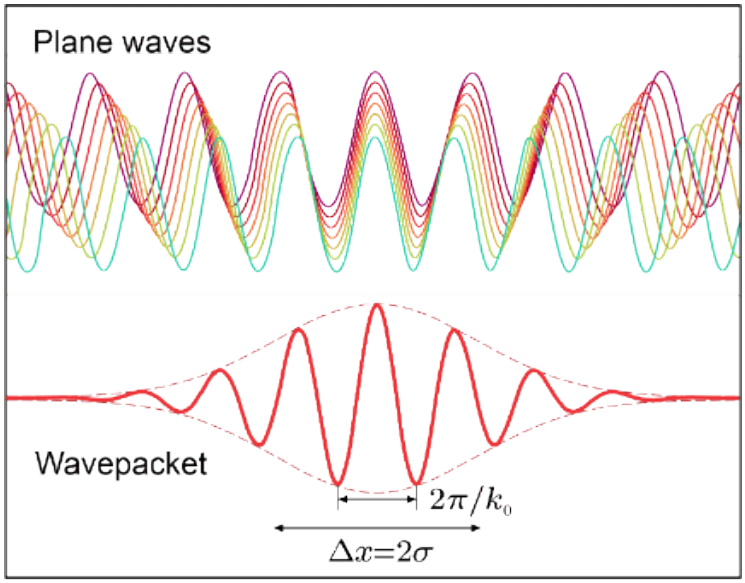


Figure 4.2.2. Illustration of how a localized free-particle wavepacket is obtained from a superposition of plane waves, defining the key variables for a Gaussian wavepacket.

The momentum representation is particularly useful for constructing and propagating wavepackets, since a wavepacket with well-defined position and momentum requires a continuous distribution of plane waves. Making use of eq. (4.1.7), we can express the

superposition of plane waves as an integral over the distribution of coefficients in k-space, $c(k)$.

$$|\varphi(k)\rangle = \int_{-\infty}^{+\infty} c\left(k'\right)|k'\rangle\, dk' = c(k) \tag{4.2.7}$$

From eq. (4.2.3), we see that the k-space wavefunction amplitude directly reflects the distribution function. The corresponding x -space wavefunction is obtained by Fourier transform

$$|\psi(x)\rangle = \frac{1}{\sqrt{2\pi}} \int_{-\infty}^{+\infty} c(k) e^{ikx}|k\rangle\, dk \tag{4.2.8}$$

From this we can see that in the free-particle basis the x space wavefunction is just the Fourier transform of the distribution of expansion coefficients in k space $c(k)$.

This page titled 4.2: Free-Particle Eigenstates is shared under a CC BY-NC-SA 4.0 license and was authored, remixed, and/or curated by Andrei Tokmakoff via source content that was edited to the style and standards of the LibreTexts platform.

4.3: Free-Particle Wavepacket

In this section, we describe the dynamics of a free particle wavepacket that is localized in space and moves with time. To start we need to construct a wavepacket that describes the initial state of the system $\varphi_0(k)$. A square-integrable free-particle wavefunction can be described by any k space distribution of $c(k)$ that vanish at $\pm\infty$, and here we will concentrate on Gaussian distribution of free particle eigenfunctions of the form

$$c(k) = B\exp\left[-\sigma^2(k-k_0)^2/2\right] \tag{4.3.1}$$

This distribution's most probable wavenumber is k_0, and the dimensions or width of the wavepacket in k- and x-space is governed by σ. Such a distribution is pictured in Figure 4.3.1. From eq. (4.2.8), a properly normalized distribution requires that $(2\pi)^{-1}\int|c(k)|^2\,dk = 1$, meaning in eq. (4.3.1) the normalization constant $B = \sqrt{\sigma\sqrt{\pi}}$. Using eq. (4.2.8) we determine the initial wavepacket in position space as

$$|\psi_0(x)\rangle = (\sqrt{\pi}\sigma)^{-1/2}e^{\mathrm{i}k_0x}e^{-x^2/2\sigma^2} \tag{4.3.2}$$

from which we see that the x-space wavepacket is also initially a Gaussian with a breadth given by the standard deviation σ and modulated by a spatially varying phase factor that varies with k_0.

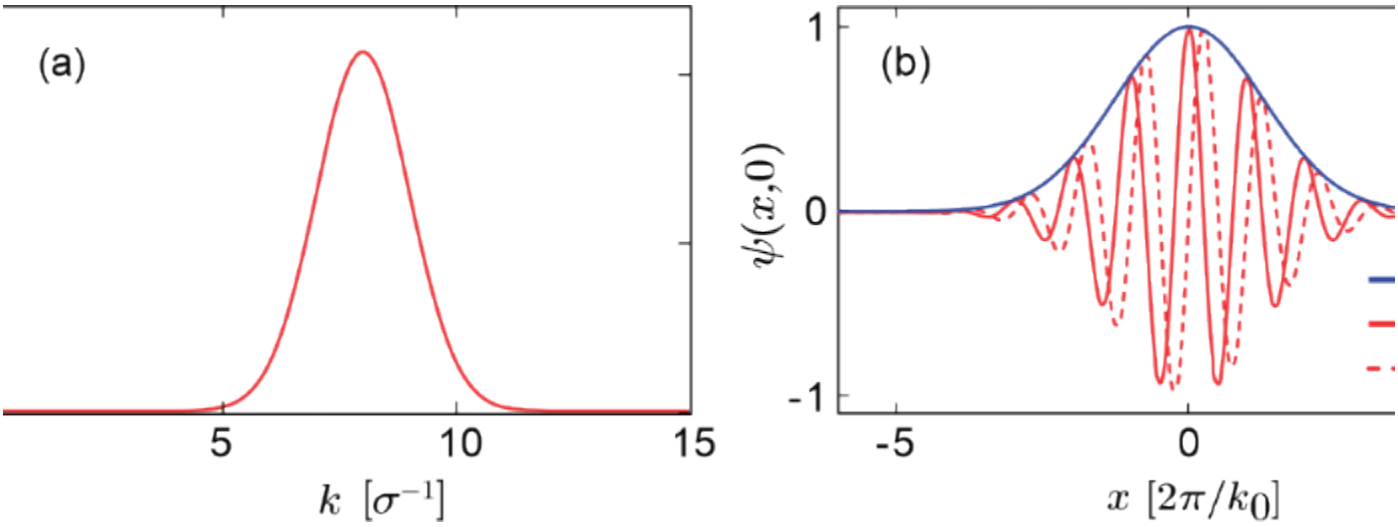


Figure 4.3.1. Initial wavepacket (a) Gaussian k-space distribution $\varphi_0(k)$ with $k_0\sigma = 8$. (b) Initial complex wavepacket in x-space, $\psi_0(x)$

The time-dependent wavefunction is easiest to evaluate in k-space using the time propagator in eq. (4.2.4), i.e. $|\varphi(t)\rangle = \hat{U}\,|\varphi_0\rangle$, and therefore the real space wavepacket is

$$\begin{aligned}|\psi(x,t)\rangle &= \frac{1}{\sqrt{2\pi}}\int_{-\infty}^{+\infty}dk\,\hat{U}(k,t)\,|\varphi_0(k)\rangle\,e^{\mathrm{i}kx}\\ &= \frac{1}{\sqrt{2\pi}}\int_{-\infty}^{+\infty}dk\,c(k)\exp\left[\mathrm{i}(kx-\omega_k t)\right]\end{aligned} \tag{4.3.3}$$

where the wavenumber dependent angular frequency ω_k is given by eq. (4.2.6). We can evaluate this integral analytically, but let's first proceed with an approximation that works for relatively narrow distributions in k, and expand ω_k about k_0

$$\begin{aligned}\omega_k &= \omega_0 + \left.\frac{\partial\omega_k}{\partial k}\right|_{k_0}(k-k_0) + \cdots\\ &= \omega_0 + v_g(k-k_0) + \cdots\end{aligned} \tag{4.3.4}$$

The leading term $\omega_0 = \hbar k_0^2/2m$ is the angular frequency corresponding to the peak of the k space distribution, and the expansion coefficient $v_g = \hbar k_0/m$ is known as the *group velocity*. Then from eq. (4.3.3) we obtain

$$|\psi(x,t)\rangle = (\sqrt{\pi}\sigma)^{-1/2} e^{\mathrm{i}(k_0 x - \omega_0 t)} \exp\left[-(x - v_g t)^2 / 2\sigma^2\right] \tag{4.3.5}$$

and the probability density is

$$|\psi(x,t)|^2 = (\sqrt{\pi}\sigma)^{-1} \exp\left[-(x - v_g t)^2 / \sigma^2\right] \tag{4.3.6}$$

The time evolution of the wavepacket described in Figure 4.3.1 is plotted in Figure 4.3.3. The peak of the Gaussian probability density moves in x like a classical particle with a constant group velocity v_g and width σ. However, the phase of the wavepacket, $\phi = (k_0 x - \omega_0 t)$, which governs the points of constant phase, such as wave crests in the packet, increases at half that rate, the phase velocity $v_p = \omega/k$, as illustrated in Figure 4.3.4.

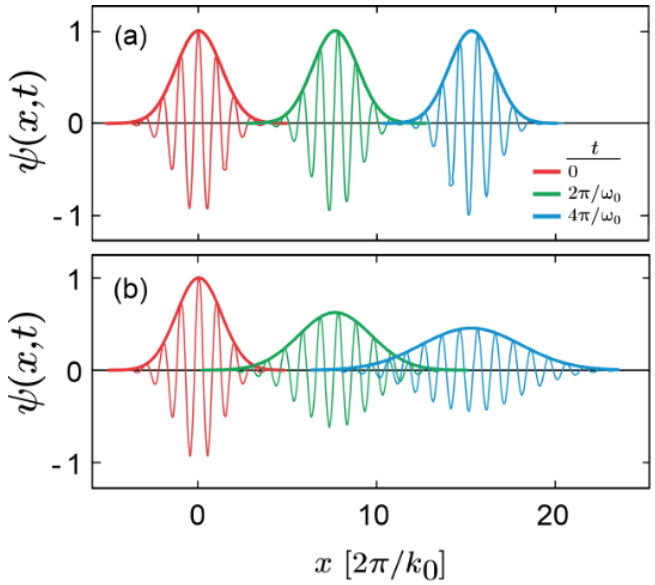


Figure 4.3.2. Time-evolution of wavepacket in x-space, showing $\mathrm{Re}[\psi(x,t)]$ and envelope $|\psi(x,t)|$ shown at time points $t = n2\pi/\omega_0$ with $n = 0, 1, 2$. Wavepacket initial conditions are those shown in Figure 4.3.1 with $k_0\sigma = 8$. (a) No dispersion case (b) With dispersion $(\beta = \pi v_g/k_0)$

Video

This interactive element is not available in this format. Visit the link or scan the QR code to access it online.

View this Video online

Figure 4.3.3. Animation of free particle wavepacket. Copyright © 2025 Andrei Tokmakoff

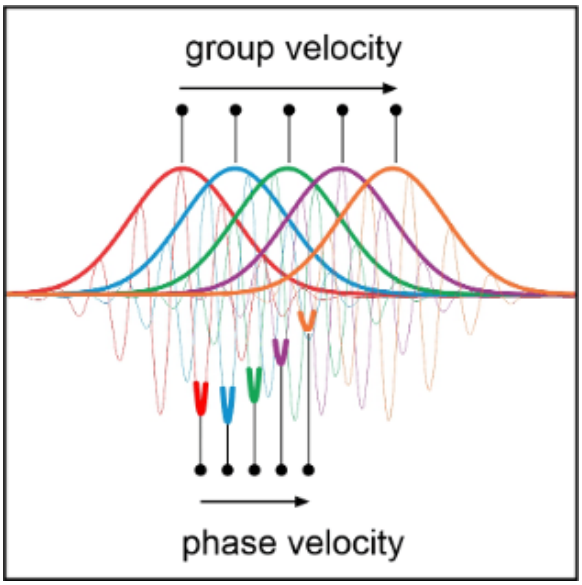


Figure 4.3.4. Wavepackets at equally spaced time points illustrating the group velocity v_g which tracks the peak $\langle x(t)\rangle$ of the wavepacket, and the phase velocity v_p, which tracks the points of constant phase.

More generally, since the group velocity also varies with k, one needs to account for group velocity dispersion, β. Then one can add the third term to expansion of ω_k in eq. (4.3.4), $\beta = \left(\partial^2\omega/\partial k^2\right)\big|_{k_0} = \hbar^2/m$, and the new expressions for the time-evolution of the wavepacket take the form of eq. (4.3.6) but with the substitution $\sigma \to \sqrt{\sigma^2 + \mathrm{i}\hbar t/m}$. The full expressions are as follows

$$|\psi(x,t)\rangle = \sqrt{\frac{\sigma}{\sqrt{\pi}\left(\sigma^2 + \mathrm{i}\hbar t/m\right)}}\, e^{\mathrm{i}(k_0 x - \omega_0 t)} \exp\left[\frac{-\left(x - v_g t\right)^2}{2\left(\sigma^2 + \mathrm{i}\hbar t/m\right)}\right] \tag{4.3.7}$$

$$|\psi(x,t)|^2 = \sqrt{\frac{\sigma}{\sqrt{\pi}\left(\sigma^4 + \hbar^2 t^2/m^2\right)}} \exp\left[\frac{-\sigma^2\left(x - v_g t\right)^2}{2\left(\sigma^4 + \hbar^2 t^2/m^2\right)}\right] \tag{4.3.8}$$

As seen in Figure 4.3.2b, with dispersion the peak of the wavepacket $\langle x\rangle$ still moves at the classical group velocity and the width increases in time. As seen from eq. (4.3.8), the width of the probability density $\sigma\sqrt{1 + \hbar^2 t^2 \sigma^{-4} m^{-2}}$ grows linearly at a rate proportional to the k-space distribution width, σ^{-1}, at long times.

This page titled 4.3: Free-Particle Wavepacket is shared under a CC BY-NC-SA 4.0 license and was authored, remixed, and/or curated by Andrei Tokmakoff via source content that was edited to the style and standards of the LibreTexts platform.

4.4: Readings

Position and Momentum Representation

1. Baym, G. *Lectures on Quantum Mechanics*; W.A. Benjamin, 1969. DOI: 10.1201/9780429499265
2. Gasiorowicz, S. *Quantum Physics*, 3rd ed.; Wiley, 2003.
3. Sakurai, J. J. *Modern Quantum Mechanics*, rev. ed.; Addison-Wesley, 1994.
4. Tannor, D. J. *Introduction to Quantum Mechanics: A Time-Dependent Perspective*; University Science Books, 2007; ch 3.

Free-Particle Wavepacket

1. Ashby, N.; Miller, S. C. *Principles of Modern Physics*; Holden-Day, 1970; ch 6.
2. Bittner, E. R. *Quantum dynamics: applications in biological and materials systems*; CRC Press, 2010; p 136. DOI: 10.1201/b15835
3. Griffiths, D. J. *Introduction to Quantum Mechanics*, 2nd ed.; Pearson Prentice Hall, 2005; ch 2.

This page titled 4.4: Readings is shared under a CC BY-NC-SA 4.0 license and was authored, remixed, and/or curated by Andrei Tokmakoff.

5: ADIABATIC APPROXIMATION

5.1: Adiabatic Processes

5.2: Born–Oppenheimer Approximation

5.3: Nonadiabatic Coupling

5.4: Diabatic and Adiabatic States

5.5: Landau–Zener Transition Probability

5.6: Adiabaticity criterion

5.7: Readings

This page titled 5: Adiabatic Approximation is shared under a CC BY-NC-SA 4.0 license and was authored, remixed, and/or curated by Andrei Tokmakoff via source content that was edited to the style and standards of the LibreTexts platform.

5.1: Adiabatic Processes

An adiabatic process is one that occurs so slowly that a system's internal degrees of freedom can fully and continuously adapt to externally driven changes. In quantum mechanics, the adiabatic approximation refers to those solutions to the Schrödinger equation that use a time-scale separation between fast and slow degrees of freedom to assert that slowly moving particles are effectively static on the timescale of motion by fast particles. Therefore, slow particles evolve under the influence of fully equilibrated fast particles. The adiabatic approximation allows one to find approximate wavefunctions that are product states in the fast and slow degrees of freedom.

Perhaps the most fundamental and commonly used version is the Born-Oppenheimer Approximation (BOA), which underlies much of how we conceive of molecular electronic structure and is the basis of potential energy surfaces. The BOA assumes that the motion of electrons is much faster than nuclei due to their large difference in mass, and therefore electrons adapt very rapidly to any changes in nuclear geometry. That is, the electrons "adiabatically follow" the nuclei. As a result, we can solve for the electronic state of a molecule for fixed nuclear configurations. Gradually stepping nuclear configurations and solving for the energy leads to an adiabatic potential energy surface. Much of our descriptions of chemical reaction dynamics is presented in terms of propagation on these potential energy surfaces. The barriers on these surfaces are how we describe the rates of chemical reactions and transition state. The trajectories along these surfaces are used to describe mechanism.

More generally, the adiabatic approximation is applied in other contexts in which there is a time-scale separation between fast and slow degrees of freedom. For instance, in the study of vibrational dynamics when the bond vibrations of molecules occur much faster than the intermolecular motions of a liquid or solid. This assumption is inherent in classical molecular dynamics force fields with fixed bond lengths. It is also generally implicit in a separation of the Hamiltonian into a system and a bath, a method we will often use to solve condensed matter problems. As widely used as the adiabatic approximation is, there are times when it breaks down, and it is important to understand when this approximation is valid, and the consequences of when it is not. This will be particularly important for describing time-dependent quantum mechanical processes involving transitions between potential energy sources.

In the context of quantum mechanics, adiabatic dynamics refers to time-dependent changes to the Hamiltonian from an initial state $H_i(t_0)$ to a final form $H_f(t_f)$ that occur slowly enough that a particle initially in the n^{th} eigenstate remains in that eigenstate throughout the process. We have already encountered this. For instance, we saw in the Example in Section 3.6 that when we squeeze and release the potential of a harmonic oscillator on a time scale that is much longer that the inverse of its frequency ($\sigma\Omega \gg 1$), that a system prepared on the ground state does not transfer any population to other eigenstates. The wavefunction adapts to the stiffening potential and then returns to its original state as the compression is released. Here the adiabatic time-scale separation is between the slow application of the external potential and the fast oscillation period of the oscillator.

An adiabatic process is therefore fully reversible. That is, after propagating the system forward under our time-dependent Hamiltonian from initial state $\psi_i(t_i = 0)$ to the final state $\psi_f(t_f)$, we can reverse the dynamics by switching the sign of the Hamiltonian's time-arguments, and propagate forward in time, but return to the initial state unchanged: $\psi_i(2t_f)$. More formally, the adiabatic approximation means that the Hamiltonian commutes with itself for all times.

In practice, this means that we can compute adiabatic dynamics with a time-dependent Hamiltonian by taking small time steps and solve the time-independent Schrödinger equation at each step to obtain slowly evolving eigenstates and energy eigenvalues.

$$H(t)\psi_n(t) = E_n(t)\psi_n(t) \tag{5.1.1}$$

As we discussed in Section 2.5, the time-propagator in the adiabatic picture is expressed in the time-evolving energy eigenvalues

$$\hat{U}(t, t_0) = \sum_n |n\rangle\langle n| \exp\left[-\frac{\mathrm{i}}{\hbar}\int_{t_0}^{t} E_n(t')\,dt'\right] \tag{5.1.2}$$

The eigenstate amplitudes of a superposition do not change, but only acquire a time-dependent phase

$$|\Psi(t, t_0)\rangle = \sum_n c_n \exp\left[-\frac{\mathrm{i}}{\hbar}\int_{t_0}^{t} E_n(t')\,dt'\right] |n\rangle \tag{5.1.3}$$

Adiabatic dynamics such as this are widely used, for instance in semiclassical methods, empirical valence bond dynamics, and ab initio molecular dynamics.

This page titled 5.1: Adiabatic Processes is shared under a CC BY-NC-SA 4.0 license and was authored, remixed, and/or curated by Andrei Tokmakoff via source content that was edited to the style and standards of the LibreTexts platform.

5.2: Born–Oppenheimer Approximation

Now we would like to add the position variables into our discussion. Before continuing further, it is helpful to review the Born-Oppenheimer Approximation (BOA). Although the BOA does not explicitly involve time as a variable, it incorporates the adiabatic approximation implicitly by neglecting the kinetic energy of the nuclei. For a molecular system, the Hamiltonian can be written in terms of the kinetic energy T of the nuclei (N) and electrons (e) and the potential energy V for the Coulomb interactions of these particles

$$\begin{aligned}\hat{H} &= \hat{T}_e + \hat{T}_N + \hat{V}_{ee} + \hat{V}_{NN} + \hat{V}_{eN} \\ &= -\sum_{i=1}^{n} \frac{\hbar^2}{2m_e}\nabla_i^2 - \sum_{J=1}^{N} \frac{\hbar^2}{2M_J}\nabla_J^2 \\ &\quad + \frac{1}{4\pi\varepsilon_0}\sum_{\substack{i,j=1 \\ j>i}}^{n} \frac{e^2}{|\mathbf{r}_i - \mathbf{r}_j|} + \frac{1}{4\pi\varepsilon_0}\sum_{\substack{IJJ=1 \\ J>I}}^{N} \frac{Z_I Z_J e^2}{|\mathbf{R}_I - \mathbf{R}_J|} - \frac{1}{4\pi\varepsilon_0}\sum_{i=1}^{n}\sum_{J=1}^{N} \frac{Z_J e^2}{|\mathbf{r}_i - \mathbf{R}_J|}\end{aligned} \tag{5.2.1}$$

Here and in the following, we will use lowercase variables to refer to electrons and uppercase to nuclei. The variables $n, i, \mathbf{r}, \nabla_r^2$, and m_e refer to the number, index, position, Laplacian, and mass of electrons, respectively, and $N, J, \mathbf{R}$, and M refer to the nuclei. e is the electron charge, and Z is the atomic number of the nucleus. Note, this Hamiltonian does not include relativistic effects such as spin-orbit coupling.

The time-independent Schrödinger equation is

$$\hat{H}(\hat{\mathbf{r}}, \hat{\mathbf{R}})\Psi(\hat{\mathbf{r}}, \hat{\mathbf{R}}) = E\Psi(\hat{\mathbf{r}}, \hat{\mathbf{R}}) \tag{5.2.2}$$

$\Psi(\hat{\mathbf{r}}, \hat{\mathbf{R}})$ is the total vibronic wavefunction, where "vibronic" refers to the combined electronic and nuclear eigenstates. Exact solutions using the molecular Hamiltonian are intractable for most problems of interest, so we turn to simplifying approximations. The BOA is motivated by noting that the nuclei are far more massive than an electron ($m_\mathrm{e} \ll M_\mathrm{I}$). With this criterion, and when the distances separating particles is not unusually small, the kinetic energy of the nuclei is small relative to the other terms in the Hamiltonian. Physically, this means the electrons move and adapt rapidly-adiabatically-in response to shifting nuclear positions. This offers an avenue to solving for Ψ by fixing the position of the nuclei, solving for the electronic wavefunctions ψ_i, and then iterating for varying $\mathbf{R}$ to obtain effective electronic potentials on which the nuclei move.

Since it is fixed for the electronic calculation, we proceed by treating $\mathbf{R}$ as a parameter rather than an operator, setting the nuclear kinetic energy to zero, and solve the electronic TISE:

$$\hat{H}_\mathrm{el}(\hat{\mathbf{r}}, \mathbf{R})\psi_i(\hat{\mathbf{r}}, \mathbf{R}) = U_i(\mathbf{R})\psi_i(\hat{\mathbf{r}}, \mathbf{R}) \tag{5.2.3}$$

where U_i is the electronic energy eigenvalue for the fixed nuclei. The electronic Hamiltonian in the BOA is

$$\hat{H}_\mathrm{el} = \hat{T}_e + \hat{V}_{ee} + \hat{V}_{eN} \tag{5.2.4}$$

In eq. (5.2.3), ψ_i is the electronic wavefunction for fixed $\mathbf{R}$, with $i = 0$ referring to the electronic ground state. Repeating this calculation for varying $\mathbf{R}$, we obtain $U_i(\mathbf{R})$, an effective or mean-field potential for the electronic states on which the nuclei can move. These are the adiabatic (or BornOppenheimer) potential energy surfaces illustrated in Figure 5.2.1.

For the nuclear degrees of freedom, we can define a Hamiltonian for the i^{th} electronic potential energy surface (PES):

$$\hat{H}_{\mathrm{Nuc},i} = \hat{T}_N + U_i(\hat{R}) \tag{5.2.5}$$

which satisfies a TISE for the nuclear wave functions $\Phi(R)$:

$$\hat{H}_{\mathrm{nuc},i}\Phi_{iJ}(R) = E_{iJ}\Phi_{iJ}(R) \tag{5.2.6}$$

Here J refers to the J^{th} eigenstate for nuclei evolving on the i^{th} PES. Equation (5.2.5) is referred to as the Born-Oppenheimer (BO) Hamiltonian.

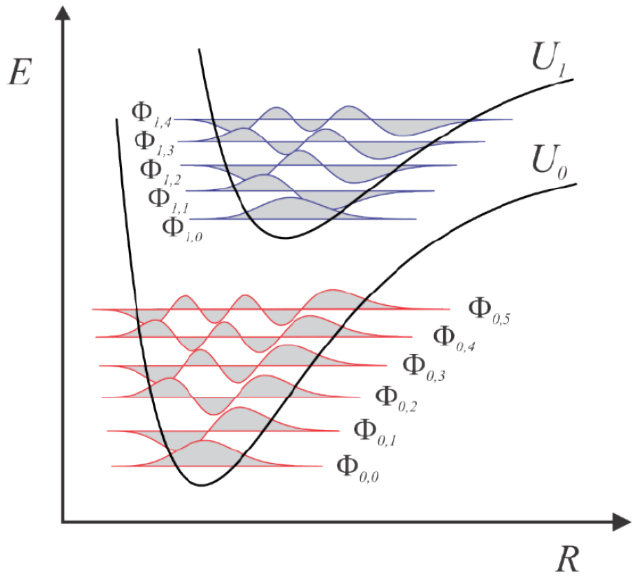


Figure 5.2.1. Illustration of Born-Oppenheimer potential energy surfaces, U_0 and U_1, for a diatomic molecule as a function of the interatomic distance R, and the nuclear eigenstates Φ plotted at their respective energy eigenvalues on those surfaces.

The BOA effectively separates the nuclear and electronic contributions to the wavefunction, allowing us to express the total wavefunction as a product of these contributions $\Psi(\mathbf{r},\mathbf{R}) = \Phi(\mathbf{R})\psi(\mathbf{r},\mathbf{R})$ and the eigenvalues as sums over the electronic and nuclear contribution: $E = E_N + E_e$. The BOA does not treat the nuclei classically. However, it is the basis for semiclassical dynamics methods in which the nuclei evolve classically on a potential energy surface and interact with quantum electronic states. If we treat the nuclear dynamics classically, then the electronic Hamiltonian can be thought of as depending on the classical nuclear positions $\mathbf{R}$ and time based on the nuclear velocities or momenta.

This page titled 5.2: Born–Oppenheimer Approximation is shared under a CC BY-NC-SA 4.0 license and was authored, remixed, and/or curated by Andrei Tokmakoff via source content that was edited to the style and standards of the LibreTexts platform.

5.3: Nonadiabatic Coupling

Even without the BO approximation, we note that the nuclear-electronic product states form a complete basis in which to express the total vibronic wavefunction:

$$\Psi(\mathbf{r},\mathbf{R}) = \sum_{i,J} c_{i,J}\Phi_{i,J}(\mathbf{R})\psi_i(\mathbf{r},\mathbf{R}) \tag{5.3.1}$$

We can therefore use this form to investigate the consequences of the BOA. For a given vibronic state, the action of the Hamiltonian on the wavefunction in the TISE is

$$\hat{H}\Psi_{i,J} = \left(\hat{T}_N(\mathbf{R}) + \hat{H}_{\text{el}}(\mathbf{R})\right)\Phi_{i,J}(\mathbf{R})\psi_i(\mathbf{R}) \tag{5.3.2}$$

Expanding the Laplacian in the nuclear kinetic energy (T_N) via the chain rule using $\nabla^2 AB = (\nabla^2 A)B + 2(\nabla A)\nabla B + A\nabla^2 B$, we obtain an expression with three terms

$$\begin{aligned}\hat{H}\Psi_{i,J} = \Phi_{i,J}(\mathbf{R})\left(\hat{T}_N(\mathbf{R}) + U_i(\mathbf{R})\right)\psi_i(\mathbf{R}) \\ - \sum_I^{\text{nuclei}} \frac{\hbar^2}{M_I}\nabla_I\Phi_{i,J}(\mathbf{R})\nabla_I\psi_i(\mathbf{R}) \\ - \sum_I^{\text{nuclei}} \frac{\hbar^2}{2M_I}\Phi_{i,J}(\mathbf{R})\nabla_I^2\psi_i(\mathbf{R})\end{aligned} \tag{5.3.3}$$

Note here the sum over index I is over the mass and thereby the kinetic energy of nucleus I, whereas J is the index of the nuclear eigenstate (quantum number). This expression is exact for vibronic problems and is referred to as the coupled channel Hamiltonian. Note that if we set the last two terms in eq. (5.3.3) to zero, we are left with the Hamiltonian we used in the BOA, eq. (5.2.5). Therefore, the last two terms describe deviations from the BOA, and are referred to as nonadiabatic terms. These depend on the spatial gradient of the wavefunction in the region of interest, and act to couple adiabatic BO states.

The coupled channel Hamiltonian has a form that is reminiscent of a perturbation theory Hamiltonian in which the Born-Oppenheimer states play the role of the zero-order Hamiltonian being perturbed ay a nonadiabatic coupling V:

$$\hat{H} = \hat{H}_{\text{BO}} + \hat{V} \tag{5.3.4}$$

To investigate this relationship further, it is helpful to write this Hamiltonian in its matrix form. We obtain the matrix elements by sandwiching the Hamiltonian between two projection operators and evaluating

$$\hat{H}_{i',J',i,J} = \iint d\mathbf{r}\, d\mathbf{R}\, \Psi^*_{i',J'}(\mathbf{r},\mathbf{R})\hat{H}(\mathbf{r},\mathbf{R})\Psi_{i,J}(\mathbf{r},\mathbf{R}) \tag{5.3.5}$$

Making use of eq. (5.3.3) we find that the Hamiltonian can be expressed in three terms

$$\begin{aligned}\hat{H}_{i',J',i,J} = \int d\mathbf{R}\, \Phi^*_{i',J'}(\mathbf{R})\left(\hat{T}_N(\mathbf{R}) + U_i(\mathbf{R})\right)\Phi_{i,J}(\mathbf{R})\,\delta_{i',i} \\ - \sum_I \frac{\hbar^2}{M_I}\int d\mathbf{R}\, \Phi^*_{i',J'}(\mathbf{R})\nabla_I\Phi_{i,J}(\mathbf{R})\cdot\mathbf{F}_{i',i}(\mathbf{R}) \\ - \sum_I \frac{\hbar^2}{2M_I}\int d\mathbf{R}\, \Phi^*_{i',J'}(\mathbf{R})\Phi_{i,J}(\mathbf{R})\mathbf{G}_{i',i}(\mathbf{R})\end{aligned} \tag{5.3.6}$$

where

$$\mathbf{F}_{i,i}(\mathbf{R}) = \int d\mathbf{r}\, \psi^*_i(\mathbf{r},\mathbf{R})\nabla_I\psi_i(\mathbf{r},\mathbf{R}) \tag{5.3.7}$$

$$\mathbf{G}_{i',i}(\mathbf{R}) = \int d\mathbf{r}\, \psi^*_{i'}(\mathbf{r},\mathbf{R})\nabla_I^2\psi_i(\mathbf{r},\mathbf{R}) \tag{5.3.8}$$

The first term in eq. (5.3.6) gives the BO Hamiltonian, and the next two terms are nonadiabatic interactions that mix adiabatic

states and depend on the spatial variation of the nuclear and electronic wavefunctions. In the latter two terms, $\mathbf{F}$ is referred to as the nonadiabatic, first-order, or derivative coupling, and $\mathbf{G}$ is the second-order nonadiabatic coupling or diagonal BO correction. Although they are evaluated by integrating over electronic degrees of freedom, both depend parametrically on the position of the nuclei. In most circumstances the last term is much smaller than the other two, so that we can concentrate on the second term in evaluating couplings between adiabatic states. For our purposes, we can write the nonadiabatic coupling in eq. (5.3.4) as

$$\hat{V}_{i',J',i,J}(\mathbf{R}) = -\sum_I \frac{\hbar^2}{M_I} \int d\mathbf{R}\, \Phi^*_{i',J'}(\mathbf{R}) \nabla_I \Phi_{i,J}(\mathbf{R}) \cdot \mathbf{F}_{i',i}(\mathbf{R}) \tag{5.3.9}$$

This emphasizes that the coupling between surfaces depends parametrically on the nuclear positions, the gradient of the electronic and nuclear wavefunctions, and the spatial overlap of those wavefunctions.

This page titled 5.3: Nonadiabatic Coupling is shared under a CC BY-NC-SA 4.0 license and was authored, remixed, and/or curated by Andrei Tokmakoff via source content that was edited to the style and standards of the LibreTexts platform.

5.4: Diabatic and Adiabatic States

Although the adiabatic surfaces are the most commonly calculated, they may not be the most useful for describing chemical processes. As an example, consider the potential energy curves in Figure 5.4.1a for the diatomic NaCl. The chemically distinct potential energy surfaces one is likely to discuss have distinct atomic or ionic character. These "diabatic" curves, or "diabats" focus on physical effects by fixing their electronic configuration but are not eigenstates. The ionic diabatic surface for $\mathrm{Na}^+ + \mathrm{Cl}^-$ is positively sloped for separated ions due to the Coulomb attraction between them, which draws them together to a stable configuration at R_{eq} at a point where attractive interactions are balanced by repulsive forces. However, the neutral atoms ($\mathrm{Na}^0 + \mathrm{Cl}^0$) exhibit weaker interactions, and their diabat is negatively sloped for closely spaced atoms. Within the framework of a coupled two-diabat system, the corresponding adiabatic surfaces from the BO Hamiltonian are obtained by diagonalizing the R -dependent Hamiltonian:

$$U_{\pm}(R) = \frac{1}{2}\left(U_a(R) + U_b(R)\right) \pm \frac{1}{2}\left[\left(U_a(R) - U_b(R)\right)^2 + 4\left|V_{ab}(R)\right|^2\right]^{1/2} \tag{5.4.1}$$

and will exhibit an avoided crossing where the electronic energy between corresponding diabatic states is equal, for states with the proper symmetry (Figure 5.4.1b). As expected from our earlier discussion of the two-level system, the splitting at the crossing ($U_a(R) = U_b(R)$) would be approximately $2V_{ab}$, twice the coupling between diabatic states, for this example.

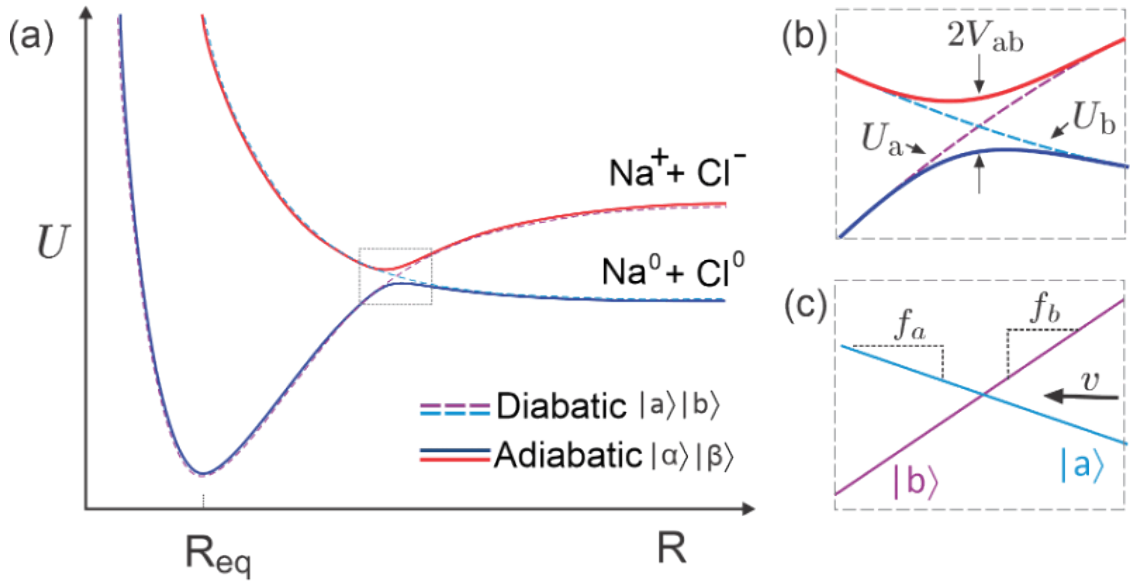


Figure 5.4.1. (a) The potential energy surface for the diatomic NaCl, showing the adiabatic curves (solid) that arise from mixing of ionic (U_a) and neutral (U_b) diabatic surfaces (dashed). (b) Inset showing the avoided crossing of adiabats. (c) Variables used in Landau-Zener expression.

The adiabatic potential energy surfaces are important in interpreting the reaction dynamics, as can be illustrated with the reaction between Na and Cl atoms. If the neutral atoms are prepared on the ground state at large separation and slowly brought together, the atoms are weakly repelled until the separation reaches the transition state $R^{\ddagger}$. Here we cross into the regime where the ionic configuration has lower energy, and transfer of an electron from Na^0 to Cl^0 will lead to an ionic bond with separation R_{eq}. Note that at $R^{\ddagger}$ the adiabatic state is a superposition with neutral and ionic character.

Although only one set of adiabatic surfaces exists, diabatic states can be constructed in many ways. In practice, diabatic states are chosen so that the nonadiabatic electronic couplings in eq. (5.3.7) are zero, which is accomplished by requiring that the wavefunctions to be independent of R, so that their gradients vanish. In the example above, the diabatic curves are constructed to keep the electron configuration or ionic charge fixed as a function of R. Although adiabats that exhibit an avoided crossing remain energetically separated, nonadiabatic coupling still allows these surfaces to influence one another at a lower level. The nonadiabatic derivative coupling between adiabats can be computed directly from the overlap of the BO wavefunctions and their gradient, or it can be obtained from the shape of the crossing diabats and the transformation between states. For a two adiabatic potential energy surfaces in one dimension, the nonadiabatic coupling is $F_{\alpha\beta} = \left\langle \psi_\alpha \middle| \frac{\partial}{\partial R} \psi_\beta \right\rangle$, and for the case of two coupled diabatic states the nonadiabatic coupling can be expressed in terms of the mixing angle θ as

$$F_{\alpha\beta} = 2 \sin\theta \cos\theta \frac{\partial \theta}{\partial R} \tag{5.4.2}$$

Despite the expectation that adiabats remain energetically separated, it is still possible for two adiabatic states to cross. Mathematically this requires that the energies of the adiabatic states be degenerate ($E_\alpha = E_\beta$) and the coupling at that configuration be zero ($V_{\alpha\beta} = V_{\beta\alpha} = 0$). This isn't possible for a one-dimensional problem, such as the NaCl example above, unless symmetry dictates that the nonadiabatic coupling vanishes. To accomplish this for a Hermitian coupling operator we need two independent nuclear coordinates, which enable us to independently tune the adiabatic splitting and coupling. This leads to a single point in the two-dimensional space at which degeneracy exists, known as a conical intersection.

This page titled 5.4: Diabatic and Adiabatic States is shared under a CC BY-NC-SA 4.0 license and was authored, remixed, and/or curated by Andrei Tokmakoff via source content that was edited to the style and standards of the LibreTexts platform.

5.5: Landau–Zener Transition Probability

Okay, so what does the previous discussion mean for dynamics? While the BOA never explicitly addresses electronic or nuclear dynamics, neglecting the nuclear kinetic energy to obtain potential energy surfaces has implicit dynamical consequences. As we discussed for our NaCl example, moving the neutral atoms together slowly allows electrons to completely equilibrate about each forward step, resulting in propagation on the adiabatic ground state. In the opposite limit, we also know that if the atoms were incident on each other so fast (with such high kinetic energy) that the electron did not have time to transfer at the crossing, that the system would pass smoothly through the crossing along the diabatic surface. In fact, it is expected that the atoms would collide and recoil before electron transfer could happen. This implies that there is an intermediate regime in which the velocity of the system is such that the system will split and follow both surfaces to some degree.

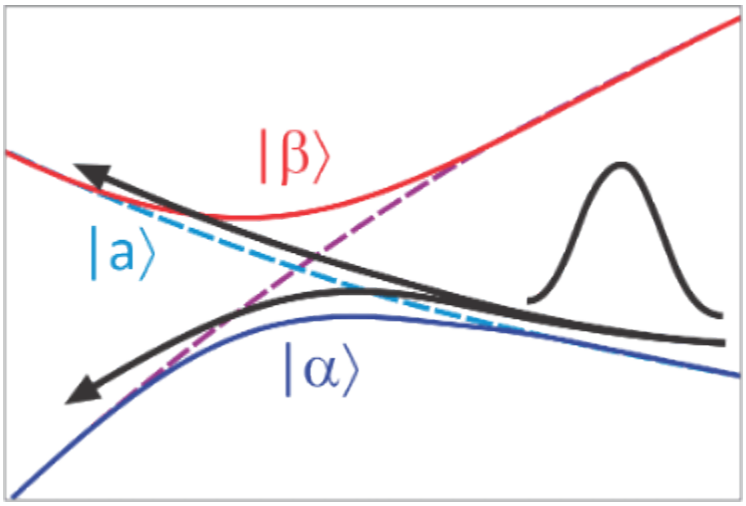


Figure $5.5.1$. Illustration of an incident wavepacket on the neutral surface with two possible outcomes: possible evolution on the neutral diabatic $|a\rangle$ or electron transfer from the the adiabatic surface $|\alpha\rangle$

How do we define "fast" and "slow" for such questions? Speaking qualitatively this is determined by the strength of coupling between states. We know that two coupled states exchange amplitude at a rate dictated by the Rabi frequency Ω_R, which in turn depends on the energy splitting and coupling of the states. For systems in which there is significant nonperturbative transfer of population between two states a and b, the time-scale over which this can occur is approximately $\Delta t \approx 1/\Omega_R \approx \hbar/V_{ab}$. This is not precise, but it provides a reasonable starting point for discussing "slow" versus "fast". "Slow" in an adiabatic sense would mean that a time-dependent interaction act on the system over a period such that $\Delta t \ll \hbar/V_{ab}$. In the case of our NaCl example, we would be concerned with the time-scale over which the atoms pass through the crossing region between diabatic states, which is determined by the incident velocity between atoms.

We can look at this more quantitatively for the curve crossing example by considering the probability that a system prepared on one diabatic surface transfers to another after passing through the degeneracy point $(E_a = E_b)$. To simplify this problem we first assume that the slopes of the diabatic surfaces $(f_i = \partial E_i/\partial R)$ in the vicinity of the degeneracy point vary linearly with R, as shown in Figure 5.4.1c, and that the coupling between surfaces V_{ab} is a constant that is independent of R and time. Next, to link position, time, and energy variables, we assume that the system passes through this point with constant velocity $v = \partial R/\partial t$. From these variables, we can describe the time-dependent energy splitting between states as

$$\begin{aligned} E_{ab}(t) &= (E_a - E_b) = vt\,(f_a - f_b) \\ &= \dot{E}t \end{aligned} \tag{5.5.1}$$

Here $\dot{E} = dE_{ab}/dt$ is the constant time rate of change in the energy splitting and we have set $t = 0$ to coincide with the degeneracy point.

One can calculate the probability of crossing from surface a to b for a trajectory that passes through the crossing by initiating the system in state a and calculating the expansion coefficient in state b subject to the time-dependent energies of the states. Since

the solution is a bit involved,[1][2][3] we only quote the result obtained when integrating the coupled differential equations for the state a and b expansion coefficients to $t \to \infty$:

$$P_{ba} = 1 - \exp\left[-\frac{2\pi V_{ab}^2}{\hbar|\dot{E}|}\right] \tag{5.5.2}$$

and $P_{aa} = 1 - P_{ba}$. This expression can be written in a useful form if we define the interaction period at the crossing, τ_{int}, as the ratio of the coupling to the splitting sweep rate

$$\tau_{\text{int}} = \frac{|V_{ab}|}{|\dot{E}|} \tag{5.5.3}$$

and the Rabi frequency at the degeneracy point, i.e. the coupling, as

$$\Omega_0 = \frac{|V_{ab}|}{\hbar} \tag{5.5.4}$$

to give:

$$P_{ba} = 1 - \exp\left[-2\pi\Omega_0\tau_{\text{LT}}\right] \tag{5.5.5}$$

Now we see if the interaction period is large compared to the Rabi frequency, $\tau_{\text{int}}\Omega_0 \gg 1$, then we obtain the result expected for the adiabatic dynamics $P_{ba} \approx 1$, and in the opposite limit the system remains on the diabatic surface, i.e. $P_{ba} \approx 0$. This is essentially the same result that we argued for heuristically above. Equation (5.5.2) is the Landau-Zener expression for the transition probability, and is generally applicable to two state problems involving a linear time sweep of the energy splitting through the degeneracy point. What this expression says in the context between curve crossing is that we can extract the branching of population between diabatic states (within the approximations made) knowing the slopes of the potentials at their crossing point, the coupling, and the velocity of an incident wavepacket.

References

(1) Ho, L. T. A.; Chibotaru, L. F. A simple derivation of the Landau-Zener formula. *Physical Chemistry Chemical Physics* **2014**, *16* (15), 6942-6945. DOI: 10.1039/c4cp00262h

(2) Wittig, C. The Landau-Zener Formula. *Journal of Physical Chemistry B* **2005**, *109* (17), 8428-8430. DOI: 10.1021/jp040627u

(3) Zener, C. Non-adiabatic crossing of energy levels. *Proceedings of the Royal Society A* **1932**, *137* (833), 696-702. DOI: 10.1098/rspa.1932.0165

This page titled 5.5: Landau–Zener Transition Probability is shared under a CC BY-NC-SA 4.0 license and was authored, remixed, and/or curated by Andrei Tokmakoff via source content that was edited to the style and standards of the LibreTexts platform.

5.6: Adiabaticity criterion

Now let's investigate more generally the factors that determine whether dynamics proceed adiabatically and when we need to consider nonadiabatic couplings. Since the adiabatic states $\Psi_\alpha(t) \equiv |\alpha\rangle$ are orthogonal for all times, the adiabatic time propagator, eq. (5.5.1), can be used to express the time-dependent wavefunction as

$$\Psi(t) = \sum_\alpha b_\alpha(t) \exp\left[-\frac{\mathrm{i}}{\hbar}\int_0^t E_\alpha(t)\,dt'\right]|\alpha\rangle \tag{5.6.1}$$

Although these are adiabatic states, we recognize that the expansion coefficients b_α can be time-dependent in the general case. So, we would like to investigate the factors that govern this time-dependence. To make the notation more compact, let's define the time-rate of change of the eigenfunction as

$$|\dot{\alpha}\rangle = \frac{\partial}{\partial t}|\Psi_\alpha(t)\rangle \tag{5.6.2}$$

If we substitute the general solution eq. (5.6.1) into the TDSE, we get

$$\mathrm{i}\hbar\sum_\alpha\left(\dot{b}_\alpha|\alpha\rangle + b_\alpha|\dot{\alpha}\rangle - \frac{\mathrm{i}}{\hbar}E_\alpha b_\alpha|\alpha\rangle\right)\exp\left[-\frac{\mathrm{i}}{\hbar}\int_0^t E_\alpha(t)\,dt'\right] = \sum_\alpha b_\alpha E_\alpha|\alpha\rangle\exp\left[-\frac{\mathrm{i}}{\hbar}\int_0^t E_\alpha(t)\,dt'\right] \tag{5.6.3}$$

Note, the third term on the left-hand side equals the right-hand term. Acting on both sides from the left with $\langle\beta|$ leads to

$$-\dot{b}_\beta\exp\left[-\frac{\mathrm{i}}{\hbar}\int_0^t E_\beta(t)\,dt'\right] = \sum_\alpha b_\alpha\langle\beta|\dot{\alpha}\rangle\exp\left[-\frac{\mathrm{i}}{\hbar}\int_0^t E_\alpha(t)\,dt'\right] \tag{5.6.4}$$

We can break up the terms in the summation into one for the target state $|\beta\rangle$ and one for the remaining states.

$$-\dot{b}_\beta = b_\beta\langle\beta|\dot{\beta}\rangle + \sum_{\alpha\neq\beta} b_\alpha\langle\beta|\dot{\alpha}\rangle\exp\left[-\frac{\mathrm{i}}{\hbar}\int_0^t dt' E_{\alpha\beta}(t')\right] \tag{5.6.5}$$

where $E_{\alpha\beta}(t) = E_\alpha(t) - E_\beta(t)$.

The adiabatic approximation applies when we can neglect the summation in eq. (5.6.5), or equivalently when $\langle\beta|\dot{\alpha}\rangle \ll \langle\beta|\dot{\beta}\rangle$ for all $|\alpha\rangle$. In that case, the system propagates on the adiabatic state $|\beta\rangle$ independent of the other states: $\dot{b}_\beta = -b_\beta\langle\beta|\dot{\beta}\rangle$. The evolution of the coefficients is

$$\begin{aligned} b_\beta(t) &= b_\beta(0)\exp\left[-\int_0^t \left\langle\beta(t')|\dot{\beta}(t')\right\rangle dt'\right] \\ &\approx b_\beta(0)\exp\left[\frac{\mathrm{i}}{\hbar}\int_0^t E_\beta(t')\,dt'\right] \end{aligned} \tag{5.6.6}$$

Here we note that in the adiabatic approximation $E_\beta(t) = \langle\beta(t)|H(t)|\beta(t)\rangle$. Equation (5.6.6) indicates that in the adiabatic approximation the population in the states never changes, only their phase.

The second term on the right in eq. (5.6.5) describes the nonadiabatic effects, and the overlap integral

$$\langle\beta|\dot{\alpha}\rangle = \left\langle\Psi_\beta\middle|\frac{\partial\Psi_\alpha}{\partial t}\right\rangle \tag{5.6.7}$$

determines the magnitude of this effect. $\langle\beta|\dot{\alpha}\rangle$ is known the nonadiabatic coupling (even though it refers to couplings between adiabatic surfaces), or as the geometrical phase. Note the parallels here to the expression in eq. (5.3.7) for the nonadiabatic coupling in evaluating the validity of the Born-Oppenheimer approximation, however, here the gradient of the wavefunction is evaluated in time rather than the nuclear position. We can make some connections between these two results by linking the gradient variables through the momentum of the particles involved.

So, when can we neglect the nonadiabatic effects? We can obtain an expression for the nonadiabatic coupling by expanding

$$\frac{\partial}{\partial t}\left[H|\alpha\rangle = E_\alpha|\alpha\rangle\right] \tag{5.6.8}$$

and acting from the left with $\langle\beta|$, which for $\alpha \neq \beta$ leads to

$$\langle\beta|\dot{\alpha}\rangle = \frac{\langle\beta|\dot{H}|\alpha\rangle}{E_\alpha - E_\beta} \tag{5.6.9}$$

For adiabatic dynamics to hold $\langle\beta|\dot{\alpha}\rangle \ll \langle\beta|\dot{\beta}\rangle$, and so we can say

$$\frac{\langle\beta|\dot{H}|\alpha\rangle}{E_\alpha - E_\beta} \ll -\frac{\mathrm{i}}{\hbar}E_\beta \tag{5.6.10}$$

So how accurate is the adiabatic approximation for a finite time-period over which the systems propagates? We can evaluate eq. (5.6.5), assuming that the system is prepared in state $|\alpha\rangle$ and that the occupation of this state never varies much from one. Then the occupation of any other state can be obtained by integrating over a period τ as

$$\begin{aligned} \dot{b}_\beta &= \langle\beta \mid \dot{\alpha}\rangle \exp\left[-\frac{\mathrm{i}}{\hbar}\int_0^\tau dt' E_{\alpha\beta}(t')\right] \\ b_\beta &\approx \mathrm{i}\hbar\frac{\langle\beta|\dot{H}|\alpha\rangle}{E_{\alpha\beta}^2}\left\{\exp\left[-\frac{\mathrm{i}}{\hbar}E_{\alpha\beta}\tau\right] - 1\right\} \\ &= 2\hbar\frac{\langle\beta|\dot{H}|\alpha\rangle}{E_{\alpha\beta}^2}e^{-\frac{\mathrm{i}}{\hbar}E_{\alpha\beta}\tau}\sin\left(\frac{E_{\alpha\beta}\tau}{2\hbar}\right) \end{aligned} \tag{5.6.11}$$

Here I used $e^{\mathrm{i}\theta} - 1 = 2\mathrm{i}e^{\mathrm{i}\theta/2}\sin(\theta/2)$. For $|b_\beta| \ll 1$, we expand the $\sin$ term and find

$$\left\langle \Psi_\beta \left| \frac{\partial H}{\partial t} \right| \Psi_\alpha \right\rangle \ll \frac{E_{\alpha\beta}}{\tau} \tag{5.6.12}$$

This is the criterion for adiabatic dynamics. It says that the rate at which the non-adiabatic coupling matrix elements change must be slow compared to the energy splitting between adiabatic states over that interaction period τ.

References

(1) Truhlar, D. D. Potential Energy Surfaces. *Encyclopedia of Physical Science and Technology*; 3rd ed.; Meyers, R. A., Ed.; Vol. 13; Academic Press, 2001; pp 9-17.

(2) Tully, J. C. Perspective: Nonadiabatic Dynamics Theory. *Journal of Chemical Physics* **2012**, *137*, 22A301. DOI: 10.1063/1.4757762

This page titled 5.6: Adiabaticity criterion is shared under a CC BY-NC-SA 4.0 license and was authored, remixed, and/or curated by Andrei Tokmakoff via source content that was edited to the style and standards of the LibreTexts platform.

5.7: Readings

Adiabatic Processes

1. Tannor, D. J. *Introduction to Quantum Mechanics: A Time-Dependent Perspective*; University Science Books, 2007; ch 9 and ch 12.

Landau–Zener Transition Probability

1. Ho, L. T. A.; Chibotaru, L. F. A simple derivation of the Landau-Zener formula. *Physical Chemistry Chemical Physics* **2014**, *16* (15), 6942-6945. DOI: 10.1039/c4cp00262h
2. Wittig, C. The Landau-Zener Formula. *Journal of Physical Chemistry B* **2005**, *109* (17), 8428-8430. DOI: 10.1021/jp040627u
3. Zener, C. Non-adiabatic crossing of energy levels. *Proceedings of the Royal Society A* **1932**, *137* (833), 696-702. DOI: 10.1098/rspa.1932.0165

Adiabaticity criterion

1. Truhlar, D. D. Potential Energy Surfaces. *Encyclopedia of Physical Science and Technology*; 3rd ed.; Meyers, R. A., Ed.; Vol. 13; Academic Press, 2001; pp 9-17. DOI: 10.1016/B0-12-227410-5/00606-2
2. Tully, J. C. Perspective: Nonadiabatic Dynamics Theory. *Journal of Chemical Physics* **2012**, *137*, 22A301. DOI: 10.1063/1.4757762

This page titled 5.7: Readings is shared under a CC BY-NC-SA 4.0 license and was authored, remixed, and/or curated by Andrei Tokmakoff.

6: CLASSICAL DESCRIPTION OF SPECTROSCOPY

6.1: Introduction

6.2: Absorption by a Driven Oscillator

6.3: Complex formulation of the driven dipole oscillator

6.4: Response of an Impulsively Driven Oscillator

6.5: Polarizability

6.6: Appendix- Laplace Transform Solution for the Driven Damped Oscillator

6.7: Readings

This page titled 6: Classical Description of Spectroscopy is shared under a CC BY-NC-SA 4.0 license and was authored, remixed, and/or curated by Andrei Tokmakoff via source content that was edited to the style and standards of the LibreTexts platform.

6.1: Introduction

One of the most important topics in time-dependent quantum mechanics is the description of spectroscopy, which is the study of matter through its interaction with electromagnetic radiation or, as we refer to it here, light. Classically, light-matter interactions result from an oscillating electromagnetic field driving the motion of the charged particles that constitute the matter, either bound electrons or nuclei. We observe these processes either through changes to the incident light induced by the matter, such as absorption of the light or the emission of new light fields, or by light-induced changes to the matter, such as ionization and photochemistry. By studying light-matter interaction as a function of the control variables for the light (intensity, frequency, polarization, phase, etc.), we can deduce molecular properties of the matter. Given the many variables governing the light, the matter, and the form of the light-matter interactions, there are countless types of spectroscopy which offer different types of molecular information. Ultimately, though, experimental spectra must be interpreted within the context of a model, making an accurate theoretical description of the physical process governing light-matter interaction vitally important.

The traditional quantum mechanical treatment of spectroscopy draws on the Golden Rule to describe the rates of light absorption or emission, and while we will discuss this, it results in a static representation of a dynamic process. Dynamically, an oscillating light field exerts forces that drive the charged particles within molecules with the same oscillatory motion. When the frequency of the light matches natural resonance conditions, this motion leads to efficient exchange of energy between the light and matter, allowing for efficient absorption of light. This dynamical picture emerges from a time-domain description of spectroscopy, which shares many similarities to a classical description of spectroscopy. There is much physical intuition to be gained from the classical description, such as the concepts of resonance, polarizability, and the Fourier transform relationships between time-domain and frequency-domain spectroscopy. For that reason, we will start our discussion of spectroscopy with a simple classical description of absorption.

This page titled 6.1: Introduction is shared under a CC BY-NC-SA 4.0 license and was authored, remixed, and/or curated by Andrei Tokmakoff via source content that was edited to the style and standards of the LibreTexts platform.

6.2: Absorption by a Driven Oscillator

The classical description of spectroscopy begins with the observations that (a) atoms and molecules are composed of charged particles and (b) an electromagnetic field can interact with the atom or molecule by exerting a force on these charges. The size and influence of the force exerted on the molecules depends on the form of the potential binding the charges together, the magnitude of the charges, and the strength of the external field. The simplest model needs to account for the light, the charged particles that constitute the matter, and the light-matter interactions. The driven harmonic oscillator model expresses these elements in terms of Newton's equation of motion $F = ma$ and forms a steppingstone toward more detailed treatments of light-matter interactions.

Charged particle in a harmonic potential

Let's start by discussing the matter. While a static electric field ($\mathcal{E}_0$) can exert a force on any charge q, i.e. $F = q\mathcal{E}_0$, the efficient transfer of energy between matter and oscillating electromagnetic radiation comes from resonance—the sustained periodic displacement of the charge that matches the driving electric field. The key requirement for resonance is that the charged particles are bound. The many electrons and nuclei in molecules feel a restoring force when a field pushes them away from their equilibrium configuration, whether that is the balance of the attractive and repulsive forces that govern the positions of nuclei or the distribution of electrons about the center of mass of a molecule. Even in magnetic resonance experiments, the fixed magnetic field of the spectrometer imposes a restoring force that aligns spins to be interrogated with resonant magnetic fields.

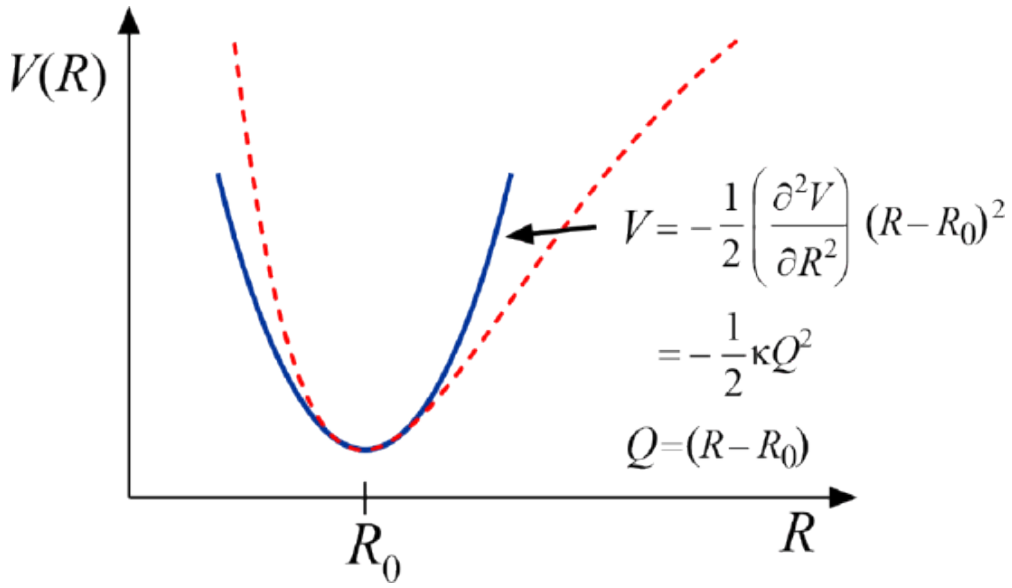


Figure 6.2.1: Harmonic approximation to a bound potential for small displacements from the equilibrium position x_0.

The simplest way of representing this problem is to consider the behavior of a single charged particle of mass m with charge q held within a harmonic potential Figure 6.2.1—often called the Lorentz model or the electron-on-a-spring model. However, this model is just as applicable to a molecule with multiple bound charges that has an equilibrium configuration R_0—for instance, the bond length of a diatomic molecule. Generally, the potential energy of a bound particle (or molecule) $V(R)$ will have a minimum at R_0. For small variations in the position of the particle near R_0, we can perform an expansion of $V(R)$ about R_0. The leading term takes on a parabolic form:

$$V(R) \approx \frac{1}{2}\left(\frac{\partial^2 V}{\partial R^2}\right)_{R=R_0}(R-R_0)^2 \tag{6.2.1}$$

This is just the potential energy for a harmonic oscillator. Therefore, we describe the matter in our model using the harmonic potential

$$V = \frac{1}{2}\kappa Q^2 \tag{6.2.2}$$

where the displacement coordinate $Q = R - R_0$. The force constant κ is determined by the curvature of the potential near the minimum

$$\kappa = \left(\frac{\partial^2 V}{\partial R^2}\right)_{R=R_0} \tag{6.2.3}$$

When the charged particle is displaced from equilibrium, the restoring force is

$$F_{\text{res}} = -\frac{\partial V}{\partial Q} = -\kappa Q \tag{6.2.4}$$

This is the classic linear restoring force expression expected from Hooke's Law.

Without any further input into the model, Newton's equation of motion is

$$F_{\text{res}} = ma \tag{6.2.5}$$

or

$$m\frac{\partial^2 Q}{\partial t^2} + \kappa Q = 0 \tag{6.2.6}$$

To solve this equation we apply the boundary conditions, setting the position Q_0 and velocity V_0 of the particle at time $t = 0$, and we obtain the following solution

$$Q(t) = Q_0 \cos(\omega_0 t) + \frac{V_0}{m\omega_0}\sin(\omega_0 t) \tag{6.2.7}$$

As illustrated in Figure 6.2.2, the particle displays simple oscillatory motion at the natural resonance frequency ω_0

$$\omega_0 = \sqrt{\frac{\kappa}{m}} \tag{6.2.8}$$

The important observation is that a displaced particle oscillates at a frequency governed by the shape of the binding potential near its minimum.

As a next step, we also add a damping force to describe the flow of energy from the oscillator into its environment. This is added in part to broaden the model's description of the matter, but it is also crucial for describing the energy flow from the light to the matter. Even if a molecule is absorbing light in isolation, the accelerating charges will radiate an electric field, thereby emitting energy that damps the amplitude of its oscillations. The simplest way to incorporate this is to recognize that damping changes the amplitude of vibration with time and is therefore proportional to the velocity of the particle ($V = \dot{Q}$). We assign a constant b, the friction coefficient, to describe the linear relation between the damping force and velocity: $F_{\text{damp}} = -b\dot{Q}$.

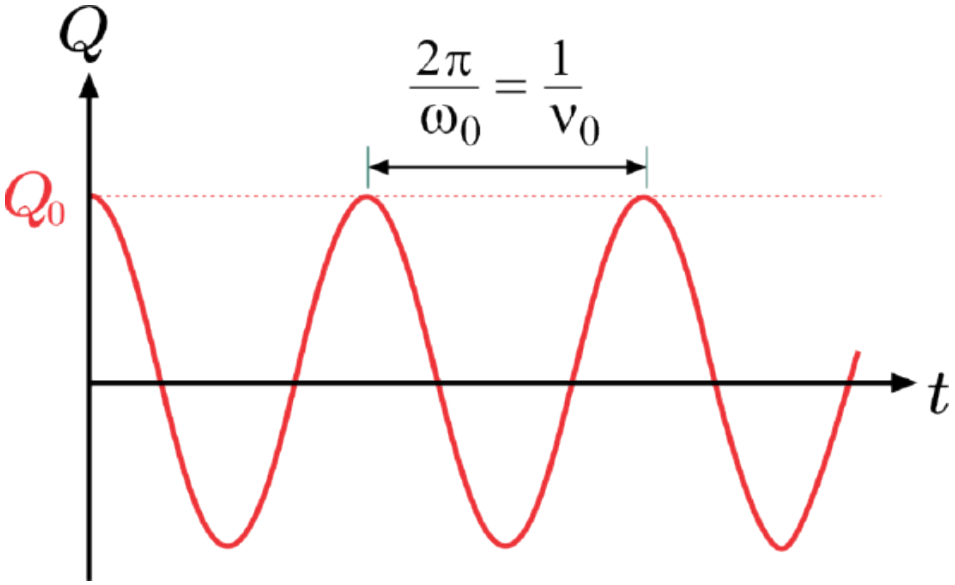


Figure 6.2.2: Time-dependence of a particle in a harmonic potential in the absence of an external force, exhibiting oscillations with a period $\tau = \nu_0^{-1}$ for a particle released from an initially displaced position $Q(0) = Q_0$ with $V_0 = 0$.

With damping, Newton's second law becomes

$$\begin{aligned} F_{\text{res}} + F_{\text{damp}} &= ma \\ -\kappa Q - b\frac{\partial Q}{\partial t} &= m\frac{\partial^2 Q}{\partial t^2} \end{aligned} \tag{6.2.9}$$

Let's re-write this equation in a manner that will simplify the notation and interpretation going forward:

$$\ddot{Q} + 2\gamma\dot{Q} + \omega_0^2 Q = 0 \tag{6.2.10}$$

Here the damping constant γ is defined as

$$\gamma = \frac{b}{2m} \tag{6.2.11}$$

For the second-order homogeneous equation such as eq. (6.2.10), we find oscillatory solutions similar to eq. (6.2.7) with modifications due to damping:

$$Q(t) = e^{-\gamma t}\left[A\cos\Omega_0 t + B\sin\Omega_0 t\right] \tag{6.2.12}$$

with $A = Q_0$ and $B = (\gamma Q_0 + V_0)\,\Omega_0^{-1}$. As example of this solution is illustrated in Figure 6.2.3. The damping force has modified the position equation in two ways. First is the exponential decrease of the oscillation amplitude over time from $e^{-\gamma t}$. Second, the particle oscillates at a reduced frequency:

$$\Omega_0 = \sqrt{\omega_0^2 - \gamma^2} \tag{6.2.13}$$

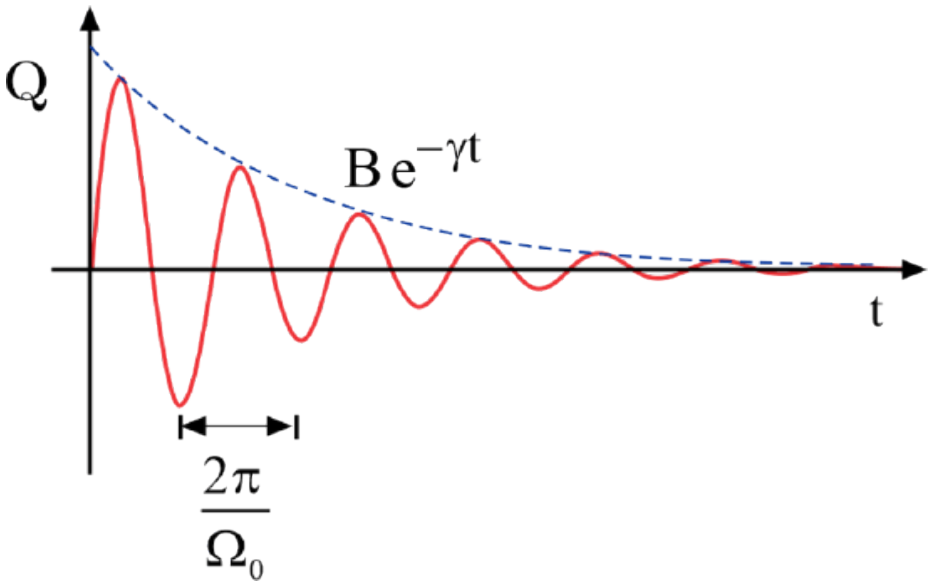


Figure 6.2.3: Example of the response of a damped oscillator initially positioned at $Q = 0$ with a positive velocity V_0.

The strength of the damping (γ) modifies the natural frequency of a bound particle from the value predicted by the curvature of the binding potential (ω_0), resulting in the reduced frequency Ω_0. However, the most common case in molecular spectroscopy is the underdamped oscillator, which occurs when the damping constant γ is much smaller than ω_0. Therefore, the reduced frequency of an underdamped oscillator is $\Omega_0 \approx \omega_0$. In this limit we can simply substitute ω_0 for Ω_0 in eq. (6.2.12) without any serious concern.

In the opposite limit of strong damping, $\gamma > \omega_0$, the oscillator's kinetic energy dissipates in a shorter time than the oscillatory period, and Ω_0 takes on imaginary values. However, we don't need to be concerned about an unphysical, imaginary oscillation because the constant B also becomes imaginary, ensuring the ultimate solution is real. Using $\cos(bi) = \cosh b$ and $\sin(bi) = \mathrm{i}\sinh b$, we can show that what was an oscillatory function in the underdamped regime becomes an exponentially damped function in the overdamped regime. That is, the term $\sin\Omega_0 t$ becomes $\sinh(\Gamma t)$, where the damping rate Γ is

$$\Gamma = \sqrt{\gamma^2 - \omega_0^2} \tag{6.2.14}$$

The general solution in the overdamped limit can be written as a sum of damped exponentials

$$\begin{aligned} Q(t) &= e^{-\gamma t}\left[A\cosh(\Gamma t) + B\sinh(\Gamma t)\right] \\ &= \frac{1}{2}(A+B)e^{-(\gamma-\Gamma)t} + \frac{1}{2}(A-B)e^{-(\gamma+\Gamma)t} \end{aligned} \tag{6.2.15}$$

A math digression

At this point, it is worth noting that the solutions to equations of the form of eq. (6.2.10) can be written multiple ways. Remember, the general solution to homogeneous linear second order differential equations can be expressed in terms of the roots to the characteristic equation $ar^2 + br + c = 0$, leading to $Q(t) = c_1 e^{r_1 t} + c_2 e^{r_2 t}$, where r_1 and r_2 are complex numbers. In the present case, we know that κ, m, and b are real, so we only have real valued solutions, resulting in forms like eq. (6.2.12).

Now, let's consider the form of eq. (6.2.7), and by extension eq. (6.2.12), using the constants A and B:

$$Q(t) = A(\omega_0 t) + B\cos(\omega_0 t) \tag{6.2.16}$$

This consists of two elements, sine and cosine, which are oscillating with the same frequency but each phase-shifted 90° from the other. The cosine is referred to as "in-phase," while sine is "in-quadrature." Signals which are in-quadrature can be re-written in terms of a single amplitude and phase using the following relationships:

$$\begin{aligned} A\sin\omega_0 t \pm B\cos\omega_0 t &= \sqrt{A^2+B^2}\,\sin(\omega_0 t \pm \beta') \qquad \beta' = \mathrm{atan}(B/A) \\ &= \sqrt{A^2+B^2}\,\cos(\omega_0 t \pm \beta) \qquad \beta = \mathrm{atan}(A/B) \end{aligned} \tag{6.2.17}$$

For instance, we can use the identities in eqn. (6.2.17) to write eqn. (6.2.12) in the form

$$Q(t) = \sqrt{A^2 + B^2} e^{-\gamma t} \cos(\Omega_0 t \pm \beta) \tag{6.2.18}$$

To convert the amplitude ($\sqrt{A^2 + B^2}$) and phase (β) back to the in-quadrature components, we can use the identities

$$\begin{aligned} \cos(\omega_0 t \pm \beta) &= \cos(\beta)\cos(\omega_0 t) \mp \sin(\beta)\sin(\omega_0 t) \\ \sin(\omega_0 t \pm \beta) &= \sin(\beta)\cos(\omega_0 t) \pm \cos(\beta)\sin(\omega_0 t) \end{aligned} \tag{6.2.19}$$

Here are a few additional trigonometric identities that prove useful in describing driven harmonic oscillator problems:

$$\begin{aligned} \cos(a + bi) &= \cos a \cosh b - \mathrm{i} \sin a \sinh b \\ \sin(a + bi) &= \sin a \cosh b + \mathrm{i} \cos a \sinh b \\ \cos(bi) &= \cosh b \\ \sin(bi) &= \mathrm{i} \sinh b \end{aligned} \tag{6.2.20}$$

Driving the oscillator sinusoidally

Now let's turn to discussing the light. Light is a traveling electromagnetic field that oscillates in time and in space and is characterized by several factors. However, in the present case, our interest is limited to the sinusoidally oscillating force that it exerts on the matter, and therefore we drop spatial variables and phase. We retain only the essential variables: the oscillating frequency ω and the amplitude of the electric field, $\mathcal{E}_0$.

$$\mathcal{E}(t) = \mathcal{E}_0 \cos(\omega t) \tag{6.2.21}$$

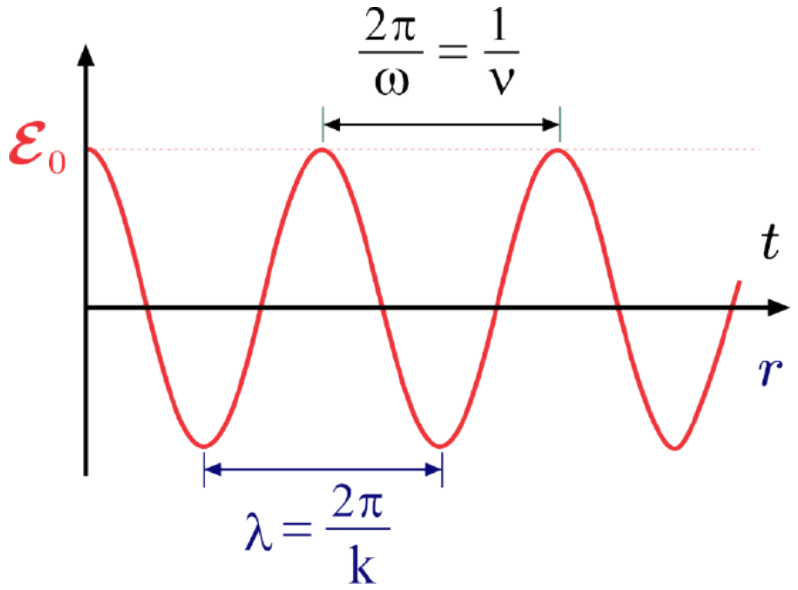


Figure 6.2.4: Sinusoidal driving field with an amplitude $\mathcal{E}_0$ and angular frequency ω.

Next, how does this field interact with the molecule's charges? We take the distribution of charge within the molecule to be defined by the dipole moment μ and the interaction potential of the field and the dipole is $V(t) = -\mu \cdot \mathcal{E}(t)$. For the case of a single particle of charge q, one can express the dipole moment as the charge times the displacement of the oscillator, $\mu = qQ$; however, this expression can also be extended to molecules with a sum over charges. The external driving force that the field exerts on the oscillator can then be calculated from $F_{\text{ext}} = -\partial V / \partial Q$, which leads to a sinusoidal form with an amplitude F_0 and a driving frequency ω.

$$F_{\text{ext}}(t) = F_0 \cos(\omega t) \tag{6.2.22}$$

Here, F_0 is the amplitude of the driving force. For a single charged particle, it would be $F_0 = q\mathcal{E}_0$, but for a molecule in three

dimensions, we express it as

$$\begin{aligned} F_0 &= \left(\frac{\partial \boldsymbol{\mu}}{\partial Q}\right) \cdot \boldsymbol{\mathcal{E}}_0 \\ &\equiv \boldsymbol{\mu}' \cdot \boldsymbol{\mathcal{E}}_0 \end{aligned} \tag{6.2.23}$$

In this expression, the dipole derivative $\boldsymbol{\mu}' = (\partial \boldsymbol{\mu}/\partial Q)$ reflects the fact that the light's forces redistribute the charges within the molecule and alter the dipole moment. That is, the field polarizes the molecule. This factor is referred to as the transition dipole moment in vibrational and electronic spectroscopy or the polarizability when discussing general distortions of electron density by electric fields. Specifically, eq. (6.2.23) indicates that two factors influence the electric field's force on the oscillator: (1) the charge displacement is proportional to the magnitude of the field, and (2) efficient interactions require alignment between the electric field polarization and the transition dipole moment because there is a dot product between the direction of charge displacement and the field. We'll drop the vector notation now for simplicity.

Adding this third force term to eq. (6.2.9) results in the driven oscillator equation

$$\ddot{Q} + 2\gamma\dot{Q} + \omega_0^2 Q = \frac{F_0}{m}\cos(\omega t) \tag{6.2.24}$$

As a result of adding a time-dependent force to eq. (6.2.10), this equation is an inhomogeneous second-order ODE. The general solution, described in an appendix, can be expressed as the sum of a steady-state solution and a transient solution. The steady-state solution is only determined by the form of the driving force, while the transient solution is determined by the initial conditions, i.e., the position and velocity of the particle at $t = 0$.

Our calculation of the absorption spectrum comes from the steady state solution to eq. (6.2.24), which assumes that the oscillator has come to equilibrium, when the continuous energy input from the electric field is in balance with the dissipation of energy caused by damping. The steady-state solution takes the form

$$Q(t) = Q_0 \cos(\omega t - \beta) \tag{6.2.25}$$

where the amplitude of the driven oscillator is

$$Q_0 = \frac{F_0}{m\sqrt{\left(\omega_0^2 - \omega^2\right)^2 + 4\gamma^2\omega^2}} \tag{6.2.26}$$

and the oscillator's phase is given by

$$\tan\beta = \frac{2\gamma\omega}{\omega_0^2 - \omega^2} \tag{6.2.27}$$

Let's look at the behavior of this oscillator, starting with the maximum displacement Q_0. Equation (6.2.26) shows that displacement is proportional to the magnitude of the light's driving force, but it also has a so-called "resonant denominator" that is dependent on the oscillator's frequency and damping constant. The highest displacements are realized on resonance, when the frequency of the driving field matches the natural frequency of the system ($\omega_0 = \omega$). One can still drive the particle off resonance, but the degree to which one can displace the particle falls off with the detuning ($\omega - \omega_0$) in a manner that depends on the damping. Damping always decreases Q_0 relative to the undamped oscillator, but this effect is most pronounced near resonance. These features are illustrated in Figure 6.2.5a.

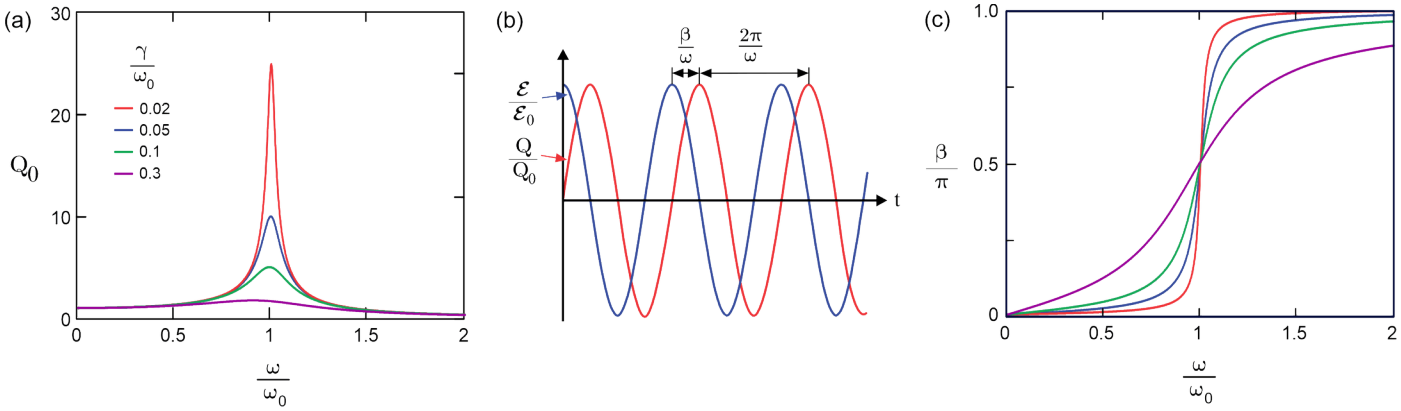


Figure 6.2.5: Steady-state solution to the sinusoidally driven underdamped harmonic oscillator. (a) Maximum displacement of the oscillator Q_0 as a function of detuning from resonance, $\omega = \omega_0$, and damping coefficient, γ. Note the asymmetry in the lineshape with a finite value of Q_0 at $\omega = 0$. (b) Illustration of the phase-shift β in the time-dependent oscillations of $Q(t)$ relative to the driving field $\mathcal{E}(t)$. (c) Magnitude of the oscillator phase relative to the driving field as a function of detuning. Different lines correspond to the different damping coefficients in (a).

From eq. (6.2.25), notice that the particle oscillates at the driving frequency ω and not at the resonance frequency ω_0, but with a phase shift β relative to the driving field. On resonance $\beta = \pi/2$, and the particle oscillates as $\sin \omega t$, lagging behind the phase of the field by 90° Figure 6.2.5b. The maximum force is exerted on the particle at $Q = 0$, the position where the velocity and kinetic energy of the particle are at maximum. The external force drops to zero when the particle reaches its classical turning points ($\pm Q_0$). The phase shift β depends on the detuning from resonance, varying from 0 to π with increasing ω Figure 6.2.5c. When $\omega \ll \omega_0$, $\beta = 0$, so the particle is in-phase with the driving field. This means that the field changes slowly, and the particle position adiabatically tracks the oscillations of the field.

Using eq. (6.2.17) we can re-write eq. (6.2.25) in terms of a cosine component that is in-phase with the driving field and a sine component that is in-quadrature ($\pi/2$ phase-shifted)

$$Q(t) = Q_0 \left[\frac{2\gamma\omega}{\sqrt{\left(\omega_0^2 - \omega^2\right)^2 + (2\gamma\omega)^2}} \sin(\omega t) + \frac{\left(\omega_0^2 - \omega^2\right)}{\sqrt{\left(\omega_0^2 - \omega^2\right)^2 + (2\gamma\omega)^2}} \cos(\omega t) \right] \tag{6.2.28}$$

This shows that the maximum amplitude of oscillation for a given driving frequency is described by the leading term in this equation.

Note that the driving field is harmonically displacing the charged particle, and therefore the external field is inducing an oscillating dipole moment of the form $\mu(t) = \mu' Q(t)$. As we will see next, the sine component is proportional to the power absorbed by the field and is referred to as the absorptive part of the oscillator response, whereas the cosine term in eq. (6.2.28) is the dispersive part that encodes the phase shift of the matter with respect to the field.

Absorption Spectrum

The absorption spectrum indicates the amount of power transferred from the light to the oscillator as a function of the incident frequency of the light, which we can calculate from the average value of the force acting on the oscillator times the velocity of the particle. The power can then be decomposed into the average force acting on an oscillator times the particle velocity. For a continuously oscillating field, the average power absorbed is obtained by averaging the steady state solution over one cycle of the field.

$$\begin{aligned} \overline{\mathcal{P}}_{\text{abs}} &= \overline{F \cdot \dot{Q}} = \frac{2\pi}{\omega} \int_0^{2\pi/\omega} F(t) \cdot \dot{Q}(t)\, dt \\ &= \frac{\gamma\omega^2 F_0^2}{m} \frac{1}{\left(\omega^2 - \omega_0^2\right)^2 + 4\omega^2\gamma^2} \end{aligned} \tag{6.2.29}$$

One observation that we can make immediately is that power absorption from the field requires $\gamma > 0$. That is, if there is no damping—no dissipation of energy by the oscillator—the energy in the driving field is not irreversibly absorbed by the oscillator

but is instead transferred back and forth between the coupled oscillator and field at steady-state. From eq. (6.2.23) we also see that the absorption of energy from the field is proportional to the square of the dipole derivative and the intensity of the electric field: $F_0^2 = (\boldsymbol{\mu}')^2 \boldsymbol{\mathcal{E}}_0^2$. Finally, note that the absorbed power is proportional to the sine term in eq. (6.2.28), which is why the sine component is often referred to as the absorptive part of the oscillator response.

For most optical and infrared spectroscopy, resonances are observed to be in the weak damping limit, $\gamma \ll \omega_0$. Under these circumstances, it is reasonable to describe the absorption spectrum by making a near-resonance approximation where $\omega_0 \approx \omega$, and we can simplify the denominator in eq. (6.2.29) as

$$\left(\omega_0^2 - \omega^2\right) = (\omega_0 + \omega)(\omega_0 - \omega) \approx 2\omega(\omega_0 - \omega) \tag{6.2.30}$$

and re-write it as

$$\overline{\mathcal{P}}_{\text{abs}} = \frac{\gamma}{2m}(\boldsymbol{\mu}')^2 \boldsymbol{\mathcal{E}}_0^2 \frac{1}{(\omega - \omega_0)^2 + \gamma^2} \tag{6.2.31}$$

This is known as a Lorentzian lineshape Figure 6.2.6. It peaks at the resonance frequency, has a full width half-maximum (FWHM) line width of 2γ, and the integrated area is $\pi(\mu')^2\mathcal{E}_0^2/4m$. This steady state model describes the behavior analyzed by frequency domain spectroscopy. In frequency domain spectroscopy, the power (or intensity) absorbed is measured as a function of a tuned monochromatic frequency. The resonances we find in the absorption data allow us to identify the molecular parameters ω_0, γ, and μ'.

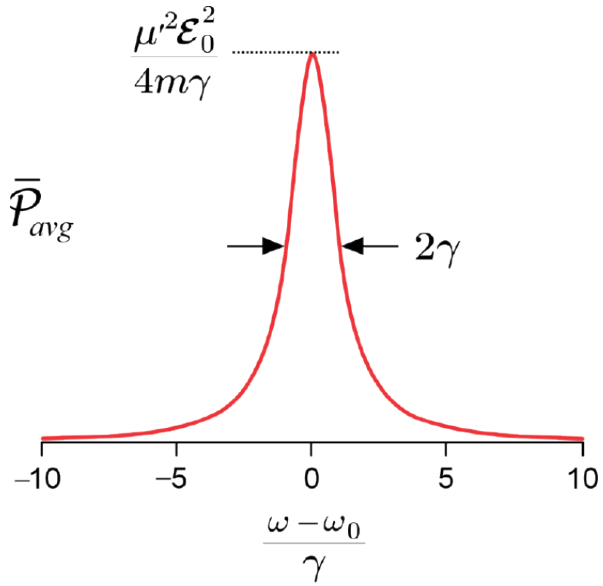


Figure 6.2.6: Lorentzian lineshape illustrating the parameters that govern linewidth and intensity in the absorption spectrum.

An experimental parameter commonly used to describe the strength of a resonance is the absorption cross-section, σ. It can be obtained by measuring the power of light absorbed relative to the incident intensity. Using the formula for the intensity of the incident light $I_0 = \frac{1}{2}\varepsilon_0 c \mathcal{E}_0^2$, and remembering that $\mu' = \partial\mu/\partial Q$ we find

$$\sigma(\omega) = \frac{\overline{\mathcal{P}}_{\text{abs}}}{I_0} = \underbrace{\frac{\pi}{mc\varepsilon_0}\left(\frac{\partial\mu}{\partial Q}\right)^2}_{\text{magnitude}} \underbrace{\frac{\gamma/\pi}{(\omega - \omega_0)^2 + \gamma^2}}_{\substack{\text{area normalized} \\ \text{lineshape}}} \tag{6.2.32}$$

This equation is written such that the overall magnitude of the power that a molecular transition can absorb is spread across an area-normalized Lorentzian lineshape. The linewidth may vary based on interactions of the molecule with its environment. As discussed in Sec. 7.6., the cross-section is proportional to the commonly used extinction coefficient, which is determined from Beer's Law. While one can directly read the parameters ω_0 and γ from the peak position and line width of an absorption spectrum, converting the absorption spectrum into a cross section or extinction coefficient allows one to obtain a quantitative measure of $(\partial\mu/\partial Q)^2$.

This page titled 6.2: Absorption by a Driven Oscillator is shared under a CC BY-NC-SA 4.0 license and was authored, remixed, and/or curated by Andrei Tokmakoff via source content that was edited to the style and standards of the LibreTexts platform.

6.3: Complex formulation of the driven dipole oscillator

In the previous section, we found that that the driven oscillator exhibits a phase shift as a function of the frequency of the driving field, and that the absorption spectrum is related to the in-quadrature ($\sin\omega t$) contribution to the oscillator displacement. These observations suggests that a complex formulation of the driven oscillator problem is mathematically useful, even if the behavior of the field, oscillator coordinate, and induced dipole are all real quantities. Indeed, this is the preferred and commonly used representation for condensed matter spectroscopy. Additionally, we noted that the effect of the driving electric field is to induce a dipole moment in the matter by displacing charges, i.e. $\mu(t) = \mu' Q(t)$. For these reasons, we will repeat our discussion of the driven oscillator here but write it instead in terms of an induced dipole driven by an electric field and using a complex formulation.

The damped oscillator equation (6.2.10) is unchanged; however, we can express the solution in a complex form. Taking the case of the underdamped oscillator ($\omega_0 > \gamma$), one obtains

$$\tilde{Q}(t) = \left(C_+ e^{-\mathrm{i}\Omega_0 t} + C_- e^{\mathrm{i}\Omega_0 t}\right) e^{-\gamma t} \tag{6.3.1}$$

where $C_\pm = \frac{1}{2}\left[Q_0 \pm V_0/\mathrm{i}\Omega_0\right]$. Here and in the following, tildes are used to remind you of complex valued quantities. We can relate the $C_\pm$ amplitudes to the amplitudes in eq. (6.2.12) through $A = \mathrm{Re}\left[C_+ + C_-\right]$ and $B = \mathrm{Im}\left[C_- - C_-\right]$. We also write the driving field in a complex form

$$\tilde{\mathcal{E}}(t) = \mathcal{E}_0 e^{\mathrm{i}\omega t} \tag{6.3.2}$$

Our prior results for the displacement of the oscillator and the driving fields are obtained by taking the real parts of these expression, i.e. $Q(t) = \mathrm{Re}[\tilde{Q}(t)]$ and $\mathcal{E}(t) = \mathrm{Re}[\mathcal{E}_0 e^{\mathrm{i}\omega t}]$. The driven dipole oscillator equation is

$$\ddot{\mu} + 2\gamma\dot{\mu} + \omega_0^2 \mu = \frac{\mu' \mathcal{E}_0}{m} e^{\mathrm{i}\omega t} \tag{6.3.3}$$

With a solution

$$\tilde{\mu}(t) = \mu' \tilde{Q}(\omega) e^{\mathrm{i}\omega t} \tag{6.3.4}$$

Here, $\tilde{Q}(\omega)$ is the oscillator's frequency-dependent amplitude function, containing the complex resonant denominator

$$\tilde{Q}(\omega) = \frac{\mu' \mathcal{E}_0}{m} \frac{1}{(\omega_0^2 - \omega^2) + 2\mathrm{i}\omega\gamma} \tag{6.3.5}$$

To obtain the induced dipole moment as a real quantity, we calculate the real part of eq. (6.3.4)

$$\mu(t) = \mathrm{Re}[\tilde{\mu}(t)] = \mathrm{Re}[\mu' \tilde{Q}(\omega) e^{\mathrm{i}\omega t}] \tag{6.3.6}$$

making use of the relationships (6.3.12) and (6.3.13) below. This results in an expression one could predict from by multiplying $Q(t)$ in eq. (6.2.28) by μ'

$$\mu(t) = \frac{(\mu')^2 \mathcal{E}_0}{m} \left[\frac{2\gamma\omega}{\left(\omega^2 - \omega_0^2\right)^2 + (2\gamma\omega)^2} \sin(\omega t) + \frac{(\omega_0^2 - \omega^2)}{\left(\omega^2 - \omega_0^2\right)^2 + (2\gamma\omega)^2} \cos(\omega t) \right] \tag{6.3.7}$$

Next, we turn to the absorption spectrum, which we can obtain in a similar manner as shown in the previous section. The energy of a dipole in an electric field is $-\mu\mathcal{E}$, and thus we can obtain the cycle-averaged power transferred to the oscillator from $\overline{\mathcal{P}}_{\mathrm{abs}} = \overline{\dot{\mu}(t)\mathcal{E}(t)}$ using eq. (6.3.7). This leads to the same expression as eq. (6.2.29):

$$\overline{\mathcal{P}}_{\mathrm{abs}} = \frac{\omega \left(\mu'\right)^2 \mathcal{E}_0^2}{2m} \frac{2\gamma\omega}{\left(\omega^2 - \omega_0^2\right)^2 + 4\omega^2\gamma^2} \tag{6.3.8}$$

As we observed before, the absorption lineshape corresponds to the amplitude factor corresponding to the in-quadrature ($\sin\omega t$) term in eq. (6.3.7).

For those with familiarity with Fourier transformations, it should be apparent that the in-phase ($\cos\omega t$) and in-quadrature ($\sin\omega t$

) amplitudes for $\tilde{Q}(\omega)$ in eq. (6.3.7) bear a close resemblance to the real and imaginary parts of the Fourier transform of the time-dependence of $\tilde{Q}(t)$ in eq. (6.3.1). This mathematical transformation between the conjugate variables ω and t is the key observation that links frequency and time-domain spectroscopy and allows one to develop a dynamical interpretation of the resonances within a frequency spectrum. We will investigate this further in the following section and return to this constantly through our discussion of spectroscopy.

Lorentzian lineshapes and driven oscillator identities

The complex Lorentzian lineshape can be written as

$$\sigma = \frac{1}{\Delta - \mathrm{i}\Gamma} \tag{6.3.9}$$

where Δ is a real number that refers to the detuning of the light field from resonance and Γ is a real number that describes damping processes that lead to line broadening. The lineshape can be decomposed into real and imaginary parts as

$$\sigma = \frac{\Delta}{\Delta^2 + \Gamma^2} + \mathrm{i}\frac{\Gamma}{\Delta^2 + \Gamma^2} \tag{6.3.10}$$

Or can be written as an amplitude and a phase ϕ

$$\sigma = \frac{1}{\sqrt{\Delta^2 + \Gamma^2}} e^{\mathrm{i}\phi} \tag{6.3.11}$$

where phase $\tan \pi\phi = \Gamma/\Delta$

Some common identities we use are:

$$\mathrm{Re}\left(\frac{1}{\omega - \omega_0 \pm \mathrm{i}\gamma}\right) = \frac{\omega - \omega_0}{(\omega - \omega_0)^2 + \gamma^2} \tag{6.3.12}$$

$$\mathrm{Im}\left(\frac{1}{\omega - \omega_0 \pm \mathrm{i}\gamma}\right) = \frac{\mp\gamma}{(\omega - \omega_0)^2 + \gamma^2} \tag{6.3.13}$$

$$\mathrm{Re}\left(\frac{1}{\omega^2 - \omega_0^2 \pm \mathrm{i}\omega\gamma}\right) = \frac{\omega^2 - \omega_0^2}{(\omega^2 - \omega_0^2)^2 + \gamma^2\omega^2} \tag{6.3.14}$$

$$\mathrm{Im}\left(\frac{1}{\omega^2 - \omega_0^2 \pm \mathrm{i}\omega\gamma}\right) = \frac{\mp\gamma\omega}{(\omega^2 - \omega_0^2)^2 + \gamma^2\omega^2} \tag{6.3.15}$$

For the driven oscillator, the complex amplitudes in the presence of a driving field are given by

$$\begin{aligned}\mathrm{Re}\left(\frac{e^{\mathrm{i}\omega t}}{\omega^2 - \omega_0^2 \pm \mathrm{i}\omega\gamma}\right) &= \mathrm{Re}\left(\frac{e^{-\mathrm{i}\omega t}}{\omega^2 - \omega_0^2 \mp \mathrm{i}\omega\gamma}\right) \\ &= \frac{(\omega^2 - \omega_0^2)\cos(\omega t) \pm \gamma\omega \sin(\omega t)}{(\omega^2 - \omega_0^2)^2 + \gamma^2\omega^2}\end{aligned} \tag{6.3.16}$$

$$\begin{aligned}\mathrm{Im}\left(\frac{e^{\mathrm{i}\omega t}}{\omega^2 - \omega_0^2 \pm \mathrm{i}\omega\gamma}\right) &= -\mathrm{Im}\left(\frac{e^{-\mathrm{i}\omega t}}{\omega^2 - \omega_0^2 \mp \mathrm{i}\omega\gamma}\right) \\ &= \frac{(\omega^2 - \omega_0^2)\sin(\omega t) \mp \gamma\omega \cos(\omega t)}{(\omega^2 - \omega_0^2)^2 + \gamma^2\omega^2}\end{aligned} \tag{6.3.17}$$

The real driven oscillator response function eq. (6.3.16) and complex lineshape are related by a Fourier-Laplace transform:

$$\frac{1}{\Omega_0}\int_0^\infty e^{-\gamma t}\,\sin(\Omega_0 t)\,e^{\pm\mathrm{i}\omega t}\,dt = \frac{1}{\Omega_0^2 + (\mathrm{i}\omega \mp \gamma)^2} = \frac{1}{\omega_0^2 - \omega^2 \mp 2\mathrm{i}\gamma\omega} \tag{6.3.18}$$

The last equality makes use of the relationship between the oscillator frequency and reduced frequency: $\Omega_0 = \sqrt{\omega_0^2 - \gamma^2}$.

This page titled 6.3: Complex formulation of the driven dipole oscillator is shared under a CC BY-NC-SA 4.0 license and was authored, remixed, and/or curated by Andrei Tokmakoff via source content that was edited to the style and standards of the LibreTexts platform.

6.4: Response of an Impulsively Driven Oscillator

Within the driven oscillator model, there are three molecular parameters that can be obtained from an absorption spectrum: ω_0 , γ, and μ'. However, these parameters can also be obtained by following a different experimental approach. We instead apply a momentary, or impulsive, driving force of magnitude F_0 to an oscillator at rest

$$F_{\text{ext}}(t) = F_0\delta(t - t_0) \tag{6.4.1}$$

Here again the applied force is related to the incident field strength through $F_0 = \mu'\mathcal{E}_0$. Although it is challenging at the molecular scale, if we can observe the motion of the bound particle following the impulse, we can in principle reveal the same information. Setting $t_0 \rightarrow 0$ in this equation and applying the initial conditions $Q(0) = 0$ and $V(0) = \dot{Q}(0) = 0$, the transient solution to eq. (6.2.24) is

$$Q(t) = \frac{F_0}{m\Omega_0} \exp(-\gamma t) \sin \Omega_0 t \tag{6.4.2}$$

The resulting exponentially damped sinusoidal oscillations are illustrated in Figure 6.4.1.

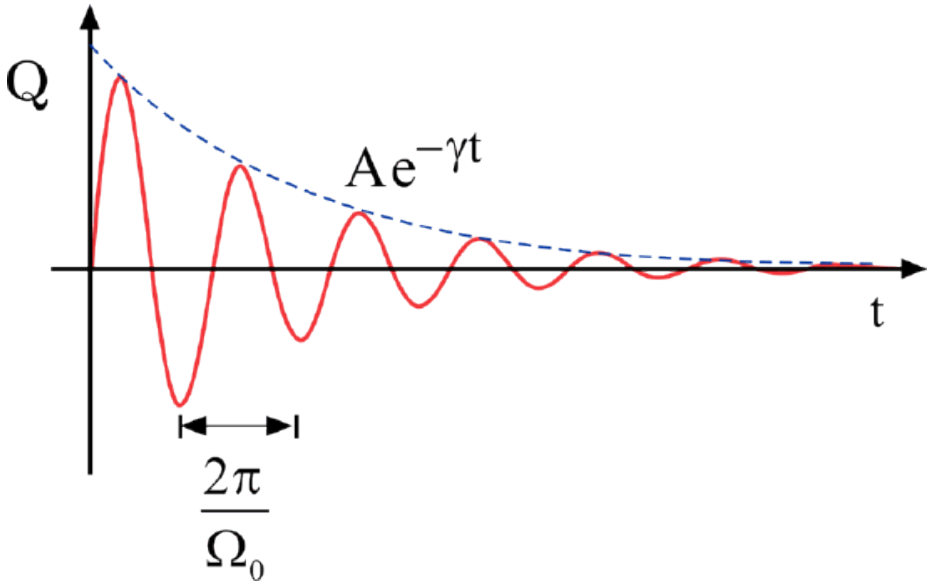


Figure 6.4.1: Transient behavior of a weakly damped oscillator abruptly kicked from its equilibrium position, $Q(0) = 0$, with an impulsive driving force.

Linear response theory provides the formal framework that relates the time-domain response of the oscillator and frequency domain representations of the absorption spectrum. We will discuss this in more detail later, but it is worth summarizing some of the results here. Starting with the time-dependent behavior, linear response theory describes the changes of a molecular variable A from an equilibrium value $\langle A \rangle$ when it is driven by a weak external force, $f(t)$. The time-dependent change of A can be written as a convolution of the time-dependent external force with the impulse response function $R(t)$.

$$\delta A(t) = \overline{A(t)} - \langle A \rangle = \int_0^\infty d\tau\, R(\tau) f(t - \tau) \tag{6.4.3}$$

Here, τ is the time interval between the application of the force and the observation of A. $R(t)$ describes the material properties and is not dependent on the force. In the limit that the driving force is a delta function perturbation, like eq. (6.4.1), the behavior of $\delta A(t)$ is directly proportional to $R(t)$.

In the case of the driven dipole oscillator, we can equate $\delta A(t)$ in eq. (6.4.3) with the magnitude of the dipole induced by the light $\mu(t) = \mu' Q(t)$ where $Q(t)$ is given by eq. (6.4.2). Comparing these equations, we can write:

$$\mu(t) = \mathcal{E}_0 R(t) \tag{6.4.4}$$

where the response function is given by

$$R(t) = \frac{\mu'^2}{m\Omega_0} \exp(-\gamma t) \sin \Omega_0 t \tag{6.4.5}$$

Here, all of the molecular terms including μ' have been folded into the response function.

Linear response theory also connects the real-valued, time-domain response function to its complex, frequency-dependent representation, the susceptibility $\tilde{\chi}(\omega)$

$$\delta\overline{A(\omega)} = \tilde{f}(\omega)\tilde{\chi}(\omega) \tag{6.4.6}$$

The function $\tilde{f}$ is a complex, frequency-domain representation of the driving force, obtained from the Fourier transform of $f(t)$. The susceptibility will play an important role in describing the how a medium is polarized in response to the application of a light field. In linear response theory, it is determined from the Fourier–Laplace transform (single-sided Fourier transform) of R.

$$\tilde{\chi}(\omega) = \int_0^\infty d\tau\, R(\tau) e^{\mathrm{i}\omega\tau} \tag{6.4.7}$$

$\tilde{\chi}$ is complex and can be written

$$\tilde{\chi}(\omega) = \chi'(\omega) + \mathrm{i}\chi''(\omega) \tag{6.4.8}$$

where χ' and χ'' are the real and imaginary parts of the susceptibility, respectively.

Returning the impulsively driven oscillator, if we apply the Fourier transform in eq. (6.4.7) to the response function in eq. (6.4.5), we find that the susceptibility of the dipole oscillator is

$$\tilde{\chi}(\omega) = \frac{\mu'^2}{m}\left[\frac{(\omega_0^2 - \omega^2)}{(\omega_0^2 - \omega^2)^2 + (2\gamma\omega)^2} + \mathrm{i}\frac{2\gamma\omega}{(\omega_0^2 - \omega^2)^2 + (2\gamma\omega)^2}\right] \tag{6.4.9}$$

We see that this expression has a similar form to the steady state time dependent behavior in eqs. (6.2.28) and (6.3.7), in which the amplitude of the real and imaginary components of the susceptibility of map onto the $\cos\omega t$ and $\sin\omega t$ terms of $Q(t)$. Both expressions reflect a frequency-dependent displacement of the oscillator which is maximized by the resonance condition $\omega = \omega_0$. The imaginary component of the susceptibility $\chi''(\omega)$ and corresponding $\sin\omega t$ time-dependence describe the resonance condition that leads to the highest oscillator displacement and largest absorption of energy by the oscillator. The real part of susceptibility χ' corresponds to off-resonance driving of the oscillator by the field and the resulting phase shift of the oscillator motion relative to its resonance condition. The absorption spectrum is then proportional to the imaginary part of the susceptibility from $P_{\mathrm{abs}}(\omega) \sim \mu'^2\mathcal{E}_0^2\ \chi''_Q(\omega)$.

The imaginary and real parts of the oscillator susceptibility are plotted in Figure 6.4.2, illustrating their corresponding absorptive and dispersive lineshapes. Importantly, this example illustrates the intrinsic Fourier transformation relationships between the dynamical behavior of matter under light excitation (time-domain spectroscopy) and the absorption spectrum (frequency-domain spectroscopy). We will investigate these relationships in more detail when we look at condensed matter problems and the quantum representation of the lineshape.

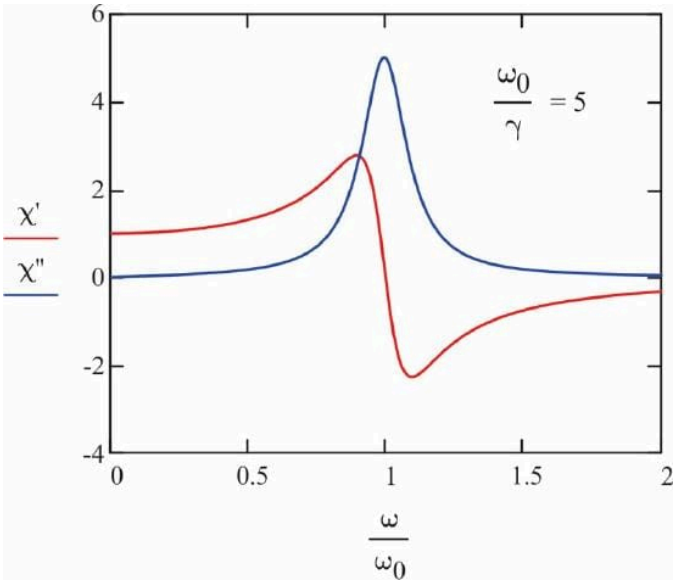


Figure 6.4.2: Illustration of the absorptive and dispersive lineshapes associated with the imaginary (blue) and real (red) parts of the susceptibility, respectfully.

This page titled 6.4: Response of an Impulsively Driven Oscillator is shared under a CC BY-NC-SA 4.0 license and was authored, remixed, and/or curated by Andrei Tokmakoff via source content that was edited to the style and standards of the LibreTexts platform.

6.5: Polarizability

Our classical description of spectroscopy and the driven oscillator model can also be used to give us insight into the light-matter interactions mediated by atomic and molecular polarizability. Polarizability refers to the ability of electromagnetic radiation to shift electron density within molecules and thereby induce dipole moments. It is a critical component of light matter interactions in the non-resonant case, i.e. in the absence of the resonant interactions that we focused on for absorption spectroscopy with $\omega \approx \omega_0$. Let's begin by using classical reasoning to understand how the bound electrons displaced by an electric field induce an electronic dipole moment and use this to define the polarizability.

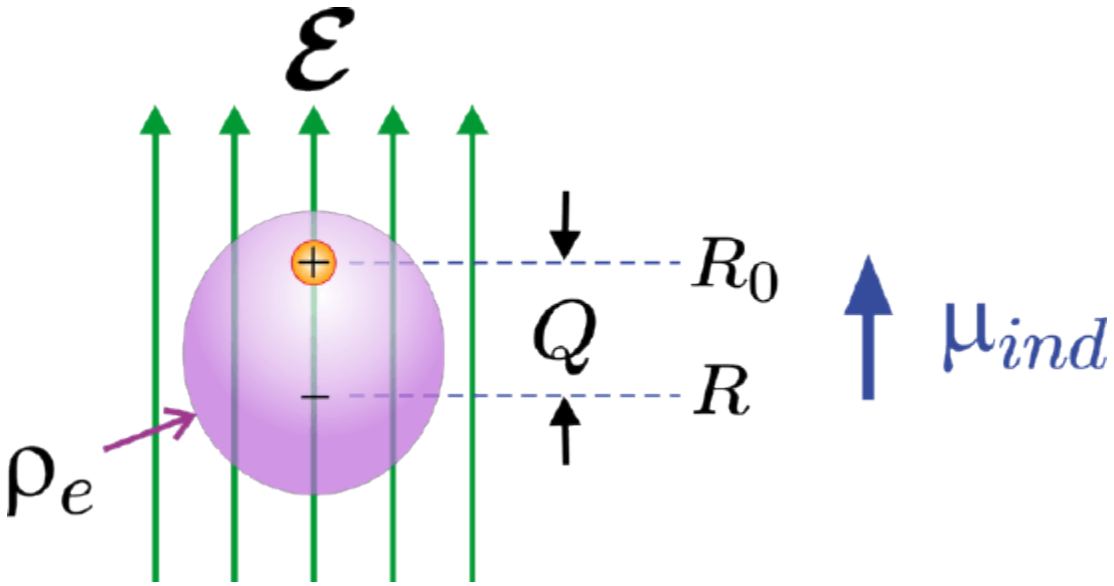


Figure 6.5.1: Illustration of how an electric field polarizes the electron density about an atom, and the variables for the classical model.

Atomic polarizability in a static field

We observe that, when an electric field is applied to an atom or molecule, it displaces charges in response to the field to lower the total energy. The distribution of bound electrons within a molecule will distort away from their equilibrium configuration, or polarize, thereby inducing a dipole moment, even in those atoms of molecules that don't have a dipole in the absence of the field. This effect is illustrated in Figure 6.5.1 for the case of an atom, showing how application of a field leads to the displacement of electron density ρ_e in the opposite direction of the field, resulting a shift of electronic charge density from a mean position R_0 to R. The relatively massive nucleus is hardly affected relative to the light electrons such that its position and thereby the center of positive nuclear charge remains at R_0. This results in an induced dipole moment that depends on the degree that electronic density is displaced, the charges on the nuclei, and the magnitude of the field. Specifically, the microscopic factor that describes the proportionality between the strength of the applied electric field $\mathcal{E}_{\text{ext}}$ and the induced dipole moment μ_{ind} is the atomic or molecular polarizability:

$$\mu_{\text{ind}} = \alpha \mathcal{E}_{\text{ext}} \tag{6.5.1}$$

The SI units for α are Cm^2V^{-1}, but it is typically quoted as the polarizability volume $\alpha/4\pi\varepsilon_0$ in units of m^3.

Let's calculate the polarizability classically by describing what happens to the charges on the application of the field. The classical dipole moment is calculated by integrating over charge densities for electrons and nuclei, but we want to just illustrate the concept with a simple classical approach. Let's imagine that an atom's electronic charge q_e is distributed uniformly through a sphere of radius a and that the nucleus is a point charge q_N. Before applying the external field $\mathcal{E}_{\text{ext}}$, the nucleus and sphere are centered at R_0. The internal electric field experienced by the nucleus as a result of electronic charge density is given by

$$\mathcal{E}_e(R) = -\frac{1}{4\pi\varepsilon_0}\frac{q_e(R-R_0)}{a^3} \tag{6.5.2}$$

We will consider small perturbative shifts in the position of the electron density, so that applying a field does not change the shape of the spherical electron density, but merely displaces it from R_0. Then, the restoring force that the electrons exert on the nucleus is $F_{e\to N}(R) = q_N\mathcal{E}_e(R)$, which we can invert to obtain the force that the nucleus exerts on the electrons

$$F_{N\to e} = -F_{e\to N} = -\frac{1}{4\pi\varepsilon_0}\frac{q_e q_N}{a^3}(R - R_0) \tag{6.5.3}$$

Note the linear form of this equation $F = -\kappa(R - R_0)$, where κ is the force constant for displacing the electron density:

$$\kappa = \frac{-q_e q_N}{4\pi\varepsilon_0 a^3} \tag{6.5.4}$$

If we now apply a uniform external electric field to the atom, its force on the electrons is

$$F_{\mathcal{E}\to e} = q_e\mathcal{E}_{\text{ext}} \tag{6.5.5}$$

We can now solve for the displacement in the electronic charge density relative to the nucleus by finding the condition where the forces on the electronic charge from the external field and from the nucleus match each other: $F_{N\to e}(R) = F_{\mathcal{E}\to e}$ or

$$-q_N\mathcal{E}_e(R) = q_e\mathcal{E}_{\text{ext}} \tag{6.5.6}$$

Substituting eq. (6.5.2) into this expression gives us an expression for the displacement of the electron density as a linear function of the applied external field:

$$R - R_0 = \frac{4\pi\varepsilon_0 a^3}{q_N}\mathcal{E}_{\text{ext}} \tag{6.5.7}$$

We also see the intuitive observation that the displacement is inversely proportional to the nuclear charge. That is, a higher positive nuclear charge makes it that much harder to displace the electrons from their equilibrium position.

From the displacement in eq. (6.5.7), we can calculate the dipole moment induced by the external field. In practice, it is proper to find the difference in electronic charge density before and after the application of the field, but we are after simple insights. We can recognize that q_e and q_N are, generally, not the charges of the bare particles, but effective charges that describe a valence electron interacting with a screened nucleus and the external field. As a result, it's effective for calculating the dipole to assume that $q_e = -q_N = q$. We also assume that the position and magnitude of q_N don't change during application of the field. In that case we can assume that the induced dipole is proportional to q_e: $\mu_{\text{ind}} = q_e(R - R_0)$. Then, from eq. (6.5.7) we find

$$\mu_{\text{ind}} = 4\pi\varepsilon_0 a^3\mathcal{E}_{\text{ext}} \tag{6.5.8}$$

As anticipated from eq. (6.5.1), we find a linear proportionality between the applied electric field and the induced dipole moment. The corresponding atomic polarizability is given by

$$\alpha = 4\pi\varepsilon_0 a^3 \tag{6.5.9}$$

This result confirms that the ability to distort the electron density of an atom is proportional to the volume of space over which it is distributed, in this case $\alpha = 3\varepsilon_0 V_{\text{atom}}$.

How well does this model do? We first have to ask, which type of radius is appropriate? Comparing the van der Waals radius ($a = 1.83$ Å) and covalent radius ($a = 0.96$ Å) for atomic argon results in polarizability volumes of $\alpha/4\pi\varepsilon_0 = 6.13$ Å^3 and 0.88 Å^3, which can be contrasted with the experimental value of 1.66 Å^3.(1) The same comparison done for hydrogen, with van der Waals radius (1.20 Å) and Bohr radius (0.53 Å), leads to polarizability volumes of 1.73 Å^3 and 0.15 Å^3, compared to the experimental values of 0.67 Å^3.(1) The model is satisfying in the sense that it puts us in within the correct order of magnitude and illustrates certain physical trends, but it has enough uncertainty and variation from atom to atom that that it's not very useful quantitatively. A perhaps more useful application is to invert this calculation to interpret the effective radii of the electron density that corresponds to the experimental polarizability. In that case, we find that $a = 1.18$ Å and 0.87 Å for argon and hydrogen respectively.

The extension of such classical models to molecular polarizabilities adds additional concerns that make them impractical. In addition to the variation of polarizability with different atoms and the types of bonds that they participate in, the polarizability of a molecule is anisotropic and can depend significantly on nuclear configuration. For instance, if one changes a bond length the molecular polarizability can change linearly with displacement in an analogous manner to our earlier discussion of induced dipole moments: $\alpha = \alpha_0 + \alpha' Q$, where α_0 is a static polarizability and α' is a polarizability derivative. Even so, within similar types

of molecules, the molecular polarizability does correlate strongly with molecular volumes, and models that model polarizability as classical induced dipoles remain an active area of research.

Polarizability of the driven oscillator

We have established the phenomenology for the polarizability, however in the context of a static field. For light-matter interactions, the dynamic electromagnetic field can induce dipole moments in non-polar and non-absorbing media which oscillates with the periodicity of the field. These oscillating dipoles can in turn become sources for further interactions, such as Raman or light scattering. The polarizability is similarly closely related to the dielectric susceptibility and index of refraction that govern the optical and electrical properties of condensed matter, as we will see later. Critical to all these topics is the frequency dependence of the polarizability, which we can address with the driven harmonic oscillator model. We will equate the oscillator coordinate with the degree of electronic charge displacement $Q = R - R_0$ and define the particle as a single electron with mass m_e and charge q.

The force constant κ in eq. (6.5.4) can be rewritten with eq. (6.5.9) as $\kappa = q^2/\alpha$, which allows us to calculate the resonance frequency for the bound electron cloud directly from a polarizability using $\omega_0 = \sqrt{\kappa/m_e}$, or

$$\omega_0 = \frac{q}{\sqrt{\alpha m_e}} \tag{6.5.10}$$

Let's calculate ω_e. Taking a representative polarizability volume for atoms and small molecules of $\alpha = 2.0\ \text{Å}^3$, we find a resonance frequency of $\omega_0/2\pi = 1.8 \times 10^{15}\ \text{Hz}$. This is equivalent to a period of $0.5\ \text{fs}$, or absorption at a deep-UV wavelength of $167\ \text{nm}$. Despite the limitations of classical thinking, this calculation reveals an important observation. The intrinsic resonances associated with polarizing electrons in molecules are typically of very high frequency, reflecting the extremely rapid dynamics of electrons that aren't highly delocalized. These frequencies exceed the most common range for molecular spectroscopy in the UV, visible, infrared and terahertz/microwave regimes that we use for studying the structure and dynamics of nuclei, bonds, and molecular valence electrons. Thus, within this atomic polarizability model, the influence of optical and infrared radiation on polarizable electrons in matter is typically in a regime where $\omega \ll \omega_e$.

For the interaction of the light and electron, we consider the electric field to have the same form as before; however, in this case we will take the force that the field exerts on the electron to be calculated from eq. (6.5.5), or

$$F_{\text{ext}}(t) = q\mathcal{E}_0 \cos \omega t \tag{6.5.11}$$

Thus, with the substitution of q for μ', all of the expressions that redrived for the driven oscillator response remain the same. The frequency dependent displacement of the oscillator $\tilde{Q}(\omega)$ in eq. (6.3.5) allows us to write the induced dipole moment as

$$\tilde{\mu}_{\text{ind}}(t) = \frac{q^2}{m_e} \frac{1}{(\omega^2 - \omega_0^2) + 2\text{i}\omega\gamma} \mathcal{E}_{\text{ext}}(t) \tag{6.5.12}$$

If we next compare this with the definition of the polarizability in eq. (6.5.1), we find that the polarizability is given by the complex quantity

$$\tilde{\alpha}(\omega) = \frac{q^2}{m_e} \frac{1}{(\omega^2 - \omega_0^2) + 2\text{i}\omega\gamma} \tag{6.5.13}$$

Where the real and imaginary parts of the polarizability $\tilde{\alpha}(\omega) = \alpha'(\omega) + \text{i}\alpha''(\omega)$ are the same as those given for the susceptibility in eq. (6.4.8) with the substitution of q for μ'. Note, when the complex polarizability is evaluated at zero frequency (the static limit), this expression recovers eq. (6.5.10).

So, what is the difference between the polarizability and susceptibility? Looking forward our discussion of condensed matter, α is an intrinsic molecular property whereas χ is a macroscopic property on scales much larger than the wavelength of light. In a dilute gas of N non-interacting molecules, χ is just proportional to $N\alpha$, but in condensed matter χ will also need to account for the interactions of the polarizable molecules with each other and the medium they are embedded in. Furthermore, the microscopic induced dipole in our model, μ, will be replaced by the macroscopic polarization $P = \varepsilon_0 \chi \mathcal{E}$, a dipole moment density.

More generally, the polarizability of electrons in polyatomic molecules and condensed matter is also influenced by changing nuclear positions, which we have not addressed here. Therefore the expression in eq. (6.5.12) can be interpreted more broadly. The resonance frequency ω_0 can be interpreted as any coordinate for bound charges and their natural resonance frequency that gives rise to a displacement of electron density from their average configuration, such as the vibration of molecules.

In discussing the classical driven oscillator, we have invoked two notations to represent how much charges within molecules are displaced when driven by an oscillating electric field. We used the dipole derivatives $\mu' = \partial\mu/\partial Q$ in discussing absorption spectroscopy and the magnitude of the displaced electronic charge q in discussing the polarizability α. Both have units of coulombs (C); what is the difference? Within the context of this model there isn't a significant difference, but the differences will become more apparent as we look at the molecular factors governing the interactions, whether we are near a molecular resonance, and in nonlinear spectroscopy. In practice one language is more useful for discussing resonant interactions, whereas the other is more common for off-resonant interactions.

This can be illustrated by combining both forms of the interaction in considering the light-matter interaction potential $V = -\mu\mathcal{E}$. For absorption, the force on this oscillator depends on $-\partial V/\partial Q$ and thereby μ'. This is equivalent to saying that the molecule's dipole moment varies about an average value μ_0 as the oscillator vibrates *even in the absence of a field*: $\mu = \mu_0 + \mu' Q$. In the case of the polarizability there is an additional contribution that arises with the field present—the induced dipole moment $\mu_{\mathrm{ind}} = \alpha\mathcal{E}$. Combining all of these factors, we find that the magnitude of the interaction potential is

$$\begin{aligned} V &= -\mu\mathcal{E} \\ &= -(\mu_0 + \mu' Q + \mu_{\mathrm{ind}})\,\mathcal{E} \\ &= -\mu_0\mathcal{E} - \mu' Q\mathcal{E} - \alpha\mathcal{E}^2 \end{aligned} \tag{6.5.14}$$

The second term in the interaction energy is proportional to μ' and scales linearly in $\mathcal{E}$ and Q. It results in resonant absorption at a natural frequency governed by the molecule's potential energy surface. The final term that depends on α scales as $\mathcal{E}^2$ because the electric field serves first to induce a dipole moment then exchanges energy with the oscillator via this induced dipole. This term, which describes Raman spectroscopy and light scattering, is most likely to dominate when we have strong electric fields and are far from resonance.

References

(1) Experimental Polarizabilities. *Computational Chemistry Comparison and Benchmark DataBase*, National Institute of Standards and Technology: 2022. https://cccbdb.nist.gov/expdatax.asp

This page titled 6.5: Polarizability is shared under a CC BY-NC-SA 4.0 license and was authored, remixed, and/or curated by Andrei Tokmakoff via source content that was edited to the style and standards of the LibreTexts platform.

6.6: Appendix- Laplace Transform Solution for the Driven Damped Oscillator

The equation of motion for the driven oscillator is

$$\ddot{x} + 2\gamma\dot{x} + \omega_0^2 x = \frac{F_0}{m}\cos\omega t \tag{6.6.1}$$

with initial conditions $x(0) = x_0$ and $\dot{x}(0) = v_0$.

The Laplace transform $\mathcal{L}$ of a time-domain function $f(t)$ is defined as:

$$\mathcal{L}\{f(t)\} = F(s) = \int_0^\infty e^{-st} f(t)\, dt \tag{6.6.2}$$

where s is a complex variable that is conjugate to t. The Laplace transform assists in solving differential equations in t (where $t \geqslant 0$), by converting them into algebraic equations in s. We can readily incorporate initial conditions as $s(0)$, and it's particularly useful for use with step and impulsive response problems.

The inverse Laplace transform from the s domain to the time domain, $f(t) = \mathcal{L}^{-1}\{F(s)\}$, is defined by

$$f(t) = \frac{1}{2\pi \mathrm{i}} \int_{c-\mathrm{i}\infty}^{c+\mathrm{i}\infty} e^{st} F(s)\, ds \tag{6.6.3}$$

where c is a real number chosen so that singularities in $F(s)$ are to the left of the line $\mathrm{Re}(s) = c$, and the integral is taken along the line in the complex plane $s = c + \mathrm{i}\omega$.

For our equation, the Laplace transform for the time dependent terms in eq. (6.6.1) are:

$$\begin{aligned} \mathcal{L}\{\dot{x}\} &= sX(s) - x_0 \\ \mathcal{L}\{\ddot{x}\} &= s^2X(s) - sx_0 - v_0 \\ \mathcal{L}\{\cos(\omega t)\} &= \frac{s}{s^2+\omega^2} \end{aligned} \tag{6.6.4}$$

So in the s domain eq. (6.6.1) becomes

$$s^2X(s) - sx_0 - v_0 + 2\gamma\left(sX(s) - x_0\right) + \omega_0^2 X(s) = \frac{F_0}{m}\frac{s}{s^2+\omega^2} \tag{6.6.5}$$

We can now solve for $X(s)$:

$$X(s) = \frac{\frac{F_0}{m}\frac{s}{s^2+\omega^2} + sx_0 + v_0 + 2\gamma x_0}{s^2 + 2\gamma s + \omega_0^2} \tag{6.6.6}$$

As a next step let's split this result into two parts. The first term in the numerator is the "homogeneous term" that results in transient behavior dependent on the initial conditions with $F_0 = 0$. The "particular term" are the remaining terms in the numerator, and these describe the steady-state behavior from the driving term.

$$\begin{aligned} X(s) &= \frac{sx_0 + v_0 + 2\gamma x_0}{s^2 + 2\gamma s + \omega_0^2} + \frac{F_0}{m}\frac{s}{\left(s^2+\omega^2\right)\left(s^2 + 2\gamma s + \omega_0^2\right)} \\ &= X_h(s) + X_p(s) \end{aligned} \tag{6.6.7}$$

So the time-domain solution will be obtained from the inverse Laplace transform of these two terms:

$$x(t) = x_h(t) + x_p(t) \tag{6.6.8}$$

For the homogeneous part, $X_h(s)$, we recognize that the denominator has roots determined by

$$\begin{aligned} 0 &= s^2 + 2\gamma s + \omega_0^2 \\ &= (s+\gamma)^2 + \left(\omega_0^2 - \gamma^2\right) \\ &= (s+\gamma)^2 + \Omega^2 \end{aligned} \tag{6.6.9}$$

where the reduced frequency $\Omega = \sqrt{\omega_0^2 - \gamma^2}$ and $\omega_0 > \gamma$. Why do we care about the roots? The Laplace inverse transform uses the fact that each simple pole (root) in s corresponds to a term in the time domain. A simple pole at $s = a$ gives a term e^{at}. When inverting something like

$$\frac{1}{(s+\gamma)^2 + \Omega^2} \tag{6.6.10}$$

which has complex poles at

$$s = -\gamma \pm \mathrm{i}\Omega \tag{6.6.11}$$

The inverse Laplace transform then results in damped oscillatory terms, $e^{-\gamma t}\cos(\Omega t)$ and $e^{-\gamma t}\sin(\Omega t)$:

$$\mathcal{L}^{-1}\left\{\frac{s+\gamma}{(s+\gamma)^2 + \Omega^2}\right\} = e^{-\gamma t}\cos(\Omega t) \tag{6.6.12}$$

$$\mathcal{L}^{-1}\left\{\frac{\Omega}{(s+\gamma)^2 + \Omega^2}\right\} = e^{-\gamma t}\sin(\Omega t) \tag{6.6.13}$$

So we can write the homogeneous term in eq. (6.6.7) as

$$X_h(s) = \frac{sx_0 + v_0 + 2\gamma x_0}{s^2 + 2\gamma s + \omega_0^2} = \frac{x_0(s+\gamma) + (v_0 + \gamma x_0)}{(s+\gamma)^2 + \Omega^2} \tag{6.6.14}$$

This leads to the inverse Laplace transform

$$x_h(t) = e^{-\gamma t}\left[x_0\cos(\Omega t) + \frac{v_0 + \gamma x_0}{\Omega}\sin(\Omega t)\right] \tag{6.6.15}$$

For the particular part (the steady-state solution):

$$X_p(s) = \frac{F_0}{m}\frac{s}{(s^2+\omega^2)\left(s^2 + 2\gamma s + \omega_0^2\right)} \tag{6.6.16}$$

we need to rewrite this in a form that allows us to make use of the following inverse transforms:

$$\mathcal{L}^{-1}\left\{\frac{s}{s^2+\omega^2}\right\} = \cos(\omega t) \tag{6.6.17}$$

$$\mathcal{L}^{-1}\left\{\frac{1}{s^2+\omega^2}\right\} = \frac{\sin(\omega t)}{\omega} \tag{6.6.18}$$

$$\mathcal{L}^{-1}\left\{\frac{s+\gamma}{(s+\gamma)^2 + \Omega^2}\right\} = e^{-\gamma t}\cos(\Omega t) \tag{6.6.19}$$

$$\mathcal{L}^{-1}\left\{\frac{1}{(s+\gamma)^2 + \Omega^2}\right\} = \frac{e^{-\gamma t}\sin(\Omega t)}{\Omega} \tag{6.6.20}$$

To use these, we can solve for the partial fraction decomposition of eq, (6.6.16) :

$$\frac{s}{(s^2+\omega^2)\left(s^2 + 2\gamma s + \omega_0^2\right)} = \frac{As + B}{s^2+\omega^2} + \frac{Cs + D}{s^2 + 2\gamma s + \omega_0^2} \tag{6.6.21}$$

To find A, B, C, D, we multiply both sides by the denominator on the left and equate coefficients by orders in s. It takes some effort, but you find

$$
\begin{aligned}
A &= -C = \frac{\omega^2 - \omega_0^2}{\left(\omega_0^2 - \omega^2\right)^2 + 4\gamma^2\omega^2} \\
B &= -\frac{2\gamma\omega^2}{\left(\omega_0^2 - \omega^2\right)^2 + 4\gamma^2\omega^2} \\
D &= \frac{2\gamma\omega_0^2}{\left(\omega_0^2 - \omega^2\right)^2 + 4\gamma^2\omega^2}
\end{aligned}
\tag{6.6.22}
$$

We also recognize that the terms involving C and D in the time domain will result in damped terms that decay as $e^{-\gamma t}$, and so the A and B terms are the ones that will give the steady-state behavior. So, for long times such that $\gamma t \gg 1$,

$$
x_p(t) = \frac{F_0}{m}\left[A\cos(\omega t) + \frac{B}{\omega}\sin(\omega t)\right] \tag{6.6.23}
$$

You can combine these into a single cosine via a phase shift as we described in Section 6.2.

$$
x_p(t) = \frac{F_0/m}{\sqrt{\left(\omega_0^2 - \omega^2\right)^2 + 4\gamma^2\omega^2}}\cos(\omega t - \phi) \tag{6.6.24}
$$

where

$$
\phi = \arctan\left(\frac{2\gamma\omega}{\omega_0^2 - \omega^2}\right) \tag{6.6.25}
$$

Combining the homogeneous and particular results, the final general solution is

$$
x(t) = e^{-\gamma t}\left[x_0\cos(\Omega t) + \frac{v_0 + \gamma x_0}{\Omega}\sin(\Omega t)\right] + \frac{F_0/m}{\sqrt{\left(\omega_0^2 - \omega^2\right)^2 + 4\gamma^2\omega^2}}\cos(\omega t - \phi) \tag{6.6.26}
$$

Impulse response

Now let's work the same problem for the impulsive driving force, also known as the Green's function for the system. We take the driving force to be a delta function application of a force of magnitude F_0 at time $t = 0$. The equation of motion is

$$
\ddot{x} + 2\gamma\dot{x} + \omega_0^2 x = \frac{F_0}{m}\delta(t) \tag{6.6.27}
$$

with initial conditions $x(0) = 0$ and $\dot{x}(0) = 0$.

We take the Laplace transform using the earlier expressions and $\mathcal{L}\{\delta(t)\} = 1$, which results in

$$
\left[s^2 + 2\gamma s + \omega_0^2\right] X(s) = \frac{F_0}{m} \tag{6.6.28}
$$

We again re-write $s^2 + 2\gamma s + \omega_0^2 = (s+\gamma)^2 + \Omega^2$ with $\Omega = \sqrt{\omega_0^2 - \gamma^2}$. Then, with the inverse transform

$$
\mathcal{L}^{-1}\left\{\frac{1}{(s+a)^2 + \Omega^2}\right\} = \frac{1}{\Omega}e^{-at}\sin(\Omega t) \tag{6.6.29}
$$

this leads to

$$
x(t) = \frac{F_0}{m\Omega}e^{-\gamma t}\sin(\Omega t) \qquad t \geqslant 0 \tag{6.6.30}
$$

This is the impulse response function

Let's repeat this for the case of the overdamped oscillator, for which $\gamma^2 > \omega_0^2$. In this case we are looking for the roots of the characteristic equation:

$$s^2 + 2\gamma s + \omega_0^2 = 0 \tag{6.6.31}$$

$$s_\pm = -\gamma \pm \sqrt{\gamma^2 - \omega_0^2} \equiv -\gamma \pm \Lambda \tag{6.6.32}$$

where the reduced damping constant $\Lambda = \sqrt{\gamma^2 - \omega_0^2} > 0$ and the roots are real and negative. As above, we use the partial fractions decomposition to rewrite the Laplace transform as

$$\begin{aligned} X(s) &= \frac{F_0}{m}\frac{1}{\left[s^2 + 2\gamma s + \omega_0^2\right]} \\ &= \frac{F_0/m}{(s - s_+)(s - s_-)} \\ &= \frac{A}{s - s_+} + \frac{B}{s - s_-} \end{aligned} \tag{6.6.33}$$

Solving for A and B, we find

$$\begin{aligned} A &= \frac{F_0/m}{2\Lambda} \\ B &= -\frac{F_0/m}{2\Lambda} \end{aligned} \tag{6.6.34}$$

Now we make use of the inverse Laplace transform

$$\mathcal{L}^{-1}\left\{\frac{1}{s - a}\right\} = e^{at} \tag{6.6.35}$$

To obtain

$$\begin{aligned} x(t) &= \frac{F_0}{m}\frac{1}{2\Lambda}\left[e^{s_+ t} - e^{s_- t}\right] \\ &= \frac{F_0}{m}\frac{1}{2\Lambda}\left[e^{(-\gamma+\Lambda)t} - e^{(-\gamma-\Lambda)t}\right] \\ &= \frac{F_0}{m\Lambda}e^{-\gamma t}\sinh(\Lambda t) \end{aligned} \tag{6.6.36}$$

This function rises from 0 as Λt reaches a maximum when $\Lambda t = \tanh^{-1}\Lambda/\gamma$, and exponentially decays to zero as $e^{-\gamma t}$.

This page titled 6.6: Appendix- Laplace Transform Solution for the Driven Damped Oscillator is shared under a CC BY-NC-SA 4.0 license and was authored, remixed, and/or curated by Andrei Tokmakoff.

6.7: Readings

Absorption by a driven oscillator

1. Siegman, A. E. *Lasers*; University Science Books, 1986.
2. Yariv, A. *Optical Electronics*, 4th ed.; Saunders College, 1991. DOI: 10.7907/5r87-m275

Complex formulation of the driven dipole oscillator

1. Chong, Y. D. Complex oscillations. *Complex Methods for the Sciences*; LibreTexts, 2021.

Polarizability

1. Griffiths, D. J. *Introduction to Electrodynamics*, 3rd ed.; Prentice-Hall, 1999.
2. Jackson, J. D. *Classical Electrodynamics*, 2nd ed.; Wiley, 1975
3. McHale, J. L. *Molecular Spectroscopy*, 1st ed.; Prentice-Hall, 1999.
4. Parson, W. W. *Modern optical spectroscopy:with exercises and examples from biophysics and biochemistry*, 2nd ed.; Springer, 2015. DOI: 10.1007/978-3-540-37542-5

This page titled 6.7: Readings is shared under a CC BY-NC-SA 4.0 license and was authored, remixed, and/or curated by Andrei Tokmakoff.

7: INTERACTION OF LIGHT AND MATTER

7.1: Introduction

7.2: Electromagnetic Plane Waves

7.3: Classical Light–Matter Interactions

7.4: Electric Dipole Hamiltonian

7.5: The Dipole Operator and Transition Dipole Matrix Elements

7.6: Absorption Cross Section

7.7: Quantitative Examples of Light-Matter Interactions

7.8: Appendix- Electromagnetic Fields and Potentials

7.9: Appendix- Magnetic Dipole and Electric Quadrupole Transitions

7.10: Readings

This page titled 7: Interaction of Light and Matter is shared under a CC BY-NC-SA 4.0 license and was authored, remixed, and/or curated by Andrei Tokmakoff via source content that was edited to the style and standards of the LibreTexts platform.

7.1: Introduction

From the classical model of spectroscopy, we have gained considerable insight and developed some intuition into the way matter absorbs light. Most of what we learned from that model will also hold true in quantum mechanical systems, but now the mathematical formalism and the physical representation of the matter is different. One important difference is that quantum mechanics builds on Hamilton's formulation of classical mechanics, rather than Newton's. The more significant differences are: (1) quantum mechanics constrains the energies allowed by a system and (2) the positions of the charged particle are represented probabilistically through a wavefunction. However, the resonant interaction, through which oscillating electromagnetic fields displace the bound charges in molecules, remains qualitatively the same.

Quantum mechanically, we will describe spectroscopy as a light-induced perturbation that couples quantum states of the matter. In the most general form, the Hamiltonian for the light-matter interaction would be

$$H = H_M + H_L + H_{LM} \tag{7.1.1}$$

Here H_M is the Hamiltonian encompassing the matter and can be time-dependent. In condensed phases, the matter is composed of numerous interacting molecules, some elements of which may or may not be influenced by the light. However, our starting point is to describe simple, isolated molecules to which we assign a time-independent Hamiltonian H_0. In eq. (7.1.1), H_L is the Hamiltonian for the electromagnetic field, and H_{LM} reflects its time-dependent interaction with the matter. A fully quantum mechanical treatment of H_L would describe light in terms of photons (as we do in Chapter 9), but we will here work with a semiclassical treatment in which the matter is described quantum mechanically and the electromagnetic field classically.

For the moment, we are only interested in the effect that the light has on the matter, so we assume that the electromagnetic field is simply a time-dependent potential that acts on the matter and is not influenced by the matter in return. In other words, we can ignore H_L, and replace H_{LM} with the interaction potential $V(t)$, so that the Hamiltonian assumes the familiar form

$$H \approx H_0 + V(t) \tag{7.1.2}$$

This form, of course, is exactly what we need to solve problems in the interaction picture, as discussed in Chapter 3.

As anticipated from our discussion of the driven two-level system and the Golden Rule, light acts to resonantly couple two quantum states. The resulting coherent superposition state will oscillate at the frequency of the driving electric field and have a time-dependent wavefunction that encodes sinusoidal variations in the probability density, thereby describing the oscillating position of the charged particles.

The key formal result from this chapter is the Electric Dipole Hamiltonian (EDH), an expression for the interaction potential $V(t)$ in eq. (7.1.2) that describes light-matter interaction in a manner similar to our classical treatment: through the displacement of charged particles. To obtain the EDH, we start by developing a classical Hamiltonian from the classical force experienced by a charged particle in an electromagnetic field, and then quantize the Hamiltonian by substituting the quantum operators for the particles of the matter:

$$\begin{aligned} p &\rightarrow -\mathrm{i}\hbar\hat{\nabla} \\ r &\rightarrow \hat{r} \end{aligned} \tag{7.1.3}$$

In the following three sections, we work through two steps to get to the EDH. We begin by reviewing the classical description of electromagnetic fields in terms of a vector potential. Next, we describe how the electromagnetic vector potential interacts with charged particles, first classically and then quantum mechanically. We then use the remaining sections to describe what the EDH means for the absorption of light.

This page titled 7.1: Introduction is shared under a CC BY-NC-SA 4.0 license and was authored, remixed, and/or curated by Andrei Tokmakoff via source content that was edited to the style and standards of the LibreTexts platform.

7.2: Electromagnetic Plane Waves

As a starting point, it is helpful to review the classical description of electromagnetic fields. In the appendix (Sec. 7.8), you will find a derivation of the plane wave solutions to the vector potential and electric and magnetic fields from Maxwell's equations; however, if this material is unfamiliar it is also helpful to review this material in other sources.(1)(2)(3) We will summarize this content for the case of free electromagnetic plane waves (i.e., in a vacuum), which can be used as a basis set for more complex waveforms.

The starting point for any discussion of electromagnetic waves is Maxwell's equations, which provide the unified formalism for describing the correlated behavior of dynamic electric and magnetic fields in matter. They can be applied on both a microscopic, molecular scale and developed into a continuum description on a macroscopic scale and thus form an effective basis for translating molecular phenomena between these limits. One of the important insights into electromagnetic radiation that emerges is that the electric field $\mathcal{E}(\mathbf{r},t)$ far away from charges and currents can be described by the wave equation

$$\nabla^2\mathcal{E}-\frac{1}{c^2}\frac{\partial^2\mathcal{E}}{\partial t^2}=0 \tag{7.2.1}$$

where c is the speed of light, which is related to the fundamental permittivities by

$$c=\frac{1}{\sqrt{\varepsilon_0\mu_0}} \tag{7.2.2}$$

This equation has many possible solutions satisfied by a field that is a function of the argument $(r-ct)$. Of particular interest to us are plane wave solutions of the form

$$\boldsymbol{\mathcal{E}}(\mathbf{r},t)=\tilde{\boldsymbol{\mathcal{E}}}_0e^{\mathrm{i}(\mathbf{k}\cdot\mathbf{r}-\omega t)} \tag{7.2.3}$$

which describe a wave of frequency ω traveling in the direction of the wavevector $\mathbf{k}$ at the speed of light. k is the wavenumber, which is related to the spatial oscillation of the field with a period (i.e. wavelength) of $\lambda=2\pi/k$. For any value of k, there are positive and negative wavevectors. Then the sinusoidal argument can take the form $(\mathrm{i}\mathbf{k}\cdot\mathbf{r}-\mathrm{i}\omega t)$ to describe propagation in the $\mathbf{k}$ direction, and $(-\mathrm{i}\mathbf{k}\cdot\mathbf{r}-\mathrm{i}\omega t)$ for backward propagating in the $-\mathbf{k}$ direction.

The wavevector and frequency are not independent but are governed by the dispersion relationship

$$k=|\mathbf{k}|=\frac{\omega}{c} \tag{7.2.4}$$

Writing $(kr-\omega t)$ as $k(r-ct)$ shows that the wavefronts of the plane waves described by (7.2.3) move with a phase velocity of c, the speed of light.

Note that when writing eq. (7.2.3) in complex form, it is understood that one should calculate the real part of this equation to obtain the real electric field. Although the real part is the physically observable field, the complex form serves many practical mathematical benefits when describing the superposition of waves and is particularly important in the quantum description of the light field.

Maxwell's equations describe the electric and magnetic fields of the light $(\mathcal{E},\mathcal{B})$, but, rather than fields, our Hamiltonian formulation of quantum mechanics requires a time-dependent potential. Fortunately, classical electromagnetic fields that vary in time and space are commonly represented through a vector potential A and a scalar potential φ using the relations

$$\boldsymbol{\mathcal{E}}=-\frac{\partial\mathbf{A}}{\partial t}-\nabla\varphi \tag{7.2.5}$$

$$\boldsymbol{\mathcal{B}}=\nabla\times\mathbf{A} \tag{7.2.6}$$

For electrostatics, the electric field is related to the electrostatic potential through $\mathcal{E}=-\nabla\varphi$, however, for a field that varies in both time and space, the electrodynamic potential must be expressed in terms of both $\mathbf{A}$ and φ. While the electric and magnetic fields of an electromagnetic wave are both vector quantities expressed in terms of six spatial variables (the x, y, and z components of $\mathcal{E}$ and $\mathcal{B}$) in addition to time, these are not independent variables. Maxwell's equations constrain them, allowing a potential representation with four variables (A_x, A_y, A_z, and φ). But these four variables are still not yet uniquely determined. There are

different potentials that can result in the same fields, and thus we have the freedom to select a gauge as a constraint that allows us to uniquely describe the electromagnetic wave. In our case we choose the Coulomb gauge

$$\nabla \cdot \mathbf{A} = 0 \tag{7.2.7}$$

which leads to a wave equation for the vector potential of a free electromagnetic wave in the absence of charges and currents:

$$\nabla^2 \mathbf{A} - \varepsilon_0 \mu_0 \frac{\partial^2 \mathbf{A}}{\partial t^2} = 0 \tag{7.2.8}$$

This, of course has the same form and properties as eq. (7.2.1)

For the case of plane waves, the solution to eq. (7.2.8) can be written as

$$\mathbf{A}\left(\mathbf{r}, t\right) = \tilde{A}_0 \hat{\varepsilon} e^{\mathrm{i}(\mathbf{k}\cdot\mathbf{r} - \omega t)} \tag{7.2.9}$$

and the real-valued vector potential is obtained as

$$\mathbf{A} = A_0 \hat{\varepsilon} \cos\left(\mathbf{k}\cdot\mathbf{r} - \omega t\right) \tag{7.2.10}$$

where $A_0 = |\tilde{A}_0|$, and the vector potential is directed along the polarization unit vector $\hat{\varepsilon}$. Since $\nabla \cdot \mathbf{A} = 0$, the polarization is orthogonal to the direction of propagation ($\mathbf{k} \cdot \hat{\varepsilon} = 0$), meaning it is a transverse electric field.

Using eq. (7.2.5) and eq. (7.2.6) we can obtain plane wave expressions for the electric and magnetic fields from the vector potential in eq. (7.2.9)

$$\boldsymbol{\mathcal{E}} = \mathrm{i}\omega \tilde{A}_0 \hat{\varepsilon} e^{\mathrm{i}(\mathbf{k}\cdot\mathbf{r} - \omega t)} \tag{7.2.11}$$

$$\boldsymbol{\mathcal{B}} = \mathrm{i}(\mathbf{k} \times \hat{\varepsilon}) \tilde{A}_0 e^{\mathrm{i}(\mathbf{k}\cdot\mathbf{r} - \omega t)} \tag{7.2.12}$$

We can see that eq. (7.2.11) has the same form as eq. (7.2.3), which allows us to see that the amplitudes of the fields are related to the vector potential as

$$\tilde{\boldsymbol{\mathcal{E}}}_0 = \mathrm{i}\omega \tilde{A}_0 \hat{\varepsilon} \tag{7.2.13}$$

$$\tilde{\boldsymbol{\mathcal{B}}}_0 = \mathrm{i}(\mathbf{k} \times \hat{\varepsilon}) \tilde{A}_0 \tag{7.2.14}$$

We observe that the electric field is polarized along the same direction as the vector potential, whereas the orientation of the magnetic field lies in the direction $\mathbf{k} \times \hat{\varepsilon}$. That is the electric field polarization and magnetic field polarization are orthogonal, and both are orthogonal to $\mathbf{k}$. For brevity it can sometimes be useful to define $\hat{b}$, a unit vector along the magnetic field polarization: $\hat{b} = \left[(\mathbf{k} \times \hat{\varepsilon}) / |\mathbf{k}|\right] = \hat{k} \times \hat{\varepsilon}$.

The leading factor of i in equations (7.2.11) and (7.2.12) doesn't mean that these quantities are imaginary; they are real. It helps to re-write them in real form:

$$\boldsymbol{\mathcal{E}} = \hat{\varepsilon} \mathcal{E}_0 \sin\left(\mathbf{k}\cdot\mathbf{r} - \omega t\right) \tag{7.2.15}$$

$$\boldsymbol{\mathcal{B}} = \hat{b} \mathcal{B}_0 \sin\left(\mathbf{k}\cdot\mathbf{r} - \omega t\right) \tag{7.2.16}$$

where the field amplitudes $\mathcal{E}_0 = |\tilde{\boldsymbol{\mathcal{E}}}_0|$ and $\mathcal{B}_0 = |\tilde{\boldsymbol{\mathcal{B}}}_0|$, and the relative amplitudes are related by the speed of light: $\mathcal{E}_0 / \mathcal{B}_0 = \omega / k = c$. By comparing these equations with eq. (7.2.10) we also see that the vector potential oscillates as $\cos\left(\omega t\right)$, whereas the electric and magnetic fields oscillate in-phase with each other as $\sin\left(\omega t\right)$. In other words, the potential and fields oscillate in-quadrature with each other—phase shifted by $\pi/2$. Thus, the additional factor of i in the complex amplitudes in eqs. (7.2.13) and (7.2.14) are indicative of the quadrature phase shift between the fields and the vector potential. We will encounter this representation of the in-quadrature phase relationship between two complex oscillating functions at various times in our discussion of spectroscopy.

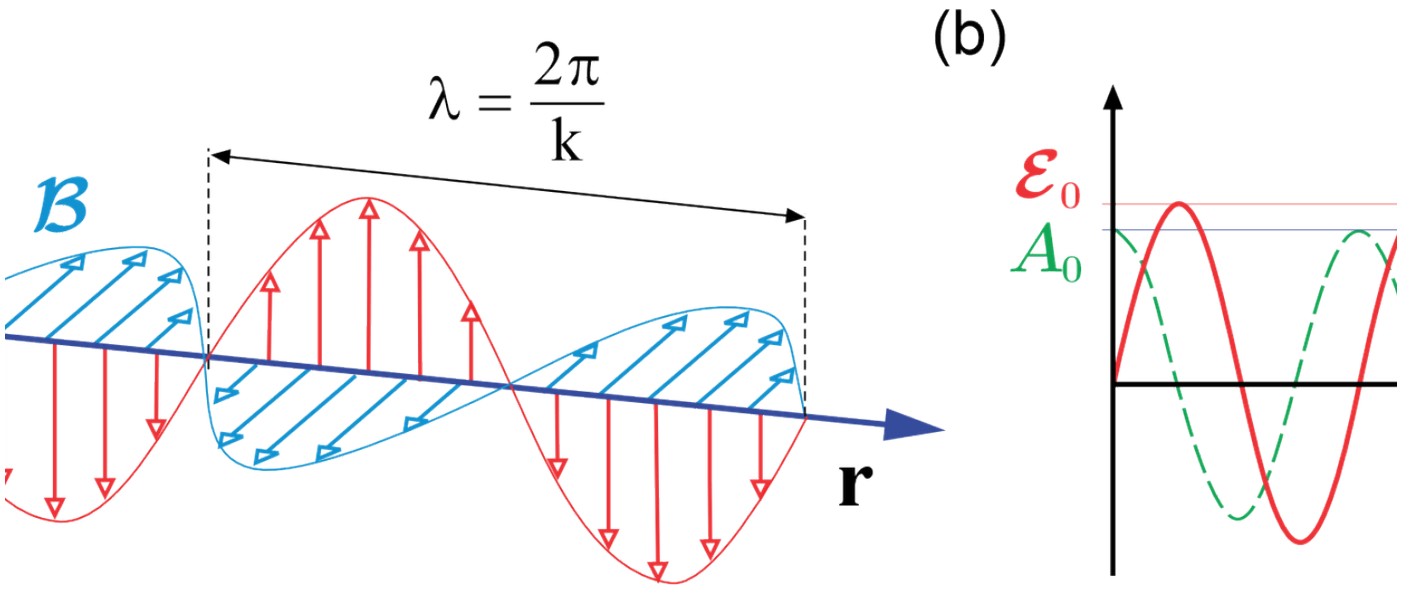


Figure 7.2.1: (a) Properties of linearly polarized free plane electromagnetic wave in space. The electric field (red) and magnetic field (blue) oscillate in phase with orthogonal polarization perpendicular to the direction of travel, $\mathbf{k}$. Waves travel with a velocity c and have a spatial periodicity, or wavelength, $\lambda = 2\pi/k$. (b) In time, oscillations of the electric field are phase-shifted with respect to the vector potential (green) by $\pi/4$ and have a period $2\pi/\omega$ Time and space variables are related by $\omega = kc$ and in vacuum $rt = c$.

Since electromagnetic fields carry energy, we need ways of describing a field's energy content and its energy flux, or rate of energy flow, in a manner that is experimentally accessible. The energy flux through a given area within a given time interval is given by the Poynting vector, which points in the direction of wave-propagation:

$$\mathbf{S} = \varepsilon_0 c^2 \mathcal{E} \times \mathcal{B} \tag{7.2.17}$$

This function oscillates with time as $\sin^2 \omega t$, so we determine the intensity I (or irradiance) by averaging the magnitude of $\mathbf{S}$ over one cycle of the field to find

$$I = \langle \mathbf{S} \rangle = \frac{1}{2} \varepsilon_0 c \mathcal{E}_0 \qquad (\mathrm{Wm}^{-2}) \tag{7.2.18}$$

The peak value of S is twice this time-averaged value.

Recognizing that the wave moves at the speed of light, we can obtain an alternate, time-independent interpretation of the field's energy content by dividing the energy flux per unit area (I) by the speed at which the wave travels (c). This results in an energy density for the field:

$$U = \frac{1}{2} \varepsilon_0 \mathcal{E}_0^2 \qquad (\mathrm{Jm}^{-3}) \tag{7.2.19}$$

The energy density U is important in the quantum description of light, when energy is expressed in terms of the number of photons—each with energy $\hbar\omega$—within a finite volume.

The electromagnetic plane waves described above are monochromatic waves in a vacuum and extended over all space. They have an exactly defined frequency, wavevector, and polarization vector. Similar to our discussion of free-particle eigenstates and wavepackets, we recognize that such a wave—extended over all space—does not exist in nature, and that realistic light fields are not monochromatic and have characteristics that vary in time and space. However, realistic electromagnetic fields can be expressed as a linear superposition of monochromatic waves. Indeed, monochromatic waves are a continuous orthonormal basis set by which we can express the general solution to eq. (7.2.8). As a periodic function, this is done effectively in k-space, using a Fourier transform to express the vector potential (or electric field) in terms of a k-space distribution function.

The vector potential basis set, also known as the *modes* of the radiation field, are defined as

$$\mathbf{A}_{\mathbf{k},\varepsilon}(\mathbf{r},t) = \hat{\varepsilon}_k \tilde{A}_{k,\varepsilon} e^{\mathrm{i}(\mathbf{k}\cdot\mathbf{r}-\omega_k t)} + \hat{\varepsilon}_k \tilde{A}^*_{k,\varepsilon} e^{-\mathrm{i}(\mathbf{k}\cdot\mathbf{r}-\omega_k t)} \tag{7.2.20}$$

Each plane wave mode is indexed by its wavevector k and polarization ε. We denote the dependence of frequency on wavevector by using the notation ω_k. For free electromagnetic waves in vacuum, $\omega = kc$ for all k, but we can already anticipate using dispersion relationships $\omega(k)$ to define more complex relations between ω and k in our description of electromagnetic waves in condensed matter. We also index the polarization vector in eq. (7.2.20) as $\hat{\varepsilon}_k$ since the general polarization state is expressed in term of a sum of contributions from two orthogonal transverse modes (i.e. $\hat{z}$ and $\hat{y}$ if the wave is traveling along $\hat{x}$). However, we will drop these indices if we are not describing polarization phenomena.

We can describe a general waveform in time and space by integrating waves of the form (7.2.20) over a mode amplitude distribution $\tilde{\mathbf{A}}(\mathbf{k})$

$$\mathbf{A}(\mathbf{r},t) = \frac{1}{(2\pi)^{3/2}} \int_{-\infty}^{+\infty} \tilde{\mathbf{A}}(\mathbf{k}) e^{-\mathrm{i}\omega_k t} e^{\mathrm{i}\mathbf{k}\cdot\mathbf{r}}\, d\mathbf{k} + \text{c.c.} \tag{7.2.21}$$

In defining $\tilde{\mathbf{A}}(\mathbf{k})$ we added a factor of $(2\pi)^{-3/2}$ as anticipated for Fourier transform relations in 3D. Then we can invert this equation to show that the k-space amplitude distribution is given by the Fourier transformation of the real space amplitude distribution at $t = 0$, $\mathbf{A}(\mathbf{r}) = \mathbf{A}(\mathbf{r},0)$,

$$\tilde{\mathbf{A}}(\mathbf{k}) = \frac{1}{(2\pi)^{3/2}} \int_{-\infty}^{+\infty} \mathbf{A}(\mathbf{r}) e^{-\mathrm{i}\mathbf{k}\cdot\mathbf{r}}\, d\mathbf{r} \tag{7.2.22}$$

It is therefore reasonable for us to equate $\tilde{\mathbf{A}}(\mathbf{k})$ with $A_{\mathbf{k},\varepsilon}$.

References

(1) Cohen-Tannoudji, C.; Diu, B.; Laloë, F. Quantum Mechanics; Wiley, 1977.

(2) Griffiths, D. J. *Introduction to Electrodynamics*, 3rd ed.; Prentice-Hall, 1999.

(3) Jackson, J. D. *Classical Electrodynamics*, 2nd ed.; Wiley, 1975.

This page titled 7.2: Electromagnetic Plane Waves is shared under a CC BY-NC-SA 4.0 license and was authored, remixed, and/or curated by Andrei Tokmakoff via source content that was edited to the style and standards of the LibreTexts platform.

7.3: Classical Light–Matter Interactions

As our first step toward a quantum model of light-matter interactions, we outline the derivation of a classical Hamiltonian in terms of the vector potential to describe how charged particles interact with an electromagnetic field. We start with the Lorentz expression for force that an electromagnetic field exerts on a particle with charge q and moving at velocity $\mathbf{v}$:

$$\mathbf{F} = q\left(\mathcal{E} + \mathbf{v} \times \mathcal{B}\right) \tag{7.3.1}$$

For most classical particles, the magnitude of the first term, the force from Coulomb's Law, far exceeds the second. Since the magnetic and electric field components of an electromagnetic wave scale in magnitude as $\mathcal{B}_0/\mathcal{E}_0 = 1/c$, their contributions to the force on a charged particle scale as ν/c, which is only significant for relativistic particles.

The derivation takes a sequence of steps to translate the forces described by eq. (7.3.1) into the potential energies used in Lagrangian mechanics and then into a Hamiltonian. In the first step, the Lorentz force can be related to the vector and scalar potentials using eqs. (7.2.7) and eq. (7.2.8). Writing eq. (7.3.1) for one dimension (x) in terms of the Cartesian components of $\mathcal{E}$, $\mathbf{v}$, and $\mathcal{B}$, we get:

$$F_x = q\left(\mathcal{E}_x + v_y\mathcal{B}_z - v_z\mathcal{B}_y\right) \tag{7.3.2}$$

With $\mathcal{E}_x = -\frac{\partial\varphi}{\partial x} - \frac{\partial A_x}{\partial t}$; $\mathcal{B}_z = \frac{\partial A_y}{\partial x} - \frac{\partial A_x}{\partial y}$; and $\mathcal{B}_y = \frac{\partial A_x}{\partial z} - \frac{\partial A_z}{\partial x}$.

In Lagrangian mechanics, this force can be expressed in terms of the total potential energy $\mathcal{U}$, which in the x dimension is

$$F_x = -\frac{\partial\mathcal{U}}{\partial x} + \frac{d}{dt}\left(\frac{\partial\mathcal{U}}{\partial v_x}\right) \tag{7.3.3}$$

By equating these forms of the force, we can show that the potential energy function is given by

$$\mathcal{U} = q\varphi - q\mathbf{v}\cdot\mathbf{A} \tag{7.3.4}$$

This result is derived elsewhere (1)(2) and is readily confirmed by inserting it into eq. (7.3.3).

We can now write a Lagrangian in terms of the kinetic and potential energy of the particle

$$L = T - \mathcal{U} \tag{7.3.5}$$

$$L = \frac{1}{2}m\mathbf{v}^2 + q\mathbf{v}\cdot\mathbf{A} - q\varphi \tag{7.3.6}$$

Then, the classical Hamiltonian is related to the Lagrangian as

$$\begin{aligned} H &= \mathbf{p}\cdot\mathbf{v} - L \\ &= \mathbf{p}\cdot\mathbf{v} - \frac{1}{2}m\mathbf{v}^2 - q\mathbf{v}\cdot\mathbf{A} - q\varphi \end{aligned} \tag{7.3.7}$$

To simplify the Hamiltonian, we note that the momentum of the particle is calculated from

$$\mathbf{p} = \frac{\partial L}{\partial\mathbf{v}} = m\mathbf{v} + q\mathbf{A} \tag{7.3.8}$$

which allows us to express the velocity of the particle as

$$\mathbf{v} = \frac{1}{m}(\mathbf{p} - q\mathbf{A}) \tag{7.3.9}$$

Substituting this velocity expression, eq. (7.3.9) into eq. (7.3.7), we find

$$H = \frac{1}{m}\mathbf{p}\cdot(\mathbf{p} - q\mathbf{A}) - \frac{1}{2m}(\mathbf{p} - q\mathbf{A})^2 - \frac{q}{m}(\mathbf{p} - q\mathbf{A})\cdot A + q\varphi \tag{7.3.10}$$

$$H = \frac{1}{2m}\left[\mathbf{p} - q\mathbf{A}(\mathbf{r},t)\right]^2 + q\varphi(\mathbf{r},t) \tag{7.3.11}$$

This is the classical Hamiltonian for a particle in an electromagnetic field, expressed in terms of the vector potential. In the Coulomb gauge used for our description of electromagnetic waves, $\varphi = 0$, and the last term is dropped.

What we observe in eq. (7.3.11) is that the electromagnetic vector potential influences the momentum of the charged particle, and we expect that this light-driven momentum will add to the internal momentum of bound particles in the absence of the field. The Hamiltonian for a single charged particle in a bound potential $\mathcal{U}_0(\mathbf{r})$ in the absence of an external field is

$$H_0 = \frac{\mathbf{p}^2}{2m} + \mathcal{U}_0(\mathbf{r}) \tag{7.3.12}$$

In the presence of the field, we can account for its time-dependent influence on the momentum of the particle as

$$H = \frac{1}{2m}(\mathbf{p} - q\mathbf{A}(\mathbf{r},t))^2 + \mathcal{U}_0(\mathbf{r}) \tag{7.3.13}$$

Expanding this Hamiltonian, we can re-write it in a form that emphasizes the field-induced changes to the particle.

$$H = H_0 - \frac{q}{2m}(\mathbf{p}\cdot\mathbf{A} + \mathbf{A}\cdot\mathbf{p}) + \frac{q^2}{2m}|\mathbf{A}|^2 \tag{7.3.14}$$

Here we are expressing the second term on the right with the expectation that $\mathbf{p}$ and $\mathbf{A}$ do not commute. It also indicates that the interaction strength depends not only on the magnitude of the vector potential, but that it only acts to alter the particle momentum in the direction of the vector potential's polarization.

Generally, the momenta and binding energies in H_0 make it the energetically dominant term in eq. (7.3.14), and $\mathbf{A}$ is small enough that it does not significantly change the potential experienced by the molecule. Since the last term is proportional to $\mathbf{A}^2$, it is small compared to the cross term, which is proportional to $\mathbf{A}$. For such weak electromagnetic fields, we can drop the $\mathbf{A}^2$ term, and the resulting Hamiltonian for light-matter interactions maps directly onto problems that we can formulate in the interaction picture:

$$H = H_0 + V(t) \tag{7.3.15}$$

$$V(t) = -\frac{q}{2m}(\mathbf{p}\cdot\mathbf{A} + \mathbf{A}\cdot\mathbf{p}) \tag{7.3.16}$$

The $\mathbf{A}^2$ term can become significant for extremely high field strength, when the field significantly distorts the potential binding molecules together—for instance, under ionizing conditions. Such effects would start to play a role at intensity levels $> 10^{15}$ $\mathrm{W/cm^2}$, which are present around high-energy and tightly-focused pulsed, femtosecond lasers.

References

(1) Cohen-Tannoudji, C.; Diu, B.; Laloë, F. *Quantum Mechanics, Volume 3: Fermions, Bosons, Photons, Correlations, and Entanglement*; Wiley, 2019; p 1492.

(2) Schatz, G. C.; Ratner, M. A. *Quantum Mechanics in Chemistry*; Dover Publications, 2002; pp 82-83.

This page titled 7.3: Classical Light–Matter Interactions is shared under a CC BY-NC-SA 4.0 license and was authored, remixed, and/or curated by Andrei Tokmakoff via source content that was edited to the style and standards of the LibreTexts platform.

7.4: Electric Dipole Hamiltonian

We are now ready to obtain the semi-classical Hamiltonian for a particle in an electromagnetic field by substituting the quantum mechanical momentum operator for the classical momentum in eq. (7.3.16). The vector potential $\mathbf{A}$ remains classical and only modulates the interaction strength:

$$\hat{\mathbf{p}} = -\mathrm{i}\hbar\nabla \tag{7.4.1}$$

$$V(t) = \frac{\mathrm{i}\hbar}{2m} q\left(\nabla\cdot\mathbf{A} + \mathbf{A}\cdot\nabla\right) \tag{7.4.2}$$

In the semiclassical case, we can show that $\nabla\cdot\mathbf{A} = \mathbf{A}\cdot\nabla$. Remembering that this product will be evaluated operating on a wavefunction, we can use the chain rule to write: $\nabla\cdot(\mathbf{A}\left|\psi\right\rangle) = (\nabla\cdot\mathbf{A})\left|\psi\right\rangle + \mathbf{A}\cdot(\nabla\left|\psi\right\rangle)$. Since $\nabla\cdot\mathbf{A} = 0$, the first term is zero.

With both terms in eq. (7.4.2) equal, the interaction potential is:

$$V(t) = -\frac{q}{m}\mathbf{A}\cdot\hat{\mathbf{p}} \tag{7.4.3}$$

$$V(t) = -\frac{q}{2m}(\hat{\varepsilon}\cdot\hat{\mathbf{p}})\left(\tilde{A}_0 e^{\mathrm{i}(\mathbf{k}\cdot\mathbf{r}_j-\omega t)} + \tilde{A}_0^* e^{-\mathrm{i}(\mathbf{k}\cdot\mathbf{r}-\omega t)}\right) \tag{7.4.4}$$

We can generalize eq. (7.4.3) for the case of multiple charged particles, as would be appropriate for a molecular Hamiltonian, by summing the interaction over the charges:

$$V(t) = -\sum_j \frac{q_j}{m_j}\mathbf{A}\left(\mathbf{r}_j, t\right)\cdot\hat{\mathbf{p}}_j \tag{7.4.5}$$

$$V(t) = -\sum_j \frac{q_j}{2m_j}(\hat{\varepsilon}\cdot\mathbf{p}_j)\left(\tilde{A}_0 e^{\mathrm{i}(\mathbf{k}\cdot\mathbf{r}_j-\omega t)} + \tilde{A}_0^* e^{-\mathrm{i}(\mathbf{k}\cdot\mathbf{r}_j-\omega t)}\right) \tag{7.4.6}$$

Generally, it is possible to neglect the dependence of the interaction potential on the wave vector ($\mathbf{k}$) when the wavelength of the field is much larger than the molecules we are interrogating. That is as $\lambda\to\infty$, $\mathbf{k}\to 0$. To look at this a bit closer, let's define $\mathbf{r}_0$ as the center of mass of a molecule, r_i as the position of charge i within the molecule, and $\delta\mathbf{r}_i = \mathbf{r}_i - \mathbf{r}_0$ as the distance between charge i and the center of mass. Therefore:

$$e^{\mathrm{i}\mathbf{k}\cdot\mathbf{r}_i} = e^{\mathrm{i}\mathbf{k}\cdot\mathbf{r}_0}e^{\mathrm{i}\mathbf{k}\cdot\delta\mathbf{r}_i} \tag{7.4.7}$$

The typical wavelengths used in spectroscopy—UV, visible, and infrared—are measured in hundreds to thousands of nanometers—orders of magnitude larger than the dimensions that describe the charge distributions of single molecules. Under those circumstances $\mathbf{k}\cdot\delta\mathbf{r}_i \ll 1$ and $e^{\mathrm{i}k\cdot\delta r_i}\to 1$. The term $e^{\mathrm{i}k\cdot r_0}$ is just a constant phase factor which we can set to $\mathbf{r}_0 = 0$ for an isolated molecule. The result is that the $\mathbf{k}\cdot\mathbf{r}$ terms in eq. (7.4.6) vanish. This is known as the electric dipole approximation.

There are circumstances, though, where one needs to retain the spatial dependence for certain other types of light-matter interactions, for instance when the electric or magnetic field gradient matters on the molecular scale. If so, we can expand $e^{\mathrm{i}k\cdot r}$ as

$$e^{\mathrm{i}\mathbf{k}\cdot\mathbf{r}} \approx 1 + \mathrm{i}\mathbf{k}\cdot\mathbf{r} - \frac{1}{2}[\mathbf{k}\cdot\mathbf{r}]^2 + \cdots \tag{7.4.8}$$

The leading term leads to the electric dipole transitions that we concern ourselves with here. The second term gives rise to (a) electric quadrupole transitions, (b) charge distribution interacting with the gradient of electric fields, and (c) magnetic dipole transitions, which are described in the appendix. These effects are typically smaller than electric dipole interactions by a factor of 10^3 but play important roles in describing the influence of magnetic fields or electron angular momentum of atomic and molecular spectroscopy, and in the origin of differential absorption of left- and right-circularly polarized light in circular dichroism spectroscopy.

For a single charged particle, the interaction Hamiltonian in eq. (7.4.8) in the electric dipole approximation is

$$V(t) = -\frac{q}{2m}(\hat{\varepsilon}\cdot\hat{\mathbf{p}})\left(\tilde{A}_0 e^{-\mathrm{i}\omega t} + \tilde{A}_0^* e^{\mathrm{i}\omega t}\right) \tag{7.4.9}$$

or more simply

$$V(t) = V_0 \cos \omega t \tag{7.4.10}$$

with

$$V_0 = -\frac{A_0 q}{m}(\hat{\varepsilon} \cdot \hat{\mathbf{p}}) \tag{7.4.11}$$

We can also express the EDH in terms of the light's electric field. Using eq. (7.2.13) we obtain

$$V(t) = -\frac{q}{2\mathrm{i}m\omega}(\hat{\varepsilon} \cdot \hat{\mathbf{p}}) \left(\tilde{\mathcal{E}}_0 e^{-\mathrm{i}\omega t} - \tilde{\mathcal{E}}_0^* e^{\mathrm{i}\omega t} \right) \tag{7.4.12}$$

As expected, the electric field is phase shifted with respect to the vector potential so that

$$V(t) = V_0 \sin \omega t \tag{7.4.13}$$

with

$$V_0 = -\frac{\mathcal{E}_0 q}{\omega m}(\hat{\varepsilon} \cdot \hat{\mathbf{p}}) \tag{7.4.14}$$

This is the electric dipole Hamiltonian which describes how the momentum of charged particles is influenced by a sinusoidally modulated, time-dependent electric field. We see that the interaction of light with matter in eq. (7.3.14) has now been cast into the familiar form $H = H_0 + V_0 \sin \omega t$ where V_0 is given by eq. (7.4.13) or equivalently eq. (7.4.10). The operators describing the charged particles—$\mathbf{p}$ in this case—only influence the strength of the interaction, V_0, and the time-dependence to this interaction is only due to the sinusoidal variation of the external field.

As anticipated, the interaction of light and matter using the electric dipole Hamiltonian is perfectly suited to describe spectroscopy in the interaction picture. To calculate the rates of absorption or emission by the matter, we can turn to the Golden rule expression for the rates of population transfer between initial (ℓ) and final (k) eigenstates of H_0 induced by a harmonic potential $V(t)$, which we derived in Section 3.7:

$$w_{k\ell} = \frac{\pi}{2\hbar} |V_{k\ell}|^2 \left[\delta(E_k - E_\ell - \hbar\omega) + \delta(E_k - E_\ell + \hbar\omega) \right] \tag{7.4.15}$$

From this expression we already know that there is a resonance requirement that matches the transition energy gap to the frequency of the driving field: $E_k - E_\ell = \pm\hbar\omega$. The next step is to evaluate the EDH matrix elements $V_{k\ell}$ to understand the factors that influence the strength of this interaction.

This page titled 7.4: Electric Dipole Hamiltonian is shared under a CC BY-NC-SA 4.0 license and was authored, remixed, and/or curated by Andrei Tokmakoff via source content that was edited to the style and standards of the LibreTexts platform.

7.5: The Dipole Operator and Transition Dipole Matrix Elements

We now turn to calculating the matrix element $V_{k\ell}$ which dictates how strongly the electromagnetic wave interacts with the charged particles. For the moment, we will neglect the vector nature of this interaction. Recognizing that potential is real but the matrix elements complex, we start with eq. (7.4.12), and write the matrix elements for the case of a single bound charged particle as

$$V_{k\ell} = -\frac{q}{\mathrm{i}m\omega}\,\tilde{\mathcal{E}}_0 \langle k|\,\hat{\mathbf{p}}\,|\ell\rangle \tag{7.5.1}$$

To evaluate the matrix elements of the momentum operator, it is helpful to use the commutator relationship between a particle's position and Hamiltonian which holds for central potential Hamiltonians of the form eq. (7.3.12):

$$\left[\hat{\mathbf{r}}, \hat{H}_0\right] = \frac{\mathrm{i}\hbar\hat{\mathbf{p}}}{m} \tag{7.5.2}$$

Solving for $\hat{p}$ in this expression, we can evaluate the matrix element in eq. (7.5.1) as

$$\begin{aligned}\langle k|\,\hat{\mathbf{p}}\,|\ell\rangle &= \frac{m}{\mathrm{i}\hbar}\left\langle k\left|\,\hat{\mathbf{r}}\hat{H}_0 - \hat{H}_0\hat{\mathbf{r}}\,\right|\ell\right\rangle \\ &= \frac{m}{\mathrm{i}\hbar}\left(\langle k|\,\hat{\mathbf{r}}\,|\ell\rangle\, E_\ell - E_k\,\langle k|\,\hat{\mathbf{r}}\,|\ell\rangle\right) \\ &= \mathrm{i}m\omega_{k\ell}\,\langle k|\,\hat{\mathbf{r}}\,|\ell\rangle\end{aligned} \tag{7.5.3}$$

So, by substituting back into eq. (7.5.1), we have

$$V_{k\ell} = -q\,\langle k|\,\hat{\mathbf{r}}\,|\ell\rangle\,\frac{\omega_{k\ell}}{\omega}\tilde{\mathcal{E}}_0 \tag{7.5.4}$$

For the case of many charged particles eq. (7.5.4) can be written

$$V_{k\ell} = -\frac{\omega_{k\ell}}{\omega}\tilde{\mathcal{E}}_0 \sum_j q_j\,\langle k|\,\hat{\mathbf{r}}_j\,|\ell\rangle \tag{7.5.5}$$

In this form, we observe that the matrix elements are related to a sum over the charge and position of the constituent particles; that is, the spatial distribution of charge within a molecule, or dipole moment. Therefore, it is helpful to define the dipole operator

$$\hat{\boldsymbol{\mu}} = \sum_j q_j\hat{\mathbf{r}}_j \tag{7.5.6}$$

The dipole operator $\hat{\mu}$ is the quantum analog of the classical dipole moment μ, which describes the distribution of charge density ρ in the molecule:

$$\mu = \int dr\, r\rho(r) \tag{7.5.7}$$

The strength of interaction between light and matter in eq. (7.5.5)

$$V_{k\ell} = -\frac{\omega_{k\ell}}{\omega}\tilde{\mathcal{E}}_0\mu_{k\ell} \tag{7.5.8}$$

is now proportional to matrix elements in the dipole operator

$$\mu_{k\ell} = \langle k|\,\hat{\boldsymbol{\mu}}\,|\ell\rangle \tag{7.5.9}$$

which is known as the transition dipole moment. The magnitudes of the transition dipole matrix elements dictate whether there can be efficient absorption of light, which requires a change of molecular distribution of charge between $|k\rangle$ and $|\ell\rangle$. This matrix element is the foundation underlying the spectroscopic selection rules, which describe what light-driven transitions are allowed. We will look into this is some detail in Chapter 10.

We can now add back the vector nature of the light-matter interaction. From eq. (7.4.12) we see that V_0 depends on the alignment of the light's electric field with the dipole moment, $\mathcal{E}_0\hat{\varepsilon}\cdot\hat{\boldsymbol{\mu}} = \boldsymbol{\mathcal{E}}_0\cdot\hat{\boldsymbol{\mu}}$, so the corresponding matrix elements are

$$V_{k\ell} = -\frac{\omega_{k\ell}}{\omega}(\boldsymbol{\mathcal{E}}_0\cdot\boldsymbol{\mu}_{kl}) \tag{7.5.10}$$

Substituting this into the Golden Rule eq. (7.4.15) leads to an expression for the rate of transitions between quantum states induced by the light field:

$$\begin{aligned} w_{k\ell} &= \frac{\pi}{2\hbar}|\mathcal{E}_0|^2\,\frac{\omega_{k\ell}^2}{\omega^2}|\boldsymbol{\mu}_{kl}|^2\left[\delta(E_k - E_\ell - \hbar\omega) + (E_k - E_\ell + \hbar\omega)\right] \\ &= \frac{\pi}{2\hbar^2}|\mathcal{E}_0|^2\,|\boldsymbol{\mu}_{kl}|^2\left[\delta(\omega_{k\ell} - \omega) + \delta(\omega_{k\ell} + \omega)\right] \end{aligned} \tag{7.5.11}$$

We observe that the resonance condition $E_k - E_\ell = \pm\hbar\omega$ dictates that the frequency ratio $\omega_{k\ell}/\omega = 1$, and therefore this factor can be dropped from the original expression.

Note that the electric dipole interaction potential used to obtain eq. (7.5.10) is essentially the same as the well-known potential energy for a dipole in an electric field:

$$V = -\boldsymbol{\mu}\cdot\boldsymbol{\mathcal{E}} \tag{7.5.12}$$

This raises the question, why did we go through all the effort to derive the electric dipole Hamiltonian when we simply could have quantized the classical energy of a dipole in a field? Remember that our original expression for the interaction of a charged particle with an electromagnetic field, eq. (7.3.14) is valid for light-matter interactions under any conditions, and we made a number of additional assumptions in obtaining the EDH, eq. (7.4.9). We assumed interactions occur with weak classical resonant electric fields. We neglected magnetic fields, spin, and the gradient or curl of the electric field. Remember also that the classical expression was derived for static electric fields rather than time-varying electromagnetic fields. What we have learned are the conditions under which it is possible to quantize eq. (7.5.12) to obtain electric dipole transitions.

Equation (7.5.11) shows that the rates of absorption and stimulated emission by the matter is related to the square of the electric field amplitude (or intensity), and the modulus squared of the matrix element connecting the initial and final states. For a molecular system, this expression can be summed over all of the states participating in the interaction with the electric field. If the system is initially in the ground state $|g\rangle$, this sum is over all excited states $\{|e\rangle\}$, and only the absorption terms remain. To calculate an absorption spectrum, we have to remember that this reflects the power or rate of energy change by the system, which reflects the rate of transitions from g to e and the energy change accompanying that transition $\hbar\omega_{eg}$:

$$\overline{\mathcal{P}}_{\text{abs}}(\omega_{eg}) = \dot{E}(\omega_{eg}) = \hbar\omega_{eg}w_{eg} \tag{7.5.13}$$

Then, if the intensity of the light is constant with frequency, the absorption spectrum is

$$\overline{\mathcal{P}}_{\text{abs}}(\omega) = \frac{\pi\omega}{2\hbar}|\mathcal{E}_0|^2\sum_e|\boldsymbol{\mu}_{eg}|^2\,\delta(\omega_{eg} - \omega) \tag{7.5.14}$$

This shows that the Golden Rule absorption spectrum is a series of delta function resonances at frequencies equal to the transition energies ($\omega = \omega_{eg}$).

What we can see thus far is that the Golden Rule approach outlined here results in a description of two important features of a quantum absorption spectrum: (1) the absorption spectrum identifies resonances that are related to the energy gap between initial and final states, $E_k - E_\ell = \pm\hbar\omega$, and (2) the strength of the interaction of the light and matter and therefore the peak height is proportional to the square of the transition dipole matrix element connecting the initial and final state $|\mu_{eg}|^2$. What is missing at this point is any description of lineshape that we observed in the classical driven oscillator model. We will address this last point after we look at how the transition dipole moment influences absorption spectra in practice.

This page titled 7.5: The Dipole Operator and Transition Dipole Matrix Elements is shared under a CC BY-NC-SA 4.0 license and was authored, remixed, and/or curated by Andrei Tokmakoff via source content that was edited to the style and standards of the LibreTexts platform.

7.6: Absorption Cross Section

We are now prepared to describe how strongly a particular molecular transition will absorb light using experimentally accessible variables. The transition rates induced by a resonant electromagnetic field, eq. (7.5.11), can be rewritten with the experimentally accessible I, the intensity of the light, can be rewritten with the experimentally accessible intensity of the field using the relation $I = \frac{1}{2}\varepsilon_0 c \mathcal{E}_0^2$. When the field is on resonance ($\omega_{k\ell} = \omega$), this gives

$$w_{k\ell} = \frac{\pi}{\varepsilon_0 c \hbar^2} I \left| \langle k | \, \hat{\varepsilon} \cdot \hat{\boldsymbol{\mu}} \, | \ell \rangle \right|^2 \tag{7.6.1}$$

The square of the transition dipole matrix element is the fundamental molecular property that determines the light matter interaction, but in practice we also need to understand the alignment of the molecular transition dipole moment with the polarization of the electric field. While this can be defined for a single molecule, the molecules in a macroscopic sample are not necessarily uniformly aligned with the polarization of the light or with each other. For the particular case that we have a linearly polarized light source interacting with an ensemble of molecules with a uniform distribution of orientations, we can perform an average over alignment angles θ between the field polarization and the transition dipole moment:

$$\left| \langle k | \, \hat{\varepsilon} \cdot \hat{\boldsymbol{\mu}} \, | \ell \rangle \right|^2 = |\mu_{k\ell}|^2 \left\langle \cos^2 \theta \right\rangle = \frac{1}{3} |\mu_{k\ell}|^2 \tag{7.6.2}$$

This result predicts that the rate of absorption should be a factor of three lower than perfectly aligned transition dipoles:

$$w_{k\ell} = \frac{\pi}{3\varepsilon_0 c \hbar^2} I \left| \boldsymbol{\mu}_{k\ell} \right|^2 \tag{7.6.3}$$

Now let's relate the transition rates to a quantity that we can directly measure and that is not dependent on properties of the light: the absorption cross section, σ. We obtain σ by taking the total energy absorbed by the transition per unit time ($\mathrm{J\ \ s^{-1}}$) and normalize it relative to the incident intensity of the field ($\mathrm{J\ s^{-1}\ cm^{-2}}$). Since the rate of energy absorption is the rate of transitions from eq. (7.6.1) times the energy change for that transition $\hbar\omega_{k\ell}$ we have

$$\begin{aligned} \sigma &= \frac{\hbar \omega w_{k\ell}}{I} \\ &= \frac{\pi \omega}{3\varepsilon_0 c \hbar} |\boldsymbol{\mu}_{k\ell}|^2 \end{aligned} \tag{7.6.4}$$

Note σ has units of $\mathrm{cm^2}$. It is often said that the cross-section is the "fractional area" of the incident electromagnetic wave that a molecule will absorb, but don't take that too literally. It is not related to real molecular dimensions. The absorption cross-section is a measure of how well a particular molecular resonance absorbs a frequency of light. Note also that the golden rule rate for absorption is the same as the rate for stimulated emission. Therefore, the cross-section for these processes is also the same. For two states, g and e, with $E_g < E_e$

$$\sigma_{eg} = \sigma_{ge} \tag{7.6.5}$$

Comparing eq. (7.6.4) with the absorption cross-section for the classical driven oscillator in eq. (6.2.32), we observe that the quantum transition dipole moment and the classical dipole derivatives play the same role in governing the strength of the molecular response to the light. We will see more precisely in the next chapter how these two quantities both encode the same displacement of charges within a molecule when interacting with an electromagnetic field.

An alternate representation of the strength of the absorption interaction is the Einstein B coefficient, which relates the absorption rate to the energy density of the electromagnetic field $\mathcal{U}$

$$w_{k\ell} = B_{k\ell} \mathcal{U}(\omega_{k\ell}) \tag{7.6.6}$$

With the energy density given by eq. (7.2.19), we find

$$B_{k\ell} = \frac{\pi}{3\varepsilon_0 \hbar^2} |\boldsymbol{\mu}_{k\ell}|^2 \tag{7.6.7}$$

and the absorption cross-section is related to the B coefficient by $\sigma = \hbar\omega B_{k\ell}/c$. As with the cross-section, the B coefficients for absorption and stimulated emission are the same: $B_{eg} = B_{ge}$.

Let's remember that these expressions were derived for a single delta-function transition interacting on resonance with a monochromatic electromagnetic wave. They take on considerably more complexity when we start accounting for realistic lineshapes with a distribution of absorbing frequencies and realistic electromagnetic fields in which the energy is distributed across a finite band of frequencies. Furthermore, one must remember that these expressions derive from a specific set of units. Expressions for B and σ vary considerably in the literature, because they depend on whether it is derived using angular or normal frequency, cgs or SI units, and whether intensity is defined through the electric field amplitude or time-averaged value.(1) If one wishes to be quantitative, it is important to be aware of how such expressions were obtained.

To see how this is related to typical absorption measurements, we can use a phenomenological approach to calculate the change in the intensity of the incident light, I, due to absorption as it passes through a sample of absorbing molecules:

$$\frac{dI}{dx} = -N\sigma I \tag{7.6.8}$$

Here N is the molecular concentration in cm^{-3}, and the cross-section is quoted in cm^2. Assuming an incident intensity I_0 and integrating eq. (7.6.8) over a path length L, we can obtain the transmission, or fraction of light intensity propagated through the sample, as

$$T = \frac{I}{I_0} = e^{-N\sigma L} \tag{7.6.9}$$

The transmission of light through the sample decays exponentially as a function of path length. Note that a continuum description of absorption is characterized by an absorption coefficient α with units of cm^{-1}, which is related to the absorption cross-section as $\alpha = N\sigma$, or $T = e^{-\alpha L}$.

Equation (7.6.9) can also be written in terms of the familiar Beer-Lambert Law:

$$A = -\log\frac{I}{I_0} = \epsilon C L \tag{7.6.10}$$

Where A is the absorbance and C is the sample concentration in $\mathrm{mol\ L}^{-1}$, which is related to the number density via Avogadro's number N_A,

$$C[\mathrm{mol\,L^{-1}}] = 1000\frac{N[\mathrm{cm^{-3}}]}{N_A} \tag{7.6.11}$$

In eq. (7.6.10), the characteristic molecular quantity that describes the sample's ability to absorb the light is ϵ, the molar decadic extinction coefficient, given in $\mathrm{L\ mol^{-1}\ cm^{-1}}$. With these units, we see that we can equate ϵ with the cross section as

$$\epsilon = \frac{N_A\sigma}{2303} \tag{7.6.12}$$

As we saw in our discussion of the classical driven oscillator, when an absorption peak has a finite linewidth, the magnitude of the transition dipole moment is reflected in the total area underneath the molecule's absorption lineshape. To quantitatively determine the absorption cross-sections or the magnitude of the transition dipole matrix element from absorption spectra one needs to integrate the absorbed power over the entire lineshape. In the case of the extinction coefficient one can determine the magnitude of the transition dipole moment in Debyes (D) from the following expression:(2)(3)

$$\begin{aligned} |\mu_{k\ell}|^2 &= \frac{3\varepsilon_0\hbar c\,2303}{2\pi^2 N_A} n\int\frac{\epsilon(\nu)}{\nu}\,d\nu \\ &= 9.186\times10^{-3}\,\frac{\mathrm{D}^2}{\mathrm{L\,mol^{-1}\,cm^{-1}}}\,n\int\frac{\epsilon(\nu)}{\nu}\,d\nu \end{aligned} \tag{7.6.13}$$

Here the absorption spectrum is expressed in molar decadic units and the frequency ν in wavenumbers (cm^{-1}). We have included the index of refraction n used in calculations from solution phase spectra. As a final note, this is an appropriate formula for direct measurements in the time or frequency domain. There are additional considerations if the absorption spectrum was obtained with a dispersive spectrometer as a function of wavelength.

References

(1) Hilborn, R. C. Einstein coefficients, cross sections, *f* values, dipole moments, and all that. *American Journal of Physics* **1982**, *50* (11), 982-986. DOI: 10.1119/1.12937

(2) Herzberg, G. *Molecular Spectra and Molecular Structure*; Prentice-Hall, 1939; p 261.

(3) McHale, J. L. *Molecular Spectroscopy*, 1st ed.; Prentice-Hall, 1999.

This page titled 7.6: Absorption Cross Section is shared under a CC BY-NC-SA 4.0 license and was authored, remixed, and/or curated by Andrei Tokmakoff via source content that was edited to the style and standards of the LibreTexts platform.

7.7: Quantitative Examples of Light-Matter Interactions

How strong is the interaction of light and matter in typical molecular spectroscopy? How do the light's source and intensity—also known as irradiance—alter the nature of the interaction? When is it proper to call an interaction perturbative? To answer these questions, we will be informed by a more quantitative approach. For different scenarios, we will calculate electric field strengths, transition dipole moments, and Rabi frequencies to observe how much these quantities can vary.

Electric Fields

We will begin by analyzing some common light sources to find the magnitude of the electric fields $\mathcal{E}_0$ they generate. Remember that light's electric field is treated classically in our semiclassical description of the light-matter interaction, so the frequency of the light isn't explicitly needed for this calculation.

Weak continuous fields

First, consider a continuous wave laser source providing weak excitation with a power of $P = 1\ \mu\text{W}$. Since the electric field is related to the intensity or energy density, we must specify the area through which this power passes in the sample. If this light is focused to a radius of $w_0 = 100\ \mu\text{m}$, using the power per unit area $I = P/\mathcal{A} = P/\pi w_0^2$ we can estimate the intensity of the source at the focus, which gives $3.2 \times 10^{-3}\ \text{W cm}^{-2}$ (Figure 7.7.1). Using $I = \frac{1}{2}\varepsilon_0 c\,|\mathcal{E}_0|^2$ leads to the conclusion that the magnitude of the electric field at the focus is $\mathcal{E}_0 = 155\ \text{V m}^{-1}$.

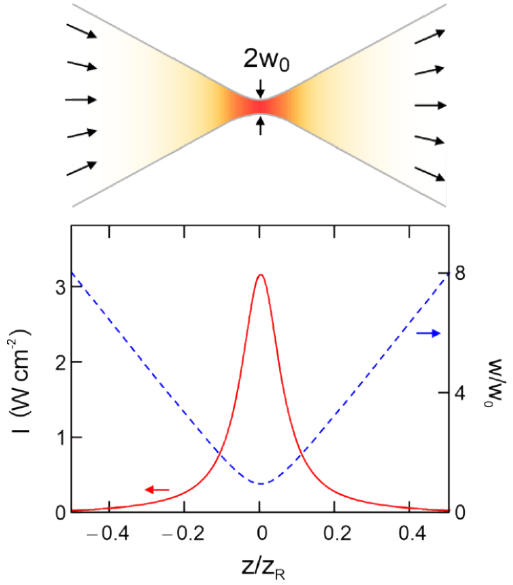


Figure 7.7.1: Illustration of the change in beam size w and intensity I on focusing a $1\ \mu\text{W}$ beam to a waist of $w_0 = 100\ \mu\text{m}$. Z_R is set by the optics used by the instrument, typically tens of mm.

Let's compare this electric field with that of sunlight. The solar irradiance at the top of the atmosphere is typically quoted as $0.13\ \text{W cm}^{-2}$. Although this intensity is higher than that of the laser source, it is spread over the spectrum of a $5800\ \text{K}$ blackbody source. To make a closer comparison to the bandwidth of a laser source, we can divide the sunlight spectrum into nanometer wavelength intervals and find the irradiance of each. The maximum intensity of any nanometer range of the spectrum is $I = 1.8 \times 10^{-4}\ \text{W cm}^{-2}$ and the corresponding electric field is $\mathcal{E}_0 = 8.7\ \text{V m}^{-1}$.

Short pulsed fields

Second, consider a commonly available ultrafast laser source with a pulse energy of $E = 100\ \text{nJ}$ and a pulse length of $\Delta\tau = 100\ \text{fs}$ which we focus to a radius of $100\ \mu\text{m}$. The magnitude of the electric field is time-dependent, and the energy is distributed through the pulse. To keep the example as simple as possible, let's assume that the energy is distributed uniformly over the pulse length,

leading to a peak fluence (energy flux) of $E/\Delta t = 10^6$ W. At the focus, this results in a peak intensity of $I_{\text{peak}} = 3.2$ GW cm^{-2} and a corresponding peak electric field of $\mathcal{E}_{\text{peak}} = 1.5 \times 10^8$ V m^{-1}.

We see that the magnitude of the field generated by a laser can vary by many orders of magnitude depending on the pulse characteristics and focusing of the beams. How high is the magnitude of this field? Certainly high enough to make it very useful for ultrafast nonlinear spectroscopy, but generally not high enough to ionize molecules, which typically requires intensities that are greater yet by factor of 10^4 to 10^5. As a point of context, remember that the binding energy for the electron in hydrogen atom is $E_{\text{bind}} = 13.6$ eV and the average distance separating the proton and electron is $a_0 = 0.53$ Å, suggesting that the field strength one would need to remove the electron $\mathcal{E}_0$ is no less than $a_0 E_{\text{bind}} = 3 \times 10^{11}$ V m^{-1}.

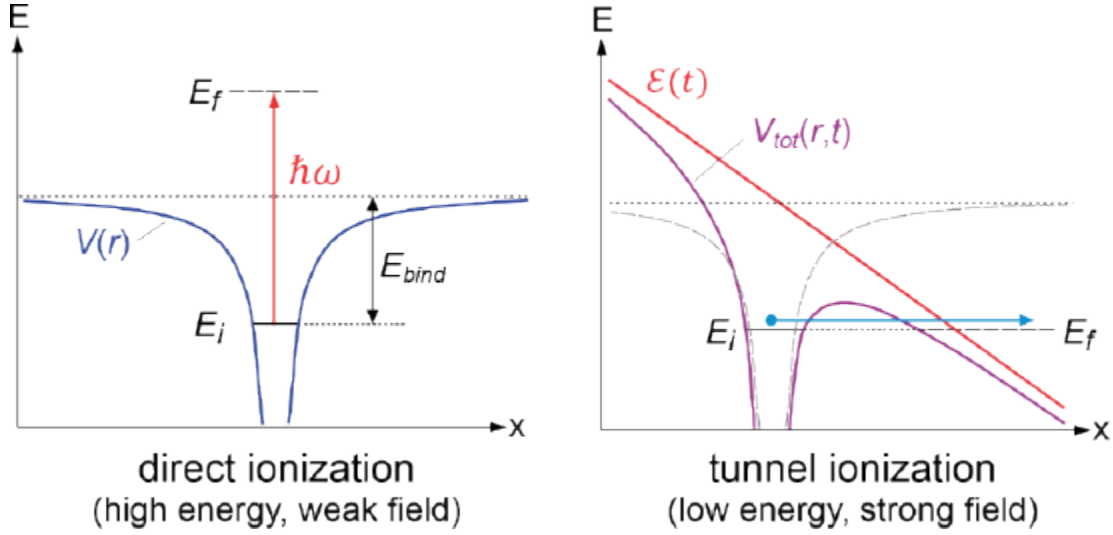


Figure 7.7.2: Illustration of atomic ionization processes with weak and strong electric fields. Direct ionization requires quantum mechanical transitions from the initial bound state the electron to a final continuum state using a photon whose energy exceeds the binding energy of the electron ($E_f - E_i = \hbar\omega$). Tunnel ionization occurs when the electric field of the light is strong enough that it distorts the Coulomb potential $V(r)$ experienced by the bound electron. If the light is polarized along $\hat{x}$, the net potential experienced by an electron becomes $V_{\text{tot}}(r,t) = V(r) - ex\mathcal{E}(t)$, which creates the possibility of the electron tunneling into a continuum state with $E_f = E_i$.

In reality, the ionization of atoms and molecules can proceed through multiple different mechanisms. What we typically think of ionization by light is a resonant interaction with photons that exceed the binding energy of the electron ($E_{\text{bind}} < \hbar\omega$). In the case of hydrogen atoms, this corresponds to energies in excess of 13.6 eV or a corresponding wavelength of 91 nm—deep into the vacuum ultraviolet. These resonant ionization processes do not require strong electric fields. Strong field ionization can occur at much lower photon energies through a mechanism known as tunnel ionization (Figure 7.7.2b). This refers to a process in which the electric field distorts the coulomb potential that binds the electrons, creating a possibility for electrons to tunnel through an induced barrier into free space.

Transition dipole moment

Some of the strongest molecular transitions are found in commonly used visible dyes and fluorophores families, with peak molar extinction coefficient values of $\epsilon = 0.8 - 2.6 \times 10^5$ M^{-1} cm^{-1}, whereas strong IR vibrational absorptions have a peak value of $\epsilon = 10^3$M^{-1} cm^{-1}. Typical molar extinction coefficients for vibrational and electronic transitions have extinction coefficients in the range $\epsilon = 10^1$–10^5 M^{-1} cm^{-1}.

In calculating the transition dipole moment, we must account for the linewidth of the absorption peak over which this absorption is spread. As illustrated in Figure 7.7.3

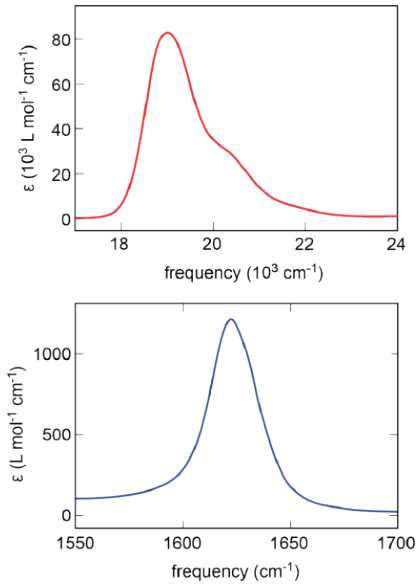


Figure 7.7.3: Absorption spectra and molar extinction coefficients for two strong transitions (top) Visible electronic absorption spectrum for dilute solution of rhodamine 6G in acetonitrile. Integration over this lineshape using eq. (7.6.13) results in a transition dipole moment of $1.2\ \mathrm{D}$. (bottom) Infrared vibrational absorption spectrum of the carbonyl stretching vibration of N-methylacetamide in $\mathrm{D_2O}$, which corresponds to a transition dipole moment of $0.3\ \mathrm{D}$.

Rabi Frequency

The strength of the light-matter interaction can be accurately characterized by the Rabi frequency, Ω_R. In Sec. 3.3 we demonstrated how applying a resonant sinusoidal potential will drive population back and forth between the initial and final state with a periodicity of $\sin \Omega_R t$. When the electromagnetic field is on resonance with the molecular transition, the Rabi frequency is directly proportional to on the light's electric field amplitude and the magnitude of the transition dipole moment

$$\Omega_R = \frac{|\mu_{k\ell}|\,\mathcal{E}_0}{\hbar} \tag{7.7.1}$$

The time it takes to invert the population—that is, for the probability amplitude of the initial state to be transferred to the final state under continuous illumination—is $\tau_{\mathrm{inv}} = \pi/\Omega_R$. In the case of the perturbative Golden Rule formalism that we have been discussing, the field induces transitions at a rate proportional to the square of the Rabi Frequency. From eq. (7.6.3), we find

$$w_{k\ell} = \frac{4\pi}{3\varepsilon_0 c}\Omega_R^2 \tag{7.7.2}$$

Let's calculate the Rabi frequencies corresponding to the electric fields and transition dipole moments described in the two previous sections. Let's first consider a case corresponding to a fluorophore with a strong electronic transition between electronic ground and excited state, with a transition dipole moment of $\mu_{eg} = 3.0\ \mathrm{D}$. For a resonant absorption interaction with a continuous wave field of $\mathcal{E}_0 = 155\ \mathrm{V\ m^{-1}}$, the Rabi frequency is $\Omega_R = 1.5 \times 10^7\ \mathrm{s^{-1}}$, indicating that the population can be transferred from the ground to the excited state within $\tau_{\mathrm{inv}} = 210\ \mathrm{ns}$ under continuous illumination. In practice, this does not happen. The radiative relaxation rate of the electronically excited state is far too fast. A typical fluorescence lifetime is 1–$5\ \mathrm{ns}$, so under illumination with this source the system reaches a steady state with only a small population in the excited state.

Turning to the case of the femtosecond pulse with $\mathcal{E}_{\mathrm{peak}} = 1.5 \times 10^8\ \mathrm{V\ m^{-1}}$ interacting with the same transition dipole moment, the Rabi frequency increases many orders of magnitude to $\Omega_R = 1.5 \times 10^{13}\ \mathrm{s^{-1}}$ and τ_{inv} is approximately $200\ \mathrm{fs}$. Now the interaction is so strong during the short period of pulsed illumination that the rate of absorption far exceeds the rate of radiative relaxation. Half of the population initially in the ground state is transferred to the excited state over the $100\ \mathrm{fs}$ pulse length. This is a regime where one should be skeptical of the validity of first-order perturbation theory and the Golden Rule, since we are seeing substantial changes in the initial populations and stimulated emission is ignored. If we compare the pulsed laser source interacting with a weaker vibrational transition dipole moment with $\mu_{eg} = 0.3\ \mathrm{D}$, the Rabi decreases proportionately to $\Omega_R = 1.5 \times 10^{12}\ \mathrm{s^{-1}}$ and τ_{inv} is approximately $2000\ \mathrm{fs}$. Only 5% of the probability amplitude has been shifted from ground to excited state, which is in line with the assumptions of perturbation theory.

When using pulsed electromagnetic fields, the amount of population transferred from the ground to the excited state is another important indicator of the light-matter interaction's strength. To describe this, we can borrow some of the language and concepts used in magnetic resonance spectroscopy. Consider a square pulse: an electric field $\mathcal{E}_0 \cos \omega t$ that is switched on abruptly, applied for a period Δt, and then switched off abruptly. The amount of population shifted to the excited state is $\sin(\Omega_R \Delta t)$, and therefore once can define an angle $\theta = \Omega_R \Delta t$ that describes how the probability amplitude is distributed between states. A π pulse applied to a two-level system initially in the ground state inverts the population, putting it into the excited state. A 2π pulse inverts and returns the population to the ground state. A $\pi/2$ pulse creates an equally weighted superposition of ground and excited states.

This page titled 7.7: Quantitative Examples of Light-Matter Interactions is shared under a CC BY-NC-SA 4.0 license and was authored, remixed, and/or curated by Andrei Tokmakoff via source content that was edited to the style and standards of the LibreTexts platform.

7.8: Appendix- Electromagnetic Fields and Potentials

Wave Equations and Electromagnetic Fields

Here we review the derivation of the vector potential, electric field, and magnetic field for electromagnetic plane waves propagating in free space. The starting point for all discussions of electromagnetic waves is Maxwell's equations in vacuum, also known as the microscopic form, which are in SI units:

$$\nabla \cdot \mathcal{B} = 0 \tag{7.8.1}$$

$$\nabla \cdot \mathcal{E} = \frac{\rho}{\varepsilon_0} \tag{7.8.2}$$

$$\nabla \times \mathcal{E} = -\frac{\partial \mathcal{B}}{\partial t} \tag{7.8.3}$$

$$\nabla \times \mathcal{B} = \mu_0 \mathbf{J} + \varepsilon_0 \mu_0 \frac{\partial \mathcal{E}}{\partial t} \tag{7.8.4}$$

The four vector variables here are $\mathcal{E}$, the electric field ($\mathrm{V\ m^{-1}}$); $\mathcal{B}$, the magnetic flux density ($\mathrm{C\ m^{-2}}$); $\mathbf{J}$, the current density ($\mathrm{A\ m^{-2}}$); ρ, the charge density ($\mathrm{C\ m^{-3}}$). The fundamental constants are ε_0, the electrical vacuum permittivity ($8.85419 \times 10^{-12}\ \mathrm{F\ m^{-1}}$), and μ_0, the magnetic vacuum permittivity ($1.256637 \times 10^{-6}\ \mathrm{N\ A^{-2}}$), which are related to the speed of light in a vacuum by

$$c = \frac{1}{\sqrt{\varepsilon_0 \mu_0}} \tag{7.8.5}$$

In vacuum, the magnetic field $\mathbf{H}$ ($\mathrm{A\ m^{-2}}$) is directly proportional to $\mathcal{B}$: $\mathcal{B} = \mu_0 \mathbf{H}$. We are interested in describing $\mathcal{E}$ and $\mathcal{B}$ in terms of $\mathbf{A}$, the magnetic vector potential ($\mathrm{V\ s\ m^{-1}}$), and φ, the scalar electrostatic potential ($\mathrm{J\ c^{-1}}$).

To start, let's review some basic properties of vector and scalar fields. A field $\mathbf{F}(\mathbf{r})$ associates a physical property to different points in space, and may be time dependent. A scalar field assigns a number to each point in space, whereas a vector field assigns a vector. The divergence of a vector field

$$\nabla \cdot \mathbf{F} = \frac{\partial F_x}{\partial x} + \frac{\partial F_y}{\partial y} + \frac{\partial F_z}{\partial z} \tag{7.8.6}$$

is a scalar. For a scalar field ϕ, the gradient

$$\nabla \phi = \frac{\partial \phi}{\partial x}\hat{x} + \frac{\partial \phi}{\partial y}\hat{y} + \frac{\partial \phi}{\partial z}\hat{z} \tag{7.8.7}$$

is a vector for the rate of change at one point in space. Here $\hat{x}^2 + \hat{y}^2 + \hat{z}^2 = \hat{r}^2$ are unit vectors. Also, the curl

$$\nabla \times \mathbf{F} = \begin{vmatrix} \hat{x} & \hat{y} & \hat{z} \\ \frac{\partial}{\partial x} & \frac{\partial}{\partial y} & \frac{\partial}{\partial z} \\ F_x & F_y & F_z \end{vmatrix} \tag{7.8.8}$$

is a vector whose x, y, and z components are the circulation of the field about that component.

Some useful identities from vector calculus that we will use are

$$\nabla \cdot (\nabla \times \mathbf{F}) = 0 \tag{7.8.9}$$

$$\nabla \times (\nabla \phi) = 0 \tag{7.8.10}$$

$$\nabla \times (\nabla \times \mathbf{F}) = \nabla (\nabla \cdot \mathbf{F}) - \nabla^2 \mathbf{F} \tag{7.8.11}$$

To obtain the wave equation for the electric field, we can substitute eq. (7.8.2) and (7.8.3) in eq. (7.8.11) with $\mathbf{F} = \mathcal{E}$ to obtain:

$$-\frac{\partial (\nabla \times \mathcal{B})}{\partial t} = \frac{\nabla \rho}{\varepsilon_0} - \nabla^2 \mathcal{E} \tag{7.8.12}$$

Substituting eq. (7.8.4) into this expression gives

$$\nabla^2 \mathcal{E} - \varepsilon_0 \mu_0 \frac{\partial^2 \mathcal{E}}{\partial t^2} = \frac{\nabla \rho}{\varepsilon_0} + \mu_0 \frac{\partial \mathbf{J}}{\partial t} \tag{7.8.13}$$

This is the inhomogeneous wave equation for the electric field. In the absence of charges and currents, the terms on the right-hand side are zero, and we obtain the wave equation for the free electric field:

$$\nabla^2 \mathcal{E} - \varepsilon_0 \mu_0 \frac{\partial^2 \mathcal{E}}{\partial t^2} = 0 \tag{7.8.14}$$

This form of a wave equation has as solutions functions of the form $\mathcal{E}(x - vt)$ that propagate in the x direction with a velocity of magnitude $v = (\varepsilon_0 \mu_0)^{-1/2}$. In vacuum that velocity is the speed of light, c.

$$c = \frac{1}{\sqrt{\varepsilon_0 \mu_0}} \tag{7.8.15}$$

In spherical coordinates, solutions to eq. (7.8.14) take the form $\frac{1}{r}\mathcal{E}\left(r - vt\right)$.

To obtain the plane wave solutions to eq. (7.8.14), we posit solutions with a form that separates the spatial and temporal variables:

$$\mathcal{E}(\mathbf{r}, t) = \mathcal{E}(\mathbf{r}) e^{\mathrm{i}\omega t} \tag{7.8.16}$$

The real electric field is understood to be obtained from $\mathrm{Re}\left[\mathcal{E}(\mathbf{r}, t)\right]$. Substituting (7.8.16) into (7.8.14) we obtain an equation for the spatial part of the field:

$$\nabla^2 \mathcal{E}(\mathbf{r}) - k^2 \mathcal{E}(\mathbf{r}) = 0 \tag{7.8.17}$$

where $k^2 = \omega^2 c^2$. This equation has solutions of the form $\mathcal{E}(\mathbf{r}) = \mathcal{E}_0 e^{-\mathrm{i}\mathbf{k}\cdot\mathbf{r}}$, which have a periodicity in space governed by the wavevector $\mathbf{k}$. The solution allows positive and negative values of the wavevector but requires that $\mathbf{k}$ and frequency are related by the dispersion relationship

$$|\mathbf{k}| = \frac{\omega}{c} = \frac{2\pi}{\lambda} \tag{7.8.18}$$

where λ is the wavelength of light.

With these results for $\mathcal{E}(\mathbf{r})$ one finds that the resulting solutions to the wave-equation (7.8.14) have the sinusoidal form

$$\mathcal{E}(\mathbf{r}, t) = \tilde{\mathcal{E}}_0 e^{\mathrm{i}(\mathbf{k}\cdot\mathbf{r} - \omega t)} \tag{7.8.19}$$

with the complex amplitude $\tilde{\mathcal{E}}_0$. The real part is calculated as:

$$\mathrm{Re}[\mathcal{E}(\mathbf{r}, t)] = \frac{1}{2}\tilde{\mathcal{E}}_0 e^{\mathrm{i}(\mathbf{k}\cdot\mathbf{r} - \omega t)} + \frac{1}{2}\tilde{\mathcal{E}}_0^* e^{-\mathrm{i}(\mathbf{k}\cdot\mathbf{r} - \omega t)} \tag{7.8.20}$$

Alternatively, we can express this as:

$$\mathcal{E}(\mathbf{r}, t) = \mathcal{E}_0 \cos\left(\mathbf{k}\cdot\mathbf{r} - \omega t - \alpha\right) \tag{7.8.21}$$

Here the phase factor α is added to illustrate that sine function solutions ($\alpha = \pi/2$) are equally valid. This is possible because one can add an arbitrary phase factor $e^{-\mathrm{i}\alpha}$ to eq. (7.8.16), which simply carries through.

Equations (7.8.20) and (7.8.21) describe a monochromatic plane wave of frequency ω traveling in the direction of the wavevector $\mathbf{k}$ at the speed of light. For any value of k, there are positive and negative solutions, for which the sinusoidal argument can take the form $(\mathrm{i}\mathbf{k}\cdot\mathbf{r} - \mathrm{i}\omega t)$ to describe propagation in the $\mathbf{k}$ direction and $(-\mathrm{i}\mathbf{k}\cdot\mathbf{r} - \mathrm{i}\omega t)$ for backward propagating in the $-\mathbf{k}$ direction. Additionally, Maxwell's equation with zero charge density, $\nabla\cdot\mathcal{E} = 0$, dictates that these waves satisfy $\mathbf{k}\cdot\mathcal{E}_0 = 0$, so the electric fields are oriented perpendicular to the direction of travel, i.e. transverse waves.

A similar approach using the other two Maxwell equations can be used to obtain the wave equation for the magnetic field. For a free electromagnetic wave, we find

$$\nabla^2 \mathcal{B} - \varepsilon_0 \mu_0 \frac{\partial^2 \mathcal{B}}{\partial t^2} = 0 \tag{7.8.22}$$

This is the same wave equation as that for the electric field and therefore must have the same solutions:

$$\mathcal{B}(\mathbf{r}, t) = \mathcal{B}_0 e^{\mathrm{i}(\mathbf{k}\cdot\mathbf{r} - \omega t)} + \mathcal{B}_0^* e^{-\mathrm{i}(\mathbf{k}\cdot\mathbf{r} - \omega t)} \tag{7.8.23}$$

or

$$\mathcal{B}(\mathbf{r}, t) = \mathcal{B}_0 \cos\left(\mathbf{k}\cdot\mathbf{r} - \omega t - \alpha\right)$$

There are similar constraints on the constants $\mathcal{B}_0$, $\mathbf{k}$, and ω.

Maxwell's equations (7.8.3) and (7.8.4) dictate that $\mathcal{E}$ and $\mathcal{B}$ are not independent of each other. If we substitute the solutions eq. (7.8.20) and (7.8.23) into these equations, we find that the frequency wavevector and phase of the waves must be the same for $\mathcal{E}$ and $\mathcal{B}$ and that

$$\mathbf{k} \times \mathcal{E}_0 = \omega \mathcal{B}_0 \tag{7.8.24}$$

$$\mathbf{k} \times \mathcal{B}_0 = -\mu_0 \varepsilon_0 \omega \mathcal{E}_0 \tag{7.8.25}$$

Thus, the orientation of the magnetic field is perpendicular to the electric field and the direction of propagation ($\mathbf{k} \perp \mathcal{E} \perp \mathcal{B}$). These expressions hold for all plane waves. Taking the absolute value of eq. (7.8.24) and using eq. (7.8.15) and (7.8.18), we find that the magnitude of the magnetic and electric fields are related by the speed of light:

$$\frac{\mathcal{E}_0}{\mathcal{B}_0} = c \tag{7.8.26}$$

Separately, one can show that the Poynting vector describing the wave's energy flux is $\mathbf{S} = \varepsilon_0 c^2 (\mathcal{E} \times \mathcal{B})$. $\mathbf{S}$ is parallel to $\mathbf{k}$ and gives the rate of energy passage through a given area per unit time ($\mathrm{W\ cm^{-2}}$). One calculates the intensity or irradiance as the value obtained by averaging $\mathbf{S}$ over one cycle of the field: $I = \langle S \rangle = \frac{1}{2} \varepsilon_0 c \mathcal{E}_0^2$.

Vector Potential

We now introduce the magnetic vector potential $\mathbf{A}(\mathbf{r}, t)$ and a electrostatic scalar potential $\varphi(\mathbf{r}, t)$, which we will relate to $\mathcal{E}$ and $\mathcal{B}$. We start by recognizing that any vector field F can be written in terms of a vector potential and scalar potential according to

$$\mathbf{F} = \nabla \Phi + \nabla \times \mathbf{A} \tag{7.8.27}$$

Since the magnetic field has no divergence, $\nabla \cdot \mathcal{B} = 0$, and eq. (7.8.9) indicates that $\nabla \cdot (\nabla \times \mathbf{A}) = 0$, we can relate the vector potential and magnetic field through

$$\mathcal{B} = \nabla \times \mathbf{A} \tag{7.8.28}$$

Inserting this into eq. (7.8.3) and rewriting, we can relate the electric field and vector potential:

$$\nabla \times \left[\mathcal{E} + \frac{\partial \mathbf{A}}{\partial t} \right] = 0 \tag{7.8.29}$$

Comparing eqs. (7.8.29) and (7.8.10) allows us to state that a scalar product exists such that

$$\mathcal{E} = -\frac{\partial \mathbf{A}}{\partial t} - \nabla \varphi \tag{7.8.30}$$

This equation shows that, when the vector potential is independent of time, we recover the expected relationship between the electric field and the gradient of the electrostatic potential: $\mathcal{E} = -\nabla \varphi$. Summarizing our results, we see that the potentials $\mathbf{A}$ and φ determine the fields $\mathcal{B}$ and $\mathcal{E}$:

$$\mathcal{B}(\mathbf{r}, t) = \nabla \times \mathbf{A}(\mathbf{r}, t) \tag{7.8.31}$$

$$\mathcal{E}(\mathbf{r}, t) = -\nabla \varphi(\mathbf{r}, t) - \frac{\partial}{\partial t} \mathbf{A}(\mathbf{r}, t) \tag{7.8.32}$$

We are interested in determining the classical wave equationS for $\mathbf{A}$ and φ. Using eq. (7.8.31), differentiating eq. (7.8.32), and substituting into eq. (7.8.4), we obtain

$$\nabla \times (\nabla \times \mathbf{A}) + \varepsilon_0 \mu_0 \left(\frac{\partial^2 \mathbf{A}}{\partial t^2} + \nabla \frac{\partial \varphi}{\partial t} \right) = \mu_0 \mathbf{J} \tag{7.8.33}$$

Using eq. (7.8.11),

$$\left[-\nabla^2 \mathbf{A} + \varepsilon_0 \mu_0 \frac{\partial^2 \mathbf{A}}{\partial t^2} \right] + \nabla \left(\nabla \cdot \mathbf{A} + \varepsilon_0 \mu_0 \frac{\partial \varphi}{\partial t} \right) = \mu_0 \mathbf{J} \tag{7.8.34}$$

From eq. (7.8.30), we have

$$\nabla \cdot \boldsymbol{\mathcal{E}} = -\frac{\partial \nabla \cdot \mathbf{A}}{\partial t} - \nabla^2 \varphi \tag{7.8.35}$$

and using eq. (7.8.2),

$$\frac{-\partial \nabla \cdot \mathbf{A}}{\partial t} - \nabla^2 \varphi = \frac{\rho}{\varepsilon_0} \tag{7.8.36}$$

To continue, we must specify the divergence of A in order to uniquely specify the vector potential. Notice from eqs. (7.8.31) and (7.8.32) that we only need to specify four field components ($A_x,\ A_y,\ A_z,\ \varphi$) to determine all six $\mathcal{E}$ and $\mathcal{B}$ components. But $\mathcal{E}$ and $\mathcal{B}$ do not uniquely determine $\mathbf{A}$ and φ. So we can construct $\mathbf{A}$ and φ in any number of ways without changing $\mathcal{E}$ and $\mathcal{B}$. Notice that if we change $\mathbf{A}$ by adding $\nabla\chi$, where χ is any scalar function of $\mathbf{r}$ and t, $\mathcal{B}$ will not change ($\nabla \times (\nabla \cdot \mathcal{B}) = 0$). Adding $\nabla\chi$ will change $\mathcal{E}$ by $(-\frac{\partial}{\partial t}\nabla\chi)$, but we can change φ to $\varphi' = \varphi - (\partial\chi/\partial t)$. Then $\mathcal{E}$ and $\mathcal{B}$ will both be unchanged. This property of changing representation (changing the gauge) without changing $\mathcal{E}$ and $\mathcal{B}$ is known as gauge invariance. We can define a gauge transformation with

$$\mathbf{A}'(\mathbf{r}, t) = \mathbf{A}(\mathbf{r}, t) + \nabla\chi(\mathbf{r}, t) \tag{7.8.37}$$

$$\varphi'(\mathbf{r}, t) = \varphi(\mathbf{r}, t) - \frac{\partial}{\partial t}\chi(\mathbf{r}, t) \tag{7.8.38}$$

Up to this point, $\mathbf{A}'$ and φ' are undetermined. Let's choose a χ such that:

$$\nabla \cdot \mathbf{A} + \varepsilon_0 \mu_0 \frac{\partial \varphi}{\partial t} = 0 \tag{7.8.39}$$

This is known as the Lorentz condition (gauge). It is selected so that when we insert it into eq. (7.8.33), the second term of the left hand side vanishes, and we are left with

$$-\nabla^2 \mathbf{A} + \varepsilon_0 \mu_0 \frac{\partial^2 \mathbf{A}}{\partial t^2} = \mu_0 \mathbf{J} \tag{7.8.40}$$

Similarly, inserting eq. (7.8.39) into eq. (7.8.35) gives

$$\nabla^2 \varphi - \varepsilon_0 \mu_0 \frac{\partial^2 \varphi}{\partial t^2} = -\frac{\rho}{\varepsilon_0} \tag{7.8.41}$$

Equations (7.8.40) and (7.8.41) are inhomogeneous wave equations for $\mathbf{A}$ and φ, with the current density and charge density as source terms, so this gauge is useful when describing time-varying charges. Within the Lorentz gauge, we can still arbitrarily add another χ; it must only satisfy eq. (7.8.39). If we substitute eqs. (7.8.37) and (7.8.38) into eq. (7.8.41), we see that χ follows the wave equation

$$\nabla^2 \chi - \varepsilon_0 \mu_0 \frac{\partial^2 \chi}{\partial t^2} = 0 \tag{7.8.42}$$

So we can make further choices or add constraints to $\mathbf{A}$ and φ, as long as they obey eq. (7.8.42).

In the Coulomb gauge, we set

$$\nabla \cdot \mathbf{A} = 0 \tag{7.8.43}$$

which is selected so that insertion into eq. (7.8.35) gives the Poisson equation for the scalar potential: $\nabla^2\varphi = -\rho/\varepsilon_0$. This means treating static charge distributions is straightforward. A special case of the Coulomb gauge is the Gibbs gauge, which sets $\varphi = 0$ and can be used for free electromagnetic waves in the absence of charges and currents. The challenge for general solutions in the Coulomb gauge is that the vector potential wave equation has a more complicated form. From eq. (7.8.33):

$$\nabla^2\mathbf{A} - \varepsilon_0\mu_0\frac{\partial^2\mathbf{A}}{\partial t^2} = -\mu_0\,\mathbf{J} + \varepsilon_0\mu_0\nabla\left(\frac{\partial\varphi}{\partial t}\right) \tag{7.8.44}$$

One can simplify this equation further by recognizing that the currents can be separated into a sum of longitudinal and transverse contributions, $\mathbf{J} = \mathbf{J}_\parallel + \mathbf{J}_\perp$, which correspond to the components that are curl free $(\nabla\times\mathbf{J}_\parallel = 0)$ and divergence free $(\nabla\cdot\mathbf{J}_\perp)$. Jackson shows how the second term on the right hand side of eq. (7.8.44) is equal to $\mu_0\mathbf{J}_\parallel$,(1) meaning that the source term for the wave equation of $\mathbf{A}$ purely arises from the transverse current:

$$\nabla^2\mathbf{A} - \varepsilon_0\mu_0\frac{\partial^2\mathbf{A}}{\partial t^2} = -\mu_0\mathbf{J}_\perp \tag{7.8.45}$$

Indeed, we will see that using the Coulomb gauge results in electric fields that are purely transverse.

In isolation, the vector potential is far from any currents, and the wave equation for the free vector potential becomes:

$$\nabla^2\mathbf{A} - \varepsilon_0\mu_0\frac{\partial^2\mathbf{A}}{\partial t^2} = 0 \tag{7.8.46}$$

Noting $\varepsilon_0\mu_0 = c^2$, we see this is an equation for a wave propagating at the speed of light. As described in the previous section, we look for harmonic plane wave solutions to this equation and find

$$\mathbf{A}(r,t) = \tilde{\mathbf{A}}_0 e^{\mathrm{i}(\mathbf{k}\cdot\mathbf{r}-\omega t)} \tag{7.8.47}$$

where $\tilde{\mathbf{A}}_0$ is a complex vector amplitude. Alternatively, we can write a solution in real form:

$$\mathbf{A} = \mathbf{A}_0\sin(\omega t - \mathbf{k}\cdot\mathbf{r} + \alpha) \tag{7.8.48}$$

Here α is an arbitrary constant phase, so a cosine solution is obtained by setting $\alpha = \pi/2$ or, equivalently, setting $\tilde{\mathbf{A}}_0 = \mathbf{A}_0 e^{\mathrm{i}\alpha}$. As before, $\mathbf{k}$ is the wave vector which points along the direction of propagation and has a magnitude

$$k^2 = \omega^2\mu_0\varepsilon_0 = \frac{\omega^2}{c^2} \tag{7.8.49}$$

which allows for positive and negative wavenumbers. Since $\nabla\cdot\mathbf{A} = 0$ (see eq. (7.8.43)), $-\mathbf{k}\cdot\mathbf{A}_0\cos(\omega t - \mathbf{k}\cdot\mathbf{r} + \alpha) = 0$. Therefore,

$$\mathbf{k}\cdot\mathbf{A}_0 = 0 \tag{7.8.50}$$

This indicates that the vector potential is oriented perpendicular to the direction of wave propagation ($\mathbf{k}\perp\mathbf{A}_0$).

Finally, we can obtain the electric and magnetic field from eqs. (7.8.31) and (7.8.32) with $\nabla\varphi = 0$

$$\mathcal{E} = -\frac{\partial\mathbf{A}}{\partial t} \tag{7.8.51}$$

$$\mathcal{B} = \nabla\times\mathbf{A} \tag{7.8.52}$$

The expressions corresponding to the real form of $\mathbf{A}$ in eq. (7.8.48) are

$$\mathcal{E} = -\omega\mathbf{A}_0\cos(\omega t - \mathbf{k}\cdot\mathbf{r} + \alpha) \tag{7.8.53}$$

$$\mathcal{B} = -(\mathbf{k}\times\mathbf{A}_0)\cos(\omega t - \mathbf{k}\cdot\mathbf{r} + \alpha) \tag{7.8.54}$$

and the expressions corresponding to the complex form in eq. (7.8.47) are

$$\tilde{\mathcal{E}} = -\mathrm{i}\omega\tilde{\mathbf{A}}_0\, e^{\mathrm{i}(k\cdot r-\omega t)} = -\mathrm{i}\omega\tilde{\mathbf{A}} \tag{7.8.55}$$

$$\tilde{\mathcal{B}} = -\mathrm{i}\,(\mathbf{k}\times\mathbf{A}_0)\, e^{\mathrm{i}(k\cdot r-\omega t)} = -\mathrm{i}\left(\mathbf{k}\times\tilde{\mathbf{A}}\right) \tag{7.8.56}$$

From eq. (7.8.53), we observe that the electric field is parallel with the vector potential ($\mathcal{E}\parallel\mathbf{A}_0$), and the magnetic field is

perpendicular to the electric field and the direction of propagation $(\mathbf{k} \perp \mathcal{E} \perp \mathcal{B})$, consistent to what we observed in the previous section.

References

(1) Jackson, J. D. *Classical Electrodynamics*, 2nd ed.; Wiley, 1975.

This page titled 7.8: Appendix- Electromagnetic Fields and Potentials is shared under a CC BY-NC-SA 4.0 license and was authored, remixed, and/or curated by Andrei Tokmakoff via source content that was edited to the style and standards of the LibreTexts platform.

7.9: Appendix- Magnetic Dipole and Electric Quadrupole Transitions

The leading term in the expansion of $e^{\mathrm{i}\mathbf{k}\cdot\mathbf{r}}$ in the light-matter interaction Hamiltonian, eq. (7.4.6), resulted in electric dipole transitions, also known as E1 transitions. The second term

$$V^{(2)}(t) = -\mathrm{i}\frac{q}{m}\tilde{A}_0(\hat{\varepsilon}\cdot\mathbf{p})(\mathbf{k}\cdot\mathbf{r})e^{-\mathrm{i}\omega t} \tag{7.9.1}$$

leads to magnetic dipole (M1) and electric quadrupole (E2) transitions, which we will describe here. To start, let's look at the product $(\hat{\varepsilon}\cdot\mathbf{p})(\mathbf{k}\cdot\mathbf{r})$, which is now a function of two quantum operators, $\mathbf{p}$ and $\mathbf{r}$. The first term selects the projection of the particle's momentum onto the direction of the field polarization. The second describes how the time-dependent position of the charge is projected along the direction of field propagation. Therefore, this term accounts for the motion and position of the charged particle in two orthogonal directions. To look closer, let's consider the case that we have a plane wave polarized in the x direction and propagating along z. In that case this product is

$$(\hat{\varepsilon}\cdot\mathbf{p})(\mathbf{k}\cdot\mathbf{r}) \to zp_x$$

(Remember: since the directions are orthogonal, the operators commute, and the order doesn't matter). You may note that this type of product appears in the orbital angular momentum operator $L_y = zp_x - xp_z$, and indeed angular momentum is the type of operator that is expected to influence a particle's position and momentum in both x and z dimensions. We therefore expect that, in evaluating the matrix elements $\langle k|zp_x|\ell\rangle$, there might be contributions from $\langle k|L_y|\ell\rangle$ and a second factor. The trick to making this work is to write the operator in the form zp_x

$$zp_x = \frac{1}{2}(zp_x - xp_z) + \frac{1}{2}(zp_x + xp_z)$$

This strategy results in a symmetrized and anti-symmetrized operators that will commute. The first term is what we expected, $\frac{1}{2}L_y$. The second term can be simplified using the expression for a particle in a central potential: $[H_0, xz] = -\mathrm{i}\hbar(zp_x + xp_z)/m$. Then the resulting matrix elements of $V^{(2)}$ can be written as

$$\langle k|zp_x|\ell\rangle = \frac{1}{2}\langle k|L_y|\ell\rangle + \frac{\mathrm{i}m}{2\hbar}\langle k|xz|\ell\rangle \tag{7.9.2}$$

So, what do these terms indicate? the leading term describes the orbital angular momentum in y—the direction in which the magnetic field is polarized—and this can be expressed in terms of a magnetic dipole moment. The second term represents simultaneous charge displacements in the z and x directions, and this can be expressed as an electric quadrupole moment. With this insight, we can return to the original expression and work through the problem more generally.

First, we can rewrite the operator product in eq. (7.9.2) using the outer product $\mathbf{pr}$

$$(\hat{\varepsilon}\cdot\mathbf{p})(\mathbf{k}\cdot\mathbf{r}) = \hat{\varepsilon}\cdot(\mathbf{pr})\cdot\mathbf{k} \tag{7.9.3}$$

Written explicitly, this is

$$\hat{\varepsilon}\cdot(\mathbf{pr})\cdot\mathbf{k} = \begin{pmatrix} \varepsilon_x & \varepsilon_y & \varepsilon_z \end{pmatrix}\begin{pmatrix} p_xr_x & p_xr_y & p_xr_z \\ p_yr_x & p_yr_y & p_yr_z \\ p_zr_x & p_zr_y & p_zr_z \end{pmatrix}\begin{pmatrix} k_x \\ k_y \\ k_z \end{pmatrix} \tag{7.9.4}$$

Alternatively, this could be written $\sum_n^m \varepsilon_m(p_mr_n)k_n$, where the indices $m, n = \{x, y, z\}$. We can now rewrite the product of operators $\mathbf{pr}$ as a sum of symmetrized and antisymmetrized terms:

$$\hat{\varepsilon}\cdot(\mathbf{pr})\cdot\mathbf{k} = \frac{1}{2}\hat{\varepsilon}\cdot(\mathbf{pr}-\mathbf{rp})\cdot\mathbf{k} + \frac{1}{2}\hat{\varepsilon}\cdot(\mathbf{pr}+\mathbf{rp})\cdot\mathbf{k} \tag{7.9.5}$$

We now have two commuting terms which will allow us to separate $V^{(2)}(t)$ into two contributions: $V^{(2)}_{\mathrm{mag}}$ gives rise to magnetic dipole transitions, and $V^{(2)}_Q$ leads to electric quadrupole transitions:

$$V^{(2)}(t) = V^{(2)}_{\text{mag}}(t) + V^{(2)}_{Q}(t) \tag{7.9.6}$$

Let's now discuss and simplify these two terms to make them more intuitive. Considering the leading term in (7.9.5), we can use the vector identity $(A \times B) \cdot (C \times D) = (A \times C)(B \times D) - (A \times D)(B \times C)$ to write this expression in terms of the orbital angular momentum $\mathbf{L}$

$$\begin{aligned} \frac{1}{2}\hat{\varepsilon} \cdot (\mathbf{pr} - \mathbf{rp}) \cdot \mathbf{k} &= \frac{1}{2}\left[(\hat{\varepsilon} \cdot \mathbf{p})(\mathbf{r} \cdot \mathbf{k}) - (\hat{\varepsilon} \cdot \mathbf{r})(\mathbf{p} \cdot \mathbf{k})\right] \\ &= \frac{1}{2}\left[(\mathbf{k} \cdot \hat{\varepsilon}) \cdot (\mathbf{r} \times \mathbf{p})\right] \\ &= \frac{1}{2}(\mathbf{k} \times \hat{\varepsilon}) \cdot \mathbf{L} \end{aligned} \tag{7.9.7}$$

Since the vector $\mathbf{k} \times \hat{\varepsilon}$ describes the direction of the magnetic field $\mathcal{B}$, and the amplitude of the magnetic field and vector potential are related by $\tilde{A}_0 = \tilde{\mathcal{B}_0}/\mathrm{i}k$, we can write

$$V^{(2)}_{\text{mag}}(t) = -\frac{e}{2m}\mathcal{B}(t) \cdot \mathbf{L} \tag{7.9.8}$$

with $\mathcal{B}(t) = \hat{b}\tilde{\mathcal{B}_0}e^{-\mathrm{i}\omega t}$. We are dealing with electron orbital angular momentum, so we have set $q = e$. Using the definition of the Bohr magneton

$$\mu_B = \frac{e\hbar}{2m} \approx 9.274 \times 10^{-24}\,\mathrm{J\,T^{-1}}$$

and the magnetic dipole operator

$$\boldsymbol{\mu}_{\text{mag}} = -\frac{e}{2m}\mathbf{L} = -\mu_B\frac{\mathbf{L}}{\hbar}$$

we can see that the magnetic dipole interaction with the electromagnetic field is

$$V^{(2)}_{\text{mag}}(t) = -\mathcal{B}(t) \cdot \boldsymbol{\mu}_{\text{mag}} \tag{7.9.9}$$

This is the same form that we found for electric dipole interactions with the electric field.

Remember that we have not included electron spin $\mathbf{S}$ in our derivations of the light-matter interactions. Including magnetic field interactions with electron spin in the original Hamiltonian leads to a more general form in which $\mathcal{B} \cdot \mathbf{L}$ in eq. (7.9.8) is replaced with $\mathcal{B} \cdot (\mathbf{L} + g_e\mathbf{S})$, where the electron factor g is $g_e \approx 2$. As a result, there are two contributions to the magnetic dipole moment: one from the electron orbital angular momentum and one from the electron spin angular momentum: $\boldsymbol{\mu}_{\text{mag}} = \boldsymbol{\mu}_L + \boldsymbol{\mu}_S$.

Turning to electric quadrupole transitions, we can simplify the expression $(\mathbf{pr} + \mathbf{rp})$ in eq. (7.9.5) by substituting the identity $\mathbf{p} = \mathrm{i}m\left[H_0, \mathbf{r}\right]/\hbar$:

$$\mathbf{pr} + \mathbf{rp} = \frac{\mathrm{i}m}{\hbar}\left[\left[H_0, \mathbf{r}\right]\mathbf{r} - \mathbf{r}\left[\mathbf{r}, H_0\right]\right] = \frac{-\mathrm{i}m}{\hbar}\left[\mathbf{rr}, H_0\right] \tag{7.9.10}$$

The resulting matrix element for this operator is $\langle k|\left[\mathbf{rr}, H_0\right]|\ell\rangle = \hbar\omega_{k\ell}\langle k|\mathbf{rr}|\ell\rangle$. Here, $\mathbf{rr}$ is an outer product of two vectors, which is proportional to the quadrupole moment. In a system with spherical symmetry, the dipole moment describes charge displacements introduce an asymmetry in the charge distribution, which generates a force or torque in an external electric field. Quadrupole moments involve changes in the charge displacement that introduce asymmetry with no net dipole and no net force on an external electric field. This quadrupole moment is obtained from $\mathbf{Q} = q\mathbf{rr}$, which can be written as a second rank tensor (3×3 matrix) $Q_{m,n} = \sum_{m,n} qr_m r_n$, where $m, n = \{x, y, z\}$. Motivated by the classical definition, with the recognition that $\mathbf{Q}$ is a traceless matrix ($\sum_m Q_{mm} = 0$), we define the quadrupole moment for many charges (i) as

$$Q_{m,n} = \sum_i q_i\left(3r_{m,i} \cdot r_{n,i} - r_i^2\delta_{m,n}\right) \qquad m, n = \{x, y, z\} \tag{7.9.11}$$

We can now express the interaction potential of the quadrupole moment with an electric field using $\tilde{A}_0 = \tilde{E}_0/\mathrm{i}\omega$

$$\begin{aligned} V_Q^{(2)}(t) &= -\mathrm{i}\frac{q}{2m}\tilde{\mathbf{A}}_0 \cdot (\mathbf{pr} + \mathbf{rp}) \cdot \mathbf{k} e^{-\mathrm{i}\omega t} \\ &= -\frac{1}{2\mathrm{i}\hbar\omega}\tilde{\mathbf{E}}_0 \cdot [\mathbf{Q}, H_0] \cdot \mathbf{k} e^{-\mathrm{i}\omega t} \end{aligned} \tag{7.9.12}$$

Then, the transition quadrupole matrix element can be evaluated as

$$\begin{aligned} \left\langle k \left| V_Q^{(2)} \right| \ell \right\rangle &= \frac{\mathrm{i}\tilde{E}_0\omega_{k\ell}}{2\omega} \langle k | \hat{\varepsilon} \cdot \mathbf{Q} \cdot \hat{k} | \ell \rangle \\ &= \frac{\mathrm{i}\tilde{E}_0\omega_{k\ell}}{2\omega}\mathbf{Q}_{k,\ell} \end{aligned} \tag{7.9.13}$$

What are the selection rules for these light-matter interaction mechanisms? Let's consider the example of atomic spectroscopy. The selection rules for electric-dipole (or E1) transitions between states k and ℓ dictates that states ℓ and k have to be of opposite parity and that the changes in angular momentum quantum numbers are $\Delta\ell = \pm 1$ and $\Delta m_\ell = 0, \pm 1$. For magnetic dipole (M1) and electric quadrupole (E2) transitions, states ℓ and k have to be of the same parity, and the allowed changes in quantum numbers are $\Delta\ell = \pm 1$ and $\Delta m_\ell = 0, \pm 1$.

This page titled 7.9: Appendix- Magnetic Dipole and Electric Quadrupole Transitions is shared under a CC BY-NC-SA 4.0 license and was authored, remixed, and/or curated by Andrei Tokmakoff via source content that was edited to the style and standards of the LibreTexts platform.

7.10: Readings

Electromagnetic Fields, Potentials, and Waves

1. Cohen-Tannoudji, C.; Diu, B.; Laloë, F. *Quantum Mechanics*; Wiley, 1977.
2. Griffiths, D. J. *Introduction to Electrodynamics*, 3rd ed.; Prentice-Hall, 1999.
3. Jackson, J. D. *Classical Electrodynamics*, 2nd ed.; Wiley, 1975.
4. Struve, W. S. *Fundamentals of Molecular Spectroscopy*; Wiley, 1989.

Classical Light–Matter Interactions

1. Cohen-Tannoudji, C.; Diu, B.; Laloë, F. *Quantum Mechanics*; Wiley, 1977.
2. Jackson, J. D. *Classical Electrodynamics*, 2nd ed.; Wiley, 1975.
3. McHale, J. L. *Molecular Spectroscopy*, 1st ed.; Prentice-Hall, 1999.
4. Merzbacher, E. *Quantum Mechanics*, 3rd ed.; Wiley, 1998.
5. Sakurai, J. J. *Modern Quantum Mechanics*, rev. ed.; Addison-Wesley, 1994; p 1492.
6. Schatz, G. C.; Ratner, M. A. *Quantum Mechanics in Chemistry*; Dover Publications, 2002; pp 82-83.

Appendix- Magnetic Dipole and Electric Quadrupole Transitions

1. Baym, G. *Lectures on Quantum Mechanics*; W.A. Benjamin, 1969. DOI: 10.1201/9780429499265
2. Struve, W. S. *Fundamentals of Molecular Spectroscopy*; Wiley, 1989.

This page titled 7.10: Readings is shared under a CC BY-NC-SA 4.0 license and was authored, remixed, and/or curated by Andrei Tokmakoff.

8: EMISSION OF RADIATION

8.1: Classical rate of light emission
8.2: Radiation from an Oscillating Dipole
8.3: Appendix- Wave equation with a source
8.4: Readings

This page titled 8: Emission of Radiation is shared under a CC BY-NC-SA 4.0 license and was authored, remixed, and/or curated by Andrei Tokmakoff via source content that was edited to the style and standards of the LibreTexts platform.

8.1: Classical rate of light emission

Using spectroscopy to study molecular properties has two basic modalities. We can investigate changes to the properties of electromagnetic fields once they have passed through matter (for instance through absorption measurements), or we can study light emitted by the matter. Thus, studying emitted radiation is the complementary second half of spectroscopy. However, these two spectroscopic modalities are not as distinct as one might think, but rather two sides of the same coin. The incident and emitted fields are closely coupled, with oscillating charged particles being both the consequence of a driving electromagnetic field and the source of a charge current that re-radiates light. Here we will discuss some of the factors needed to describe emission of light from oscillating charges, starting with classical observations and describing the radiation of electromagnetic fields from a dipole emitter.

In our discussion of the classical driven oscillator, we have seen that a resonant electromagnetic field can drive a bound charged particle to oscillate at the driving frequency. The sinusoidal oscillation of this charge should similarly in the emission of radiation, even after switching off the field, since accelerated charges radiate an electromagnetic field. At distances far from the source, this radiated field is calculated as

$$\mathcal{E}_{\text{rad}}(\mathbf{r},t') = \frac{q}{4\pi\varepsilon_0 c^2}\left.\frac{d\hat{r}^2}{dt^2}\right|_{t'} \tag{8.1.1}$$

Here $\mathbf{r}$ is the distance from the source to the observer, $\hat{r}$ is the unit vector in that direction, and $\mathcal{E}$ is evaluated at the retarded time $t' = t - (r/c)$, to account for the time it takes for the field to propagate at the speed of light from the source to the observer. The emitted radiation are spherical waves radiated into three dimensions, which we will describe for a point dipole emitter in the following section.

We also learned from our driven oscillator model that a driven oscillator will absorb energy from the driving field when it is near resonance. To reach a steady state solution, the energy absorbed must be balanced by energy dissipation. We accounted for this phenomenologically by adding a damping constant γ to the equation of motion. For molecules in condensed matter, one can imagine irreversible processes by which this energy might be dissipated as heat, but for an isolated molecule or atom radiating this energy into an electromagnetic field is far more likely. Although it is possible to formulate the forces on the driven oscillator to properly account for the emission of radiation, the nuances needed to handle that problem are best reviewed elsewhere.(1) We can, however, calculate in a straightforward manner the power radiated into all directions by an oscillator in the absence of damping. This is essentially what one would expect when the damping is weak enough to neglect and when the driving field is strong enough to neglect its depletion due to absorption. In that limit, the radiated power is governed by the Larmor formula

$$\overline{\mathcal{P}}_{\text{rad}} = \frac{\mu'^2}{6\pi\varepsilon_0 c^3}\left|\ddot{Q}\right|^2 \tag{8.1.2}$$

where $\ddot{Q}$ is the acceleration of the bound particle. This leads to(2)(2)

$$\overline{\mathcal{P}}_{\text{rad}} = \frac{\mu'^4 E_0^2}{12\pi\varepsilon_0 m^2 c^3}\frac{\omega^4}{\left(\omega_0^2-\omega^2\right)^2+4\gamma^2\omega^2} \tag{8.1.3}$$

As before, μ' is the dipole derivative for displacing the charged oscillator, and E_0 is the amplitude of the incident driving field.

With these results in hand, it is possible to calculate the classical scattering cross section (σ_{sc}), which describes the power radiated by the dipole into all directions, relative to the incident intensity of the electric field driving the oscillator:

$$\sigma_{\text{sc}}(\omega) = \frac{\overline{\mathcal{P}}_{\text{rad}}}{I_0} \tag{8.1.4}$$

With $I_0 = \frac{1}{2}\varepsilon_0 c E_0^2$, we obtain

$$\sigma_{\text{sc}}(\omega) = \frac{\mu'^4}{12\pi\varepsilon_0^2 m^2 c^4}\frac{\omega^4}{\left(\omega_0^2-\omega^2\right)^2+4\gamma^2\omega^2} \tag{8.1.5}$$

Note that the leading factor in this equation has units of m^2, while the second term is a unitless lineshape function. If we take μ'

to be the electron charge e, we can see that this factor is proportional to the square of the so-called classical electron radius $r_e = e^2/\left[4\pi\varepsilon_0 m_e c^2\right] \approx 3\times10^{-15}$ m. Thus, the magnitude of this scattering cross section is governed by a prefactor that is very small, on the order of 10^{-24} cm^2. In contrast, molecular electronic absorption cross-sections are on the order of $10^{-16}-10^{-18}$cm^2. The prefactor in eq. (8.1.5) gives the scattering cross-section directly for scattered light with frequencies that are significantly greater than the resonance frequency ($\omega \gg \omega_0$).

We can use eq. (8.1.5) to describe Raleigh scattering, the non-resonant scattering of light by polarizable molecules when the scattered radiation is at much lower frequencies that the electronic absorption. In that limit, $\omega \ll \omega_0$, and we can set $\gamma \to 0$ to give:

$$\sigma_{\mathrm{sc}}(\omega) = \frac{\mu'^4}{12\pi\varepsilon_0^2 m^2 c^4}\frac{\omega^4}{\omega_0^4} \tag{8.1.6}$$

This expression illustrates the high order ω^4 scaling of the efficiency of Raleigh and non-resonant Raman scattering. Raleigh scattering of solar radiation from the atmosphere is considered responsible for the appearance of a blue sky.

The driven oscillator model can also be used to calculate the damping coefficient for classical radiative relaxation, although this requires a more sophisticated accounting for the forces that give rise to the radiative power loss.(1) This results in

$$\gamma_{\mathrm{rad}} = \frac{\mu'^2\omega^2}{6\pi m\varepsilon_0 c^3} \tag{8.1.7}$$

How good are the classical predictions? Using the charge of an electron for μ', electron mass, and an oscillation frequency corresponding to visible radiation ($\omega/2\pi = 10^{15}$ Hz), we find a radiative lifetime of $\tau_{\mathrm{rad}} = \gamma_{\mathrm{rad}}^{-1} = 4\times10^{-9}$ s. This is the same order of magnitude as the lifetimes of atomic excited states. As we have noted previously for classical models, this is satisfying in that it gets close to proper values, but this calculation bypasses many details regarding the true nature of atom-field interactions, leading to limited predictive capability. For instance, the quantum calculation of the spontaneous emission rate scales as ω^3 as opposed to the ω^2 scaling here.

References

(1) Griffiths, D. J. *Introduction to Electrodynamics*, 3rd ed.; Prentice-Hall, 1999.

(2) An, K. *Fundamentals of Laser Physics*; World Scientific, 2023. DOI: 10.1142/13112

(2) Stenzel, O. *Light-matter interaction: a crash course for students of optics, photonics and materials science*; Springer, 2022. DOI: 10.1007/978-3-030-87144-4

This page titled 8.1: Classical rate of light emission is shared under a CC BY-NC-SA 4.0 license and was authored, remixed, and/or curated by Andrei Tokmakoff via source content that was edited to the style and standards of the LibreTexts platform.

8.2: Radiation from an Oscillating Dipole

In addition to accounting for the radiative rate of energy loss by a driven oscillator, we are interested in describing the radiation pattern of the emitted wave in three dimensions. This requires us to solve the problem of an oscillating charge coupled to an electromagnetic radiation field using Maxwell's equations, which can be reviewed in any electrodynamics text.(1)(2) Here we will summarize the steps and results for the far-field emission of radiation by an oscillating point dipole, using a notation more applicable to molecular spectroscopy. This dipole acts as a source of charge current which is coupled to the electromagnetic vector potential.

The dipole oscillator refers to two equal and oppositely signed charges $\pm q$ displaced from each other along the z axis by a distance R_0. The static dipole moment $\mathbf{m}_0 = qR_0\hat{\mathbf{z}}$, however, does not radiate a field; only time-dependent potentials can act as a source. To introduce the time-dependence, we take the bond length and therefore the magnitude of the dipole moment to oscillate sinusoidally at a frequency ω_0, as we would expect for the motion of bound charges induced by a driving field:

$$\mathbf{m}(t) = m_0 + \hat{\mathbf{z}}m' \cos(\omega t) \tag{8.2.1}$$

For small changes in bond length, this overall variation in the dipole moment amplitude can be expressed using the dipole derivatives, $\mu' = (\partial m/\partial Q)$, and oscillator displacement, $Q = R - R_0$, that we used in the driven oscillator model. Thus, $m' = \mu' Q$.

A point dipole refers to the limiting behavior of this dipole as d approaches zero (but remember that $d = 0$ result in no dipole potential and no radiation!). This is equivalent to the observer position $\mathbf{r}$ being much larger than d. Additionally, we will be describing the behavior in the far-field. This refers to the observer being at much longer distances from the dipole than the wavelength of the radiated light, $r \gg c/\omega = \lambda$.

To couple this dipole to an electromagnetic field we turn to the wave-equation for the vector potential A in the presence of a charge current is

$$\nabla^2 \mathbf{A} - \varepsilon_0 \mu_0 \frac{\partial^2 \mathbf{A}}{\partial t^2} = -\mu_0 \mathbf{J} \tag{8.2.2}$$

J is the transverse current density, which we obtain from the time-derivative of the oscillating dipole

$$\mathbf{J}(t) = \frac{d\mathbf{m}}{dt} = -\hat{\mathbf{z}}m'\omega \sin(\omega t) \tag{8.2.3}$$

Thus, the current is proportional to the momentum of the charged particle: $\mathbf{J} = \mu' \mathbf{p}$. Solutions for $\mathbf{A}$ from eq. (8.2.9) will oscillate at the same frequency as $\mathbf{J}$. Furthermore, by virtue of the dipole's alignment along z, the magnitude of $\mathbf{A}$ can only depend on r and the polar angle θ, resulting in solutions of the form $\mathbf{A}(\mathbf{r}, t) = \mathbf{A}(r, \theta) \sin \omega t$. As described in the appendix, in the far field the vector potential for sinusoidally oscillating potentials can be calculated from

$$\mathbf{A}(\mathbf{r}, t) = \frac{\mu_0}{4\pi r} \int \mathbf{J}(\mathbf{r}', t')\, d\mathbf{r}' \tag{8.2.4}$$

In this case, the integration is performed along z over the length of the dipole. Since the action of emitted electromagnetic radiation propagates at the speed of light c from the dipole at the origin to the observer at radial distance r, the resulting expression is evaluated in terms of the retarded time

$$t' = t - \frac{r}{c} \tag{8.2.5}$$

The resulting spherical waveform describing the vector potential is oriented along $\hat{z}$ and propagates spherically, dropping in magnitude radially as $1/r$:

$$\mathbf{A}(r, \theta, t) = -\hat{\mathbf{z}} \frac{\mu_0 m' \omega}{4\pi r} \sin\left(\omega\left(t - \frac{r}{c}\right)\right) \tag{8.2.6}$$

To briefly summarize an involved derivation in spherical coordinates ($\hat{z} = \hat{r}\cos\theta - \hat{\theta}\sin\theta$), the vector potential can be used to calculate the magnetic field from $\mathcal{B} = \nabla \times \mathbf{A}$ and then the electric field follows from $\dot{\mathcal{E}} = c^2 \nabla \times \mathcal{B}$:(3)

$$\mathcal{E}_{\text{rad}}(r,\theta,t) = -\hat{\theta}\frac{\mu_0 m'\omega^2}{4\pi}\frac{\sin\theta}{r}\cos\left(\omega\left(t-\frac{r}{c}\right)\right) \tag{8.2.7}$$

The radiation pattern for the electric field emitted by the point dipole is illustrated in Figure 8.2.1. It has a $\sin\theta$ angular dependence leading to a maximum perpendicular to the dipole and is independent of the azimuthal angle ϕ. These are spherical waves rather than plane waves, with wavefronts that have a donut shape with a maximum in the xy plane. With increasing distance the curvature of these wavefronts appears to decrease to an observer in the xy plane. Notice that the magnitude of the field drops with distance as $1/r$, a slow drop-off that allows for long range propagation from a point source (i.e., we can see stars!).

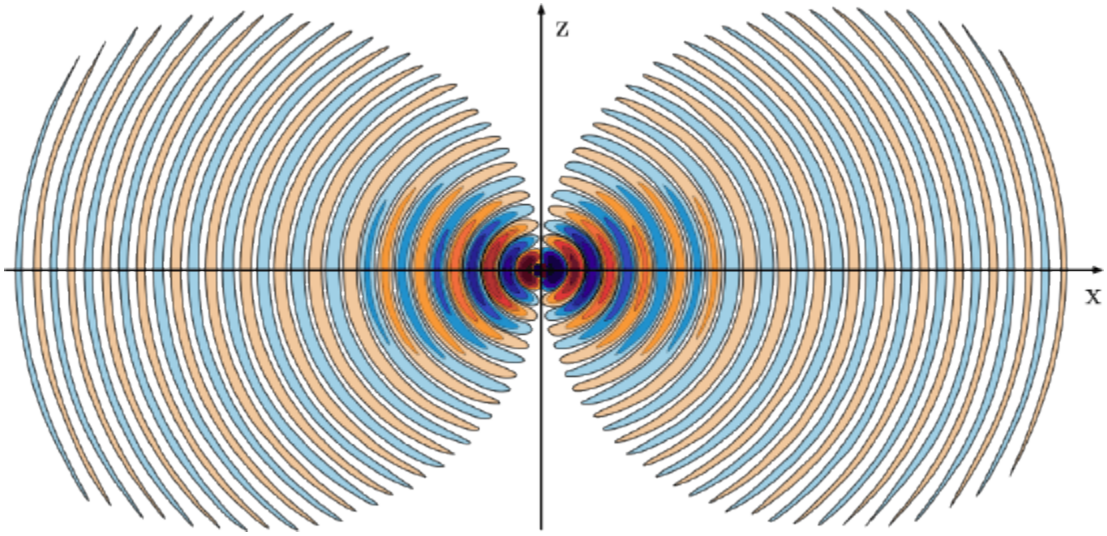


Figure 8.2.1: Far-field electric field contours in the z, x plane for radiation emitted by an oscillating point dipole positioned at the origin and oriented along z.

Video

This interactive element is not available in this format. Visit the link or scan the QR code to access it online.

View this Video online

Figure 8.2.2: Far Field

Video

This interactive element is not available in this format. Visit the link or scan the QR code to access it online.

View this Video online

Figure 8.2.3: Near Field

Now consider the phase relationships between the different quantities we have investigated (Figure 8.2.4). Remembering our

results from the driven oscillator model, when we are on resonance, the motion of the bound particle $Q(t)$ is in-quadrature to the excitation field $\mathcal{E}_{\rm ex}(t)$. So, a resonant external field from a plane wave traveling along x and oscillating as $\sin(\omega t)$ will induce oscillations in $Q(t)$ positioned at $x = 0$ that oscillate along z as $\cos\omega t$, as in eq. (8.2.1). Then, notice the leading minus sign in eq. (8.2.7), which indicates that the radiated electric field is oscillating out-of-phase with the respect to the oscillation of the dipole in eq. (8.2.1), since $-\cos\omega t = \cos(\omega t + \pi)$. Of course the radiated field is emitted as spherical waves into three dimensions. Focusing on the behavior along the x axis, we see a sequence of sequential phase shifts through the variables that dictate the light-matter interaction. On resonance, $Q(t)$ tracks the incident field with a phase-shift of $\pi/2$ reflecting that the maximum force on the particle and its highest velocity are present at the highest driving field. The current and vector potential lag $Q(t)$ by another $\pi/2$ phase-shift since they are proportional to the velocity $\dot{Q}$. Finally, the radiated field $\mathcal{E}_{\rm rad}(t)$ experiences another phase shift of $\pi/2$ relative to $A(t)$, leading to a total phase shift of π between Q and $\mathcal{E}_{\rm rad}$.

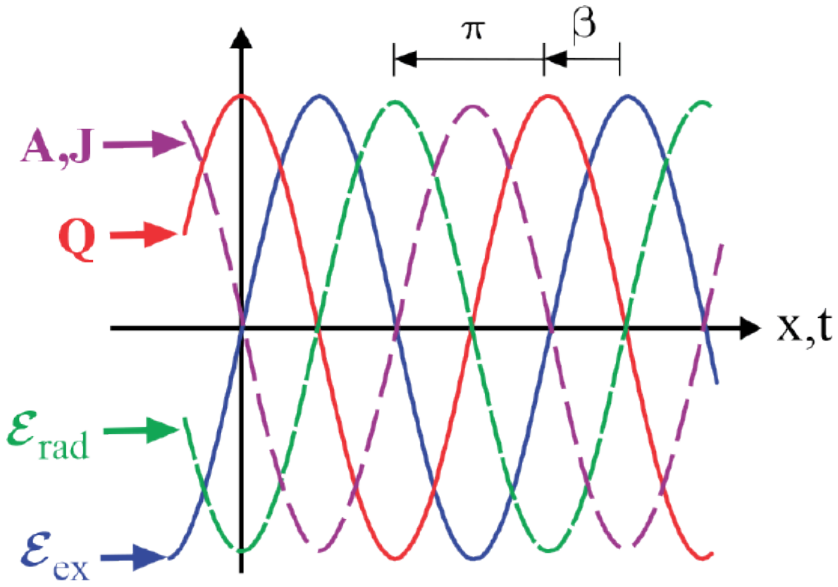


Figure 8.2.4: The time-dependent behaviors of the different functions are linked by a phase relationship. Writing the general sinusoidal behavior as $\cos(\omega t - \phi)$, the phase shifts ϕ for the different quantities is: $\phi = \pi/2$ for $\mathcal{E}_{\rm ex}$, $\phi = 0$ for Q on resonance but generally by a phase $\beta = \arctan(\chi''/\chi')$; $\phi = -\pi/2$ for $\mathbf{A}$ and $\mathbf{J}$; $\phi = -\pi$ for $\mathcal{E}_{\rm rad}$.

By cycle-averaging the Poynting vector, we can obtain the average power radiated into a solid angle per unit time.

$$I_{\rm avg}(r,\theta) = \frac{m'^2\omega^4}{32\pi^2\varepsilon_0 c^3}\frac{\sin^2\theta}{r} \tag{8.2.8}$$

This expression can be integrated over all directions to obtain the total power emitted from the dipole, from which we recover eq. (8.1.3):

$$\bar{\mathcal{P}}_{\rm rad} = \frac{m'^2\omega^4}{12\pi\varepsilon_0 c^3} \tag{8.2.9}$$

We can observe that there is a close interplay between the fields that are driving the charges of the system, the absorption of light by the driven dipole, and the radiation emitted by the dipole because of that interaction. The radiative damping of a driven oscillator leads to the observation that the steady state rate of absorption of energy by the oscillator must be matched by the rate of energy radiation by the oscillator. The second important phenomenon is the phase relationship between the driving field and the radiated field, which can lead to interference effects in between the transmitted and radiated field in the far field. In the current case, the spherical waves radiated by the dipole will have an angular dependence to its interference with a plane wave driving field. As we will see, these phase relationships play an important role in condensed phase spectroscopy where the macroscopic polarization of the sample takes the place of the driven dipole. There we will also need to be concerned of the action of the oscillating dipoles on each other and the field as it travels through the sample. Absorption spectroscopy can be conceived of as a destructive interference effect between the radiated and transmitted fields, whereas scattering of light results from the background free re-emission of radiation into all directions. In nonlinear spectroscopy, phase-matching conditions that depend on the incident wave-vectors of two or more fields can result in coherent signal emission into background free directions. When discussing condensed phase spectroscopy, we use will return to Maxwell's Equations and incorporate the polarization of the medium as a source term for the electromagnetic wave equations.

References

(1) Griffiths, D. J. *Introduction to Electrodynamics*, 3rd ed.; Prentice-Hall, 1999.

(2) Jackson, J. D. *Classical Electrodynamics*, 2nd ed.; Wiley, 1975.

(3) Wolski, A. Theory of Electromagnetic Fields. *arXiv* **2014**. DOI: 10.48550/arXiv.1111.4354

This page titled 8.2: Radiation from an Oscillating Dipole is shared under a CC BY-NC-SA 4.0 license and was authored, remixed, and/or curated by Andrei Tokmakoff via source content that was edited to the style and standards of the LibreTexts platform.

8.3: Appendix- Wave equation with a source

Let's consider the effect of time-dependent charges and currents on the equations for the scalar electrostatic potential φ and vector potential $\mathbf{A}$. We begin with the wave equations for the electrostatic potential and vector potential derived in Sec. 7.8:

$$\nabla^2\varphi - \varepsilon_0\mu_0\frac{\partial^2\varphi}{\partial t^2} = -\frac{\rho}{\varepsilon_0} \tag{8.3.1}$$

$$\nabla^2\mathbf{A} - \varepsilon_0\mu_0\frac{\partial^2\mathbf{A}}{\partial t^2} = -\mu_0\mathbf{J} \tag{8.3.2}$$

ρ is the charge density and $\mathbf{J}$ is the transverse current density. The vector and scalar potential are related by

$$\nabla\cdot\mathbf{A} = -\varepsilon_0\mu_0\frac{\partial\varphi}{\partial t} \tag{8.3.3}$$

The general solutions to eq. (8.3.1) and (8.3.3) are(1)

$$\varphi(\mathbf{r},t) = \int\frac{\rho(\mathbf{r}',t')}{4\pi\varepsilon_0|\mathbf{r}-\mathbf{r}'|}\,d\mathbf{r}' \tag{8.3.4}$$

$$\mathbf{A}(\mathbf{r},t) = \int\frac{\mu_0\mathbf{J}(\mathbf{r}',t')}{4\pi|\mathbf{r}-\mathbf{r}'|}\,d\mathbf{r}' \tag{8.3.5}$$

Since the emitted electromagnetic radiation propagates at the speed of light c from the source at position r' to the observer at radial distance r, these expressions are evaluated using in terms of the retarded time

$$t' = t - \frac{|r-r'|}{c} \tag{8.3.6}$$

Thus eqs. (8.3.4) and (8.3.5) are known as the retarded potentials.

We will consider specific solutions in which the sources have a sinusoidal time dependence. We take ρ and $\mathbf{J}$ to also have a sinusoidal time-dependence of the form $\rho(\mathbf{r},t') = \rho(\mathbf{r})e^{\mathrm{i}\omega t'}$ and $\mathbf{J}(\mathbf{r},t') = \mathbf{J}(\mathbf{r})e^{\mathrm{i}\omega t'}$, where it is understood that, to obtain the real charge density or current density, one calculates the real part of the corresponding complex quantity. This results in vector and scalar potentials that have a similar form $\mathbf{A}(\mathbf{r},t) = \mathbf{A}(\mathbf{r})e^{\mathrm{i}\omega t}$ and $\varphi(\mathbf{r},t) = \varphi(\mathbf{r})e^{\mathrm{i}\omega t}$. Then from eqs. (8.3.1) and (8.2.2) we are left with equations for the spatial amplitudes

$$\nabla^2\mathbf{A}(\mathbf{r}) + \mathbf{k}^2\mathbf{A}(\mathbf{r}) = -\mu_0\mathbf{J}(\mathbf{r}) \tag{8.3.7}$$

$$\nabla^2\varphi(\mathbf{r}) + \mathbf{k}^2\varphi(\mathbf{r}) = -\frac{\rho(\mathbf{r})}{\varepsilon_0} \tag{8.3.8}$$

Here $k = \omega/c$.

Recognizing that the retarded potentials can be written as

$$\begin{aligned}\rho\left(r,t'\right) &= \rho(r)\exp\left[\mathrm{i}\omega t'\right]\\ &= \rho(r)\exp\left[\mathrm{i}\omega t\right]\exp\left[-\mathrm{i}\omega\left|r-r'\right|/c\right]\\ &= \rho(r)\exp\left[\mathrm{i}\omega t\right]\exp\left[-ik\left|r-r'\right|\right]\end{aligned} \tag{8.3.9}$$

equations (8.3.4) and (8.3.5) for sinusoidal sources become:

$$\varphi(\mathbf{r},t) = \int\rho(\mathbf{r}',t')\frac{e^{\mathrm{i}k|\mathbf{r}-\mathbf{r}'|}}{4\pi\varepsilon_0|\mathbf{r}-\mathbf{r}'|}\,d\mathbf{r}' \tag{8.3.10}$$

$$\mathbf{A}(\mathbf{r},t) = \int\mathbf{J}(\mathbf{r}',t')\frac{\mu_0 e^{\mathrm{i}k|\mathbf{r}-\mathbf{r}'|}}{4\pi|\mathbf{r}-\mathbf{r}'|}\,d\mathbf{r}' \tag{8.3.11}$$

We now turn to the case in which the emission is observed on distance scales that greatly exceed the size of the radiation source. Then we can approximate that $|r-r'| \approx r$, so the remaining terms in r can be factored out of the integral

$$\varphi(\mathbf{r},t)=\frac{e^{\mathrm{i}kr}}{4\pi\varepsilon_0\mathbf{r}}\int\rho(\mathbf{r}',t')\,d\mathbf{r}' \tag{8.3.12}$$

$$\mathbf{A}(\mathbf{r},t)=\frac{\mu_0 e^{\mathrm{i}kr}}{4\pi\mathbf{r}}\int\mathbf{J}(\mathbf{r}',t')\,d\mathbf{r}' \tag{8.3.13}$$

If we also calculate the potentials in the far field, that is at distances r that exceed the wavelength of the emitted light ($r \gg c/\omega = \lambda$), then we can expand and set $e^{ikr} \rightarrow 1$. Then we can calculate the scalar and vector potentials from

$$\varphi(\boldsymbol{r},t)=\frac{1}{4\pi\varepsilon_0 r}\int\rho(\boldsymbol{r}',t')\,d\boldsymbol{r}' \tag{8.3.14}$$

$$\boldsymbol{A}(\boldsymbol{r},t)=\frac{\mu_0}{4\pi r}\int\boldsymbol{J}(\boldsymbol{r}',t')\,d\boldsymbol{r}' \tag{8.3.15}$$

To describe fields emitted by electric dipoles, we return to eq. (8.3.4) and use the continuity equation between the charge density $\boldsymbol{\rho}(r)$ and the divergence of the current

$$\mathrm{i}\omega\boldsymbol{\rho}(\mathbf{r})=\nabla\cdot\mathbf{J} \tag{8.3.16}$$

to rewrite the integrand as $-\mathrm{i}\omega\mathbf{r}\mathbf{m}(\mathbf{r})$, where $\mathbf{m}(\mathbf{r})$ is the electric dipole moment

$$\mathbf{m}(\mathbf{r})=\int\mathbf{r}\rho(\mathbf{r})\,d\mathbf{r} \tag{8.3.17}$$

This allows one to express the vector potential as

$$\mathbf{A}(\mathbf{r})=-\mathrm{i}\frac{\omega\mu_0}{4\pi}\mathbf{m}\frac{e^{\mathrm{i}kr}}{r} \tag{8.3.18}$$

The magnetic field can be calculated from the vector potential as

$$\boldsymbol{\mathcal{B}}=\nabla\times\mathbf{A} \tag{8.3.19}$$

and the electric field at a distance far from the source is obtained from

$$\boldsymbol{\mathcal{E}}=\frac{\mathrm{i}\mu_0}{\omega}\nabla\times\boldsymbol{\mathcal{B}} \tag{8.3.20}$$

which yield

$$\boldsymbol{\mathcal{B}}=k^2(\hat{\mathbf{r}}\times\boldsymbol{\mu})\frac{e^{\mathrm{i}kr}}{r}$$

$$\boldsymbol{\mathcal{E}}=\left(\frac{1}{\mathrm{c}}\right)\boldsymbol{\mathcal{B}}\times\hat{\mathbf{r}}$$

References

(1) Rana, F. *Lecture 28: Antennas and Radiation and the Hertzian Dipole*. https://courses.cit.cornell.edu/ece303/Lectures/

This page titled 8.3: Appendix- Wave equation with a source is shared under a CC BY-NC-SA 4.0 license and was authored, remixed, and/or curated by Andrei Tokmakoff via source content that was edited to the style and standards of the LibreTexts platform.

8.4: Readings

Dipole Radiation

1. Feyman, R.; Leighton, R.; Sands, M. Electromagnetic Radiation. *The Feynman Lectures on Physics, Volume I*; New Millennium ed.; Basic Books, 2006. https://www.feynmanlectures.caltech.edu/I_28.html
2. Fitzpatrick, R. *The Hertzian Dipole*. 2006. https://farside.ph.utexas.edu/teaching/em/lectures/node94.html
3. Griffiths, D. J. *Introduction to Electrodynamics*, 3rd ed.; Prentice-Hall, 1999.
4. Jackson, J. D. *Classical Electrodynamics*, 3rd ed.; Wiley, 1998.

This page titled 8.4: Readings is shared under a CC BY-NC-SA 4.0 license and was authored, remixed, and/or curated by Andrei Tokmakoff.

9: QUANTUM ELECTROMAGNETIC FIELD

9.1: Introduction

9.2: Hamiltonian for quantized electromagnetic field

9.3: Electromagnetic field

9.4: Light-Matter Interactions and Spontaneous Emission

9.5: Coherent States

9.6: Readings

This page titled 9: Quantum Electromagnetic Field is shared under a CC BY-NC-SA 4.0 license and was authored, remixed, and/or curated by Andrei Tokmakoff via source content that was edited to the style and standards of the LibreTexts platform.

9.1: Introduction

Spontaneous emission processes like fluorescence are defined by the release of incoherent radiation from excited molecules when a light field is absent. A light field may be used to excite a molecule but then turned off prior to emission. Energy from other sources—perhaps thermal or mechanical—can also result in an excited state molecule which returns to equilibrium through radiative emission. Classically, this process can be described as the radiation of an electromagnetic field from a oscillating dipole, as discussed in Sec. 8.2. In a classical oscillator, the continuous emission of radiation from the oscillating charge displacement will lead to gradual damping of the magnitude of the oscillation. However, we understand molecularly that a quantum transition involves discrete jumps in the energy from an initial to a final state. The principle of energy conservation is preserved by the Golden Rule resonance condition, which indicates that the energy change in the matter is proportional to frequency of the driving field:

$$E_f - E_i = \hbar\omega \tag{9.1.1}$$

To discuss discrete changes in the state of light during an absorption or emission process, we must invoke a quantized radiation field. The discrete changes in the energy of the matter are matched by equal and opposite changes in the energy of the field. While the particles of matter each jump and fall in energy, the field changes energy through the absorption or emission of a photon, the quantum particle of the electromagnetic field.

We will describe in this chapter how one develops a quantum mechanical Hamiltonian for the electromagnetic field and the electromagnetic Hamiltonian's effects on changes in the state of the combined matter-light system. The important insight that enables this is a close connection between the energy of light expressed as harmonic plane waves and the energy of a quantum harmonic oscillator.

At the most basic level, we formulate the quantum mechanics of light-matter interactions through a Hamiltonian composed of separable Hamiltonians, one for the matter H_M and one for light H_L. These sub-systems interact through a light-matter interaction Hamiltonian H_{LM}:

$$H_{\text{tot}} = H_M + H_L + H_{LM} \tag{9.1.2}$$

Our semiclassical description of light-matter interactions in Sec. 7.4, was obtained using our typical technique of applying quantum mechanical principles to classical results. Quantizing the interaction between a classical electromagnetic vector potential and a charged particle results in the interaction Hamiltonian:

$$H_{LM}(t) = -\frac{q}{m}\mathbf{A}(t)\cdot\mathbf{p} \tag{9.1.3}$$

We can continue to build on this result, which holds true in the Coulomb gauge. What we are seeking now is a description of the Hamiltonian for the light, written in terms of a quantum vector potential.

As we do this, we must keep in mind the existing stipulations on our solutions. We have a Schrödinger equation to solve. H_L will be used to describe the wavefunction for the light, but photons are not infinitely extended plane waves. They are traveling wavepackets that one can characterize as a superposition of plane waves (see our prior discussion of wavepackets in Sec. 4.3). Since the basis set used for classical electromagnetic waveforms is the superposition of plane waves, to create a quantum mechanical description of light we will work in a quantized representation of this basis set: the quantum vector potential. The vector potential basis set is the sum of a radiation field over a continuum of plane wave modes. It is defined as:

$$\mathbf{A}_{\mathbf{k},\sigma}(\mathbf{r},t) = \sum_{k,\sigma}\hat{\varepsilon}_{k,\sigma}\,\tilde{A}_{k,\sigma}\,e^{\mathrm{i}(\mathbf{k}\cdot\mathbf{r}-\omega_k t)} + \hat{\varepsilon}_{k,\sigma}\,\tilde{A}^*_{k,\sigma}\,e^{-\mathrm{i}(\mathbf{k}\cdot\mathbf{r}-\omega_k t)} \tag{9.1.4}$$

Each mode is indexed by its wavenumber k as well as by the polarization index $\sigma = 1, 2$, indicating the two orthogonal transverse modes that contribute to the polarization vector $\hat{\varepsilon}_k$. The notation ω_k denotes the dependence of frequency on wavevector, which is $\omega_k = kc$ in the case of free electromagnetic waves.

This page titled 9.1: Introduction is shared under a CC BY-NC-SA 4.0 license and was authored, remixed, and/or curated by Andrei Tokmakoff via source content that was edited to the style and standards of the LibreTexts platform.

9.2: Hamiltonian for quantized electromagnetic field

The energy density is the starting point for connecting the energy in an electromagnetic wave to its fields.

$$\mathcal{U} = \frac{1}{2}\varepsilon_0 \boldsymbol{\mathcal{E}}^2 + \frac{1}{2\mu_0}\boldsymbol{\mathcal{B}}^2 = \frac{1}{2}\varepsilon_0 \left(\boldsymbol{\mathcal{E}}^2 + c^2 \boldsymbol{\mathcal{B}}^2\right) \tag{9.2.1}$$

The energy of the electromagnetic field can then be obtained by integrating over a volume, which gives the classical Hamiltonian of the electromagnetic field.

$$H_L = \frac{1}{2}\varepsilon_0 \int d^3r \left(\boldsymbol{\mathcal{E}}^2 + c^2 \boldsymbol{\mathcal{B}}^2\right) \tag{9.2.2}$$

This Hamiltonian can be expressed in the vector potential basis set, using the expressions that connect $\mathbf{A}$ with the fields that we derived earlier: $\boldsymbol{\mathcal{E}} = -\dot{\mathbf{A}}$ and $\boldsymbol{\mathcal{B}} = \nabla \times \mathbf{A}$.

$$H_L = \frac{1}{2}\varepsilon_0 \int d^3r \left(\dot{\mathbf{A}}^2 + c^2 \left|\nabla \times \mathbf{A}\right|^2\right) \tag{9.2.3}$$

The second term in the integral can be further simplified if we work with plane wave solutions such as eq. (9.1.4). Then, for a single wave mode, $\int d^3r \left|\nabla \times \mathbf{A}\right|^2$ can be evaluated to give $k^2 \int d^3r \; A^2$. This leads to our working expression for the classical Hamiltonian in terms of the electromagnetic vector potential:

$$H_L = \int d^3r \, \frac{1}{2}\varepsilon_0 \left[\dot{\mathbf{A}}_k^2 + \omega_k^2 \mathbf{A}_k^2\right] \tag{9.2.4}$$

This integral can be evaluated for a large cubic volume V, assuming periodic boundary conditions that allow an integral number of half wavelengths within the walls. The resulting energy in the single mode wave, averaged over time, is

$$\bar{E}_k = 2\varepsilon_0 \omega_k^2 \left|\mathbf{A}_k\right|^2 = 2\varepsilon_0 |\boldsymbol{\mathcal{E}}_k|^2 \tag{9.2.5}$$

Note the similarity of the Hamiltonian in eq. (9.2.4) to that for a continuum of harmonic oscillators with varying frequency:

$$\begin{aligned} H_{\mathrm{HB}} &= \sum_j \frac{1}{2}\frac{p_j^2}{m_j} + \frac{1}{2} m_j \omega_j^2 x_j^2 \\ &= \sum_j \frac{1}{2}\left(\dot{q}_j^2 + \omega_j^2 q_j^2\right) \end{aligned} \tag{9.2.6}$$

The abbreviation H_{HB} is applied to this Hamiltonian because it is identical in form to a harmonic bath Hamiltonian. We will use the harmonic bath later to describe the continuum states of a condensed matter environment in a statistical manner. In mapping eq. (9.2.4) to eq. (9.2.6), $\mathbf{A}$ plays the role of the reduced oscillator coordinate $q = \hat{x}/\sqrt{m}$, $\dot{\mathbf{A}}$ is its conjugate momentum $m\dot{q} = \sqrt{m}\dot{x}$, and the integral over volume replaces the sum over modes that vary in frequency. It therefore follows quite naturally that one can express the quantum Hamiltonian for an electromagnetic field in terms of a continuum of harmonic oscillator modes with frequencies of ω_k. Going even further, we can use second quantization expressions for the harmonic oscillator to express the vector potential as

$$A_k = \sqrt{\frac{\hbar}{2\omega_{\mathrm{k}}}}\left(\hat{a}_{k,\sigma}^{\dagger} + \hat{a}_{k,\sigma}\right) \tag{9.2.7}$$

$$\dot{A}_k = \mathrm{i}\sqrt{\frac{\hbar\omega_{\mathrm{k}}}{2}}\left(\hat{a}_{k,\sigma}^{\dagger} - \hat{a}_{k,\sigma}\right) \tag{9.2.8}$$

and the Hamiltonian becomes

$$H_L = \sum_{k,\sigma} \hbar\omega_k \left(\hat{a}_{k,\sigma}^{\dagger}\hat{a}_{k,\sigma} + \frac{1}{2}\right) \tag{9.2.9}$$

Here $\hat{a}^{\dagger}_{k,\sigma}$ and $\hat{a}_{k,\sigma}$ are creation and annihilation operators for the light quanta (photons) in the mode with wavevector k and polarization state σ. These obey the commutation relation $\left[\hat{a}_{k',\sigma'}, \hat{a}^{\dagger}_{k,\sigma}\right] = \delta_{k,k'}\delta_{\sigma,\sigma'}$.

The connection between the classical and quantum Hamiltonians for the electromagnetic field is presented quite loosely here, but eq. (9.2.9) can be rigorously derived from eq. (9.2.4) using the vector potential for a continuum of plane waves.(1) Within this formalism, the one can define a vector potential operator that satisfies eq. (9.2.4) as

$$\mathbf{A}(\mathbf{r},t) = \sum_{k,\sigma}\sqrt{\frac{\hbar}{2\varepsilon_0 V\omega_k}}\left(\hat{\varepsilon}_{k,\sigma}\hat{a}_{k,\sigma}e^{\mathrm{i}(\mathbf{k}\cdot\mathbf{r}-\omega t)} + \hat{\varepsilon}^{*}_{k,\sigma}\hat{a}^{\dagger}_{k,\sigma}e^{-\mathrm{i}(\mathbf{k}\cdot\mathbf{r}-\omega t)}\right) \tag{9.2.10}$$

V is the quantization volume, and the factor of $1/\sqrt{V}$ ensures the orthonormality of the plane wave basis set when integrating over a volume:

$$\int d^3r\,\frac{e^{-\mathrm{i}\mathbf{k}\cdot\mathbf{r}}}{\sqrt{V}}\frac{e^{\mathrm{i}\mathbf{k}'\cdot\mathbf{r}}}{\sqrt{V}} = \delta_{k,k'} \tag{9.2.11}$$

In eq. (9.2.10), $\mathbf{A}^2$ is an energy density which must then be integrated over V.

The operators for the vector potential described in eq. (9.2.7), $\mathbf{A}(\mathbf{r})$, and the Hamiltonian are both time-independent. However, in the Heisenberg or interaction pictures, these operators adopt the conventional time-dependence of the harmonic oscillator raising and lowering operators when evaluating $\mathbf{A}(\mathbf{r},t) = e^{-\mathrm{i}H_L t/\hbar}\mathbf{A}(\mathbf{r})e^{\mathrm{i}H_L t/\hbar}$. This results in the expected time-dependence in eq. (9.2.10). We also find that the operators corresponding to the electric and magnetic fields are

$$\begin{aligned}
\boldsymbol{\mathcal{E}}(\mathbf{r},t) &= \mathrm{i}\sum_{k,\sigma}\sqrt{\frac{\hbar\omega_k}{2\varepsilon_0 V}}\left(\hat{\varepsilon}_{k,\sigma}\hat{a}_{k,\sigma}e^{\mathrm{i}(\mathbf{k}\cdot\mathbf{r}-\omega_k t)} - \hat{\varepsilon}^{*}_{k,\sigma}\hat{a}^{\dagger}_{k,\sigma}e^{-\mathrm{i}(\mathbf{k}\cdot\mathbf{r}-\omega_k t)}\right)\\
\boldsymbol{\mathcal{B}}(\mathbf{r},t) &= \mathrm{i}\sum_{k,\sigma}\sqrt{\frac{\hbar}{2\varepsilon_0 V\omega_k}}\left(\mathbf{k}\times\hat{\varepsilon}_{k,\sigma}\right)\left(\hat{a}_{k,\sigma}e^{\mathrm{i}(\mathbf{k}\cdot\mathbf{r}-\omega_k t)} - \hat{a}^{\dagger}_{k,\sigma}e^{-\mathrm{i}(\mathbf{k}\cdot\mathbf{r}-\omega_k t)}\right)
\end{aligned} \tag{9.2.12}$$

Substituting these relationships into the Hamiltonian for the classical radiation field, eq. (9.2.2), leads directly to the quantum version, eq. (9.2.9).

Along similar lines to the calculation of the energy of the field in this section, one can also compute the momentum associated with the electromagnetic wave. The classical momentum is obtained from the Poynting vector using $\mathbf{p}_L = \varepsilon_0\int d^3r\ \boldsymbol{\mathcal{E}}\times\boldsymbol{\mathcal{B}}$. Expressing this in terms of the vector potential and evaluating this for the plane wave modes gives:(1)

$$\mathbf{p}_L = \sum_{k,\sigma}\hbar\mathbf{k}\hat{a}^{\dagger}_{k,\sigma}\hat{a}_{k,\sigma} \tag{9.2.13}$$

References

(1) Townsend, J. S. *A Modern Approach to Quantum Mechanics*, 2nd ed.; University Science Books, 2012.

This page titled 9.2: Hamiltonian for quantized electromagnetic field is shared under a CC BY-NC-SA 4.0 license and was authored, remixed, and/or curated by Andrei Tokmakoff via source content that was edited to the style and standards of the LibreTexts platform.

9.3: Electromagnetic field

One can anticipate many, but not all, consequences of the Hamiltonian, eq. (9.2.9), on our description of the field wavefunction from what we already know about quantum harmonic oscillators. Harmonic oscillators have equidistant energy levels, and the state of the oscillator can be specified by the number of excitations in the oscillator $|n\rangle$. Therefore, the state of a single electromagnetic mode k can be specified by the number of excitations (quanta) in that mode, N_k. Since the electromagnetic modes form an orthonormal basis, the total wavefunction of the light $|\varphi_L\rangle$ can be expressed in product states for the number of excitations in each of the modes:

$$|\varphi_L\rangle = |N_1, N_2, N_3, ...\rangle \tag{9.3.1}$$

The ground state of the electromagnetic field, the vacuum state, where all N_k = 0.

$$|0\rangle = |0_1, 0_2, 0_3, ...\rangle \tag{9.3.2}$$

Wavefunctions of this form are referred to as Fock states. In this framework, the creation and annihilation operators act to raise or lower the number of excitations in a specific mode:

$$\begin{aligned} \hat{a}_k^\dagger |N_1, N_2, ... N_k ...\rangle &= \sqrt{N_k + 1}\, |N_1, N_2, ... N_k + 1 ...\rangle \\ \hat{a}_k |N_1, N_2, ... N_k ...\rangle &= \sqrt{N_k}\, |N_1, N_2, ... N_k - 1 ...\rangle \end{aligned} \tag{9.3.3}$$

The occupation of each mode can be related to the ground state through repeated application of the creation operator:

$$|N_k\rangle = \frac{\left(\hat{a}_k^\dagger\right)^{N_k}}{\sqrt{N_k!}} |0_k\rangle \tag{9.3.4}$$

One can define a single mode number operator

$$\hat{N}_{k,\sigma} = \hat{a}_{k,\sigma}^\dagger \hat{a}_{k,\sigma} \tag{9.3.5}$$

that gives you the number of excitations in mode k:

$$\hat{N}_{k,\sigma} |\varphi_L\rangle = N_{k,\sigma} |\varphi_L\rangle \tag{9.3.6}$$

That is, $N_{k,\sigma}$ is the eigenvalue for the number operator $\hat{N}_{k,\sigma}$, and can take on integer values such that $N_{k,\sigma} = 0, 1, 2, ...$ The total number of excitations in the field is then given by the total number operator

$$\hat{N} = \sum_{k,\sigma} \hat{N}_{k,\sigma} \tag{9.3.7}$$

The energy associated with the excitations of a specific mode is the energy eigenvalue $E_{k,\sigma}$, obtained from solving $H_L |\varphi_L\rangle = E_L |\varphi_L\rangle$.

$$E_{k,\sigma} = \hbar\omega_k \left(N_{k,\sigma} + \frac{1}{2}\right) \tag{9.3.8}$$

The energy depends on the number of quanta occupying the mode, multiplied by the energy of each quantum, plus a ground state zero-point energy of $\hbar\omega_k/2$. The total electromagnetic energy of the light is obtained from the expectation value of the Hamiltonian, which involves a sum over all modes:

$$E_L = \langle H_L \rangle = \sum_{k,\sigma} \left(N_{k,\sigma} + \frac{1}{2}\right) \hbar\omega_k \tag{9.3.9}$$

This does lead to a problem—if there are no bounds on the number of modes, a light field with no photons has infinite energy! That is, $E_0 = \sum_{k,\sigma} \frac{1}{2}\hbar\omega_k \to \infty$. Since we are unable to measure the absolute energy of the ground state and can only ascertain the differences of energy between states, we won't view this as a serious problem. For our purposes, it will serve to set the ground state energy to zero. There are ways of dealing with this divergence problem through renormalization, but that is beyond our

scope. It's good to remember that this is still just a model.

To describe the combined state of the light and matter, the total Hamiltonian given by eq. (9.1.2) can be expressed as a joint light-matter system, $H_0 = H_L + H_M$, and the interaction between the two:

$$\begin{aligned} H_{\text{tot}} &= H_M + H_L + H_{LM} \\ &= H_0 + H_{LM} \end{aligned} \tag{9.3.10}$$

This is a useful partitioning when the light-matter interactions are weak and lends itself to working in the interaction picture. If the matter is described by the wavefunction $|\psi_M\rangle$, where $H_M |\psi_M\rangle = E_M |\psi_M\rangle$, then the total state of the joint light-matter system $|\Psi\rangle$ can be expressed in terms of product states

$$|\Psi\rangle = |\psi_M \varphi_L\rangle \tag{9.3.11}$$

Each state $|\Psi\rangle$ is an eigenstate of H_0, and the energy of the system is the sum of the energies for the light and matter, $E = E_L + E_M$.

Now consider how to describe changes to the state of the system that are driven by light-matter interactions. For any transition in the matter from an initial state $|\ell\rangle$ to a final state $|m\rangle$—both eigenstates of H_M—we expect an associated transition in the light field of equal and opposite energy. For such a transition, we can express the initial and final states of the total light-matter system as:

$$\begin{aligned} |i\rangle &= |\ell; N_1, N_2, N_3 \ldots, N_k, \ldots\rangle \\ |f\rangle &= |m; N_1, N_2, N_3, \ldots, N_k \pm 1, \ldots\rangle \end{aligned} \tag{9.3.12}$$

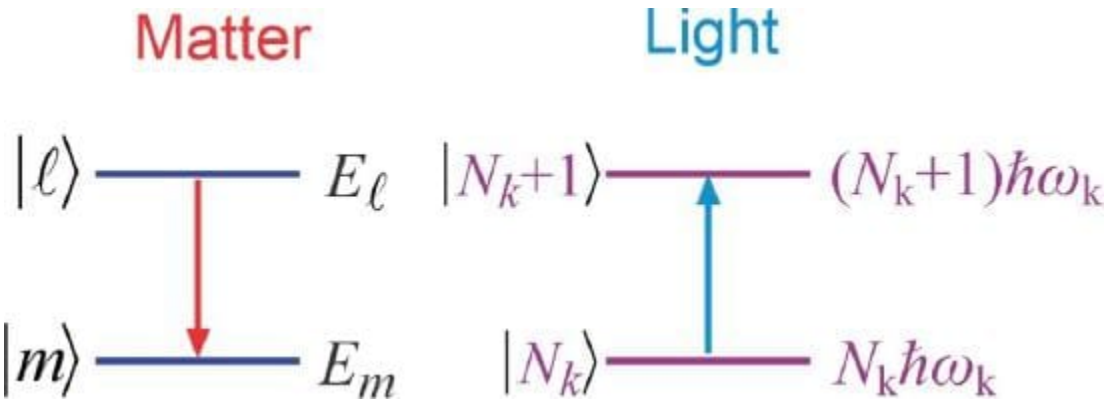


Figure 9.3.1: Energy diagram of the joint light+matter system, illustrating the changes in state accompanying a spontaneous emission event. The initial state of the system is $|i\rangle = |\ell, N_k\rangle$ and the final state of the system is $|f\rangle = |m, N_k + 1\rangle$.

The change in the light field is observed in the occupation of mode k, which transition from N_k to $N_k \pm 1$. In the final state $N_k \pm 1$, a "+" refers to emission (an increase in the number of photons in the field), and "−" refers to absorption (a decrease in the number of photons). The energies of these the initial and final states of the system are obtained by summing over the total energy of the matter and electromagnetic field.

$$E_i = \langle i| H_0 |i\rangle = E_\ell + \sum_j N_j \hbar\omega_j \tag{9.3.13}$$

$$E_f = \langle f| H_0 |f\rangle = E_m + \sum_j N_j \hbar\omega_j \pm \hbar\omega_k \tag{9.3.14}$$

The total energy change of the matter-light system is $E_f - E_i = E_m - E_\ell \pm \hbar\omega_k$. The Golden Rule description of transition rates enforces the resonance condition $E_f - E_i = 0$. Thus, the energy change in the matter is the opposite to the change of energy of the light: $E_m - E_\ell = \mp\hbar\omega_k$.

This page titled 9.3: Electromagnetic field is shared under a CC BY-NC-SA 4.0 license and was authored, remixed, and/or curated by Andrei Tokmakoff via source content that was edited to the style and standards of the LibreTexts platform.

9.4: Light-Matter Interactions and Spontaneous Emission

With our expressions for the quantum vector potential, we can now turn to evaluating the rates of absorption and emission processes. If we insert our expression for $\mathbf{A}$, eq. (9.2.10), into the interaction Hamiltonian for the interaction of the radiation field with a single charged particle, eq. (9.1.3), we obtain

$$H_{LM}(t) = -\sum_{k,\sigma} \frac{q}{m}\sqrt{\frac{\hbar}{2\varepsilon_0 V\omega_k}}\left[\left(\hat{\varepsilon}_{k,\sigma}\cdot\hat{\mathbf{p}}\right)\hat{a}_{k,\sigma}e^{\mathrm{i}(\mathbf{k}\cdot\hat{\mathbf{r}}-\omega t)} + \left(\hat{\varepsilon}^{*}_{k,\sigma}\cdot\hat{\mathbf{p}}\right)\hat{a}^{\dagger}_{k,\sigma}e^{-\mathrm{i}(\mathbf{k}\cdot\hat{\mathbf{r}}-\omega t)}\right] \tag{9.4.1}$$

In writing this, it is worth remembering that the field operators $\hat{a}$ and the matter operators $\hat{p}$ commute. As written, this Hamiltonian expresses the energy density associated with the light-matter interaction, and the energy would be obtained by integrating over the quantization volume V:

$$H_{LM} = -\int_V d^3r\,\frac{q}{m}\mathbf{A}\cdot\mathbf{p} \tag{9.4.2}$$

Now let's calculate matrix elements in H_{LM}, working in the electric dipole approximation where $e^{\mathrm{i}k\cdot r}\approx 1$. To avoid enumerating the full state of the light field, we will look specifically at changes to a single mode $|N_j\rangle$ that accompanies a transition in the matter from initial state $|\ell\rangle$ to final state $|m\rangle$. What is apparent from the annihilation and creation operators is that the two terms in eq. (9.4.1) describe transitions in the joint light-matter system that result in absorption (first term on the right) and emission (second term on the right). Let's drop the polarization factors for now and look at each of these processes separately.

To describe an absorption process, we can specify the initial state as $|i\rangle = |\ell, N_j\rangle$ and the final state as $|f\rangle = |m, N_j - 1\rangle$. Then the matrix element in the light-matter interaction is calculated as

$$\langle f|\,H_{LM}\,|i\rangle = -\frac{q}{m}\sqrt{\frac{\hbar}{2\varepsilon_0 V\omega_j}}\,\langle m|\,\hat{p}\,|\ell\rangle\,\langle N_j - 1|\,\hat{a}_j\,|N_j\rangle\,e^{-\mathrm{i}\omega_j t} \tag{9.4.3}$$

Drawing on our earlier discussion of the electric dipole matrix elements, we apply the identity $\hat{p}_{m\ell} = \mathrm{i}m\omega_{m\ell}\hat{r}_{m\ell}$ and the definion of the dipole operator, $\boldsymbol{\mu} = q\mathbf{r}$. Then the square of the matrix element is

$$|\langle f|\,H_{LM}\,|i\rangle|^2 = \frac{\hbar\omega_{m\ell}^2}{2\varepsilon_0\omega_j V}N_j\,|\boldsymbol{\mu}_{m\ell}|^2 \tag{9.4.4}$$

This squared matrix element dictates the rates of absorption from the field when evaluating Fermi's Golden Rule. We observe that this is proportional to the square of the transition dipole moment $\boldsymbol{\mu}_{m\ell}$, as we observed in our semiclassical description, and to the energy in the light field, as reflected in the N_j number of photons in mode j.

Now we can use the Golden Rule to calculate the rate of absorption from the field:

$$w_{m\ell}^{\mathrm{abs}} = \frac{2\pi}{\hbar}|\langle f\,|H_{LM}(t)|\,i\rangle|^2\,\delta(E_f - E_i) \tag{9.4.5}$$

Substituting eq. (9.4.4) and the energies of the initial and final states, $E_i = E_\ell + N_j\hbar\omega_j$ and $E_f = E_m + (N_j - 1)\hbar\omega_j$, we obtain

$$\begin{aligned} w_{m\ell}^{\mathrm{abs}} &= \frac{2\pi}{\hbar}\left[\frac{N_j\hbar\omega_{m\ell}^2}{2\varepsilon_0 V\omega_j}|\boldsymbol{\mu}_{m\ell}|^2\right]\,\delta(E_m - E_\ell - \hbar\omega_j) \\ &= \frac{\pi\,|\boldsymbol{\mu}_{m\ell}|^2}{\varepsilon_0\hbar^2}\frac{N_j\hbar\omega_j}{V}\,\delta(\omega_{m\ell} - \omega_j) \end{aligned} \tag{9.4.6}$$

This expression has been written to imply the resonance condition $\omega_{m\ell} = \omega_j$. If we remember that the energy density U of the electromagnetic field for modes of frequency ω_j is based on the number of photons occupying the quantization volume

$$U(\omega_j) = \frac{N_j\hbar\omega_j}{V} \tag{9.4.7}$$

then the rate of absorption can be written in a form we saw previously—the product of the Einstein B coefficient and the light

energy density at the transition frequency.

$$w_{m\ell}^{\text{abs}} = B_{m\ell} U\left(\omega_{m\ell}\right) \tag{9.4.8}$$

$B_{m\ell}$ is typically quoted as being a factor 3 less, which results from orientationally averaging the projection of the transition dipole moment onto the field polarization over an isotropic distribution, $\left|\hat{\varepsilon}_k \cdot \boldsymbol{\mu}_{m\ell}\right|^2 = \left|\mu_{m\ell}\right|^2/3$. This gives:

$$B_{m\ell} = \frac{\pi}{3\varepsilon_0 \hbar^2} \left|\mu_{m\ell}\right|^2 \tag{9.4.9}$$

It is also possible to see how the intensity of the light manifests in eq. (9.4.3) if we remember the classical relation between the intensity and energy density $I = cU$. Since the energy density and electric field are related by $U(\omega_j) = \frac{1}{2}\varepsilon_0 \left|\mathcal{E}_j\right|^2$, we recover the original semiclassical expression for the rate of absorption that we calculated in Section 7.6.

$$w_{m\ell}^{\text{abs}} = \frac{\pi}{2\hbar^2} \left|\boldsymbol{\mu}_{m\ell}\right|^2 \left|\boldsymbol{\mathcal{E}}(\omega_{m\ell})\right|^2 \tag{9.4.10}$$

Now let's repeat our methods of matrix element and transition rate evaluation for these emission processes. The initial and final states are $|i\rangle = |\ell, N_j\rangle$ and $|f\rangle = |m, N_j + 1\rangle$, indicating that the number of light quanta in the field mode j will increase on emission. In this case, the total energy of photons with energy $\hbar\omega_j$ created in the field will match the loss of energy in the matter. Therefore, $\left(E_m - E_\ell\right)/\hbar = \omega_{m\ell} < 0$. The matrix element is

$$\langle f| H_{LM} |i\rangle = -\frac{q}{m}\sqrt{\frac{\hbar}{2\varepsilon_0 V \omega_j}} \langle m| \hat{\mathbf{p}} |\ell\rangle \langle N_j + 1| \hat{a}_i^\dagger |N_j\rangle e^{\mathrm{i}\omega_j t} \tag{9.4.11}$$

which results in a squared matrix element

$$\left|\langle f| H_{LM} |i\rangle\right|^2 = \frac{\hbar\omega_{m\ell}^2}{2\varepsilon_0 \omega_j V} \left(N_j + 1\right) \left|\boldsymbol{\mu}_{m\ell}\right|^2 \tag{9.4.12}$$

Evaluating the Golden Rule rate of emission leads to

$$w_{m\ell}^{\text{em}} = \frac{\pi \left|\boldsymbol{\mu}_{m\ell}\right|^2}{\varepsilon_0 \hbar^2} \frac{\left(N_j + 1\right)\hbar\omega_j}{V} \delta(\omega_{m\ell} + \omega_j) \tag{9.4.13}$$

We observe that when $N_j \gg 1$, the rates of stimulated emission match what we previously saw in Section 7.6, as they are proportional to $B_{m\ell} U(-\omega_{m\ell})$. The delta function ensures that the photon created in mode j has the same energy as the energy lost in the downward $|\ell\rangle \to |m\rangle$transition in the matter, $-\omega_{m\ell} = \omega_j$.

The squared matrix element takes the same form as the absorption expression, though with a rate that depends on $N_j + 1$ rather than just N_j. That is, there is the possibility for a light-matter interaction even if there are initially no photons in the mode $(N_j = 0)$. Even when no electromagnetic radiation is present the presence of excited states in the matter allows a photon to be created in the field. Unlike the classical radiation from a dipole, this spontaneous emission step occurs in a single quantal step that creates a photon while annihilating an excitation in the matter.

Separating the contributions from stimulated and spontaneous emission processes, the rate of emission can be written

$$w_{m\ell}^{\text{em}} = B_{m\ell} U(-\omega_{m\ell}) + A_{m\ell} \tag{9.4.14}$$

The $B_{m\ell}$ coefficient is given by eq. (9.4.9), and the rate of spontaneous emission is given by the Einstein $A_{m\ell}$ coefficient

$$A_{m\ell} = \frac{\pi\omega \left|\mu_{m\ell}\right|^2}{3\varepsilon_0 \hbar V} \tag{9.4.15}$$

As with the expression for the $B_{m\ell}$ coefficient in eq. (9.4.9), the factor of 3 here arises from performing an orientational average over an isotropic distribution of dipole orientations. When we equate the inverse of the quantization volume $1/V$ with the density of states for photon modes:

$$\frac{1}{V} = g(\omega) = \frac{\omega^2}{\pi^2 c^3} \tag{9.4.16}$$

we find the common expression for the rate of spontaneous emission:

$$w_{m\ell}^{\text{spont}} = A_{m\ell} = \frac{\omega^3 \left|\mu_{m\ell}\right|^2}{3\pi\varepsilon_0 \hbar c^3} \tag{9.4.17}$$

and we observe that $A_{m\ell} = \hbar\omega^3 B_{m\ell}/\pi^2 c^3$.

The A coefficient can be used to calculate the power that is radiated spontaneously from an excited state by multiplying the emission rate and the energy of a light quantum: $\bar{\mathcal{P}}_{\text{rad}} = \hbar\omega A_{m\ell}$. This expands to

$$\bar{\mathcal{P}}_{\text{rad}} = \frac{\omega^4 \left|\mu_{m\ell}\right|^2}{3\pi\varepsilon_0 c^3} \tag{9.4.18}$$

This expression looks remarkably similar to the expression for the power radiated by a Hertzian dipole. In this case, the transition dipole matrix element plays the role of the classical dipole amplitude.

The A coefficient also allows one to compute the rate of radiative relaxation from the excited state of an atom or molecule. For instance, let's look at the radiative emission rate for the hydrogen $2p \rightarrow 1s$. This has a transition dipole moment of ~ 1 D and a transition energy of $E_i - E_f = 10.2$ eV. Using $\omega = (E_i - E_f)/\hbar$, eq. (9.4.16) gives $A = 5 \times 10^9$ s^{-1}. The picosecond to nanosecond regime is typical for the radiative lifetimes of electronic transitions between molecular singlets states. In practice, excited states typically have numerous possible radiative relaxation pathways to different lower energy states. As a result, the radiative lifetimes of excited states are calculated as a sum over all possible downward transitions for the matter from the initial state:

$$\tau_{\text{rad}}^{-1} = \sum_m A_{m\ell} \tag{9.4.19}$$

Note also that the radiative relaxation rate in eq. (9.4.16) scales as ω^3. Thus, while the picosecond to nanosecond regime may be common for electronic transitions, vibrational transitions can have infrared radiative lifetimes in the microsecond to millisecond regime.

Finally, there is the question of how radiative relaxation influences the final state of the light field. We observed in our discussion of the classical driven oscillator that energy dissipation processes, including radiative relaxation, result in a broadening of absorption lineshapes. We will take up the distribution of final photon states and its effect on emission lineshapes in our discussion of irreversible relaxation in Chapter 11.

This page titled 9.4: Light-Matter Interactions and Spontaneous Emission is shared under a CC BY-NC-SA 4.0 license and was authored, remixed, and/or curated by Andrei Tokmakoff via source content that was edited to the style and standards of the LibreTexts platform.

9.5: Coherent States

What is a photon, really? What can we say without digging deeply into quantum optics? What we have seen so far is that it is the elementary excitation of the quantum electromagnetic field, with an energy of $\hbar\omega_k$. But photons are also quasiparticles with momentum $\hbar k$. They are created (or annihilated) through their interactions with matter (or each other). The "creation" and "annihilation" operators $\hat{a}_k^\dagger$ and $\hat{a}_k$ seen in the second quantization of a field are not only "raising" and "lowering" operators that influence the quantum state and energy of a harmonic oscillator. The operators represent the quite literal creation and destruction of photons. From the Hamiltonian, eq. (9.2.9), we can conclude that photons are bosons (integer spin particles) subject to the commutator relationships $\left[\hat{a}_{k,\sigma}, \hat{a}_{k',\sigma'}^\dagger\right] = \delta_{kk'}\delta_{\sigma\sigma'}$ and $\left[\hat{a}_{k,\sigma}, \hat{a}_{k',\sigma'}\right] = \left[\hat{a}_{k,\sigma}^\dagger, \hat{a}_{k',\sigma'}^\dagger\right] = 0$.

What makes photons challenging to discuss is defining their wavefunction in space and time. In section 9.3, the creation of a photon was associated with the occupation of a single mode of the radiation field. A photon in a single mode is associated with a plane electric field of precise k and ω_k that is extended over all space. As an eigenstate of H_L, it is a stationary state. Such states don't exist in reality.

Consider the emission of a photon from the excited state of an atom. Photons are emitted in a short window of time following the atomic excitation. They then travel through space, and one can accurately determine their arrival times at a detector or their emitted frequency. Thus, realistic photons emitted from atoms are wavepackets of the electromagnetic field that are localized in time and space with a group velocity that propagates at the speed of light. Many repeated experiments on identically prepared systems demonstrate that there are some variations in the variables that govern the state of the photon. Thinking about laser sources, photons can be quasi-monochromatic or pulsed–localized in time. There are finite dimensions to a real photon's electromagnetic field in time, energy, frequency, space, and wavevector.

To think about this, let's look at the single photon wavepacket.(1) If we denote as $|1_k\rangle$ the single photon state with one photon in mode k and zero photons in all others, then the wavepacket is a superposition of many single photon states

$$|\varphi\rangle = \sum_k C_k |1_k\rangle \tag{9.5.1}$$

where the probability density is normalized so that the coefficients are normalized: $\sum_k |C_k|^2 = 1$. If we calculate the expectation value of the total number operator, we find that it represents a single photon: $\langle\varphi|\hat{N}|\varphi\rangle = 1$. The wavepacket is an eigenstate of the number operator, but not of the field operators since multiple values of $\mathbf{k}$ are involved. For instance, the momentum of the field is now $\langle\varphi|\hat{p}_L|\varphi\rangle = \sum_k |C_k|^2 \hbar\mathbf{k}$, reflecting an average over the probability density defined by C_k. As a superposition state, the wavepacket is not stationary, and the intensity of the wave speed of light, as we learned from the expectation value of the electric field. For a photon traveling in the x direction:

$$\mathcal{E}(x,t) = \mathrm{i}\sum_k \sqrt{\frac{\hbar kc}{2\varepsilon_0 V}}\hat{a}_k e^{\mathrm{i}(kx-\omega_k t)} \tag{9.5.2}$$

$$\mathcal{E}^2 = \langle\varphi|\mathcal{E}^2|\varphi\rangle = \frac{\hbar c}{2\varepsilon_0 V}\sum_k \left|C_k k e^{\mathrm{i}k(x-ct)}\right|^2 \tag{9.5.3}$$

This is known as a quasi-classical state becaus when used to compute expectation values for operators corresponding to classical observables, it produces what we would expect of an electromagnetic field.

There are many ways to realize the form of a single photon wavepacket, but additional complexity arises in multiphoton wavefunctions. Returning to single mode wavefunctions, let's remember that the general Fock state $|\varphi_L\rangle = |N_1, N_2, N_3, ...\rangle$ is shorthand for a tensor product. Each mode itself has an infinite number of eigenfunctions and number eigenvalues, so the most general form of a multi-photon light field also can involve superposition states of the mode eigenfunctions. Let's look a bit further at these superposition states, now allowing for multiple photons within a single mode. Here we will drop the mode indices ($N_k \rightarrow N$) and look at the superposition of mode states with different photon number:

$$|\alpha\rangle = \sum_{N=0}^{\infty} C_N |N\rangle \tag{9.5.4}$$

The number of photons in this mode will be obtained from the expectation value of the number operator: $\langle\alpha|\hat{N}|\alpha\rangle$.

A state $|\alpha\rangle$ is commonly referred to as a coherent state if it is the eigenstate of the annihilation operator:

$$\hat{a}\,|\alpha\rangle = \alpha\,|\alpha\rangle \tag{9.5.5}$$

Let's investigate what this means by determining the eigenvalue α. Although α can be complex, its magnitude equals the square root of the mean number of photons in the mode. Acting on this equation from the left with $\langle N_k - 1|$ gives us the recurrence relationship $\sqrt{N}C_N = \alpha C_{N-1}$. Repeated insertion of this formula into itself allows you to find

$$C_N = \frac{\alpha^N}{\sqrt{N!}}C_0 \tag{9.5.6}$$

Then using eq. (9.5.4) and the normalization condition $\langle\alpha|\alpha\rangle = 1$ we can find $C_0 = \exp(-|\alpha|^2/2)$. This leads to the general representation of a single mode coherent state

$$|\alpha\rangle = e^{-|\alpha|^2/2}\sum_{N=0}^{\infty}\frac{\alpha^N}{\sqrt{N!}}\,|N\rangle \tag{9.5.7}$$

Using the operator $\hat{N} = \hat{a}^\dagger\hat{a}$, the expectation value for the number operator follows immediately from eq. (9.5.5):

$$\langle N\rangle = \langle\alpha|\,\hat{N}\,|\alpha\rangle = |\alpha|^2 \tag{9.5.8}$$

A coherent state has an uncertainty in the photon number which we can describe through the variance: $\langle N^2\rangle - \langle N\rangle^2 = |\alpha|^2$. To calculate the probability of finding N photons in a coherent state we project $|\alpha\rangle$ onto eigenstate $|N\rangle$:

$$P(N) = |\langle N|\alpha\rangle|^2 \tag{9.5.9}$$

Using eq. (9.5.7) leads to

$$\begin{aligned} P(N) &= \frac{e^{-|\alpha|^2}\,|\alpha|^{2N}}{N!} \\ &= \frac{e^{-\langle N\rangle}\,\langle N\rangle^N}{N!} \end{aligned} \tag{9.5.10}$$

Therefore the occupation of photons in the mode follows a Poisson distribution. Even coherent, single-mode light sources with fixed intensity have a natural variation in photon number, with a mean value of $\langle N\rangle$ and a root-mean-square distribution that is $\sqrt{\langle N\rangle}$.

The emergence of a Poisson distribution for the occupation of harmonic oscillator states is one that we have encountered before, when calculating Franck-Condon factors for displaced harmonic oscillators. In that case, the displacement operator $\hat{D}(\lambda) = \exp\left[-i\hat{p}\lambda/\hbar\right]$ was used to generate a displacement of one harmonic oscillator relative to another in the position representation. Overlap integrals with the raising and lowering operator formalism could be applied there. The same concepts apply to generating coherent states. One finds that a coherent state is generated by applying the displacement operator $\hat{D}(\alpha) = \exp[\alpha\hat{a}^\dagger - \alpha^*\hat{a}]$ to the vacuum state: $|\alpha\rangle = \hat{D}(\alpha)\,|0\rangle$

References

1. Fabre, C.; Treps, N. Modes and states in quantum optics. *Reviews of Modern Physics* **2020**, *92* (3), 035005. DOI: 10.1103/RevModPhys.92.035005

This page titled 9.5: Coherent States is shared under a CC BY-NC-SA 4.0 license and was authored, remixed, and/or curated by Andrei Tokmakoff via source content that was edited to the style and standards of the LibreTexts platform.

9.6: Readings

Introduction

1. Baym, G. *Lectures on Quantum Mechanics*; W.A. Benjamin, 1969. DOI: 10.1201/9780429499265
2. Heitler, W. *The Quantum Theory of Radiation*, 3rd ed.; Dover Publications, 1984.
3. Loudon, R. *The Quantum Theory of Light*, 3rd ed.; Oxford University Press, 2000. DOI: 10.1093/oso/9780198501770.001.0001
4. Scully, M. O.; Zubairy, M. S. *Quantum Optics*; Cambridge University Press, 1997. DOI: 10.1017/CBO9780511813993

Coherent States

1. Baym, G. *Lectures on Quantum Mechanics*; W.A. Benjamin, 1969. DOI: 10.1201/9780429499265
2. Cohen-Tannoudji, C.; Diu, B.; Laloë, F. *Quantum Mechanics*; Wiley, 1977.
3. Heitler, W. *The Quantum Theory of Radiation*, 3rd ed.; Dover Publications, 1984.
4. Loudon, R. *The Quantum Theory of Light*, 3rd ed.; Oxford University Press, 2000. DOI: 10.1093/oso/9780198501770.001.0001
5. Scully, M. O.; Zubairy, M. S. *Quantum Optics*; Cambridge University Press, 1997. DOI: 10.1017/CBO9780511813993

This page titled 9.6: Readings is shared under a CC BY-NC-SA 4.0 license and was authored, remixed, and/or curated by Andrei Tokmakoff.

10: TRANSITION DIPOLE MOMENT AND SELECTION RULES

10.1: The Molecular Transition Dipole Moment
10.2: Selection Rules in the Electric Dipole Approximation
10.3: Molecular Electronic Spectroscopy and Franck Condon Factors
10.4: Appendix - Rotational Transition Matrix Elements
10.5: Readings

This page titled 10: Transition Dipole Moment and Selection Rules is shared under a CC BY-NC-SA 4.0 license and was authored, remixed, and/or curated by Andrei Tokmakoff via source content that was edited to the style and standards of the LibreTexts platform.

10.1: The Molecular Transition Dipole Moment

We can now move on to discuss the molecular factors that governs the strength of the light-matter interaction for transitions between two quantum states, which is contained in the transition dipole matrix element, $\boldsymbol{\mu}_{k\ell} = \langle k|\boldsymbol{\mu}|\ell\rangle$, or transition dipole moment. The dipole operator $\boldsymbol{\mu}$ itself can in some respects be expressed relatively simply: it describes how the charges of the particles are distributed in the molecule. In the body-fixed frame centered at $\mathbf{r}_0$ it can be expressed as a sum over the position of all charged particles of the system

$$\boldsymbol{\mu} = \sum_i q_i(\mathbf{r}_i - \mathbf{r}_0) \tag{10.1.1}$$

or by integrating of the distribution of charge density ρ

$$\boldsymbol{\mu} = \int d\mathbf{r}\, \mathbf{r}\rho(\mathbf{r}) \tag{10.1.2}$$

From this convention we see that the dipole moment vector points from the negative to the positive charge. For polyatomic molecules the dipole operator is sometimes partitioned into a sum of nuclear and electronic contributions, by summing over the position (R_j) of different nuclear charges ($Z_j e$) and the positions (r_i) of the electrons:

$$\hat{\boldsymbol{\mu}} = -\sum_i e\hat{\mathbf{r}}_i + \sum_j Z_j e\hat{\mathbf{R}}_j \tag{10.1.3}$$

The permanent dipole moment for the molecule—that is the time-invariant quantity that describes the asymmetry in a molecule's charge distribution—can be calculated as the expectation value of the dipole operator. The dipole moment and transition dipole matrix element have historically been quoted in the cgs units of Debye (D) where $1\ \mathrm{D} = 3.336 \times 10^{-30}\ \mathrm{C}\cdot\mathrm{m}$. Two fundamental charges of $+e$ and $-e$ separated by $1\ \text{Å}$ have a dipole moment of $4.8\ \mathrm{D}$.

Although there are challenges dealing with many electrons and nuclei, the complexity of dealing with the dipole operator arises because the position and motions of these many particles are not independent. Consider the transition dipole moment between two electronic states $|g\rangle$ and $|e\rangle$. Since the dipole operator depends on the position of multiple nuclei and electrons, calculating $\langle e|\mu|g\rangle$ involves integrals not only over the electronic wavefunction, but over numerous vibrational, and rotational wavefunctions, even when these contributions are separable as $|g\rangle = |\psi_{\mathrm{elec},g}\,\varphi_{\mathrm{nuc},g}\,D_{\mathrm{rot},g}\rangle$.

Much like dealing with the Schrödinger equation for the molecular Hamiltonian, we need to develop strategies for simplifying the interaction of a molecular dipole moment with light for specific applications. Let's investigate the strategies for evaluating the transition dipole matrix elements for a series of different cases, starting with simple models where we can focus on specific types of interactions, and building up from there. What we will find it that often stringent requirements emerge on which quantum states the light can couple in absorption and emission processes. "Selection rules" are those criteria that determine whether a transition dipole matrix element is zero or not, or equivalently whether a quantum transition is "allowed" or not.

This page titled 10.1: The Molecular Transition Dipole Moment is shared under a CC BY-NC-SA 4.0 license and was authored, remixed, and/or curated by Andrei Tokmakoff via source content that was edited to the style and standards of the LibreTexts platform.

10.2: Selection Rules in the Electric Dipole Approximation

Here we will investigate the transition dipole moment for three simple cases in which we focus on a matrix element that is for a purely vibrational, rotational, or electronic transition. This will provide us with several important insights that govern more complex transitions involving all three degrees of freedom. The first case is for vibrations in which focus is only on how the transition dipole moment is affected by the change in charge distribution as a molecule vibrates. The second focuses only on rotation, where a permanent dipole is fixed in the molecular frame, but its projection onto the electric field polarization varies as it rotates. Last, the electronic transitions in a hydrogen atom illustrates how the transition dipole moments are governed by the electron's orbital angular momentum.

Vibrational selection rules for a diatomic molecule

First, let's consider the vibrational selection rules for a diatomic molecule for which the two atoms are bound by a harmonic potential. To build a dipole operator we can assume that the two atoms have equal and opposite partial charges q on each atomic site ($q_1 = -q_2 = q$). Using the transformation from atomic positions $(\mathbf{r}_1, \mathbf{r}_2)$ into internal coordinates ($\mathbf{x} = \mathbf{r}_2 - \mathbf{r}_1$), the electric dipole Hamiltonian describing the electric field interacting with two atoms can be expressed in the same form but in terms of one diatomic vibration, with reduced mass m_R and vibrational momentum $\mathbf{p}_x$:

$$V = \sum_{j=1,2} \frac{q_j}{\omega m_j} (\mathbf{E} \cdot \mathbf{p}_\mathbf{r})_j = \frac{q}{\omega m_R} (\mathbf{E} \cdot \mathbf{p}_\mathbf{x}) \tag{10.2.1}$$

In this process, the nuclear Hamiltonian also transformed into a one-dimensional vibrational Hamiltonian $H_0 = p_x^2/2m_R + V(x)$ whose eigenstates we use to evaluate the transition dipole matrix elements. The general relation for the matrix elements $m_R \omega_{k\ell} \mathbf{r}_{k\ell} = -i\mathbf{p}_{k\ell}$ is used to justify the familiar form of the interaction potential $V = -\boldsymbol{\mu} \cdot \mathbf{E}$. If the equilibrium bond length is x_0, then the permanent dipole moment for the molecule is $\boldsymbol{\mu}_0 = q\,\mathbf{x}_0$. Note the electric dipole Hamiltonian vanishes in this transformation if the partial charges are equal, indicating that a homonuclear diatomic will not interact with light through this mechanism.

While $\boldsymbol{\mu}_0$ is a vector, it is not an operator, and any matrix element of interest in the vibrational eigenstates would be zero: $\mu_k \ell = \mu_0 \langle k|\ell\rangle = \mu_0 \delta_{k,\ell}$. Absorption by vibrations requires the light to move the molecular charge distribution by changing the bond length against the restoring force of the oscillator. In general a molecular dipole moment can vary considerably as the positions of nuclei change, however, for small-amplitude vibrations we expect that the dipole moment can be described by expanding it in the vibrational displacement around the equilibrium bond length x_0.

$$\boldsymbol{\mu} = \boldsymbol{\mu}_0 + \left.\frac{\partial \boldsymbol{\mu}}{\partial x}\right|_{x=x_0} (x - x_0) + \cdots \tag{10.2.2}$$

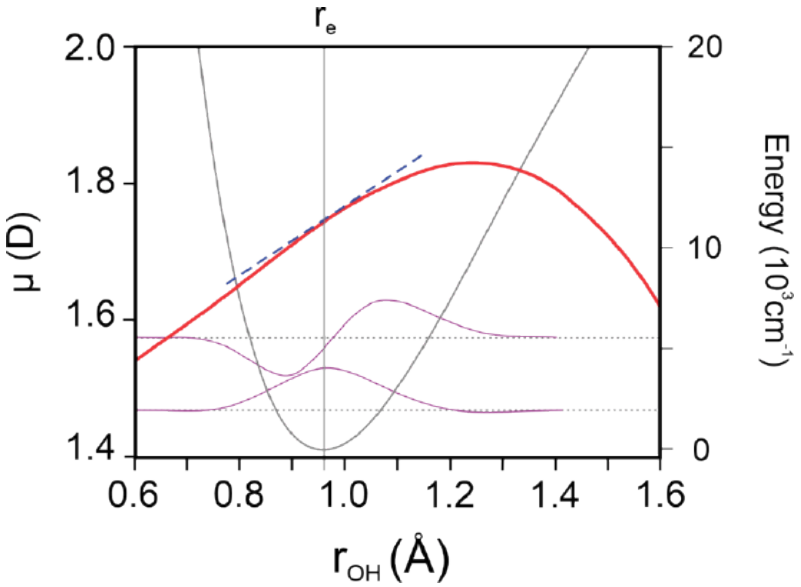


Figure 10.2.1: Variation of the dipole moment of HDO as a function of the O–H bond displacement (red) and the dipole derivative evaluated at the equilibrium bond length r_e (blue). Also shown are the O–H vibrational potential and the energies and wavefunctions for the $n = 0$ and 1 eigenstates. Figure adapted from Theulé, P. C., et al. *J. Chem. Phys.* 2005, **122**, 124312.

This behavior is illustrated in fig. (10.2.1). Now the vibrational displacement x is an operator, and the magnitude of the dipole change is given by the derivative of the dipole moment with regard to x evaluated at x_0. The dipole derivative $\partial\boldsymbol{\mu}/\partial x$ governs how much the dipole moment changes as the bond stretches, which can arise both from the change in separation between fixed charges and from charge redistribution as the bond lengthens. Then the vibrational transition dipole moment $\boldsymbol{\mu}_{n',n} = \langle n'|\boldsymbol{\mu}|n\rangle$ involves a product of the dipole derivatives and the matrix elements in x.

$$\boldsymbol{\mu}_{n',n} = \frac{\partial\boldsymbol{\mu}}{\partial x}\langle n'|x|n\rangle \tag{10.2.3}$$

Note that the transition dipole moment is a vector quantity that indicates the net direction of the change of charge distribution with the displacement of the vibration. In the case of a diatomic, there no choice, but for the vibration to induce change displacement in the same direction as the bond and permanent dipole moment, but in polyatomic molecules $\partial\boldsymbol{\mu}/\partial x$ need not be parallel to $\boldsymbol{\mu}_0$. As an example, consider the bending vibration of CO_2.

If we assume that the vibrations of the system are described in terms of harmonic oscillator eigenstates $|n\rangle$, we obtain

$$\mu_{n',n} = \frac{\partial\boldsymbol{\mu}}{\partial x}\sqrt{\frac{\hbar}{2m_R\omega_0}}\left[\sqrt{n+1}\,\delta_{n',n+1} + \sqrt{n}\,\delta_{n',n-1}\right] \tag{10.2.4}$$

The selection rules for the transition dipole moment in the harmonic approximation only allows the light to couple vibrational states that differ by one quantum ($n' = n \pm 1$), and the absorption strength for allowed transitions is governed by the square of the dipole derivative: $|\boldsymbol{\mu}_{n,\,n\pm1}|^2 \sim (\partial\mu/\partial x)^2$. In practice, most internal molecular vibrations of interest are not thermally populated, which results in absorption only $n = 0 \rightarrow n' = 1$ transitions. Anharmonicity of the vibrational potential loosens these selection rules and leads to the possibility of $n' > n \pm 1$ transitions.

Rotational selection rules for a rigid diatomic molecule

By construction, the rotation of a rigid molecule does not allow changes in bond length such as those in eq. (10.2.5). Rather, we express the permanent dipole moment as a product of its magnitude and a unit vector specifying its orientation, $\boldsymbol{\mu}_0 = \mu_0\hat{u}$, and focus our attention on the projection of the dipole moment $\hat{u}$ onto the electric field polarization vector $\hat{\varepsilon}$ in the electric dipole Hamiltonian, $(\hat{u}\cdot\hat{\varepsilon})$. In the case of a linear diatomic molecule interacting with linearly polarized light, the rotating molecule's dipole moment projects onto the electric field as $(\hat{u}\cdot\hat{\varepsilon}) = \cos\theta$. The matrix elements connecting initial and final rotational states are evaluated in the basis of spherical harmonics $Y_{J,M}(\theta,\phi) = |JM\rangle$

$$\boldsymbol{\mu}_{if} = \boldsymbol{\mu}_0\,\langle J'M'|\,\hat{u}\cdot\hat{\varepsilon}\,|JM\rangle \tag{10.2.5}$$

where we are using primes to label the final state. To evaluate the matrix element, we start by expressing the dot-product as a first-order spherical harmonic using $\cos\theta = \sqrt{\frac{4\pi}{3}}Y_{1,0}$:

$$\langle J'M'|\,(\hat{u}\cdot\hat{z})\,|JM\rangle = \sqrt{\frac{4\pi}{3}}\int d\Omega\; Y^*_{J',M'}Y_{1,0}Y_{J,M} \tag{10.2.6}$$

where the integral over spherical angles has been abbreviated as

$$\int d\Omega = \frac{1}{4\pi}\int_0^{2\pi} d\varphi \int_0^{\pi} \sin\theta\; d\theta \tag{10.2.7}$$

Integrals of this sort are common in describing the coupling of angular momenta and for evaluating matrix elements involving angular motion such as these. The solutions can be expressed in terms of Clebsch-Gordon coefficients $\langle J_2M_2; J_1M_1|J_3M_3\rangle$:

$$\int d\Omega\; [Y_{J_3,\,M_3}]^*\;\; Y_{J_1,\,M_1}Y_{J_2,\,M_2} = \sqrt{\frac{(2J_1+1)\,(2J_2+1)}{4\pi\,(2J_3+1)}}\,\langle J_20;\,J_10\mid J_30\rangle\,\langle J_2M_2;\,J_1M_1\mid J_3M_3\rangle \tag{10.2.8}$$

For the current example, eq. (10.2.6) with $J_1 = 1$ and $M_1 = 0$, we have

$$\langle J',m'|\,\hat{\mu}\cdot\hat{z}\,|J,m\rangle = \mu_0\left(\frac{2J+1}{2J'+1}\right)^{\frac{1}{2}}\langle J0;10|J'0\rangle\,\langle Jm;10|J'm'\rangle \tag{10.2.9}$$

and we find that these coefficients are only non-zero when $J' = J \pm 1$ and $M' = M$:

$$\langle J'M'|\,\hat{u}\cdot\hat{z}\,|JM\rangle = \begin{cases} \sqrt{\frac{(J+1)^2-M^2}{4(J+1)^2-1}} & \text{if } J' = J+1 \\ \sqrt{\frac{J^2-M^2}{4J^2-1}} & \text{if } J' = J-1 \end{cases} \tag{10.2.10}$$

Once again, strict selection rules limiting the allowed transitions to changes in one quantum of angular momentum ($\Delta J = \pm 1$, $\Delta M = 0$) are observed for the rigid rotor.

Beyond diatomic molecules interrogated with linearly polarized light, the evaluation of the transition dipole matrix elements becomes considerably more complicated, both for describing the rotational behavior of the molecule in the body-fixed frame ($\hat{a}$, $\hat{b}$, $\hat{c}$) and its transformation into the laboratory frame ($\hat{x}$, $\hat{y}$, $\hat{z}$). However, the essence of evaluating rotational matrix elements for the transformation between coordinate systems using Clebsch-Gordon coefficients remains the same. These extensions are described in detail elsewhere.

Clebsch-Gordon Identities(2)(3)

The Clebsch-Gordon coefficients that emerge from the integral over $Y^*_{J_3,M_3}Y_{J_1,M_1}Y_{J_2,M_2}$ are written in different forms including $\langle J_2M_2; J_1M_1 \mid J_3M_3\rangle$ or $C(J_1, J_2, J_3; M_1, M_2, M_3)$. Some useful identities that emerge are:

1. Since the Clebsch-Gordon coefficients are real, $\langle J_2M_2; J_1M_1 \mid J_3M_3\rangle = \langle J_3M_3 \mid J_2M_2; J_1M_1\rangle$
2. $|J_2 - J_1| \leq J_3 \leq (J_2 + J_1)$
3. $M_3 = M_1 + M_2$. This reflects the conservation of the z component of the angular momentum.
4. $\langle J_2, 0; J_1, 0 \mid J_3, 0\rangle = 0$, unless $J_1 + J_2 + J_3$ is even. This is the parity conservation statement.

For evaluating transition dipole matrix elements for electric dipole transitions with linear polarization ($J_1 = 1$, $M_1 = 0$), one finds:

$$\begin{aligned}\langle J_2 M; 1,0 \mid (J_2+1)\, M\rangle &= \sqrt{\frac{(J_2-M+1)\,(J_2+M+1)}{(2J_2+1)\,(J_2+1)}} \\ \langle J_2 M; 1,0 \mid J_2 M\rangle &= \frac{M}{\sqrt{J_2\,(J_2+1)}} \\ \langle J_2 M; 1,0 \mid (J_2-1)\, M\rangle &= -\sqrt{\frac{(J_2-M)\,(J_2+M)}{J_2\,(2J_2+1)}}\end{aligned} \tag{10.2.11}$$

Selection rules for atomic spectroscopy

For simplicity, let's limit ourselves to the transition dipole interactions of linearly polarized electromagnetic waves with a one-electron hydrogen atom, neglecting electron spin. Then we can specify the state of the system through the atomic orbitals, $|n\ell m\rangle = R_{n,\ell}(r)Y_{\ell,m}(\theta,\phi)$. The transition dipole matrix element is $\langle n'\ell'm'_\ell|\,\boldsymbol{\mu}\cdot\hat{\varepsilon}\,|n\ell m_\ell\rangle$, where the interaction of the radially bound electron with z-polarized light is $\boldsymbol{\mu}\cdot\hat{\varepsilon} = e(\mathbf{r}\cdot\hat{z}) = e\mathbf{r}\cos\theta = e\mathbf{r}\sqrt{4\pi/3}\;Y_{1,0}$. This expression expresses the interaction as a product of radial and angular functions, which allows us to partition the matrix element into the product of radial and angular integrals:

$$\langle n'\ell'm'_\ell|\boldsymbol{\mu}\cdot\hat{\varepsilon}|n\ell m_\ell\rangle = \sqrt{\frac{4\pi}{3}}\mathcal{R}_{n'\ell',\,n\ell}\,\langle \ell', m'|\,Y_{1,0}\,|\ell, m\rangle \tag{10.2.12}$$

The radial integral is given by

$$\mathcal{R}_{n'\ell',\,n\ell} = \int_0^\infty r^3 R_{n'\ell'}(r)R_{n\ell}(r)dr \tag{10.2.13}$$

The orientational integral is evaluated in the same way as the rigid rotor matrix element, leading to expressions of the same form as eq. (10.2.10). As for the rigid rotor, the interaction with linearly polarized light results in the requirement that $\Delta\ell = \pm 1$ and $\Delta m = 0$ for electric dipole transitions. In the process of calculating transition rates, one typically sums over contributions from the transitions to all degenerate m' states, which leads to(4)

$$\begin{aligned}\sum_{m'_\ell}\left|\langle n'\ell'm'_\ell|\boldsymbol{\mu}\cdot\hat{\varepsilon}|n\ell m_\ell\rangle\right|^2 &= \frac{1}{3}\frac{\ell+1}{2\ell+1}(\mathcal{R}_{n'\ell',\,n\ell})^2 \qquad \ell' = \ell+1 \\ &= \frac{1}{3}\frac{\ell}{2\ell+1}(\mathcal{R}_{n'\ell',\,n\ell})^2 \qquad \ell' = \ell-1\end{aligned} \tag{10.2.14}$$

To calculate interactions in three dimensions with arbitrary polarization of the light field, we decompose the polarization vector into its x, y, and z components ($\hat{\varepsilon} = \varepsilon_x + \varepsilon_y + \varepsilon_z$) as described in the appendix and express the orientational projection factor ($\hat{u}\cdot\hat{\varepsilon}$) in terms of spherical harmonics with $\ell = 1$ and $m = 0, \pm 1$

$$\begin{aligned}\hat{u}\cdot\hat{\varepsilon} &= \varepsilon_x\sin\theta\cos\varphi + \varepsilon_y\sin\theta\sin\varphi + \varepsilon_z\cos\theta \\ \hat{u}\cdot\hat{\varepsilon} &= \sqrt{\frac{4\pi}{3}}\left[\varepsilon_z Y_{1,0} + \left(\frac{\varepsilon_x + \mathrm{i}\varepsilon_y}{\sqrt{2}}\right)Y_{1,-1} + \left(\frac{-\varepsilon_x + \mathrm{i}\varepsilon_y}{\sqrt{2}}\right)Y_{1,+1}\right]\end{aligned} \tag{10.2.15}$$

Then, the matrix elements connecting initial and final states $|i\rangle = |n\ell m_\ell\rangle$ and $|f\rangle = |n'\ell'm'\rangle$ are

$$\begin{aligned}\langle f|\,\hat{\varepsilon}\cdot\mathbf{r}\,|i\rangle =& \sqrt{\frac{(2\ell+1)}{(2\ell'+1)}}\langle \ell' 0 \mid 10; \ell 0\rangle\mathcal{R}_{n'\ell',\,n\ell} \\ &\cdot\left[\varepsilon_z\langle \ell' m'|1,0;\ell m\rangle + \left(\frac{-\varepsilon_x + i\varepsilon_y}{\sqrt{2}}\right)\langle \ell' m' \mid 1,1;\ell m\rangle + \left(\frac{\varepsilon_x + i\varepsilon_y}{\sqrt{2}}\right)\langle \ell' m' \mid 1,-1;\ell m\rangle\right]\end{aligned} \tag{10.2.16}$$

Note that the angular coefficients for the second and third terms correspond to the polarization conditions for right and left circularly polarized light. As a result, the matrix elements for experiments with circularly polarized electromagnetic fields light result in allowed transitions with $\Delta m = \pm 1$.

From the examples above, we can make some general observations regarding how symmetry dictates the electric dipole selection rules in one electron atoms. The initial and final states for a transition dipole matrix element must have the opposite parity (u versus g symmetry). States with even parity ($\mathcal{P} = +1$ or g symmetry) are unchanged when we invert the sign of r ($r \to -r$), in contrast to odd parity ($\mathcal{P} = -1$ or u symmetry). Since the dipole operator ($\mu \sim r$) is odd, the initial and final states must have

opposite symmetry for the integral to be non-zero. In atomic spectroscopy, the parity for radial wavefunctions is always even, and thus the parity of the atomic wavefunctions is governed by the parity of the spherical harmonics: $\mathcal{P}(Y_{\ell,m}) = (-1)^{\ell}$. This results in $\Delta m_{\ell} = 0, \pm 1$, $\Delta \ell = \pm 1$ selection rules for atomic spectroscopy. For the case of magnetic dipole transitions and electric quadrupole transitions in atomic spectroscopy, the initial and final states have to be of same parity, resulting in the selection rules: $\Delta m_{\ell} = 0, \pm 1$, $\Delta \ell = \pm 1$.

References

Adapted from:
(1) Theulé, P.; Callegari, A.; Rizzo, T. R.; Muenter, J. S. Dipole moments of HDO in highly excited vibrational states measured by Stark induced photofragment quantum beat spectroscopy. *Journal of Chemical Physics* **2005**, *122* (12), 124312. DOI: 10.1063/1.1864912

(2) Rose, M. E. *Elementary Theory of Angular Momentum*; Dover Publications, 1995.

(3) Zare, R. N. *Angular Momentum: Understanding Spatial Aspects in Chemistry and Physics*; Wiley, 1988.

(4) Merzbacher, E. *Quantum Mechanics*, 3rd ed.; Wiley, 1998.

This page titled 10.2: Selection Rules in the Electric Dipole Approximation is shared under a CC BY-NC-SA 4.0 license and was authored, remixed, and/or curated by Andrei Tokmakoff via source content that was edited to the style and standards of the LibreTexts platform.

10.3: Molecular Electronic Spectroscopy and Franck Condon Factors

Turning to molecular electronic spectroscopy, we will account for the role of the molecular vibrations in calculating the transition dipole moment. While the pure electronic transition dipole matrix element can be obtained by integrating the dipole operator over the initial and final electronic wavefunctions as $\langle\psi_f|\,\mu\,|\psi_i\rangle$, in practice the variation of the molecular dipole moment with the displacement of molecular vibrations has a strong effect on the absorption and emission spectra. We start by describing the state of the system with the Born-Oppenheimer approximation. As we saw in Chapter 5, the molecular wavefunction Ψ can be expanded in terms of product states in the electronic ψ_m and nuclear $\varphi_{m,n}$ eigenfunctions:

$$\Psi_{m,n}(\mathbf{r},\mathbf{R}) = \psi_m(\hat{\mathbf{r}},\mathbf{R})\varphi_{m,n}(\hat{\mathbf{R}}) \tag{10.3.1}$$

Here the electronic wavefunctions are functions of the electron positions $\mathbf{r}$, an operator, which themselves depend parametrically on the fixed position of the nuclei $\mathbf{R}$, a number.

The dipole operator is given by eq. (10.1.3)

$$\boldsymbol{\mu} = -e\sum_i \mathbf{r}_i + e\sum_J Z_J\mathbf{R}_J = \boldsymbol{\mu}_{\text{elec}} + \boldsymbol{\mu}_{\text{nuc}} \tag{10.3.2}$$

For electronic spectroscopy, the transition dipole moment connecting an initial and final state $\langle\Psi_{m',n'}|\,\boldsymbol{\mu}\,|\Psi_{m,n}\rangle$ can then be written as

$$\mu_{m',n',m,n} = \left\langle\varphi_{m',n'}(\hat{\mathbf{R}}')\psi_{m'}(\hat{\mathbf{r}}',\mathbf{R}')\,\middle|\,\boldsymbol{\mu}(\mathbf{r},\mathbf{R})\,\middle|\,\varphi_{m,n}(\hat{\mathbf{R}})\psi_m(\hat{\mathbf{r}},\mathbf{R})\right\rangle \tag{10.3.3}$$

where primes refer to the final state. Substituting eq. (10.3.2) into eq. (10.3.3) we find

$$\mu_{m',n',m,n} = \delta_{m,m'}\,\langle\varphi_n'|\,\boldsymbol{\mu}_{\text{nuc}}\,|\varphi_n\rangle + \left\langle\varphi_{m',n'}(\hat{\mathbf{R}}')\psi_{m'}(\hat{\mathbf{r}}',\mathbf{R}')\right|\boldsymbol{\mu}_{\text{elec}}\left|\varphi_{m,n}(\hat{\mathbf{R}})\psi_m(\hat{\mathbf{r}},\mathbf{R})\right\rangle \tag{10.3.4}$$

The first term only depends on the nuclear dipole operator and involves no change of electronic state, and is responsible for infrared vibrational spectroscopy. The second term describes electronic electric dipole transitions involving changes in electronic and nuclear configuration, i.e. vibronic transitions. Since most circumstances involve initial excitation from the electronic ground state, we now designate that state g and the final electronically excited state e.

Closely related to the Born-Oppenheimer approximation is the Condon approximation. Given the slow motion of the nuclei relative to that of the electrons, this approximation states that the nuclei do not move on the time-scale of the electronic transition from ground to excited states. That is, $\mathbf{R}' = \mathbf{R}$. This allows us to separate the electronic and vibrational contributions into a product of two terms

$$\mu_{e,n',g,n} = \langle\psi_e(\hat{\mathbf{r}}',\mathbf{R})\,|\,\boldsymbol{\mu}_{\text{elec}}\,|\,\psi_g(\hat{\mathbf{r}},\mathbf{R})\rangle\left\langle\Phi_{e,n'}(\hat{\mathbf{R}})\,\middle|\,\Phi_{g,n}(\hat{\mathbf{R}})\right\rangle \tag{10.3.5}$$

The first term is the electronic transition dipole matrix element, which is dependent on the configurations of the nuclei on excitation. For most purposes, we can assume that it doesn't vary much with $\mathbf{R}$, and use the average value, which we designate as μ_{eg}. The second term is not a matrix element, but an overlap integral between the nuclear wavefunctions in the initial and final electronic state. This is known as the nuclear overlap integral or Franck-Condon Factor, $\langle n'|n\rangle$. We therefore write the electronic transition probability as proportional to

$$|\mu_{e,n',g,n}|^2 = |\mu_{eg}|^2\,|\langle n'|n\rangle|^2 \tag{10.3.6}$$

Although the evaluation of the electronic transition dipole moment and Franck-Condon factor (FCF) is a complex calculation, one can make a number of important qualitative observations. The electronic transition dipole moment characterizes the magnitude of the change in the electronic charge distribution that accompanies the change in electronic state. As before, absorption of light requires the motion of charge, which requires a change of parity between $|g\rangle$ and $|e\rangle$. That is, a change between $u \leftrightarrow g$ symmetry.

Changes in electronic charge distribution between electronic surfaces mean that the nuclei will adapt to a new set of electronic

interactions that will result in a changed nuclear geometry. Therefore, the minimum energy configuration in the final electronic excited state will have nuclei that are displaced relative to the ground state. It is reasonable to assume that efficient resonant absorption of light by electronic transitions will also result in a large displacement of the nuclei between the $|g\rangle$ and $|e\rangle$ states, which will be reflected in large FCFs.

It is instructive to calculate the FCFs for the case of a single vibrational mode, as expected for a diatomic molecule. The simplest model is to assume that the vibration is harmonic and that its frequency is unchanged between the ground and electronic excited state; only the minimum of the harmonic potential is shifted to a different bond length. If the difference in displacement along the vibrational coordinate x between the ground and excited state is d, then the FCF is $\langle\varphi_{n'}(x-d)|\varphi_n(x)\rangle$, where φ_n are the harmonic oscillator eigenfunctions. If we define the x-displacement operator as $\hat{D}(x) = \exp\left(-\mathrm{i}\hat{p}_x d/\hbar\right)$, then the wavefunctions for the displaced oscillator are obtained from $|\varphi_n(x-d)\rangle = \hat{D}(d)\,|\varphi_n(x)\rangle$, and the FCF is obtained from $\langle\varphi_{n'}|\,\hat{D}(d)\,|\varphi_n\rangle$. Taking the initial state to be the ground vibrational state, $n=0$, then we can calculate the FCF for transition to state n' as

$$\langle n'|\,\hat{D}(d)\,|0\rangle = e^{-\underset{\sim}{d}}\frac{\underset{\sim}{d}^{n'}}{n'!} \tag{10.3.7}$$

▶ **See derivation of** 10.3.7

Using $\hat{p} = \mathrm{i}\sqrt{\frac{m\hbar\omega_0}{2}}\left(\hat{a}^\dagger - \hat{a}\right)$ and defining the dimensionless displacement is $\underset{\sim}{d} = d\sqrt{\frac{m\omega_0}{2\hbar}}$ we can write the FCF as

$$\begin{aligned}\langle n|\,\hat{D}\,|0\rangle &= \langle n|\,e^{-\mathrm{i}\hat{p}_x d/\hbar}\,|0\rangle \\ &= \langle n|\,e^{\underset{\sim}{d}(\hat{a}^\dagger - \hat{a})}\,|0\rangle\end{aligned} \tag{10.3.8}$$

Since the raising and lowering operators don't commute, we expand the exponential term using

$$e^{\hat{A}+\hat{B}} = e^{\hat{A}}e^{\hat{B}}e^{-\frac{1}{2}[\hat{A},\hat{B}]}$$

and $[\hat{a}^\dagger, \hat{a}] = -1$. This gives:

$$\begin{aligned}\langle n|\,\hat{D}\,|0\rangle &= \langle n|\,e^{\underset{\sim}{d}\hat{a}^\dagger}e^{-\underset{\sim}{d}\hat{a}}e^{-\underset{\sim}{d}^2/2}\,|0\rangle \\ &= e^{-\underset{\sim}{d}^2/2}\,\langle n|\,e^{\underset{\sim}{d}\hat{a}^\dagger}e^{-\underset{\sim}{d}\hat{a}}\,|0\rangle\end{aligned} \tag{10.3.9}$$

Since the exponential operator on the right is expanded as

$$e^{-\underset{\sim}{d}\hat{a}} = 1 - \underset{\sim}{d}\hat{a} + \cdots$$

and lowering $|0\rangle$ leads to the null ket:

$$\begin{aligned}\langle n|\,\hat{D}\,|0\rangle &= e^{-\underset{\sim}{d}^2/2}\,\langle n|\,e^{\underset{\sim}{d}\hat{a}^\dagger}\,|0\rangle \\ &= e^{-\underset{\sim}{d}^2/2}\,\langle n|\sum_{i=0}^{\infty}\frac{1}{i!}\left(\underset{\sim}{d}\hat{a}^\dagger\right)^i|0\rangle = e^{-\underset{\sim}{d}^2/2}\,\langle n|\sum_{m=0}^{\infty}\frac{1}{m!}\underset{\sim}{d}^m\sqrt{m!}\,|m\rangle \\ &= e^{-\underset{\sim}{d}^2/2}\,\langle n|\sum_{m=0}^{\infty}\frac{1}{\sqrt{m!}}\underset{\sim}{d}^m\,|m\rangle \\ &= e^{-\underset{\sim}{d}^2/2}\frac{\underset{\sim}{d}^n}{\sqrt{n!}}\end{aligned} \tag{10.3.10}$$

where the dimensionless displacement $\underset{\sim}{d} = d\sqrt{m\omega_0/2\hbar}$, and m and ω_0 are the mass and fundamental frequency of the harmonic oscillator. Unlike transitions within the same electronic state, vibronic transitions are allowed between all pairs of vibrational states on the ground and electronic excited state, and the probability of that transition is related to the difference in nuclear displacement between the two states. The probability for the $n=0$ to n' transition is proportional to the square of the FCF

$$I_{n',0} = \left|\left\langle n'\middle|\,\hat{D}\,\middle|0\right\rangle\right|^2 = e^{-S}\frac{S^{n'}}{n'!} \tag{10.3.11}$$

which is expressed in terms of the Huang-Rhys parameter, $S = \underset{\sim}{d}^2$, a general measure of the displacement of the excited state

nuclear potential and the strength of vibronic interaction. Note that the variation of transition probability with n' follows a Poisson distribution of intensities. This reflects that the sum of all vibronic transition probabilities is unity: $\sum_{n,n'} I_{n,n'} = 1$. The FCF describes how the electronic transition dipole transition probability is distributed amongst the various vibronic transitions, as illustrated in Figure 10.3.1.

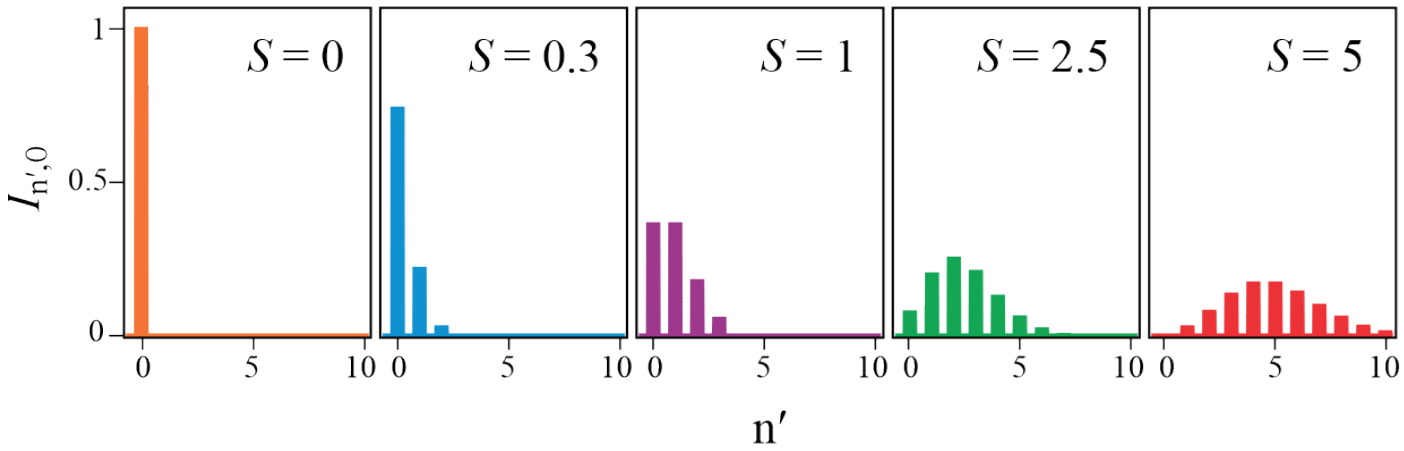


Figure 10.3.1: Illustration of the distribution of intensity amongst different $n = 0 \rightarrow n'$ transitions for different values of the Huang-Rhys parameter.

This page titled 10.3: Molecular Electronic Spectroscopy and Franck Condon Factors is shared under a CC BY-NC-SA 4.0 license and was authored, remixed, and/or curated by Andrei Tokmakoff via source content that was edited to the style and standards of the LibreTexts platform.

10.4: Appendix - Rotational Transition Matrix Elements

In calculating matrix elements involving rotation or orbital angular momentum, one often comes across integrals over a product of three spherical harmonics:

$$\int d\Omega \left[Y_{J_3}^{M_3}(\theta,\phi)\right]^* Y_{J_1}^{M_1}(\theta,\phi) Y_{J_2}^{M_2}(\theta,\phi) \tag{10.4.1}$$

where the integral over spherical angles has been abbreviated as

$$\int d\Omega = \frac{1}{4\pi}\int_0^{2\pi} d\phi \int_0^{\pi} \sin\theta \, d\theta \tag{10.4.2}$$

To evaluate such integrals, one can take advantage of a reduction formula that relates the product of two spherical harmonics to an expansion in single harmonics, where the expansion factors are related to Clebsch Gordon Coefficients (CGCs):

$$Y_{J_1}^{M_1} Y_{J_2}^{M_2} = \sum_{J_3,M_3} \sqrt{\frac{(2J_1+1)\,(2J_2+1)}{4\pi\,(2J_3+1)}} \left\langle J_1 0; J_2 0 | L 0 \right\rangle \left\langle J_1 M_1; J_2 M_2 | J_3 M_3 \right\rangle Y_{J_3}^{M_3} \tag{10.4.3}$$

With this reduction formula and the orthonormality of spherical harmonics, one obtains the general solution:

$$\int d\Omega \left[Y_{J_3}^{M_3}\right]^* Y_{J_1}^{M_1} Y_{J_2}^{M_2} = \sqrt{\frac{(2J_1+1)\,(2J_2+1)}{4\pi\,(2J_3+1)}} \left\langle J_1 0; J_2 0 | L 0 \right\rangle \left\langle J_1 M_1; J_2 M_2 | J_3 M_3 \right\rangle \tag{10.4.4}$$

These expressions can be used to calculate the rotational matrix elements for electric dipole transitions. The transition dipole orientation for interactions with linearly polarized light is calculated by decomposing the dipole orientation into the laboratory frame x, y, z directions as:

$$\begin{aligned} (\hat{\boldsymbol{\mu}} \cdot \hat{\epsilon}) &= \hat{z}\cos\theta + \hat{y}\sin\theta\sin\varphi + \hat{x}\sin\theta\cos\varphi \\ &= \hat{z}\sqrt{\frac{4\pi}{3}}Y_1^0 + \hat{x}\sqrt{\frac{2\pi}{3}}\left(Y_1^{-1} - Y_1^1\right) + \mathrm{i}\hat{y}\sqrt{\frac{2\pi}{3}}\left(Y_1^{-1} + Y_1^1\right) \end{aligned} \tag{10.4.5}$$

Looking at the leading term, the rotational matrix element for the z-projection of the dipole orientation can be evaluated by setting $(\hat{\mu}\cdot\hat{z}) = \cos\theta = \sqrt{\frac{4\pi}{3}}Y_1^0$, resulting in the integral

$$\left\langle J' M' \right| \cos\theta \left| J M \right\rangle = \sqrt{\tfrac{4\pi}{3}} \int d\Omega \, Y_{J',M'}^* Y_{1,0} Y_{J,M} \tag{10.4.6}$$

Using eq. (10.4.4) with $J_1 = 1; M_1 = 0$ gives

$$\mu_z = \left\langle J', M' \right| \cos\theta \left| J, M \right\rangle = \left(\frac{2J+1}{2J'+1}\right)^{\frac{1}{2}} \left\langle J0; 10 | J'0 \right\rangle \left\langle JM; 10 | J'M' \right\rangle \tag{10.4.7}$$

We can now simplify this using the CGCs for $J_1 = 1, M_1 = 0$. The non-zero coefficients are:

$$\begin{aligned} \left\langle J_2 M; 1, 0 | (J_2+1)\, M \right\rangle &= \sqrt{\frac{(J_2 - M + 1)\,(J_2 + M + 1)}{(2J_2+1)\,(J_2+1)}} && (\Delta J = +1, \Delta M = 0) \\ \left\langle J_2 M; 1, 0 | J_2 M \right\rangle &= \frac{M}{\sqrt{J_2\,(J_2+1)}} && (\Delta J = 0, \Delta M = 0) \\ \left\langle J_2 M; 1, 0 | (J_2-1)\, M \right\rangle &= -\sqrt{d\frac{(J_2 - M)\,(J_2 + M)}{J_2\,(2J_2+1)}} && (\Delta J = -1, \Delta M = 0) \end{aligned} \tag{10.4.8}$$

Individually, these CGCs are non-zero for $\Delta J = 0, \pm 1$ and $\Delta M = 0$, but $\Delta J = 0$, $\Delta M = 0$ doesn't involve any change of state. So, we find $\Delta J = \pm 1, \Delta M = 0$ are allowed transitions. For these two terms, the rotational transition dipole matrix elements obtained by evaluating eq. (10.4.7) are

$$\mu_z = \langle J', M' \left| \hat{r} \cdot \hat{z} \right| J, M \rangle = c^z_{J+,M} \delta_{J',J+1} \delta_{M,M'} + c^z_{J-,M} \delta_{J',J-1} \delta_{M,M'} \tag{10.4.9}$$

where the coefficients for $\Delta J = \pm 1$ transitions are:

$$\begin{aligned} c^z_{J+,M} &= \langle J+1, M \left| \hat{r} \cdot \hat{z} \right| J, M \rangle = \sqrt{\frac{(J+M+1)(J-M+1)}{(2J+1)(2J+3)}} = \sqrt{\frac{(J+1)^2 - M^2}{4(J+1)^2 - 1}} \\ c^z_{J-,M} &= \langle J-1, M \left| \hat{r} \cdot \hat{z} \right| J, M \rangle = \sqrt{\frac{(J+M)(J-M)}{(2J-1)(2J+1)}} = \sqrt{\frac{J^2 - M^2}{4J^2 - 1}} \end{aligned} \tag{10.4.10}$$

A similar process can be applied to the components of the dipole vector oriented along the x and y directions. The resulting matrix elements are non-zero for $J = J' \pm 1$ and $M = M' \pm 1$. Looking at x:

$$\begin{aligned} \mu_x = \langle J', M' | \hat{r} \cdot \hat{x} | J, M \rangle = \frac{1}{\sqrt{2}} \big(& \delta_{M',M-1} \left(c^x_{J+,M-} \delta_{J',J+1} + c^x_{J-,M-} \delta_{J',J-1} \right) \\ & - \delta_{M',M+1} \left(c^x_{J+,M+} \delta_{J',J+1} + c^x_{J-,M+} \delta_{J',J-1} \right) \big) \end{aligned} \tag{10.4.11}$$

$$\begin{aligned} \mu_y = \langle J', M' | \hat{r} \cdot \hat{y} | J, M \rangle = \frac{1}{\sqrt{2}} \big(& \delta_{M',M-1} \left(c^y_{J+,M-} \delta_{J',J+1} + c^y_{J-,M-} \delta_{J',J-1} \right) \\ & - \delta_{M',M+1} \left(c^y_{J+,M+} \delta_{J',J+1} + c^y_{J-,M+} \delta_{J',J-1} \right) \big) \end{aligned} \tag{10.4.12}$$

The coefficients for μ_x are given by:

$$\begin{aligned} c^x_{J+,M-} &= \langle J+1, M-1 \left| \hat{r} \cdot \hat{x} \right| J, M \rangle = \sqrt{\frac{(J-M+1)(J-M+2)}{2(2J+1)(2J+3)}} \\ c^x_{J-,M-} &= \langle J-1, M-1 \left| \hat{r} \cdot \hat{x} \right| J, M \rangle = \sqrt{\frac{(J+M)(J+M-1)}{2(2J-1)(2J+1)}} \\ c^x_{J+,M+} &= \langle J+1, M+1 \left| \hat{r} \cdot \hat{x} \right| J, M \rangle = \sqrt{\frac{(J+M+2)(J+M+1)}{2(2J+1)(2J+3)}} \\ c^x_{J-,M+} &= \langle J-1, M+1 \left| \hat{r} \cdot \hat{x} \right| J, M \rangle = \sqrt{\frac{(J-M)(J-M+1)}{2(2J-1)(2J+1)}} \end{aligned} \tag{10.4.13}$$

The coefficients for $\hat{y}$ are closely related those for $\hat{x}$:

$$\begin{aligned} c^y_{J+,M+} &= \langle J+1, M+1 | \hat{r} \cdot \hat{y} | J, M \rangle = \mathrm{i} c^x_{J+,M+} \\ c^y_{J+,M-} &= \langle J+1, M-1 | \hat{r} \cdot \hat{y} | J, M \rangle = -\mathrm{i} c^x_{J+,M-} \\ c^y_{J-,M+} &= \langle J-1, M+1 | \hat{r} \cdot \hat{y} | J, M \rangle = \mathrm{i} c^x_{J-,M+} \\ c^y_{J-,M-} &= \langle J-1, M-1 | \hat{r} \cdot \hat{y} | J, M \rangle = -\mathrm{i} c^x_{J-,M-} \end{aligned} \tag{10.4.14}$$

Or:

$$\begin{aligned} c^x_{J+,M\pm} &= -\mathrm{i} c^y_{J+,M\pm} \\ c^x_{J-,M-} &= \mathrm{i} c^y_{J-,M-} \end{aligned} \tag{10.4.15}$$

Returning to eq. (10.4.5), we see that the same expression can be regrouped as

$$(\hat{\boldsymbol{\mu}} \cdot \hat{\epsilon}) = \hat{z} \sqrt{\frac{4\pi}{3}} Y^0_1 - \sqrt{\frac{2\pi}{3}} Y^1_1 (\hat{x} - \mathrm{i}\hat{y}) + \sqrt{\frac{2\pi}{3}} Y^{-1}_1 (\hat{x} + \mathrm{i}\hat{y}) \tag{10.4.16}$$

Grouping by the angular momentum eigenstate illustrates why left and right circularly polarized waves, $|\pm\rangle = \frac{1}{\sqrt{2}} (\hat{x} \pm \mathrm{i}\hat{y})$, are used to induce selective changes in the spin angular momentum of electrons and a quantum electromagnetic field. Photons are spin-1 bosons that have a spin angular momentum projected in the direction of propagation: $\pm\hbar$ for left and right circularly polarized fields. Using the relationships in eq. (10.4.15) to evaluate the matrix elements for these polarization states by summing the coefficients, one finds that the left circularly polarized fields are responsible for $\Delta M = -1$ transitions whereas the right circularly polarized fields are responsible for $\Delta M = +1$. No spin changes ($\Delta M = 0$) are induced by z-polarized light. All matrix elements require a ± 1 change of J because any change in the matter's angular momentum is matched by an equal and opposite change in the photon's orbital angular momentum.

This page titled 10.4: Appendix - Rotational Transition Matrix Elements is shared under a CC BY-NC-SA 4.0 license and was authored, remixed, and/or curated by Andrei Tokmakoff via source content that was edited to the style and standards of the LibreTexts platform.

10.5: Readings

The Molecular Transition Dipole Operator and Electronic Spectroscopy

1. Struve, W. S. *Fundamentals of Molecular Spectroscopy*; Wiley, 1989.

Selection Rules

1. Atkins, P. W.; Friedman, R. *Molecular Quantum Mechanics*, 4th ed.; Oxford University Press, 2005.
2. Demtröder, W. *Laser Spectroscopy: Basic Concepts and Instrumentation*; Springer Berlin, Heidelberg, 1996; pp 80-82. DOI: 10.1007/978-3-662-08260-7
3. Flygare, W. H. *Molecular Structure and Dynamics*; Prentice-Hall, 1978.
4. Merzbacher, E. *Quantum Mechanics*, 3rd ed.; Wiley, 1998.
5. Rose, M. E. *Elementary Theory of Angular Momentum*; Dover Publications, 1995.

This page titled 10.5: Readings is shared under a license and was authored, remixed, and/or curated by Andrei Tokmakoff.

11: IRREVERSIBLE RELAXATION

11.1: Introduction
11.2: Coupling to a continuum
11.3: Spontaneous Emission
11.4: Relaxation and Line-broadening
11.5: Readings

This page titled 11: Irreversible Relaxation is shared under a CC BY-NC-SA 4.0 license and was authored, remixed, and/or curated by Andrei Tokmakoff via source content that was edited to the style and standards of the LibreTexts platform.

11.1: Introduction

There is no preferred direction to the arrow of time in isolated quantum mechanical systems. The laws governing the evolution of *isolated* systems through time are unchanged by time reversal. The TDSE is reversible, meaning that one can find solutions for propagating either forward or backward in time. If one reverses the sign of time, this is the equivalent of reversing the momenta of particles, and we should be able to trace backward to the conditions of the system at an earlier time.

In contrast, when a quantum system is not isolated, for instance through contact with another system that allows energy to flow between them, a definite direction emerges to the arrow of time, and the system's dynamics are no longer reversible. Such irreversible systems are dissipative—they decay in time from a prepared state to one where phase relationships between the basis states are lost. How does irreversible behavior, a hallmark of chemical systems, arise from the deterministic TDSE? Irreversibility is the key attribute arising from condensed phase systems, and we will it take up in more detail in later chapters. For now, the formalism we have developed will allow us to answer this question in the context of using quantum transitions from an initial state to a dense continuum of states.

To illustrate how irreversible relaxation emerges, consider an initial state coupled to a finite but growing number of randomly chosen states of nearly the same energy. Figure 11.1.1 shows the calculated probability amplitude of this initial state as the number of coupled final states increases. When there is only one final state, the exchange of probability amplitude is purely sinusoidal, as we have calculated before for a two-level system. For two final states, a somewhat more complicated beat pattern arises due to constructive and destructive interferences from different beat frequencies. As the manifold of final states increases, the variation in phases and frequencies for the exchange of amplitude gradually suppress beats. With 100 or 1000 states, recurrences in the initial state amplitude are suppressed, and an asymptotic exponential decay emerges. This observation leads us to expect that irreversible relaxation reflects the destructive interference between oscillatory exchange of amplitude of a prepared state with a closely packed manifold of accepting states. Clearly in the limit that the accepting states are truly continuous, the initial amplitude prepared in ℓ will be spread through an infinite number of continuum states.

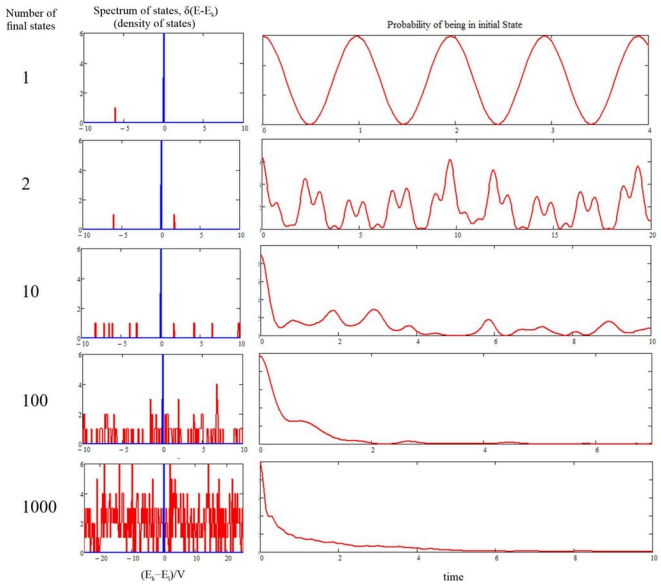


Figure 11.1.1: Illustration of the emergence of irreversible relaxation from a dense manifold of isoenergetic states k coupled to the initially prepared state ℓ.

As we discussed earlier in the context of first-order perturbation theory, when a discrete state is coupled to a continuum, the Golden Rule describes the global rate of change in probability of leaving the initial state $|\ell\rangle$ for all continuum states $|k\rangle$ as:

$$\bar{w}_{k\ell} = \frac{\partial P_\ell}{\partial t} = \frac{2\pi}{\hbar}|V_{k\ell}|^2 \rho(E_\ell) \tag{11.1.1}$$

$\rho(E_\ell)$ is the density of continuum states per unit energy interval evaluated at $E_k = E_\ell$. The transition rate $\bar{w}_{k\ell}$ is constant in time when $|V_{k\ell}|^2$ is constant in time. Under these conditions, integrating the rate equation on the left gives the probability of leaving the initial state:

$$P_\ell = 1 - \bar{w}_{k\ell} t \tag{11.1.2}$$

or equivalently of observing the system in the continuum

$$\bar{P}_k = \bar{w}_{k\ell} t \tag{11.1.3}$$

The probability of transition to the continuum varies linearly in time as shown in Figure 11.1.2. As we noted in our discussion of first-order perturbation theory, this will clearly only work for times such that $P_k(t) - P_k(0) \ll 1$.

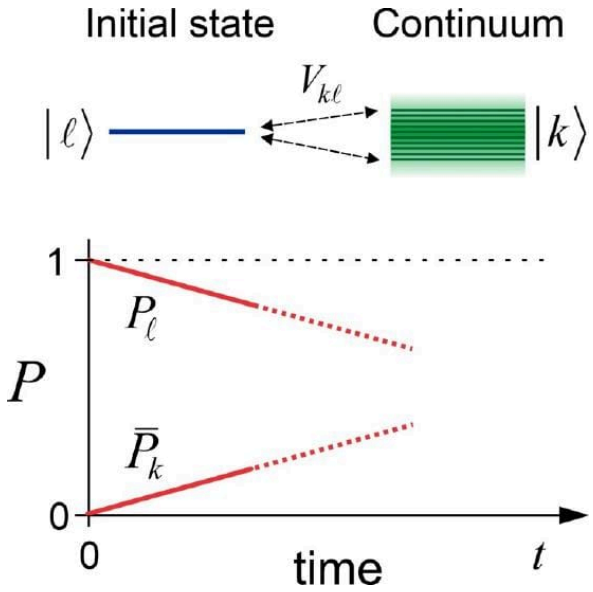


Figure 11.1.2: (Top) Illustration of the energy levels for the initial state coupled to a continuum. (Bottom) Linear change in the probability of occupying the initial state or continuum predicted from first-order perturbation theory

What long time behavior do we expect? A time-independent rate of population relaxation is one of the hallmarks of first order kinetics and exponential relaxation. Such systems follow a rate equation of the form $\partial P_\ell / \partial t = -\bar{w}_{k\ell} P_\ell$. The short-time exponential relaxation behavior out of a state ℓ, looks just like the first order result:

$$\begin{aligned} cP_\ell(t) &= \exp(-\bar{w}_{k\ell} t) \\ &= 1 - \bar{w}_{k\ell} t + \ldots \end{aligned} \tag{11.1.4}$$

We might believe that $\bar{w}_{k\ell}$ represents the slope of the relaxation behavior at $t = 0$. The reason for the timeframe limitation we had previously ($P_k(t) - P_k(0) \ll 1$) was that we did not account for depletion of initial state. This will become evident in the derivation below as we add a bit more detail to our model. Adding more detail will also reveal that the long-time relaxation behavior of state ℓ is exponential and governed by the golden rule rate.

What systems show the relaxation behavior of an initially prepared state coupled to a continuum of states? Isolated atoms and molecules undergoing spontaneous emission and other interactions with an electromagnetic field are described as coupling to a continuum of field modes. Free particles take on a continuous range of energies given by their momenta. Nuclei can take on a continuum of energies by interacting on dissociative potential energy surfaces or on bound potentials in which the energy exceeds the binding energy. The same can happen to electrons that exceed the binding energy of their molecules or materials. For a concrete example, photoionization or photodissociation of a molecule involves a light field coupling a bound state into a continuum. Other examples are common in condensed matter. The intermolecular motions of a liquid, the lattice vibrations of a crystal, or the allowed energies within the band structure of a metal or semiconductor are all examples of continua. The time-dependent behavior of molecules in condensed phases are therefore universally understood to be coupled to continua in one form or another.

This page titled 11.1: Introduction is shared under a CC BY-NC-SA 4.0 license and was authored, remixed, and/or curated by Andrei Tokmakoff via source content that was edited to the style and standards of the LibreTexts platform.

11.2: Coupling to a continuum

Let's describe the transitions from an initial state ℓ to a continuum of states $\{k\}$ under a constant perturbation. The initial state and the continuum together form a complete closed system and, in the absence of coupling, represent the eigenstates of our Hamiltonian $H_0 |n\rangle = E_n |n\rangle$:

$$1 = \sum_n |n\rangle \langle n| = |\ell\rangle \langle \ell| + \sum_k |k\rangle \langle k| \tag{11.2.1}$$

We then introduce a weak interaction between the initial state and the continuum, leading to our perturbation Hamiltonian $H = H_0 + V$. In later chapters, you will see that, when we partition $H_0 = H_S + H_B$, we can identify ℓ with the "system" and $\{k\}$ with the "bath."

Now let's make some further simplifying assumptions to aid our description. For transitions into the continuum, we will assume that all transitions are between ℓ and the continuum states, and there are no interactions between the states of the continuum: $\langle k|V|k'\rangle = V_{k,k'} = 0$. This can be rationalized by thinking of this problem as a discrete set of states interacting with a continuum of normal modes. Moreover, we will assume that the coupling interaction between the initial and continuum states is a constant for all states k: $V_{\ell k} = \langle \ell| V |k\rangle = \langle \ell| V |k'\rangle = \cdots$. For reasons that we will see later, we will also keep the diagonal matrix element $\langle \ell| V |\ell\rangle = 0$. With these assumptions, we can express the Hamiltonian for our problem as

$$\begin{aligned} H &= H_0 + V \\ H_0 &= |\ell\rangle E_\ell \langle \ell| + \sum_k |k\rangle E_k \langle k| \\ V &= \sum_k \left[|k\rangle V_{k\ell} \langle \ell| + |\ell\rangle V_{\ell k} \langle k| \right] + |\ell\rangle V_{\ell\ell} \langle \ell| \end{aligned} \tag{11.2.2}$$

We are seeking a more accurate description of the occupation of the initial and continuum states, for which we will use the interaction picture probability amplitudes

$$b_k(t) = \langle k| U_I(t, t_0) |\ell\rangle \tag{11.2.3}$$

Earlier, we saw that the exact solution to U_I was:

$$U_I(t, t_0) = 1 - \frac{\mathrm{i}}{\hbar} \int_{t_0}^{t} d\tau \, V_I(\tau) \, U_I(\tau, t_0) \tag{11.2.4}$$

This form was not very practical since U_I is a function of itself. For first-order perturbation theory, we set the final term in this equation $U_I(\tau, t_0) \to 1$. Here, in order to keep the feedback between $|\ell\rangle$ and the continuum states, we keep it as is and develop the expression a bit further. Substituting this expression into eq. (11.2.3), we get

$$b_k(t) = \langle k|\ell\rangle - \frac{\mathrm{i}}{\hbar} \int_{t_0}^{t} d\tau \, \langle k| V_I(\tau) U_I(\tau, t_0) |\ell\rangle \tag{11.2.5}$$

Next, inserting the completeness expression eq. (11.2.1) into the matrix element and recognizing $k \neq \ell$,

$$b_k(t) = -\frac{\mathrm{i}}{\hbar} \sum_n \int_{t_0}^{t} d\tau \, e^{\mathrm{i}\omega_{kn}\tau} V_{kn} b_n(\tau) \tag{11.2.6}$$

Note, V_{kn} is not a function of time. Equation (11.2.6) expresses the occupation of state k in terms of the full history of the system from $t_0 \to t$, with amplitude flowing back and forth between the states n. Equation (11.2.6) is just the integral form of the coupled differential equations that we used before:

$$\mathrm{i}\hbar \frac{\partial b_k}{\partial t} = \sum_n e^{\mathrm{i}\omega_{kn}t} V_{kn} b_n(t) \tag{11.2.7}$$

These exact forms allow for feedback between all the states, in which the amplitudes b_k depend on all other states. Since you only feed from ℓ into k, we can remove the summation in (11.2.6) and express the complex amplitude of one state within the continuum as

$$b_k = -\frac{\mathrm{i}}{\hbar} V_{k\ell} \int_{t_0}^{t} d\tau \, \mathrm{i} e^{\mathrm{i}\omega_{k\ell}\tau} b_\ell(\tau) \tag{11.2.8}$$

We want to calculate the rate of transition away from $|\ell\rangle$, including feeding from the continuum back into the initial state. From eq. (11.2.7) we can separate the sum over all states (n) into two terms involving the continuum and the initial state:

$$\mathrm{i}\hbar \frac{\partial}{\partial t} b_\ell = \sum_{k \neq \ell} e^{\mathrm{i}\omega_{\ell k} t} V_{\ell k} b_k + V_{\ell\ell} b_\ell \tag{11.2.9}$$

Now substituting (11.2.8) into (11.2.9) and setting $t_0 = 0$:

$$\frac{\partial b_\ell}{\partial t} = -\frac{1}{\hbar^2} \sum_{k \neq \ell} |V_{k\ell}|^2 \int_0^t b_\ell(\tau) e^{\mathrm{i}\omega_{k\ell}(\tau - t)} \, d\tau - \frac{\mathrm{i}}{\hbar} V_{\ell\ell} b_\ell(t) \tag{11.2.10}$$

This is an integro-differential equation that describes how the time-development of b_ℓ depends on the entire history of the system. Note we have a pair of time variables that indicate the flow of the probability amplitude: τ notes the flow from ℓ to k, and t notes the flow from k back to ℓ.

The next assumption is that b_ℓ varies slowly enough that we can discard it. While b_ℓ is a function of time, in the interaction picture it evolves slowly compared to the $\omega_{k\ell}$ oscillations, so we can remove it from the integral. This is effectively a weak coupling statement: $\hbar\omega_{k\ell} \gg V_{k\ell}$.

$$\frac{\partial b_\ell}{\partial t} = b_\ell \left[-\frac{1}{\hbar^2} \sum_{k \neq \ell} |V_{k\ell}|^2 \int_0^t e^{\mathrm{i}\omega_{k\ell}(\tau - t)} \, d\tau - \frac{\mathrm{i}}{\hbar} V_{\ell\ell} \right] \tag{11.2.11}$$

Now, we want the long-time evolution of b_ℓ such that $\omega_{k\ell} t \gg 1$, so we will investigate the integration limit $t \to \infty$. By switching variables using $t' = \tau - t$, the integral can be rewritten as:

$$\int_0^t e^{\mathrm{i}\omega_{k\ell}(\tau - t)} \, d\tau = \int_0^t e^{\mathrm{i}\omega_{k\ell} t'} \, dt' \tag{11.2.12}$$

A note on complex integration

This is a good point to discuss the complex integration of the function $\int_0^t e^{\mathrm{i}\omega t'} dt'$ and its limit at $t \to \infty$. This integral is oscillatory, with a result that diverges at $\omega = 0$, but we deal this by introducing a small positive factor ε into the exponential and later take the limit $\varepsilon \to 0$.

$$\lim_{\varepsilon \to 0^+} \int_0^\infty e^{(\mathrm{i}\omega - \varepsilon)t'} dt' = -\lim_{\varepsilon \to 0^+} \frac{1}{\mathrm{i}\omega - \varepsilon} \tag{11.2.13}$$

$$= \lim_{\varepsilon \to 0^+} \left(\frac{\varepsilon}{\omega^2 + \varepsilon^2} + \mathrm{i} \frac{\omega}{\omega^2 + \varepsilon^2} \right) \tag{11.2.14}$$

Eq. (11.2.14) shows the real and imaginary parts separated. We can see that the leading term in eq. (11.2.14) can be expressed as a delta function using

$$\lim_{\varepsilon \to 0^+} \left(\frac{\varepsilon}{\omega^2 + \varepsilon^2} \right) = \pi \delta(\omega) \tag{11.2.15}$$

The second term is known as the Cauchy Principle Part:

$$\lim_{\varepsilon \to 0^+} \left(\frac{\omega}{\omega^2 + \varepsilon^2} \right) = \mathbb{P}\left(\frac{1}{\omega} \right) \tag{11.2.16}$$

where

$$\mathbb{P}\left(\frac{1}{x} \right) = \begin{cases} \frac{1}{x} & \text{if } x \neq 0 \\ 0 & \text{if } x = 0 \end{cases} \tag{11.2.17}$$

Combining terms, we find that

$$\lim_{t\to\infty}\int_0^t e^{\mathrm{i}\omega t'}dt' = \pi\delta(\omega) - \mathrm{i}\mathbb{P}\frac{1}{\omega} \tag{11.2.18}$$

This is one of the interesting ways in which the delta function can be used to resolve complex integration problems and factors of $1/x$ that involve a divergence at $x = 0$. For instance, resonant denominators for the driven harmonic oscillator in the limit of no damping can be resolved using

$$\lim_{\gamma\to 0^+}\frac{1}{\omega \pm \mathrm{i}\gamma} = \mathbb{P}\left(\frac{1}{\omega}\right) \mp \mathrm{i}\pi\delta(\omega)$$

The identities above also allow us to obtain another important delta function identity:

$$\delta(\omega) = \frac{1}{2\pi}\int_{-\infty}^{\infty} e^{\mathrm{i}\omega t'}dt'$$

This is obtained by splitting the integral into negative and positive t' integrations

$$\int_{-\infty}^{\infty} e^{\mathrm{i}\omega t'}dt' = -\int_0^{\infty} e^{-\mathrm{i}\omega t''}dt'' + \int_0^{\infty} e^{\mathrm{i}\omega t'}dt'$$

and applying eq. (11.2.18).

Using eq. (11.2.18), eq. (11.2.11) can be evaluated in the limit $t \to \infty$, and becomes

$$\frac{\partial b_\ell}{\partial t} = b_\ell\left[\underbrace{-\frac{\pi}{\hbar^2}\sum_{k\neq\ell}|V_{k\ell}|^2\,\delta(\omega_{k\ell})}_{\text{Term 1, } \bar{w}_{k\ell}} \underbrace{-\frac{\mathrm{i}}{\hbar}\left(V_{\ell\ell} + \mathbb{P}\sum_{k\neq\ell}\frac{|V_{k\ell}|^2}{E_k - E_\ell}\right)}_{\text{Term 2}}\right] \tag{11.2.19}$$

The right-hand side of this equation has been grouped into two terms, the first real and the second imaginary. Note that Term 1 is simply the Golden Rule rate for leaving the initial state, written explicitly as a sum over the continuum of all possible final states, $\bar{w}_{k\ell} = \sum_k w_{k\ell}$. Since the manifold of final states is so dense and uniform that they are only distinguishable by their energy, we can express this sum as an integral over the density of states of the continuum $\rho(E_\ell)$. That is, we make the substitution:

$$\sum_{k\neq\ell}\delta(\omega_{k\ell}) \to \int dE_k\,\hbar\,\rho(E_k = E_\ell) \tag{11.2.20}$$

Then the relaxation rate is given by

$$\bar{w}_{k\ell} = \frac{2\pi}{\hbar}|V_{k\ell}|^2\,\rho(E_\ell) \tag{11.2.21}$$

Term 2 in eq. (11.2.19) is an energy term. It is the shift or correction of the energy of the initial state E_ℓ that arises from coupling with the continuum due to second-order, time-independent perturbation theory.

$$\Delta E_\ell = \langle\ell|\,V\,|\ell\rangle + \sum_{k\neq\ell}\frac{|\langle k|\,V\,|\ell\rangle|^2}{E_k - E_\ell} \tag{11.2.22}$$

Combining these results, we find that the time evolution of b_ℓ is governed by a simple first-order differential equation

$$\frac{\partial b_\ell}{\partial t} = b_\ell\left(-\frac{\bar{w}_{k\ell}}{2} - \frac{\mathrm{i}}{\hbar}\Delta E_\ell\right) \tag{11.2.23}$$

This can be integrated using the initial condition $b_\ell(0) = 1$ to find the time-dependent probability amplitude of the initial state ℓ as

$$b_\ell(t) = \exp\left(-\frac{\bar{w}_{k\ell}t}{2} - \frac{\mathrm{i}}{\hbar}\Delta E_\ell t\right) \tag{11.2.24}$$

If we calculate the time-dependent probability of observing the system in the initial state, we have

$$P_\ell = |c_\ell|^2 = \exp\left[-\bar{w}_{k\ell} t\right] \tag{11.2.25}$$

The probability of observing the system in state ℓ decays exponentially because the probability amplitude is being distributed among the continuum states! This is a manner of irreversible relaxation from an initially prepared state. For completeness, we can switch from the interaction picture back to the Schrödinger Picture using $c_\ell = b_\ell e^{-iE_\ell t/\hbar}$:

$$c_\ell(t) = \exp\left[-\left(\frac{\bar{w}_{k\ell}}{2} + \mathrm{i}\frac{E'_\ell}{\hbar}\right) t\right] \tag{11.2.26}$$

where the corrected energy of state ℓ is:

$$E'_\ell \equiv E_\ell + \Delta E_\ell \tag{11.2.27}$$

The solutions to the TDSE are expected to be complex and oscillatory. What we see here is a real-valued relaxation component in addition to the imaginary phase factor, resulting in the probability decays exponentially from initial state. We also find, quite remarkably, that the Golden Rule relaxation rate derived from first order perturbation theory, which is only supposed to hold for negligibly small changes in $P_\ell(t) \approx 1$, actually properly predicts the exponential rate constant describing the long-time relaxation to $P_\ell = 0$ as $t \to \infty$.

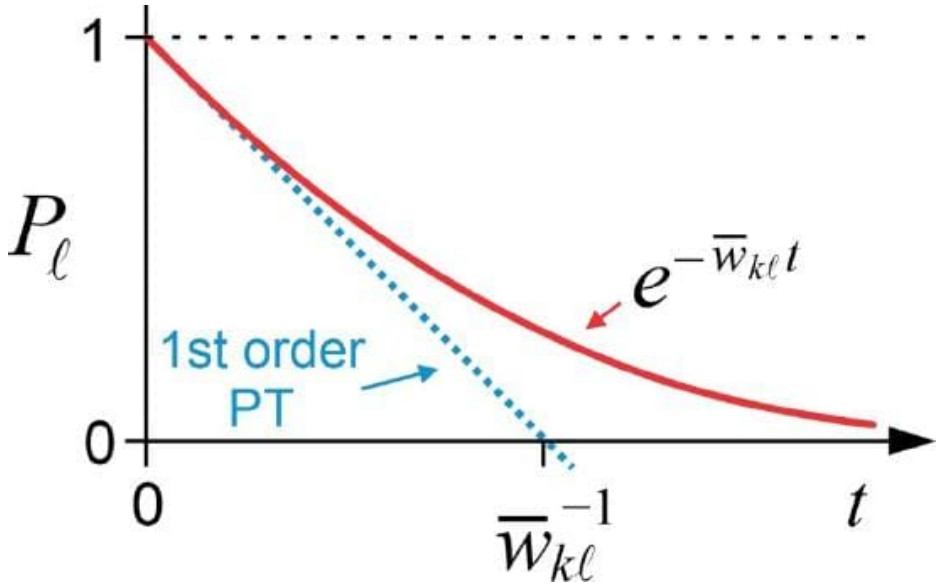


Figure 11.2.1: Illustration of the predicted exponential decay in probability of occupying the initial state given by eq. (11.2.25) compared to the linear decay predicted by eq. (11.1.2) and first order perturbation theory.

Now, what can we say about the continuum states? What is the probability that we observe the system in a particular state of the continuum given that we were initially in state ℓ? Substituting eq. (11.2.24) into eq. (11.2.8) gives us an expression for the probability amplitude of state k:

$$\begin{aligned} b_k(t) &= -\frac{\mathrm{i}}{\hbar}\int_0^t V_{k\ell} e^{\mathrm{i}\omega_{k\ell}\tau} b_\ell(\tau) d\tau \\ &= V_{k\ell}\frac{1 - \exp\left(-\frac{\bar{w}_{k\ell}}{2}t - \frac{i}{\hbar}\left(E'_\ell - E_k\right)t\right)}{E_k - E'_\ell + \mathrm{i}\hbar\bar{w}_{k\ell}/2} \\ &= V_{k\ell}\frac{1 - c_\ell(t)}{E_k - E'_\ell + \mathrm{i}\hbar\bar{w}_{k\ell}/2} \end{aligned} \tag{11.2.28}$$

In this expression, the term $1 - c_\ell(t)$ shows that b_k grows in exponentially at a rate $\bar{w}_{k\ell}$. If we investigate the long-time limit $(t \to \infty)$, we find that the final probability of occupying that state is:

$$P_k(E_k) = \frac{|V_{k\ell}|^2}{\left(E_k - E'_\ell\right)^2 + (\hbar\bar{w}_{k\ell})^2/4} \tag{11.2.29}$$

The probability density for occupying states within the continuum after relaxing from state ℓ is a Lorentzian distribution with

maximum probability centered at E'_ℓ (Figure 11.2.2). The width of the distribution is proportional to $\bar{w}_{k\ell}$, which is proportional to $|V_{k\ell}|^2 \rho(E_\ell)$, the coupling to the continuum and density of states.

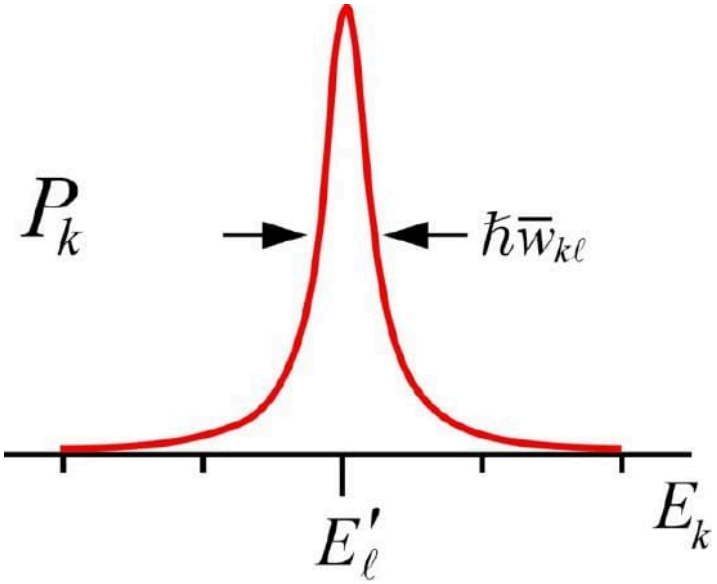


Figure 11.2.2: Probability distribution of final states in the continuum after irreversible relaxation from state ℓ.

This page titled 11.2: Coupling to a continuum is shared under a CC BY-NC-SA 4.0 license and was authored, remixed, and/or curated by Andrei Tokmakoff via source content that was edited to the style and standards of the LibreTexts platform.

11.3: Spontaneous Emission

As an application of the model described in the previous section, let's consider the spontaneous emission of light from an atom. In fact, the model was introduced by Weisskopf and Wigner for this very purpose to explain the line-broadening in atomic emission spectra.(1) In this case, we take the Hamiltonian of the system to be the sum of Hamiltonians for the atom and the electromagnetic field. The atom is represented as a two-level system with a ground and an excited state. The light is represented by the continuum of quantized electromagnetic modes of frequency ω_j, described in Section 9.3. Putting these together, the minimalist Hamiltonian is:

$$H_0 = H_{\text{atom}} + H_{\text{light}} = |e\rangle\, E_e\, \langle e| + |g\rangle\, E_g\, \langle g| + \sum_j n_j \hbar\omega_j \tag{11.3.1}$$

where $E_e > E_g$, and the number operator in the electromagnetic modes is $n_j = a_j^\dagger a_j$. To couple the atom and field, we can use the electric dipole Hamiltonian:

$$\hat{V} = -\hat{\mu}\hat{\mathcal{E}} \tag{11.3.2}$$

where quantized electric field operator is

$$\hat{\mathcal{E}} = \sum_j \mathcal{E}_j \left(a_j^\dagger + a_j\right) \tag{11.3.3}$$

and $\mathcal{E}_j = \sqrt{\hbar\omega_j/2\varepsilon_0 V}$. Note that the quantum field operator is written in a time-independent form, only acting to raise and lower the number of photons in the field, because it is expressed in the Schrödinger representation. The time-dependence of the field operator that we expect emerges when we calculate the electric dipole Hamiltonian in the interaction picture using

$$\hat{\mathcal{E}}(t) = e^{\mathrm{i}H_{\text{light}}t/\hbar}\hat{\mathcal{E}}e^{-\mathrm{i}H_{\text{light}}t/\hbar} = \sum_j \mathcal{E}_j \left(\hat{a}_j^\dagger e^{i\omega_j t} + \hat{a}_j e^{-i\omega_j t}\right) \tag{11.3.4}$$

For spontaneous emission, we will consider the case of the emission of light from an excited state of an atom in the absence of an electric field. Since the state of the system is specified as the product state of the atom and light, the initial state of the system is the excited state of the atom, with no photons in the radiation field, $|\ell\rangle = |e, 0\rangle$, and the final state of the system is the atom in the ground state with a photon in mode j of the field, $|k\rangle = |g, 1_j\rangle$. The corresponding energies of these states are $E_\ell = E_e$ and $E_k = E_g + \hbar\omega_j$, so the energy change between the initial and final state of the joint atom-light system is

$$E_k - E_\ell = \hbar\omega_{k\ell} = E_g - E_e + \hbar\omega_j = \hbar\left(\omega_{ge} + \omega_j\right) \tag{11.3.5}$$

Since $E_e > E_g$, we anticipate a resonant light-matter interaction when $-\omega_{ge} = \omega_{eg} = \omega_j$.

The coupling of the atom to the continuum of electromagnetic modes is described in the interaction picture with

$$V_I(t) = e^{\mathrm{i}H_0 t/\hbar}\hat{V}e^{-\mathrm{i}H_0 t/\hbar} \tag{11.3.6}$$

using the matrix elements in the eigenstates of H_0: $\langle k|\, V_I(t)\, |\ell\rangle$. To calculate this matrix element, we remember that the dipole operator is only an operator in the H_{atom} space and the field operator only acts on the electromagnetic modes.

$$\begin{aligned}\langle k|\, V_I(t)\, |\ell\rangle &= -\langle g|\, e^{\mathrm{i}H_{\text{atom}}t/\hbar}\hat{\mu}\, e^{-\mathrm{i}H_{\text{atom}}t/\hbar}\, |e\rangle\, \langle 1_j|\, e^{\mathrm{i}H_{\text{light}}t/\hbar}\hat{\mathcal{E}}e^{-\mathrm{i}H_{\text{light}}t/\hbar}\, |0\rangle \\ &= -e^{\mathrm{i}\omega_{ge}t}\,\hat{\mu}_{ge}\,\langle 1_j|\,\hat{\mathcal{E}}(t)\,|0\rangle\end{aligned} \tag{11.3.7}$$

$\hat{\mathcal{E}}(t)$ is given by eq. (11.3.4). Since the leading term on the right hand side of eq. (11.3.4) creates photons in the field and is therefore responsible for emission, whereas the second term describes absorption, we retain only the first term and obtain

$$\langle k|\, V_I(t)\, |\ell\rangle = -\hat{\mu}_{ge}\sum_j \mathcal{E}_j\, e^{\mathrm{i}(\omega_j+\omega_{ge})t} \tag{11.3.8}$$

Here we used $\langle n_j + 1|\, a_j^\dagger\, |n_j\rangle = \sqrt{n}$. The exponential argument in this equation is what we expect for a resonant emission process when $\omega_j = \omega_{eg}$.

In the context the Weisskopf-Wigner description, spontaneous emission is described as the exchange of probability amplitude between the initial and final state. The coupling of the atom to the field results in a cyclic flow of amplitude from the excited state of the atom to a mode of the electromagnetic field with a ground state atom then back to an atom in its excited state. The coupling results in a wavefunction for the system that is a superposition of these states:

$$|\psi(t)\rangle = b_{e,0}\,|e,0\rangle + \sum_j b_{g,j}\,|g,1_j\rangle \tag{11.3.9}$$

This time-dependent superposition acts as a source of dipole emission, although not in the classical sense of an oscillating dipole that radiates a field, but a quantum time-dependent probability that the atom and photon field are either in one state or the other. Here the state of the field is a coherent one-photon state that is a superposition of electromagnetic modes. The continuum of modes to which the atom can couple leads to the gradual loss of amplitude in the initial state and the dissipation of that energy into the field. The probability of observing the photon in a particular mode of the field follows the distribution function in eq. (11.2.29).

In completing the description of spontaneous emission, we find that the rate equation for the probability amplitude of the atom in its excited state follows eq. (11.2.23):

$$\frac{\partial b_e}{\partial t} = b_e\left(-\frac{\bar{w}}{2} - \frac{\mathrm{i}}{\hbar}\Delta E_e\right) \tag{11.3.10}$$

The rate of irreversible relaxation due to spontaneous emission is calculated from the Golden Rule:

$$\bar{w} = \frac{2\pi}{\hbar}|V_{g,1;e,0}|^2\,\rho\left(E_{eg} = E_j\right) \tag{11.3.11}$$

The calculation is the same as our calculation of the Einstein A coefficient in Section 9.4. Using the squared matrix element:

$$|V_{g,1;e,0}|^2 = \frac{|\mu_{eg}|^2}{6\varepsilon_0\hbar V}\hbar\omega_j \tag{11.3.12}$$

and the density of states of electromagnetic modes:

$$g\left(\omega\right) = V\omega^2/\pi^2c^3 \tag{11.3.13}$$

we obtain

$$\bar{w} = \frac{\omega^3\,|\mu_{eg}|^2}{3\pi\varepsilon_0\hbar c^3} = A_{eg} \tag{11.3.14}$$

The energy shift of the atom's excited state energy due to its interaction with the electromagnetic field is given by eq. (11.2.22).

This sum over continuum states can also be expressed as an integral over the photon density of states

$$\begin{aligned}\Delta E_e &= \mathbb{P}\int d\omega_j\,\rho\left(\omega_j\right)\frac{|V_{g,1;e,0}|^2}{\hbar\left(\omega_{ge}+\omega_j\right)}\\ &= \mathbb{P}\int d\omega\,\frac{\omega^3\,|\mu_{eg}|^2}{6\hbar\varepsilon_0c^3}\frac{1}{(\omega-\omega_{eg})}\end{aligned} \tag{11.3.15}$$

This integral isn't much use in this form since it diverges, and more advanced renormalization methods are required to evaluate the energy level shift. Nonetheless, it predicts a weak perturbation to atomic energy levels arising from the coupling of the electron to the electromagnetic field. Such a shift was observed in atomic hydrogen by Willis Lamb in 1947. Lamb's investigations were part of an effort to confirm the fine structure predicted by Dirac's relativistic model of atoms, which adds another layer of considerations to our non-relativistic treatment. Lamb's experiments became part of early studies into the interactions of electrons with the vacuum radiation field, which one now explains as arising from the electron's interactions with the vacuum fluctuations of the field. Lamb shared the 1955 Nobel Prize in Physics for his investigations into atomic spectra.(2)(3)

References

(1) Weisskopf, V.; Wigner, E. Berechnung der natürlichen Linienbreite auf Grund der Diracschen Lichttheorie. *Zeitschrift für Physik* **1930**, *63*, 54-73. DOI: 10.1007/BF01336768

(2) A nice description of the history of atomic spectroscopy, including the Lamb shift:

Hänsch, T. W.; Schawlow, A. L.; Series, G. W. The Spectrum of Atomic Hydrogen. *Scientific American* **1979**, *240* (3), 94-111. DOI: 10.1038/scientificamerican0379-94

(3) See also Lamb's Nobel Prize Lecture:

Lamb, W. E. *Fine Structure of the Hydrogen Atom*. Presented at Nobel Prize Awards 1955, Stockholm, December 12, 1955 (Nobel Prize in Physics lecture 1955). https://www.nobelprize.org/prizes/physics/1955/lamb/lecture/

This page titled 11.3: Spontaneous Emission is shared under a CC BY-NC-SA 4.0 license and was authored, remixed, and/or curated by Andrei Tokmakoff via source content that was edited to the style and standards of the LibreTexts platform.

11.4: Relaxation and Line-broadening

In our discussion of the classical absorption of light, we found that a mechanism of energy dissipation was required for the oscillator to reach a steady-state rate of energy absorption from the light field. In the absence of relaxation, which we added through a phenomenological damping constant, the energy of the oscillator would continue to rise indefinitely while the field is present. This relaxation process can be radiative, through the re-emission of light from the oscillator or through non-radiative channels.

Our quantum mechanical description of absorption in the context of perturbation theory avoided this difficulty by asserting that the calculated rate of absorption is small enough that we can neglect the actual changes of population in the ground and excited state. Unfortunately, in the process we discarded a physical property of all classical and quantum systems that has an important influence on light-matter interactions. Now, with a basic description of irreversible relaxation due to coupling to a continuum, we can build a model to describe the effect of relaxation on the quantum absorption lineshape.

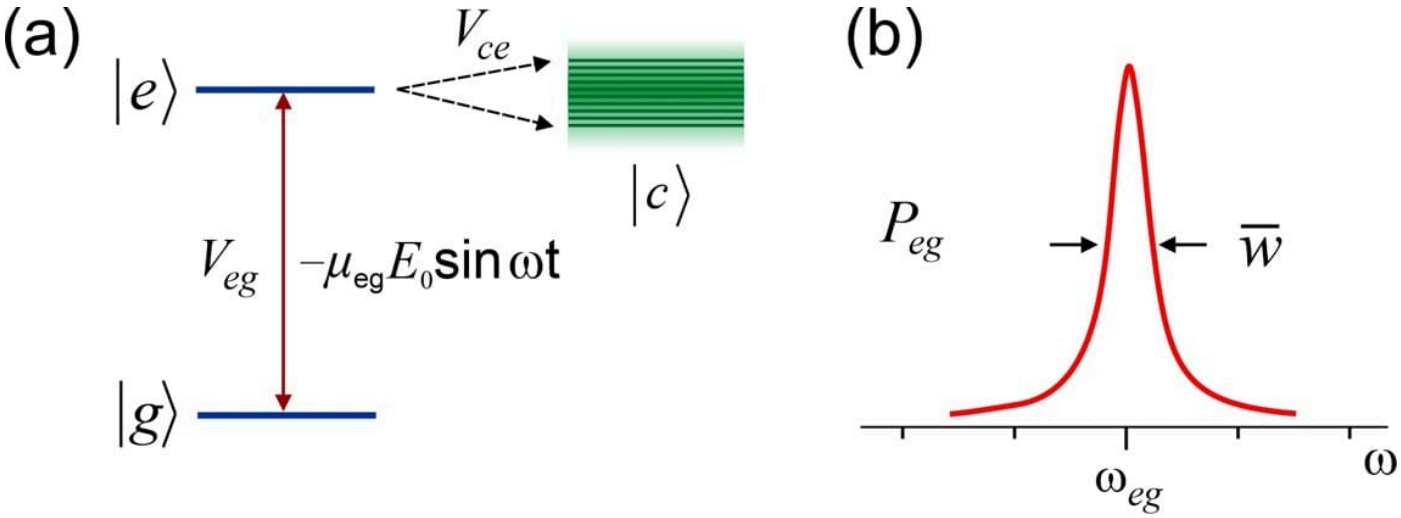


Figure 11.4.1: (a) Energy level diagram illustrating the initial and final states coupled by the oscillating electromagnetic field and the interaction of the final state $|k\rangle$ with the continuum of states $\{|n\rangle\}$. (b) The frequency-dependent probability distribution for steady state rates of absorption to the state k.

So, let's now describe the rate of absorption between a ground state $|g\rangle$ and excited state $|e\rangle$ for the case that $|e\rangle$ is coupled to a continuum of states $\{|c\rangle\}$, as illustrated in Figure 11.4.1a. It doesn't matter whether the continuum interacts with g or e; the results one obtains are the same. Our approach is to describe this with the first-order perturbation theory expressions for the probability amplitude of state e under the influence of a resonant field that couples g and e:

$$\frac{\partial}{\partial t} b_e = -\frac{\mathrm{i}}{\hbar} e^{\mathrm{i}\omega_{eg}t} V_{eg}(t) \tag{11.4.1}$$

The light-matter interaction potential is given by the transition dipole interaction with the electric field:

$$V_{eg}(t) = -\mu_{eg} E_0 \sin \omega t \tag{11.4.2}$$

To add irreversible relaxation to the description of b_e, we will draw on the irreversible relaxation model above. The expected influence of the continuum in eq. (11.2.23)—neglecting ΔE, the second-order correction to the energy of state e due to the interaction continuum—is given by

$$\frac{\partial b_e}{\partial t} = -\frac{1}{2} \bar{w} b_e \tag{11.4.3}$$

$\bar{w}$ is the Golden Rule rate of transitions from e to all continuum states, given by eq. (11.2.21):

$$\bar{w} = \frac{2\pi}{\hbar} |V_{ce}|^2 \rho(E_e) \tag{11.4.4}$$

V_{ce} is the constant coupling matrix element, describing the interaction of the excited state with a continuum state. Adding this additional relaxation term to equation for b_e, eq. (11.4.1) gives

$$\frac{\partial}{\partial t}\, b_e = -\frac{\mathrm{i}}{\hbar} e^{\mathrm{i}\omega_{eg}t} V_{eg}(t) - \frac{1}{2}\bar{w}\, b_e \tag{11.4.5}$$

Note that we now have imaginary and real terms on the right-hand side, so we expect solutions to this differential equation that are oscillatory and damped. Substituting eq. (11.4.2) into (11.4.5) and expressing $\sin \omega t$ in complex form, we obtain

$$\frac{\partial}{\partial t}\, b_e = \frac{\mu_{eg} E_0}{2\hbar} \left[e^{\mathrm{i}(\omega_{eg}+\omega)t} - e^{\mathrm{i}(\omega_{eg}-\omega)t} \right] - \frac{\bar{w}}{2} b_e(t) \tag{11.4.6}$$

The addition of a relaxation term results in a differential equation that has a steady state solution. The general solution for a differential equation of the form

$$\dot{y} + \alpha y = \beta\, e^{\mathrm{i}\gamma t} \tag{11.4.7}$$

is

$$y(t) = A e^{-\alpha t} + \frac{\beta\, e^{\mathrm{i}\gamma t}}{\alpha + \mathrm{i}\gamma} \tag{11.4.8}$$

where the first term is the transient solution, and the second term gives the steady-state behavior for $t \to \infty$. Focusing on the steady-state behavior, we find that the time-dependent change in b_e has the two expected terms which are related to absorption and simulation emission:

$$b_e(t) = \frac{\mu_{eg} E_0}{2\mathrm{i}\hbar} \left[\frac{e^{\mathrm{i}(\omega_{eg}-\omega)t}}{\bar{w}/2 + \mathrm{i}\,(\omega_{eg} - \omega)} - \frac{e^{\mathrm{i}(\omega_{eg}+\omega)t}}{\bar{w}/2 + \mathrm{i}\,(\omega_{eg} + \omega)} \right] \tag{11.4.9}$$

If we only focus only on the first absorption term, we can calculate the probability of absorption from the ground to the excited state for a given frequency of light:

$$P_{eg}(\omega) = |b_e|^2 = \frac{E_0^2 \left|\mu_{eg}\right|^2}{4\hbar^2} \frac{1}{\left(\omega_{eg} - \omega\right)^2 + \bar{w}^2/4} \tag{11.4.10}$$

The frequency dependence of the transition probability, shown in Figure 11.4.1b, is a Lorentzian lineshape peaked on resonance ($\omega_{eg} = \omega$) with a linewidth $\bar{w}$ (full width at half maximum, FWHM). Note that this expression indicates that it is possible for light to induce transitions from the ground to the excited state even when ω is not equal to ω_{eg}, as long as the detuning $(\omega_{k\ell} - \omega)$ is on the order of $\bar{w}_{nk}$. This is an important feature of light absorption similar to the classical model that is not captured by our quantum discussion of absorption in the context of the golden rule.

Although $P_{eg}(\omega)$ is not strictly an absorption spectrum, as we have previously calculated from the rate of energy uptake from the electric field, it is an effective proxy for one. Under the steady state conditions used here, the time-averaged rate of energy absorption from g to e is equal to the rate of energy dissipation from e into the continuum. Therefore $\hbar\omega P_{eg}(\omega)$ reflects the energy that being shifted from the ground to the excited state under steady-state conditions when irradiated with a monochromatic wave. What is important to take away from this it that the absorption lineshape is a fundamental property of the dynamics of the system—in this case energy, dissipation. As we will see going forward, other molecular factors also influence the linewidth; otherwise it would be possible to measure a linewidth and immediately know the energy dissipation rate for the states that are being driven by the electromagnetic wave. However, one can immediately say that the linewidth puts an upper bound on the rate of energy dissipation from those states.

This page titled 11.4: Relaxation and Line-broadening is shared under a CC BY-NC-SA 4.0 license and was authored, remixed, and/or curated by Andrei Tokmakoff via source content that was edited to the style and standards of the LibreTexts platform.

11.5: Readings

Coupling to a continuum

1. Cohen-Tannoudji, C.; Diu, B.; Laloë, F. *Quantum Mechanics*; Wiley, 1977; p 1344.
2. Merzbacher, E. *Quantum Mechanics*, 3rd ed.; Wiley, 1998; p 510.
3. Nitzan, A. *Chemical dynamics in condensed phases: Relaxation, transfer and reactions in condensed molecular systems*; Oxford University Press, 2006; p 305. DOI: 10.1093/oso/9780198529798.001.0001
4. Schatz, G. C.; Ratner, M. A. *Quantum Mechanics in Chemistry*; Dover Publications, 2002; ch 9.

This page titled 11.5: Readings is shared under a license and was authored, remixed, and/or curated by Andrei Tokmakoff.

12: QUANTUM STATISTICAL MECHANICS FOR CONDENSED MATTER

12.1: Concepts for Condensed Matter
12.2: Statistics of Ensembles
12.3: Equilibrium Systems
12.4: Mixed States
12.5: The Density Matrix
12.6: Time-Dependence of the Density Matrix
12.7: Readings

This page titled 12: Quantum Statistical Mechanics For Condensed Matter is shared under a CC BY-NC-SA 4.0 license and was authored, remixed, and/or curated by Andrei Tokmakoff via source content that was edited to the style and standards of the LibreTexts platform.

12.1: Concepts for Condensed Matter

We are now transitioning to the description of time-dependent quantum mechanics in condensed phases of matter. This will require a shift in how we think about and describe quantum systems. The main distinction is that the quantum system is no longer isolated. Whether we discuss hard materials, such as solids and nanomaterials, or soft matter, such as liquids and polymers, condensed matter is made of densely packed atomic or molecular constituents that have strong interactions, shaping the matter's physical properties. For instance, in semiconductors, covalent interactions give rise to the band structure, which reflects the delocalized states of valence electrons and phonons. Even with weaker interactions found in molecular condensed phases, wavefunctions can be extended in space over regions far larger than the fundamental building blocks. Furthermore, these delocalized states are highly dynamic. Phonons and collective liquid motions involve fluctuations on varying time and distance scales and can modify the state of any one molecule embedded in this medium in a time-dependent fashion. Whether we study the medium directly or a molecule embedded within it, the description of quantum states in condensed matter is strongly influenced by their dynamic medium.

To this point, our quantum description of molecular behavior has been precisely defined by a single wave-function—a *pure state*—that evolves deterministically according to the time-dependent Schrödinger equation. If we prepare an isolated molecule in a specific pure state, it will remain there indefinitely without external intervention, evolving in a perfectly predictable manner. We have been able to describe how one can use an external potential to prepare, interact with, and observe such an isolated quantum system, for instance in spectroscopy, which we calculate using matrix elements in an interaction potential.

In condensed matter, the eigenstates of the full Hamiltonian are *mixed state*s which reflect the environment's influence on the observed degrees of freedom of the system. The degrees of freedom within the environment are so many and so continuous that it isn't possible or even desirable to specify and analyze these mixed states. Furthermore, for ensembles of molecules, different molecules have different quantum states that reflect the details of their short-range molecular interactions. These circumstances have several consequences that require new concepts and methods, which we will outline and then work through in the following chapters.

In studying condensed matter, we typically want to describe and observe a small set of coordinates within surroundings that we cannot observe directly but which do influence the system of interest. These circumstances give rise to a common form of the Hamiltonian known as the *system-bath Hamiltonian*:

$$H = H_S + H_B + H_{SB} \tag{12.1.1}$$

This equation states that we will partition all degrees of freedom for the medium's particles such that we place a small number of directly observed coordinates into the *system*, H_S, and we put the vast number of remaining coordinates that we do not observe into the *bath*, H_B. Since the system is not isolated and exchanges energy and possibly matter with the bath, it is often referred to as an *open quantum system*. In condensed phases, the bath is typically a continuum of states that arises from the collective, delocalized states of the medium in which the system is embedded. The third term, H_{SB}, is the system-bath interaction that describes the influence of the bath on the system and vice versa. In particular, it will introduce a time-dependence to the observed system. Because it describes the interaction, H_{SB} will be a function of both system and bath coordinates. When we interact with and observe the system, we will be calculating matrix elements in system operators, and the bath's dynamic influence on the system is described by matrix elements in H_{SB}.

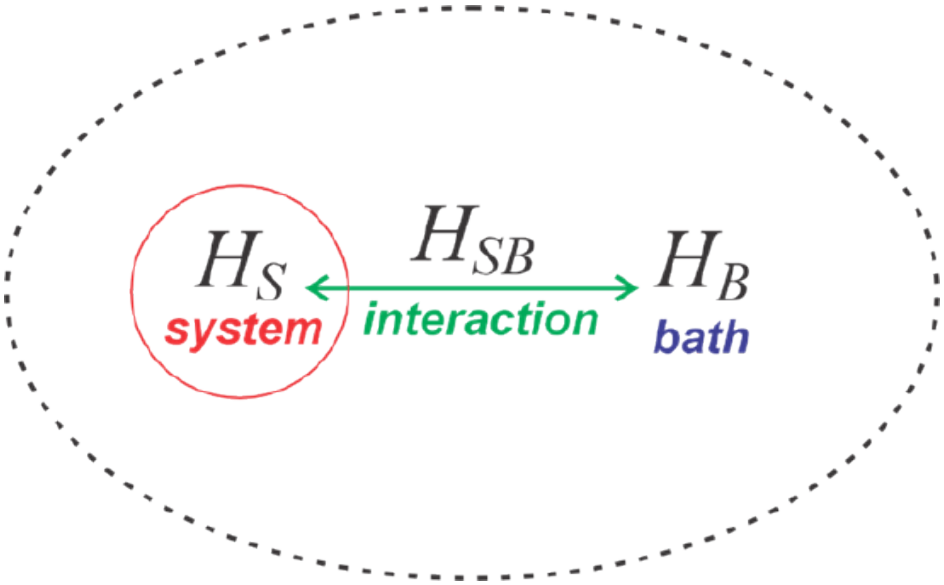


Figure 12.1.1

The term *bath*, drawn from thermodynamics, hints at some of the assumptions we make in using the system-bath Hamiltonian. First, we conceive of the bath as being a continuum of states so vast that the influence of the system on it is negligible. Equilibrium states in condensed matter are systems with kinetic energy, which is statistically distributed throughout intra- and intermolecular degrees of freedom. The ground state of an isolated quantum system is a pure, stationary state, whereas condensed matter is inherently dynamic and fluctuates due to its thermal energy. The different internal energies associated with different molecules in the condensed phase indicate that a statistical approach will be important to describing the state of an open quantum system, rather than a single wavefunction. As a result, the use of the system-bath Hamiltonian indicates an incorporation of statistical mechanics into our work, allowing the bath to be described only statistically—for instance through a density of states, a temperature, and a Boltzmann distribution.

The use of statistical mechanics also indicates that we will be dealing with ensembles of molecules in different quantum states, so we will need to perform averages over the expectation value of system operators. Thus, there are two levels of statistics one encounters in condensed phase quantum mechanics, often unstated and taken as understood. The first is the statistical interpretation of quantum mechanical probability densities and expectation values, which also applies to pure quantum states: one can only predict the distribution of likely outcomes for a series of measurements. The second is that different molecules within a sample exist in different mixed quantum states such that an expectation value also needs to be averaged over an ensemble. The impracticality of using mixed eigenstates for condensed phases along with the multiple layers of statistical averaging prompts the need for tools like the density matrix, which we take up in section 5 of this chapter.

The striking dynamical consequence of the intermolecular interactions in condensed matter is that quantum systems become irreversible and unpredictable. This is remarkable because the time-dependent Schrödinger equation is deterministic. Unitary time evolution allows us to describe the state of the system in the past or future with arbitrary accuracy, akin to classical systems evolving under Newton's equations of motion. In contrast, when a quantum system is in contact with another system that has many degrees of freedom, a definite direction emerges for time, i.e., "the arrow of time." A prepared molecular quantum state spontaneously and irreversibly loses energy to its environment, and the phase relationships that characterize quantum coherences change in ultimately unpredictable ways.

Irreversible behavior will be distinguished in two principal ways: fluctuations and dissipation. *Fluctuations* refer to unpredictable, random, or "stochastic" changes in the system's time-dependent properties. Although these may occur under any conditions, we will typically reserve the term "fluctuations" for spontaneous thermal fluctuations at equilibrium. Such fluctuations occur as a result of energy being spontaneously shifted between the system and the bath. Fluctuations occur on varying timescales, varying from slow enough they seem static to so fast that one can only observe average behavior. While *dephasing* often refers to the gradual phase randomization of synchronized oscillations among many identically prepared systems, it also describes the inherent unpredictability of a single system's phase fluctuating randomly over time. We will use the term *decoherence* to refer to the latter case when distinguishing it from general dephasing.

The second manifestation of irreversibility is *dissipation*, the process by which energy deposited into an observed system leaks irreversibly into the environment. We have already seen that a single quantum system coupled to a continuum can undergo

irreversible relaxation, and we have considered the importance of a broad continuum of states in generating exponential relaxation. This is a phenomenon that happens even in a molecular system in a vacuum, as illustrated by spontaneous emission from an isolated excited state coupled to the continuum of quantum electromagnetic modes. Going forward, we will describe analogous processes in which the continuum will arise from the condensed medium.

In our language the processes of fluctuation and dissipation are connected to equilibrium and nonequilibrium states, respectively. An *equilibrium* system is one in which the macroscopic properties are invariant with time; however, they are microscopically dynamic. Over a long enough time period, they naturally fluctuate through all the configurations available in the system. The term *nonequilibrium state*s refers to systems that have been acted on externally, moving them from equilibrium by changing the populations or energies of the quantum states available to the system. For nonequilibrium states, we will be interested in *relaxation* processes, which refer to the time-dependent processes involved in re-equilibrating the system. We will use "dissipation" to refer to the redistribution of energy as a nonequilibrium state returns toward a thermal distribution. However, we also use the term relaxation for other processes, such as the orientation randomization of an initially aligned system. In our later discussion of the fluctuation-dissipation theorem, we will discover the relationship between the equilibrium fluctuations of a system within a bath and the dissipation of energy from the system to the bath.

In spectroscopy, fluctuations and dissipation manifest distinctly in the experimental observables, making spectroscopy the most important tool to study condensed phase dynamics. As a result, we will closely tie our presentation of condensed phase quantum mechanics to the description of linear absorption spectroscopy. To analyze these phenomena, we rely on correlation functions, response functions, and linear response theory. Correlation functions describe the spontaneous fluctuations of systems at equilibrium that result from their interactions with the environment. Response functions describe how systems behave when external potentials push them out of equilibrium. Linear response theory describes the circumstances under which one can relate response functions to correlation functions. Together, correlation functions, response functions, and the density matrix form a set of interwoven tools that are essential for describing time-dependent quantum mechanics and spectroscopy of all kinds in condensed phases. These concepts will be developed over the following chapters, but first we will define additional foundational concepts and tools for condensed phase statistical mechanics.

This page titled 12.1: Concepts for Condensed Matter is shared under a CC BY-NC-SA 4.0 license and was authored, remixed, and/or curated by Andrei Tokmakoff via source content that was edited to the style and standards of the LibreTexts platform.

12.2: Statistics of Ensembles

With the need to describe ensembles, let's begin by reviewing the statistical description of a system. The variable A, which can be a classical dynamical variable or quantum expectation value, is observed to take on a distribution of different values. The basic statistical properties of this distribution can be described in terms of the mean and mean-square values of A, as determined from a large number of measurements:

$$\langle A \rangle = \frac{1}{N} \sum_{i=1}^{N} A_i \tag{12.2.1}$$

$$\langle A^2 \rangle = \frac{1}{N} \sum_{i=1}^{N} A_i^2 \tag{12.2.2}$$

Here, the summation over i refers to averaging over N independent measurements. In fact, this is how the expectation value of a quantum operator is defined—as the average value of A or A^2 obtained from many measurements on identically prepared pure states. For an ensemble, the states are drawn from a distribution of states. Alternatively, we can determine the same properties from:

$$\langle A \rangle = \sum_{j=1}^{M} P_j A_j \tag{12.2.3}$$

$$\langle A^2 \rangle = \sum_{j=1}^{M} P_j A_j^2 \tag{12.2.4}$$

Now the sum over j refers to a sum over the M possible values that A can take, weighted by P_j, the probability of observing a particular value A_j. Naturally, $\sum_j P_j = 1$. While the result of these discrete averages is the same regardless of the method we use, it can be practical to use one form over the other. For instance, in calculating ensemble averages, we typically specify the probability of occupying a particular state P_j. When we want to distinguish the methods, we will use $\bar{A}$ to refer to that average from a sum of repeated measurements and $\langle A \rangle$ to refer to an average over probability distributions.

When the accessible values come from a continuous distribution—as opposed to a discrete distribution—we now describe the internal variable with a distribution function, $P(A)$, which characterizes the probability of observing A between A and $A + dA$ with $\int P(A)\ dA = 1$. $P(A)$ is also known as the probability density since its units are A^{-1}. The statistics of A are now described in terms of the *moments* of the distribution function. The first and second moment are just the mean and mean-squared values of A

$$\langle A \rangle = \int dA\, AP(A) \tag{12.2.5}$$

$$\langle A^2 \rangle = \int dA\, A^2 P(A) \tag{12.2.6}$$

The breadth of the distribution function for A is captured in the variance of the distribution

$$\sigma^2 = \langle A^2 \rangle - \langle A \rangle^2 \tag{12.2.7}$$

σ is known as the standard deviation.

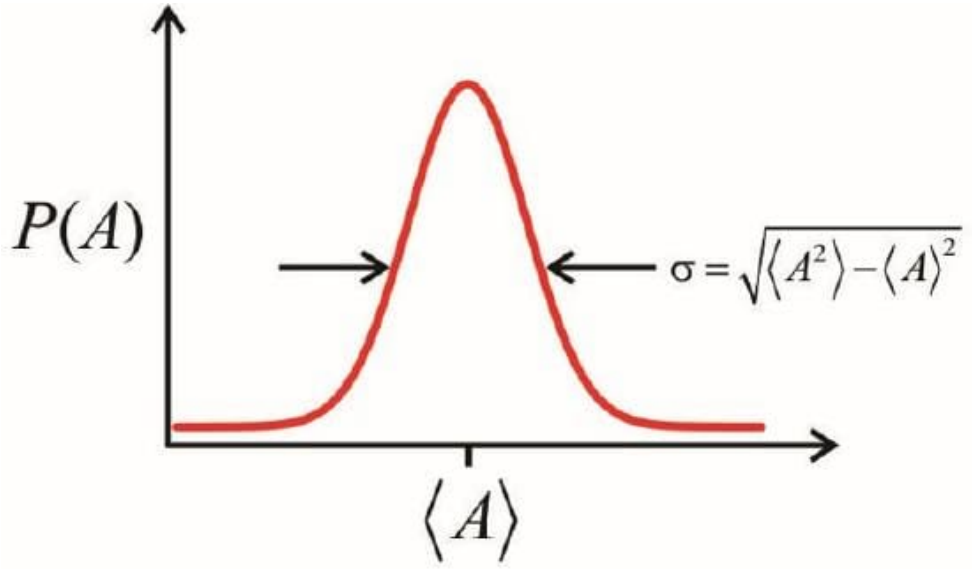


Figure 12.2.2: A simple normalized probability distribution function for the variable A is statistically described through its first and second moments, $\langle A\rangle$ and $\langle A^2\rangle$.

These concepts can be generalized to a time-dependent probability density to describe the dynamical properties of the system. This function, written either $P(A,t;A_0,t_0)$ or just $P(A,t)$, is a conditional probability for observing the particle between A and $A+dA$ at a time point t, given that it was initially at A_0 at an earlier time t_0. We obtain the global probability density, $P(A)$, by integrating $P(A,t)$ over time. For instance, the average and mean-square displacement of a particle at time t', given that it started at $x=0$ at $t=0$, are

$$\begin{aligned}\langle x(t')\rangle &= \int dx\, x(t')P(x,t')\\ \left\langle x^2(t')\right\rangle &= \int dx\, x^2(t')P(x,t')\end{aligned} \tag{12.2.8}$$

When discussing quantum systems, the key distinction between calculating statistical averages over classical probability distributions $P(x)$ and the quantum expectation values for pure states is that the quantum expectation value is the intrinsic uncertainty in a perfectly defined state, whereas the classical average is over the uncertainty in defining the state. When we deal with quantum statistical mechanics of mixed states, we need to be concerned about both types of these types of statistical descriptions. The first level is the inherent uncertainty in quantum mechanical observables. A fundamental postulate is that the expectation value of an operator $\langle\hat{A}\rangle = \langle\psi|\,\hat{A}\,|\psi\rangle$ is the mean value of A obtained over many observations on identically prepared systems $|\psi\rangle$. $\langle A\rangle$ represents the fundamental quantum uncertainty in a measurement of a precisely defined pure state with wave-like character. Given a basis set $|n\rangle$, we can calculate it as

$$\langle A\rangle = \langle\psi|\,\hat{A}\,|\psi\rangle = \sum_{m,n} c_n c_m^*\,\langle m|\,\hat{A}\,|n\rangle \tag{12.2.9}$$

where c_n describes the complex expansion coefficients. The second layer of statistical averaging is the uncertainty in defining the state of a system in an ensemble. A probability density P can be used to define possible outcomes of expectation value measurements on different initial systems $\left|\psi^{(j)}\right\rangle$:

$$\langle\langle A\rangle\rangle = \sum_j P_j \left\langle\psi^{(j)}\right|\hat{A}\left|\psi^{(j)}\right\rangle \tag{12.2.10}$$

Here the double bracket notation is written to emphasize the two layers of averaging, but we take this to be understood moving forward. In calculating averages over probability densities, it is more common to assume that a common basis set applies to all realizations of the wavefunction, and therefore one can apply the statistical averages to the expansion coefficients. Then eq. (12.2.10) is written

$$\langle A\rangle = \sum_{m,n} \langle c_n c_m^*\rangle\,\langle m|\,\hat{A}\,|n\rangle \tag{12.2.11}$$

where $\langle c_n c_m^* \rangle$ are the statistically averaged expansion coefficients, which we will see are the elements of a density matrix.

The statistical relationships above can be extended to two variables using a joint probability distribution, $P(A, B)$, which characterizes the probability of observing both A between A and $A + dA$ and B between B and $B + dB$. The statistical relationship between the variables can also be quantified by calculating moments of $P(A, B)$, either by summing or integrating over A and B. The most important measure is the correlation function

$$C_{AB} = \langle AB \rangle - \langle A \rangle \langle B \rangle \tag{12.2.12}$$

This is the *covariance*—the variance for a bivariate distribution—which measures the correlation between the variables A and B. That is, for a specific value of A, what are the associated statistics for B? To interpret this, it helps to define a correlation coefficient

$$r = \frac{C_{AB}}{\sigma_A \sigma_B} \tag{12.2.13}$$

where σ_A and σ_B are the standard deviations for the probability densities $P(A)$ and $P(B)$. The correlation coefficient r can take on values from $+1$ to -1. If $r = 1$ then there is perfect correlation between the two distributions. If the variables A and B depend on a common internal variable in the same way, then they are correlated. If no statistical relationship exists between the two distributions, then they are uncorrelated, $r = 0$, and $\langle AB \rangle = \langle A \rangle \langle B \rangle$. It is also possible that the distributions depend in an equal and opposite manner on an internal variable, in which case we call them anti-correlated with $r = -1$.

This page titled 12.2: Statistics of Ensembles is shared under a CC BY-NC-SA 4.0 license and was authored, remixed, and/or curated by Andrei Tokmakoff via source content that was edited to the style and standards of the LibreTexts platform.

12.3: Equilibrium Systems

The discussion above applies equally to the averages over equilibrium and non-equilibrium ensembles, but our most common statistical average will be over a quantum mechanical ensemble at thermal equilibrium. An equilibrium system is one in which the macroscopic properties (i.e., the intensive variables) are invariant with time. There are no steady state concentration or energy gradients (currents) in the system. Although they are macroscopically invariant, equilibrium states are microscopically dynamic. Over a long enough time period, they naturally explore all of the configurations available in the system.

In our discussion of averaging over molecular states in dilute solutions above, and comparing eq. (12.2.01) with eq. (12.2.03), we implied that the contribution from each molecule to the average is statistically equivalent, i.e. $P(A) = 1/N$. This applies to a microcanonical ensemble (N, V, E) in which any realization of a system at fixed energy is equally probable, and the statistical weight is the inverse of the number of microstates: $P = 1/\Omega$. In the case of a system in contact with a heat bath with fixed temperature T rather than energy, we seek to describe the probability of the system accessing a state n with energy E_n.

Classically, a system at equilibrium adopts a distribution of thermally accessible configurations, which we can describe as a canonical ensemble (N, V, T). The probability density of this ensemble can be specified through a temperature T and the Hamiltonian H. The canonical equilibrium probability density is a function of the full phase space coordinates $(\mathbf{q}, \mathbf{p})$:

$$P_{\text{eq}}(\mathbf{q}, \mathbf{p}) = \frac{e^{-\beta H(\mathbf{q},\mathbf{p})}}{Z} \tag{12.3.1}$$

where $\beta = (k_B T)^{-1}$, and Z is the partition function

$$Z = \int d\mathbf{p} \int d\mathbf{q}\, e^{-\beta H} \tag{12.3.2}$$

We can calculate the equilibrium ensemble average value of an internal variable A by averaging realizations of A over phase space:

$$\langle A \rangle = \int d\mathbf{p} \int d\mathbf{q}\, A\left(\mathbf{p}, \mathbf{q}\right) P_{\text{eq}}\left(\mathbf{p}, \mathbf{q}\right) \tag{12.3.3}$$

To obtain the probability density as a function of a subset of these coordinates, x, the probability distribution can be determined from

$$P_{\text{eq}}(x) = \frac{e^{-\beta H(x)}}{Z} \tag{12.3.4}$$

Now the assumption is that x and their conjugate momenta are separable from the remaining q and p, and the Hamiltonian $H(x)$ has been reduced by integration over the other degrees of freedom.

In the quantum mechanical case, we start by recognizing that building a quantum canonical ensemble implies that the Hamiltonian can be separated into many identical molecular subsystems that are in contact with a heat bath—for instance, non-interacting molecules in solution. If the eigenstates of the system Hamiltonian are $|n\rangle$ and the temperature of the bath is T, then the probability of occupying state $|n\rangle$ in the canonical ensemble is given by the expectation value of the equilibrium probability density, which is a Boltzmann weight:

$$P_n = \frac{1}{Z} \langle n | \, e^{-\beta \hat{H}} \, | n \rangle = \frac{e^{-\beta E_n}}{Z} \tag{12.3.5}$$

The partition function in this case comes from summing over the Boltzmann weights:

$$Z = \sum_n P_n \tag{12.3.6}$$

The ensemble-average quantum mechanical expectation value for the operator $\hat{A}$ is then obtained by the expectation values for states $|n\rangle$ weighted by their Boltzmann weight:

$$\langle A \rangle = \sum_n P_n \langle n | \hat{A} | n \rangle \tag{12.3.7}$$

P_n is the equilibrium population of state n.

Other notable examples of probability distribution functions are the Fermi-Dirac distribution function for indistinguishable fermions occupying a state of energy E:

$$Z = 1 + e^{-\beta(E-E_F)} \tag{12.3.8}$$

$$P(E) = \frac{1}{e^{\beta(E-E_F)} + 1} \tag{12.3.9}$$

where E_F is the Fermi energy (chemical potential). The Bose-Einstein probability for the probability of n indistinguishable bosons of energy E_1 occupying the same state

$$Z = \left(1 - e^{-\beta E_1}\right)^{-1} \tag{12.3.10}$$

$$P(E_n) = e^{-\beta E_n}\left(1 - e^{-\beta E_1}\right) \tag{12.3.11}$$

with energy $E_n = nE_1$. Ensemble averages are again computed with eq. (12.3.7).

This page titled 12.3: Equilibrium Systems is shared under a CC BY-NC-SA 4.0 license and was authored, remixed, and/or curated by Andrei Tokmakoff via source content that was edited to the style and standards of the LibreTexts platform.

12.4: Mixed States

Let's look a bit further into the origin of mixed states and their intrinsically statistical nature. To this point we have discussed the time-dependent quantum mechanical properties of *pure states*, which are characterized by a single wavefunction derived from a Hamiltonian that specifies all particles and fields in the system of interest. In condensed phases, molecules interact with one another, and as a result no two molecules have the same state. We cannot write down an exact Hamiltonian for these problems because we cannot (and actually do not want to) specify the states of all degrees of freedom. It is more practical to concentrate our attention on one, or a few, degrees of freedom that are directly observed in a measurement and describe the influence of the surroundings on the observed degrees of freedom in a statistical manner. These observations lead to the concept of *mixed states* and statistical mixtures. A mixed state refers to any case in which we don't have complete information on the observed system of interest and must instead describe its properties and behavior statistically. The most common example is a system at thermal equilibrium, but it applies to any large set of independently prepared states that have no phase relationship with each other.

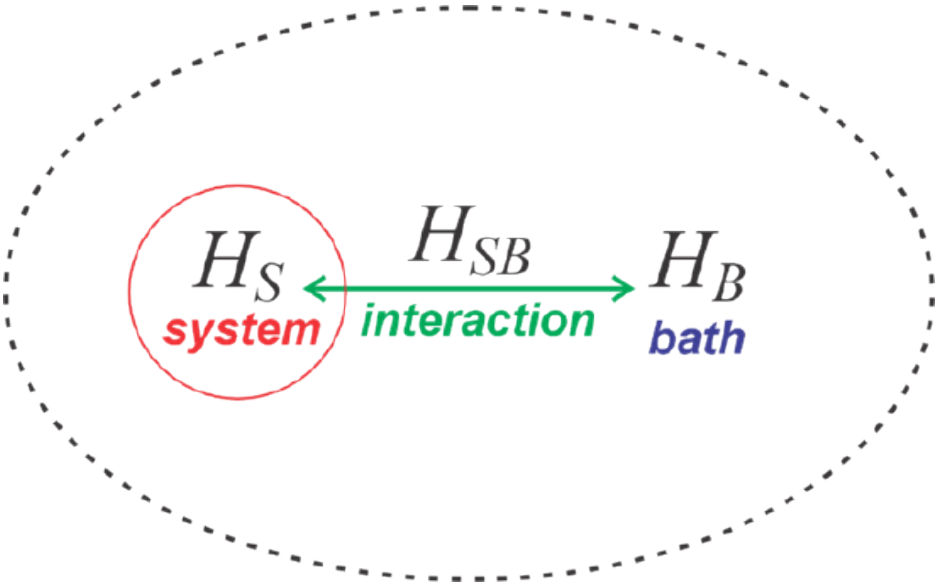


Figure 12.4.1

How does a system get into a mixed state? Generally, if you have two systems and you put these in contact with each other, the interaction between the two will lead to a new joint system that is inseparable. Consider two systems described by H_S and H_B. The eigenstates of H_S are $|n\rangle$ and those of H_B are $|\alpha\rangle$. Before these systems interact, the Hamiltonian is

$$H_0 = H_S + H_B \tag{12.4.1}$$

and the state of the joint system $|\psi_0\rangle$ can be described as an expansion in product states of $|n\rangle$ and $|\alpha\rangle$.

$$|\psi_0\rangle = |\psi_S^0\rangle\,|\psi_B^0\rangle \tag{12.4.2}$$

$$|\psi_S^0\rangle = \sum_n s_n\,|n\rangle \qquad |\psi_B^0\rangle = \sum_\alpha b_\alpha\,|\alpha\rangle \tag{12.4.3}$$

$$|\psi_0\rangle = \sum_{n,\alpha} s_n b_\alpha\,|n\alpha\rangle \tag{12.4.4}$$

where s and b are expansion coefficients. After these states are allowed to interact, we have a new state $|\psi(t)\rangle$. The new mixed state can still be expressed in the zero-order basis, although this does not represent the eigenstates of the new Hamiltonian with the interaction H_{SB}:

$$H = H_0 + H_{SB} \tag{12.4.5}$$

$$|\psi(t)\rangle = \sum_{n,\alpha} c_{n,\alpha}\,|n\alpha\rangle \tag{12.4.6}$$

For any point in time, $c_{n,\alpha}$ is the complex amplitude for the basis state $|n\alpha\rangle$. The coefficient $c_{n,\alpha}$ encodes $P_{n,\alpha} = |c_{n,\alpha}|^2$, the joint probability for finding particle of $|\psi_S\rangle$ in state $|n\rangle$ and simultaneously finding particle of $|\psi_B\rangle$ in state $|\alpha\rangle$. Generally speaking, any time after bringing the systems in contact $c_{n,\alpha} \neq s_n b_\alpha$.

In the case of experimental observables, we are typically able to observe or manipulate one H_S, the "system", and are blind to the other H_B, the "bath". In condensed phases, the bath has vastly more degrees of freedom and is treated as a continuum. The key property of a mixed state or statistical mixture is that we don't precisely know the state of the bath. For instance, in an equilibrium system, all we can do is specify the probability that the system occupies a state $|n\rangle$, averaged over all possible states of the bath:

$$P_n = \sum\nolimits_\alpha |c_{n,\alpha}|^2 = \overline{|c_n|^2} \tag{12.4.7}$$

Here averaging over the bath removes the pureness of the state since we have lost information on the states of the bath. We refer to P_n as the *population* of state n.

Now let's look at how this emerges by describing ensembles. Imagine a dilute room temperature solution of molecules within a weakly interacting solvent, or equivalently. The key observation here is that the solute molecules can be treated as being completely independent entities that have no interactions with each other—only with the liquid. As a result, no quantum mechanical phase relationship exists between solute molecules. In isolation, each solute molecule has the same molecular Hamiltonian H_{mol} and eigenfunctions

$$H_{\text{mol}} |n\rangle = E_n |n\rangle \tag{12.4.8}$$

As a result of their interaction with the solvent, the unique state of molecule i within the solution will be described by the wavefunction $|\psi^{(i)}\rangle$, which we will expand in this isolated molecule eigenbasis. This is reasonable for weak solute-solvent interactions, but generally one wants to ensure that the isolated system Hilbert space provides a complete basis for describing the system once you put it in the condensed phase. Once in the liquid, the details of the amplitudes of the eigenstates at any moment will differ from one molecule to the next depending on the time-dependent local environment.

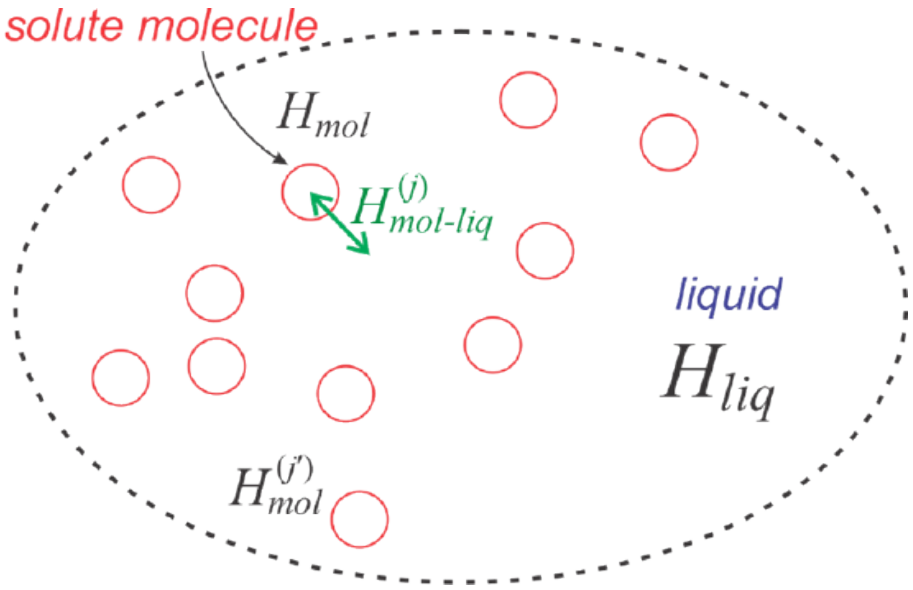


Figure 12.4.2

To describe the solution, we introduce a Hamiltonian for the pure liquid H_{liq} into which we wrap all of the solvent degrees of freedom and which we have only minimal statistical information about. Finally, there is a solute-solvent interaction Hamiltonian $H^{(i)}_{\text{mol–liq}}$ which describes how these interactions influence the state of a specific solute molecule indexed j. Thus, the Hamiltonian for any individual molecule is

$$H^{(i)} = H_{\text{mol}} + H_{\text{liq}} + H^{(i)}_{\text{mol–liq}} \tag{12.4.9}$$

To build a statistical description of the system, we don't need to treat each molecule separately, only describe the variety of possible molecular interactions with the liquid. If we average eq. (12.4.9) over all molecules, we can obtain the Hamiltonian:

$$\begin{aligned} H &= \frac{1}{N}\sum_{j=1}^{N} H^{(i)} \\ &= H_{\text{mol}} + H_{\text{liq}} + \bar{H}_{\text{mol–liq}} \end{aligned} \tag{12.4.10}$$

where $\bar{H}_{\text{mol–liq}}$ describes the average influence of the liquid on the solute. This Hamiltonian takes the form of the system-bath Hamiltonian in eq. (12.1.1), in which a molecular solute's interactions with its surroundings are treated in a statistical manner.

We now turn our attention to the expectation values that we would measure in an experiment. First, we recognize that for the individual molecule i, the expectation value for an operator would be expressed as

$$\langle A\rangle^{(i)} = \left\langle \psi^{(i)} \right| \hat{A} \left| \psi^{(i)} \right\rangle \tag{12.4.11}$$

In the case of the ensemble, we would also average the expectation value over the N molecules.

$$\langle A\rangle = \frac{1}{N}\sum_{i=1}^{N} \langle A\rangle^{(i)} \tag{12.4.12}$$

Equivalently, this could be expressed as an average over the probability that a molecule is described by wavefunction $\left|\psi^{(j)}\right\rangle$

$$\langle A\rangle = \sum_{j=1}^{M} P_j \left\langle \psi^{(j)} \right| \hat{A} \left| \psi^{(j)} \right\rangle = \sum_{j=1}^{M} P_j \langle A\rangle^{(j)} \tag{12.4.13}$$

Since the isolated molecular eigenstates (n) and the liquid (α) states form a complete basis set, the pure state of molecule i can be expressed as an expansion in this basis:

$$\left|\psi^{(i)}\right\rangle = \sum_{a,\alpha} c_{a,\alpha}^{(i)} \left|n\alpha\right\rangle \tag{12.4.14}$$

Expanding eq. (12.4.12) with the use of eqs. (12.4.11) and (12.4.14) gives us the expectation value

$$\langle A\rangle = \frac{1}{N}\sum_{i=1}^{N}\sum_{n,m}\sum_{\alpha,\beta} c_{m,\beta}^{(i)} \left(c_{n,\alpha}^{(i)}\right)^{*} \langle n\alpha| \hat{A} \left|m\beta\right\rangle \tag{12.4.15}$$

This is an excruciating combination of sums over molecules, system eigenstates, and bath states, which reflects the daunting pure-state representation of the expectation value. However, for a mixed state we will average over the possible configurations of the bath and their influence on the different molecules. This results in an average of the product of complex system eigenfunction amplitudes for the system states:

$$\langle c_m c_n^*\rangle = \frac{1}{N}\sum_{i=1}^{N}\sum_{\alpha,\beta} c_{m,\beta}^{(i)} \left(c_{n,\alpha}^{(i)}\right)^{*} \tag{12.4.16}$$

We also take the operator $\hat{A}$ to only be a function of the system coordinates, so that $\langle n\alpha| \hat{A} \left|m\beta\right\rangle = \langle n| \hat{A} \left|m\right\rangle$. Then the expectation value for the mixed state ensemble is

$$\langle A\rangle = \sum_{n,m} \langle c_m c_n^*\rangle \langle n| \hat{A} \left|m\right\rangle \tag{12.4.17}$$

The quantity $\langle c_n c_m^*\rangle$ specifies the mixed state of the system. We retain information on the average state of solute molecules while losing precise information about the liquid environment. We will associate $\langle c_n c_m^*\rangle$ with the matrix elements of the density matrix or density operator ρ that we describe in the following section:

$$\rho_{mn} = \langle c_m c_n^*\rangle \tag{12.4.18}$$

Substituting this definition into eq. (12.4.17), we find that the expectation value becomes

$$\begin{aligned}\langle A\rangle &= \sum_{n,m}\rho_{mn}A_{nm}\\ &= \sum_{m}\langle m|\,\rho A\,|m\rangle\\ &= Tr\left[\rho A\right]\end{aligned} \tag{12.4.19}$$

where the trace $\mathrm{Tr}\left(\cdots\right)=\sum_m\langle m|\cdots|m\rangle$ refers to summing over the diagonal elements of a matrix.

It may not be obvious how eq. (12.4.17) relates to the expected expression for an ensemble-averaged expectation value in eq. (12.3.07)

$$\langle A\rangle = \sum_{n} P_n\,\langle n|\,\hat{A}\,|n\rangle \tag{12.4.20}$$

The difference is that eq. (12.4.17) applies to all systems, including non-equilibrium ones. Remember, in an equilibrium system we are dealing with a statistical mixture in which no coherences or phase relationships between members of the ensemble are present. The lack of coherence is the property that allows the equilibrium ensemble average of $\langle c_n c_m^*\rangle$ to be equated with the thermal population p_n. To evaluate this average, we recognize that these are complex numbers and that the equilibrium ensemble average of the expansion coefficients is equivalent to phase averaging over the expansion coefficients. Since at equilibrium all phases are equally probable,

$$\langle c_n c_m^*\rangle_{\mathrm{eq}} = \frac{1}{2\pi}\int_0^{2\pi} c_n c_m^*\,d\phi = \frac{1}{2\pi}\,|c_n|\,|c_m|\int_0^{2\pi} e^{-\mathrm{i}\phi_{nm}}\,d\phi_{nm} = |c_n|\,|c_m|\,\delta(\phi_n-\phi_m) \tag{12.4.21}$$

where $c_n=|c_n|\,e^{\mathrm{i}\phi_n}$ and $\phi_{nm}=\phi_n-\phi_m$. The integral is quite clearly zero unless $\phi_n=\phi_m$, giving an equilibrium average consistent with eq. (12.3.05):

$$\langle c_n c_m^*\rangle_{\mathrm{eq}} = |c_n|^2 = P_n = \frac{e^{-\beta E_n}}{Z} \tag{12.4.22}$$

This page titled 12.4: Mixed States is shared under a CC BY-NC-SA 4.0 license and was authored, remixed, and/or curated by Andrei Tokmakoff via source content that was edited to the style and standards of the LibreTexts platform.

12.5: The Density Matrix

In the previous section, we learned that the density matrix can encode the state of a quantum ensemble for which we have only an average description of how the environment influences the ensemble's properties. We are now prepared to use those insights to define the density matrix and investigate its properties and use.

The density matrix or density operator is an alternative to the wavefunction for representing the state of a quantum system. The name "density matrix" derives from its quantum role as a probability distribution function $P(A)$. For pure states, the density matrix and wavefunctions are functionally equivalent, but one gains significant practical advantages using the density matrix for describing mixed states and certain time-dependent problems—particularly irreversible relaxation and nonlinear spectroscopy in the condensed phase.

To start our discussion, let's consider pure states. The density matrix is defined as the outer product of the wavefunction and its Hermitian conjugate.

$$\rho \equiv |\psi\rangle \langle\psi| \tag{12.5.1}$$

Thus, if you specify a possible state of a particle $|\phi\rangle$, the expectation value $\langle\phi|\rho|\phi\rangle = |c_\phi|^2$ gives the probability of finding the particle in state $|\phi\rangle$. If the wavefunction for the system is expanded in the basis $|n\rangle$

$$|\psi\rangle = \sum_n c_n |n\rangle \tag{12.5.2}$$

the density matrix is given by

$$\begin{aligned} \rho &= \sum_{n,m} c_n c_m^* |n\rangle \langle m| \\ &\equiv \sum_{n,m} \rho_{nm} |n\rangle \langle m| \end{aligned} \tag{12.5.3}$$

where the density matrix elements are $\rho_{nm} = c_n c_m^*$. The diagonal density matrix elements $(n = m)$ describe the probability of occupying a particular state, since $\rho_{nn} = c_n c_n^* = P_n$. Off-diagonal elements $(n \neq m)$ are complex and will be used to describe coherent superposition states. Note that the density matrix is not specific to a particular basis set and can be transformed between basis sets with the unitary transformations that we apply to other operators.

Expectation values for an operator A are obtained by taking a trace of the product of A and ρ. This can be seen by substituting eq. (12.5.2) into $\langle A\rangle = \langle\psi| A |\psi\rangle$ to give

$$\begin{aligned} \langle A\rangle &= \sum_{n,m} \rho_{nm} A_{mn} \\ &= \mathrm{Tr}\left[\rho A\right] \end{aligned} \tag{12.5.4}$$

The trace function refers to summing over the diagonal elements of the matrix, $\mathrm{Tr}[\cdots] = \sum_m \langle m| \cdots |m\rangle$. Note that $\mathrm{Tr}\left[A\rho\right] = \mathrm{Tr}\left[\rho A\right]$. Since probabilities must be normalized, $\mathrm{Tr}\left(\rho\right) = 1$.

For mixed states, the density matrix is again defined as an outer product, but eq. (12.5.1) must be statistically averaged over different possible realizations of the wavefunction:

$$\rho \equiv \sum_j P_j \left|\psi^{(j)}\right\rangle \left\langle\psi^{(j)}\right| \tag{12.5.5}$$

This definition presupposes that we have defined a statistical mixture of independent systems in the state $\left|\psi^{(j)}\right\rangle$.(1) Again we choose to expand the wavefunction using eq. (12.5.2), with the knowledge that the $|n\rangle$ basis is complete

$$\begin{aligned} \rho &= \sum_{n,m} \langle c_n c_m^*\rangle |n\rangle \langle m| \\ &\equiv \sum_{n,m} \rho_{nm} |n\rangle \langle m| \end{aligned} \tag{12.5.6}$$

Now the density matrix elements are assigned to the statistically averaged product of expansion coefficients:

$$\rho_{nm} = \langle c_n c_m^* \rangle = \sum_j P_j c_n^{(j)} c_m^{*(j)} \tag{12.5.7}$$

The expectation value of an operator for the mixed state is given by:

$$\langle A \rangle = \sum_j P_j \left\langle \psi^{(j)} \right| \hat{A} \left| \psi^{(j)} \right\rangle \tag{12.5.8}$$

When expanded, we find that the expectation values are calculated in the same way as pure states:

$$\begin{aligned} \langle A \rangle &= \sum_{n,m} \langle c_n c_m^* \rangle A_{mn} \\ &= \mathrm{Tr}\left[\hat{\rho}\hat{A}\right] \end{aligned} \tag{12.5.9}$$

By comparing this equation to the classical determination of the mean value of A in eq. (12.2.3), we can see how the density matrix functions as a quantum probability distribution function $P(A)$.

As we discussed in the last section, the mixed-state density matrix naturally emerges from the system-bath Hamiltonian by statistically averaging the system-bath interactions H_{SB} over the states of the bath. Let's investigate how this occurs. Using the separation of system (a) and bath (α) degrees of freedom, the expectation value of an operator A can be expressed with the product states $|a\alpha\rangle$ as

$$\begin{aligned} \langle A \rangle &= \langle \psi | A | \psi \rangle \\ &= \sum_{\substack{a,\alpha \\ b,\beta}} c_{b,\beta} c_{a,\alpha}^* \langle a\alpha | A | b\beta \rangle \end{aligned} \tag{12.5.10}$$

We consider the operator A to only be a function of the system coordinates. This is typical of experimental measurements, for instance performing spectroscopy of the system through interaction of the dipole operator. Then we can average the expectation value of A over the bath degrees of freedom. Equation (12.5.10) becomes

$$\begin{aligned} \langle A \rangle &= \sum_{\substack{a,\alpha \\ b,\beta}} c_{b,\beta} c_{a,\alpha}^* \langle a | A | b \rangle \delta_{\alpha,\beta} \\ &= \sum_{a,b} \left(\sum_\alpha c_{b,\alpha} c_{a,\alpha}^* \right) A_{ab} \\ &= \sum_{a,b} \langle c_b c_a^* \rangle A_{ab} \end{aligned} \tag{12.5.11}$$

Here the bath-average of the product of system expansion coefficients takes the same form as eq. (12.5.7):

$$\langle c_b c_a^* \rangle = \sum_\alpha c_{b,\alpha} c_{a,\alpha}^* \Leftrightarrow \sum_j P_j c_n^{(j)} c_m^{*(j)} \tag{12.5.12}$$

Hence these two ways of interpreting mixed states, (1) an average over the configurations of an invisible bath versus (2) a probabilistic description of possible states of the system, are equivalent.

Using the formalism of the system-bath Hamiltonian has the added benefit of separating out the observed system states and operators from the bath coordinates that we are blind to. We can use eq. (12.5.11) to define a density matrix for the system degrees of freedom ρ_S (also called the reduced density matrix, σ) where the density matrix elements are given by eq. (12.5.12):

$$(\rho_S)_{b,a} = \langle c_b c_a^* \rangle \tag{12.5.13}$$

The system density matrix (or reduced density matrix) is obtained from the density matrix for the full Hamiltonian, $\rho_{b\beta,a\alpha}$, by performing a partial trace over the bath degrees of freedom:

$$\begin{aligned} (\rho_s)_{b,a} &= \sum_{\alpha,\beta} \langle b\beta | \rho | a\alpha \rangle \delta_{\alpha,\beta} \\ \rho_s &\equiv \mathrm{Tr}_B(\rho) \end{aligned} \tag{12.5.14}$$

Here $\mathrm{Tr}_B(\ldots) = \sum_\alpha \langle\alpha|\ldots|\alpha\rangle$. The expectation value of the system operators is then calculated from ρ_S in the same way as before:

$$\begin{aligned}\langle A\rangle &\equiv \sum_{a,b} (\rho_S)_{ba} A_{ab} \\ &= \mathrm{Tr}\left[\rho_S A\right]\end{aligned} \tag{12.5.15}$$

Generally speaking, the term density matrix is used interchangeably for either the reduced or complete density matrix unless the distinction is relevant to the discussion. Distinguishing the reduced density matrix plays an important role in the study of irreversible relaxation processes, in which energy flows from the system to the bath (Chapter 11). Although we cast this discussion in terms of the system-bath Hamiltonian, the strategies we outlined are generally applicable when one wants to separate a Hamiltonian into sub-systems and focus on one subsystem while averaging over the influence of the others.

Equilibrium Density Matrix

For a statistical mixture at thermal equilibrium, the equilibrium density matrix for the canonical ensemble is defined in the same manner as the classical probability density:

$$\rho_{\mathrm{eq}} = \frac{e^{-\beta H}}{Z} \tag{12.5.16}$$

As before, Z is the partition function and $\beta = (k_B T)^{-1}$. We can obtain an equilibrium expectation value of A by averaging over the thermal occupation of quantum states using

$$\langle A\rangle = \mathrm{Tr}\left(\rho_{\mathrm{eq}} A\right) \tag{12.5.17}$$

In the eigenbasis $\{|n\rangle\}$, with $\hat{H}|n\rangle = E_n|n\rangle$, ρ_{eq} is a diagonal matrix characterized by Boltzmann weighted populations in the quantum states:

$$\left(\rho_{\mathrm{eq}}\right)_{nm} = \frac{1}{Z}\langle n| e^{-\beta\hat{H}} |m\rangle = \frac{e^{-\beta E_n}}{Z}\delta_{nm} = p_n \delta_{nm} \tag{12.5.18}$$

$$\rho_{nn} = \frac{e^{-\beta E_n}}{Z} \tag{12.5.19}$$

Note also that

$$Z = \mathrm{Tr}\left(e^{-\beta\hat{H}}\right) = \sum_n e^{-\beta E_n} \tag{12.5.20}$$

Properties of the density matrix

These properties follow from the definitions above:

1. ρ is Hermitian since $\rho^*_{nm} = \rho_{mn}$
2. $\mathrm{Tr}(\rho) = 1$, since probability must be normalized.
3. We can ascertain the degree of a quantum state's "purity" from

$$\mathrm{Tr}\left(\rho^2\right)\begin{cases} = 1 & \text{for pure states} \\ < 1 & \text{for mixed states}\end{cases} \tag{12.5.21}$$

In addition, when working with the density matrix, it is convenient to make note of these trace properties:

1. The trace over a product of matrices is invariant to cyclic permutation of the matrices:

$$\mathrm{Tr}(ABC) = \mathrm{Tr}(CAB) = \mathrm{Tr}(BCA) \tag{12.5.22}$$

2. From this result, we see that the trace is invariant to unitary transformation:

$$\mathrm{Tr}\left(S^\dagger A S\right) = \mathrm{Tr}\left(S^{-1} A S\right) = Tr(A) \tag{12.5.23}$$

3. If the density matrix is expressed in product states, the full trace can also be calculated by tracing individually over each subspace: and multiplying the results

$$\mathrm{Tr}\,(A \times B) = Tr(A)Tr(B) \tag{12.5.24}$$

References

(1) This definition encompasses pure states; for instance, if we want to specify a single wavefunction $\psi^{(j')}$: $P_j = \delta_{j,j'}$.

This page titled 12.5: The Density Matrix is shared under a CC BY-NC-SA 4.0 license and was authored, remixed, and/or curated by Andrei Tokmakoff via source content that was edited to the style and standards of the LibreTexts platform.

12.6: Time-Dependence of the Density Matrix

Just as the wavefunction is a dynamic entity, the density matrix is also time-dependent, with dynamical properties that mirror those we derived for wavefunctions. We recognize that, generally, the Schrödinger wavefunction expansion coefficients c_n in the expressions earlier in this chapter are time-dependent. For the case of a time-independent Hamiltonian, the expansion coefficients in the eigenbasis are

$$c_n(t) = c_n(0) \exp\left[-\mathrm{i}E_n t/\hbar\right] \tag{12.6.1}$$

and the time-dependence of the density matrix elements for a pure state can be expressed as

$$\rho_{nm}(t) = c_n(t)c_m^*(t) = c_n c_m^* \exp[-\mathrm{i}\omega_{nm}t] \tag{12.6.2}$$

As before, the energy splitting between eigenstates is

$$\omega_{nm} = \frac{E_n - E_m}{\hbar} \tag{12.6.3}$$

One can see that the diagonal elements of ρ are time-invariant and the off-diagonal matrix elements oscillate at an angular frequency ω_{nm}.

For the time-dependent Hamiltonian, we can derive an equation of motion for the density matrix in a straightforward manner: by time-differentiating our original definition of the density matrix $\rho = |\psi\rangle\langle\psi|$ and substituting the time-dependent Schrödinger equation

$$\begin{aligned}\frac{\partial \rho}{\partial t} &= \frac{\partial}{\partial t}\left[|\psi\rangle\langle\psi|\right] \\ &= \left[\frac{\partial}{\partial t}|\psi\rangle\right]\langle\psi| + |\psi\rangle\frac{\partial}{\partial t}\langle\psi| \\ &= -\frac{\mathrm{i}}{\hbar}H|\psi\rangle\langle\psi| + \frac{\mathrm{i}}{\hbar}|\psi\rangle\langle\psi|H\end{aligned} \tag{12.6.4}$$

Thus, the density matrix evolves according to

$$\frac{\partial \rho}{\partial t} = -\frac{\mathrm{i}}{\hbar}[H, \rho] \tag{12.6.5}$$

Equation (12.6.5) is the Liouville-Von Neumann equation, which we observe is isomorphic to the Heisenberg equation of motion. Using the mixed state definition of the density matrix, one can show that eq. (12.6.5) also applies to mixed states.

As one would expect from the definition of the density matrix $\rho = |\psi\rangle\langle\psi|$, the solution to (12.6.5) is

$$\rho(t) = U\rho_0 U^\dagger \tag{12.6.6}$$

where ρ_0 represents the state of the system at t_0, and U is the time-evolution operator

$$U = \exp_+\left[-\frac{\mathrm{i}}{\hbar}\int_0^t d\tau\, H(\tau)\right] \tag{12.6.7}$$

One can interpret the density matrix in eq. (12.6.6) in terms of the outer product of a wavefunction with its Hermitian conjugate, except that each of these wavefunctions have been individually propagated forward in time. U is used to propagate the *ket* wavefunction and $U^\dagger$ to propagate the *bra* wavefunction. However, in the density matrix representation, the pair of time-propagators represent the application of a unitary transformation to the operator ρ that moves it forward in time.

Taken together, eq. (12.6.6) and the cyclic invariance of the trace imply that the time-dependent expectation value of an operator can be calculated either by propagating the density matrix in time, similar to the Schrödinger picture, or by propagating the operator in time, as expected for the Heisenberg picture:

$$\begin{aligned}\left\langle \hat{A}(t) \right\rangle &= \mathrm{Tr}\left[\hat{A}\rho(t)\right] \\ &= \mathrm{Tr}\left[\hat{A}U\rho_0 U^\dagger\right] = \mathrm{Tr}\left[U^\dagger \hat{A} U \rho_0\right] \\ &= \mathrm{Tr}\left[\hat{A}(t)\rho_0\right]\end{aligned} \tag{12.6.8}$$

Example: Time dependence of a two-level system

We can revisit the time dependence of a two-level system using the density matrix representation for a mixed state. We will calculate the time-dependence of the population of the two states after applying a constant coupling potential to a system. We start with two states a and b at thermal equilibrium. The Hamiltonian is

$$H_0 = \begin{pmatrix} E_a & 0 \\ 0 & E_b \end{pmatrix} \tag{12.6.9}$$

The initial state of the density matrix is diagonal with the equilibrium populations in the two states given by Boltzmann weights, $p_n = e^{-\beta E_n}/Z$,

$$\rho_0 = \begin{pmatrix} p_a & 0 \\ 0 & p_b \end{pmatrix} \tag{12.6.10}$$

As expected for a normalized wavefunction, $\mathrm{Tr}\,(\rho_0) = p_a + p_b = 1$.

At time $t = 0$, a constant potential coupling the two states is applied to the system and the total Hamiltonian for $t \geq 0$ is

$$H = H_0 + V = \begin{pmatrix} E_a & 0 \\ 0 & E_b \end{pmatrix} + \begin{pmatrix} 0 & V_{ab} \\ V_{ba} & 0 \end{pmatrix} = \begin{pmatrix} E_a & V_{ab} \\ V_{ba} & E_b \end{pmatrix} \tag{12.6.11}$$

We can calculate the time-evolution of the system from eq. (12.6.6) using the time-propagator $e^{-\mathrm{i}Ht/\hbar}$. However, a matrix exponential is evaluated far more easily in the eigenbasis, where it takes on a diagonal form.

To diagonalize the Hamiltonian, we previously rewrote it in terms of the mixing angle θ, defined by $\tan 2\theta = |V_{ab}|/\Delta$ where $\Delta = (E_a - E_b)/2$. Then

$$H = E\,\mathbf{I} + \Delta \begin{pmatrix} 1 & \tan 2\theta \\ \tan 2\theta & -1 \end{pmatrix} \tag{12.6.12}$$

and $E = (E_a + E_b)/2$. The transformation that diagonalizes the Hamiltonian and its inverse are

$$S = \begin{pmatrix} \cos\theta & -\sin\theta \\ \sin\theta & \cos\theta \end{pmatrix} \qquad S^{-1} = \begin{pmatrix} \cos\theta & \sin\theta \\ -\sin\theta & \cos\theta \end{pmatrix} \tag{12.6.13}$$

$$\tilde{H} = SHS^{-1} = \begin{pmatrix} \epsilon_+ & 0 \\ 0 & \epsilon_- \end{pmatrix} \tag{12.6.14}$$

The resulting eigenvalues for the two eigenstates $|\pm\rangle$ are $\varepsilon_\pm = E \pm \Delta \sec 2\theta$. Note that a tilde is being used to indicate a matrix in the eigenbasis. In the eigenbasis, the time propagator is diagonal:

$$\tilde{U} = \begin{pmatrix} \exp[-\mathrm{i}\varepsilon_+ t/\hbar] & 0 \\ 0 & \exp[-\mathrm{i}\varepsilon_- t/\hbar] \end{pmatrix} \tag{12.6.15}$$

We also apply the transformation to the initial density matrix:

$$\tilde{\rho}_0 = S\rho_0 S^{-1} = \begin{pmatrix} p_a - \delta p\,\cos^2\theta & -\frac{1}{2}\,\delta p\,\sin 2\theta \\ -\frac{1}{2}\,\delta p\,\sin 2\theta & p_b + \delta p\,\cos^2\theta \end{pmatrix} \tag{12.6.16}$$

where $\delta p = p_a - p_b$ is the initial population difference between the states. Then we can propagate the system forward in time in the eigenbasis:

$$\tilde{\rho}(t) = \tilde{U}\tilde{\rho}_0\tilde{U}^\dagger = \begin{pmatrix} p_a - \delta p\, \cos^2\theta & -\frac{1}{2}\,\delta p\, \sin 2\theta e^{-\mathrm{i}\Omega t} \\ -\frac{1}{2}\,\delta p\, \sin 2\theta e^{\mathrm{i}\Omega t} & p_b + \delta p\, \cos^2\theta \end{pmatrix} \tag{12.6.17}$$

Here the time evolution is governed by the frequency $\Omega = (\epsilon_+ - \epsilon_-)/2\hbar = \sqrt{\Delta^2 + V^2}$. We can see that, in this eigenbasis, the populations of the eigenstates (diagonal elements) are time-independent—as expected for stationary states. However, we are interested in the time-dependence of the populations of the initial zero-order states. To understand those, we transform back into the zero-order basis:

$$\rho\,(t) = S^{-1}\tilde{\rho}\,(t)\,S \tag{12.6.18}$$

To understand how the population in the a and b states evolve with time, we look at the diagonal elements, which we can express in terms of either the mixing angle or our original variables:

$$\begin{aligned} \rho_{aa}(t) &= p_a - \delta p \sin^2 2\theta \sin^2 \Omega t \\ &= p_a - \delta p \frac{V^2}{V^2 + \Delta^2} \sin^2 \Omega t \end{aligned} \tag{12.6.19}$$

$$\begin{aligned} \rho_{bb}(t) &= p_b + \delta p \sin^2 2\theta \sin^2 \Omega t \\ &= p_b + \delta p \frac{V^2}{V^2 + \Delta^2} \sin^2 \Omega t \end{aligned} \tag{12.6.20}$$

We observe that the populations of the a and b states start at their initial values and then shift in a sinusoidal fashion from the initially most populated state to the least populated state with a sinusoidal time-dependence whose time-scale and magnitude depends on the mixing angle, i.e. the coupling strength. The time-dependence is similar to what we calculated for the pure states, but because we have a mixed state that has a probability of initially occupying state a or b, the coupling shifts population both upward and downward in energy. Note that the trace over the density matrix remains constant with time: $\mathrm{Tr}\,(\rho(t)) = \rho_{aa}(t) + \rho_{bb}(t) = p_a + p_b = 1$

Density Matrix in the Interaction Picture

Similarly to wavefunctions, we can also formulate the density operator in the interaction picture for problems in which the Hamiltonian can be expressed in terms of $H = H_0 + V(t)$—the system of interest H_0 under the influence of an external potential $V(t)$. This proves useful for perturbation theory applications, and it is commonly used in spectroscopy. The interaction picture density operator is defined as the outer product of interaction picture wavefunctions:

$$\rho_I = |\psi_I\rangle\,\langle\psi_I| \tag{12.6.21}$$

Using our original transformation between the Schrödinger and interaction picture wavefunctions

$$|\psi_I(t)\rangle = U_0^\dagger\,|\psi_S(t)\rangle = U_I\,|\psi_0\rangle \tag{12.6.22}$$

We obtain the transformation between the Schrödinger and interaction pictures as $\rho_I(t) = U_0^\dagger \rho_S(t) U_0$ where $U_0 = e^{-\mathrm{i}H_0 t/\hbar}$. The time evolution of the density matrix then is

$$\rho_I(t) = U_I^\dagger \rho_0 U_I \tag{12.6.23}$$

where $\rho_0 = |\psi_0\rangle\,\langle\psi_0|$ and the interaction picture time propagator is

$$U_I(t) = \exp_+\left[-\frac{\mathrm{i}}{\hbar}\int_0^t d\tau\, V_I(\tau)\right] \tag{12.6.24}$$

and, as before, $V_I = U_0^\dagger V U_0$. Note, in the interaction picture the expectation value of an operator is given by:

$$\langle A\rangle = \mathrm{Tr}\,[\rho_I A_I] \tag{12.6.25}$$

and the equation of motion for ρ_I is

$$\frac{\partial \rho_I}{\partial t} = -\frac{\mathrm{i}}{\hbar}\,[V_I, \rho_I] \tag{12.6.26}$$

The formal solution to equation (12.6.26) is obtained by integrating in time from t_0 to t to obtain

$$\rho_I(t) = \rho_I(t_0) - \frac{\mathrm{i}}{\hbar}\int_{t_0}^{t} dt' \left[V_I(t'), \rho_I(t')\right] \tag{12.6.27}$$

As we found in our discussion of the time-propagator earlier, this exact solution is not particularly useful, since $\rho_I(t)$ is expressed as a function of itself inside the integral $\rho_I(t')$. However, this form lends itself well to a series expansion that is useful for perturbation theory. Repeated substitution of $\rho_I(t)$ in eq. (12.6.27) into itself on the right hand side gives the perturbation series expansion

$$\begin{aligned}\rho_I(t) = \rho_0 &- \frac{\mathrm{i}}{\hbar}\int_{t_0}^{t} dt_1 \left[V_I(t_1), \rho_0\right] \\ &+ \left(-\frac{\mathrm{i}}{\hbar}\right)^2 \int_{t_0}^{t} dt_2 \int_{t_0}^{t_2} dt_1 \left[V_I(t_2), \left[V_I(t_1), \rho_0\right]\right] + \cdots \\ &+ \left(-\frac{\mathrm{i}}{\hbar}\right)^n \int_{t_0}^{t} dt_n \int_{t_0}^{t_n} dt_{n-1} \ldots \int_{t_0}^{t_2} dt_1 \left[V_I(t_n), \left[V_I(t_{n-1}), \left[\ldots, \left[V_I(t_1), \rho_0\right] \ldots\right]\right]\right] \\ &+ \cdots\end{aligned} \tag{12.6.28}$$

$$\rho_I(t) = \rho^{(0)} + \rho^{(1)} + \rho^{(2)} + \cdots + \rho^{(n)} + \cdots \tag{12.6.29}$$

This expression, known as a Magnus expansion, writes the density matrix as a sum of contributions, where each term is labeled as $\rho^{(n)}$, the n^{th}-order expansion of the density matrix. This perturbative expansion will play an important role later in the description of nonlinear spectroscopy. An n^{th} order expansion term will be proportional to the observed polarization in an n^{th} order nonlinear spectroscopy, and the commutators observed in eq. (12.6.28) are closely related to nonlinear response functions.

This page titled 12.6: Time-Dependence of the Density Matrix is shared under a CC BY-NC-SA 4.0 license and was authored, remixed, and/or curated by Andrei Tokmakoff via source content that was edited to the style and standards of the LibreTexts platform.

12.7: Readings

The Density Matrix

1. Blum, K. *Density Matrix Theory and Applications*; Plenum Press, 1981.
2. Mukamel, S. *Principles of Nonlinear Optical Spectroscopy*; Oxford University Press, 1995.

This page titled 12.7: Readings is shared under a license and was authored, remixed, and/or curated by Andrei Tokmakoff.

13: CORRELATION FUNCTIONS

13.1: Classical Time-Correlation Functions
13.2: Examples of Classical Time-Correlation Functions
13.3: Calculating the Correlation Function from a Discrete Trajectory
13.4: Quantum Time-Correlation Functions
13.5: Transition Rates from Time Correlation Functions
13.6: Appendix- Weiner-Khinchin Theorem and the Power Spectrum
13.7: Readings

This page titled 13: Correlation Functions is shared under a CC BY-NC-SA 4.0 license and was authored, remixed, and/or curated by Andrei Tokmakoff via source content that was edited to the style and standards of the LibreTexts platform.

13.1: Classical Time-Correlation Functions

Time-correlation functions are an effective and intuitive way of representing the dynamics of a system, and they are one of the most common tools of time-dependent quantum mechanics. They are applicable to any time-dependent process but are most commonly used to describe fluctuations and other irreversible processes in condensed phases. We can and will use them to describe the deterministic oscillatory behavior of pure-quantum states; however, our work is motivated by finding a general tool that will help us deal with the inherent thermal motions of molecular systems at equilibrium. These correlation functions provide a statistical description of the time evolution of an internal variable within an ensemble. We will use them extensively in the description of spectroscopy, relaxation phenomena, and the loss of state memory in a fluctuating environment.

Specifically, we are interested in characterizing the microscopic fluctuations of a molecular variable embedded in an actively evolving environment. Although macroscopic properties of equilibrium systems do not change, they are dynamic, with molecules constantly exploring the range of configurations that are thermally accessible to them. For chemical problems in the condensed phase, we constantly encounter the problem of fluctuations in dynamical variables arising from their interactions with the environment. Figure 13.1.1 illustrates a trajectory for the time-dependent fluctuations in the value of a molecular variable A about an average value $\langle A \rangle$ for one member of an equilibrium ensemble. The time-evolution is unpredictable, but over a long enough period of time, we can determine that the observed values of A are sampled from a distribution function $P(A)$. Such a system, in which the time-dependence is unpredictable but the statistics over long periods of time remain unchanged is known as stationary. The noisy nature of the fluctuations in $A(t)$ seems to leave little information about molecular dynamics, but looking over shorter periods of time, it is clear that there is a distinct trajectory—a time-sequence of events—as $A(t)$ evolves. It takes finite periods of time to sample values of A. The dynamics are somewhat but not entirely random since they are a consequence of the time-dependent interactions of a molecule with its environment.

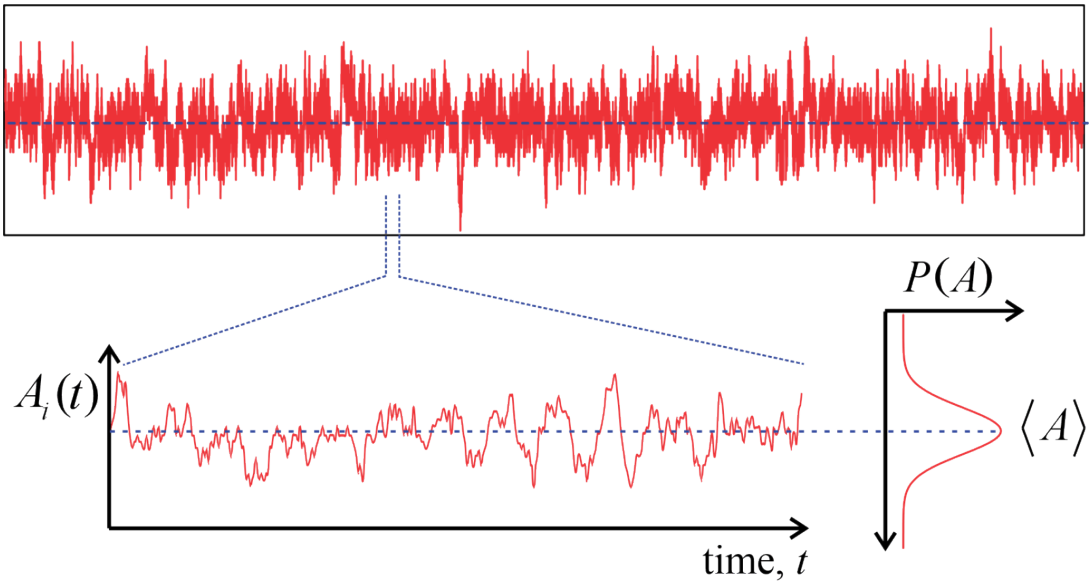


Figure 13.1.1: Illustration of a trajectory of time dependent observations of the value of the molecular variable A for one member of an ensemble at thermal equilibrium.

Correlation functions provide a way of characterizing the spontaneous and unpredictable character of a system's time-evolution and thereby describing the molecular behavior that underlies these fluctuations. We can provide a statistical description of the characteristic time scales and amplitudes to these changes by comparing the value of A at time t with the value of A at a later time, t'. With that in mind, we define a time-correlation function (TCF) as a time-dependent quantity, $A(t)$, multiplied by that quantity at some later time, $A(t')$, and average these observations over an equilibrium ensemble:

$$C_{AA}(t,t') \equiv \langle A(t)\, A(t') \rangle_{\text{eq}} \tag{13.1.1}$$

Why this form? Note that the variance of A is used to characterize the distribution in the values of A that are allowed in a system, but if we calculate the mean square value of A at two different time-points rather than the same point, we introduce a microscopic time-variable to average over.

The classical form of the correlation function is evaluated using an integral over phase space:

$$C_{AA}(t,t') = \int d\mathbf{p} \int d\mathbf{q}\, A(\mathbf{p},\mathbf{q};t) A(\mathbf{p},\mathbf{q};t')\, P_{\text{eq}}(\mathbf{p},\mathbf{q}) \tag{13.1.2}$$

where P_{eq} is the equilibrium probability density. The quantum correlation function can be evaluated by performing a thermal average over the expectation value of the product of operators, using wavefunctions or the density matrix:

$$\begin{aligned} C_{AA}(t,t') &= \sum_n P_n \langle n| A(t)A(t') |n\rangle \\ &= Tr\left[\rho_{\text{eq}} A(t) A(t')\right] \end{aligned} \tag{13.1.3}$$

Here $P_n = e^{-\beta E_n}/Z$ and ρ_{eq} is the equilibrium density matrix. Equations (13.1.2) and (13.1.3) are auto-correlation functions, which correlate the same variable at two points in time, but one can also define a *cross-correlation* function that describes the correlation of two different variables in time

$$C_{AB}(t,t') \equiv \langle A(t) B(t')\rangle \tag{13.1.4}$$

So, what does a time-correlation function tell us? Qualitatively, a TCF describes how long a given property of a system persists until it is averaged out by microscopic motions and interactions with its surroundings. It describes how and when a statistical relationship has vanished. We can use correlation functions to describe various time-dependent chemical processes. For instance, we will use $\langle \mu(t)\mu(0)\rangle$—the dynamics of the molecular dipole moment—to describe absorption spectroscopy. We will also use them for relaxation processes induced by the interaction of a system and bath: $\langle H_{SB}(t) H_{SB}(0)\rangle$. Classically, you can use TCFs to characterize transport processes. For instance, a diffusion coefficient is related to the velocity correlation function for the diffusing particle: $\mathscr{D} = \frac{1}{3}\int_0^\infty dt\ \langle v(t)v(0)\rangle$.

Properties of Correlation Functions

There are several properties of correlation functions for random fluctuations in the variable A at thermal equilibrium that can be deduced from the definitions above.

1. When evaluated at $t = t'$, we obtain the mean square value of A, which is also the maximum amplitude. This is positive for an autocorrelation function and independent of time.

$$C_{AA}(t,t) = \langle A(t)\, A(t)\rangle = \left\langle A^2\right\rangle \geqslant 0 \tag{13.1.5}$$

2. For long time separations between observations ($t - t' \to \infty$), thermal fluctuations act to randomize the system, and the two values of A become uncorrelated. Thus, the correlation function in this limit is just the mean value of A squared:

$$\lim_{t'\to\infty} C_{AA}(t,t') = \langle A(t)\rangle \langle A(t')\rangle = \langle A\rangle^2 \tag{13.1.6}$$

3. Since correlation functions characterize equilibrium systems whose statistical properties are stationary, these functions are also stationary. That means they do not depend on the absolute point of observation (t and t'), but rather the time interval between observations ($\tau = t - t'$). A stationary random process means that the reference point can be shifted by an arbitrary value T without changing the properties of the ensemble:

$$C_{AA}(t,t') = C_{AA}(t+T, t'+T) \tag{13.1.7}$$

So, by choosing $T = -t'$, we see that the TCF is only a function of one variable, τ:

$$C_{AA}(t,t') = C_{AA}(t-t',0) = C_{AA}(\tau) \tag{13.1.8}$$

Although the time-dependent form of $C_{AA}(\tau)$ can vary, the properties defined so far are illustrated by the example in Figure 13.1.2.

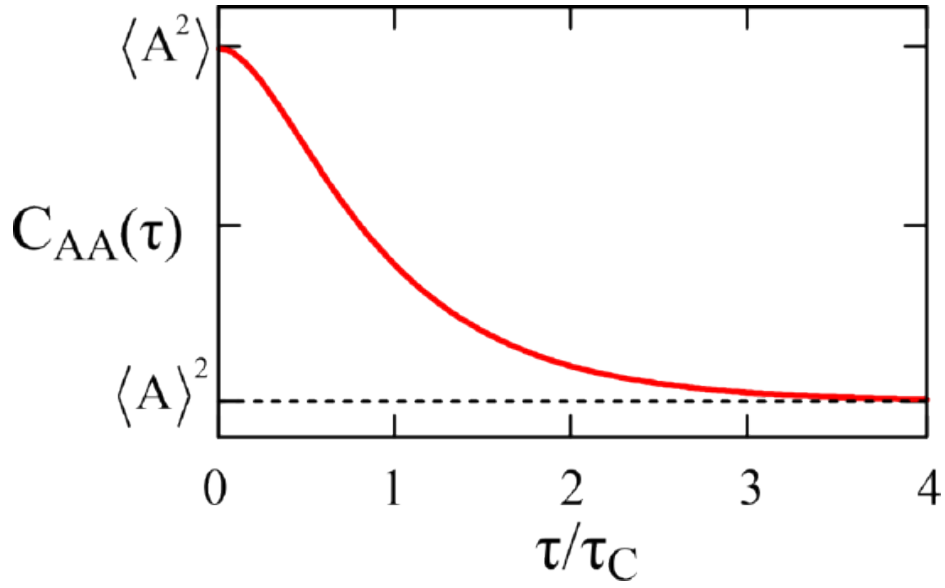


Figure 13.1.2: A hypothetical time-autocorrelation function for a molecular variable A.

Implicit in this statement is an understanding that we take the time-average value of A to be equivalent to the equilibrium ensemble average value of A, i.e., the system is ergodic (see box below). So, the correlation of fluctuations can be expressed as either a time-average over the trajectory of one molecule

$$\overline{A(\tau)A(0)} = \lim_{T\to\infty} \frac{1}{T} \int_0^T dt\, A\,(t+\tau)\, A(t) \tag{13.1.9}$$

or an equilibrium ensemble average

$$\langle A(\tau)A(0)\rangle = \sum_n \frac{e^{-\beta E_n}}{Z}\, \langle n|\, A(\tau)A(0)\,|n\rangle \tag{13.1.10}$$

The time-averaging in eq. (13.1.9) is the calculation that is used in analyzing trajectories and which averages over the noisy dynamics to reveal the statistically relevant correlations in time-dependent behavior of $A(t)$.

4. Classical correlation functions are real and even in time:

$$\begin{aligned} \langle A(t)\, A(t')\rangle &= \langle A(t')A(t)\rangle \\ C_{AA}(\tau) &= C_{AA}(-\tau) \end{aligned} \tag{13.1.11}$$

5. When we observe fluctuations in A about an average $\langle A\rangle$, we often redefine the correlation function in terms of the deviation from average

$$\delta A \equiv A - \langle A\rangle \tag{13.1.12}$$

Then the TCF becomes:

$$C_{\delta A\delta A}(\tau) = \langle \delta A(\tau)\delta A(0)\rangle = C_{AA}(\tau) - \langle A\rangle^2 \tag{13.1.13}$$

The result of subtracting $\langle A\rangle^2$ is that the long-time limit $\lim_{\tau\to\infty}\ C_{\delta A\delta A}(\tau) = 0$ when correlation is lost, and the zero time value is just the variance in A

$$C_{\delta A\delta A}(0) = \left\langle \delta A^2\right\rangle = \left\langle A^2\right\rangle - \langle A\rangle^2 \tag{13.1.14}$$

6. The decay of the correlation function to zero quantifies the time scale for the loss of memory of the initial value of A . The characteristic time scale for this relaxation is the correlation time, τ_c. There are many possible forms to *correlation functions*, and several time scales may exist, but if the correlation has a simple monotonic decay, one can calculate τ_c by integrating the TCF:

$$\tau_c = \frac{1}{\langle \delta A^2 \rangle} \int_0^\infty dt \, \langle \delta A(t) \delta A(0) \rangle \tag{13.1.15}$$

You can confirm that this works by using an exponential form: $C(t) = C(0) \exp(-t/\tau_c)$.

Definition: Ergodic Systems

As illustrated in Figure 13.1.1, over a long enough time period we expect that one molecule in a homogeneous medium will be able to sample all available configurations of the system with a probability given by the probability density function $P(A)$. That is, a normalized histogram of all observations of A gives $P(A)$. Such a system is referred to as *ergodic*. Specifically, in an ergodic system, it is possible to statistically describe the properties of the internal variable A by either (1) averaging over all values of A sampled by a member of the ensemble over a long period, or (2) averaging over the realizations of A for the entire ensemble at one point in time. That is, the statistics for A can be expressed as a time-average or an ensemble average. For an equilibrium system, the ensemble average value of A can be computed from

$$\langle A \rangle = \sum_n \frac{e^{-\beta E_n}}{Z} \langle n | A | n \rangle \tag{13.1.16}$$

and the time average, designated with a bar rather than brackets, can be computed from

$$\bar{A} = \lim_{T \to \infty} \frac{1}{T} \int_0^T dt \, A_i(t) \tag{13.1.17}$$

These quantities are equal for an ergodic system: $\langle A \rangle = \bar{A}$.

Equilibrium systems are ergodic, and non-ergodic systems are not at equilibrium. Examples of non-ergodic systems whose macroscopic properties do not change with time include kinetically trapped systems, where molecules don't have enough thermal energy to equilibrate as observed in glasses and polymers, and open systems under steady-state conditions that are maintained by a constant flux of energy or matter between the system and surroundings. From eq. (13.1.17), we see that the term ergodic also carries a dynamical connotation. A system is ergodic if one member of the ensemble has evolved long enough to sample the equilibrium probability distribution. Experimental observations on one particle for shorter time scales are measurements on a nonequilibrium system, since they effectively measure the system with a bias toward the sampled states.

This page titled 13.1: Classical Time-Correlation Functions is shared under a CC BY-NC-SA 4.0 license and was authored, remixed, and/or curated by Andrei Tokmakoff via source content that was edited to the style and standards of the LibreTexts platform.

13.2: Examples of Classical Time-Correlation Functions

Example 1: Velocity autocorrelation function for gas

Consider a dilute gas of molecules which have a Maxwell–Boltzmann distribution of velocities. We focus on the component of the molecular velocity along the $\hat{x}$ direction, v_x. We know that the average velocity is $\langle v_x \rangle = 0$. The velocity correlation function is

$$C_{v_x v_x}(\tau) = \langle v_x(\tau) v_x(0) \rangle \tag{13.2.1}$$

From the equipartition principle, we know the average translational kinetic energy is $\frac{1}{2} m \langle v_x^2 \rangle = k_B T/2$, so the zero-time value of the correlation function is

$$C_{v_x v_x}(0) = \langle v_x^2(0) \rangle = \frac{k_B T}{m} \tag{13.2.2}$$

For time scales that are short compared to collisions between molecules (Figure 13.2.1a), the velocity of any given molecule remains constant and unchanged, so the correlation function for the velocity is also unchanged, remaining at $k_B T/m$. This non-interacting regime corresponds to the behavior of an ideal gas.

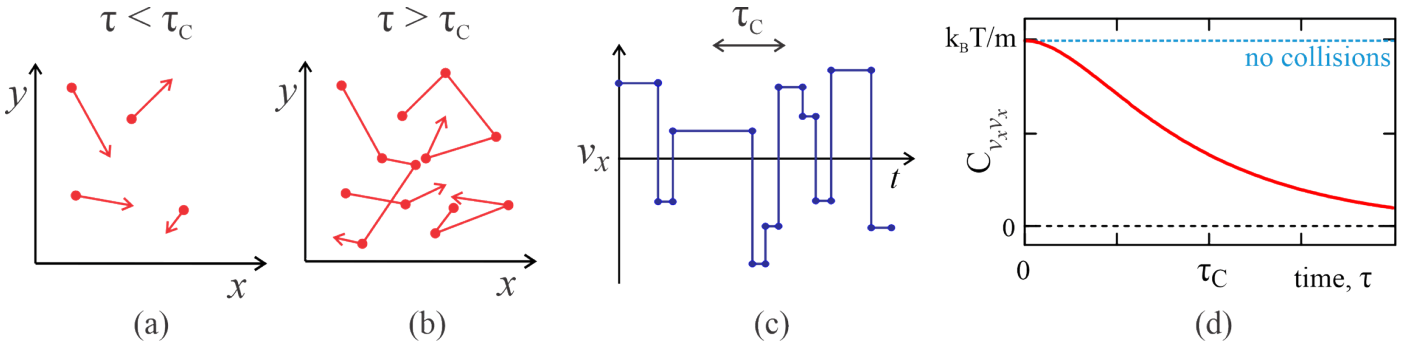


Figure 13.2.1: Molecular velocities in a gas. For a short period of time, the velocities of individual molecules are unchanged (a), but for times greater than the mean time between collisions the velocities are randomized (b). (c) Trajectory of velocities sampled by a single molecule through a series of collisions, with the approximate scale of the correlation time. (d) The corresponding velocity autocorrelation function, indicating that it would not decay without collisions.

For any real gas, there will be collisions that randomize the direction and speed of the molecules (Figure 13.2.1b), so that any molecule over a long enough time will sample the various velocities within the Maxwell–Boltzmann distribution. From the trajectory of x velocities for a given molecule (Figure 13.2.1c) we can calculate $C_{v_x v_x}(\tau)$ using a time-averaging approach. The correlation function will drop with a correlation time τ_c, which is related to mean time between collisions. After multiple collisions, the correlation with the initial velocity is lost and $C_{v_x v_x}(\tau)$ approaches $\langle v_x \rangle^2 = 0$. Finally, we can determine the diffusion constant for the gas, which relates the time and mean square displacement of the molecules: $\langle x^2(t) \rangle = 2\mathscr{D}_x t$. If we assume that the correlation function drops exponentially with a correlation time τ_c, we can use the Kubo formula to find the diffusion constant in the x dimension:

$$\mathscr{D}_x = \int_0^\infty dt \, \langle v_x(t) v_x(0) \rangle = \frac{k_B T \tau_c}{m} \tag{13.2.3}$$

For independent diffusion in x, y, and z dimensions, the diffusion constant in 3D is $\mathscr{D}_{3D} = \frac{1}{3}(\mathscr{D}_x + \mathscr{D}_x + \mathscr{D}_x)$. In viscous fluids τ_c/m is called the mobility, μ.

Example 2: Dipole rotational correlation function

Consider the classical correlation function for the rotating dipole moment of a polar diatomic molecule in a dilute gas. If we consider this a rigid rotating object, we can decompose the dipole $\boldsymbol{\mu}$ into a constant magnitude and a direction unit vector: $\boldsymbol{\mu} = \mu_0 \cdot \hat{u}$. Since these variables are separable, the correlation function is also separable into terms for the magnitude and orientation.

$$\begin{aligned} C_{\mu\mu}(t) &= \langle \boldsymbol{\mu}(t)\, \boldsymbol{\mu}(0) \rangle \\ &= \langle \mu_0^2 \rangle \, \langle \hat{u}(t) \cdot \hat{u}(0) \rangle \\ &= \langle \mu_0^2 \rangle \, \langle \cos\theta(t) \rangle \end{aligned} \tag{13.2.4}$$

This correlation function projects the time-dependent orientation of the dipole onto its original direction, and it therefore depends on the cosine of the angle of rotation $\theta(t)$. As illustrated in Figure 13.2.2, free rotational motion by one molecule results in oscillations that depend on the molecule's angular velocity ω_A through $\theta(t) = \omega_A t$. Oscillations to negative values occur when the dipoles are oriented anti-parallel to their original direction.

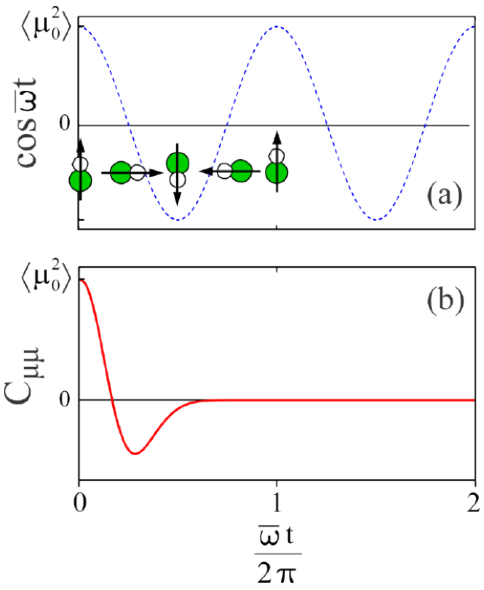


Figure 13.2.2: (a) Time-dependent dipole orientation factor $\cos\theta(t)$ for a molecule rotating in a plane with angular velocity $\bar{\omega}_A = \sqrt{k_B T/I}$ (b) Rotational correlation function after averaging over the Boltzmann distribution of angular frequencies for $I\bar{\omega}_A^2 = k_B T$.

While this behavior is characteristic of any one molecule, the correlation function is computed by averaging over the Boltzmann distribution of angular velocities. At equilibrium, the average kinetic energy per rotational degree of freedom, $\frac{1}{2}k_B T$, is equal to the moment of inertia and average angular velocity, $\frac{1}{2}I\langle\omega_A^2\rangle$. Thus one might expect that the period of oscillations in the correlation function, $\tau = 2\pi/\omega_A$, can be related to the molecule's moment of inertia by $\tau \sim 2\pi\,(I/k_B T)^{-1/2}$. In fact, when we average over the distribution $P\,(\omega_A) \sim \exp(-I\omega_A^2/2k_B T)$, the resulting correlation function appears critically damped with one oscillation (Figure 13.2.2). In this case, the observed damping is not a result of irreversible relaxation. It reflects the broad distribution of rotational frequencies present at thermal equilibrium and the resulting destructive interference between rotors spinning at different speeds. This is an example of when an apparent dynamical effect is merely a result of averaging over an ensemble with highly varying behavior; this gives rise to inhomogeneous broadening in spectroscopy, as we will discuss in Chapter 15.

Independent of this damping, we know that the correlation function will relax to zero because all orientations of the gas phase molecules are equally probable, and therefore $\langle\hat{u}\rangle^2 = 0$. In a real gas, the collisional damping effects described in Example 1 are also a source of relaxation to the correlation function.

Example 3: Harmonic oscillator correlation function

The time-dependent motion of a harmonic vibrational mode is given by Newton's law in terms of the acceleration and restoring force as $m\ddot{q} = -m\omega^2 q$ or $\ddot{q} = -\omega^2 q$, with the solution $q(t) \;= q_0 \cos\omega_0 t + (p_0/m\omega_0)\sin\omega_0 t$. The two terms reflect how the energy in an oscillator is divided between the constantly exchanging potential and kinetic energy of the particle. Therefore an ensemble average needs to consider the thermal distribution of both position and momentum of the oscillator. For this average, it is helpful to rewrite the solution in terms of an amplitude and phase:

$$q(t) = \sqrt{q_0^2 + \left(\frac{p_0}{m\omega_0}\right)^2}\cos(\omega_0 t + \beta) \qquad \beta = \operatorname{atan}\left(\frac{p_0}{q_0 m\omega_0}\right) \tag{13.2.5}$$

Then the correlation function for the harmonic oscillator coordinate is

$$\begin{aligned} C_{qq}(t) &= \langle q(t)\, q(0)\rangle \\ &= \left\langle q_0^2 + \left(\frac{p_0}{m\omega_0}\right)^2 \right\rangle \langle \cos(\beta)\cos(\omega_0 t + \beta)\rangle \end{aligned} \tag{13.2.6}$$

We have written this as an equilibrium average over two terms: the first reflects a thermal average over the oscillator amplitude, and the second averages over the phase of oscillation (β) of different members of the ensemble. For the leading term, we note that average total kinetic and potential energy for the oscillator is k_BT: $\left\langle \frac{1}{2}m\omega_0^2 q^2 + \frac{1}{2m}p^2 \right\rangle = k_BT$. Therefore, we know that the mean square oscillator amplitude is determined by:

$$\left\langle q_0^2 + \left(\frac{p_0}{m\omega_0}\right)^2 \right\rangle = \frac{2k_BT}{m\omega_0^2} \tag{13.2.7}$$

For the second term in eq. (13.2.6), we average the product of cosines by integrating over phases between $\beta = 0$ and 2π to obtain $\frac{1}{2}\cos\omega_0 t$. This leads to our final correlation function.

$$C_{qq}(t) = \frac{k_BT}{m\omega_0^2}\cos\omega_0 t \tag{13.2.8}$$

Note that the denominator here is also the force constant for the oscillator, $\kappa = m\omega_0^2$. We observe that the average behavior of the harmonic oscillator thermal ensemble is to oscillate undamped with an amplitude that increases with temperature. No damping is observed because there is no time-dependent perturbations to the phase of individual oscillators. If the ensemble also reflected a distribution of frequencies (for constants), then an average over those frequencies would lead to apparent (inhomogeneous) damping of the correlation function similar to Example 2.

We can use the same reasoning to calculate the velocity autocorrelation function for the harmonic oscillator and obtain

$$C_{vv}(t) = \frac{k_BT}{m}\cos\omega_0 t \tag{13.2.9}$$

Note, $C_{vv}(t) = \omega_0^2 C_{qq}(t)$. This reflects a general property regarding derivatives of classical correlation functions. Since $v = \dot{q}$, the velocity autocorrelation function can be related to the second derivative of the position autocorrelation function. There are some subtleties to this relation, described in the box below. The velocity autocorrelation function plays an important role in characterizing a continuum of harmonic modes, such as phonons. Noting that the Fourier transform of eq. (13.2.9) gives $\tilde{C}_{vv}(\omega) = (k_BT/m)\,\delta(\omega - \omega_0)$, we can integrate this over a frequency-dependent density of states $g(\omega_0)$ to show that $\tilde{C}_{vv}(\omega)$ is proportional to the density of states. This leads to the following Fourier transform relationship between the velocity autocorrelation function and the density of states for a continuum of harmonic modes:

$$g(\omega) = \frac{m}{2\pi k_BT}\mathrm{Re}\left[\int_0^\infty C_v(t)e^{-\mathrm{i}\omega t}\,dt\right] \tag{13.2.10}$$

Exercise 13.2.1

Taking time-derivatives of time-correlation functions is particularly helpful for relating position correlation functions to those involving velocity or momentum. To understand how a time-derivative is evaluated, it is helpful to return to the original definition for a stationary process:

$$C(t_1, t_2) = \langle A(t_1)\, A(t_2)\rangle = \langle A(0)A(t_2 - t_1)\rangle \tag{13.2.11}$$

The correlation function only depends on the time interval between observations. Therefore we express it in terms of $\tau = t_2 - t_1$, but time-derivatives with respect to τ require that we differentiate with respect to t_2 and t_1 points: $\frac{d}{d\tau} = \frac{\partial}{\partial t_2} - \frac{\partial}{\partial t_1}$. When applied to $C(t_1, t_2)$ we obtain

$$\frac{d}{d\tau}\langle A(t_1)\, A(t_2)\rangle = \left\langle A(t_1)\,\dot{A}(t_2)\right\rangle - \left\langle \dot{A}(t_1)\, A(t_2)\right\rangle \tag{13.2.12}$$

If this expression is to maintain equivalence for a stationary system that is dependent only on τ, the following equalities must apply:

$$\dot{C}(\tau) \equiv \frac{d}{d\tau} C(\tau) = \left\langle A(0)\dot{A}(\tau) \right\rangle = -\left\langle \dot{A}(0)A(\tau) \right\rangle \tag{13.2.13}$$

We also can see that the time-derivative is an odd function of time: $\dot{C}(\tau) = -\dot{C}(-\tau)$. Note that these are no longer autocorrelation functions, since one is calculating the correlation of A with its time derivative.

If we extend this reasoning to second derivatives, another set of relationships emerges. Expanding the second derivative in the same manner,

$$\ddot{C}(\tau) \equiv \frac{d^2}{d\tau^2} C(\tau) \tag{13.2.14}$$

we find

$$\ddot{C}(\tau) = \left\langle A(0)\ddot{A}(\tau) \right\rangle = \left\langle \ddot{A}(0)A(\tau) \right\rangle = -\left\langle \dot{A}(0)\dot{A}(\tau) \right\rangle \tag{13.2.15}$$

The second derivative is even in time: $C(\tau) = C(-\tau)$. We see this relationship play out in the position and velocity autocorrelation functions above. Since $C_{vv}(\tau) = \langle \dot{x}(\tau)\dot{x}(0) \rangle$, we find that, for the harmonic oscillator, $C_{vv}(\tau) = -\ddot{C}_{xx}(\tau) = \omega^2 C_{xx}(\tau)$.

This page titled 13.2: Examples of Classical Time-Correlation Functions is shared under a CC BY-NC-SA 4.0 license and was authored, remixed, and/or curated by Andrei Tokmakoff via source content that was edited to the style and standards of the LibreTexts platform.

13.3: Calculating the Correlation Function from a Discrete Trajectory

While time and the correlation function are both continuous variables, in practice, correlation functions are commonly determined from a time-average over a long sequence of discretely sampled data points. In molecular dynamics simulations or single molecule experiments, measurements of atomic positions, momenta, or fluorescence intensity are recorded as a trajectory. The data are a sequence of consecutive observations with short, fixed time intervals. To see how the classical correlation function is obtained, let's translate eq. (13.1.09) for use with such a discretely sampled trajectory.

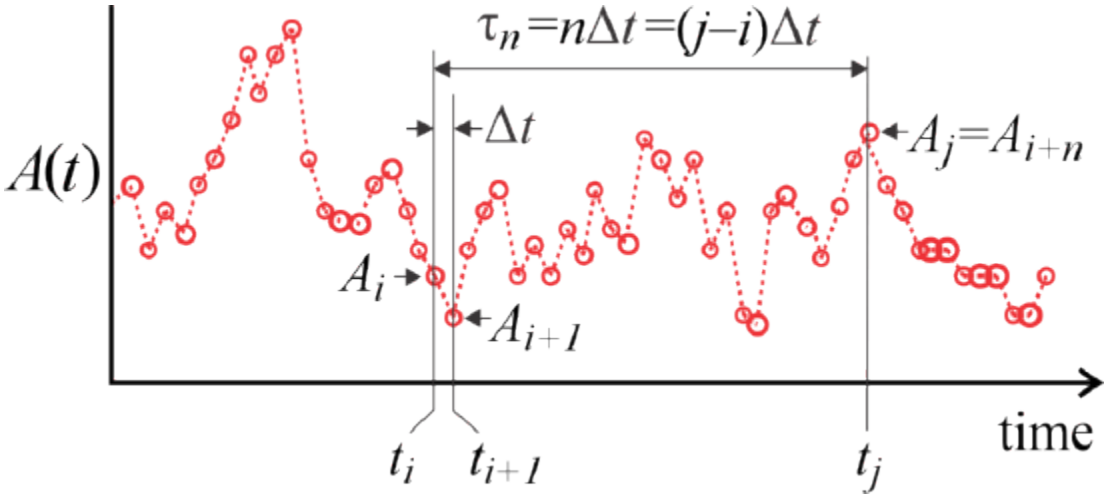


Figure 13.3.1: $A(t)$ trajectory indicating variables used in numerically calculating a time-averaged correlation function.

The trajectory consists of N observations of the dynamical variable A at series of time points t_i (Figure 13.3.1). The separation between time points is $t_{i+1} - t_i = \Delta t$, and the length of the trajectory is $T = N\Delta t$. We define a time interval between observations, $\tau_n = t_j - t_i = n\Delta \mathrm{t}$, where $n = |j - i|$ is the index marking the separation of time-steps along the trajectory. Then, we can approximate the integral in eq. (13.1.09) by a sum:

$$C_{AA}(\tau_n) = \lim_{T\to\infty} \frac{1}{T} \sum_{i=1}^{N} \Delta t\, A(t_i) A(t_i + \tau_n) = \lim_{N\to\infty} \frac{1}{N} \sum_{i=1}^{N} A_i A_{i+n} \tag{13.3.1}$$

Here, the value of A observed at time t_i is designated A_i.

In practice, the length of the trajectory N is finite, limiting the possible pairs of t_i and t_j. For each time interval (n), there are a different number of observation pairs to average across. For the maximum delay $\tau_n = T$, we only have one data pair: the first and last observations. This pair has an index of $n = N - 1$. The greatest number of pairwise products—N, to be precise—are possible when the time points are equal ($t_i = t_j$ and $n = 0$). Therefore, for a given delay τ_n, the number of pairwise products is $N - n$. So we can write eq. (13.3.1) as

$$C_{AA}(\tau) = C(n) = \frac{1}{N-n} \sum_{i=1}^{N-n} A_{i+n} A_i \tag{13.3.2}$$

Note, this is a classical correlation function that is even in time, so this expression need only be calculated for positive values of n, for which $t_j \geq t_i$.

As an example, consider the following calculation for fluctuations in a vibrational frequency $\omega(t)$. The trajectory, pictured in Figure 13.3.2a, consists of a $T = 655$ ps trajectory of more than 65500 consecutive frequencies $\omega(t_i)$ separated by $\Delta t = 10$ fs. These frequencies fluctuate between 3220–3270 cm^{-1}, with a mean value of $\langle\omega\rangle = 3244$ cm^{-1}. This trajectory illustrates that there are fast fluctuations on femtosecond time scales, while the behavior is seemingly random on 50 picosecond time scales. After converting the trajectory to a variation of the frequency from the mean, $\delta\omega(t_i) = \omega(t_i) - \langle\omega\rangle$, the frequency correlation function is determined from eq. (13.3.2), with the substitution $\delta\omega(t_i) \to A_i$. The resulting correlation function, $C_{\delta\omega\delta\omega}(\tau)$, is shown in Figure 13.3.2b.

If we consider the correlation function over the full $655\ \mathrm{ps}$ window of the calculation, we can see that the correlation function averages to zero on the time scale of 10^4–10^5 femtoseconds. However, when we expand the first $5\ \mathrm{ps}$, we observe a smooth decay of the correlation function, signifying the loss of memory in the fluctuating frequency on the 10^3 femtosecond time scale. From eq. (13.1.15), we find that the correlation time is $\tau_C = 785\ \mathrm{fs}$. On top of the smooth decay, the correlation function exhibits damped beats with a period of $\sim 300\ \mathrm{fs}$. These indicate that underlying dynamic processes are acting to weakly modulate the time dependent frequency $\omega(t)$. The zero-time value of the correlation function gives the variance in the frequency as $C_{\delta\omega\delta\omega}(0) = \langle \delta\omega^2 \rangle = \langle \omega^2 \rangle - \langle \omega \rangle^2 = 27\ \mathrm{cm}^{-2}$, or a standard deviation in $P(\omega)$ of approximately $5\ \mathrm{cm}^{-1}$.

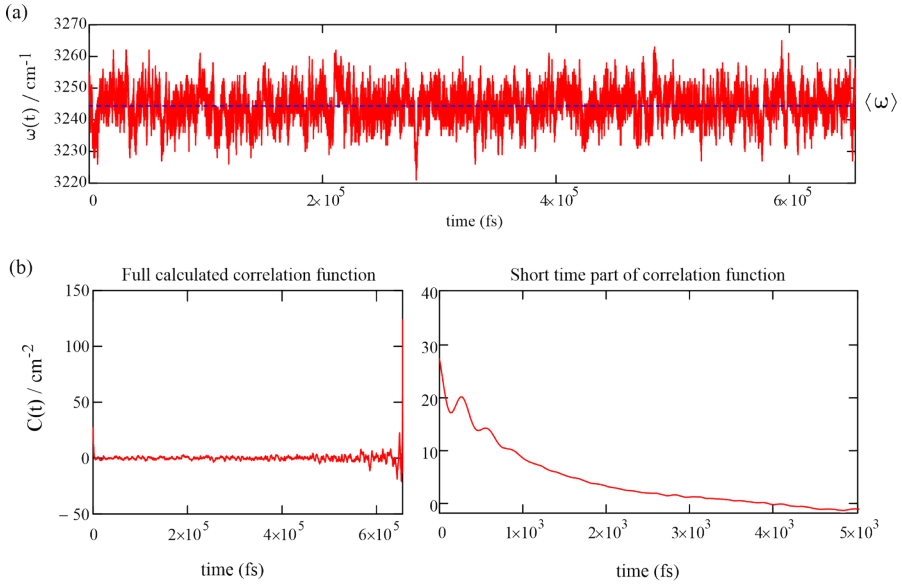


Figure 13.3.2: (a) $640\ \mathrm{ps}$ trajectory of time-dependent vibrational frequencies spaced by $10\ \mathrm{fs}$. (b) Frequency autocorrelation function $C(t)$ calculated from this trajectory, showing the full calculated $C(t)$ over the $640\ \mathrm{ps}$ range on the left, and a zoom in of the first $5\ \mathrm{ps}$ on the right.

This page titled 13.3: Calculating the Correlation Function from a Discrete Trajectory is shared under a CC BY-NC-SA 4.0 license and was authored, remixed, and/or curated by Andrei Tokmakoff via source content that was edited to the style and standards of the LibreTexts platform.

13.4: Quantum Time-Correlation Functions

Quantum time-correlation functions may be written $C_{AA}(\tau) = \langle A(\tau)A(0)\rangle$. They are computed as the expectation value of a product of time-dependent Hermitian operators, which are evaluated at two times and averaged over an equilibrium ensemble:

$$C_{AA}(\tau) = \sum_n p_n \langle n| \hat{A}(\tau)\hat{A}(0) |n\rangle \tag{13.4.1}$$

where $p_n = e^{-\beta E_n}/Z$. Note that convention has the time-ordering from right to left. Again, τ is the time interval between the first and second time points. In the density matrix representation, we have

$$C_{AA}(\tau) = \mathrm{Tr}\left[\hat{A}(\tau)\hat{A}(0)\rho_{\mathrm{eq}}\right] \tag{13.4.2}$$

where ρ_{eq} is the equilibrium density matrix. Naturally, the time-dependent operators in the correlation function invoke a Heisenberg representation of the operators, although in almost all cases we will be using correlation functions with interaction picture operators $A_I(t) \ = e^{\mathrm{i}H_0 t}Ae^{-\mathrm{i}H_0 t}$. In the classical case, the time-ordering of the variables didn't matter, since it was real and even in time, but we will now need to watch the time-ordering of the quantum mechanical operators and define C_{AA} with right-to-left time-ordering, as if there is a sequence of interactions on the *ket* $|n\rangle$.

If we evaluate eq. (13.4.1) for a time-independent Hamiltonian in the Schrödinger picture using the eigenbasis $|n\rangle$, inserting a projection operator leads to

$$\begin{aligned} C_{AA}(\tau) &= \sum_n p_n \langle n| U^\dagger(\tau)AU(\tau)A |n\rangle \\ &= \sum_{n,m} p_n \langle n| A |m\rangle \langle m| A |n\rangle e^{-\mathrm{i}\omega_{mn}\tau} \end{aligned} \tag{13.4.3}$$

$$C_{AA}(\tau) = \sum_{n,m} p_n |A_{mn}|^2 e^{-\mathrm{i}\omega_{mn}\tau} \tag{13.4.4}$$

This eigenfunction form shows simple unitary time-evolution with no irreversible behavior. The correlation function is a superposition of complex, undamped oscillations at all energy splittings, weighted by the squared matrix element that couples the states and the equilibrium population of states. The superposition state described by the correlation function persists indefinitely. While this form isn't representative of condensed matter problems, it can prove useful for gas phase molecular ensembles that are composed of weakly damped, non-interacting molecules, and we will make use of it in describing properties of correlation functions. As we will see in later chapters, the addition of irreversible processes in condensed phases will lead to an additional real-valued term in the exponential in eq. (13.4.4) that damps these oscillations.

Properties of Quantum Correlation Functions

Although we have not yet introduced irreversible processes, there are a number of properties that can already be deduced from the definition of quantum correlation functions. For instance, in writing eq. (13.4.1), we already recognized that correlation functions are stationary. This can be demonstrated by manipulating the time-evolution operators in the Schrödinger representation:

$$\begin{aligned} \langle A(t)A(t')\rangle &= \left\langle U^\dagger(t)AU(t)U^\dagger(t')AU(t')\right\rangle \\ &= \left\langle U(t')U^\dagger(t)AU(t)U^\dagger(t')A\right\rangle \\ &= \left\langle U^\dagger\left(t-t'\right)AU\left(t-t'\right)A\right\rangle \\ &= \left\langle A\left(t-t'\right)A(0)\right\rangle \end{aligned} \tag{13.4.5}$$

This leads us to use the same time interval notation as before: $\tau = t - t'$.

The most striking difference with classical correlation functions is that quantum correlation functions are complex, not real nor even in time. Again using the properties of the time-evolution operator, we can show that inverting the order of the operators is the same as taking the correlation function's complex conjugate:

$$\langle A(0)A(\tau)\rangle = \langle A(\tau)A(0)\rangle^* = \langle A(-\tau)A(0)\rangle \tag{13.4.6}$$

or, in short,

$$C^*_{AA}(\tau) = C_{AA}(-\tau) \tag{13.4.7}$$

Since it is complex, you cannot directly measure a quantum correlation function, but observables are often related to the real or imaginary part of correlation functions. The real and imaginary parts of $C_{AA}(t)$ can be separated as

$$C_{AA}(t) = C'_{AA}(t) + \mathrm{i}C''_{AA}(t) \tag{13.4.8}$$

and computed from:

$$\begin{aligned} C'_{AA}(t) &= \frac{1}{2}\left[C_{AA}(t) + C^*_{AA}(t)\right] = \frac{1}{2}\left[\langle A(t)A(0)\rangle + \langle A(0)A(t)\rangle\right] \\ &= \frac{1}{2}\left\langle [A(t), A(0)]_+ \right\rangle \end{aligned} \tag{13.4.9}$$

$$\begin{aligned} C''_{AA}(t) &= \frac{1}{2}\left[C_{AA}(t) - C^*_{AA}(t)\right] = \frac{1}{2}\left[\langle A(t)A(0)\rangle - \langle A(0)A(t)\rangle\right] \\ &= \frac{1}{2}\left\langle [A(t), A(0)] \right\rangle \end{aligned} \tag{13.4.10}$$

In eq. (13.4.9), $[A, B]_+ \equiv AB + BA$ is known as the *anticommutator* (sometimes written $\{A, B\}$), and C'_{AA} is also known as a *symmetrized* correlation function, whereas C''_{AA} is *anti-symmetrized*.

As illustrated in Figure 14.4.1, the real part is even in time, $C'_{AA}(-\tau) = C'_{AA}(\tau)$, and can be expanded as Fourier series in cosines, whereas the imaginary part is odd, $C''_{AA}(-\tau) = -C''_{AA}(\tau)$, and can be expanded in sines. We will see later that the magnitude of the real part grows with temperature, but the imaginary does not. At 0 K, the real and imaginary components have equal amplitudes, but as one approaches the classical (high temperature) limit, the real part dominates the imaginary.

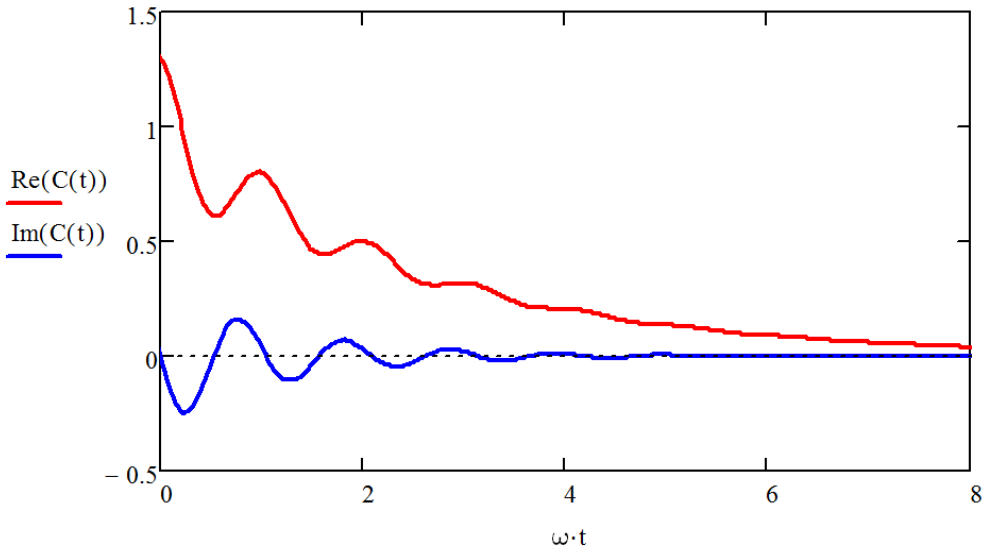


Figure 13.4.1: Illustration of the real and imaginary components of a quantum time correlation function.

We will also see in our discussion of linear response in Section 14.6 that C'_{AA} and C''_{AA} are directly proportional to the step response function S and the impulse response function R, respectively. R describes how a system is driven away from equilibrium by an external potential, while S describes the relaxation of the system back to equilibrium after a potential holding it away from equilibrium is released. Classically, the two are related by $R \propto \partial S/\partial t$.

Spectral representation of correlation functions (1)

Since time and frequency are conjugate variables, we can also define the correlation function in the frequency domain by the

Fourier transformation of the time correlation function. There can be practical advantages to using one representation over another; for instance, a spectrum may be a simpler way of representing complex beating patterns in time, or time-domain convolution can turn into a simple product in frequency space. Transformation between the two also allows us to make direct connections between the dynamical processes captured by time-correlation function and the spectra observed by certain experiments.

The Fourier transform and its inverse are defined as

$$C_{AA}(\omega) = \tilde{\mathcal{F}}\left[C_{AA}(t)\right] = \int_{-\infty}^{+\infty} dt\, \mathrm{e}^{\mathrm{i}\omega t}\, C_{AA}(t) \tag{13.4.11}$$

$$C_{AA}(t) = \tilde{\mathcal{F}}^{-1}\left[C_{AA}(\omega)\right] = \frac{1}{2\pi}\int_{-\infty}^{+\infty} d\omega\, \mathrm{e}^{-\mathrm{i}\omega t}\, C_{AA}(\omega) \tag{13.4.12}$$

In eq. (13.4.11), $C_{AA}(\omega)$ is known as the power spectrum. Even if $C_{AA}(t)$ is a complex correlation function, the power spectrum is real and positive. To show this, we split the integral in (13.4.11) into one for negative times and one for positive times and then use the property for Hermitian operators $C_{AA}(-t) = C^{*}_{AA}(t)$ to show

$$C_{AA}(\omega) = 2\,\mathrm{Re}\int_{0}^{\infty} e^{\mathrm{i}\omega t}\, C_{AA}(t)\, dt \tag{13.4.13}$$

We will also make use of the Fourier-Laplace transform or single-sided Fourier transform of the correlation function

$$\tilde{C}_{AA}(\omega) = \int_{0}^{\infty} e^{\mathrm{i}\omega t}\, C_{AA}(t)\, dt \tag{13.4.14}$$

This transform, which we distinguish by the tilde over the C, differs only in the lower limit of the integral, but proves to be important when we restrict time to be positive, as is the case for response functions. This frequency domain representation is complex, with real and imaginary components that we separate as:

$$\tilde{C}_{AA}(\omega) = C'_{AA}(\omega) + \mathrm{i}C''_{AA}(\omega) \tag{13.4.15}$$

Figure 14.4.2 shows examples of the real and imaginary parts of a frequency-domain correlation function that corresponds to the complex time-correlation function in Figure 14.4.1. Note that the complex nature of $C_{AA}(t)$ means that $C'_{AA}(\omega)$ and $C''_{AA}(\omega)$ are not even and odd in frequency, as they would be for a classical real correlation function.

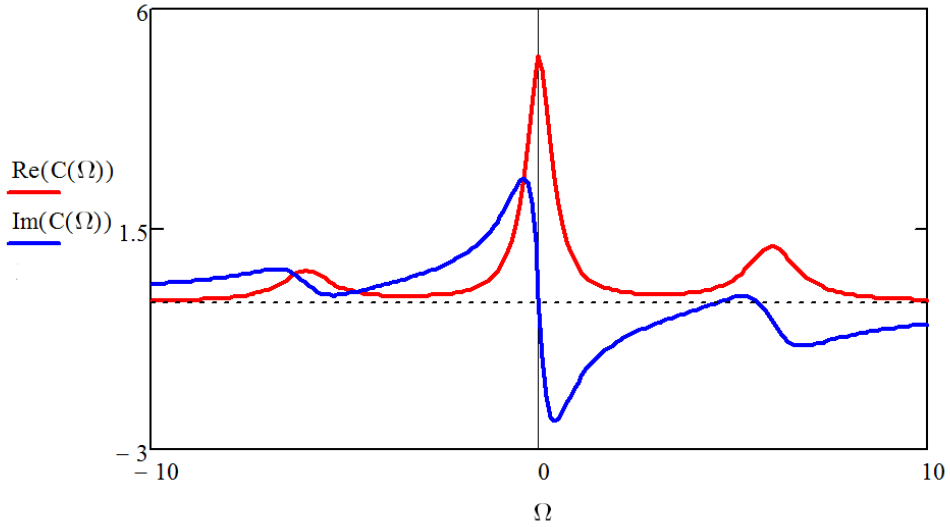


Figure 13.4.2: Real and imaginary parts of a frequency-domain correlation function $\tilde{C}(\omega)$ that corresponds to the complex time-correlation function in Figure 14.4.1. Note that the spectra are not even or odd functions of frequency

Returning to the eigenstate expression of the correlation function for a time-independent Hamiltonian in eq. (13.4.4), we can evaluate the Fourier transform of $C_{AA}(\tau)$ to give

$$C_{AA}(\omega) = \sum_{n,m} p_n \left|A_{mn}\right|^2 \delta(\omega - \omega_{mn}) \tag{13.4.16}$$

Note that this expression looks very similar to the Golden Rule transition rate that we derived from first-order perturbation theory. In fact, we will see in Section 13.5 that the Fourier transform of time-correlation functions evaluated at the energy gap between the initial and final states gives the same Golden Rule transition rate between those states: $C_{AA}(\omega_{mn}) \propto \bar{w}_{mn}$.

Although eq. (13.4.16) has no explicit time dependence, the ensemble average over states $|n\rangle$ occupied at equilibrium does enforce a time ordering of sorts. $\tilde{C}_{AA}(\omega)$ is a spectrum that quantifies the influence of the operator A in coupling initial state n to final state m as a function of the energy difference between the states. This expression applies to an ensemble at finite temperature with population in thermally accessible states, so it applies to initial states that are either lower or higher in energy than the final states. This is reflected by the negative and positive frequencies, respectively. Since the initial state population drops with increasing energy, for a given energy gap C_{AA} is smaller at negative frequencies than positive ones. If we compare the correlation function for two states n and m, we find that their ratio is proportional to a Boltzmann factor evaluated at the energy gap E_{mn}:

$$\frac{C_{AA}(\omega_{nm})}{C_{AA}(\omega_{mn})} = \frac{P_m}{P_n} = e^{-\beta E_{mn}} \tag{13.4.17}$$

Anticipating Section 13.5, where we will show that $C_{AA}(\omega_{mn})$ is related to the rate of transitions from n to m, the ratio of C_{AA} in eq. (13.4.17) between negative and positive frequencies is also related to the rates of upward and downward transitions:

$$\frac{\bar{w}_{ij}}{\bar{w}_{ji}} = \frac{P_j}{P_i} = e^{-\beta E_{ji}} \tag{13.4.18}$$

This is the principle of detailed balance, which relates upward and downward transition rates at equilibrium to the difference in thermal occupation between states.

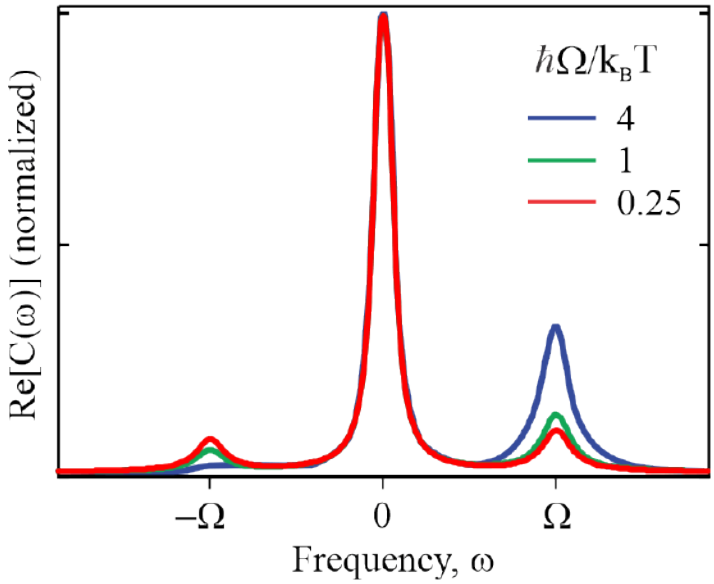


Figure 13.4.3: Influence of temperature on the shape of the real part of $\tilde{C}(\omega)$.

We can establish further relationships between the complex, real, and imaginary parts of the complex frequency domain representation. Equation (13.4.17) can be written as

$$\tilde{C}_{AA}(\omega) = e^{\beta\hbar\omega}\tilde{C}_{AA}(-\omega) \tag{13.4.19}$$

which illustrates how temperature influences the asymmetry of the spectrum. As illustrated in Figure 14.4.3, the ratio of positive and negative peaks is equal in the high temperature limit ($\hbar\omega \ll k_B T$) but strongly favors the positive frequency peak for $\hbar\omega \gg k_B T$. This relationship, together with a Fourier transform of eq. (13.4.7),

$$C^*_{AA}(\omega) = C_{AA}\left(-\omega\right) \tag{13.4.20}$$

allows us to obtain other relationships linking the real and imaginary components. The symmetrized and anti-symmetrized frequency domain correlation functions that correspond to the time-domain expressions in eqs. (13.4.9) and (13.4.10) are

$$\tilde{C}_{AA}(\omega) \pm \tilde{C}_{AA}(-\omega) = \left(1 \pm e^{-\beta\hbar\omega}\right)\, \tilde{C}_{AA}(\omega) \tag{13.4.21}$$

This results in the real and imaginary components:

$$\tilde{C}'_{AA}(\omega) = \frac{1}{2}\tilde{C}_{AA}(\omega)\left(1 + e^{-\beta\hbar\omega}\right) \tag{13.4.22}$$

$$\tilde{C}''_{AA}(\omega) = \frac{1}{2}\tilde{C}_{AA}(\omega)\left(1 - e^{-\beta\hbar\omega}\right) \tag{13.4.23}$$

The components can be related as

$$C'_{AA}(\omega) = \coth\left(\beta\hbar\omega/2\right) C''_{AA}(\omega) \tag{13.4.24}$$

Thus, specifying any one representation of the spectrum is sufficient to determine the others. Equation (13.4.22) is sometimes used to construct a quantum correlation function from a classical correlation function, with the assumption that the classical correlation function can be equated with the real quantum correlation function.

Example: Harmonic oscillator correlation functions

As an example, we show different ways of evaluating the correlation function for the position of an ensemble of quantum harmonic oscillators

$$C_{xx}(t) = \langle \hat{x}(t)\hat{x}(0)\rangle \tag{13.4.25}$$

For this model, the position operator can be expressed in terms of raising and lower operators as

$$\hat{x} = \sqrt{\hbar/2m\omega_0}\left(a + a^\dagger\right) \tag{13.4.26}$$

The Hamiltonian $H = \hbar\omega_0(a^\dagger a + \frac{1}{2})$ has energy eigenvalues $E_n = n\hbar\omega_0 + 1/2$, so that the energy gap between initial and final states is $\omega_{mn} = (m-n)\,\omega_0$. For an equilibrium ensemble, the Bose-Einstein probability distribution is $P_n = e^{-\beta n\hbar\omega_0}\left(1 - e^{-\beta\hbar\omega_0}\right)$, and

$$\bar{n} = \sum\nolimits_n nP_n = \left(e^{\beta\hbar\omega_0} - 1\right)^{-1} \tag{13.4.27}$$

is the average occupation number for a Bose-Einstein distribution.

1) Schrodinger representation. We evaluate the correlation function using eq. (13.4.4). The matrix elements in the position operator x_{mn} are

$$\langle m|\,\hat{x}\,|n\rangle = \sqrt{\frac{\hbar}{2m\omega_0}}\left[\sqrt{n+1}\,\delta_{n+1,m} + \sqrt{n}\,\delta_{n-1,m}\right] \tag{13.4.28}$$

which are nonzero for $m = n \pm 1$. Then eq. (13.4.4) becomes

$$\begin{aligned} C_{xx}(\tau) &= \sum_{n,m} P_n\,|A_{mn}|^2\, e^{-\mathrm{i}(m-n)\omega_0\tau} \\ &= \sum_{n,m} P_n \frac{\hbar}{2m\omega_0}\left[(n+1)\delta_{n+1,m} + n\delta_{n-1,m}\right] e^{-\mathrm{i}\omega_{mn}\tau} \\ &= \sum_n \frac{e^{-\beta n\hbar\omega_0}}{1 - e^{-\beta\hbar\omega_0}} \frac{\hbar}{2m\omega_0}\left[(n+1)e^{-\mathrm{i}\omega_0\tau} + ne^{\mathrm{i}\omega_0\tau}\right] \\ &= \frac{\hbar}{2m\omega_0}\left[(\bar{n}+1)e^{-\mathrm{i}\omega_0\tau} + \bar{n}e^{\mathrm{i}\omega_0\tau}\right] \end{aligned} \tag{13.4.29}$$

The final line is the complex form, which we can separate into real and imaginary components:

$$\begin{aligned} C_{xx}(\tau) &= C'_{xx}(\tau) + \mathrm{i}C''_{xx}(\tau) \\ &= \frac{\hbar}{2m\omega_0}\left[(2\bar{n}+1)\cos\omega_0 t - \mathrm{i}\sin\omega_0 t\right] \end{aligned} \tag{13.4.30}$$

In the classical high-temperature limit ($\bar{n} \approx k_B T/\hbar\omega_0$), $\bar{n} \gg 1$, and the correlation function becomes entirely real: $C_{xx}(\tau) = (k_B T/m\omega_0^2)\cos\omega_0 t$. This is the same as we obtained in our earlier example, eq. (14.2.08).

2) Heisenberg Representation. Starting with eq. (13.4.1), we can draw on the time-dependence of the position operator that we evaluated in Section 2.6.

$$\hat{x}(t) = \sqrt{\frac{\hbar}{2m\omega_0}}\left(a^\dagger e^{\mathrm{i}\omega_0 t} + a e^{-\mathrm{i}\omega_0 t}\right) \tag{13.4.31}$$

The product $\hat{x}(t)\hat{x}(0)$ leads to four terms, of which only two will contribute to the expectation value:

$$C_{xx}(\tau) = \sum_n P_n \frac{\hbar}{2m\omega_0}\left\langle n\right| aa^\dagger e^{-\mathrm{i}\omega_0 t} + a^\dagger a e^{\mathrm{i}\omega_0 t}\left|n\right\rangle \tag{13.4.32}$$

This leads immediately to eq. (13.4.29). Note that $\left\langle aa^\dagger\right\rangle = \bar{n}+1$ and $\left\langle a^\dagger a\right\rangle = \bar{n}$.

The power spectrum for the position correlation function is obtained by Fourier transforming eq. (13.4.29)

$$C_{xx}(\omega) = \frac{\hbar}{2m\omega_0}\left[(\bar{n}+1)\,\delta(\omega-\omega_0) + \bar{n}\delta(\omega+\omega_0)\right] \tag{13.4.33}$$

This spectrum has two delta function peaks at $\omega = \pm\omega_0$. These temperature-dependent peak heights differ but become equal as $T \to \infty$. We will investigate the properties of this spectral function further in Chapter 17.

References

(1) Mukamel, S. *Principles of Nonlinear Optical Spectroscopy*; Oxford University Press, 1995.

This page titled 13.4: Quantum Time-Correlation Functions is shared under a CC BY-NC-SA 4.0 license and was authored, remixed, and/or curated by Andrei Tokmakoff via source content that was edited to the style and standards of the LibreTexts platform.

13.5: Transition Rates from Time Correlation Functions

We have previously seen that the first-order perturbation theory transition rates can be related to the Fourier transform of the time-dependent external potential, when the transform is evaluated at the energy gap between the initial and final state. We will now expand on this observation to describe the ensemble-average rates of the transitions that naturally occur within an equilibrium ensemble. We will show that these transition rates can be expressed in a time-domain picture through a time-correlation function for the interaction between states.

When a potential V is applied to a system described by the Hamiltonian H_0, the transition rate from system state n to state m is given by the state-to-state form of the Golden Rule:

$$w_{mn} = \frac{2\pi}{\hbar} |V_{mn}|^2 \, \delta\left(E_m - E_n\right) \tag{13.5.1}$$

We are interested in calculating the average rates of transition between states of the system under equilibrium conditions. We will look specifically at the case of a system at thermal equilibrium, in which the initially populated state n is coupled to all possible final states m. Averaging this over the equilibrium thermal population of initial states gives the net rates of transition out of states with energy E_n to states with energy E_m

$$\bar{w}_{mn} = \frac{2\pi}{\hbar} \sum_{m,n} p_n \, |V_{mn}|^2 \, \delta\left(E_m - E_n\right) \tag{13.5.2}$$

where $p_n = e^{-\beta E_n}/Z$. From this expression we can observe the principle of detailed balance, which applies to all equilibrium systems. If we consider the relative transition rate between two states at thermal equilibrium, eq. (13.5.2) shows us that the ratio of the transition rates between two states must be inversely proportional to the ratio of the populations in those states

$$\frac{\bar{w}_{mn}}{\bar{w}_{nm}} = \frac{p_n}{p_m} = e^{-\beta E_{nm}} \tag{13.5.3}$$

Equivalently, the flux of population leaving state i for j matches that of the reverse direction: $p_m \bar{w}_{mn} = p_n \bar{w}_{nm}$.

To express the rates of transitions in eq. (13.5.2) in the time-domain, we convert the energy conservation statement $\delta\left(E_m - E_n\right) = \delta\left(\omega_{mn}\right)/\hbar$ to the time domain using the definition of the delta function

$$\delta(\omega) = \frac{1}{2\pi} \int_{-\infty}^{+\infty} dt \, e^{\mathrm{i}\omega t} \tag{13.5.4}$$

giving

$$\bar{w}_{mn} = \frac{1}{\hbar^2} \sum_{m,n} p_n \, |V_{mn}|^2 \int_{-\infty}^{+\infty} dt \, e^{\mathrm{i}(E_m - E_n)t/\hbar} \tag{13.5.5}$$

Writing the matrix elements explicitly, and recognizing that in the interaction picture $e^{-\mathrm{i}H_0 t/\hbar} \, |\ell\rangle = e^{-\mathrm{i}E_\ell t/\hbar} \, |\ell\rangle$, we have

$$\bar{w}_{mn} = \frac{1}{\hbar^2} \sum_{m,n} p_n \int_{-\infty}^{+\infty} dt \, e^{\mathrm{i}(E_m - E_n)t/\hbar} \, \langle n \, | V | \, m \rangle \, \langle m | \, V \, | n \rangle \tag{13.5.6}$$

$$= \frac{1}{\hbar^2} \sum_{m,\ell} p_n \int_{-\infty}^{+\infty} dt \; \langle n \, | V | \, m \rangle \, \langle m | \, e^{\mathrm{i}H_0 t/\hbar} \, V \, e^{-\mathrm{i}H_0 t/\hbar} \, | n \rangle \tag{13.5.7}$$

Then, recognizing the resolution of the identity $\sum_m |m\rangle \langle m| = 1$

$$\bar{w}_{mn} = \frac{1}{\hbar^2} \sum_{n} p_n \int_{-\infty}^{+\infty} dt \, \langle n | \, V_I(0) V_I(t) \, | n \rangle \tag{13.5.8}$$

$$\bar{w}_{mn} = \frac{1}{\hbar^2} \int_{-\infty}^{+\infty} dt \, \langle V_I(t) V_I(0) \rangle \tag{13.5.9}$$

As before, $V_I(t) = e^{\mathrm{i}H_0 t/\hbar} V e^{-\mathrm{i}H_0 t/\hbar}$. The final expression, eq. (13.5.9), indicates that integrating over the correlation function for the

time-dependent interaction between the initial state and its surroundings results in the transfer rate.

This is a more general expression than one might assume. Although the derivation emphasized specific eigenstates, eq. (13.5.9) indicates that knowledge of a time-dependent interaction potential of any sort can be used to calculate transition rates from the time-correlation function for that potential. Consider the correlation function for an arbitrary time-dependent potential:

$$C_{VV}(t) = \langle V_I(t) V_I(0) \rangle \tag{13.5.10}$$

Using the system eigenstates, this correlation function can be expressed as eq. (14.4.4).

$$\begin{aligned} C_{VV}(t) &= \sum_{n,m} p_n \langle n | V_I(t) V_I(0) | n \rangle \\ &= \sum_{n,m} p_n |V_{nm}|^2 e^{\mathrm{i}\omega_{nm}t} \end{aligned} \tag{13.5.11}$$

Now, following eq. (14.4.11), we can Fourier transform this time-correlation function and apply the delta function identity, eq. (13.5.4), to obtain the frequency-domain correlation function:

$$\begin{aligned} \tilde{C}_{VV}(\omega) &= \sum_{n,m} p_n |V_{nm}|^2 \int_{-\infty}^{+\infty} dt\, e^{\mathrm{i}\omega t} e^{-\mathrm{i}\omega_{mn}t} \\ &= \sum_{n,m} p_n |V_{nm}|^2 \delta(\omega_{mn} - \omega) \end{aligned} \tag{13.5.12}$$

Comparing this expression with eq. (13.5.2), we find that one can calculate average transition rates between two states from a correlation function. This is done by Fourier transforming the time-correlation function and evaluating the resulting frequency domain correlation function at the energy gap between the initial and final states:

$$\bar{w}_{mn} = \frac{1}{\hbar^2} \tilde{C}_{VV}(\omega_{mn}) \tag{13.5.13}$$

We can apply the same reasoning to describe the rates of transition induced by a harmonic perturbation which we derived earlier:

$$\bar{w}_{k\ell} = \frac{\pi}{2\hbar^2} \sum_{\ell,k} p_\ell |V_{k\ell}|^2 [\delta(\omega_{k\ell} - \omega) + \delta(\omega_{k\ell} + \omega)] \tag{13.5.14}$$

This results in a similar expression for the transition rate, again in terms of a Fourier transform over an interaction potential time-correlation function:

$$\begin{aligned} \bar{w} &= \frac{1}{\hbar^2} \int_{-\infty}^{+\infty} dt\, e^{-\mathrm{i}\omega t} \langle V_I(0) V_I(t) \rangle \\ &= \frac{1}{\hbar^2} \int_{-\infty}^{+\infty} dt\, e^{\mathrm{i}\omega t} \langle V_I(t) V_I(0) \rangle \end{aligned} \tag{13.5.15}$$

We will look at this closer at the consequences for spectroscopy in the following chapter.

This page titled 13.5: Transition Rates from Time Correlation Functions is shared under a CC BY-NC-SA 4.0 license and was authored, remixed, and/or curated by Andrei Tokmakoff via source content that was edited to the style and standards of the LibreTexts platform.

13.6: Appendix- Weiner-Khinchin Theorem and the Power Spectrum

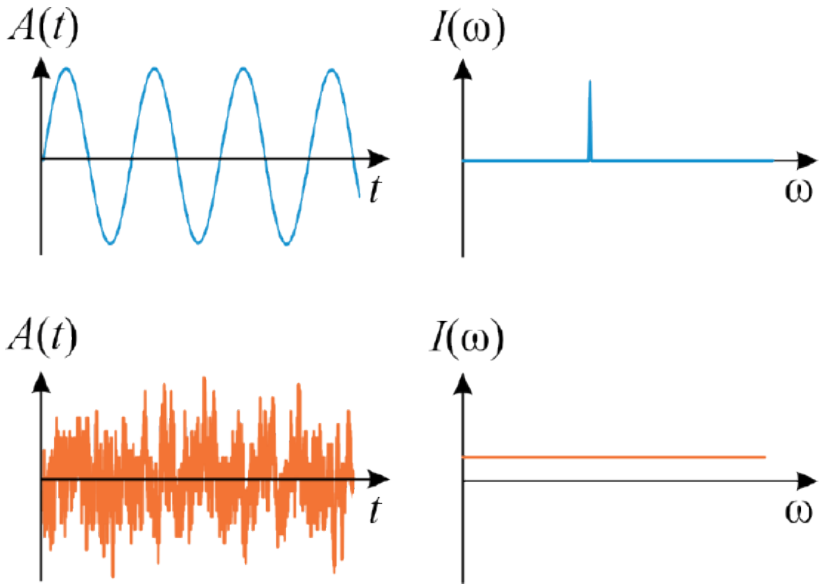


Figure 13.6.1: The time-dependence and power spectrum of a periodic process (top) and white noise (bottom).

For a stationary random process or simple periodic motion, the dynamical variable will fluctuate about an average value. As a result, the trajectory $A(t)$ can be represented in the frequency domain through Fourier analysis. The existence of a Fourier transform requires that the process $A(t)$ has finite energy, and therefore $\int_{-\infty}^{\infty} |A(t)|^2 \, dt$ is finite. The power spectrum of such a process $I(\omega)$ shows how the power associated with $A(t)$ is distributed among different frequency components of the signal. Wiener–Khinchin theorem states that the power spectrum of a stationary random process can be expressed in terms of the autocorrelation function of the Fourier transform of the autocorrelation function of $A(t)$:

$$C_{AA}(t) = \langle A^*(0)A(t)\rangle \tag{13.6.1}$$

$$I(\omega) = \left\langle |A(\omega)|^2 \right\rangle = \int_{-\infty}^{\infty} C_{AA}(t) e^{i\omega t} \, dt \tag{13.6.2}$$

Furthermore, the integrated power is equal whether calculated in the time or frequency domain (Parseval's theorem):

$$\int_{-\infty}^{\infty} |A(t)|^2 \, dt = \frac{1}{2\pi} \int_{-\infty}^{\infty} |A(\omega)|^2 \, d\omega \tag{13.6.3}$$

The power spectrum of a single, purely sinusoidal process will be a delta function with a height determined by the modulation amplitude of the signal (Figure 14.6.1). "White-noise" refers to the case in which the power spectrum is flat across all frequencies; i.e., there is no spectral correlation to the power spectrum

$$\left\langle |A(\omega)|^2 \right\rangle = \langle A(\omega) A(\omega')\rangle \, \delta(\omega - \omega') \tag{13.6.4}$$

$$\langle A(\omega)\rangle = 0 \tag{13.6.5}$$

In general, "noise" implies a random and unpredictable (or stochastic) nature to the process. In general, physical processes arise from atomic and molecular motions that have specific dynamical timescales and the power spectrum is characteristic of those dynamics in much the same way that a correlation function is.

Derivation of Weiner-Khinchin Theorem

Let's demonstrate that the power spectrum for stochastic stationary fluctuations $A(t)$ is given by the Fourier transform of the correlation function for the observed variable:

$$I_{AA}(\omega) = \int_{-\infty}^{\infty} C_{AA}(t)\, e^{\mathrm{i}\omega t}\, dt \tag{13.6.6}$$

where $I_{AA}(\omega) = \left\langle |A(\omega)|^2 \right\rangle$. We start with the observation that one can Fourier analyze the frequency components in $A(t)$ over time with

$$A(\omega) = \lim_{T\to\infty} \frac{1}{T} \int_0^T A(t)\, e^{\mathrm{i}\omega t}\, dt \tag{13.6.7}$$

The power spectrum is given by the integral:

$$I(\omega) = \langle A^*(\omega) A(\omega) \rangle = \lim_{T\to\infty} \frac{1}{T^2} \int_0^T dt_1 \int_0^T dt_2\, \overline{A^*(t_1) A(t_2)}\, \exp\left[-\mathrm{i}\omega\,(t_1 - t_2)\right] \tag{13.6.8}$$

Since this is a stationary process we can rewrite the correlation function in terms of the time interval

$$t_1 - t_2 = \tau \tag{13.6.9}$$

$$C_{AA}(\tau) = \langle A^*(t_1 - t_2) A(0) \rangle = \langle A^*(\tau) A(0) \rangle \tag{13.6.10}$$

To evaluate the integral, we break it into two parts: (1) for $t_1 > t_2$ and (2) for $t_1 < t_2$.

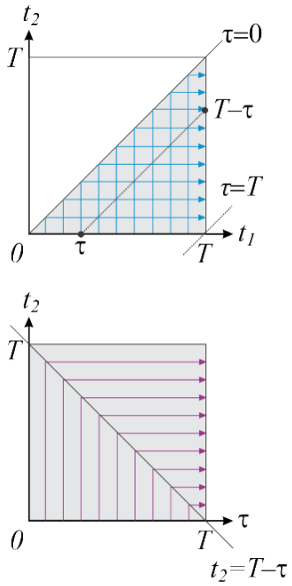


Figure 13.6.2: Illustration of the change of integration variables from t_1 and t_2 to t_2 and τ.

We start with integral (1) for $t_1 > t_2$, illustrated by the space shaded in Figure 14.6.2. To enforce the time-ordering, we change the limit on the first integral to t_1:

$$I^{(1)}(\omega) = \lim_{T\to\infty} \frac{1}{T^2} \int_0^T dt_1 \int_0^{t_1} dt_2\, C_{AA}(\tau) \exp[-\mathrm{i}\omega\tau] \tag{13.6.11}$$

Then we change integration variables from t_1 and t_2 to τ and t_2. Since $t_1 = \tau + t_2$, $dt_1 = d\tau$. Consider how the integration limits change. When $t_1 = T$ then $t_2 = T - \tau$, but when $t_1 = 0$, $t_2 = 0$ and $\tau = 0$, so the integration limits on t_2 are switched to

$$\begin{aligned} I^{(1)}(\omega) &= \lim_{T\to\infty}\frac{1}{T^2}\int_0^T d\tau \int_0^{T-\tau} dt_2\, C_{AA}(\tau)\exp[-\mathrm{i}\omega\tau] \\ &= \lim_{T\to\infty}\frac{1}{T^2}\int_0^T d\tau\,(T-\tau)C_{AA}(\tau)\exp[-\mathrm{i}\omega\tau] \\ &= \lim_{T\to\infty}\frac{1}{T}\int_0^T d\tau\left(1-\frac{\tau}{T}\right)C_{AA}(\tau)\exp[-\mathrm{i}\omega\tau] \end{aligned} \tag{13.6.12}$$

As long as $\lim_{t\to\infty} C_{AA}(t)$ decays to a constant so that the integral converges, then the limit $\lim_{T\to\infty}$ ensures that $(1-\frac{\tau}{T})\to 1$ and

$$I^{(1)}(\omega) = \lim_{T\to\infty}\frac{1}{T}\int_0^T d\tau\, C_{AA}(\tau)\exp[-\mathrm{i}\omega\tau] = \int_0^\infty d\tau\, C_{AA}(\tau)\exp[-\mathrm{i}\omega\tau] \tag{13.6.13}$$

This is the result for integral (1).

Now turning to integral (2), we have $t_2 > t_1$ and since τ is defined the same way it is always negative and varies from $-t_2$ to 0. We can express $\exp\left[-\mathrm{i}\omega\left(t_1-t_2\right)\right]$ in eq. (13.6.8) as $\exp\left[\mathrm{i}\omega\tau\right]$ and the correlation function as:

$$C_{AA} = \langle A^*(t_1-t_2)A(0)\rangle = \langle A^*(-\tau)A(0)\rangle = C_{AA}(-\tau) \tag{13.6.14}$$

Then, the integral we have is

$$I^{(2)}(\omega) = \lim_{T\to\infty}\frac{1}{T^2}\int_0^T dt_2\int_0^{t_2} dt_1\, C_{AA}(-\tau)\exp[\mathrm{i}\omega\tau] \tag{13.6.15}$$

Now, since t_1 precedes t_2 we change integration variables from t_1 and t_2 to τ and t_1, with $dt_2 = -d\tau$. Again, consider how the integration limits change. When $t_2 = T$ then $t_2 = T-\tau$, but when $t_1 = 0$, $t_2 = 0$ and $\tau = 0$, so the integration limits on t_1 are the same as we saw before:

$$\begin{aligned} I^{(2)}(\omega) &= \lim_{T\to\infty}\frac{1}{T^2}\int_0^T d\tau \int_0^{T-\tau} dt_1\, C_{AA}(-\tau)\exp[\mathrm{i}\omega\tau] \\ &= \lim_{T\to\infty}\frac{1}{T^2}\int_0^T d\tau\,(T-\tau)C_{AA}(-\tau)\exp[\mathrm{i}\omega\tau] \\ &= \int_0^\infty d\tau\, C_{AA}(-\tau)\exp[\mathrm{i}\omega\tau] \end{aligned} \tag{13.6.16}$$

This is the result for integral (2). Now we can add the results (1) and (2) together:

$$I(\omega) = \int_0^\infty d\tau\, C_{AA}(\tau)\exp[-\mathrm{i}\omega\tau] + \int_0^\infty d\tau\, C_{AA}(-\tau)\exp[\mathrm{i}\omega\tau] \tag{13.6.17}$$

Converting the second integral integration limits to $-\infty\to 0$ ($-\tau\to\tau$) we get

$$I(\omega) = \int_{-\infty}^\infty d\tau\, C_{AA}(\tau)\exp[-\mathrm{i}\omega\tau] \tag{13.6.18}$$

This isn't specific to how we defined τ, and it is equivalent to write $I(\omega) = \int_{-\infty}^{\infty} d\tau\ C_{AA}(\tau)\exp[\mathrm{i}\omega\tau]$.

This page titled 13.6: Appendix- Weiner-Khinchin Theorem and the Power Spectrum is shared under a CC BY-NC-SA 4.0 license and was authored, remixed, and/or curated by Andrei Tokmakoff via source content that was edited to the style and standards of the LibreTexts platform.

13.7: Readings

1. Berne, B. J. Time-Dependent Properties of Condensed Media. *Physical chemistry:an advanced treatise. Vol. 8B, Liquid state*; Eyring, H., Henderson, D., Jost, W., Eds.; Vol. 8B; Academic Press, 1971; pp 540-716.
2. Berne, B. J.; Pecora, R. *Dynamic Light Scattering: With applications to chemistry, biology, and physics*; R.E. Krieger Publishing Co., 1990.
3. Chandler, D. *Introduction to Modern Statistical Mechanics*; Oxford University Press, 1987.
4. Kubo, R.; Toda, M.; Hashitsume, N. *Statistical Physics II: Nonequilibrium Statistical Mechanics*, 2nd ed.; Springer Berlin Heidelberg, 1991. DOI: 10.1007/978-3-642-58244-8
5. Mazenko, G. *Nonequilibrium Statistical Mechanics*; Wiley-VCH, 2006. DOI: 10.1002/9783527618958
6. McHale, J. L. *Molecular Spectroscopy*, 1st ed.; Prentice-Hall, 1999.
7. McQuarrie, D. A. *Statistical Mechanics*; Harper & Row, 1976.
8. Mukamel, S. *Principles of Nonlinear Optical Spectroscopy*; Oxford University Press, 1995.
9. Schatz, G. C.; Ratner, M. A. *Quantum Mechanics in Chemistry*; Dover Publications, 2002.
10. Wang, C. H. *Spectroscopy of Condensed Media: Dynamics of Molecular Interactions*; Academic Press, 1985. DOI: 10.1016/B978-0-12-734780-6.X5001-8
11. Zwanzig, R. *Nonequilibrium Statistical Mechanics*; Oxford University Press, 2001. DOI: 10.1093/oso/9780195140187.001.0001

This page titled 13.7: Readings is shared under a CC BY-NC-SA 4.0 license and was authored, remixed, and/or curated by Andrei Tokmakoff via source content that was edited to the style and standards of the LibreTexts platform.

14: LINEAR RESPONSE THEORY

14.1: Classical Linear Response Theory
14.2: Example- Response of a damped harmonic oscillator
14.3: The Response Function and Energy Absorption
14.4: Quantum Linear Response Functions
14.5: Nonlinear response functions
14.6: Relaxation of a Prepared State
14.7: Example- Response of an abruptly shifted oscillator
14.8: Readings

This page titled 14: Linear Response Theory is shared under a CC BY-NC-SA 4.0 license and was authored, remixed, and/or curated by Andrei Tokmakoff via source content that was edited to the style and standards of the LibreTexts platform.

14.1: Classical Linear Response Theory

(1) Correlation functions provide a statistical description of the dynamics of molecular variables under equilibrium conditions, but it remains unclear how they are related to experimental observables. You have probably sensed this from the fact that correlation functions are *complex*, but observables must be real. Also, correlation functions describe equilibrium dynamics, but, realistically, acting on a system with external forces or potentials moves the system away from equilibrium, resulting in a non-equilibrium state. What happens as a result? These questions fall into the realm of nonequilibrium statistical mechanics, an area of active research for which formal theories are limited and approximation methods are the primary tools. Linear response theory is the primary approximation method, which describes the evolution away or toward equilibrium under perturbative conditions.

We will use linear response theory to describe an experimental observable. Specifically, this will tell us how an equilibrium system changes in response to an applied force. The real, observable quantity that will describe this is a *response function*. We will go on to show how it is related to correlation functions. Embedded in this discussion is a particularly important observation: when the changes away from equilibrium are small, the dynamics of the equilibrium system dictate the nonequilibrium response of the system! Thus, knowledge of equilibrium dynamics is useful in predicting the outcome of nonequilibrium processes.

So, the question is, "How does the system respond if you drive it away from equilibrium?" We will examine the case in which an equilibrium system, described by a Hamiltonian H_0, interacts weakly with an external agent, described by H_I. The system is moved away from equilibrium by the external agent, and the system absorbs energy from the external agent. How do we describe the time-dependent properties of the system? We first take the external agent to interact with the system through an internal, dynamical variable A, and the time-dependent action of the external agent is $f(t)$. The influence of the external agent on the system is linearly proportional to A, or $H_I = -f(t)A$. So, the Hamiltonian for this problem is given by

$$H = H_0 - f(t)A \tag{14.1.1}$$

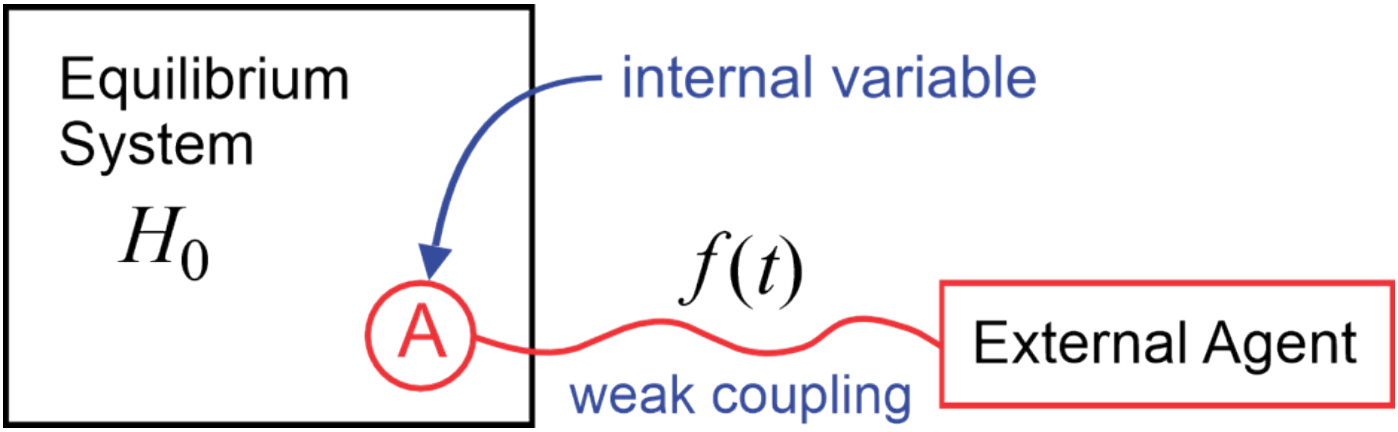


Figure 14.1.1: The linear response system-agent interaction.

Although our current discussion is for a classical Hamiltonian, one might already anticipate that this would be dealt with quantum mechanically in the interaction picture, with A being a system operator. Some examples may help put these variables in more concrete terms. For instance, if the internal variable is the position of a particle x, then $f(t)$ describes the time-dependent force being exerted on the particle. The internal variable may be the position, velocity, or angular momentum of charges or spins in the system interacting with an external electric or magnetic field. While H_I can typically be described as an external potential V, with $f = -\partial V/\partial A$ being an external force, the interaction of the external agent with the system can also be a kinetic energy coupling. Since H_I describes work being done on the system by the agent, this framework can also be used to think about the flow of heat into or out of the system.

Let's now consider the process of introducing the external agent to the system. The system described by H_0 is initially a thermally equilibrated ensemble, and the internal variable can be characterized by its ensemble average value $\langle A \rangle$. The external agent is then turned on at time t_0. We assume that the external agent has the same interaction H_I with each member of the ensemble, although initial states within the ensemble may vary. For $t > t_0$, the system begins moving away from equilibrium. The state of the internal variable is changing with time, but we can still statistically characterize it by averaging over the nonequilibrium ensemble. This average is designated $\overline{A(t)}$, and $\langle A \rangle \neq \overline{A}$ as a result of the interaction.

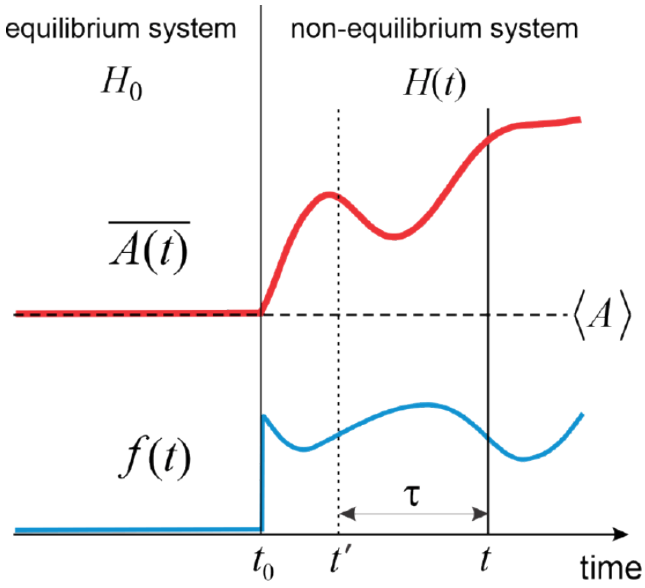


Figure 14.1.2: Illustration of the time-evolution of an internal variable A after applying an external agent at time t_0.

How do we formulate the behavior of $\overline{A(t)}$? For a weak interaction with the external agent, in which the magnitude of H_I is much smaller that the internal energies described by H_0, we can describe the non-equilibrium behavior $\overline{A(t)}$ by performing an expansion in powers of $f(t)$ about the equilibrium value $\langle A \rangle$. For small changes, the leading terms in such an expansion should capture most of the dynamics of $\overline{A(t)}$. The first two expansion terms are independent of f (zero-order terms) and linearly proportional to $f(t)$

$$\overline{A(t)} = \left(\text{terms } f^{(0)}\right) + \left(\text{terms } f^{(1)}\right) + \ldots \tag{14.1.2}$$

The leading term in this expansion is independent of f and should therefore be the initial average value $\langle A \rangle$. The remaining terms describe the deviation from equilibrium behavior at time t, that is

$$\delta\overline{A(t)} = \overline{A(t)} - \langle A \rangle \tag{14.1.3}$$

Linear response theory is concerned with describing the second term in eq. (14.1.2), in which the change in A is linearly proportional to f. Of course, describing $\overline{A(t)}$ for an arbitrary $f(t)$ means that we have to integrate over the full history of the time-dependent interactions with the system from t_0 to t. So, as a starting point we can express eq. (14.1.2) as

$$\overline{A(t)} = \langle A \rangle + \int_{t_0}^{t} dt' R(t,t') f(t') + \ldots \tag{14.1.4}$$

The right-hand side contains $R(t,t')$, the linear response function, which is sometimes denoted $\phi(t)$ or $\chi(t)$. This is the quantity that contains all microscopic information on the system's dynamics as it propagates from the point of application of the force t' to the point of observation of the system t. Describing R is the focus of our attention here. Note that the linear response assumption made in writing this equation is that the response function itself is only a function of A, not f. This allows it to be described entirely by the properties of the system, independent of the external agent. Also, since the response function is directly proportional to an observable internal variable, R must be a real function.

Properties of the response function

Even with the limited statements we have made to set up the problem, there are several properties that we can deduce about the response function:

1. Causal: Causality refers to the common-sense observation that the system cannot respond before the force has been applied. Therefore $R(t,t') = 0$ for $t' > t$, and t is the upper integration limit. Also, the system was initially at equilibrium, and we want to account for any possible time dependence to $f(t)$, so the lower integration limit is set as $t_0 = -\infty$. Then the time-dependent change in A is expressed by applying the integration limits to eq. (14.1.4):

$$\delta\overline{A(t)} = \overline{A(t)} - \langle A \rangle = \int_{-\infty}^{t} dt_0 \, R\left(t, t'\right) f(t') \tag{14.1.5}$$

While causality is implied by the integration limit, we can also make the statement of causality explicit by writing the linear response function as $\Theta\left(t - t'\right) R\left(t, t'\right)$, where we have introduced the unit step response function:

$$\Theta\left(t - t'\right) \equiv \begin{cases} 0 & \text{for } t < t' \\ 1 & \text{for } t \geq t' \end{cases} \tag{14.1.6}$$

2. Stationary: Similarly to our discussion of correlation functions, the time-dependence of the system only depends on the time interval between the application of a potential and the observation. Therefore, we write $R\left(t, t'\right) = R\left(t - t'\right)$, and eq. (14.1.5) becomes

$$\delta\overline{A(t)} = \int_{-\infty}^{t} dt' R\left(t - t'\right) f\left(t'\right) \tag{14.1.7}$$

Rather than using absolute time points, we define the time interval $\tau = t - t'$, which allows us to write (14.1.7) as

$$\delta\overline{A(t)} = \int_{0}^{\infty} d\tau \, R(\tau) f\left(t - \tau\right) \tag{14.1.8}$$

This expression says that the observed response is a convolution of the system's material response and the applied force's time-development.

3. Impulse response: Note that if one applies a delta function perturbation:

$$f(t) = f_0 \, \delta\left(t - t_0\right) \tag{14.1.9}$$

then the observed change in eq. (14.1.8) is directly proportional to the response function

$$\delta\overline{A(t)} = f_0 \, R\left(t - t_0\right) \tag{14.1.10}$$

Thus, R is often referred to as the *impulse response function*. An impulse response kicks the system away from the equilibrium established under H_0, so $R(\tau)$ will always rise from zero. Since the time-evolution for $t > t_0$ is under H_0, $\overline{A(t)}$ will always return to $\langle A \rangle$, and $R(\tau)$ will ultimately return to zero. In other words, $R(\tau)$ will be a function that can be expanded in sines. This means the response to an arbitrary $f(t)$ can be described through a Fourier analysis, suggesting that a spectral representation of the response function would be useful.

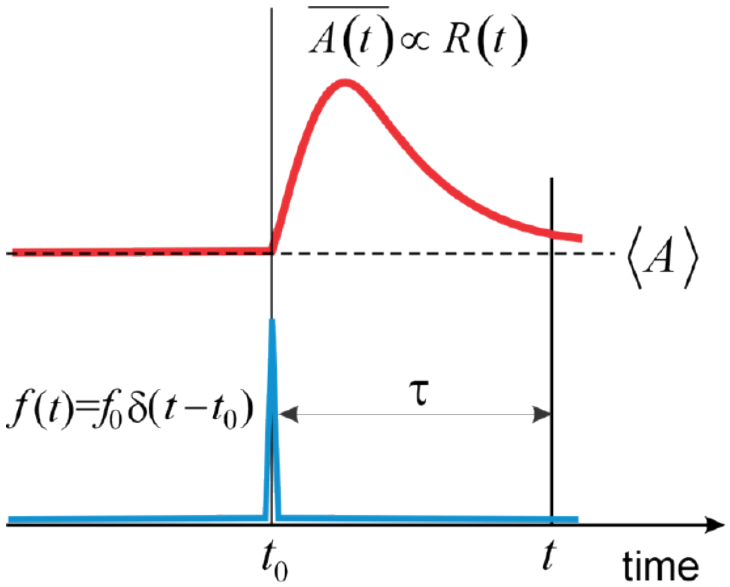


Figure 14.1.3: Impulse perturbation experiment.

The susceptibility

Since the observed temporal behavior of the nonequilibrium system is only linearly dependent on $f(t)$, the time-dependence of $\overline{A(t)}$ can be Fourier analyzed. There are incentives to express the response function in the frequency domain as a spectral response function, or *susceptibility*, $\chi(\omega)$. We start with eq. (14.1.8) and Fourier transform both sides:

$$\begin{aligned}\delta\overline{A(\omega)} &\equiv \int_{-\infty}^{+\infty} dt\, \delta\overline{A(t)} e^{\mathrm{i}\omega t} \\ &= \int_{-\infty}^{+\infty} dt \left[\int_0^{\infty} d\tau\, R(\tau) f(t-\tau)\right] e^{\mathrm{i}\omega t}\end{aligned} \tag{14.1.11}$$

Now we insert $e^{-\mathrm{i}\omega\tau} e^{+\mathrm{i}\omega\tau} = 1$ and collect terms in τ and t to find

$$\delta\overline{A(\omega)} = \int_{-\infty}^{+\infty} dt \int_0^{\infty} d\tau\, R(\tau) f\,(t-\tau)\, e^{\mathrm{i}\omega(t-\tau)} e^{\mathrm{i}\omega\tau} \tag{14.1.12}$$

$$= \int_{-\infty}^{+\infty} dt' e^{\mathrm{i}\omega t'} f(t') \int_0^{\infty} d\tau\, R(\tau) e^{\mathrm{i}\omega\tau} \tag{14.1.13}$$

or

$$\delta\overline{A(\omega)} = f(\omega)\tilde{\chi}(\omega) \tag{14.1.14}$$

In eq. (14.1.13) we switched variables, setting $t' = t - \tau$. The first term in eq. (14.1.14), $f(\omega)$, is a frequency domain power spectrum of the driving force, obtained from the Fourier transform of $f(t')$. The second term, $\chi(\omega)$, is the susceptibility, which is defined as the Fourier-Laplace transform (single-sided Fourier transform) of the impulse response function. Switching between time and frequency domains shows that a convolution of the force and response function in time, eq. (14.1.8), leads to the product of the force and susceptibility spectra in frequency, eq. (14.1.14). This is a manifestation of the convolution theorem, which states that a convolution of time-domain functions is the same as multiplying their Fourier transforms and performing an inverse Fourier transform on the product:

$$A(t) \otimes B(t) \equiv \int_{-\infty}^{\infty} d\tau\, A\,(t-\tau)\, B(\tau) = \int_{-\infty}^{\infty} d\tau\, A(\tau) B\,(t-\tau) = \mathcal{F}^{-1}\left[\tilde{A}(\omega)\tilde{B}(\omega)\right] \tag{14.1.15}$$

Here $\otimes$ refers to convolution, $\tilde{A}(\omega) = \mathcal{F}[A(t)]$, $\mathcal{F}[\cdots]$ is a Fourier transform, and $\mathcal{F}^{-1}[\cdots]$ is an inverse Fourier transform.

Although $R(\tau)$ is a real function, the susceptibility $\tilde{\chi}(\omega)$ is complex. We can separate the real and imaginary parts as

$$\chi(\omega) = \chi'(\omega) + \mathrm{i}\chi''(\omega) \tag{14.1.16}$$

Since

$$\tilde{\chi}(\omega) = \int_0^{\infty} d\tau\, R(\tau) e^{\mathrm{i}\omega\tau} \tag{14.1.17}$$

and R is real, the real and imaginary contributions are obtained from cosine or sine transforms of the response functions

$$\chi' = \int_0^{\infty} d\tau\, R(\tau) \cos\omega\tau \tag{14.1.18}$$

$$\chi'' = \int_0^{\infty} d\tau\, R(\tau) \sin\omega\tau \tag{14.1.19}$$

From this we find that χ' and χ'' are even and odd functions of frequency

$$\chi'(\omega) = \chi'(-\omega) \tag{14.1.20}$$

$$\chi''(\omega) = -\chi''(-\omega) \tag{14.1.21}$$

and the complex susceptibility has the property

$$\tilde{\chi}(-\omega) = \tilde{\chi}^*(\omega) \tag{14.1.22}$$

Notice also that eq. (14.1.22) allows us to write the real and imaginary form as

$$\chi'(\omega) = \frac{1}{2}\left[\tilde{\chi}(\omega) + \tilde{\chi}(-\omega)\right] \tag{14.1.23}$$

$$\chi''(\omega) = \frac{1}{2\mathrm{i}}\left[\tilde{\chi}(\omega) - \tilde{\chi}(-\omega)\right] \tag{14.1.24}$$

Examples of the relationships between χ' and χ'' are shown in Figure 14.1.4 for underdamped and overdamped oscillators.

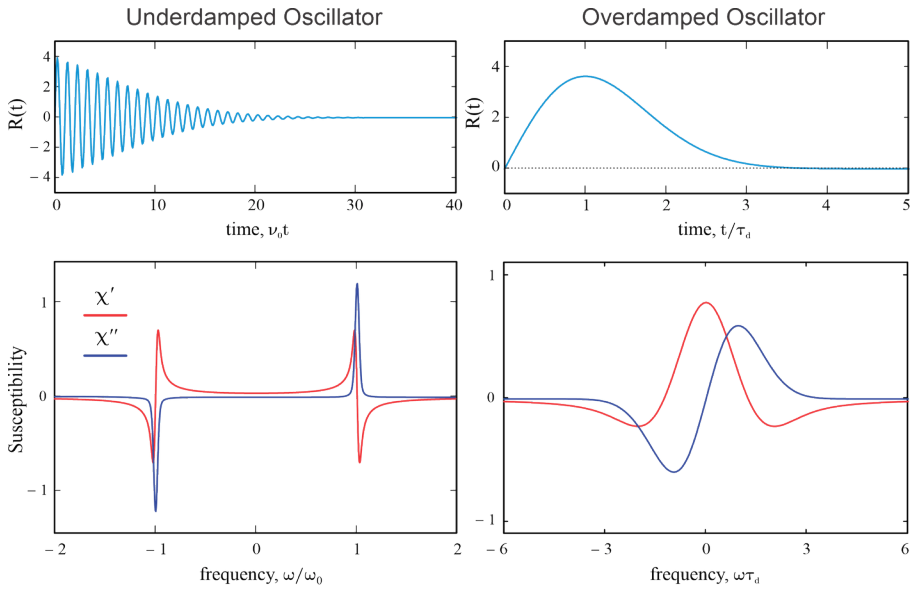


Figure 14.1.4: Examples of response functions and their corresponding real and imaginary susceptibilities. (Left) High frequency underdamped oscillator with time dependence $R(t) \sim \sin(\omega_0 t)\exp(-\gamma t)$. (Right) Example of a low frequency overdamped response function $R(t) \sim t\exp\left(-t^2/2\tau_d^2\right)$.

Kramers-Krönig relations

Since they are cosine and sine transforms of the same function, $\chi'(\omega)$ is not independent of $\chi''(\omega)$. The two are related by the Kramers–Krönig relationships:(2)

$$\chi'(\omega) = \frac{1}{\pi}\mathbb{P}\int_{-\infty}^{+\infty}\frac{\chi''(\omega')}{\omega' - \omega}\,d\omega' \tag{14.1.25}$$

$$\chi''(\omega) = -\frac{1}{\pi}\mathbb{P}\int_{-\infty}^{+\infty}\frac{\chi'(\omega')}{\omega' - \omega}\,d\omega' \tag{14.1.26}$$

where $\mathbb{P}$ is the principal part of the integral. These are obtained by substituting the inverse sine transform of eq. (14.1.19) into eq. (14.1.18):

$$\begin{aligned}\chi'(\omega) &= \frac{1}{\pi}\int_0^{\infty} dt\cos\omega t\int_{-\infty}^{+\infty}\chi''(\omega')\sin\omega' t\,d\omega' \\ &= \frac{1}{\pi}\lim_{L\to\infty}\int_{-\infty}^{+\infty}d\omega'\,\chi''(\omega')\int_0^{L}\cos\omega t\sin\omega' t\,dt\end{aligned} \tag{14.1.27}$$

Using $\cos ax\sin bx = \frac{1}{2}\sin(a+b)x + \frac{1}{2}\sin(b-a)x$, this can be written as

$$\chi'(\omega) = \frac{1}{\pi}\lim_{L\to\infty}\mathbb{P}\int_{-\infty}^{+\infty}d\omega'\,\chi''(\omega)\frac{1}{2}\left[\frac{-\cos(\omega'+\omega)L + 1}{\omega'+\omega} - \frac{\cos(\omega'-\omega)L + 1}{\omega'-\omega}\right] \tag{14.1.28}$$

If we choose to evaluate the limit $L\to\infty$, the cosine terms are hard to deal with, but we expect they will vanish since they oscillate

rapidly. We can instead average eq. (14.1.28) over a single cycle $L = 2\pi/(\omega' - \omega)$ to obtain eq. (14.1.25). The other relation can be derived in a similar way. Note that the Kramers-Krönig relationships are another consequence of causality, which dictated the lower limit of $t_0 = 0$ on the first integral evaluated above.

Equations (14.1.25) and (14.1.26) are often represented in a different way that only relies on integrating over positive frequencies. If we separate the integrals into two parts, one over negative frequencies and the second over positive frequencies, then we can use $\chi''(\omega) = -\chi''(-\omega)$ to write eq. (14.1.25) as

$$\begin{aligned}\chi'(\omega) &= \frac{1}{\pi}\int_0^{+\infty}\frac{\chi''(\omega')}{\omega' - \omega}\,d\omega' + \frac{1}{\pi}\int_{-\infty}^{0}\frac{\chi''(\omega')}{\omega' - \omega}\,d\omega' \\ &= \frac{1}{\pi}\int_0^{+\infty}\chi''(\omega')\left(\frac{1}{\omega' - \omega} - \frac{1}{-\omega' - \omega}\right)d\omega' \\ \chi'(\omega) &= \frac{2}{\pi}\int_0^{\infty}\chi''(\omega')\frac{\omega'}{\omega'^2 - \omega^2}\,d\omega'\end{aligned} \tag{14.1.29}$$

The same approach gives the inverse relation as

$$\chi''(\omega) = -\frac{2\omega}{\pi}\int_0^{\infty}\chi'(\omega')\frac{1}{\omega'^2 - \omega^2}\,d\omega' \tag{14.1.30}$$

In practice, these relationships are difficult to apply. For instance, if one would like to accurately obtain the real susceptibility from the imaginary, one must measure χ'' over all applicable frequencies. For molecular condensed phases, this could span from the megahertz radio frequency range to the x-ray regime.

References

(1) Jensen, J.; Mackintosh, A. R. Linear Response Theory. *Rare Earth Magnetism: Structures and Excitations*; The International Series of Monographs on Physics, Clarendon Press, Oxford University Press, 1991; pp 134-162. DOI: 10.1093/oso/9780198520276.003.0003

(2) Nitzan, A., *Chemical Dynamics in Condensed Phases*. Oxford University Press: New York, 2006, pp 411-412.

This page titled 14.1: Classical Linear Response Theory is shared under a CC BY-NC-SA 4.0 license and was authored, remixed, and/or curated by Andrei Tokmakoff via source content that was edited to the style and standards of the LibreTexts platform.

14.2: Example- Response of a damped harmonic oscillator

Response Function

To calculate and apply a response function practically, we return to the driven harmonic oscillator, which we discussed in the classical model of spectroscopy. The equation of motion for a forced damped harmonic oscillator is:

$$\ddot{x} - \gamma\dot{x} + \omega_0^2 x = \frac{f(t)}{m} \tag{14.2.1}$$

$f(t)$ is the time-dependent external driving force, x is the internal coordinate, γ is the damping constant, and $\omega_0 = \sqrt{k/m}$ is the natural frequency of the oscillator.

Although $f(t)$ has an arbitrary form, to determine the response function for the position of the damped harmonic oscillator, we seek a solution to eq. (14.2.1) using an impulsive driving force: $f(t) = f_0\delta(t - t_0)$ because this results in the time-dependent position being directly proportional to the response function, $x(t) = f_0 R_{xx}(t)$. has an analytical solution for $x(t)$, from which we obtain

$$R_{xx}(\tau) = \Theta(\tau)\frac{1}{m\Omega}\exp\left(-\frac{\gamma}{2}\tau\right)\sin\Omega\tau \tag{14.2.2}$$

The reduced frequency Ω is defined as

$$\Omega = \sqrt{\omega_0^2 - \gamma^2/4} \tag{14.2.3}$$

As illustrated in Figure 14.2.1a, the response function displays weakly-damped oscillations as $\sin\Omega\tau$, which is expected because response functions should rise from $R_x(0) = 0$.

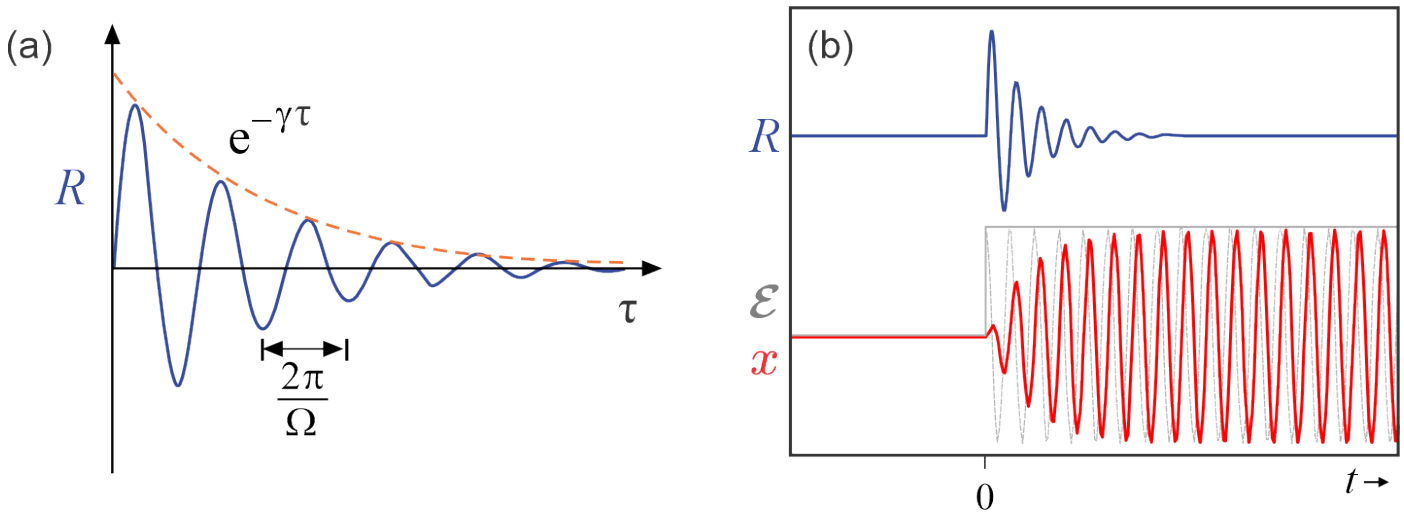


Figure 14.2.1: (a) Response function for damped harmonic oscillator. (b) Illustration of time-domain response of the driven oscillator $x(t)$ in red when driven on resonance, $\omega = \Omega$, by an oscillating driving force in grey.

We can calculate the behavior of the oscillator after turning on a sinusoidal driving field. If x represents the position of a particle with charge q, and we abruptly apply a time-dependent electric field, $E(t) = \Theta(t)E_0\cos\omega t$, the driving force on the particle is $f(t) = qE(t)$. Then the response of the oscillator is given by

$$x(t) = \int_0^\infty d\tau\, R_{xx}(\tau) f(t - \tau) \tag{14.2.4}$$

Figure 14.2.1a shows the calculation of this integral alongside the response function and the driving field. Although the field is applied instantaneously at $t = 0$, the oscillator only gradually reaches steady state oscillatory behavior, changing on the time-

scale of the damping of the response function. Also note that the sine oscillations of $x(t)$ are $90\,^{\circ}$ phase shifted from the cosine oscillations of $f(t)$.

Susceptibility

Using eq. (14.2.2), we evaluate eq. (14.1.17) and obtain the susceptibility

$$\chi(\omega) = \frac{1}{m\left(\omega_0^2 - \omega^2 - \mathrm{i}\gamma\omega\right)} \tag{14.2.5}$$

Which we can separate into an imaginary component:

$$\chi''(\omega) = \frac{\gamma\omega}{m\left[\left(\omega_0^2 - \omega^2\right)^2 + \gamma^2\omega^2\right]} \tag{14.2.6}$$

and a real part:

$$\chi'(\omega) = \frac{\omega_0^2 - \omega^2}{m\left[\left(\omega_0^2 - \omega^2\right)^2 + \gamma^2\omega^2\right]} \tag{14.2.7}$$

Note that the denominators in these expressions exhibit two resonances: one for positive frequencies where $\omega \approx \omega_0$ and one for negative frequencies with $\omega \approx -\omega_0$. The real and imaginary components are illustrated in Figure 14.2.2a, showing that positive and negative frequencies are related as $\chi'(-\omega) = \chi'(\omega)$ and $\chi''(-\omega) = -\chi''(\omega)$.

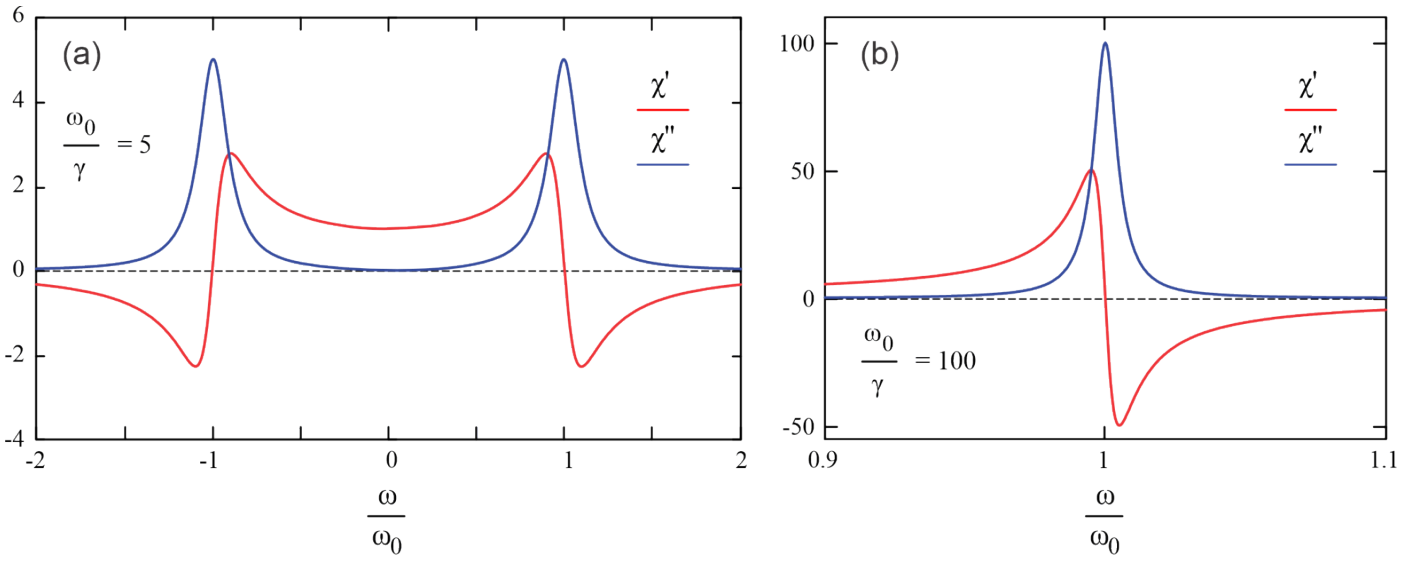


Figure 14.2.2: (a) Real and imaginary parts of the driven oscillator susceptibility. (b) Real and imaginary parts of the susceptibility in the weak damping (near resonance) approximation. Note the difference in frequency axes.

For the case of weak damping $\gamma \ll \omega_0$, which is commonly encountered in molecular spectroscopy, eq. (14.2.5) is written as a Lorentzian lineshape using the near-resonance approximation:

$$\begin{aligned} \omega^2 - \omega_0^2 &= (\omega + \omega_0)(\omega - \omega_0) \\ &\approx \begin{cases} 2\omega(\omega - \omega_0) & \omega > 0 \\ -2\omega(\omega_0 + \omega) & \omega < 0 \end{cases} \end{aligned} \tag{14.2.8}$$

For positive frequencies,

$$\chi(\omega) \approx \frac{1}{2m\omega_0}\frac{1}{\omega - \omega_0 + i\gamma/2} \qquad \omega > 0 \tag{14.2.9}$$

Then the imaginary part of the susceptibility shows a symmetric lineshape, with a linewidth of γ at full width at half maximum

(Figure 14.2.2b).

$$\chi''(\omega) \approx \frac{1}{2m\omega_0} \frac{\gamma}{(\omega - \omega_0)^2 + \gamma^2/4} \tag{14.2.10}$$

$$\chi'(\omega) \approx \frac{1}{m\omega_0} \frac{(\omega - \omega_0)}{(\omega - \omega_0)^2 + \gamma^2/4} \tag{14.2.11}$$

This page titled 14.2: Example- Response of a damped harmonic oscillator is shared under a CC BY-NC-SA 4.0 license and was authored, remixed, and/or curated by Andrei Tokmakoff via source content that was edited to the style and standards of the LibreTexts platform.

14.3: The Response Function and Energy Absorption

Let's investigate the relationship between the linear response function and the absorption of energy from the external agent. The external agent performs work on the internal variable A, and the energy needed to move A from equilibrium is ultimately dissipated into other system degrees of freedom. We can calculate the rate of energy absorption, averaged over the nonequilibrium ensemble, from the time-derivative in the expectation value of the Hamiltonian

$$\begin{aligned}\mathcal{P}_{\text{abs}} &= \frac{\partial \bar{H}}{\partial t} = -\frac{\partial f}{\partial t}\overline{A(t)} \\ &= \frac{\partial f(t)}{\partial t}\left[\langle A\rangle + \int_0^\infty d\tau\, R_{AA}(\tau) f\,(t-\tau)\right]\end{aligned} \tag{14.3.1}$$

For this example, we take the internal variable to be a dipole moment μ and the external agent to be an electromagnetic field $\mathcal{E}$, and we will relate $\dot{E}$ to the absorption cross-section σ. The Hamiltonian is

$$H = H_0 - f(t)A = H_0 - \mathcal{E}(t)\mu \tag{14.3.2}$$

We assume that the system is driven by a monochromatic electromagnetic field with a time dependence given by

$$f(t) = \mathcal{E}_0 \cos\omega t = \frac{1}{2}\left[\mathcal{E}_0 e^{-\mathrm{i}\omega t} + \mathcal{E}_0^* e^{\mathrm{i}\omega t}\right] \tag{14.3.3}$$

With such a field, energy will flow in and out of the system as it oscillates, so to obtain a time-averaged rate of energy absorption, we will want to cycle average eq. (14.3.1) over a period T:

$$\overline{\mathcal{P}}_{\text{abs}} = \frac{1}{T}\int_0^T dt\, \frac{\partial \mathcal{E}(t)}{\partial t}\left[\langle\mu\rangle + \int_0^\infty d\tau\, R_{\mu\mu}(\tau) f\,(t-\tau)\right] \tag{14.3.4}$$

There are two terms in the integral. Over many oscillations of the field, the first term here averages to zero, since $\langle A\rangle$ is constant. Inserting eq. (14.3.3) into the second term results in a transformation of the response function into a susceptibility:

$$\frac{1}{2}\int_0^\infty d\tau\, R(\tau)\left[\mathcal{E}_0 e^{-\mathrm{i}\omega(t-\tau)} + \mathcal{E}_0^* e^{\mathrm{i}\omega(t-\tau)}\right] = \frac{1}{2}\left[\mathcal{E}_0 e^{-\mathrm{i}\omega t}\chi(\omega) + \mathcal{E}_0^* e^{\mathrm{i}\omega t}\chi(-\omega)\right] \tag{14.3.5}$$

By differentiating (14.3.3) and inserting both it and (14.3.5) into eq. (14.3.4), we obtain

$$\overline{\mathcal{P}}_{\text{abs}} = -\frac{1}{4T}\int_0^T dt\, \left[-\mathrm{i}\omega\mathcal{E}_0 e^{-\mathrm{i}\omega t} + \mathrm{i}\omega\mathcal{E}_0^* e^{\mathrm{i}\omega t}\right]\left[\mathcal{E}_0 e^{-\mathrm{i}\omega t}\chi(\omega) + \mathcal{E}_0^* e^{\mathrm{i}\omega t}\chi(-\omega)\right] \tag{14.3.6}$$

The result is four terms, of which two oscillate at 2ω and two at zero frequency. Then we average this expression over one cycle of the field, setting $T = 2\pi/\omega$. The 2ω terms in the integral vanish, and the zero-frequency terms are retained because $\frac{1}{T}\int_0^T dt\ e^{-\mathrm{i}\omega t}e^{+\mathrm{i}\omega t} = 1$ and $\int_0^T dt\ e^{-\mathrm{i}\omega t}e^{-\mathrm{i}\omega t} = 0$.

The resulting rate of energy absorption from the field is given by

$$\begin{aligned}\overline{\mathcal{P}}_{\text{abs}} &= \frac{\mathrm{i}}{4}\omega\left|\mathcal{E}_0\right|^2\left[\chi(-\omega) - \chi(\omega)\right] \\ &= \frac{\omega}{2}\left|\mathcal{E}_0\right|^2\chi''(\omega)\end{aligned} \tag{14.3.7}$$

Hence the absorption of energy by the system is proportional to the imaginary part of the susceptibility. Now, from the intensity of the incident field, $I = \frac{1}{2}\varepsilon_0 c\mathcal{E}_0^2$, the absorption cross-section is

$$\sigma(\omega) = \frac{\overline{\mathcal{P}}_{\text{abs}}}{I} = \frac{\omega}{\varepsilon_0 c}\chi''(\omega) \tag{14.3.8}$$

This is a general result that is not specific to the current example. An external agent's interaction with an internal variable induces energy absorption in the system that is proportional to the imaginary part of the susceptibility. Although it is not addressed in the derivation, the energy absorbed must ultimately be dissipated into the system degrees of freedom. Therefore χ'' is also

associated with describing the dissipation of energy.

Next, let's relate the imaginary part of the susceptibility to the underlying correlation function $C_{AA}(t)$. Using the definition of $\chi''(\omega)$, eq. (15.1.24), the relation of the complex susceptibility to the response function, eq. (15.1.17), $\tilde{\chi}(\omega) = \int_0^\infty d\tau\ R(\tau)e^{i\omega\tau}$, and the relationship of $R(\tau)$ to the imaginary part of $C_{AA}(t)$, one can show

$$\begin{aligned}\chi''(\omega) &= \frac{1}{2\hbar}\left[\int_{-\infty}^{\infty} d\tau \left(C_{AA}(\tau) - C_{AA}\left(-\tau\right)\right) e^{i\omega\tau}\right] \\ &= \frac{1}{2\hbar}\left(C_{AA}(\omega) - C_{AA}(-\omega)\right)\end{aligned} \tag{14.3.9}$$

That is, $\chi''(\omega)$ is proportional to the difference in Fourier transform power spectra for the correlation function $C_{AA}(t)$ evaluated at ω and $-\omega$. These terms are related by the detailed balance expression $C_{AA}(-\omega) = e^{-\beta\hbar\omega}C_{AA}(\omega)$, and therefore

$$\chi''(\omega) = \frac{1}{2\hbar}C_{AA}(\omega)\left(1 - e^{-\beta\hbar\omega}\right) \tag{14.3.10}$$

This page titled 14.3: The Response Function and Energy Absorption is shared under a CC BY-NC-SA 4.0 license and was authored, remixed, and/or curated by Andrei Tokmakoff via source content that was edited to the style and standards of the LibreTexts platform.

14.4: Quantum Linear Response Functions

To develop a quantum description of the linear response function, we start by recognizing that the response of a system to an applied external agent is a problem we can solve in the interaction picture. Our time-dependent Hamiltonian is the same as before:

$$H(t) = H_0 - f(t)\hat{A} = H_0 + V(t) \tag{14.4.1}$$

H_0 is the material Hamiltonian for the equilibrium system. The external agent acts on the equilibrium system through $\hat{A}$, an operator in the system states, with a time-dependence described by $f(t)$. We take $V(t)$ to induce only small changes and treat this problem with perturbation theory in the interaction picture.

We want to describe the nonequilibrium response $\overline{A(t)}$, which we will get by ensemble averaging the time-dependent expectation value of $\hat{A}(t)$. Remember, the expectation value for a pure state in the interaction picture is

$$\begin{aligned} \langle A(t)\rangle &= \langle \psi_I(t)|\, A_I(t)\, |\psi_I(t)\rangle \\ &= \langle \psi_0|\, U_I^\dagger A_I U_I\, |\psi_0\rangle \end{aligned} \tag{14.4.2}$$

and the interaction picture Hamiltonian corresponding to eq. (14.4.1) is

$$\begin{aligned} V_I(t) &= U_0^\dagger(t) V(t) U_0(t) \\ &= -f(t) A_I(t) \end{aligned} \tag{14.4.3}$$

with

$$A_I(t) = U_0^\dagger \hat{A} U_0 \tag{14.4.4}$$

Equation (14.4.2) shows us that the nonequilibrium state of the system—characterized by $|\psi_I(t)\rangle$—can be related to the initial state of the system $|\psi_0\rangle$ through the time-propagator. Thus the nonequilibrium expectation value $\overline{A(t)}$ can be obtained by performing an equilibrium average over the expectation value of $U_I^\dagger A_I U_I$ in (14.4.2):

$$\overline{A(t)} = \sum_n p_n \langle n|\, U_I^\dagger A_I U_I\, |n\rangle \tag{14.4.5}$$

Here, $|n\rangle$ are eigenstates of H_0. Working with the first-order solution to $U_I(t)$

$$U_I(t - t_0) = 1 + \frac{\mathrm{i}}{\hbar}\int_{t_0}^{t} dt' f(t') A_I(t') \tag{14.4.6}$$

we can now calculate the value of the operator A at time t, integrating over the history of the applied interaction $f(t')$:

$$\begin{aligned} A(t) &= U_I^\dagger A_I U_I \\ &= \left\{1 - \frac{\mathrm{i}}{\hbar}\int_{t_0}^{t} dt' f(t') A_I(t')\right\} A_I(t) \left\{1 + \frac{\mathrm{i}}{\hbar}\int_{t_0}^{t} dt' f(t') A_I(t')\right\} \end{aligned} \tag{14.4.7}$$

We then expand this and retain only the leading term, which is independent of $f(t')$, plus the two terms that are linear in f:

$$\begin{aligned} A(t) &\cong A_I(t) + \frac{\mathrm{i}}{\hbar}\int_{t_0}^{t} dt' f(t') \left\{A_I(t) A_I(t') - A_I(t') A_I(t)\right\} \\ &= A_I(t) + \frac{\mathrm{i}}{\hbar}\int_{t_0}^{t} dt' f(t') \left[A_I(t), A_I(t')\right] \end{aligned} \tag{14.4.8}$$

Since f is only the time-dependence of the external agent and commutes with A, we were able to factor it out in the second term. This leaves the difference between two products of operators that differ in their time ordering. The stationary properties of the time-evolution operator mean that we can re-write the commutator: $[A_I(t), A_I(t')] = [A_I(t - t'), A_I(0)]$. We then switch variables from t' to the time interval $\tau = t - t'$. Since we are interested in describing a system initially at equilibrium, we also set $t_0 = -\infty$. Then eq. (14.4.8) can be re-written as

$$A(t) = A_I(t) + \frac{\mathrm{i}}{\hbar}\int_0^\infty d\tau\, f(t-\tau)\,[A_I(\tau), A_I(0)] \tag{14.4.9}$$

This equation describes the time-evolution of the operator A for a pure state. We can now calculate the expectation value of A by performing the ensemble average described in eq. (14.4.5). Noting that the force is applied equally to each member of the ensemble, we obtain

$$\overline{A(t)} = \langle A\rangle + \frac{\mathrm{i}}{\hbar}\int_0^\infty d\tau\, f(t-\tau)\,\langle[A_I(\tau), A_I(0)]\rangle \tag{14.4.10}$$

The first term on the right-hand side is independent of f, so it comes from an equilibrium ensemble average for the expectation value of A:

$$\langle A(t)\rangle = \sum_n p_n \langle n\,|A_I|\,n\rangle = \langle A\rangle \tag{14.4.11}$$

The second term is just an equilibrium ensemble average over the commutator in $A_I(t)$:

$$\langle[A_I(\tau), A_I(0)]\rangle = \sum_n p_n \langle n\,|[A_I(\tau), A_I(0)]|\,n\rangle \tag{14.4.12}$$

Comparing eq. (14.4.10) with the expression for the linear response function, eq. (14.1.8), we find that the quantum linear response function is

$$R_{AA}(\tau) = \begin{cases} \frac{\mathrm{i}}{\hbar}\langle[A_I(\tau), A_I(0)]\rangle & \tau \geqslant 0 \\ 0 & \tau < 0 \end{cases} \tag{14.4.13}$$

It is sometimes written with the unit step function to enforce causality:

$$R_{AA}(\tau) = \frac{\mathrm{i}}{\hbar}\Theta(\tau)\,\langle[A_I(\tau), A_I(0)]\rangle \tag{14.4.14}$$

although the causal requirement that $\tau \geq 0$ will generally be taken as understood. The important thing to note is that, in a system under the influence of a weak external potential, the time-development is governed by the dynamics of the equilibrium system under H_0.

The linear response function is therefore proportional to the difference of two correlation functions with the order of the operators interchanged, i.e. the anti-symmetrized correlation function we discussed in the last chapter

$$R_{AA}(\tau) = \frac{\mathrm{i}}{\hbar}\Theta(\tau)\,\{\langle A_I(\tau)A_I(0)\rangle - \langle A_I(0)A_I(\tau)\rangle\} \tag{14.4.15}$$

As an observable quantity, we know that A is a Hermitian operator, and therefore $C_{AA}(-\tau) = C^*_{AA}(\tau)$. So, we can say that $R(\tau)$ is related to the imaginary part of the correlation function $C''(\tau)$

$$\begin{aligned} R_{AA}(\tau) &= \frac{\mathrm{i}}{\hbar}\Theta(\tau)\,(C_{AA}(\tau) - C_{AA}(-\tau)) \\ &= \frac{\mathrm{i}}{\hbar}\Theta(\tau)\,(C_{AA}(\tau) - C^*_{AA}(\tau)) \\ &= -\frac{2}{\hbar}\Theta(\tau)C''_{AA}(\tau) \end{aligned} \tag{14.4.16}$$

As we expect for an observable, the response function is real.

If we express the correlation function as an expansion in eigenstates,

$$C_{AA}(\tau) = \sum_{n,m} p_n\,|A_{mn}|^2\,e^{-\mathrm{i}\omega_{mn}\tau} \tag{14.4.17}$$

then

$$R_{AA}(\tau) = \frac{2}{\hbar}\Theta(\tau)\sum_{n,m} p_n \left|A_{mn}\right|^2 \sin\omega_{mn}\tau \tag{14.4.18}$$

We see that $R(\tau)$ can be expanded in sines—an odd function of time. This reflects that fact that the impulse response function (the deviation from equilibrium) must have a value of 0 at $t = t_0$ then move away from 0 at the point where the external potential is applied.

The same approach can be used to describe the response function in the density matrix formalism. Again, working in the interaction picture, we can calculate the non-equilibrium value of A after the application of the external agent. The density matrix representation of eq. (14.4.5) is

$$\overline{A(t)} = \mathrm{Tr}\left(A_I(t)\rho_I(t)\right) \tag{14.4.19}$$

To first order, the time-evolution of the density matrix in the interaction picture is

$$\rho_I(t) = \rho_I(t_0) - \frac{\mathrm{i}}{\hbar}\int_{t_0}^{t} dt' \left[V_I(t'), \rho_I(t_0)\right] \tag{14.4.20}$$

The initial state of the system is thermal equilibrium, so $\rho_I\left(t_0\right) = \rho_{\mathrm{eq}}$. Setting $t_0 = -\infty$ and substituting into eq. (14.4.19), we find that the change induced in the ensemble-averaged expectation value of A is

$$\begin{aligned}\delta\overline{A(t)} &= \mathrm{Tr}\left\{A_I(t)\left(\frac{-\mathrm{i}}{\hbar}\right)\int_{-\infty}^{t} dt'\left(-f(t')\right)\left[V_I(t'), \rho_{\mathrm{eq}}\right]\right\} \\ &= \int_{-\infty}^{t} dt' f(t')\frac{\mathrm{i}}{\hbar}\mathrm{Tr}\left\{A_I(t)\left[A_I(t'), \rho_{\mathrm{eq}}\right]\right\}\end{aligned} \tag{14.4.21}$$

Defining the time interval $\tau = t - t'$, and exchanging the order of operators, $A\left[B, C\right] = \left[A, B\right]C$,

$$\delta\overline{A(t)} = \frac{\mathrm{i}}{\hbar}\int_{0}^{\infty} d\tau\, f(t-\tau)\,\mathrm{Tr}\left(\left[A_I(\tau), A_I(0)\right]\rho_{\mathrm{eq}}\right) \tag{14.4.22}$$

This takes the same form as eq. (14.4.10), and we see that the linear response function is given by

$$R_{AA}(\tau) = \frac{\mathrm{i}}{\hbar}\Theta(\tau)\,\mathrm{Tr}\left(\left[A_I(\tau), A_I(0)\right]\rho_{\mathrm{eq}}\right) \tag{14.4.23}$$

This page titled 14.4: Quantum Linear Response Functions is shared under a CC BY-NC-SA 4.0 license and was authored, remixed, and/or curated by Andrei Tokmakoff via source content that was edited to the style and standards of the LibreTexts platform.

14.5: Nonlinear response functions

If the internal variable of the system does not respond linearly to the application of the external agent, the principles that we discussed in prior sections can be extended to include nonlinear terms, as long as the interaction remains perturbative. That is, we can include the expansion in higher orders of $f(t)$ in our description of $\overline{A(t)}$ in eq. (14.1.04), which will ultimately be implemented using higher order perturbation theory expansions.

To illustrate how this reasoning works, let's look at the second-order term in eq. (14.1.04):

$$\delta\overline{A(t)}^{(2)} = \int dt_1 \int dt_2\, R^{(2)}(t;t_1,t_2) f_1(t_1) f_2(t_2) \tag{14.5.1}$$

We can write the Hamiltonian as $H = H_0 - f_1(t_1)\hat{A} - f_2(t_2)\hat{A}$. Equation (14.5.1) is meant to account for changes to A caused by two external forces, f_1 and f_2, applied at times t_1 and t_2 on a system that was initially at equilibrium. These forces can be two distinct agents acting on the same variable, or by setting $f_1 = f_2$ we can simply be talking about a quadratic dependence of f on A. Again, the time-dependence of either $f_n(t)$ can be arbitrarily complex, and we will integrate over the entire history of the application of two external forces up to the time of observation t (Figure 14.5.1).

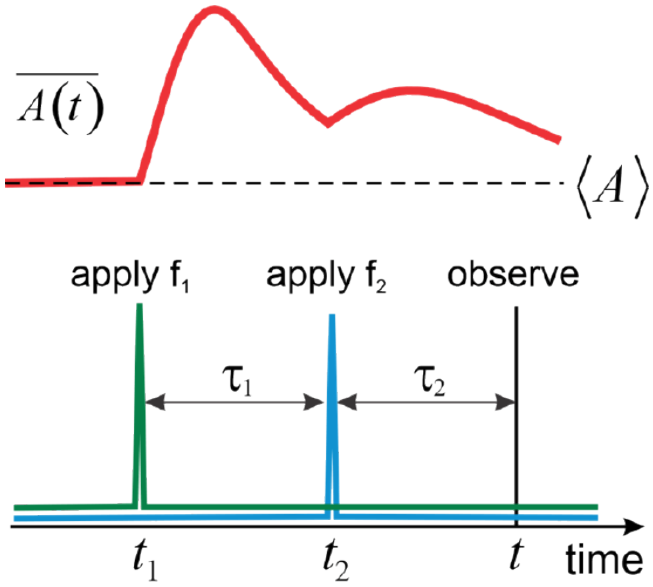


Figure 14.5.1: Variables describing the second order response of an internal variable to two independent impulses.

The second-order response function is formulated to enforce causality through a time ordering that requires (1) that all forces must be applied before a response is observed and (2) that the application of f_1 must precede f_2. That is, $t \geqslant t_2 \geqslant t_1$, which we enforce with the time-ordering of the integration limits. We will call the system stationary so that we are only concerned with the time intervals between consecutive interaction times. We expect that eq. (14.5.1) will take the form

$$\delta\overline{A(t)}^{(2)} = \int_{-\infty}^{t} dt_2 \int_{-\infty}^{t_2} dt_1\, R^{(2)}(t-t_2, t_2-t_1) f_1(t_1) f_2(t_2) \tag{14.5.2}$$

We define the intervals between adjacent interactions

$$\begin{aligned} \tau_1 &= t_2 - t_1 \\ \tau_2 &= t - t_2 \end{aligned} \tag{14.5.3}$$

Switching integration variables from t_1 and t_2 to τ_1 and τ_2, we find

$$\delta\overline{A(t)}^{(2)} = \int_0^{\infty} d\tau_1 \int_0^{\infty} d\tau_2\, R^{(2)}(\tau_1,\tau_2)\, f_1(t-\tau_1-\tau_2) f_2(t-\tau_2) \tag{14.5.4}$$

In this expression, the time arguments for f_1 and f_2 ensure the proper time ordering and that τ_1 preceeds τ_2.

We can follow most of the same reasoning as in Sec. 14.3, keeping terms to second order, to derive the quantum mechanical form of the second-order (nonlinear) response function. At this point, there are enough integrals and time-ordered operators to worry about in the derivation that it becomes easier to use a density matrix approach. We will again evaluate eq. (14.3.19), making use of the series expansion of the interaction picture density matrix. Taking the system to be initially at equilibrium, the expansion to second order is

$$\begin{aligned}\rho_I(t) &= \rho_{\text{eq}} - \frac{\text{i}}{\hbar}\int_{-\infty}^{t} dt_1\,[V_I(t_1),\rho_{\text{eq}}] + \left(\frac{-\text{i}}{\hbar}\right)^2 \int_{-\infty}^{t} dt_2 \int_{-\infty}^{t_2} dt_1\,[V_I(t_2),[V_I(t_1),\rho_{\text{eq}}]] + \ldots \\ &= \rho_I^{(0)} + \rho_I^{(1)} + \rho_I^{(2)} + \ldots\end{aligned} \tag{14.5.5}$$

The linear response function is obtained from $\rho_I^{(1)}$, while the second-order corrections to the changes in $A(t)$, denoted $\overline{A^{(2)}(t)}$, come from inserting $\rho_I^{(2)}$ into eq. (14.3.19):

$$\begin{aligned}\overline{A^{(2)}(t)} &= \text{Tr}\left(A_I(t)\rho_I^{(2)}(t)\right) \\ &= \text{Tr}\left\{A_I(t)\left(-\frac{\text{i}}{\hbar}\right)^2 \int_{-\infty}^{t} dt_2 \int_{-\infty}^{t_2} dt_1\,[A_I(t_2),[A_I(t_1),\rho_{\text{eq}}]]\,(-f_2(t_2))\,(-f_1(t_1))\right\} \\ &= \left(\frac{\text{i}}{\hbar}\right)^2 \int_{-\infty}^{t} dt_2 \int_{-\infty}^{t_2} dt_1\,\text{Tr}\left(A_I(t)\,[A_I(t_2),[A_I(t_1),\rho_{\text{eq}}]]\right) f_2(t_2) f_1(t_1)\end{aligned} \tag{14.5.6}$$

Switching time variables to the time intervals in eq. (14.5.3), we find:

$$\overline{A^{(2)}(t)} = \left(\frac{\text{i}}{\hbar}\right)^2 \int_0^{\infty} d\tau_2 \int_0^{\infty} d\tau_1\,\text{Tr}\left(A_I(t)\,[A_I(\tau_2),[A_I(\tau_1),\rho_{\text{eq}}]]\right) f_2\left(t-\tau_2\right) f_1\left(t-\tau_2-\tau_1\right) \tag{14.5.7}$$

Comparing this result with eq. (14.5.4), we can see that the second order response function is given by the nested commutator products within the trace. Rewriting the nested commutator products as

$$A_I(t)\,[A_I(\tau_2),[A_I(\tau_1),\rho_{\text{eq}}]] = [[A_I(\tau_2),A_I(\tau_1)]\,,A_I\,(0)]\,\rho_{\text{eq}} \tag{14.5.8}$$

we find that the response function is

$$R^{(2)}(\tau_1,\tau_2) = \left(\frac{\text{i}}{\hbar}\right)^2 \text{Tr}\left([[A_I(\tau_2),A_I(\tau_1)]\,,A_I(0)]\,\rho_{\text{eq}}\right) \tag{14.5.9}$$

Equivalently, we can write

$$R^{(2)}(\tau_1,\tau_2) = \left(\frac{\text{i}}{\hbar}\right)^2 \langle[[A_I(\tau_2),A_I(\tau_1)]\,,A_I(0)]\rangle \tag{14.5.10}$$

If one expands the nested commutator in eq. (14.5.10), one finds that there are four separate correlation functions that vary by the time-ordering of the operators. For Hermitian operators, only two of these correlation functions are independent, and the other two are their complex conjugates. We will discuss the interpretation of nonlinear response functions and define nonlinear susceptibilities when we take up nonlinear spectroscopy.

This page titled 14.5: Nonlinear response functions is shared under a CC BY-NC-SA 4.0 license and was authored, remixed, and/or curated by Andrei Tokmakoff via source content that was edited to the style and standards of the LibreTexts platform.

14.6: Relaxation of a Prepared State

The impulse response function $R_{AA}(t)$ describes the behavior of a system being driven away from equilibrium by the application of an external force to the internal variable A. Here we want to investigate how knowledge of $R_{AA}(t)$ helps solve a related problem: the relaxation of a prepared state back to equilibrium (Figure 14.6.1). In this scenario, the external agent again interacts through the internal variable A, but by applying a constant potential the system is initially held away from equilibrium. The Hamiltonian is $H = H_0 - f_0 A$, and the ensemble average of A is $\langle A \rangle_0$. At time t_0, the external potential is released, and the system relaxes to its equilibrium state under the Hamiltonian H_0, where the average value of A is $\langle A \rangle_{\text{eq}}$. The change in A over the course of the relaxation is thus

$$\delta \bar{A}_0 = \langle A \rangle_0 - \langle A \rangle_{\text{eq}} \tag{14.6.1}$$

The time-dependent relaxation behavior of A for $t > t_0$ is characterized by the step response function $S_{AA}(t)$, which is the function we want to describe.

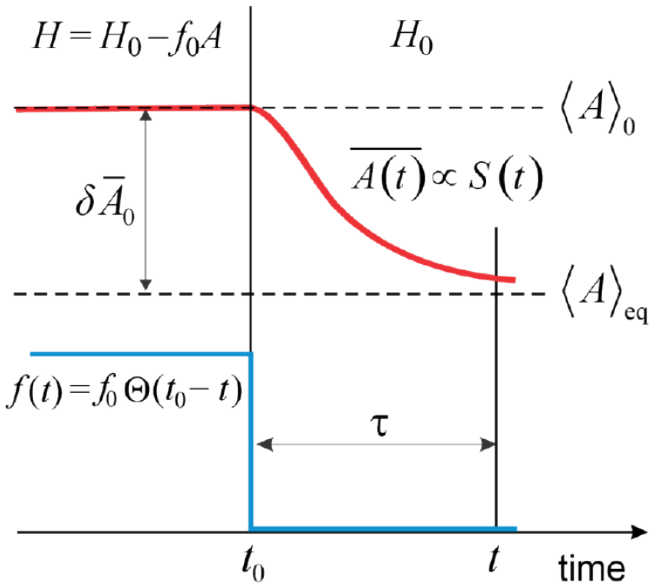


Figure 14.6.1: The step-response relaxation experiment.

In the perturbative limit, one can anticipate that the form of the impulse response function and the step response functions are related. Just as we expect that the impulse response to rise from zero at $\tau = 0$ and be expressed as an odd function in time due to the finite time it takes for molecules to respond to an applied force, the step response should decay from a positive value at $\tau = 0$ and look even in time (Figure 14.6.2). We also know that a unit step function $\Theta(t - t')$ is obtained by time integrating over the delta function $\delta(t - t')$, so we can already anticipate that $R_{AA}(t)$ is proportional to $\dot{S}_{AA}(t)$.

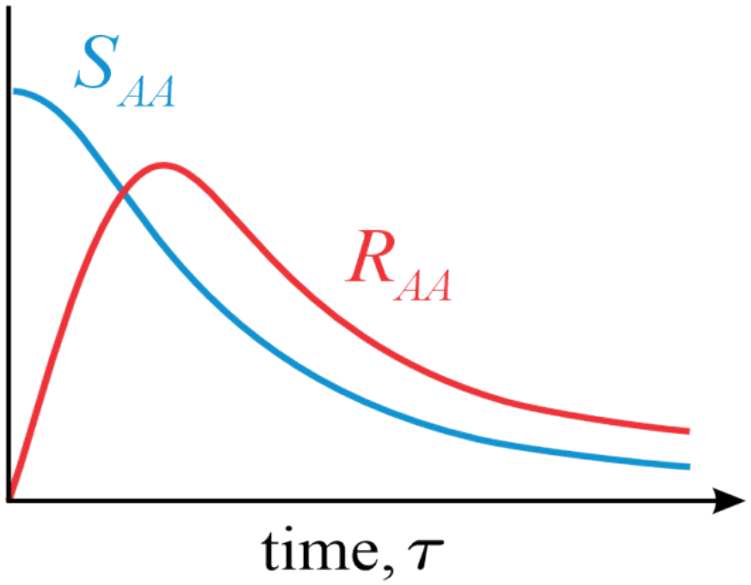


Figure 14.6.2: Illustration of derivative relationship between the impulse and step response functions.

In the classical case, these relationships hold in a direct manner. The time-dependent relaxation of A is directly proportional to the correlation function

$$\delta\overline{A(t)} = \frac{f_0}{k_B T}\langle A(0)A(t)\rangle \tag{14.6.2}$$

The classical correlation function is real and even, and the linear response function is given by

$$R(\tau) = \left.\frac{\partial\overline{A(t)}}{\partial t}\right|_{f=0} = \frac{1}{k_B T}\frac{\partial}{\partial t}\langle A(0)A(t)\rangle \tag{14.6.3}$$

Here the magnitude of the perturbation is small, so the ensemble average of the correlation function in these expressions can be performed over the equilibrium ensemble described by H_0. From these relationships we can conclude that

$$\delta\overline{A(t)} = f_0 S_{AA}(t) \tag{14.6.4}$$

and that the extent of the prepared system's relaxation after a period t is related to a time integral over the response function

$$S_{AA}(0) - S_{AA}(t) = \int_0^t d\tau\, R_{AA}(\tau) \tag{14.6.5}$$

Let's think a bit about what this equation means. The left-hand side measures how far toward equilibrium a non-equilibrium ensemble has relaxed. The right-hand side indicates that this is due to the cumulative (time-integrated) fluctuations of the system acting on the system, represented by the response function. This result is pointing toward a fundamental relationship between dissipating energy, as captured by the step-response function, and the natural noisy fluctuations of the system in the response function. This time-domain representation is one way to represent the fluctuation-dissipation theorem, which fundamentally links the fluctuations of an equilibrium environment to the ability to relax from a prepared state that is not too far removed from equilibrium.

Equation (14.6.5) has additional practical uses. It can be used to calculate $S_{AA}(t)$ from $R_{AA}(t)$. It also forms a way of directly connecting experimental measurements of $\overline{A(t)}$ with the response functions. We observe that time-dependent measurements of the extent of relaxation back to equilibrium $\overline{S}(t)$ can be related to the normalized step response function and area normalized impulse response function:

$$\overline{S}(t) = \frac{\delta\overline{A(t)}}{\delta\bar{A}_0} = \frac{\langle A\rangle_0 - \overline{A(t)}}{\langle A\rangle_0 - \langle A\rangle_{\text{eq}}} = \frac{S_{AA}(0) - S_{AA}(t)}{S_{AA}(0) - S_{AA}(\infty)} = \frac{\int_0^t d\tau\, R(\tau)}{\int_0^\infty d\tau\, R_{AA}(\tau)} \tag{14.6.6}$$

Let's turn to describing quantum step response functions. We will begin empirically with a few observations. First, response

functions must be real since they are related to experimental observables of the internal variable A, but quantum correlation functions are complex, with the property $C(-t) = C^*(t)$. We have already seen that quantum impulse response functions R_{AA} are related to the antisymmetrized correlation function for A, and since A is Hermitian, this is the imaginary part of the correlation function, C''_{AA}. The step response function should be real and even, $S_{AA}(t) = S_{AA}(-t)$. Thus it stands to reason that the step response function will be proportional to the symmetrized correlation function, $C^{(+)}_{AA}$, which is the real part of the correlation function, C'_{AA}:

$$\begin{aligned} C^{(+)}_{AA}(\tau) &= \frac{1}{2}\left(\langle A_I(\tau)A_I(0)\rangle + \langle A_I(0)A_I(\tau)\rangle\right) \\ &= \frac{1}{2}\left(C_{AA}(\tau) + C_{AA}(-\tau)\right) \\ &= \frac{1}{2}\left(C_{AA}(\tau) + C^*_{AA}(\tau)\right) \\ &= C'_{AA}(\tau) \end{aligned} \tag{14.6.7}$$

Let's test whether the derivative of $C^{(+)}_{AA}$ is related to the impulse response function $R_{AA}(\tau)$.

$$\begin{aligned} \frac{\partial C^{(+)}_{AA}}{\partial \tau} &= \frac{1}{2}\frac{\partial}{\partial \tau}\langle A(\tau)A(0) + A(0)A(\tau)\rangle \\ &= \frac{1}{2}\left\langle \dot{A}(\tau)A(0) + A(0)\dot{A}(\tau)\right\rangle \end{aligned} \tag{14.6.8}$$

Into this equation we substitute the Heisenberg equation of motion for the interaction picture $-\mathrm{i}\hbar\dot{A} = [H_0, A]$, expand the resulting terms, and cyclically rearrange them—as one can for traces (thermal averages)—to find

$$\begin{aligned} \frac{\partial C^{(+)}_{AA}}{\partial \tau} &= \frac{1}{2}\frac{\mathrm{i}}{\hbar}\langle H_0A(\tau)A(0) - H_0A(0)A(\tau) + H_0A(\tau)A(0) - H_0A(0)A(\tau)\rangle \\ &= \frac{\mathrm{i}}{\hbar}\langle H_0\left[A(\tau), A(0)\right]\rangle \end{aligned} \tag{14.6.9}$$

Now we make a perturbative assumption and say that we are close enough to equilibrium (under H_0) that one can thermally average over that term to get the average energy of the system

$$H_0 = \sum\nolimits_n E_nP_n = \sum\nolimits_n E_ne^{-\beta E_n}/Z \tag{14.6.10}$$

Then,

$$\begin{aligned} \frac{\partial C^{(+)}_{AA}}{\partial \tau} &= \frac{\mathrm{i}}{\hbar}\langle H_0\rangle\langle[A(\tau), A(0)]\rangle \\ &= \langle H_0\rangle R(\tau) \end{aligned} \tag{14.6.11}$$

This equation shows that the time-derivative of the symmetrized correlation function is proportional to the impulse response function and the average thermal energy of the system $\langle H_0\rangle$. For the case of the harmonic oscillator Hamiltonian,

$$\langle H_0\rangle = \frac{\hbar\omega_0}{2}\coth\left(\frac{\beta\hbar\omega_0}{2}\right) \tag{14.6.12}$$

In the high temperature (classical) limit, $\coth(x) \to x$ and we find that

$$\frac{1}{k_BT}\frac{\partial C^{(+)}_{AA}}{\partial \tau} = R(\tau) \tag{14.6.13}$$

Comparing with eq. (14.6.3) does confirm that the symmetrized correlation function can be used to obtain the step response function S_{AA} for $\tau \geqslant 0$.

These insights can be confirmed with the derivation in the appendix below. As a result, the step response function is defined as:

$$S_{AA}(\tau) \equiv \frac{1}{\hbar}\Theta(\tau)\left\langle[A_I(\tau), A_I(0)]_+\right\rangle \tag{14.6.14}$$

where $[A, B]_+ = AB + BA$ is the anticommutator. Then we see that $S_{AA}(\tau)$ is related to the real part of the correlation function

$C'_{AA}(\tau)$ through

$$S_{AA}(\tau) = \frac{2}{\hbar}\Theta(\tau)C'_{AA}(\tau) \tag{14.6.15}$$

From the eigenstate representation of the correlation function,

$$C(\tau) = \sum_{n,m} p_n \left|A_{mn}\right|^2 e^{-\mathrm{i}\omega_{mn}\tau} \tag{14.6.16}$$

we see that the step response function can be expressed as an expansion in cosines

$$S(\tau) = \frac{2}{\hbar}\Theta(\tau)\sum_{n,m} p_n \left|A_{mn}\right|^2 \cos\omega_{mn}\tau \tag{14.6.17}$$

In the frequency domain, the spectral representation of the step response function is obtained from the Fourier–Laplace transform

$$S_{AA}(\omega) = \int_0^\infty dt\, S_{AA}(t)e^{\mathrm{i}\omega t} \tag{14.6.18}$$

From the symmetrized correlation function and the detailed balance condition we find

$$\begin{aligned} S_{AA}(\omega) &= \frac{1}{2}\left[C_{AA}(\omega) + C_{AA}(-\omega)\right] \\ &= \frac{1}{2}\left(1 + e^{-\beta\hbar\omega}\right)C_{AA}(\omega) \end{aligned} \tag{14.6.19}$$

Now, we can relate this to the expression for the imaginary part of the susceptibility, eq. (14.4.10)

$$\chi''_{AA}(\omega) = \frac{1}{2\hbar}\left(1 - e^{-\beta\hbar\omega}\right)C_{AA}(\omega) \tag{14.6.20}$$

Combining these, we obtain the relationship(1)

$$\chi''_{AA}(\omega) = \frac{1}{\hbar}\tanh\left(\frac{\beta\hbar\omega}{2}\right)S_{AA}(\omega) \tag{14.6.21}$$

This is the formal expression for the fluctuation-dissipation theorem proven in 1951 by Callen and Welton. It followed an observation made many years earlier (1930) by Lars Onsager for which he was awarded the 1968 Nobel Prize in Chemistry: "The relaxation of macroscopic nonequilibrium disturbance is governed by the same laws as the regression of spontaneous microscopic fluctuations in an equilibrium state."

Noting that $\tanh(x) \to x$ for $x \gg 1$, we see that in the high temperature (classical) limit

$$\chi''_{AA}(\omega) = \frac{\omega}{2k_BT}S_{AA}(\omega) \tag{14.6.22}$$

Appendix: Derivation of step response function

We can show more directly how the impulse and step response are related. To begin, let's consider the Hamiltonian for the step response experiment,

$$H = \begin{cases} H_0 - f_0 A & t < 0 \\ H_0 & t \geqslant 0 \end{cases} \tag{14.6.23}$$

Here $f_0 A$ is the external potential that holds the system away from the equilibrium under H_0, A is the internal variable that is held away from equilibrium, and f_0 is the proportionality factor that describes the magnitude and time-dependence of the external potential. We start by writing the expectation values of the internal variable A for the system equilibrated under H at time $t = 0$ and under H_0 at $t = \infty$ by performing an equilibrium ensemble average:

$$\langle A\rangle_0 = \left\langle \frac{e^{-\beta(H_0 - f_0 A)}}{Z_0} A \right\rangle \qquad Z_0 = \left\langle e^{-\beta(H_0 - f_0 A)} \right\rangle \tag{14.6.24}$$

$$\langle A\rangle_{\text{eq}} = \left\langle \frac{e^{-\beta H_0}}{Z_{\text{eq}}} A \right\rangle \qquad Z_{\text{eq}} = \left\langle e^{-\beta H_0} \right\rangle \tag{14.6.25}$$

where $\beta = 1/k_B T$. If we make the *classical* linear response approximation, which states that when the applied potential $f_0 A$ is very small relative to H_0, then

$$e^{-\beta(H_0 - f_0 A)} \approx e^{-\beta H_0}\left(1 + \beta f_0 A\right) \tag{14.6.26}$$

and $Z_0 \approx Z_{\text{eq}}$. The magnitude of the perturbation is

$$\delta A = \langle A\rangle_0 - \langle A\rangle_{\text{eq}} \approx \beta f_0 \left\langle A^2 \right\rangle \tag{14.6.27}$$

and the time-dependent relaxation is given by the classical correlation function

$$\delta\overline{A(t)} = \beta f_0 \langle A(0) A(t)\rangle \tag{14.6.28}$$

For a description that works for the quantum case, let's start with the system under H_0 at $t = -\infty$, ramp up the external potential at a slow rate η to allow the system to adiabatically equilibrate along with the changing potential. Then at $t = 0$, we abruptly shut off the external potential and watch the system. We are interested in describing the behavior of the system in the adiabatic limit that $\eta \to 0$. The Hamiltonian for the system is

$$H = \begin{cases} H_0 + f_0 A e^{\eta t} & t < 0 \\ H_0 & t \geqslant 0 \end{cases} \tag{14.6.29}$$

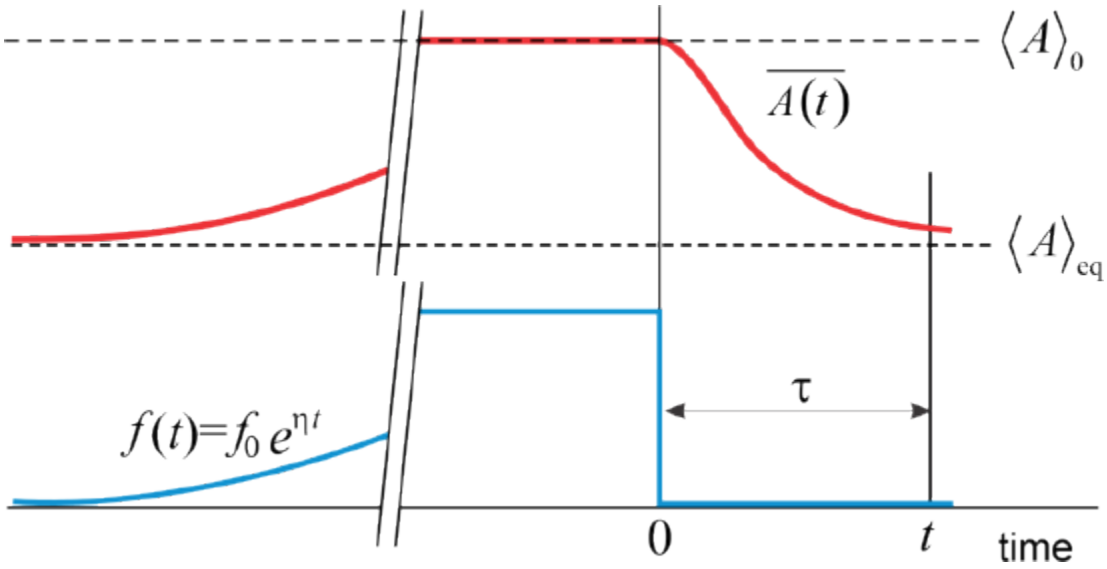


Figure 14.6.3: Adiabatic preparation of the step-response experiment.

We can now write the time-dependence of the system as the external force is gradually applied by convoluting the impulse response function R_{AA} with $f(t)$ for $t < 0$:

$$\delta\overline{A(t)} = \overline{A(t)} - \langle A\rangle_{\text{eq}} = \lim_{\eta \to 0} \int_{-\infty}^{0} dt' R_{AA}\left(t - t'\right) e^{\eta t'} f_0 \tag{14.6.30}$$

Since the response function is proportional to the imaginary part of the correlation function $C''_{AA}(\tau)$, we can express $R_{AA}(t - t')$ as an inverse Fourier transform over the $C''_{AA}(\omega)$:

$$R(t) = \frac{2}{\hbar} C''(t) = \frac{2}{\hbar}\frac{1}{2\pi} \int_{-\infty}^{\infty} d\omega\, C''(\omega) e^{-\mathrm{i}\omega t} \tag{14.6.31}$$

Substituting this into (14.6.30) allows us to evaluate the integral over t'. We obtain

$$\begin{aligned}\overline{\delta A(t)} &= \lim_{\eta\to 0}\frac{f_0}{2\pi}\frac{2}{\hbar}\int_{-\infty}^{0}dt'\int_{-\infty}^{\infty}d\omega\, e^{(\eta+i\omega)t'}e^{-i\omega t}C''(\omega) \\ &= \frac{f_0}{2\pi}\frac{2}{\hbar}\int_{-\infty}^{\infty}d\omega\, P\left(\frac{1}{\omega}\right)C''(\omega)e^{-i\omega t}\end{aligned} \tag{14.6.32}$$

We next use the correlation function identity relating real and imaginary spectra, $C'(\omega) = C''(\omega)/\omega$, to write the results in terms of the real part of the correlation function:

$$\begin{aligned}\overline{\delta A(t)} &= \frac{f_0}{2\pi}\frac{2}{\hbar}\int_{-\infty}^{\infty}d\omega\, C'(\omega)e^{i\omega t} \\ &= f_0\frac{2}{\hbar}C'(t)\end{aligned} \tag{14.6.33}$$

This result shows that the step response relaxation is governed by the real part of the correlation function. A more detailed derivation of this result is found in Mazenko.(2)

References

(1) Likharev, K. K. Fluctuation-dissipation Theorem. *Essential Graduate Physics - Quantum Mechanics*; LibreTexts. https://phys.libretexts.org/Bookshelves/Quantum_Mechanics/Essential_Graduate_Physics_-_Quantum_Mechanics_(Likharev)/07%3A_Open_Quantum_Systems/7.04%3A_Fluctuation-dissipation_Theorem

(2) Mazenko, G. *Nonequilibrium Statistical Mechanics*; Wiley-VCH, 2006. DOI: 10.1002/9783527618958

This page titled 14.6: Relaxation of a Prepared State is shared under a CC BY-NC-SA 4.0 license and was authored, remixed, and/or curated by Andrei Tokmakoff via source content that was edited to the style and standards of the LibreTexts platform.

14.7: Example- Response of an abruptly shifted oscillator

To illustrate how the step response works in practice, let's work through examples based on the quantum harmonic oscillator. Consider an ensemble of oscillators after the particles have been released from a non-equilibrium position. What is the time-dependent behavior of the ensemble position? As a starting point, let's look at the classical damped oscillator. From eq. (14.2.02), the response function is

$$R(\tau) = \frac{1}{m\Omega}\sin\Omega\tau e^{-\Gamma\tau} \tag{14.7.1}$$

where $\Omega = \sqrt{\omega_0^2 + \Gamma^2}$. This describes the behavior of the particle in response to a kick from its equilibrium position. The step response function characterizes the behavior when a particle is released from a non-equilibrium position. It is obtained from eq. (14.6.05)

$$S_{AA}(0) - S_{AA}(t) = \frac{1}{m\left(\Gamma^2+\Omega^2\right)}\left(1 - e^{-\Gamma\tau}\cos\Omega\tau - \frac{\Gamma}{\Omega}e^{-\Gamma\tau}\sin\Omega\tau\right) \tag{14.7.2}$$

and the normalized step response function from eq. (14.6.06) is

$$\overline{S}(t) = \left(\cos\Omega\tau - \frac{\Gamma}{\Omega}\sin\Omega\tau\right)e^{-\Gamma\tau} \tag{14.7.3}$$

In the limit of weak damping, $\Gamma \ll \omega$, we get the expected behavior

$$\bar{S}(t) = \cos\omega_0 t\, e^{-\Gamma t} \tag{14.7.4}$$

If the system is released from $q = d$, the relaxation behavior will be given by $\delta\bar{q}(t) = d\bar{S}(t) = d\cos\omega_0 t\ \ e^{-\Gamma t}$. These functions are compared in Figure 14.7.1, illustrating how impulse responses and step response functions are odd and even in time, respectively, and how their oscillatory behavior can be expressed in sines and cosines, respectively.

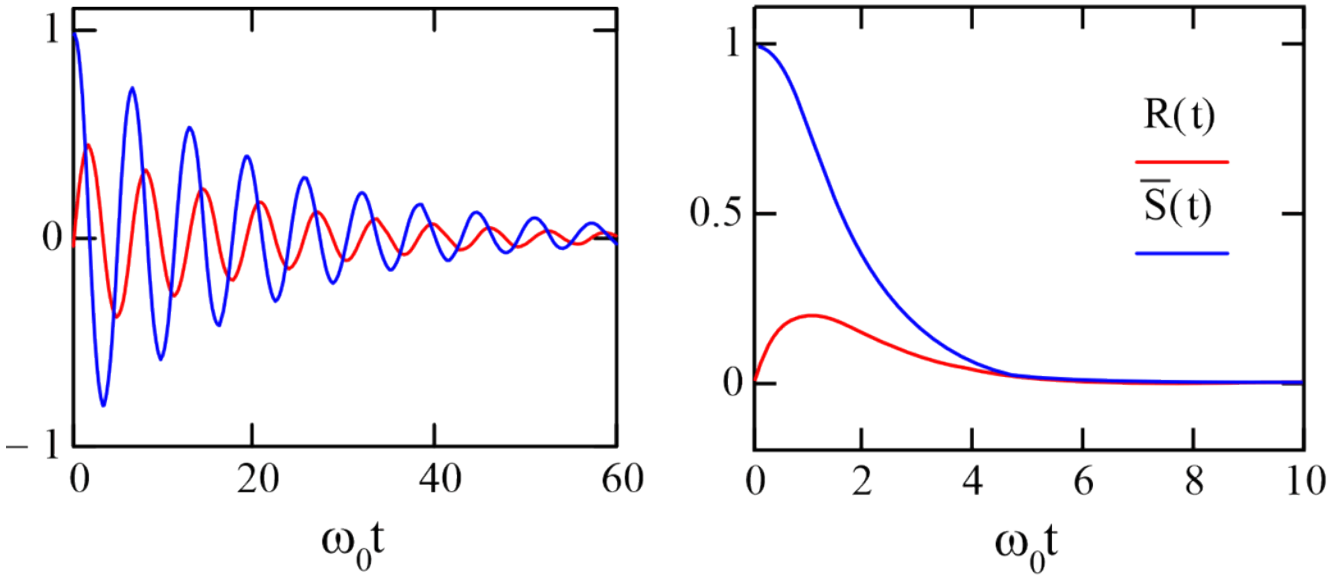


Figure 14.7.1: Examples of the impulse and step response functions for (left) an underdamped oscillator $\omega_0/\Gamma = 20$, and (right) a critically damped oscillator.

Turning to the quantum harmonic oscillator, we first calculate the position response function R_{qq}, which we obtain from the imaginary part of the correlation function, C''_{qq}, using eq. (14.3.16),

$$R(\tau) = -\frac{2}{\hbar}C''(\tau) \tag{14.7.5}$$

In Sec. 13.4 we found that oscillator position autocorrelation function is given by

$$\begin{aligned} C_{qq}(\tau) &= C'_{qq}(\tau) + \mathrm{i}C''_{qq}(\tau) \\ &= \frac{\hbar}{2m\omega_0}\left[(2\bar{n}+1)\cos\omega_0 t - \mathrm{i}\sin\omega_0 t\right] \end{aligned} \tag{14.7.6}$$

where $\bar{n} = \left(e^{\beta\hbar\omega_0} - 1\right)^{-1}$. So, the response function is

$$R_{qq}(\tau) = \frac{1}{m\omega_0}\sin\omega_0 t \tag{14.7.7}$$

As expected, the position correlation function of an ensemble of undamped harmonic oscillator oscillates indefinitely. It may seem odd in some respects to use this as an example because without irreversible relaxation some of the properties of response functions we discussed earlier don't apply, such as $\lim_{t\to\infty} R(t) = 0$. This isn't a serious concern because all real systems are ultimately irreversible. Without fully justifying it here, the response function for a harmonic oscillator that is weakly damped as a result of being coupled to a continuum is

$$R_{qq}(\tau) = \frac{1}{m\omega_0}\sin\omega_0 t\,\mathrm{e}^{-\gamma t} \tag{14.7.8}$$

Note that this has exactly the same form as the classical response function.

The general response of the oscillator to an externally applied potential is given by eq. (14.3.10)

$$\overline{\delta q(t)} = \int_0^\infty d\tau\, f(t-\tau)R(\tau) \tag{14.7.9}$$

So, if an impulsive kick is applied to an equilibrium ensemble of oscillators at $\langle q\rangle_{\mathrm{eq}} = 0$, then $f(t) = f_0\delta(t)$, and the time-dependent displacement from equilibrium is

$$\overline{\delta q(t)} = f_0 R_{qq}(t) = \frac{f_0}{m\omega_0}\sin\omega_0 t \tag{14.7.10}$$

Or, in the case of the weakly damped oscillator, we obtain

$$\overline{\delta q(t)} = f_0 R_{qq}(t) = \frac{f_0}{m\omega_0}\sin\omega_0 t\,\mathrm{e}^{-\gamma t} \tag{14.7.11}$$

Notice that the units of C_{qq} are m^2 and R_{qq} is in $\mathrm{s}^2/\mathrm{kg} = \mathrm{m/N}$, and f_0 is a force in N. This looks exactly as we would expect for the impulse response of the classical oscillator. A positive force f_0 pushes the oscillator to positive displacement and initiates oscillatory motion with a maximum average amplitude of $f_0/m\omega_0$.

The step response function is obtained by inserting the quantum correlation function into eq. (14.6.15)

$$\begin{aligned} S_{AA}(t) &= \frac{2}{\hbar}C'_{AA}(t) \\ &= \frac{(2\bar{n}+1)}{m\omega_0}\cos\omega_0 t \end{aligned} \tag{14.7.12}$$

The corresponding time-dependent behavior of an oscillator released from the position $q = d$ is then

$$\begin{aligned} \overline{\delta q(t)} &= f_0 S_{AA}(t) \\ &= \frac{f_0}{m\omega_0}(2\bar{n}+1)\cos\omega_0 t \\ &= d\cos\omega_0 t \end{aligned} \tag{14.7.13}$$

In the last line, the boundary conditions dictate that $d = (f_0/m\omega_0)\,(2\overline{n}+1)$, and f_0 is the force applied to the oscillators to hold their mean position at $q = d$. The time-dependent expectation value for the position starts at $q = d$ and oscillates back and forth about $q = 0$ between $q = \pm d$.

We can approach this problem in a different manner and calculate the oscillator behavior directly from the impulse response function. We take the equilibrium Hamiltonian to be $H_0 = \frac{1}{2}p^2 + \frac{1}{2}m\omega_0^2 q^2$ with a mean position $\langle q\rangle_{\mathrm{eq}} = 0$. An external potential has

been applied to the oscillator, holding its position at $\langle q \rangle_0 = d$. At time $t = 0$, the external potential is abruptly shut off. We can express the time-dependent Hamiltonian as

$$H = \frac{p^2}{2m} + \frac{1}{2} m\omega_0^2 q_t^2 \tag{14.7.14}$$

where

$$q_t = \begin{cases} q - d & \text{for } t < 0 \\ q & \text{for } t \geqslant 0 \end{cases} \tag{14.7.15}$$

We can expand this expression to help write it in the form we used in our linear response discussion:

$$H = H_0 - \Theta(-t)\frac{1}{2} m\omega_0^2 \left(2dq - d^2\right) \tag{14.7.16}$$

To focus on the time-dependence, we will drop the constant factor of $\frac{1}{2} m\omega_0^2 d^2$ for simplicity. This factor matters when calculating the potential energy dissipated by the shifted oscillator, but it does not influence the time-dependence. So we have

$$H = H_0 - f(t)q \tag{14.7.17}$$

$$f(t) = \Theta(-t) f_0 \qquad f_0 = m\omega_0^2 d \tag{14.7.18}$$

Again, we can calculate how the system evolves under H_0 with the response function, using

$$\overline{\delta q(t)} = \int_0^\infty d\tau \, R(\tau) f(t - \tau) \tag{14.7.19}$$

Now, inserting eq. (14.7.18) has the effect of changing the lower integration limit:

$$\begin{aligned} \overline{\delta q(t)} &= \int_t^\infty d\tau \, R(\tau) f_0 \\ &= \omega_0 d \int_t^\infty \sin \omega_0 \tau \, d\tau \end{aligned} \tag{14.7.20}$$

This integral can be solved by introducing the damping factor $e^{-\gamma t}$ and afterwards taking the limit $\gamma \to 0$.

$$\begin{aligned} \overline{\delta q(t)} &= \omega_0 d \lim_{\gamma \to 0} \int_t^\infty \sin \omega_0 \tau e^{-\gamma \tau} d\tau \\ &= d \cos \omega_0 t \end{aligned} \tag{14.7.21}$$

We calculate the time-dependent displacement of the oscillator from $\overline{q(t)} = \langle q \rangle_{\text{eq}} + \overline{\delta q(t)}$. We observe now that the expectation value for the position where it was held at $q = d$ and oscillates at a frequency ω_0 about $\tilde{q} = 0$ between the turning points $q = \pm\, d$.

The same problem can be applied to the step-up response, in which the oscillator is initially at equilibrium and the potential is abruptly shifted to $q = d$ at $t = 0$. This has the effect of changing the integration limits in eq. (14.7.19) from 0 to t, giving

$$\overline{\delta q(t)} = d\left(1 - \cos \omega_0 t\right) \tag{14.7.22}$$

When the potential is applied, the particle is set into motion, moving positively and oscillating about $q = d$ between the turning points $q = 0$ and $2d$ at a frequency ω_0.

In some respects, one might be surprised to find that the behavior we see is identical to that of a classical particle. We went through the effort of calculating the quantum correlation function thermally averaged over an ensemble at finite temperature and integrating over the response function to describe the non-equilibrium behavior of the ensemble, yet we ended up with results that don't seem to have any quantum behavior left. Though, you may be less surprised if you recall that in our discussion of Ehrenfest's theorem the quantum oscillator's position and momentum expectation values had dynamics that mirrored classical dynamics. Quantum mechanics does still appear when you calculate other properties of the oscillator or when discussing the magnitude of the forces or potentials needed to prepare the non-equilibrium state, as observed in eq. (14.7.13).

This page titled 14.7: Example- Response of an abruptly shifted oscillator is shared under a CC BY-NC-SA 4.0 license and was authored, remixed, and/or curated by Andrei Tokmakoff via source content that was edited to the style and standards of the LibreTexts platform.

14.8: Readings

General References

These texts are excellent learning resources and general references that broadly cover classical and quantum mechanical linear response theory and the fluctuation-dissipation relationship.

1. Berne, B. J.; Pecora, R. *Dynamic Light Scattering: With applications to chemistry, biology, and physics*; R.E. Krieger Publishing Co., 1990.
2. Chandler, D. *Introduction to Modern Statistical Mechanics*; Oxford University Press, 1987.
3. McQuarrie, D. A. *Statistical Mechanics*; Harper & Row, 1976.
4. Nitzan, A. *Chemical dynamics in condensed phases: Relaxation, transfer and reactions in condensed molecular systems*; Oxford University Press, 2006. DOI: 10.1093/oso/9780198529798.001.0001
5. Slichter, C. P. *Principles of Magnetic Resonance, with Examples from Solid State Physics*; Harper & Row, 1963.
6. Wang, C. H. *Spectroscopy of Condensed Media: Dynamics of Molecular Interactions*; Academic Press, 1985. DOI: 10.1016/B978-0-12-734780-6.X5001-8
7. Zwanzig, R. *Nonequilibrium Statistical Mechanics*; Oxford University Press, 2001. DOI: 10.1093/oso/9780195140187.001.0001

More advanced

1. Berne, B. J. Time-Dependent Properties of Condensed Media. *Physical chemistry:an advanced treatise. Vol. 8B, Liquid state*; Eyring, H., Henderson, D., Jost, W., Eds.; Vol. 8B; Academic Press, 1971; pp 540-716.
2. Mazenko, G. *Nonequilibrium Statistical Mechanics*; Wiley-VCH, 2006. DOI: 10.1002/9783527618958
3. Jensen, J.; Mackintosh, A. R. Linear Response Theory. *Rare Earth Magnetism: Structures and Excitations*; The International Series of Monographs on Physics, Clarendon Press, Oxford University Press, 1991; pp 134-162. DOI: 10.1093/oso/9780198520276.003.0003
4. Kubo, R.; Toda, M.; Hashitsume, N. *Statistical Physics II: Nonequilibrium Statistical Mechanics*, 2nd ed.; Springer Berlin Heidelberg, 1991. DOI: 10.1007/978-3-642-58244-8
5. Mukamel, S. *Principles of Nonlinear Optical Spectroscopy*; Oxford University Press, 1995.

Classic Papers

1. Kubo, R. Statistical-Mechanical Theory of Irreversible Processes. I. General Theory and Simple Applications to Magnetic and Conduction Problems. *Journal of the Physical Society of Japan* **1957**, *12*, 570-586. DOI: 10.1143/JPSJ.12.570.
    - Kubo's detailed presentation of theoretical principles that relate the equilibrium fluctuations of a system to the linear response function via the fluctuation-dissipation theorem.
2. Callen, H. B.; Welton, T. A. Irreversibility and Generalized Noise. *Physical Review* **1951**, *83* (1), 34-40. DOI: 10.1103/PhysRev.83.34.
    - First derivation of the commonly used form of the fluctuation-dissipation theorem.

This page titled 14.8: Readings is shared under a CC BY-NC-SA 4.0 license and was authored, remixed, and/or curated by Andrei Tokmakoff via source content that was edited to the style and standards of the LibreTexts platform.

15: TIME-DOMAIN SPECTROSCOPY

15.1: Absorption Spectra from Time-Correlation Functions
15.2: Describing Diverse Spectroscopies with the Dipole Correlation Function
15.3: Vibrational and Rotational Spectroscopy
15.4: Line Broadening Mechanisms
15.5: Readings

This page titled 15: Time-Domain Spectroscopy is shared under a CC BY-NC-SA 4.0 license and was authored, remixed, and/or curated by Andrei Tokmakoff via source content that was edited to the style and standards of the LibreTexts platform.

15.1: Absorption Spectra from Time-Correlation Functions

Our classical model of spectroscopy was rooted in a dynamical description of the motion of charged particles in response to an oscillating electric field. The classical description illustrates the connection between the absorption spectrum and the dynamics of a driven oscillator's dipole moment, and it provides the Fourier transform relationships that allow one to relate these two representations of the molecular behavior. In contrast, our quantum mechanical description of absorption using the Golden Rule resulted in a delta function resonance condition, which hides any time-dependent description of motion.

Now that we are equipped with time-correlation functions and response functions, we are in a position to build some dynamical perspectives back into our quantum understanding of spectroscopy. An alternative quantum approach to spectroscopy is to recognize that the features of a spectrum are just a frequency domain representation of the underlying molecular dynamics. Here we will discuss the case of resonant light absorption through electric dipole transitions by drawing upon the new tools we have developed, such as the expression of Golden Rule rates via Fourier transforms of time-correlation functions, the acquisition of response functions using time-correlation functions, and the relationship between the absorption cross section and the imaginary part of the susceptibility. These will allow us to reveal how an absorption spectrum reflects the dynamical motions of molecular dipole moments within an equilibrium ensemble.

Since we are discussing absorption spectroscopy, we will describe the interaction between a molecular system and an electromagnetic field through the electric dipole Hamiltonian

$$\begin{aligned} H &= H_0 + V(t) \\ &= H_0 - \boldsymbol{\mu} \cdot \boldsymbol{\mathcal{E}}(t) \end{aligned} \tag{15.1.1}$$

From a linear response perspective, the dipole operator μ is the internal variable being driven by an external electromagnetic field $\mathcal{E}(t) = \mathcal{E}_0 \sin \omega t$. As we showed previously, when induced by a monochromatic field, the golden rule rates of absorption and stimulated emission between an initial state $|\ell\rangle$ and final state $|k\rangle$ are given by

$$w_{k\ell} = \frac{\pi}{2\hbar^2} |\mathcal{E}_0|^2 \left|\boldsymbol{\mu}_{kl}\right|^2 \left[\delta\left(\omega_{k\ell} - \omega\right) + \delta\left(\omega_{k\ell} + \omega\right)\right] \tag{15.1.2}$$

where $\boldsymbol{\mu}_{k\ell} = \langle k| \boldsymbol{\mu} |\ell\rangle$ is the transition dipole matrix element.

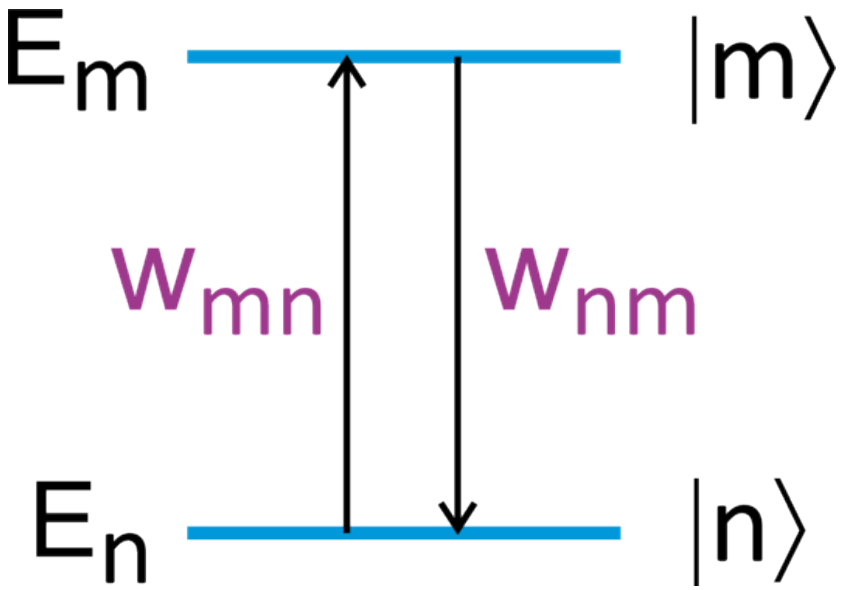


Figure 15.1.1: The net rate of absorption depends on the difference of absorption and stimulated emission processes connecting pairs of upper (m) and lower (n) states.

Let's apply these expressions to an equilibrium ensemble of molecules, which initially populate a distribution of thermally accessible quantum states with a probability $p_\ell = \exp[-\beta E_\ell]$. Since molecules at non-zero temperatures can initially occupy excited states, we need to consider that incident light can either be absorbed, resulting in transition from lower molecular energy

levels (n) to higher ones (m), or it can stimulate emission from excited states downward in energy (Figure 15.1.1). We will obtain the electromagnetic field's net rate of energy loss from the difference between the two processes. To calculate the rates of absorption and stimulated emission, we will sum the golden rule expression for the rates of transition between initial and final states (ℓ and k) over all possible lower and upper energy levels (n and m), stipulating that $E_m > E_n$. Then, as this system is an ensemble, these two processes need to be weighted by the equilibrium population of the initial states, p_ℓ. The net rate of energy absorption from the radiation field is given by

$$\begin{aligned}\overline{\mathcal{P}}_{\text{abs}}(\omega) &= \sum_{\ell,k=\{m,n\}} p_\ell w_{k\ell} \hbar\omega_{k\ell} \\ &= \sum_{n,m} p_n w_{mn} \hbar\omega_{mn} + p_m w_{nm} \hbar\omega_{nm}\end{aligned} \tag{15.1.3}$$

In evaluating the sum over all states, the term containing ω_{mn} is positive, describing absorption, whereas the term with ω_{nm} is negative and denotes stimulated emission.

To correlate the behavior of the ensemble with an observed absorption spectrum, we would like to calculate the absorption cross-section σ. The absorption cross-section describes the rate of energy absorption $\overline{\mathcal{P}}_{\text{abs}}(\omega)$ relative to the intensity of light incident on the sample, I:

$$\sigma_{eg}(\omega) = \frac{\overline{\mathcal{P}}_{\text{abs}}(\omega)}{I} \tag{15.1.4}$$

Inserting eq. (15.1.2), (15.1.4), and $I = \frac{1}{2}\varepsilon_0 c \mathcal{E}_0^2$ into this expression, and remembering that ω_{mn} is positive while ω_{nm} is negative, we obtain the expression

$$\sigma(\omega) = \frac{\pi\omega}{\varepsilon_0 \hbar c} \sum_{n,m} \left[p_n \left|\boldsymbol{\mu}_{mn}\right|^2 \delta\left(\omega_{mn} - \omega\right) \; - p_m \left|\boldsymbol{\mu}_{nm}\right|^2 \delta\left(\omega_{nm} + \omega\right) \right] \tag{15.1.5}$$

We can simplify this further by noting that the two terms can be related using $\delta\left(\omega_{nm} + \omega\right) = \delta\left(\omega_{mn} - \omega\right)$, which both indicate how close the frequency is to resonance. This results in

$$\sigma(\omega) = \frac{\pi\omega}{\varepsilon_0 \hbar c} \sum_{n,m} \left(p_n - p_m\right) \left|\boldsymbol{\mu}_{mn}\right|^2 \delta\left(\omega_{mn} - \omega\right) \tag{15.1.6}$$

This expression matches our intuition that the net rate of energy absorption depends on the population difference between upper and lower states: $p_n - p_m$. Since \(E_n

$$p_n - p_m = p_n \left(1 - e^{-\beta\hbar\omega_{mn}}\right) \tag{15.1.7}$$

Under perturbative conditions, where the absorption of light does not significantly alter the distribution of population through the system (i.e. heat it!), we can write the cross section as

$$\sigma(\omega) = \frac{\pi\omega}{\varepsilon_0 \hbar c} \left(1 - e^{-\beta\hbar\omega}\right) \sum_{n,m} p_n \left|\boldsymbol{\mu}_{mn}\right|^2 \delta\left(\omega_{mn} - \omega\right) \tag{15.1.8}$$

These perturbative conditions are consistent with linear response theory.

Thinking back to our discussion of correlation functions, we notice terms in equations (15.1.5), (15.1.6), and (15.1.8) that look like the eigenstate representations of two power spectra (frequency domain correlation functions). Let's look into these, starting with the power spectrum $C_{\mu\mu}(\omega)$ that we see in eq. (15.1.8):

$$C_{\mu\mu}(\omega) = \sum_{n,m} p_n \left|\boldsymbol{\mu}_{mn}\right|^2 \delta\left(\omega_{mn} - \omega\right) \tag{15.1.9}$$

This power spectrum reports on the strength of the light-matter interaction as a function of the frequency of the light. In Section 13.4, we showed that this expression is the Fourier transform of the dipole correlation function

$$C_{\mu\mu}(t) = \sum_{n,m} p_n \left|\boldsymbol{\mu}_{mn}\right|^2 \exp\left(\mathrm{i}\omega_{mn} t\right) \tag{15.1.10}$$

Let's extract a more useful formula for the cross-section using the procedure we described in Section 13.5 to recover the dipole

correlation function. We start by representing the delta function in eq. (15.1.9) with a Fourier transform of a complex exponential:

$$\delta\left(\omega-\omega_{mn}\right)=\frac{1}{2\pi}\int_{-\infty}^{+\infty}dt\,e^{\mathrm{i}(\omega-\omega_{mn})t} \tag{15.1.11}$$

Inserting this into eq. (15.1.9) and expanding the transition dipole matrix elements gives

$$C_{\mu\mu}(\omega)=\frac{1}{2\pi}\int_{-\infty}^{+\infty}dt\sum_{n,m}p_n\left\langle n\right|\boldsymbol{\mu}\left|m\right\rangle\left\langle m\right|\boldsymbol{\mu}\left|n\right\rangle e^{\mathrm{i}(\omega-\omega_{mn})t} \tag{15.1.12}$$

In the eigenstate representation, the oscillatory time-dependence of $e^{-\mathrm{i}\omega_{mn}t}$ is a representation of the dynamics described by the system time-evolution operator, $U_0\left|n\right\rangle=e^{-\mathrm{i}H_0t/\hbar}\left|n\right\rangle=e^{-\mathrm{i}E_nt/\hbar}\left|n\right\rangle$, This allows us to rewrite eq. (15.1.12) as

$$C_{\mu\mu}(\omega)=\frac{1}{2\pi}\int_{-\infty}^{+\infty}dt\sum_{n,m}p_n\left\langle n\left|U_0^\dagger\boldsymbol{\mu}U_0\right|m\right\rangle\left\langle m\left|\boldsymbol{\mu}\right|n\right\rangle e^{\mathrm{i}\omega t} \tag{15.1.13}$$

This transformation leads to a time-dependent dipole operator in the interaction picture: $\boldsymbol{\mu}_I(t)=U_0^\dagger\boldsymbol{\mu}U_0$. We can also remove the sum over m, since this is just the identity projection operator $\sum_m\left|m\right\rangle\left\langle m\right|=1$. We now have

$$C_{\mu\mu}(\omega)=\frac{1}{2\pi}\int_{-\infty}^{+\infty}dt\sum_{n}p_n\left\langle n\right|\boldsymbol{\mu}_I(t)\boldsymbol{\mu}_I(0)\left|n\right\rangle e^{\mathrm{i}\omega t} \tag{15.1.14}$$

The expression in the integral is just the dipole-dipole time-correlation function as we originally defined it in Section 13.4.

$$\begin{aligned}C_{\mu\mu}(t)&=\sum_n p_n\left\langle n\right|\boldsymbol{\mu}_I(t)\boldsymbol{\mu}_I(0)\left|n\right\rangle\\&=\left\langle\boldsymbol{\mu}_I(t)\boldsymbol{\mu}_I(0)\right\rangle\end{aligned} \tag{15.1.15}$$

Thus, the power spectrum $C_{\mu\mu}(\omega)$ is actually the Fourier transform of $C_{\mu\mu}(t)$

$$C_{\mu\mu}(\omega)=\frac{1}{2\pi}\int_{-\infty}^{+\infty}dt\,e^{\mathrm{i}\omega t}\left\langle\boldsymbol{\mu}_I(t)\boldsymbol{\mu}_I(0)\right\rangle \tag{15.1.16}$$

Furthermore, this power spectrum is directly related to the absorption spectrum described by eq. (15.1.8):

$$\sigma(\omega)=\frac{\omega}{2\varepsilon_0\hbar c}\left(1-e^{-\beta\hbar\omega}\right)\int_{-\infty}^{+\infty}dt\,e^{\mathrm{i}\omega t}\left\langle\boldsymbol{\mu}_I(t)\boldsymbol{\mu}_I(0)\right\rangle \tag{15.1.17}$$

Equation (15.1.17) indicates that the absorption spectrum can be obtained from the autocorrelation function of the dipole operator, which is an equilibrium property that describes the spontaneous, time-dependent behavior of the system's dipole moments in the absence of an electromagnetic field. The use of first-order perturbation theory in deriving this expression indicates that this information is sufficient to calculate how electromagnetic radiation interacts with the system—a manifestation of linear response theory and the fluctuation-dissipation theorem.

So how is eq. (15.1.17) related to a response function? If we return to the two terms in eq. (15.1.5), we notice that the first term describing absorption contains the correlation function we just described in eq. (15.1.16), but the second term describing stimulated emission, while similar, is a bit different. If we repeat the steps above, we can express the second term as a correlation function with the dipole operators reversed

$$\sum_{n,m}p_m\left|\boldsymbol{\mu}_{mn}\right|^2\delta\left(\omega_{nm}+\omega\right)=\frac{1}{2\pi}\int_{-\infty}^{+\infty}dt\,e^{\mathrm{i}\omega t}\left\langle\boldsymbol{\mu}_I(0)\boldsymbol{\mu}_I(t)\right\rangle \tag{15.1.18}$$

So, the expression for the cross section in eq. (15.1.5) results in two terms in the anti-symmetrized correlation function, giving the response function:

$$\begin{aligned}\sigma(\omega)&=\frac{\omega}{2\varepsilon_0\hbar c}\left[\int_{-\infty}^{\infty}dt\,e^{\mathrm{i}\omega t}\left(\left\langle\boldsymbol{\mu}_I(t)\boldsymbol{\mu}_I(0)\right\rangle-\left\langle\boldsymbol{\mu}_I(0)\boldsymbol{\mu}_I(t)\right\rangle\right)\right]\\&=\frac{\omega}{2\varepsilon_0\hbar c}\int_{-\infty}^{\infty}dt\,e^{\mathrm{i}\omega t}\left\langle\left[\boldsymbol{\mu}_I(t),\boldsymbol{\mu}_I(0)\right]\right\rangle\end{aligned} \tag{15.1.19}$$

If we remember that switching the order of a pair of operators is the same at taking their Hermitian conjugate, we recognize that this cross-section is a real-valued function. Using our expression for the linear response function, $R_{\mu\mu}(t) = -\frac{\mathrm{i}}{\hbar}\Theta(t)\left\langle[\boldsymbol{\mu}_I(t), \boldsymbol{\mu}_I(0)]\right\rangle$, we find

$$\sigma(\omega) = \frac{\mathrm{i}\omega}{\varepsilon_0 c}\int_{-\infty}^{\infty} dt\, e^{\mathrm{i}\omega t} R_{\mu\mu}(t) \tag{15.1.20}$$

Since the response function is related to the imaginary part of the correlation function:

$$R(\tau) = -\frac{\mathrm{i}}{\hbar}\left(C_{\mu\mu}(\tau) - C^*_{\mu\mu}(\tau)\right) = \frac{2}{\hbar}\mathrm{Im}C_{\mu\mu}(\tau) \tag{15.1.21}$$

we also obtain the result from Section 14.3: the absorption spectrum is proportional to the imaginary part of the susceptibility:

$$\sigma(\omega) = \frac{\omega}{\varepsilon_0 c}\chi''(\omega) \tag{15.1.22}$$

We should also recognize that the detailed balance relationships for correlation functions, $\tilde{C}_{AA}(\omega) = e^{\beta\hbar\omega}\tilde{C}_{AA}(-\omega)$, are a consequence of the derivation above. Equations (15.1.5) and (15.1.19) can be expressed as the difference between the power spectra for absorption and stimulated emission:

$$\sigma(\omega) = \frac{\pi\omega}{\varepsilon_0\hbar c}\left[C_{\mu\mu}(\omega) - C_{\mu\mu}(-\omega)\right] \tag{15.1.23}$$

This is then related to eq. (15.1.17) through

$$C_{\mu\mu}(\omega) - C_{\mu\mu}(-\omega) = \left(1 - e^{-\beta\hbar\omega}\right)C(\omega) \tag{15.1.24}$$

Above we neglected the vector properties of the dipole operator and light field polarization $\hat{\varepsilon}$, but we can add that back into our description of the absorption lineshape to show the orientational component of the correlation function. The Fourier transform of the dipole-dipole correlation function is then expressed as

$$C_{\mu\mu}(\omega) = \frac{1}{2\pi}\int_{-\infty}^{+\infty} dt\, e^{\mathrm{i}\omega t}\left\langle\hat{\varepsilon}\cdot\boldsymbol{\mu}_I(t)\hat{\varepsilon}\cdot\boldsymbol{\mu}_I(0)\right\rangle \tag{15.1.25}$$

This notation indicates that one must evaluate the projection of the dipole operator onto the polarization vector of the incident light field at times 0 and t. If the rotational terms in the Hamiltonian H_{rot} are separable from the isotropic vibrational and electronic contributions H_{iso} that do not depend on orientation, $H_0 = H_{\mathrm{rot}} + H_{\mathrm{iso}}$, then it becomes possible to write this correlation function as a product of two correlation functions, a rotational correlation function for the orientational dynamics, and a vibronic correlation function for the isotropic dynamics: $C_{\mu\mu}(t) = C_{\mathrm{rot}}(t)C_{\mathrm{iso}}(t)$. We will look at this closer in the following section.

Here we have written dipole operators as $\boldsymbol{\mu}_I$, emphasizing the interaction picture representation. As we move forward, we will drop this notation and take it as understood that, for the purposes of spectroscopy, the dipole operator is expressed in the interaction picture and evolves under the material Hamiltonian H_0.

This page titled 15.1: Absorption Spectra from Time-Correlation Functions is shared under a CC BY-NC-SA 4.0 license and was authored, remixed, and/or curated by Andrei Tokmakoff via source content that was edited to the style and standards of the LibreTexts platform.

15.2: Describing Diverse Spectroscopies with the Dipole Correlation Function

What we now have is a general relationship showing that the absorption spectrum can be calculated from a dipole correlation function describing the evolving charge distributions within the molecules, solids, or materials of interest. Besides electric dipole transitions, we haven't specified anything about the types of charged particles and dynamics that contribute to the absorption spectrum, but this expression applies to absorption by equilibrium ensembles of any type. Since different types of molecular motion have disparate effects on the dynamics of the dipole operator, they affect different regions of the electromagnetic spectrum. We will describe specific instances of spectroscopy by identifying the molecular motions at play and correlating them with the dynamics and frequencies they influence.

Although the dipole operator provides a straightforward way to represent the charged particles of the system, its dynamics are complex, since all the motions of these electrons and nuclei depend on one another. The time-dependence of this operator depends on the full Hamiltonian for the system H_0, which must account for the dynamics of all electronic, nuclear, and spin degrees of freedom,

$$\boldsymbol{\mu}(t) = e^{\mathrm{i}H_0 t/\hbar}\boldsymbol{\mu}e^{-\mathrm{i}H_0 t/\hbar} \tag{15.2.1}$$

To make this a tractable problem, we seek strategies for writing this Hamiltonian in the form:

$$H_0 = \sum_h H_i + \sum_{i\neq j} H_{i,j} \tag{15.2.2}$$

In this expression the indices i and j refer to separable terms that result from "bright" electronic, vibrational, rotational, translational, and electronic and nuclear spin degrees of freedom ($i,j \in \{\mathrm{elec},\mathrm{vib},\mathrm{rot},t,\sigma,I\}$). The time-dependencies of these degrees of freedom directly influence the dipole moment that is being interrogated by the electromagnetic field. The i and j indices also encompass a bath representing the "dark" degrees of freedom that aren't directly resonant with the light but influence the dynamics of the dipole operators. We have seen how such a separation is accomplished in sections 10.2, 10.3, and 21.2.2. In some cases, it is because certain degrees of freedom can be considered truly independent. It is more likely, though, that we can achieve separation by invoking an adiabatic approximation. This method uses the separation of time-scales between fast and slow degrees of freedom to treat the influence of fast motions on the slow ones through a "mean field" approach. In the second term of eq. (15.2.2), $H_{i,j}$ refers to pairwise couplings between different degrees of freedom, and it emphasizes that interactions such as electron-nuclear interactions H_{e-v} and spin-orbit coupling H_{e-s}. Ideally, these terms are small, and their influence can be incorporated through perturbation theory.

In such a separable form, the general wavefunction for the system can be expressed in terms of product states combining the wavefunctions for different degrees of freedom. For a Hamiltonian that is the sum of electronic, vibrational, and rotational Hamiltonians, $H_0 = H_{\mathrm{elec}} + H_{\mathrm{vib}} + H_{\mathrm{rot}}$, the state is

$$|\psi\rangle = |\psi_{\mathrm{elec}}\psi_{\mathrm{vib}}\psi_{\mathrm{rot}}\cdots\rangle \tag{15.2.3}$$

and the dipole autocorrelation function is determined from an average over an equilibrium ensemble of such states

$$C_{\mu\mu}(t) = \sum_j P_{\mathrm{tot},j}\,\langle\psi_j|\,\boldsymbol{\mu}(t)\boldsymbol{\mu}(0)\,|\psi_j\rangle \tag{15.2.4}$$

Here, the dipole operator evolves under the full Hamiltonian H_0, and P_{tot} describes the joint probability of occupying a state with a given electronic, vibrational, and rotational character. For a separable Hamiltonian, the probability functions are also separable into a product of independent terms:

$$P_{\mathrm{tot}} = \frac{e^{-\beta H_0}}{Z_{\mathrm{tot}}} = \frac{e^{-\beta H_{\mathrm{elec}}}}{Z_{\mathrm{elec}}}\frac{e^{-\beta H_{\mathrm{vib}}}}{Z_{\mathrm{vib}}}\frac{e^{-\beta H_{\mathrm{rot}}}}{Z_{\mathrm{rot}}} = P_{\mathrm{elec}}P_{\mathrm{vib}}P_{\mathrm{rot}} \tag{15.2.5}$$

The same approximations that allow the Hamiltonian to be separated can be used to justify the partitioning of the dipole operator into independent terms that describe how the dipole moment depends on specific electronic, vibrational, or rotational degrees of freedom. We saw an example of how this can be done for the transition dipole moment in Sec. 10.3. Another strategy invokes

the Born-Oppenheimer approximation to calculate simple dipole operators for different electronic states. Later, we will show a method for decoupling rotational and vibrational dipole moments.

By applying the multiple forms of separation we have discussed—and neglecting the H_{i-j} interaction terms—the overall correlation function can be broken into a product of correlation functions from various degrees of freedom:

$$C_{\mu\mu}(t) = C_{\text{elec}}(t)C_{\text{vib}}(t)C_{\text{rot}}(t)\cdots \tag{15.2.6}$$

Each of these correlation functions are expressed in the form shown here for the vibrational states

$$\begin{aligned} C_{\text{vib}}(t) &= \sum_n P_{\text{vib},n} \left\langle \psi_{\text{vib},n} \right| e^{\mathrm{i}H_{\text{vib}}t/\hbar} \boldsymbol{\mu} e^{-\mathrm{i}H_{\text{vib}}t/\hbar} \boldsymbol{\mu} \left| \psi_{\text{vib},n} \right\rangle \\ &= \left\langle \boldsymbol{\mu}_{\text{vib}}(t) \boldsymbol{\mu}_{\text{vib}}(0) \right\rangle \end{aligned} \tag{15.2.7}$$

The total dipole correlation function can have oscillatory components at many frequencies, and its Fourier transform will give the full absorption spectrum from the ultraviolet to the microwave regions of the spectrum. Generally speaking, the highest frequency contributions (for instance electronic) will be modulated by contributions from lower frequency motions (...such as vibrations and rotations). However, each of these correlation functions can be separately analyzed to understand how they contribute to specific frequency regions of the electromagnetic spectrum, based on the transition-dipole-allowed resonances that emerge from different types of dynamics. We will look at some examples for how this plays out in the following section.

In practice, a fully separable Hamiltonian and dipole operator is often an over-simplification. Electronic, vibrational, and rotational motions are intimately linked, even when the time-scales of their motions are vastly different. Examples include Jahn-Teller distortions and Herzberg-Teller interactions between electronic and vibrational degrees of freedom, and vibrational-rotational coupling in IR spectra. Including these effects does not stop us from using this formalism; however, we account for these effects using perturbation theory in a separable basis set. For instance, vibrational-rotational couplings would result in first and second order corrections to the vibrational Hamiltonian and dipole operator, which lead to corrected energy levels and dynamics in the correlation function.

This page titled 15.2: Describing Diverse Spectroscopies with the Dipole Correlation Function is shared under a CC BY-NC-SA 4.0 license and was authored, remixed, and/or curated by LibreTexts.

15.3: Vibrational and Rotational Spectroscopy

With separable correlation functions, we can now concentrate on how different types of nuclear and electronic dynamics give rise to peaks across the electromagnetic spectrum. In the following we will look at some examples of vibrational and rotational absorption spectra for thermal ensembles of isolated (gas-phase) molecules, and the electronic spectroscopy examples will be discussed in the following chapter.

IR vibrational spectroscopy

As we originally observed in our classical model of absorption spectroscopy, absorption of mid-infrared light by vibrations arises from the light driving changes in charge distribution as a molecule vibrates. As we discussed in Section 10.2, we describe this effect by recognizing that the dipole operator depends on the displacement of nuclei. We can take the dipole moment to depend weakly on the displacement of vibrational coordinates q so that we expand the dipole operator as

$$\boldsymbol{\mu} = \boldsymbol{\mu}_0 + \boldsymbol{\mu}' q + \cdots \tag{15.3.1}$$

where $\boldsymbol{\mu}' = \partial\boldsymbol{\mu}/\partial q|_{q=q_0}$ is the dipole derivative, and $\boldsymbol{\mu}_0$ is the permanent dipole moment. Then, eq. (15.2.07) can be expressed as a correlation function in the vibrational coordinate

$$C_{\text{vib}}(\tau) = |\boldsymbol{\mu}'|^2 \langle q(t)q(0)\rangle \tag{15.3.2}$$

So, the time-dependent dynamics of the vibrational coordinate dictate the IR lineshape. Equation (15.3.2) can be used to calculate absorption spectra for classical and quantum mechanical cases.

As an example, consider the case of a quantum harmonic oscillator with Hamiltonian $H = \hbar\omega_0(a^\dagger a + \frac{1}{2})$. Using the second expansion term in eq. (15.3.1), the dipole correlation function can be written in terms of the harmonic oscillator correlation function

$$\begin{aligned} C_{\text{vib}}(\tau) &= \sum_n p_n \langle n|\, \mu(\tau)\mu(0)\, |n\rangle \\ &= \mu'^2 \sum_n p_n \langle n|\, q(\tau)q(0)\, |n\rangle \end{aligned} \tag{15.3.3}$$

We discussed how to evaluate the harmonic oscillator correlation function earlier. Using this result, the vibrational dipole correlation function is written

$$C_{\text{vib}}(\tau) = \frac{\mu'^2\hbar}{2m_R\omega_0}\left[(\bar{n}+1)e^{-i\omega_0 t} + \bar{n}e^{i\omega_0 t}\right] \tag{15.3.4}$$

where $\bar{n} = (e^{\beta\hbar\omega_0} - 1)^{-1}$ is the thermal occupation number.

This quick result, while correct, glosses over the fact that these expressions include our evaluation of the transition dipole matrix elements

$$\begin{aligned} \mu_{mn} &= \langle m|\, \mu' q\, |n\rangle \\ &= \sqrt{\frac{\mu'^2\hbar}{2m_R\omega_0}}\left(\delta_{n+1,m}\sqrt{n+1} + \delta_{n-1,m}\sqrt{n}\right) \end{aligned} \tag{15.3.5}$$

This expression reminds us of the $\Delta n = \pm 1$ selection rules, indicates that $\mu_{mn} = \mu_{nm}$, and defines the fundamental transition matrix element $\mu_{10} = \sqrt{\mu'^2\hbar/2m\omega_0}$. It also shows us how transition dipole moments scale with quantum number relative to the fundamental transition

$$|\mu_{mn}|^2 = |\mu_{10}|^2\left((n+1)\delta_{m,n+1} + n\delta_{m,n-1}\right) \tag{15.3.6}$$

We can substitute this into the eigenstate form of the dipole correlation function to get eq. (15.3.4)

$$\begin{aligned} C_{\text{vib}}(\tau) &= \sum_{n,m} p_n \left|\mu_{mn}\right|^2 e^{-\mathrm{i}\omega_{mn}t} \\ &= \left|\mu_{10}\right|^2 \left((\bar{n}+1)e^{-\mathrm{i}\omega_0 t} + \bar{n}e^{\mathrm{i}\omega_0 t}\right) \end{aligned} \tag{15.3.7}$$

The absorption lineshape is then obtained from eq. (15.1.17)

$$\sigma_{\text{vib}}(\omega) = \frac{\mu'^2}{4m_R\varepsilon_0 c}\left(1 - e^{-\beta\hbar\omega}\right)\left[(\bar{n}+1)\,\delta\left(\omega-\omega_0\right) + \bar{n}\delta\left(\omega+\omega_0\right)\right] \tag{15.3.8}$$

The leading term describes absorption from state $n \rightarrow n+1$, whereas the second term describes stimulated emission from $n \rightarrow n-1$. Most of the time, molecular vibrational frequencies are of high enough energy that the low temperature limit applies at room temperature ($\bar{n} \rightarrow 0$, $e^{-\beta\hbar\omega} \approx 0$), and we have only a single absorption peak at the fundamental transition frequency

$$\sigma_{\text{vib}}(\omega) = \frac{\mu'^2}{4m_R\varepsilon_0 c}\delta\left(\omega-\omega_0\right) \tag{15.3.9}$$

Rotational spectroscopy

Now let's consider pure rotational spectroscopy, measured in the far infrared or microwave region of the spectrum. We will look specifically at the free rotation of a rigid rotor, as is characteristic of a gas-phase diatomic molecule. The Hamiltonian is expressed in terms of the rotational angular momentum operator $\mathbf{J}$ and moment of inertia I

$$H_{\text{rot}} = \frac{\mathbf{J}^2}{2I} \tag{15.3.10}$$

and the corresponding eigenvalue equations for the rotor's angular momentum are

$$\begin{aligned} \mathbf{J}^2\left|J,M\right\rangle &= \hbar^2 J\left(J+1\right)\left|J,M\right\rangle \qquad & J &= 0,1,2... \\ \mathbf{J}_z\left|J,M\right\rangle &= M\hbar\left|J,M\right\rangle & M &= -J,-J+1,...,J \end{aligned} \tag{15.3.11}$$

J is the rotational quantum number, and M refers to its projection onto the z axis. Therefore, the energy eigenvalues for H_{rot} are

$$E_J = BJ(J+1) \tag{15.3.12}$$

where the rotational constant, here in units of joules,(1) is

$$B = \frac{\hbar^2}{2I} \tag{15.3.13}$$

The rigid rotor approximation allows one to separate the rotational Hamiltonian from the vibrational and electronic degrees of freedom and evaluate a rotational lineshape in terms of a rotational correlation function without explicitly accounting for the other degrees of freedom. The dipole moment can be written in terms of a permanent dipole moment that is a product of its magnitude μ_0 and $\hat{u}$, a unit vector that specifies its orientation:

$$\boldsymbol{\mu} = \mu_0\hat{u} \tag{15.3.14}$$

In some respects, the rigid rotor approximation can be viewed as an adiabatic approximation in which μ_0 reflects a value that is averaged over much faster electronic and vibrational degrees of freedom.

The rotational absorption lineshape will be related to the Fourier transform of the rotation correlation function for the permanent dipole vector in the laboratory frame, $\hat{\varepsilon}$, which is set by the polarization of the light.

$$C_{\text{rot}}(t) = \mu_0^2\left\langle\left(\hat{\varepsilon}\cdot\hat{u}(t)\right)\left(\hat{\varepsilon}\cdot\hat{u}(0)\right)\right\rangle \tag{15.3.15}$$

Setting the polarization of the field along the $\hat{z}$ axis such that $\left(\hat{u}\cdot\hat{z}\right) = \cos\theta$, we get

$$C_{\text{rot}}(t) = \mu_0^2\left\langle\cos\theta(t)\cos\theta(0)\right\rangle \tag{15.3.16}$$

The leading μ_0^2 term means that a permanent dipole moment is required to get absorption. Remember that $\theta(t)$ still refers to a time-dependent operator in the interaction picture, whose time-dependence is governed by the rotational Hamiltonian. That is,

$$\cos\theta(t) = e^{iH_{rot}t/\hbar}\cos\theta e^{-iH_{rot}t/\hbar} \tag{15.3.17}$$

Thus, we can already anticipate that the frequency of rotational resonances will depend on the rate of rotation, which is determined by the angular momentum and the moment of inertia. Evaluating the correlation function will require that we average over both a Boltzmann distribution for the initial occupation of rotational states and the initial orientational distribution of dipoles, which is taken as isotropic, as we expect in a gas.

Then the rotational correlation function in eq. (15.3.16) can be written as

$$C_{rot}(t) = \mu_0^2 \sum_{J,M} p_{J,M} \langle J,M| e^{iH_{rot}t/\hbar}\cos\theta e^{-iH_{rot}t/\hbar}\cos\theta |J,M\rangle \tag{15.3.18}$$

Here, $|J,M\rangle$ refers to the initial state of the system and $p_{J,M}$ is the probability of initially occupying a particular J,M level:

$$p_{J,M} = e^{-\beta E_J}/Z_{rot} \tag{15.3.19}$$

$$Z_{rot} = \sum_{J,M} e^{-\beta E_J} \tag{15.3.20}$$

To evaluate this correlation function, we can insert the identity operator $I = \sum_{J',M'} |J'M'\rangle\langle J'M'|$ where marked by the arrow in eq. (15.3.18) and apply $e^{-iH_{rot}t/\hbar}|J,M\rangle = e^{-iE_Jt/\hbar}|J,M\rangle$. We also need to evaluate the square of a matrix element of the form $\langle J'M'|\cos\theta|JM\rangle$, which we described in Sec. 10.2:

$$|\langle J',M'|\cos\theta|J,M\rangle|^2 = s^{(+)}_{J,M}\delta_{J',J+1}\delta_{M',M} + s^{(-)}_{J,M}\delta_{J',J-1}\delta_{M',M} \tag{15.3.21}$$

Here the constant coefficients are

$$s^{(+)}_{J,M} = \frac{(J+1)^2 - M^2}{4(J+1)^2 - 1} \qquad s^{(-)}_{J,M} = \frac{J^2 - M^2}{4J^2 - 1} \tag{15.3.22}$$

Equation (15.3.21) defines the rigid-rotor selection rules linking initial states $|J,M\rangle$ and final states $|J',\ M'\rangle$, where $J' = J \pm 1$ and $M' = M$. Even though the energy levels of the rigid rotor, eq. (15.3.12), are nonlinearly spaced, the restriction to changes in J by ± 1 means that the transition energies are spaced linearly in J:

$$\begin{aligned} E_{J'} - E_J &= B\left[J'(J'+1) - J(J+1)\right] \\ &= \begin{cases} 2B(J+1) & J' = J+1 \\ -2BJ & J' = J-1 \end{cases} \end{aligned} \tag{15.3.23}$$

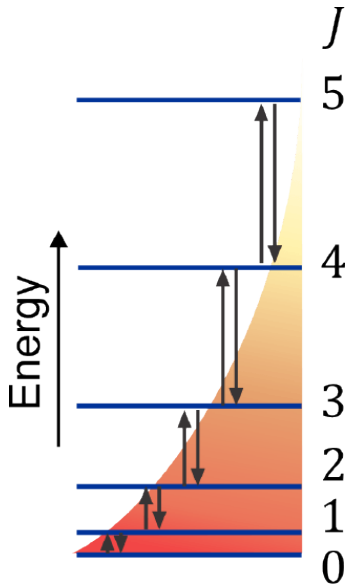


Figure 15.3.1: Rotational energy level diagram, illustrating the exponentially dropping thermal occupation of energy levels and the competing absorption and stimulated emission processes contributing at each transition frequency.

Spectroscopically, the $\Delta J = \pm 1$ changes in J correspond to the absorption or stimulated emission of radiation between adjacent energy levels (Figure 15.3.1). For gas phase molecules at room temperature, the thermally populated ensemble of rotational states extends to high J, so we can expect both processes to occur and expect that the net absorption will be related to the population difference between the upper and lower state. These steps lead to the correlation

$$C_{\text{rot}}(t) = \mu_0^2 \sum_{J,M} p_{J,M} \left(s_{J,M}^{(+)} e^{-2\text{i}(J+1)Bt/\hbar} + s_{J,M}^{(-)} e^{2\text{i}JBt/\hbar} \right) \tag{15.3.24}$$

which has two terms corresponding to the $\Delta J = \pm 1$ quantum number changes.

Let's continue by thinking about how to perform the thermal average. Since the rotational energy B isn't dependent on M, we can simplify things by performing the sum of $s_{J,M}^{(\pm)}$ coefficients over $M = -J$ to $+J$. As described in Sec. 10.2, these sums result in a factor of $(J+1)/3$ for $\Delta J = +1$ and $J/3$ for $\Delta J = -1$. With these steps, we obtain a correlation function in which we only need to sum over the initial J:

$$C_{\text{rot}}(t) = \frac{1}{3}\mu_0^2 \sum_{J} p_J \left((J+1) e^{-2\text{i}(J+1)Bt/\hbar} + J e^{2\text{i}JBt/\hbar} \right) \tag{15.3.25}$$

This is expressed in terms of the probability of being in a particular J state $p_J = e^{-\beta E_J}/Z_{\text{rot}}$. The sum over M in the rotational partition function can also be eliminated by including the degeneracy of M states for a given J: $Z_{\text{rot}} = \sum_J (2J+1) e^{-\beta E_J}$.

Using equation (15.1.16), the corresponding rotational correlation function in the frequency domain is

$$C_{\text{rot}}(\omega) = \frac{\hbar \mu_0^2}{6\pi} \sum_{J} p_J \left[(J+1)\delta\left(\hbar\omega - 2B(J+1)\right) + J\delta\left(\hbar\omega + 2BJ\right) \right] \tag{15.3.26}$$

This spectral correlation function exhibits a series of delta-function peaks spaced by $2B$, with the first term contributing peaks that arise from $\Delta J = +1$ and appear at positive frequencies for $\omega = 2B(J+1)/\hbar$, while the peaks from the second term arise from $\Delta J = -1$ and are observed at negative frequencies for $\omega = -2BJ/\hbar$. These two terms reflect the processes of absorption and stimulated emission respectively, but in this form it's not clear how the net absorption that we measure resulting from the sum of these processes comes about. This is where our expression for the cross-section, eq. (15.1.23), comes in. In calculating the imaginary part using $C_{\mu\mu}(\omega) - C_{\mu\mu}(-\omega)$, subtracting the conjugate spectrum $C_{\mu\mu}(-\omega)$ removes the stimulated emission contribution from the total absorption terms to give the net absorption. So, the absorption cross section from eq. (15.1.23) is

$$\sigma_{\text{rot}}(\omega) = \frac{\pi \mu_0^2}{6\varepsilon_0 c Z_{\text{rot}}} \omega \sum_{J} p_J \left[(J+1)\delta\left(\hbar\omega - 2B(J+1)\right) - J\delta\left(\hbar\omega + 2BJ\right) \right] \tag{15.3.27}$$

The two terms reflect the fact that each thermally populated level with $J > 0$ contributes both to absorptive and stimulated emission processes, and the observed intensity reflects the difference in populations. Since both terms enforce the $\Delta M = 0$ selection rule, we are assured that stimulated emission is properly accounted for and not solely dependent on the population of a J state.

Let's look at the behavior of the rotational correlation function and absorption spectrum as a function of temperature. In Figure 15.3.2, we plot the correlation function, the initial population of J states, and the absorption cross section using the example of a diatomic molecule that has a rotational constant of $\bar{B} = 5\ \text{cm}^{-1}$, which corresponds roughly to the value for DCL. Since the occupation of initial states is proportional to $e^{-\beta E_J} = e^{-\beta 2BJ(J+1)}$, the temperature scale that defines low and high temperature is measured with respect to $2B$, so we calculate the behavior of these functions at 1, 20, and 300 K, which correspond to $k_B T/2B$ values of 0.07, 1.4 and 21. These are shown in Figure 15.3.2.

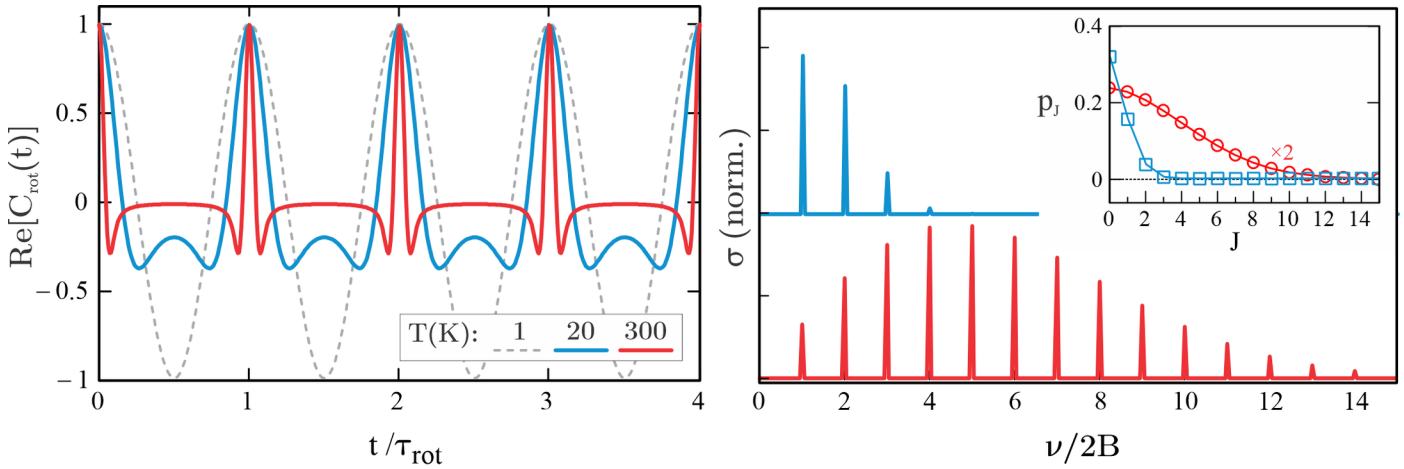


Figure 15.3.2: Temperature-dependence of rotational spectroscopy showing (left) the dipole-dipole correlation function for four rotational periods and (right) the peak normalized absorption cross section. Calculations are for a rotational constant of $B = 5\ \text{cm}^{-1}$, resulting in a rotational period of $21\ \text{ps}$. The temperatures of correspond to a relative temperature scale of $k_BT/2B = 0.07$, 1.4, and 21. Inset shows p_J, the population of initial J states.

At low temperature, all of the population that is initially in $J = 0$ and $C_{\text{rot}}(t)$ oscillates as a simple sinusoidal function with a rotational period of $\tau_{\text{rot}} = h/2B = 21\ \text{ps}$. The corresponding absorption spectrum has one resonance with an absorption frequency of $2B$, corresponding to absorption from $J = 0$ to $J' = 1$.

At the more elevated temperature of $20\ \text{K}$, on the same scale as the rotational constant, significant population is also initially observed in $J = 1$ and 2. The rotational correlation function now shows periodic peaks at τ_{rot} but without the negative excursions of a simple sinusoid. One can rationalize this by recognizing that the correlation function is expressed in terms of a sum of harmonics with a base frequency $2B$, which results in destructive interference unless $t = \tau_{\text{rot}}$. These are referred to as rotational recurrences, since they arise from the periodic realignment of dipole moments within the ensemble of molecules. The corresponding absorption spectrum is a series of resonances separated by $2B$ that reflect the weighting of these different harmonics. The spectral weights now account for the possibility of absorption and stimulated emission among the initially populated states.

Finally, at high temperature, the ensemble has rotational states initially populated to high J. It's important to remember that the energy levels of the rigid rotor are unequally spaced, meaning that at high J, the thermal population states falls off as a Gaussian in J. The net effect on $C_{\text{rot}}(t)$ is that the rotational recurrences are sharpened and that destructive interferences suppress any amplitude between them. The corresponding spectrum now has a large series of lines spaced by $2B$ that extend to a frequency of $30\bar{B} = 150\ \text{cm}^{-1}$. The envelope rises with frequency at low J due to the growing degeneracy of M states that scale as $g_M(J) = (2J + 1)$, but at high J the spectrum drops due to the falling thermal population in initial states. The high temperature behavior can be compared to the classical rotational correlation function that we described and plotted in Sec. 13.2. We find that the classical description reproduces the initial decay of the correlation function at times less that τ_{rot}, but not the recurrences. The periodic recurrences are the features that give rise to the fine structure in the rotational spectrum, and the classical correlation function recovers the overall envelope at high temperature.

Rotational-Vibrational Spectroscopy

Since we have done the work to describe the vibrational spectroscopy of a harmonic oscillator and the rotational spectroscopy of a rigid rotor, it is not much extra work to describe IR rotational-vibrational (or ro-vibrational) spectroscopy involving simultaneous transitions in vibrational and rotational quantum number. We can draw from the results above and put more attention into how separable Hamiltonians result in products of correlation functions.

We will assume a separable rigid rotor/harmonic oscillator Hamiltonian:

$$H_0 = H_{\text{rot}} + H_{\text{vib}} \tag{15.3.28}$$

with the same form as those above. An eigenstate of the system will be described by the product state labeled by the vibrational and rotational quantum numbers $|\psi\rangle = |n, J, M\rangle$, and the TISE is $H_0 |n, J, M\rangle = E_{n,J,M} |n, J, M\rangle$, with energy eigenvalues given by

$$\begin{aligned} E_{n,J} &= E_{\text{rot}} + E_{\text{vib}} \\ &= BJ\,(J+1) + \hbar\omega_0 \left(n + \frac{1}{2}\right) \end{aligned} \tag{15.3.29}$$

The transition energies in the mid-IR we will be discussing, $\Delta E = E_f - E_i$, involve changes in rotational and vibrational quantum number. Let's use a prime to index the quantum numbers for the final state and no prime for the initial: $|f\rangle = |n', J', M'\rangle$ and $|i\rangle = |n, J, M\rangle$. Let's consider the case of vibrational transitions involving a high frequency vibration with $\hbar\omega_0 \gg k_B T$, so that we only need to consider $n = 0 \to 1$ absorption from the ground vibrational state with $\Delta n = +1$. However, the temperature still exceeds the rotational energy: $k_B T \gg B$. Incorporating the rotational selection rules, $\Delta J = \pm 1$ and $\Delta M = 0$, the transition energies are

$$\begin{aligned} \Delta E &= E_{n',J'} - E_{n,J} \\ &= \hbar\omega_0 + B\,(J'\,(J'+1) - J\,(J+1)) \\ &= \begin{cases} \hbar\omega_0 + 2B(J+1) & J' = J+1 \text{ (R-branch)} \\ \hbar\omega_0 - 2BJ & J' = J-1 \text{ (P-branch)} \end{cases} \end{aligned} \tag{15.3.30}$$

As illustrated in Figure 15.3.3, the transition involves a change in vibrational and rotational quantum number, with rotational frequency shifts added to the vibrational $0 \to 1$ transition frequency ω_0. The transition frequency can involve a simultaneous increase in the vibrational and rotational state in the case of $\Delta J = +1$, and it is also possible to have a drop in rotational state, $\Delta J = -1$, accompanying the vibrational transition. Of course, a $\Delta J = -1$ transition can only occur from rotational excited states that are initially thermally populated, $J \geq 1$.

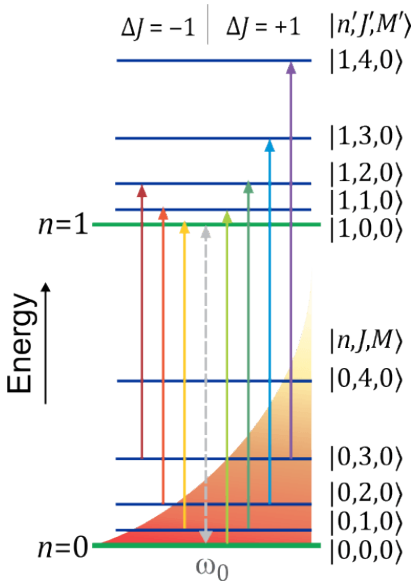


Figure 15.3.3: Transitions observed in ro-vibrational spectroscopy of diatomics with frequencies ordered left to right in increasing frequency. The fundamental vibrational transition frequency ω_0 (shown in dotted gray) is not observed.

To calculate the correlation function, we assume that the molecule's dipole moment varies linearly with the displacement of the vibration, as in eq. (15.3.1):

$$\boldsymbol{\mu} = \boldsymbol{\mu}_0 + \boldsymbol{\mu}' q + \cdots \tag{15.3.31}$$

Here again, $\boldsymbol{\mu}'$ is the dipole derivative, which we separate as a product of its magnitude and orientation:

$$\boldsymbol{\mu}' = \mu' \hat{u} \tag{15.3.32}$$

Both of these factors carry a time dependence, but since the rotational and vibrational Hamiltonians commute, we can separate the time-dependence

$$\begin{aligned} \boldsymbol{\mu}'(t) &= e^{\mathrm{i}H_0 t} \boldsymbol{\mu}' e^{-\mathrm{i}H_0 t} \\ &= e^{\mathrm{i}H_{\text{vib}} t} \mu' e^{-\mathrm{i}H_{\text{vib}} t} e^{\mathrm{i}H_{\text{rot}} t} \hat{u} e^{-\mathrm{i}H_{\text{rot}} t} \\ &= \mu'(t) \hat{u}(t) \end{aligned} \tag{15.3.33}$$

We can substitute this into the dipole correlation function, here written to emphasize the polarization of the incident light:

$$\begin{aligned} C_{\mu\mu}(\omega) &= \langle \hat{\varepsilon} \cdot \mu(t) \hat{\varepsilon} \cdot \mu(0) \rangle \\ &= \langle \mu'(t)(\hat{\varepsilon} \cdot \hat{u}(t)) \mu'(0)(\hat{\varepsilon} \cdot \hat{u}(0)) \rangle \\ &= \langle \mu'(t)\mu'(0) \rangle \langle (\hat{\varepsilon} \cdot \hat{u}(t))(\hat{\varepsilon} \cdot \hat{u}(0)) \rangle \\ &= C_{\text{vib}}(t) C_{\text{rot}}(t) \end{aligned} \tag{15.3.34}$$

The separable nature of the Hamiltonian and the fact that the rotational Hamiltonian commutes with the vibrational position operator (and vice versa) allow us to separate the total rovibrational correlation function into a product of vibrational and rotational correlation functions.

Of course, these two correlation functions are essentially identical to those we evaluated in the preceding sections. Using eq. (15.3.7) and eq. (15.3.25), and setting $\bar{n} \to 0$, we find

$$\begin{aligned} C_{\mu\mu}(t) &= \frac{1}{3}|\mu_{10}|^2 \sum_{n,J} p_n p_J \left((\bar{n}+1) e^{-\mathrm{i}\omega_0 t} + \bar{n} e^{\mathrm{i}\omega_0 t} \right) \left((J+1) e^{-2\mathrm{i}(J+1)Bt} + J e^{2\mathrm{i}JBt} \right) \\ &= \frac{\mu'^2 \hbar}{6 m_R \omega_0} \sum_J p_J \left((J+1) e^{-\mathrm{i}(\omega_0 - 2(J+1)B)t} + J e^{-\mathrm{i}(\omega_0 + 2JB)t} \right) \end{aligned} \tag{15.3.35}$$

We can see that the total dipole correlation function has a sum over two oscillating terms at the transition energies given in eq. (15.3.30) which arise from $n = 0 \to 1$ vibrational transition and the $\Delta J = +1$ and -1 changes in rotational quantum number. When we calculate our absorption cross-section using eq. (15.1.23), we obtain

$$\begin{aligned} \sigma(\omega) &= \frac{\pi\omega}{\varepsilon_0 \hbar c} \left[C_{\mu\mu}(\omega) - C_{\mu\mu}(-\omega) \right] \\ &= \frac{\mu'^2}{12 m_R \varepsilon_0 \hbar c} \left(\frac{\omega}{\omega_0} \right) \sum_J p_J \left((J+1)\delta\left(\omega - \omega_0 - 2B(J+1)\right) + J\delta\left(\omega - \omega_0 + 2JB\right) \right) \end{aligned} \tag{15.3.36}$$

We observe that we have a sum over delta function transitions for the $\Delta J = \pm 1$ terms. In this case, stimulated emission terms do not contribute since we ignored the negligibly small thermal population of the $n = 1$ vibrational level. However, it is still possible to have $\Delta J = -1$ transitions with $\Delta n = +1$ involving higher lying rotational states that are initially thermally occupied.

An example of a rovibrational infrared correlation function and absorption spectrum from this model are shown in Figure 15.3.4, using the rotational parameters from Figure 15.3.2 and a vibrational frequency of $\omega_0 = 2000 \text{ cm}^{-1}$. While the pure vibrational correlation function only oscillates at a single (high) frequency ω_0, the total correlation function is a product with the rotational correlation function. As a result, we observe a correlation function in which the high frequency vibrational oscillations are modulated by slower rotational recurrences. In the resulting absorption spectrum, we see two lobes—the P-branch ($\Delta J = -1$) and R-branch ($\Delta J = +1$)—with periodic transitions spaced by $2B$ on either side of the vibrational $0 \to 1$ transition frequency, ω_0. The lobes rise from either side of ω_0 as a result of the growth in the degeneracy of M states with increasing J; however, at higher detuning from ω_0, the lines switch to decaying as a result of decreases in thermal occupation of the initial rotational states which occur as J increases.

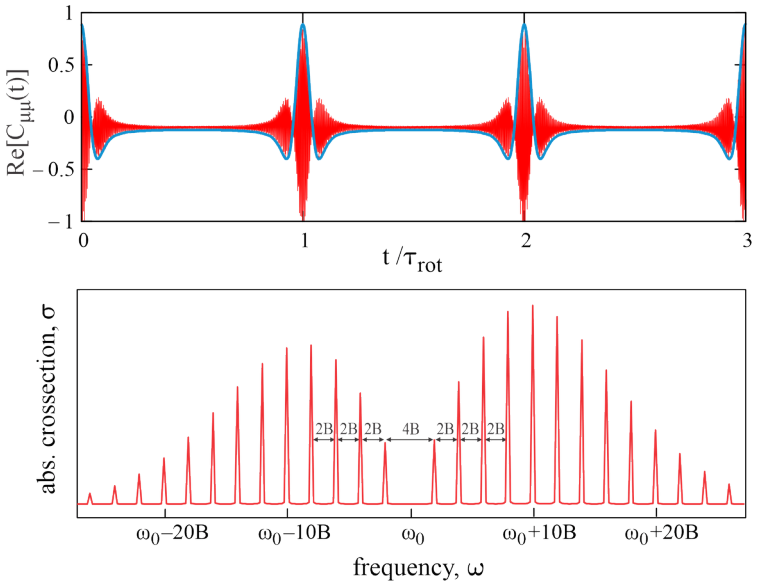


Figure 15.3.4: Rotational-vibrational spectroscopy of a diatomic molecule in the time and frequency domain using $\bar{B} = 5\ \text{cm}^{-1}$; $k_B T = 300\ \text{K}$, and $\hbar\omega_0 = 2000\ \text{cm}^{-1}$. (Top) Rovibrational correlation function, eq. (15.3.35), in red superimposed on the pure rotational correlation function in blue, showing how the rotational correlation function modulates the vibrational oscillations at ω_0. (Bottom) The corresponding absorption spectrum illustrating the band envelopes and fine structure of the P- and R-branches on the low- and high-frequency sides of the vibrational frequency.

Video

This interactive element is not available in this format. Visit the link or scan the QR code to access it online.

View this Video online

Raman spectroscopy

Although we derived a description of the absorption spectrum in terms of a correlation function for the electric dipole operator, similar forms emerge for non-resonant light-matter interactions, which we can illustrate using Raman scattering. Technically, we need second-order perturbation theory to describe Raman interactions, because the transitions are induced by two electromagnetic fields whose frequency difference equals the energy splitting between states. But we can brush over this and summarize the time-correlation function formalism by replacing the dipole operator with an induced dipole moment generated by an incident field. The incident field $\mathcal{E}_i$ polarizes the molecule, inducing a dipole moment whose magnitude is determined by the polarizability α

$$\boldsymbol{\mu}_{\text{ind}} = \boldsymbol{\alpha}\boldsymbol{\mathcal{E}}_i(t) \tag{15.3.37}$$

The scattered light field $\mathcal{E}_s$ results from an interaction with this induced dipole

$$\begin{aligned} V(t) &= -\boldsymbol{\mu}_{\text{ind}} \cdot \boldsymbol{\mathcal{E}}_s(t) \\ &= \boldsymbol{\mathcal{E}}_s(t) \cdot \boldsymbol{\alpha} \cdot \boldsymbol{\mathcal{E}}_i(t) \\ &= \mathcal{E}_s(t)\mathcal{E}_i(t)\left(\hat{\varepsilon}_s \cdot \boldsymbol{\alpha} \cdot \hat{\varepsilon}_i\right) \end{aligned} \tag{15.3.38}$$

Here we have written the polarization components of the incident (i) and scattered (s) light projecting onto the polarizability tensor α. Equation (15.3.38) leads to an expression for the Raman spectrum in terms of the time-correlation function for the polarizability :

$$\begin{aligned}\sigma(\omega) &\propto \int_{-\infty}^{+\infty} dt\, e^{\mathrm{i}\omega t} \left\langle (\hat{\varepsilon}_s \cdot \boldsymbol{\alpha}(t) \cdot \hat{\varepsilon}_i)\, (\hat{\varepsilon}_s \cdot \boldsymbol{\alpha}(0) \cdot \hat{\varepsilon}_i) \right\rangle \\ &= \int_{-\infty}^{+\infty} dt\, e^{\mathrm{i}\omega t} \left\langle \boldsymbol{\alpha}(t) \boldsymbol{\alpha}(0) \right\rangle \end{aligned} \tag{15.3.39}$$

As with the dipole operator, the time-evolution of the polarizability operator arises from the Hamiltonian for the matter in the absence of the field $\boldsymbol{\alpha}(t) = e^{\mathrm{i}H_0 t/\hbar} \boldsymbol{\alpha} e^{-\mathrm{i}H_0 t/\hbar}$. To evaluate this, the polarizability tensor can also be expanded in the nuclear coordinates, as in eq. (15.3.1),

$$\boldsymbol{\alpha} = \boldsymbol{\alpha}_0 + \left.\frac{\partial \boldsymbol{\alpha}}{\partial q}\right|_{q=q_0} q + \cdots \tag{15.3.40}$$

where the leading term would lead to Raleigh scattering and rotational Raman spectra, and the second term would give vibrational Raman scattering.

Also remember that the polarizability tensor is a second rank tensor that tells you how well a light field polarized along i can induce a dipole moment (light-field-induced charge displacement) in the s direction. For cylindrically symmetric systems which have a polarizability component $\alpha_{||}$ along the principal axis of the molecule and a component $\alpha_\perp$ perpendicular to that axis, this usually takes the form

$$\boldsymbol{\alpha} = \begin{pmatrix} \alpha_{||} & & \\ & \alpha_\perp & \\ & & \alpha_\perp \end{pmatrix} = \alpha \mathbf{I} + \frac{1}{3}\beta \begin{pmatrix} 2 & & \\ & -1 & \\ & & -1 \end{pmatrix} \tag{15.3.41}$$

where α is the isotropic component of polarizability tensor, and β is the anisotropic component.

References

(1) The traditional form for the rotational energies is expressed as a Dunham expansion in powers of $J(J+1)$ and expressed in units of wavenumbers, such that $\bar{\nu} = E_J/hc = \bar{B}J\,(J+1) + \ldots$ where $\bar{B} = h/8\pi^2 Ic$. The bar over a variable indicates the cm^{-1} units convention.

This page titled 15.3: Vibrational and Rotational Spectroscopy is shared under a CC BY-NC-SA 4.0 license and was authored, remixed, and/or curated by Andrei Tokmakoff via source content that was edited to the style and standards of the LibreTexts platform.

15.4: Line Broadening Mechanisms

The examples in the previous section illustrate how dynamical processes in thermal ensembles give rise to vibrational and rotational resonances; however, we still ended with spectra composed of delta function resonances. This is a natural consequence of a model with no damping of the correlation function. All spectra, particularly those for condensed matter but also those for the gas phase, are subject to irreversible processes that dissipate the energy absorbed from the light, even if that is purely radiative, as we saw in Sec. 11.3 and 11.4. Thus, the dynamics of irreversible dissipation processes influence the linewidth of a resonance. To illustrate, imagine that the dipole correlation function describing absorption between ground (g) and excited (e) states has an oscillatory, damped form

$$C_{\mu\mu}(t) \propto |\mu_{eg}|^2 \exp\left[-\mathrm{i}\omega_{eg}t - \Gamma t\right] \tag{15.4.1}$$

This is the same as the eigenstate correlation function expression, eq. (15.1.10), but we have added a phenomenological damping term $e^{-\Gamma t}$, where Γ is the damping rate. Then the corresponding absorption lineshape would be Lorentzian:

$$\sigma(\omega) \propto |\mu_{eg}|^2 \frac{\Gamma}{(\omega - \omega_{eg})^2 + \Gamma^2} \tag{15.4.2}$$

Thus the absorption line is broadened to a half-width at half-maximum (HWHM) of Γ. One can anticipate that measuring linewidths gives you an estimate of the relaxation rate. Indeed, the analysis of dissipative dynamics is closely related to the analysis of absorption lineshapes.

The difficulty with interpreting dynamics from absorption lineshapes is two-fold. One is practical. When multiple resonances are present, as with the rotational spectra in the previous section or with a complex polyatomic, then fast damping may result in spectral overlap. Second, and more complicated, is that numerous molecular processes can influence the lineshape, and these are generally inseparable in an absorption spectrum. These line-broadening processes can be separated into homogenous and inhomogeneous broadening. Homogenous broadening describes the dynamic processes that are intrinsic to individual constituents of the molecular system. The ensemble averaging effects that arise from the behavioral variation between different molecules are known as inhomogeneous broadening, and these mask dynamic information.

A careful assessment of these different factors is one of our primary objectives for the following chapters, but let's here catalog some of these factors.

Homogeneous broadening

Several dynamical mechanisms can contribute to the decay of a correlation function and thereby cause line-broadening. These intrinsically molecular processes are often referred to as homogeneous broadening, and, when discussed phenomenologically, they are commonly assigned a collective time scale denoted by $T_2 = \Gamma^{-1}$, a notation borrowed from NMR.

Population Relaxation. Population relaxation refers to decay of the correlation function caused by the limited lifetime of molecular states resulting from energy dissipating to the environment, often denoted T_1. The rate of population relaxation $1/T_1$ may have contributions both from the rate of radiative decay, i.e. spontaneous emission, and non-radiative processes, such as dissipating energy to other degrees of freedom or as heat.

$$\frac{1}{T_1} = \frac{1}{\tau_{\mathrm{rad}}} + \frac{1}{\tau_{\mathrm{NR}}} \tag{15.4.3}$$

The observed population relaxation depends on the sum of the relaxation rates for the upper (m) and lower states (n) according to $1/T_1 = w_{mn} + w_{nm}$. The total rate is often written $1/2T_1$, though, because when the energy splitting ω_{mn} is large compared to k_BT, only the downward rate w_{nm} contributes significantly to the population relaxation. We will take up the case of vibrational population relaxation in Chapter 18.

Dephasing. Dephasing is the randomization of phase within an ensemble caused by molecular interactions. Dephasing is a dynamic effect in which memory of a molecule's phase of oscillation is lost due to intermolecular interactions randomizing the phase, for instance through collisions in a dense gas or fluctuations induced by a solvent, as illustrated in Figure 15.4.1. The process of pure dephasing does not change the populations of the states involved. Time-averaging this behavior results in the

decay of a correlation function, which is commonly characterized by the time constant T_2^* in the phenomenological description. We will develop the formal framework for describing this in Chapter 17.

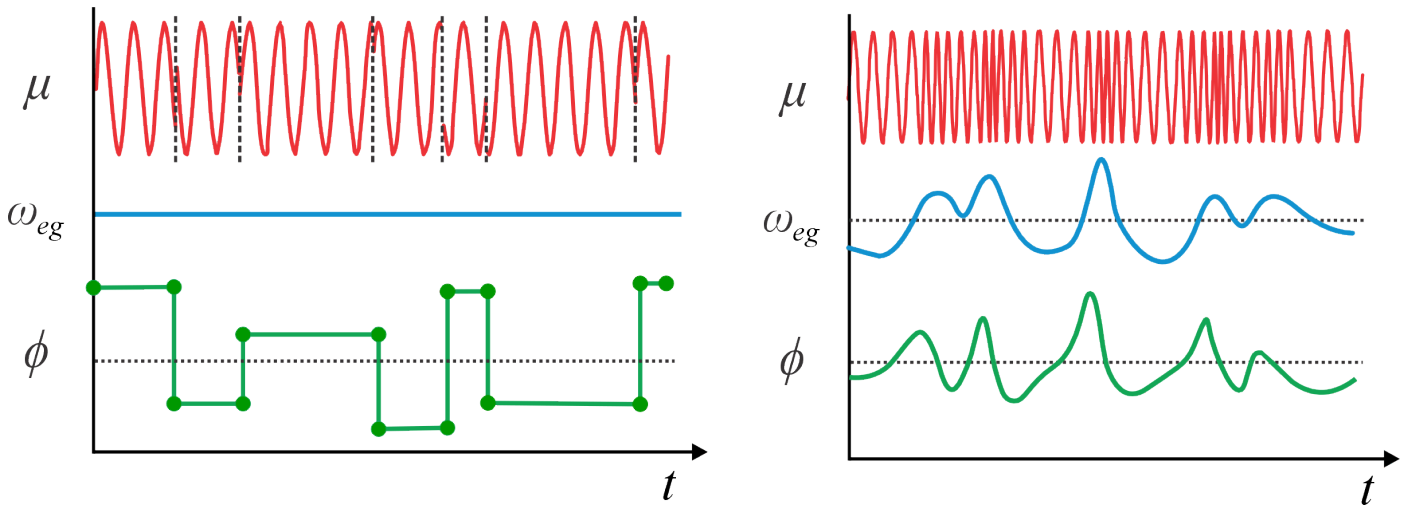


Figure 15.4.1: Illustration of dephasing induced by molecular interactions. (Left) A scenario in which the frequency of oscillation of a dipole moment ω_{eg} can remain constant, but the phase is shifted due to random perturbations. (Right) Behavior of a dipole moment μ whose frequency continuously varies around an average value, and as a result its phase $\phi = \partial\omega_{eg}/\partial t$ also varies continuously.

Orientational relaxation. Orientational relaxation (τ_{or}) also leads to decay of the dipole correlation function and thereby contributes to line-broadening. Since the correlation function depends on the projection of the dipole onto a fixed axis in the laboratory frame, the dephasing effect of the initial randomization of dipole orientations is averaged over the ensemble. We saw above how free rotational motion leads to complex rotational recurrences in the dipole correlation function, which result in a broad envelope of resonances around the lineshape of a vibrational-rotational spectrum. In solution, free rotation is interrupted and decay of the rotational correlation function is commonly treated as an orientational diffusion problem. For absorption lineshapes, the time-scale for the exponential decay of the correlation function is $\tau_{\text{or}} = 1/2D_{\text{or}}$, where D_{or} is the orientational diffusion constant.

Multiple processes. If these homogeneous processes are independent, the rates for relaxation of the correlation function in eq. (15.4.3) all contribute additively to the damping and line width caused by homogenous broadening:

$$\Gamma = \frac{1}{T_2} = \frac{1}{T_1} + \frac{1}{T_2^*} + \frac{1}{\tau_{\text{or}}} \tag{15.4.4}$$

Inhomogeneous broadening

Absorption lineshapes can also be broadened by a static distribution of frequencies; this is inhomogeneous broadening. If static environmental variations have a greater influence on the variation of absorption frequencies within the ensemble than the inherent linewidth due to homogeneous broadening, then the observed lineshape reports on the distribution of those environments (Figure 15.4.2). As a result, inhomogeneous broadening is a static ensemble averaging effect that makes it impossible to obtain dynamical content from an absorption spectrum. The origin of the inhomogeneous broadening can be molecular (for instance, lattice defects in crystals) or macroscopic (i.e., an inhomogeneous magnetic field in NMR).

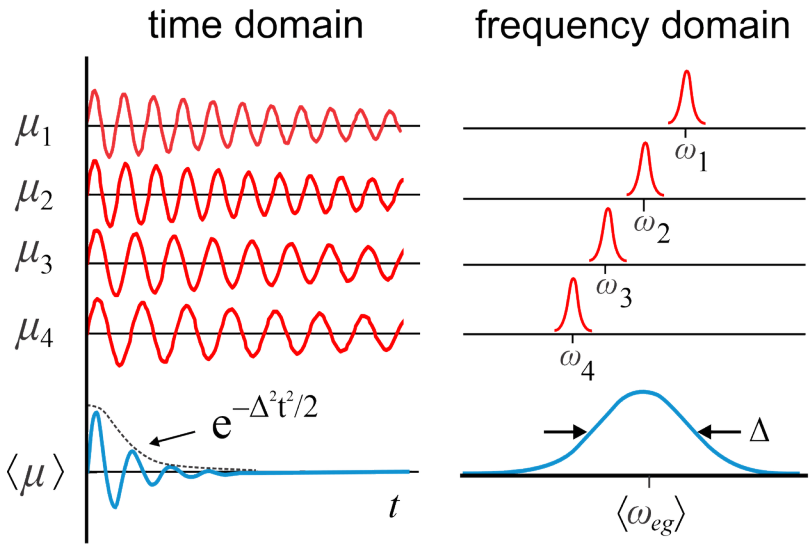


Figure 15.4.2: Illustration of how ensemble averaging over a static distribution of transition frequencies for different molecules leads to a decay of the dipole correlation function and corresponding broadening of the absorption spectrum.

To illustrate, let's consider an ensemble of molecules with transition frequencies ω_{eg} in a Gaussian distribution centered on ω_{eg}^0 with a standard deviation Δ:

$$P(\omega_{eg}) = \frac{1}{\sqrt{2\pi\Delta^2}} \exp\left[-\frac{\left(\omega_{eg}-\omega_{eg}^0\right)^2}{2\Delta^2}\right] \tag{15.4.5}$$

To calculate the correlation function, we need to integrate the dynamics of individual molecules over the distribution of transition frequencies in the ensemble. If the molecular relaxation rate is roughly constant for all members of the ensemble, then

$$C_{\mu\mu}(t) = |\mu_{eg}|^2 \int P(\omega_{eg}) \exp\left(-i\omega_{eg}t - \Gamma t\right) d\omega_{eg} \tag{15.4.6}$$

Setting the integration limits from $-\infty$ to ∞, we find that the correlation function takes the form

$$C_{\mu\mu}(t) = |\mu_{eg}|^2 \exp\left(-i\omega_{eg}^0 t - \Gamma t - \Delta^2 t^2/2\right) \tag{15.4.7}$$

This correlation function oscillates at the central transition frequency of the ensemble ω_{eg}^0 and has both exponential and Gaussian damping factors. Note, when the distribution of frequencies is very small, $\Delta \to 0$, and we obtain the correlation function we wrote before for the homogeneous case, eq. (15.4.1). On the other hand, when $\Delta \gg \Gamma$, we can neglect the Γt term in the exponential, and $C_{\mu\mu}(t)$ decays purely as a Gaussian in time. The Fourier transform then gives an absorption lineshape that is Gaussian, peaked at ω_{eg}^0 with a standard deviation linewidth of Δ, for the expected behavior in the inhomogeneous limit:

$$\sigma(\omega) \propto |\mu_{eg}|^2 \exp\left(-\frac{\left(\omega-\omega_{eg}^0\right)^2}{2\Delta^2}\right) \tag{15.4.8}$$

Total linewidth

The total linewidth of the absorption spectrum reflects contributions from all of these sources and more! Regardless of how diverse the different contributions to the dynamics of the dipole are, we will find that all line-broadening effects are ultimately expressed in terms of a time-dependent lineshape function $g(t)$. The lineshape can then be written as the Fourier transform over the oscillating transition frequency, damped and modulated by a complex $g(t)$:

$$\sigma(\omega) \propto \int_{-\infty}^{+\infty} dt\, e^{i\omega t} e^{-i\omega_{eg}t - g(t)} \tag{15.4.9}$$

For instance, in the case described by eq. (15.4.7), we would assign $g(t) = \Gamma t + \Delta^2 t^2/2$.

At the end of this discussion, one might wonder how we learn anything dynamical from absorption spectroscopy, if numerous inseparable processes contribute to broadening the spectrum. It is true, there are only limited pieces of information that one can uniquely determine from the linewidth and lineshape. This is one of the biggest motivators for using nonlinear and two-dimensional spectroscopies. These techniques allow one to isolate different dynamic contributions to a lineshape through the use of time- and/or frequency-resolved measurements involving two or more incident fields.

This page titled 15.4: Line Broadening Mechanisms is shared under a CC BY-NC-SA 4.0 license and was authored, remixed, and/or curated by Andrei Tokmakoff via source content that was edited to the style and standards of the LibreTexts platform.

15.5: Readings

1. McHale, J. L. *Molecular Spectroscopy*, 1st ed.; Prentice-Hall, 1999.
2. McQuarrie, D. A. *Statistical Mechanics*; Harper & Row, 1976; ch 21.
3. Nitzan, A. *Chemical dynamics in condensed phases: Relaxation, transfer and reactions in condensed molecular systems*; Oxford University Press, 2006. DOI: 10.1093/oso/9780198529798.001.0001
4. Schatz, G. C.; Ratner, M. A. *Quantum Mechanics in Chemistry*; Dover Publications, 2002; sec 6.2.

This page titled 15.5: Readings is shared under a CC BY-NC-SA 4.0 license and was authored, remixed, and/or curated by LibreTexts.

16: COUPLING OF ELECTRONIC AND NUCLEAR MOTION

16.1: The Displaced Harmonic Oscillator Model
16.2: Coupling to a Harmonic Bath
16.3: Semiclassical Approximation to the Dipole Correlation Function
16.4: Readings

This page titled 16: Coupling of Electronic and Nuclear Motion is shared under a CC BY-NC-SA 4.0 license and was authored, remixed, and/or curated by Andrei Tokmakoff via source content that was edited to the style and standards of the LibreTexts platform.

16.1: The Displaced Harmonic Oscillator Model

The displaced harmonic oscillator (DHO) is a widely used model that describes the coupling of nuclear motions to electronic states; however, it contains the general framework for describing molecular interactions and dynamics observed in many experiments. We will use it to describe the interactions underlying electronic absorption spectroscopy in order to understand how vibrations that alter electronic configurations can produce the vibronic structure seen in absorption spectra. The model depicts the interactions between two components: an experimentally observed quantity—here it is the "bright" electronic transition—and an environment that we don't see directly—a "dark" harmonic oscillator. Spectroscopically, it can also be used to describe wavepacket dynamics, the coupling of electronic and vibrational states to intramolecular vibrations or solvent, or the coupling of the electronic states of solids or semiconductors to phonons. Further extensions of this model can be used to describe fundamental chemical rate processes, the interactions of a molecule with a dissipative or fluctuating environment, and Marcus theory for nonadiabatic electron transfer. The common theme is an experimentally observed system coupled to dynamical nuclear degrees of freedom.

The DHO and Electronic Absorption

Molecular electronic excited states have different geometries than the ground state due to the change in electronic configuration. This interdependence between electronic energy and nuclear configuration results in a variation of the electronic energy gap between states as one stretches bonds of the molecule. We are interested in describing how this effect influences the electronic absorption spectrum, and thereby we will gain insight into how one experimentally determines the coupling between electronic and nuclear degrees of freedom. For example, consider the electronic transitions between the bound potential energy surfaces of a ground and excited state as we displace a nuclear coordinate q. As illustrated in Figure 16.1.1, the model consists of two harmonic oscillator potentials whose minima are separated vertically by an energy splitting $(E_e - E_g)$ and are shifted relative to one another by a displacement d along the coordinate q. We will calculate the absorption spectrum in the interaction picture using the time-correlation function for the dipole operator.

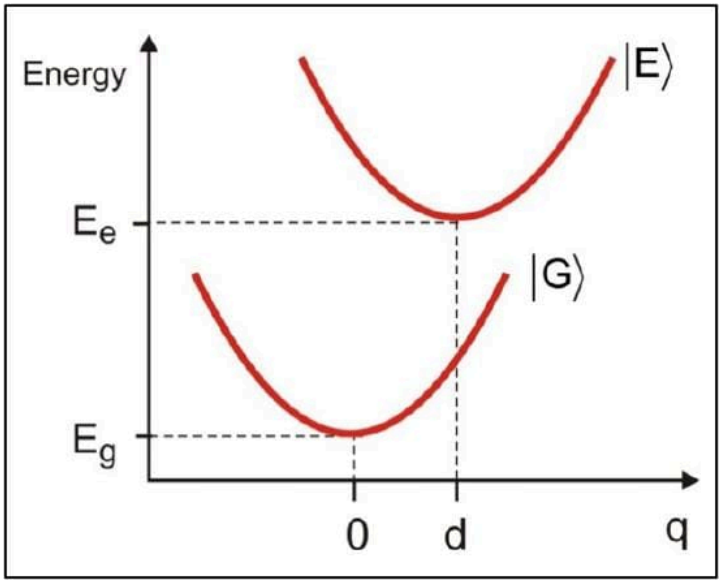


Figure 16.1.1: Key variables for the displaced harmonic oscillator model.

We start constructing the displaced harmonic oscillator model by writing a Hamiltonian that contains two terms describing the potential energy surfaces of the electronically excited state $|E\rangle$ and ground state $|G\rangle$

$$H_0 = H_G + H_E \tag{16.1.1}$$

These terms describe the dependence of the electronic energy on the displacement of a nuclear coordinate q. Since the state of the system depends on the level of vibrational excitation, we describe it as a product of the electronic and nuclear states, $|\Psi\rangle = |\psi_{\text{elec}}\Phi_{\text{nuc}}\rangle$, or more simply using the indexes $|\Psi\rangle = |a, n\rangle$. For the present case, the electronic state is indexed as $a = g$ or e, and

the vibrational state is described by the corresponding vibrational quantum number n

$$|G\rangle = |g, n_g\rangle \qquad |E\rangle = |e, n_e\rangle \tag{16.1.2}$$

Implicit in this model is the Born-Oppenheimer approximation, which allows us to separate the nuclear and electronic states and energies in H_0, i.e., $H_G|G\rangle = (E_g + E_{n_g})|G\rangle$.

The Hamiltonian for each surface contains both the electronic energy in the absence of vibrational excitation, $|a\rangle\, E_a\, \langle a|$, and a vibronic Hamiltonian that describes the change in energy with nuclear displacement, $H_a(q)$.

$$\begin{aligned} H_G &= |g\rangle\, E_g\, \langle g| + H_g(q) \\ H_E &= |e\rangle\, E_e\, \langle e| + H_e(q) \end{aligned} \tag{16.1.3}$$

For our purposes, the vibronic Hamiltonian is harmonic and has the same force constant in the ground and excited states ($\kappa = m\omega_0^2$). However, the excited state is displaced along q by d, relative to the ground state.

$$H_g = \frac{p^2}{2m} + \frac{1}{2} m\omega_0^2 q^2 \tag{16.1.4}$$

$$H_e = \frac{p^2}{2m} + \frac{1}{2} m\omega_0^2 (q-d)^2 \tag{16.1.5}$$

The operator q acts only to change the degree of vibrational excitation on the $|E\rangle$ or $|G\rangle$ surface.

To calculate the electronic absorption spectrum, we now wish to evaluate the dipole correlation function in the interaction picture:

$$\begin{aligned} C_{\mu\mu}(t) &= \langle \boldsymbol{\mu}(t)\boldsymbol{\mu}(0)\rangle \\ &= \sum_{\ell=E,G} p_\ell \left\langle \ell \left| e^{\mathrm{i}H_0 t/\hbar} \boldsymbol{\mu} e^{-\mathrm{i}H_0 t/\hbar} \boldsymbol{\mu} \right| \ell \right\rangle \end{aligned} \tag{16.1.6}$$

Here, the correlation function is evaluated as an average over the initial state of the system, $|\ell\rangle = |a, n\rangle$. Thus the p_ℓ is the joint probability of occupying a particular electronic and vibrational state, i.e., $p_\ell = p_a p_n$. Under typical conditions, the system will initially be on the ground electronic state, so that $|\ell\rangle = |G\rangle = |g, n_g\rangle$ and

$$C_{\mu\mu}(t) = \sum_{n_g} p_{n_g} \left\langle g, n_g \left| e^{\mathrm{i}H_0 t/\hbar} \boldsymbol{\mu} e^{-\mathrm{i}H_0 t/\hbar} \boldsymbol{\mu} \right| g, n_g \right\rangle \tag{16.1.7}$$

The time propagator under the molecular Hamiltonian $e^{-\mathrm{i}H_0 t/\hbar}$ can be expressed in term of contributions from evolutions on the ground and excited states:

$$e^{-\mathrm{i}H_0 t/\hbar} = |G\rangle e^{-\mathrm{i}H_G t/\hbar} \langle G| + |E\rangle e^{-\mathrm{i}H_E t/\hbar} \langle E| \tag{16.1.8}$$

We then make the Condon Approximation, which states that there is no nuclear dependence for the dipole operator. It is only an operator in the electronic states.

$$\bar{\mu} = |g\rangle\, \mu_{ge}\, \langle e| + |e\rangle\, \mu_{eg}\, \langle g| \tag{16.1.9}$$

This approximation implies that the timescale of electronic excitation that leads to transitions between electronic surfaces occurs so rapidly that there is no change in nuclear displacement. This corresponds to a vertical transition between states on the potential energy diagram.

Under typical conditions, the system will only be on the ground electronic state at equilibrium, and by substituting eqs. (16.1.8) and (16.1.9) into (16.1.6) we find:

$$C_{\mu\mu}(t) = |\mu_{eg}|^2\, e^{-\mathrm{i}(E_e - E_g)t/\hbar} \left\langle e^{\mathrm{i}H_g t/\hbar} e^{-\mathrm{i}H_e t/\hbar} \right\rangle \tag{16.1.10}$$

The leading two factors represent the electronic transition intensity and the oscillations at the pure electronic energy gap respectively, whereas the final term represents the nuclear dynamics. This final term is known as the dephasing function:

$$\begin{aligned} F(t) &= \sum_{n_g} p_{n_g} \left\langle n_g \left| e^{\mathrm{i}H_g t/\hbar} e^{-\mathrm{i}H_e t/\hbar} \right| n_g \right\rangle \\ &= \left\langle e^{\mathrm{i}H_g t/\hbar} e^{-\mathrm{i}H_e t/\hbar} \right\rangle \\ &= \left\langle U_g^\dagger U_e \right\rangle \end{aligned} \tag{16.1.11}$$

Note that, physically, the dephasing function is an overlap integral rather than an expectation value. It describes the time-dependent overlap of the nuclear wavefunction on the ground state, $|\varphi_g\rangle = \sum_{n_g} b_{n_g} |n_g\rangle$ with the time-evolution of the same wavepacket initially projected onto the excited state

$$F(t) = \langle \varphi_g(t) | \varphi_e(t) \rangle \tag{16.1.12}$$

This is a general expression that does not depend on the form of the potential. If you have knowledge of the nuclear and electronic eigenstates or the nuclear dynamics on your ground and excited state surfaces, this expression is your route to the absorption spectrum.(1)(2)

To evaluate $F(t)$, it is helpful to write the ground state nuclear Hamiltonian as

$$H_g = \hbar\omega_0 \left(a^\dagger a + \tfrac{1}{2} \right) \tag{16.1.13}$$

and express the excited state Hamiltonian in terms of H_g using the displacement operator $\hat{D}$

$$H_e = \hat{D} H_g \hat{D}^\dagger \tag{16.1.14}$$

$$\hat{D} = \exp\left(-\mathrm{i}\hat{p}d/\hbar \right) \tag{16.1.15}$$

Remember $\hat{D}$ acts on the position operator to shift it in space as:

$$\hat{D}\hat{q}\hat{D}^\dagger = \hat{q} - d \tag{16.1.16}$$

and $\hat{p}$ is only an operator in the vibrational degree of freedom. The same transformation allows us to relate the time propagators on the ground and excited states

$$e^{-\mathrm{i}H_e t/\hbar} = \hat{D} e^{-\mathrm{i}H_g t/\hbar} \hat{D}^\dagger \tag{16.1.17}$$

Substituting eq. (16.1.17) into eq. (16.1.11) allows us to rewrite eq. (16.1.11) as

$$\begin{aligned} F(t) &= \left\langle U_g^\dagger e^{-\mathrm{i}dp/\hbar} U_g e^{\mathrm{i}dp/\hbar} \right\rangle \\ &= \left\langle e^{-\mathrm{i}d\hat{p}(t)/\hbar} e^{\mathrm{i}d\hat{p}(0)/\hbar} \right\rangle \\ &= \left\langle \hat{D}(t) \hat{D}^\dagger(0) \right\rangle \end{aligned} \tag{16.1.18}$$

This transformation shifts the time-dependence to the momentum operator using

$$\hat{p}(t) = U_g^\dagger \hat{p}(0) U_g \tag{16.1.19}$$

resulting in a time-dependent displacement operator $\hat{D}(t)$ with the same physical interpretation as eq. (16.1.12). The effect of the nuclear motion on the absorption spectrum can now be expressed as a time-correlation function for the displacement of the vibration following electronic excitation.

To evaluate eq. (16.1.18) we start with the time-dependent expression for the harmonic oscillator momentum operator, expressed in raising and lowering operators,

$$\hat{p}(t) = \mathrm{i}\sqrt{\frac{m\hbar\omega_0}{2}} \left(a^\dagger e^{\mathrm{i}\omega_0 t} - a e^{-\mathrm{i}\omega_0 t} \right) \tag{16.1.20}$$

This gives the dephasing function

$$F(t) = \left\langle \left[\underset{\sim}{d} \left(a^\dagger e^{-\mathrm{i}\omega_0 t} \right) \right] \exp\left[-\underset{\sim}{d} \left(a^\dagger - a \right) \right] \right\rangle \tag{16.1.21}$$

where we have defined a dimensionless displacement variable

$$\underset{\sim}{d} = d\sqrt{\frac{m\omega_0}{2\hbar}} \tag{16.1.22}$$

Since $a^\dagger$ and a do not commute, $[a^\dagger, a] = -1$, we split the exponential operators using the identity

$$e^{\hat{A}+\hat{B}} = e^{\hat{A}}e^{\hat{B}}e^{-\frac{1}{2}\left[\hat{A},\hat{B}\right]} \tag{16.1.23}$$

or specifically for $a^\dagger$ and a,

$$e^{\lambda a^\dagger + \mu a} = e^{\lambda a^\dagger}e^{\mu a}e^{\lambda\mu/2} \tag{16.1.24}$$

Note that the third term $e^{\lambda\mu/2}$ is a constant that can be factored out. Applying this to eq. (16.1.21) leads to

$$F(t) = e^{\underset{\sim}{d}^2}\left\langle \exp\left[\underset{\sim}{d}a^\dagger e^{-i\omega_0 t}\right]\exp\left[-\underset{\sim}{d}ae^{-i\omega_0 t}\right]\exp\left[-\underset{\sim}{d}a^\dagger\right]\exp\left[\underset{\sim}{d}a\right]\right\rangle \tag{16.1.25}$$

To simplify our work further, let's specifically consider the case in which we are initially in the ground vibrational state $|n_g\rangle = |0\rangle$. Since action of the lowering operator on the ground state leads to a null vector, $a|0\rangle = 0$, and $\langle 0|\, a^\dagger = 0$, the action of the corresponding exponential operators leaves the system unchanged

$$\begin{aligned} e^{-\lambda a}|0\rangle &= |0\rangle \\ \langle 0|\, e^{\lambda a^\dagger} &= \langle 0| \end{aligned} \tag{16.1.26}$$

and

$$F(t) = e^{-\underset{\sim}{d}^2}\left\langle 0\left|\exp\left[-\underset{\sim}{d}ae^{-\mathrm{i}\omega_0 t}\right]\exp\left[-\underset{\sim}{d}a^\dagger\right]\right|0\right\rangle \tag{16.1.27}$$

In principle, these are expressions which we can evaluate by expanding the exponential operators. However, the evaluation becomes much easier if we can exchange the order of the operators. Remembering that these operators do not commute, we use

$$e^{\hat{A}}e^{\hat{B}} = e^{\hat{B}}e^{\hat{A}}e^{-\left[\hat{B},\hat{A}\right]} \tag{16.1.28}$$

We can now write

$$\begin{aligned} F(t) &= e^{-\underset{\sim}{d}^2}\left\langle 0\left|\exp\left[-\underset{\sim}{d}a^\dagger\right]\exp\left[-\underset{\sim}{d}ae^{-\mathrm{i}\omega_0 t}\right]\exp\left[-\underset{\sim}{d}^2e^{-\mathrm{i}\omega_0 t}\right]\right|0\right\rangle \\ &= \exp\left[S\left(e^{-\mathrm{i}\omega_0 t}-1\right)\right] \end{aligned} \tag{16.1.29}$$

Here we introduced the Huang-Rhys parameter, S, a dimensionless factor related to the mean square displacement

$$S = \underset{\sim}{d}^2 = d^2\frac{m\omega_0}{2\hbar} \tag{16.1.30}$$

The Huang-Rhys parameter represents the strength of the electronic states' coupling to the nuclear degree of freedom. If $S = 0$, the dynamics of the nuclei have no effect on the dipole correlation function.

With eq. (16.1.29), we have come up with a simple expression for the nuclear dynamics without ever having to explicitly calculate the position dependence of the wavefunction. That is a great example of how operator methods can greatly simplify problems in quantum mechanics!

So, finally, we return to dipole correlation function, substituting the dephasing function (16.1.29) into (16.1.10):

$$C_{\mu\mu}(t) = |\mu_{eg}|^2\exp\left[-\mathrm{i}\omega_{eg}t + S\left(e^{-\mathrm{i}\omega_0 t}-1\right)\right] \tag{16.1.31}$$

This correlation function takes a form that we will see often:

$$C_{\mu\mu}(t) = \sum_n p_n|\mu_{mn}|^2 e^{-\mathrm{i}\omega_{mn}t - g(t)} \tag{16.1.32}$$

where $g(t)$ is the lineshape function

$$g(t) = -S\left(e^{-\mathrm{i}\omega_0 t}-1\right) \tag{16.1.33}$$

As we will see later, nonlinear spectroscopy models often represent dynamic phenomena in terms of a lineshape function.

Figure 16.1.2 illustrates the form of the real and imaginary parts of these complex functions, using an electronic transition energy that is ten times higher than the vibrational frequency $\omega_{eg} = 10\omega_0$, and $S = 1$. The lineshape function $g(t)$ oscillates with the frequency of the single vibrational mode, ω_0. $F(t)$ quantifies the overlap between vibrational wavepackets on the ground and excited states, which peaks once every vibrational period. $C_{\mu\mu}(t)$ has the same information as $F(t)$, but is additionally modulated at the high frequency electronic energy gap ω_{eg}.

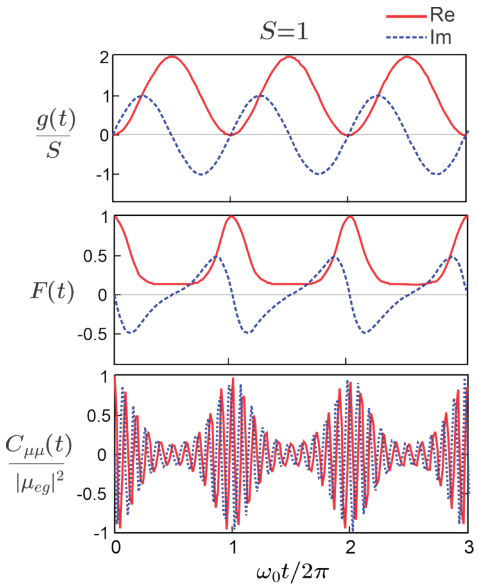


Figure 16.1.2: Time-dependence of the lineshape function, $g(t) = S(1 - \cos\omega_0 t + \mathrm{i}\sin\omega_0 t)$, dephasing function, $F(t)$, and dipole correlation function, $C_{\mu\mu}(t)$ for the displace harmonic oscillator initially in the ground electronic and vibrational states, using $S = 1$ and $\omega_{eg} = 10\omega_0$.

Absorption Lineshape and Franck-Condon Transitions

We can now study how this dynamic behavior manifests in the absorption lineshape $\sigma_{\mathrm{abs}}(\omega)$, which we obtain from a Fourier transform of the dipole correlation function in eq. (16.1.31). Separating the transformed correlation function's constant terms from the time-dependent ones, we obtain:

$$\begin{aligned}\sigma_{\mathrm{abs}}(\omega) &= \frac{1}{2\pi}\int_{-\infty}^{+\infty} dt\, e^{\mathrm{i}\omega t} C_{\mu\mu}(t) \\ &= \frac{1}{2\pi}|\mu_{eg}|^2\, e^{-S}\int_{-\infty}^{+\infty} dt\, e^{\mathrm{i}(\omega-\omega_{eg})t}\exp\left[Se^{-\mathrm{i}\omega_0 t}\right]\end{aligned} \tag{16.1.34}$$

The unusual final term—an exponential of an exponential factor—can be dealt with by expanding the leading exponential

$$\exp\left[Se^{-\mathrm{i}\omega_0 t}\right] = \sum_{n=0}^{\infty}\frac{1}{n!}S^n\left(e^{-i\omega_0 t}\right)^n \tag{16.1.35}$$

With this substitution, and remembering that $\mathcal{F}[\exp(-i\omega_0 t)] = 2\pi\delta(\omega - \omega_0)$, the absorption lineshape can be expressed as

$$\sigma_{\mathrm{abs}}(\omega) = |\mu_{eg}|^2\sum_{n=0}^{\infty} e^{-S}\frac{S^n}{n!}\delta(\omega - \omega_{eg} - n\omega_0) \tag{16.1.36}$$

As illustrated in Figure 16.1.3, the summation of delta-function peaks in this equation describes a vibrational progression that accompanies the electronic transition. The series of peaks starts with the purely electronic 0-0 transition ω_{eg} ($n_g = 0 \rightarrow n_e = 0$) and increases in frequency by integer multiples of the vibrational frequency, ω_0.

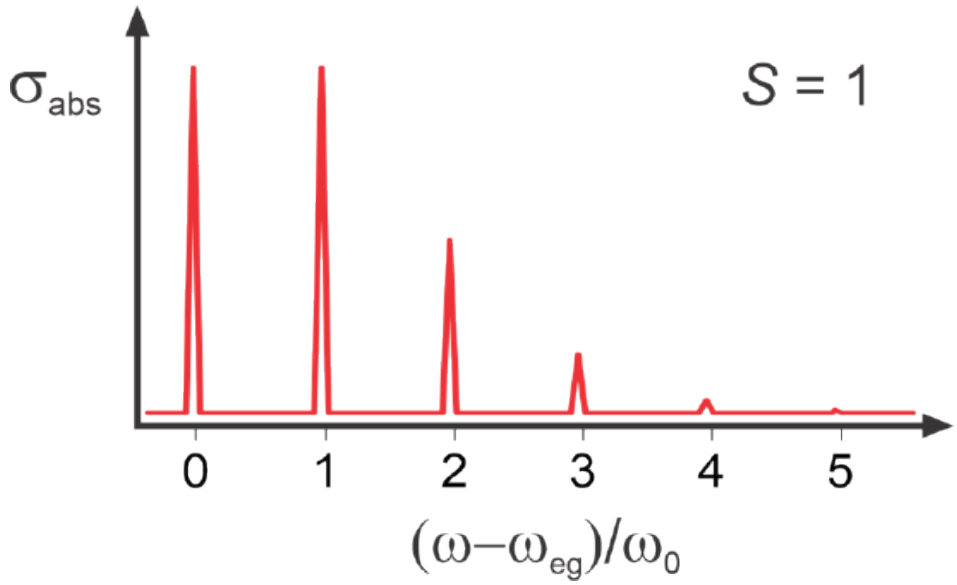


Figure 16.1.3: The absorption lineshape corresponding to the correlation function for $S = 1$ shown in Figure 16.1.2

The peaks' intensities are observed to follow a Poisson distribution. This result corresponds to the Franck-Condon integrals for the overlap of harmonic oscillator wavefunctions in the ground and displaced excited states $f_{n_g,n_e} = \langle n_g | n_e \rangle$

$$|\langle 0 \, | n \rangle|^2 = \left| \langle 0 \left| \hat{D} \right| n \rangle \right|^2 = e^{-S} \frac{S^n}{n!} \tag{16.1.37}$$

The absorption lineshape is area normalized, such that the intensity of the electronic transition dipole moment is distributed among the progression of lines:

$$\int \sigma_{\text{abs}}(\omega) \, d\omega = |\mu_{eg}|^2 \tag{16.1.38}$$

Now let's investigate how the absorption lineshape depends on S. As seen in Figure 16.1.4, for $S = 0$ there is no dependence of the electronic energy gap ω_{eg} on the nuclear coordinate, and only one resonance is observed. In this limit, the electronic energy gap is identical for any value of q, and nuclear motion has no influence on the electronic spectrum. For $S \ll 1$, the dependence of the energy gap on q is weak, and the intensity of peaks in the progression drops rapidly as S^n.

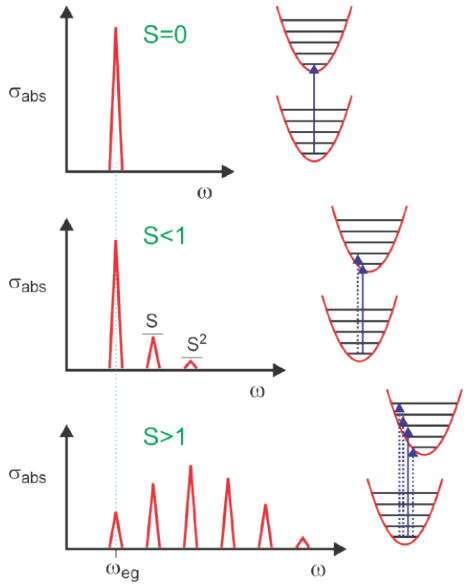


Figure 16.1.4: Illustration of the intensity variation within the vibrational procession for difference values of the Huang-Rhys factor, S.

For $S < 1$, the progression has numerous strong bands, and the most intense peak no longer corresponds to ω_{eg} but corresponds

to $n \geq 1$. The progression appears to trace a smooth curve that envelopes these transitions, which we can investigate by performing a short time expansion of the correlation function applicable for $\omega_0 t < 1$ and $S \gg 1$. If we approximate the oscillatory term in the lineshape function in eq. (16.1.34) as

$$\exp\left(-\mathrm{i}\omega_0 t\right) \approx 1 - \mathrm{i}\omega_0 t - \tfrac{1}{2}\omega_0^2 t^2 \tag{16.1.39}$$

then the lineshape envelope is

$$\begin{aligned}\sigma_{\mathrm{env}}(\omega) &= |\mu_{eg}|^2 \int_{-\infty}^{+\infty} dt\, e^{\mathrm{i}(\omega-\omega_{eg})t} e^{S(\exp(-\mathrm{i}\omega_0 t)-1)} \\ &\approx |\mu_{eg}|^2 \int_{-\infty}^{+\infty} dt\, e^{\mathrm{i}(\omega-\omega_{eg})t} e^{S(-\mathrm{i}\omega_0 t - \frac{1}{2}\omega_0^2 t^2)} \\ &= |\mu_{eg}|^2 \int_{-\infty}^{+\infty} dt\, e^{\mathrm{i}(\omega-\omega_{eg}-S\omega_0)t} e^{-\frac{1}{2}S\omega_0^2 t^2}\end{aligned} \tag{16.1.40}$$

This integral can be solved by completing the square, giving

$$\sigma_{\mathrm{env}}(\omega) = |\mu_{eg}|^2 \sqrt{\frac{2\pi}{S\omega_0^2}} \exp\left[-\frac{(\omega - \omega_{eg} - S\omega_0)^2}{2S\omega_0^2}\right] \tag{16.1.41}$$

As illustrated in Figure 16.1.5, the envelope has a Gaussian profile which is centered at the Franck–Condon vertical transition

$$\omega_{\max} = \omega_{eg} + S\omega_0 \tag{16.1.42}$$

and has a width proportional to $\sqrt{S}\omega_0$. Thus, S characterizes the expectation value for the number of vibrational quanta excited in $|E\rangle$ on absorption from the ground state. This leads us to define the average vibrational energy in $|E\rangle$ upon excitation at $q = 0$:

$$\lambda = S\hbar\omega_0 = \tfrac{1}{2}m\omega_0^2 d^2 \tag{16.1.43}$$

λ is known as the reorganization energy. This is the value of H_e at $q = 0$, which reflects the excess vibrational excitation in the excited state that occurs on a vertical transition from the ground state. This is energy that must be dissipated through vibrational relaxation on the excited state surface as the system re-equilibrates following absorption.

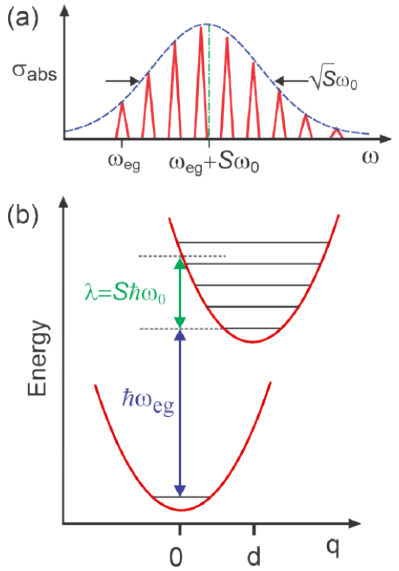


Figure 16.1.5: (a) Dependence of vibrational progression envelope on the Huang-Rhys parameter. (b) Vertical absorption transition as a sum of the electronic and excess vibrational energy.

The expansion in eq. (16.1.39) and the result of this expansion remind us that the dephasing function is a complex quantity and that the real and imaginary components impact different features of the spectrum. From eq. (16.1.40), we see that it is possible to express the dephasing function as

$$F(t) = e^{-g(t)} \tag{16.1.44}$$

where the complex quantity $g(t)$ is known as the lineshape function, with real and imaginary components $g(t) = g'(t) + \mathrm{i}g''(t)$. From eq. (16.1.40) we see that $g'(t) = \frac{1}{2}S\omega_0^2 t^2$. and $g''(t) = S\omega_0 t$. The exponential terms in the dipole correlation function can then be collected into two exponential terms for the imaginary and real terms, $C_{\mu\mu}(t) \sim e^{\mathrm{i}(\omega t - \omega_{eg} t - g'')} e^{-g'}$, which shows that g'' shifts the resonance frequency of the spectrum, but g' is a damping term that determines the linewidth and lineshape.

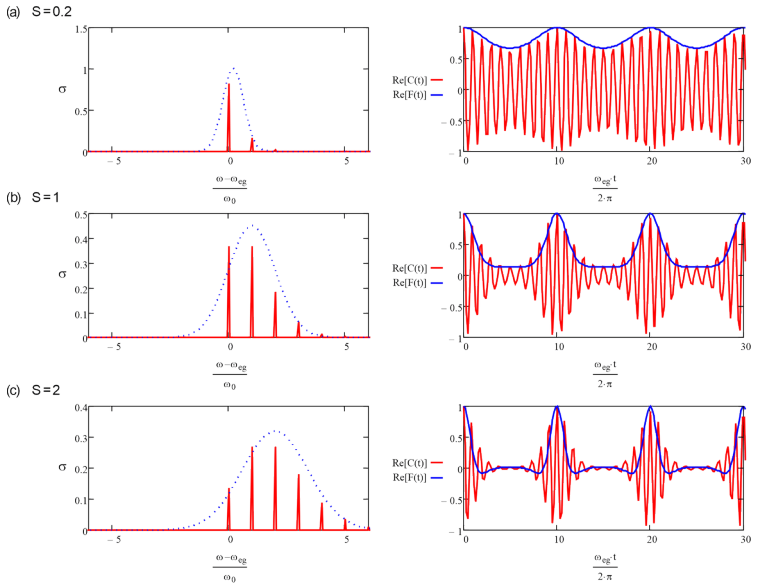


Figure 16.1.6: Examples of how the Huang-Rhys factor S influences (left) the absorption lineshape σ (16.1.36) and (right) the dipole correlation function $C_{\mu\mu}$ (16.1.31). Also shown: the Gaussian approximation of the absorption profile (16.1.41), in blue dashed lines, and the dephasing function (16.1.29), as solid blue lines.

Fluorescence

The DHO model also leads to predictions about the form of the emission spectrum from the electronically excited state. Once electronic absorption has occurred, the vibrational excitation on the excited state's potential energy surface rapidly dissipates through vibrational relaxation, typically on picosecond time scales. Vibrational relaxation leaves the system in the ground vibrational state of the electronically excited surface, with an average displacement that is larger than that of the ground state. In the absence of other non-radiative relaxation processes, the most efficient way of relaxing back to the ground state is by emission of light, i.e., fluorescence. In the Condon approximation, this occurs through vertical transitions from the excited state minimum to a vibrationally excited state on the ground electronic surface. The difference in frequency between the absorption peak and the emitted fluorescence reflects the amount of energy from the initial excitation that has dissipated into vibrational motion, on both the excited and ground states' potential energy surfaces. This difference is referred to as the Stokes shift.

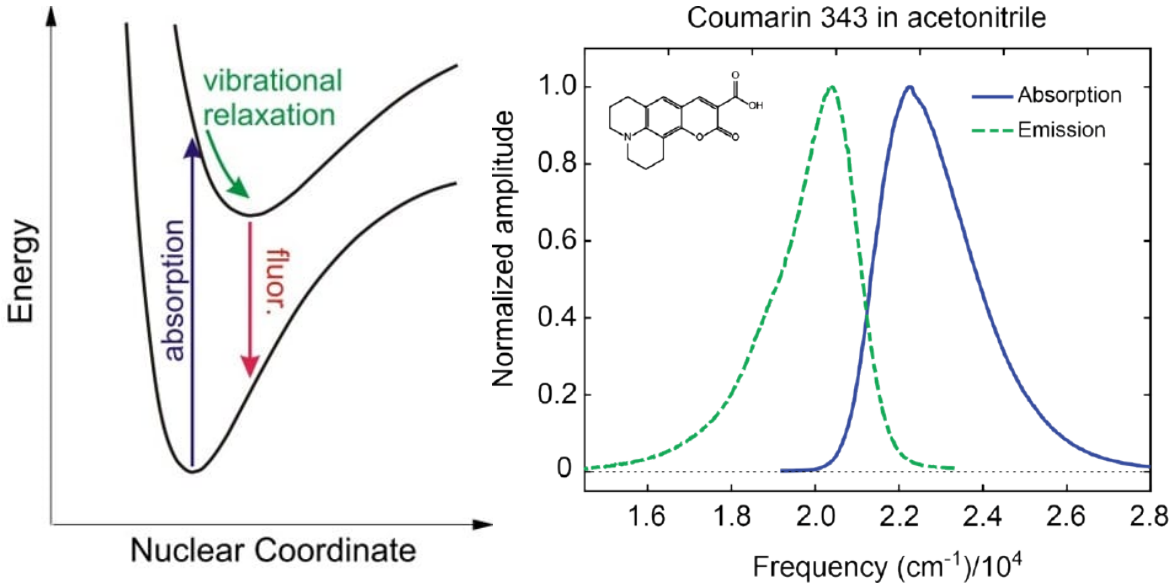


Figure 16.1.7: Vibrational relaxation processes following absorption of light lead to fluorescence emission at a lower frequency.

The emission lineshape can be obtained from the dipole correlation function using the DHO model. We assume that, following the rapid dissipation of energy λ on the excited state, the initial state before emission is equilibrated in $|e,0\rangle$ at a displacement $q=d$. Based on the energy gap at $q=d$, we see that a vertical emission from this point leaves λ as the vibrational energy that needs to be dissipated on the ground state to re-equilibrate. Therefore, we expect the Stokes shift to be 2λ (Figure 16.1.8a).

Beginning with our original derivation of the dipole correlation function and focusing on emission, we find that the dipole correlation function describing the fluorescence emission is

$$\begin{aligned} C_{\text{fl}}(t) &= \langle e,0|\,\boldsymbol{\mu}(t)\boldsymbol{\mu}(0)\,|e,0\rangle \\ &= |\mu_{eg}|^2\, e^{\mathrm{i}\omega_{eg}t}\left\langle e^{\mathrm{i}H_e t/\hbar}e^{-\mathrm{i}H_g t/\hbar}\right\rangle \\ &= |\mu_{eg}|^2\, e^{\mathrm{i}\omega_{eg}t}\left\langle U_e^{\dagger}U_g\right\rangle \end{aligned} \tag{16.1.45}$$

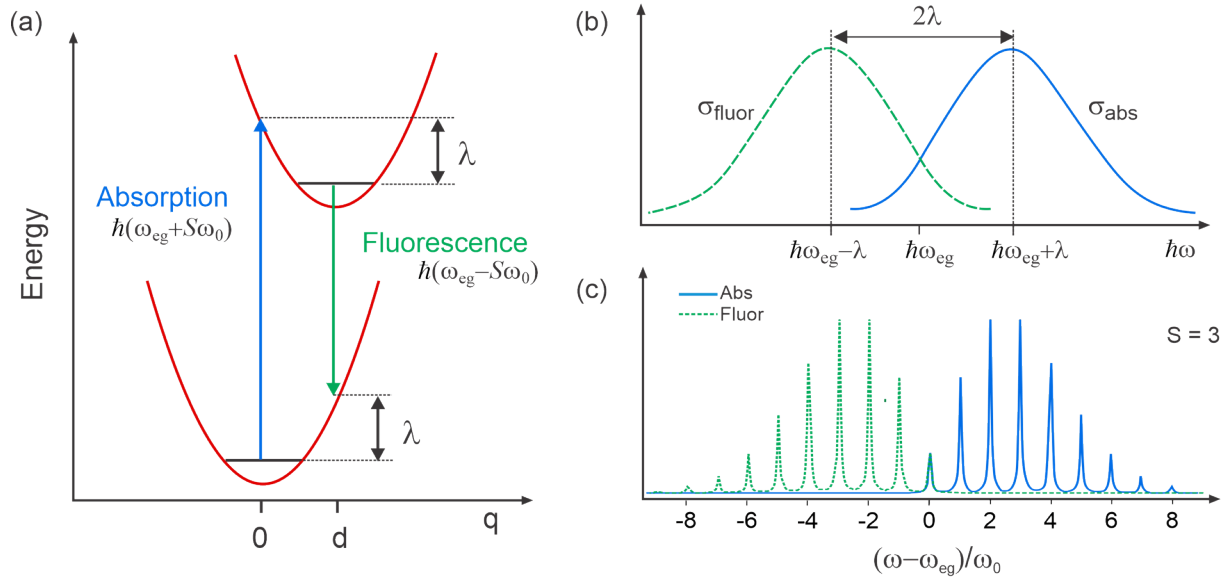


Figure 16.1.8: (a) Illustration of the DHO parameters that govern the absorption and fluorescence frequencies and the Stokes shift. (b) The expected outcome peak frequencies for the absorption and fluorescence emission envelopes. (c) Illustration of mirror image symmetry of the vibrational progression in the DHO absorption and emission spectra.

Comparing this with our expression for the dipole correlation function that we obtained for absorption from $|g,0\rangle$, $C_{\text{abs}}(t)$, in eq. (16.1.10), we find that they are related as Hermitian conjugates

$$C_{\mathrm{fl}}(t) = C^{\dagger}_{\mathrm{abs}}(t) \tag{16.1.46}$$

We can also evaluate the dephasing function for emission

$$\begin{aligned} F_{\mathrm{fl}}(t) &= \left\langle 0 \left| e^{\mathrm{i}H_e t/\hbar} e^{-\mathrm{i}H_g t/\hbar} \right| 0 \right\rangle \\ &= \exp\left[S\left(e^{\mathrm{i}\omega_0 t} - 1\right)\right] = F^{*}_{\mathrm{abs}}(t) \end{aligned} \tag{16.1.47}$$

Note also that $C^{\dagger}_{\mu\mu}(t) = C_{\mu\mu}(-t)$ and $F^{\dagger}(t) = F(-t)$. Then, we can obtain the fluorescence spectrum by Fourier transforming the dipole correlation function for the emission from $|e,0\rangle$. We follow the same strategy as shown in the previous section to find

$$\begin{aligned} \sigma_{\mathrm{fl}}(\omega) &= \int_{-\infty}^{+\infty} dt\, e^{\mathrm{i}\omega t} C_{\mathrm{fl}}(t) \\ &= |\mu_{eg}|^2 \sum_{n=0}^{\infty} e^{-S} \frac{S^n}{n!} \delta\left(\omega - \omega_{eg} + n\omega_0\right) \end{aligned} \tag{16.1.48}$$

This fluorescence emission spectrum has the same features as the absorption spectrum, although with mirror symmetry about ω_{eg} (Figure 16.1.8). A short time expansion confirms that the splitting between the peak of the absorption and emission lineshape envelopes is $2S\hbar\omega_0$, or 2λ. Further, one can establish that

$$\begin{aligned} \sigma_{\mathrm{abs}}(\omega) &= \int_{-\infty}^{+\infty} dt\, e^{\mathrm{i}(\omega-\omega_{eg})t - g(t)} \\ \sigma_{\mathrm{fl}}(\omega) &= \int_{-\infty}^{+\infty} dt\, e^{\mathrm{i}(\omega-\omega_{eg})t - g^{*}(t)} \\ g(t) &= -S\left(e^{-\mathrm{i}\omega_0 t} - 1\right) \end{aligned} \tag{16.1.49}$$

Our description of the fluorescence lineshape emerged from our semiclassical treatment of the light–matter interaction, while in practice fluorescence involves spontaneous emission of light into a quantum mechanical light field. However, though the light field must be handled differently, the form of the dipole correlation function and the resulting lineshape remain unchanged. Additionally, we assumed that there was a time scale separation between the vibrational relaxation in the excited state and the time scale of emission, so that the system can be considered equilibrated in $|e,0\rangle$. When this assumption is not valid, one must account for the more complicated possibility of emission during the relaxation process—the time-dependent Stokes shift.

References

(1) See also:
Schatz, G. C.; Ratner, M. A. *Quantum Mechanics in Chemistry*; Dover Publications, 2002; ch 9.

(2) See also:
Reimers, J. R.; Wilson, K. R.; Heller, E. J. Complex time dependent wave packet technique for thermal equilibrium systems: Electronic spectra. *Journal of Chemical Physics* **1983**, *79* (10), 4749-4757. DOI: 10.1063/1.445618

This page titled 16.1: The Displaced Harmonic Oscillator Model is shared under a CC BY-NC-SA 4.0 license and was authored, remixed, and/or curated by Andrei Tokmakoff via source content that was edited to the style and standards of the LibreTexts platform.

16.2: Coupling to a Harmonic Bath

The Hamiltonian for this displaced harmonic oscillator problem bears a notable similarity to the general form for the interaction between an electronic "system" directly observed in experiment and a harmonic oscillator "bath" with degrees of freedom that are not directly observed but influence the behavior of the system. This reasoning will be developed more carefully later for the description of fluctuations. Coupling to a continuum, or a harmonic bath, is the starting point for developing how an electronic system interacts with the continuum of intermolecular motions and phonons typical of condensed phase systems. While the Hamiltonians we have written so far describe coupling to a single bath degree of freedom, the DHO model is readily generalized to many vibrations or a continuum of nuclear motions.

So, what happens if the electronic transition is coupled to many vibrational coordinates, each with its own displacement? The extension is straightforward if we consider only two electronic states (e and g) to which we couple a set of independent modes, i.e., a bath of harmonic normal modes that interact with the system but not with each other. Then, using eq. (16.1.5), we can write the Hamiltonian for N vibrations as a sum over all the independent harmonic modes, indexed by α

$$H_e = \sum_{\alpha=1}^{N} H_e^{(\alpha)} = \sum_{\alpha=1}^{N} \left(\frac{p_\alpha^2}{2m_\alpha} + \frac{1}{2} m_\alpha \omega_\alpha^2 \left(q_\alpha - d_\alpha \right)^2 \right) \tag{16.2.1}$$

Each normal mode is written with its own distinct frequency and displacement. We can specify the state of the system in terms of product states in the electronic and nuclear occupation, i.e.,

$$\begin{aligned} |G\rangle &= |g; n_1, n_2, ..., n_N\rangle \\ &= |g\rangle \prod_{\alpha=1}^{N} |n_\alpha\rangle \end{aligned} \tag{16.2.2}$$

Additionally, we recognize that the time propagator on the electronically excited potential energy surface is a product of propagators on the potential for each normal mode coordinate.

$$U_e = \exp\left[-\frac{\mathrm{i}}{\hbar} H_e t \right] = \prod_{\alpha=1}^{N} U_e^{(\alpha)} \tag{16.2.3}$$

where

$$U_e^{(\alpha)} = \exp\left[-\frac{\mathrm{i}}{\hbar} H_e^{(\alpha)} t \right] \tag{16.2.4}$$

Similarly, for each normal mode, there is a unique Huang-Rhys factor

$$S_\alpha = d_\alpha^2 (m\omega_\alpha / 2\hbar) \tag{16.2.5}$$

dephasing function

$$F^{(\alpha)} = \left\langle \left[U_g^{(\alpha)} \right]^\dagger U_e^{(\alpha)} \right\rangle \tag{16.2.6}$$

and lineshape function $g_\alpha = -\ln F^\alpha$. The dipole correlation function is then just a product of multiple dephasing functions that characterize the time-evolution of the different vibrations.

$$C_{\mu\mu}(t) = |\mu_{eg}|^2 \, e^{-\mathrm{i}\omega_{eg} t} \cdot \prod_{\alpha=1}^{N} F^{(\alpha)}(t) \tag{16.2.7}$$

or equivalently a sum of different lineshape functions:

$$C_{\mu\mu}(t) = |\mu_{eg}|^2 \, e^{-i\omega_{eg} t - g(t)} \tag{16.2.8}$$

with

$$g(t) = -\sum_{\alpha} g_{\alpha}(t) \tag{16.2.9}$$

Taking the case that the system is initially in the ground electronic state with all normal mode vibrations in $n_{\alpha} = 0$, the initial state of the system can be written $|g, \mathbf{0}\rangle$, and the lineshape function is

$$g(t) = -\sum_{\alpha} S_{\alpha} \left(e^{-\mathrm{i}\omega_{\alpha} t} - 1\right) \tag{16.2.10}$$

In the time domain this is a complex beating pattern. In the frequency domain, this appears as a spectrum with several superimposed vibronic progressions that follow the rules developed above.

Taking this a step further, the generalization to a continuum of nuclear states emerges naturally in the frequency domain. We define a harmonic density of states, $W(\omega)$, that characterizes the continuous frequency distribution of normal modes and generalize eq. (16.2.5) to a continuously varying coupling of the electronic system to the modes, $S(\omega)$, allowing us to change the sum in eq. (16.2.9) to an integral over the density of states. For instance,

$$g(t) = \int_0^{\infty} d\omega\, W(\omega) S(\omega) \left(e^{-\mathrm{i}\omega t} - 1\right) \tag{16.2.11}$$

Here the product $W(\omega)S(\omega)$ is a coupling-weighted density of states and is commonly referred to as a *spectral density*.

This treatment establishes a bath of states with which the experimentally observed electronic transition may interact. Coupling to a bath or continuum introduces relaxation effects or damping of the electronic coherence in the absorption spectrum. You can see that, if $g(t)$ is associated with a real constant Γ that reflects an irreversible relaxation process, we obtain a Lorentzian lineshape with width Γ. This lineshape behavior emerges under certain circumstances, such as the distribution of states and coupling being large and constant, or the integration of eq. (16.2.11) over a distribution of low frequencies, such that $e^{-\mathrm{i}\omega t} \approx 1 - \mathrm{i}\omega t$. More generally, the real part of the lineshape describes damping, and the imaginary part shifts and modulates the primary frequency and leads to frequency shifts and fine structure.

An Ensemble at Finite Temperature

The single mode DHO model described above is for a pure state, but the approach can be readily extended to describe a canonical ensemble of displaced harmonic oscillators. Again, we assume that the molecular response is governed by the single mode DHO Hamiltonian. However, for a molecular ensemble, the correlation function is averaged over a thermal distribution of the initial state of the system. Taking the initial state of the system to be in the electronic ground state and that the vibrational levels (n_g) are populated following a Boltzmann distribution, the thermal distribution is:

$$p(n_g) = \frac{e^{-\beta n_g \hbar\omega_0}}{Z} \tag{16.2.12}$$

We can use this distribution to write the dipole correlation function with a thermally-averaged dephasing function:

$$C_{\mu\mu}(t) = |\mu_{eg}|^2 e^{-\mathrm{i}\omega_{eg} t} F(t) \tag{16.2.13}$$

$$F(t) = \sum_{n_g} p(n_g) \langle n_g | U_g^{\dagger} U_e | n_g \rangle \tag{16.2.14}$$

Evaluating these expressions using the strategies developed earlier in this chapter leads to

$$C_{\mu\mu}(t) = |\mu_{eg}|^2 e^{-\mathrm{i}\omega_{eg} t} \exp\left[S\left[(\bar{n}+1)\left(e^{-\mathrm{i}\omega_0 t} - 1\right) + \bar{n}\left(e^{\mathrm{i}\omega_0 t} - 1\right)\right]\right] \tag{16.2.15}$$

where $\bar{n}$ is the thermally averaged occupation number of the harmonic vibrational mode in the ground state.

$$\bar{n} = \left(e^{\beta\hbar\omega_0} - 1\right)^{-1} \tag{16.2.16}$$

The dephasing function in (16.2.15) has two terms which each correlate to different changes in the vibrational quantum number. The first is proportional to $(\bar{n}+1)$ and describes those electronic absorption events in which the vibrational quantum number increases or is unchanged ($n_e \geq n_g$). The second one is proportional to $\bar{n}$, describing those processes where the vibrational quantum number decreases or is unchanged ($n_e \leq n_g$). The latter are only allowed at elevated temperatures, where thermally

excited states are populated and are known as “hot bands.” In the low temperature limit, $\bar{n} \to 0$, and eq. (16.2.15) equals our original result, eq. (16.1.31).

Now we calculate the lineshape corresponding to the correlation function in eq. (16.2.15). If we separate the dephasing function into a product of two exponential terms and expand each of these exponentials, we can Fourier transform the result to find

$$\sigma_{\text{abs}}(\omega) = |\mu_{eg}|^2 e^{-S(2\bar{n}+1)} \sum_{j=0}^{\infty} \sum_{k=0}^{\infty} \left(\frac{S^{j+k}}{j!k!} \right) (\bar{n}+1)^j \bar{n}^k \delta\left(\omega - \omega_{eg} - (j-k)\,\omega_0\right) \tag{16.2.17}$$

Here, the summation over j describes $n_e \geq n_g$ transitions, whereas the summation over k describes $n_e \leq n_g$. For any one transition frequency, $(\omega_{eg} + n\omega_0)$, the net absorption is a sum over all possible combination of transitions within the energy splitting, given $n = (j-k)$. Again, if we set $\bar{n} \to 0$, we obtain our original result eq. (16.1.36). The contributions where \(k lead to the hot bands.

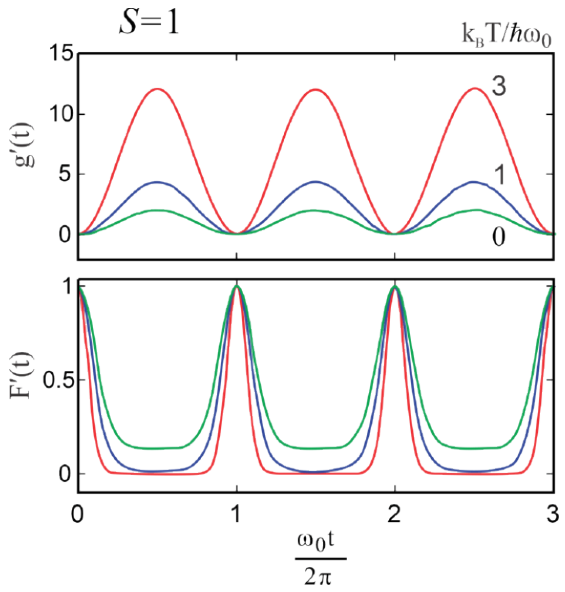


Figure 16.2.1: Examples of temperature dependence to the real part of the lineshape and dephasing functions for $S = 1$. The real part changes in amplitude, growing with temperature, whereas the imaginary part is unchanged.

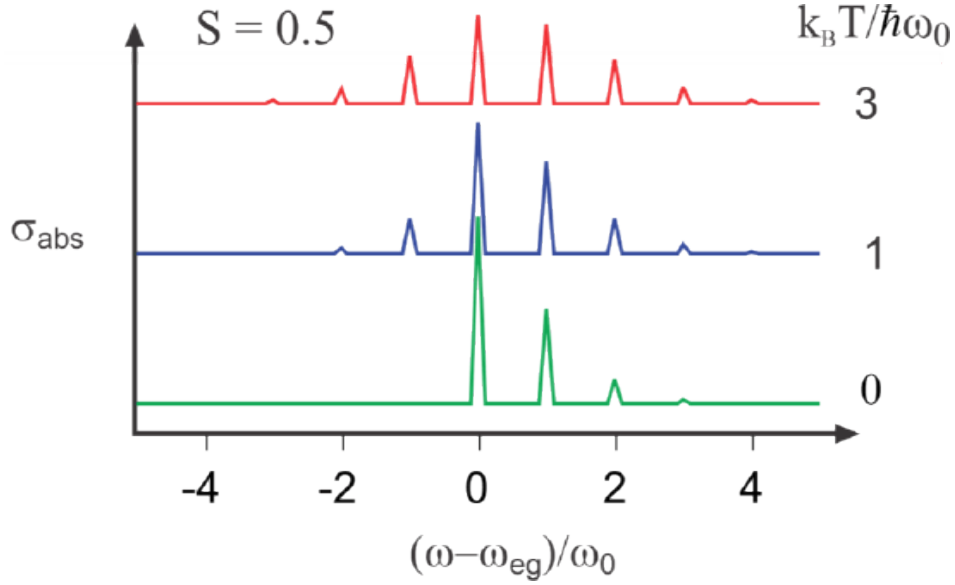


Figure 16.2.2: Examples of the vibrational progressions of the single mode DHO absorption spectrum as the temperature is increased from 0 to $3\hbar\omega_0/k_B$, illustrating the growth of hot band transitions for $\omega < \omega_{eg}$.

Combining these results with those of the previous section, we can describe the influence of temperature on the coupling of an

electronic transition to many independent normal modes or to a continuum. To achieve the former, we once again describe the system as a product state in the vibrational quantum numbers, i.e., $|E\rangle = |e; n_1, n_2, n_3 \ldots\rangle$. The resulting lineshape function is

$$g(t) = -\sum_\alpha S_\alpha \left[(\bar{n}_\alpha + 1)\left(e^{-i\omega_\alpha t} - 1\right) + \bar{n}_\alpha \left(e^{i\omega_\alpha t} - 1\right)\right] \tag{16.2.18}$$

Alternatively, we can describe coupling to a continuum by changing to an integral over a continuous frequency distribution of normal modes. This distribution is characterized by a density of states, $W(\omega)$, and frequency-dependent coupling, $S(\omega)$, leading to the lineshape

$$g(t) = -\int_0^\infty d\omega\, W(\omega)S(\omega)\left[(\bar{n}(\omega) + 1)\left(e^{-i\omega t} - 1\right) + \bar{n}(\omega)\left(e^{i\omega t} - 1\right)\right] \tag{16.2.19}$$

Similar to our earlier results, the limit $\bar{n} \to 0$ occurs at temperature $T = 0$.

Let's look at the envelope of the electronic absorption lineshape that emerges from coupling to a continuum. We begin by performing a short-time expansion on the exponential as in eq. (16.1.39)

$$F(t) = e^{-g(t)} = \exp\left[\int_0^\infty d\omega\, W(\omega)S(\omega)\left(-i\omega t - (2\bar{n} + 1)\frac{\omega^2 t^2}{2}\right)\right] \tag{16.2.20}$$

The absorption lineshape is calculated from

$$\sigma_{\text{abs}}(\omega) = \int_{-\infty}^{+\infty} dt\, e^{i(\omega - \omega_{eg})t} \exp\left[-i\langle\omega\rangle t\right] \exp\left[-\frac{1}{2}\left\langle\omega^2\right\rangle t^2\right] \tag{16.2.21}$$

where we have defined the mean vibrational excitation upon absorption as

$$\begin{aligned}\langle\omega\rangle &= \int_0^\infty d\omega\, \omega W(\omega)S(\omega) \\ &= \lambda/\hbar\end{aligned} \tag{16.2.22}$$

and

$$\left\langle\omega^2\right\rangle = \int_0^\infty d\omega\, \omega^2 W(\omega)S(\omega)\left(2\bar{n}(\omega) + 1\right) \tag{16.2.23}$$

$\left\langle\omega^2\right\rangle$ reflects the thermally averaged distribution of accessible vibrational states. After completing the square, eq. (16.2.21) gives

$$\sigma_{\text{abs}}(\omega) = |\mu_{eg}|^2 \sqrt{\frac{2\pi}{\left\langle\omega^2\right\rangle}} \exp\left[\frac{-\left(\omega - \omega_{eg} - \langle\omega\rangle\right)^2}{2\left\langle\omega^2\right\rangle}\right] \tag{16.2.24}$$

The lineshape is Gaussian, with a peak frequency at $\omega_{eg} + \langle\omega\rangle$ and a Gaussian width governed by $\left\langle\omega^2\right\rangle$. The width depends on the strength of coupling to the bath and increases with the degree of temperature-dependence, due to the thermal occupation factor in eq. (16.2.23).

This page titled 16.2: Coupling to a Harmonic Bath is shared under a CC BY-NC-SA 4.0 license and was authored, remixed, and/or curated by Andrei Tokmakoff via source content that was edited to the style and standards of the LibreTexts platform.

16.3: Semiclassical Approximation to the Dipole Correlation Function

While introducing the influence of dark degrees of freedom (the bath) on the spectroscopy of a bright state, we made some approximations that are not always valid, such as the Condon approximation and the Second Cumulant Approximation. To develop tools that allow us to work outside of these approximations, it is worth revisiting the dipole correlation function and looking at this a bit more carefully. In particular, we will discuss the semiclassical approximation, which is a useful representation of the dipole correlation function when one wants to describe the dark degrees of freedom using classical molecular dynamics simulations.

For a quantum mechanical material system interacting with a light field, the full Hamiltonian is

$$H = H_0 + V(t) \tag{16.3.1}$$

$$V(t) = -\mathbf{m} \cdot \mathcal{E}(t) \tag{16.3.2}$$

$\bar{m} = \sum_i z_i \bar{r}_i$ is the quantum mechanical dipole operator, where z_i are charges. The absorption lineshape is given by the Fourier transformation of the dipole autocorrelation function $C_{\mu\mu}$:

$$C_{\mu\mu}(\tau) = \langle \mathbf{m}(t)\mathbf{m}(0) \rangle \tag{16.3.3}$$

and the time dependence in $\bar{m}$ is expressed in terms of the usual time-propagator

$$\mathbf{m}(t) = \hat{U}_0^\dagger \mathbf{m} \hat{U}_0 \tag{16.3.4}$$

$$\hat{U}_0 = e_+^{\frac{-i}{\hbar}\int_0^t H_0(t')\,dt'} \tag{16.3.5}$$

In principle, the time development of the dipole moment for all degrees of freedom can be obtained directly from *ab initio* molecular dynamics simulations.

For a more practical expression, in which we wish to focus on only a few bright degrees of freedom, we next partition the Hamiltonian into system and bath

$$H_0 = H_S(Q) + H_B(q) + H_{SB}(Q,q) \tag{16.3.6}$$

For purposes of spectroscopy, the system that H_S refers to are those degrees of freedom (Q) with which the light interacts and in which we calculate matrix elements, while the bath described by H_B comprises all the other degrees of freedom (q). H_{SB} accounts for the interaction between the two. Although the light interaction primarily depends on how $\mathbf{m}$ varies with Q, the dipole operator remains a function of both system and bath coordinates: $\mathbf{m}(Q,q)$.

We now use the interaction picture transformation to express the time propagator under the full material Hamiltonian, $\hat{U}_0$. We can use this transformation to express it as a product of propagators for the individual terms within H_0:

$$\hat{U}_0 = U_S U_B U_{SB} \tag{16.3.7}$$

$$\hat{U}_0 = e_+^{\frac{-i}{\hbar}\int_0^t H_0\,dt'} = e^{-iH_S t} e_+^{\frac{-\mathrm{i}}{\hbar}\int_0^t H_B\,dt'} e_+^{\frac{-\mathrm{i}}{\hbar}\int_0^t \mathbf{H_{SB}}(t')dt'} \tag{16.3.8}$$

$$\mathbf{H_{SB}}(t) = e^{\mathrm{i}(H_S+H_B)t} H_{SB} e^{-\mathrm{i}(H_S+H_B)t} \tag{16.3.9}$$

Then the dipole autocorrelation function becomes

$$C_{\mu\mu} = \sum_n p_n \left\langle n \left| U_{SB}^\dagger U_B^\dagger U_S^\dagger \mathbf{m} U_S U_B U_{SB} \mathbf{m} \right| n \right\rangle \tag{16.3.10}$$

Where $p_n = \langle n | e^{-\beta H_0} | n \rangle \,/\, \mathrm{Tr}\left(e^{-\beta H_0}\right)$.

Further, to make this practical, we make an adiabatic separation between the system and bath coordinates and say that the interaction between the system and bath is weak. This allows us to write the state of the system as $|n\rangle = |a,\alpha\rangle$, a product state

comprising the system (with states a and b) and bath (with states α):

$$(H_S + H_B)\left|a,\alpha\right\rangle = (E_a + E_\alpha)\left|a,\alpha\right\rangle \tag{16.3.11}$$

With this we evaluate eq. (16.3.10) as

$$\begin{aligned} C_{\mu\mu} &= \sum_{a,\alpha} p_a p_\alpha \left\langle a,\alpha \left| U_{SB}^\dagger U_B^\dagger U_S^\dagger \mathbf{m} U_S U_B U_{SB} \mathbf{m} \right| a,\alpha \right\rangle \\ &= \sum_{\substack{a,b \\ \alpha}} p_a p_\alpha \left\langle \alpha \left| \left\langle a\right| U_{SB}^\dagger U_S^\dagger U_B^\dagger \mathbf{m} U_B U_S U_{SB} \left|b\right\rangle \mathbf{m}_{ba} \right| \alpha \right\rangle \end{aligned} \tag{16.3.12}$$

Where $\mathbf{m}_{ba} = \left\langle b\right| \mathbf{m} \left|a\right\rangle$ is the matrix element in the system states, and we have made use of the fact that H_S and H_B commute. Also, $p_a = e^{-E_a/kT}/Z_S$.

We recognize that the time propagators in the system and system-bath Hamiltonians describe time evolution at the system eigenstate energy with the addition of any modulations that the bath introduces to it

$$U_S U_{SB}\left|b\right\rangle \ = e^{-\mathrm{i}H_S t}\left|b\right\rangle e^{-\mathrm{i}\int_0^t dt' \delta E_b(t')} = \left|b\right\rangle e^{-\mathrm{i}\int_0^t dt' E_b(t')} \tag{16.3.13}$$

Thus, we can write our correlation function as

$$C_{\mu\mu} = \sum_{\substack{a,b \\ \alpha}} p_a p_\alpha \left\langle \alpha\right| e^{\mathrm{i}\int_0^t dt' E_a(t')} U_B^\dagger \mathbf{m}_{ab} U_B e^{-\mathrm{i}\int_0^t dt' E_b(t')} \mathbf{m}_{ba} \left|\alpha\right\rangle \tag{16.3.14}$$

$$C_{\mu\mu} = \left\langle \mathbf{m}_{ab}(t)\mathbf{m}_{ba}(0) e^{-\mathrm{i}\int_0^t dt' \omega_{b a}(t')} \right\rangle_B \tag{16.3.15}$$

$$\mathbf{m}_{ab}(t) = e^{-\mathrm{i}H_B t}\mathbf{m}_{ab} e^{-\mathrm{i}H_B t} \tag{16.3.16}$$

Equation (16.3.15) is the first important result of this approach. It describes a correlation function for the dipole operator in terms of an average over the time-dependent transition moment, including both its orientation and the fluctuating energy gap. The time dependence is due to the bath and $\left\langle \cdots \right\rangle_B$ refers to a trace over the bath degrees of freedom.

Let's consider the matrix elements of the quantum mechanical dipole operator. These will reflect the strength of the interaction between the electromagnetic field and the motion of the system coordinate, which may also be dependent on the bath coordinates. Since we have made an adiabatic approximation, to evaluate the matrix elements we would typically expand the dipole moment in the system degrees of freedom, Q. In the case of only one system coordinate (Q) and many bath coordinates (q_α), we can expand:

$$\mathbf{m}\left(Q,q\right) = \mathbf{m}_0 + \frac{\partial \mathbf{m}}{\partial Q} Q + \sum_\alpha \frac{\partial^2 \mathbf{m}}{\partial Q \partial q_\alpha} Q q_\alpha + \cdots \tag{16.3.17}$$

$\bar{m}_0$ is the permanent dipole moment, which we can take as a constant. In the second term, $\partial \bar{m}/\partial Q$ is the magnitude of the transition dipole moment. The third term includes the dependence of the transition dipole moment on the bath degrees of freedom, i.e., non-Condon terms. So now we can evaluate

$$\begin{aligned} \mathbf{m}_{ab} &= \left\langle a \left| \mathbf{m}_0 + \frac{\partial \mathbf{m}}{\partial Q} Q + \sum_\alpha \frac{\partial^2 \mathbf{m}}{\partial Q \partial q_\alpha} Q q_\alpha \right| b \right\rangle \\ &= \frac{\partial \mathbf{m}}{\partial Q} \left\langle a\right| Q \left|b\right\rangle + \sum_\alpha \frac{\partial}{\partial q_\alpha} \frac{\partial \mathbf{m}}{\partial Q} \left\langle a\right| Q \left|b\right\rangle \ q_\alpha \end{aligned} \tag{16.3.18}$$

We have set the matrix element in the fixed dipole moment $\left\langle a\right| \left|\mathbf{m}_0\right| \left|b\right\rangle = 0$ for simplicity. Now defining the transition dipole matrix element,

$$\bar{\mu}_{ab} = \frac{\partial \mathbf{m}}{\partial Q} \left\langle a\right| Q \left|b\right\rangle \tag{16.3.19}$$

we can write

$$\mathbf{m}_{ab} = \mathbf{m}_{ab}\left(1 + \sum_{\alpha} \frac{\partial \mathbf{m}_{ab}}{\partial q_{\alpha}} q_{\alpha}\right) \tag{16.3.20}$$

Remember that $\boldsymbol{\mu}_{ab}$ is a vector. We have found that the bath can also change the orientation of the transition dipole moment, despite the adiabatic approximation. If we want to separate the orientational and remaining dynamics, we could split the matrix element into an orientational component specified by a unit vector along $\partial \mathbf{m}/\partial Q$ and a scalar that encompasses the amplitude factors: $\boldsymbol{\mu}_{ab} = \hat{u}_{ab}\mu_{ab}$. Then eq. (16.3.15) becomes

$$C_{\mu\mu} = \left\langle \hat{u}_{ab}(t)\hat{u}_{ab}(0)\mathbf{m}_{ab}(t)\mathbf{m}_{ba}(0)e^{-\mathrm{i}\int_0^t dt'\omega_{ba}(t')} \right\rangle_B \tag{16.3.21}$$

Mixed quantum-classical spectroscopy models apply a semiclassical approximation to equation (16.3.15). Employing the semiclassical approximation means that we will replace the quantum mechanical operator $\mathbf{m}_{ab}(t)$ with a classical $\mathcal{M}_{ab}(t)$, i.e., we replace the time propagator U_B with classical propagation of the dynamics. Also, the trace over the bath in the correlation function becomes an equilibrium ensemble average over phase space.

How do you implement the semiclassical approximation? Replacing the time propagator U_B with classical dynamics amounts to integrating Newton's equations for all the bath degrees of freedom. Then you must establish how the bath degrees of freedom influence $\omega_{ba}(t)$ and $\mathbf{m}_{ab}(t)$. For the quantum operator $\mathbf{m}(Q, q, t)$, only the system coordinate Q remains quantized, and following eq. (16.3.20) we can express that the orientation and magnitude of both the dipole moment and its dynamics are dependent on the classical degrees of freedom, $\tilde{q}_{\alpha}$.

$$\mathbf{m}_{ab} = \boldsymbol{\mu}_{ab}\left(1 + \sum_{\alpha} a_{\alpha}\tilde{q}_{\alpha}\right) \tag{16.3.22}$$

a_{α} is a (linear) mapping coefficient between the bath and the transition dipole moment, $a_{\alpha} = \partial \boldsymbol{\mu}_{ab}/\partial \tilde{q}_{\alpha}$.

In practice, though use of this approximation has been handled in different ways, practical considerations have dictated that $\omega_{ba}(t)$ and $\mathbf{m}_{ab}(t)$ are not separately calculated for each time step. Instead, they are obtained from a mapping of these variables to the bath coordinates q. This mapping may be to local or collective bath coordinates, and it may be calculated to as many degrees of freedom as are necessary to obtain a highly correlated, single-valued mapping of $\omega_{ba}(t)$ and $\mathbf{m}_{ab}(t)$. Examples of these mappings include correlating ω_{ba} with the bath's electric field as it acts upon the system coordinate.

Appendix

Let's evaluate the dipole correlation function for an arbitrary H_{SB} and an arbitrary number of system eigenstates. From eq. (16.3.12) we have

$$C_{\mu\mu} = \sum_{\substack{abcd \\ \alpha}} p_a p_{\alpha} \left\langle \alpha \left| \langle a| U_{SB}^{\dagger} |c\rangle U_B^{\dagger} \langle c| U_S^{\dagger} \mathbf{m} U_S |d\rangle U_B \langle d| U_{SB} |b\rangle \langle b| \mathbf{m} |a\rangle \right| \alpha \right\rangle \tag{16.3.23}$$

$$\left\langle c \left| U_S^{\dagger} \mathbf{m} U_S \right| d \right\rangle = e^{-\mathrm{i}(E_d - E_c)t} \mathbf{m}_{cd} \tag{16.3.24}$$

$$\mathbf{m}_{cd}(t) = U_B^{\dagger} \mathbf{m}_{cd} U_B \tag{16.3.25}$$

$$\left\langle a \left| U_S B^{\dagger} \right| c \right\rangle = \langle a| e^{\mathrm{i}\int_0^t dt' \mathbf{H}_{\mathbf{SB}}(t')} |c\rangle = \exp\left[\mathrm{i}\int_0^t dt' \left[\mathbf{H}_{\mathbf{SB}}\right]_{ac}(t')\right] \tag{16.3.26}$$

$$C_{\mu\mu} = \sum_{abcd} p_a \left\langle e^{-\mathrm{i}\omega_{dc}t} e^{i\int_0^t dt' [H_{SB}]_{ac}(t')} \mathbf{m}_{cd} e^{-\mathrm{i}i\int_0^t dt' [H_{SB}]_{db}(t')} \mathbf{m}_{ba} \right\rangle_B \tag{16.3.27}$$

$$C_{\mu\mu} = \left\langle \mathbf{m}_{cd}(t)\mathbf{m}_{ba}(0) \exp\left[-\mathrm{i}\omega_{dc}t - \mathrm{i}\int_0^t dt' \left[H_{SB}\right]_{db}(t') - \left[H_{SB}\right]_{ac}(t')\right] \right\rangle_B \tag{16.3.28}$$

This page titled 16.3: Semiclassical Approximation to the Dipole Correlation Function is shared under a CC BY-NC-SA 4.0 license and was authored, remixed, and/or curated by Andrei Tokmakoff via source content that was edited to the style and standards of the LibreTexts platform.

16.4: Readings

The Displaced Harmonic Oscillator Model

1. Reimers, J. R.; Wilson, K. R.; Heller, E. J. Complex time dependent wave packet technique for thermal equilibrium systems: Electronic spectra. *Journal of Chemical Physics* **1983**, *79* (10), 4749-4757. DOI: 10.1063/1.445618
2. Mukamel, S. *Principles of Nonlinear Optical Spectroscopy*; Oxford University Press, 1995.
3. Schatz, G. C.; Ratner, M. A. *Quantum Mechanics in Chemistry*; Dover Publications, 2002.
4. Nitzan, A. *Chemical dynamics in condensed phases: Relaxation, transfer and reactions in condensed molecular systems*; Oxford University Press, 2006. DOI: 10.1093/oso/9780198529798.001.0001
5. May, V.; Kühn, O. *Charge and Energy Transfer Dynamics in Molecular Systems*; Wiley-VCH Verlag, 2011. DOI: 10.1002/9783527633791

Semiclassical Approximation to the Dipole Correlation Function

1. Auer, B. M.; Skinner, J. L. Dynamical effects in line shapes for coupled chromophores: Time-averaging approximation. *Journal of Chemical Physics* **2007**, *127* (10), 104105. DOI: 10.1063/1.2766943
2. Corcelli, S. A.; Skinner, J. L. Infrared and Raman Line Shapes of Dilute HOD in Liquid H2O and D2O from 10 to 90 °C. *Journal of Physical Chemistry A* **2005**, *109* (28), 6154-6165. DOI: 10.1021/jp0506540
3. Gorbunov, R. D.; Nguyen, P. H.; Kobus, M.; Stock, G. Quantum-classical description of the amide I vibrational spectrum of trialanine. *Journal of Chemical Physics* **2007**, *126* (5), 054509. DOI: 10.1063/1.2431803
4. Mukamel, S. *Principles of Nonlinear Optical Spectroscopy*; Oxford University Press, 1995.

This page titled 16.4: Readings is shared under a CC BY-NC-SA 4.0 license and was authored, remixed, and/or curated by LibreTexts.

17: FLUCTUATIONS AND DEPHASING

17.1: Line-broadening, dephasing, and spectral diffusion
17.2: Gaussian-Stochastic Model for Spectral Diffusion
17.3: The Energy Gap Hamiltonian
17.4: Spectral Density for Condensed Phase Spectroscopy
17.5: The Harmonic Bath's Relation to the Langevin Equation
17.6: Readings

This page titled 17: Fluctuations and Dephasing is shared under a CC BY-NC-SA 4.0 license and was authored, remixed, and/or curated by Andrei Tokmakoff via source content that was edited to the style and standards of the LibreTexts platform.

17.1: Line-broadening, dephasing, and spectral diffusion

As we have seen, experimental observables such as an electronic absorption spectrum are influenced by interactions with their environment. Here we will focus on how they are impacted by the thermal fluctuations in that environment, as is common to experiments in molecular condensed phases. Again, we will focus on absorption spectroscopy and how environmentally-induced dephasing influences the absorption lineshape. Our approach will be to calculate a dipole correlation function for a transition dipole interacting with a fluctuating environment and to show how the time scale and amplitude of fluctuations are encoded in the lineshape. Although we address spectroscopy, this approach can be applied to any such problems in which a quantum mechanical system is influenced by the thermal fluctuation of a heat bath.

Our approach is to develop a time-domain picture in which the spectroscopic transition energy gap fluctuates about an average frequency with a statistical time scale and amplitude given by the dynamics of its environment. Using the reasoning that we developed in our discussion of the Displaced Harmonic Oscillator model, we will show that this picture is equivalent to a frequency-domain representation of the coupling between a transition and a continuous distribution of harmonic modes. Thus, an absorption spectrum is a spectral representation of the dynamics experienced by an experimentally probed transition.

To begin, let's introduce some concepts that will help us describe how a chromophore's interactions with its environment influence its absorption lineshape. In the absence of interactions, a system's resonance frequency ω_{eg} and transition dipole moment μ_{eg} are fixed; however, in a condensed phase environment, the intermolecular interactions lead to changes in these observables. Time-dependent interactions with dynamically evolving surroundings are observed have a stochastic character, resulting in a fluctuating time-dependent frequency $\omega_{eg}(t)$ and dipole moment. By *stochastic* we refer to any dynamic process which includes a random component to the time-development.

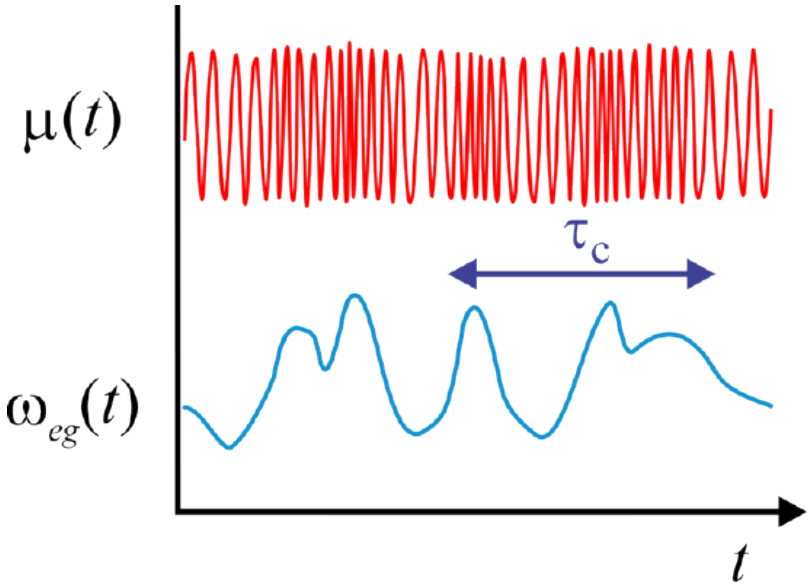


Figure 17.1.1: Time-dependent variation in the frequency of a molecule's transition dipole oscillation $\mu(t)$ because of interactions with a fluctuating environment.

Time-dependent frequency shifts result in dephasing and decoherence that contribute to the absorption lineshape. *Decoherence* refers to the process by which the frequency of a molecular transition is stochastically modulated such that the frequency $\omega_{eg}(t)$ and phase of oscillation $\phi(t) = \partial\omega_{eg}/\partial t$ become unpredictable over longer periods of time. This molecular property, shown in Figure 17.1.1, can be quantified with a time-averaged frequency correlation function

$$C_{eg}(t) = \langle \omega_{eg}(t)\omega_{eg}(0) \rangle \tag{17.1.1}$$

Dephasing, which is the term we will use, encompasses both this process and the variation of phases across an ensemble. Varying fluctuations in frequency across many members of an ensemble result in a macroscopic loss of phase correlation.

To help us describe how stochastic dephasing influences the line width and lineshape of absorption features, we will consider

it within the range of frequencies that the system samples in its dynamical evolution (Δ) and on the timescale of sampling the varying environments (τ_c). Consider the following limiting cases of line broadening, which are also compared in Figure 17.1.2:

1. **Homogeneous Broadening**. Here, the absorption lineshape is *dynamically* broadened because the dynamics of the environment modulate ω_{eg} so rapidly that the absorption spectrum effectively averages over the distribution of frequencies. This results in a linewidth that is "motionally narrowed" relative to the distribution of frequencies. The linewidth is typically quantified through the dephasing rate constant Γ or is sometimes referred to through the pure-dephasing time T_2^*.
2. **Inhomogeneous Broadening**. In this limit, the lineshape reflects an essentially *static* distribution of resonance frequencies which vary from one molecule to the other within the ensemble. The width of the absorption lineshape represents the distribution of frequencies, Δ, which arise from different structural environments available to the system.

More generally, every system lies between these limits. Given a distribution of configurations that the system can adopt—for instance, the varying solvent structures of a liquid around an electronic chromophore—a molecule in an equilibrium system will sample all configurations available to it, if observed over a long enough time. Under these circumstances, we expect that every molecule will have a different "instantaneous frequency" $\omega_i(t)$ which evolves in time through the interactions with a dynamical environment in a process known as spectral diffusion. The homogeneous and inhomogeneous extremes can be described as the limits of the time-scale τ_c on which the instantaneous frequency fluctuates across a distribution of frequencies Δ. If $\omega_i(t)$ changes rapidly relative to Δ^{-1}, the system is homogeneously broadened. If $\omega_i(t)$ changes slowly, the system is inhomogeneous. We wish to provide a general description of how these dynamical processes appear in spectroscopic observables. To do that, we will develop the tools to relate the transition frequency correlation function $C_{eg}(t)$ to the dipole correlation function $C_{\mu\mu}(t)$ that determines the absorption lineshape.

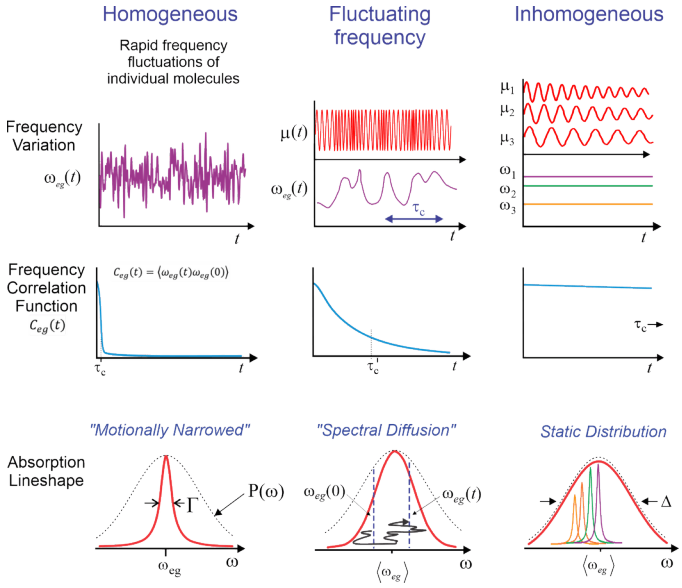


Figure 17.1.2: Summary of dephasing and line-broadening mechanisms. Homogeneous dephasing reflects rapid fluctuations of the environment which result in rapid loss of frequency correlations and motional narrowing of the absorption lineshape. Inhomogeneous broadening results from quasi-static frequencies that differ for each molecule resulting in an absorption lineshape reflecting the distribution of environments available rather than dynamics. Spectral diffusion refers to the intermediate regime in which the frequency of each molecular transition dynamically evolves on a time-scale similar to the inverse breadth of frequencies available to the system $\Delta \cdot \tau_c \approx 1$.

This page titled 17.1: Line-broadening, dephasing, and spectral diffusion is shared under a CC BY-NC-SA 4.0 license and was authored, remixed, and/or curated by Andrei Tokmakoff via source content that was edited to the style and standards of the LibreTexts platform.

17.2: Gaussian-Stochastic Model for Spectral Diffusion

We will begin with a classical description of how random fluctuations in resonance frequency influence the absorption lineshape using a model developed separately by both Philip Anderson and Ryogo Kubo in the course of their work on magnetic resonance spectroscopy. It is a Gaussian stochastic model for fluctuations, meaning that we aim to describe the time-dependence of a system that stochastically samples a Gaussian distribution of frequencies with an average value $\bar{\omega}$:

$$\omega(t) = \bar{\omega} + \delta\omega(t) \tag{17.2.1}$$

$$\overline{\delta\omega(t)} = 0 \tag{17.2.2}$$

The bar over these variables indicates a time-average, although we assume that the system is ergodic with $\bar{\omega} = \langle\omega\rangle$. The Gaussian distribution of transitions frequencies is also characterized by a variance:(1)

$$\Delta^2 = \langle\omega^2\rangle - \langle\omega\rangle^2 = \langle\delta\omega^2\rangle \tag{17.2.3}$$

The time scales for the frequency shifts will be described in terms of a frequency correlation function

$$C_{\delta\omega\delta\omega}(t) = \langle\delta\omega(t)\delta\omega(0)\rangle \tag{17.2.4}$$

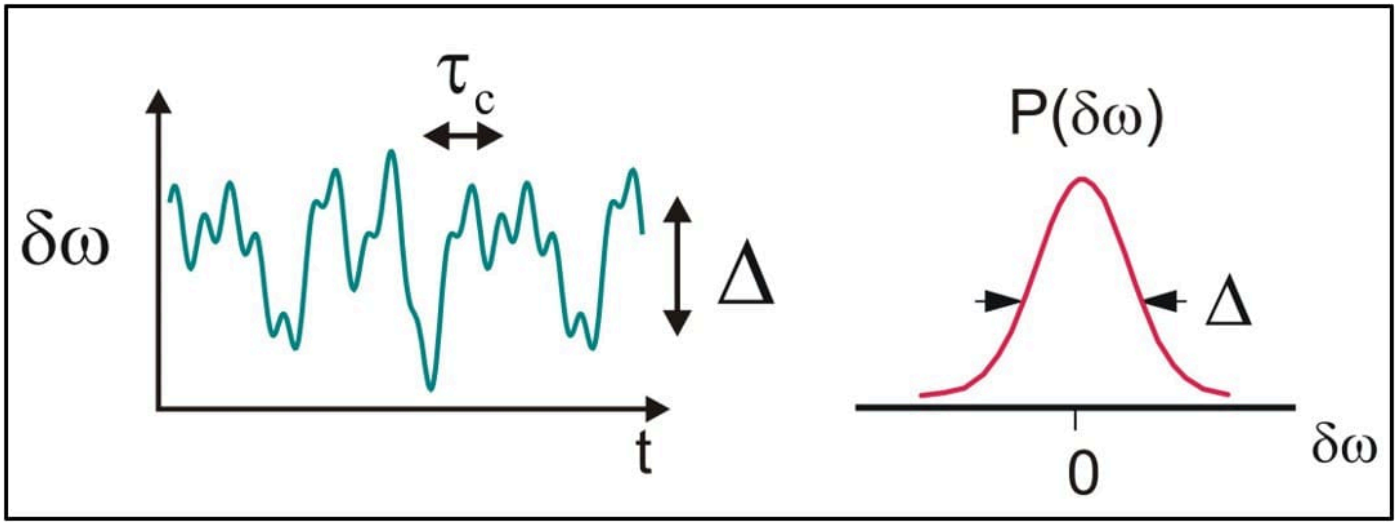


Figure 17.2.1: Variables governing the stochastic fluctuations in frequency about an average value.

Furthermore, we will describe the time scale of the fluctuations through a correlation time τ_c.

The absorption lineshape is described with a dipole time-correlation function. Let's treat the dipole moment as an internal variable to the system, the value of which depends on that of ω. Qualitatively, it is possible to write an equation of motion for μ by associating the dipole moment with the displacement of a bound particle (x) times its charge and by using our intuition regarding how the system behaves. For an unperturbed state, we say that x and therefore μ will oscillate at a frequency $\bar{\omega}$, but, with perturbations, it will vary through the distribution of available frequencies. For instance, one might expect the time-dependence to be described by $x(t) = x_0 \cos(\omega(t)t) = x_0 cos(\bar{\omega}t - \phi(t))$. For practical purposes, let's work with the complex version of this expression:

$$x(t) = x_0 e^{-i\omega(t)t} \tag{17.2.5}$$

If we differentiate this equation with respect to time and multiply by charge, we have a possible equation of motion for the stochastically modulated dipole moment.

$$\frac{\partial\mu}{\partial t} = -i\omega(t)\mu(t) \tag{17.2.6}$$

Although it is a classical equation, note the similarity to the quantum Heisenberg equation for the dipole operator: $\partial\mu/\partial t = \mathrm{i}H(t)\mu/\hbar$ The correspondence of $\omega(t)$ with $H(t)/\hbar$ offers a hint into how the quantum version of this problem will look.

The solution to eq. (17.2.6) is

$$\mu(t) = \mu(0)\exp\left[-\mathrm{i}\int_0^t d\tau\,\omega(\tau)\right] \tag{17.2.7}$$

Substituting this expression and eq. (17.2.1) into the dipole correlation function gives

$$C_{\mu\mu}(t) = |\mu|^2 e^{-\mathrm{i}\bar{\omega}t}F(t) \tag{17.2.8}$$

where

$$F(t) = \left\langle \exp\left[-\mathrm{i}\int_0^t d\tau\,\delta\omega(\tau)\right]\right\rangle \tag{17.2.9}$$

The dephasing function here is obtained by time-averaging over a trajectory, but for ergodic systems we can calculate the equilibrium average of the exponential argument over fluctuating trajectories.

The dephasing function is a bit complicated to work with as written. However, in the case of using Gaussian statistics for the fluctuations, it is possible to simplify $F(t)$ by expanding it as a *cumulant expansion of averages* (see Appendix)

$$F(t) = \exp\left[-\mathrm{i}\int_0^t d\tau'\,\langle\delta\omega(\tau')\rangle + \frac{\mathrm{i}^2}{2!}\int_0^t d\tau'\int_0^t d\tau''\,\{\langle\delta\omega(\tau')\delta\omega(\tau'')\rangle - \langle\delta\omega(\tau')\rangle\langle\delta\omega(\tau'')\rangle\}\right] \tag{17.2.10}$$

In this expression, the first term is zero, since $\langle\delta\omega\rangle = 0$. Only the second term survives for a system with Gaussian statistics.

$$F(t) = \exp\left[-\frac{1}{2}\int_0^t d\tau'\int_0^t d\tau''\,\langle\delta\omega(\tau')\,\delta\omega(\tau'')\rangle\right] \tag{17.2.11}$$

Note that this is a classical expression, so there is no time-ordering to the exponential. $F(t)$ can also be rewritten through a change of variables ($\tau = \tau' - \tau''$):

$$F(t) = \exp\left[-\int_0^t d\tau\,(t-\tau)\,\langle\delta\omega(\tau)\delta\omega(0)\rangle\right] \tag{17.2.12}$$

The dephasing function is expressed here in terms of a correlation function $C_{\delta\omega\delta\omega}$ for the fluctuations of the frequency about its average.

$$C_{\delta\omega\delta\omega}(\tau) = \langle\delta\omega(\tau)\delta\omega(0)\rangle \tag{17.2.13}$$

Note that in describing the influence of fluctuations on spectroscopy, we are now dealing with two different correlation functions: $C_{\delta\omega\delta\omega}$ and $C_{\mu\mu}$. The frequency correlation function describes how the spectroscopic transition frequency is influenced by the dynamics of molecules interacting with their surroundings, whereas the dipole correlation function describes how the system interacts with a light field and thereby with the absorption spectrum.

Although we cannot directly predict the full time-evolution of a particular molecular frequency, $C_{\delta\omega\delta\omega}(\tau)$ allows us to statistically describe the dephasing dynamics and characteristic correlation time τ_c over which the frequency of the system becomes uncorrelated with its earlier values. For short time-delays δt, the instantaneous frequency $\omega(t+\delta t)$ will remain at least partially correlated with its earlier value $\omega(t)$, meaning it retains some memory of where it previously was, statistically speaking. But once the time intervals are long enough such that $\tau \gg \tau_c$ and $C_{\delta\omega\delta\omega}(\tau)$ has decayed to zero, the system has no memory of the past and the behavior is considered Markovian. In addition to the stochastic dynamics, the frequency correlation function also describes the magnitude of the frequency excursions from the average.

To look at this behavior more closely, let's calculate the absorption lineshape for a frequency correlation function that decays exponentially, with a correlation time τ_c

$$C_{\delta\omega\delta\omega}(t) = \Delta^2\exp\left[-t/\tau_c\right] \tag{17.2.14}$$

The magnitude of the correlation function is set to correspond to the variance of the Gaussian distribution: $C_{\delta\omega\delta\omega}(0) = \langle\delta\omega^2\rangle = \Delta^2$

. Then eq. (17.2.12) gives

$$F(t) = \exp\left[-\Delta^2\tau_c^2\left(\exp\left(-t/\tau_c\right) + t/\tau_c - 1\right)\right] \tag{17.2.15}$$

which is in the form we have seen earlier $F(t) = \exp\left(-g(t)\right)$

$$g(t) = \Delta^2\tau_c^2\left(\exp\left(-t/\tau_c\right) + t/\tau_c - 1\right) \tag{17.2.16}$$

This is sometimes referred to as a Kubo lineshape function. To interpret it, let's look at its limiting forms:

1) **Long correlation times** $(t \ll \tau_c)$. In this limit, the transition frequency for one molecule within the ensemble changes slowly enough to be static on the timescale of observation. This corresponds to the inhomogeneous case and $C_{\delta\omega\delta\omega} \approx \Delta^2$. For $t \ll \tau_c$ we can perform a short time expansion of the exponential

$$e^{-t/\tau_c} \approx 1 - \frac{t}{\tau_c} + \frac{t^2}{2\tau_c^2} + \ldots \tag{17.2.17}$$

and from eq. (17.2.16) we obtain

$$g(t) = \frac{\Delta^2 t^2}{2} \tag{17.2.18}$$

Thus, the dephasing function $F(t) = \exp\left(-\Delta^2 t^2/2\right)$ and the dipole correlation function will have a Gaussian decay, with a rate given by Δ^2 for short times. This has the expected behavior for a classical correlation function, i.e., $C_{\mu\mu}(t) = C_{\mu\mu}(-t)$, even in the time domain. In this limit, the absorption spectrum is a Gaussian inhomogeneous lineshape centered at the mean frequency with a width dictated by the frequency distribution.

$$\begin{aligned}\sigma\left(\omega\right) &= \left|\mu\right|^2 \int_{-\infty}^{+\infty} dt\, e^{\mathrm{i}\omega t} e^{-\mathrm{i}\bar{\omega}t - g(t)} \\ &= \left|\mu\right|^2 \int_{-\infty}^{+\infty} dt\, e^{\mathrm{i}(\omega-\bar{\omega})t} e^{-\Delta^2 t^2/2} \\ &= \sqrt{\frac{2\pi}{\Delta^2}}\left|\mu\right|^2 \exp\left(-\frac{\left(\omega-\bar{\omega}\right)^2}{2\Delta^2}\right)\end{aligned} \tag{17.2.19}$$

2) **Short correlation times** $(t \gg \tau_c)$. This corresponds to the homogeneous limit. The frequency correlations are lost extremely quickly, and you can approximate the frequency correlation function with a delta function decay in time: $C_{\delta\omega\delta\omega}(t) = \Delta^2\delta(t)$. For $t \gg \tau_c$ we set $e^{-t/\tau_c} \approx 0$. Since $t/\tau_c \gg 1$ eq. (17.2.16) gives a lineshape function that decays linearly in time:

$$g(t) \approx -\Delta^2\tau_c t \tag{17.2.20}$$

If we define the constant

$$\Gamma \equiv \Delta^2\tau_c \tag{17.2.21}$$

we see that the dephasing function has an exponential decay:

$$F(t) = \exp\left[-\Gamma t\right] \tag{17.2.22}$$

and the corresponding absorption lineshape is Lorentzian

$$\sigma\left(\omega\right) = \left|\mu\right|^2 \frac{\Gamma}{\left(\omega-\bar{\omega}\right)^2 + \Gamma^2} \tag{17.2.23}$$

This represents the homogeneous limit. If the system explores all the available frequencies on a time scale fast compared to the inverse of the distribution ($\Delta \cdot \tau_c < 1$), then the resonance will be "motionally narrowed" into a Lorentzian lineshape.

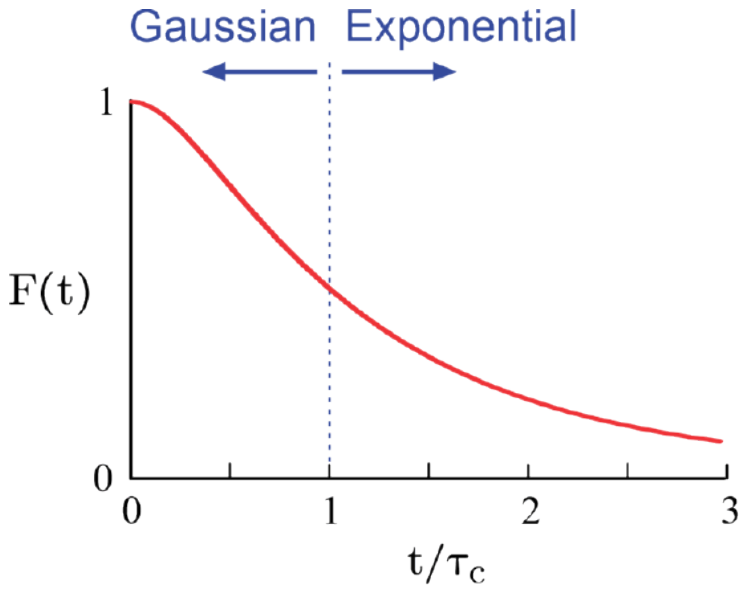


Figure 17.2.2: The dephasing function for the Gaussian stochastic lineshape, here shown for $\kappa = 0.5$, smoothly varies from a Gaussian form for $t < \tau_c$ to exponential decay for $t > \tau_c$.

More generally, the envelope of the dipole correlation function will look Gaussian at short times and exponential at long times, with the correlation time marking the separation between these regimes (Figure 17.2.2). The behavior for varying time scales of the dynamics (τ_c) are best characterized with respect to the distribution of accessible frequencies (Δ). We can define a factor

$$\kappa = \Delta \cdot \tau_c \tag{17.2.24}$$

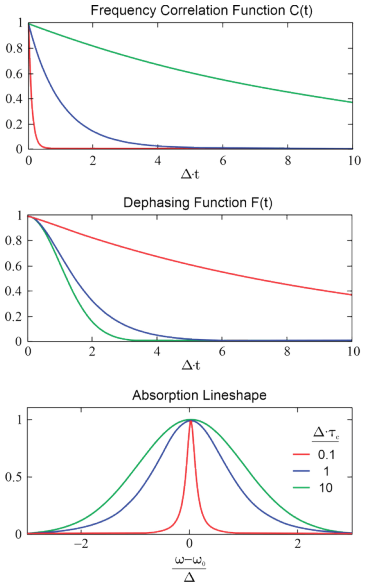


Figure 17.2.3: Illustration of the frequency correlation function $C_{\delta\omega\delta\omega}(t)$, the dephasing function $F(t)$, and absorption lineshape $\sigma(\omega)$ for the gaussian stochastic model for the fast (red), intermediate (blue), and slow (green) modulation cases.

$\kappa \ll 1$ is the fast modulation limit and $\kappa \gg 1$ is the slow modulation limit. In Figure 17.2.3, we compare how $C_{\delta\omega\delta\omega}(t)$, $F(t)$, and $\sigma(\omega)$ change as a function of κ. We see that, for a fixed distribution of frequencies Δ, increasing the time scale of fluctuations through this distribution (decreasing τ_c) gradually narrows the observed lineshape from a Gaussian distribution of static frequencies with width (FWHM) of $2.35 \cdot \Delta$ to a motionally-narrowed Lorentzian lineshape with width (FWHM) of $2\Delta^2\tau_c$.

A related motional narrowing effect is observed in the case of the NMR spectra of two species in a reversible chemical reaction. Assume we have two molecules A and B that are exchanging with a first-order rate constant k_{AB}

$$A \underset{k_{BA}}{\overset{k_{AB}}{\rightleftarrows}} B \tag{17.2.25}$$

These species are identified through two distinct resonance frequencies ω_A and ω_B. Independent of reaction kinetics, we expect two resonances at ω_A and ω_B, each with a linewidth dictated by the molecular relaxation processes for each species. Consider what happens as the exchange rates speed up to the point where the exchange rate is approximately the same as the frequency splitting between resonances, $k_{AB} \approx (\omega_A - \omega_B)$. At this point, molecules never persist long enough in one state that their dipole oscillates long enough to develop resonance at that frequency. The stochastic jumps between states rapidly modulate the observed frequency between ω_A and ω_B, resulting in line-broadening between the two frequencies. In fact, when $k_{AB} \gg (\omega_A - \omega_B)$, the two resonances "motionally narrow" together to form one resonance at the mean frequency.(2)(3)

We can obtain a general expression for the expected behavior by for the case $k_{AB} = k_{BA} = k$ and neglecting other relaxation processes. The lineshape we obtain from two equally strong resonances spaced by $2\delta\omega = (\omega_A - \omega_B)$ is then given by

$$I(\omega) = \frac{4\delta\omega^2 k}{(\omega - \delta\omega)^2(\omega + \delta\omega)^2 + 4\omega^2 k^2} \tag{17.2.26}$$

This behavior is modeled in Figure 17.2.4 for varying exchange rates relative to the energy splitting. Here, the ratio $2\delta\omega/k$ is equivalent to the ratio κ for the Gaussian-stochastic model.

Note

Want to learn more about chemical exchange lineshapes? Use this prompt in your favorite AI tool.

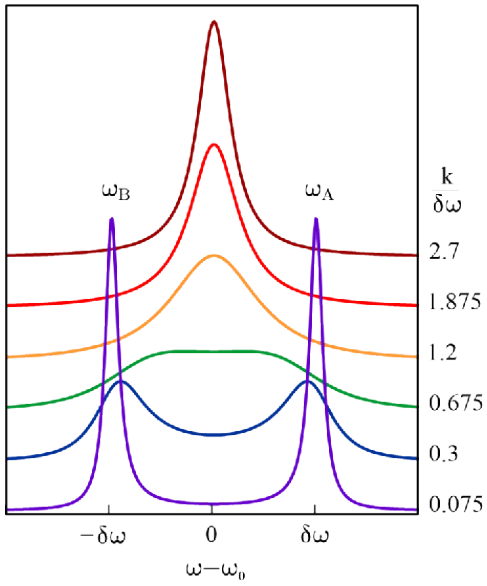


Figure 17.2.4: Motional narrowing in chemical exchange experiments. The resonances for the two exchanging species are split equally by $\pm\delta\omega = \pm|\omega_A - \omega_B|/2$ about the average frequency $\omega_0 = (\omega_A + \omega_B)/2$ and the forward and reverse rates are set equal to k.

Appendix: The Cumulant Expansion

For a statistical description of the random variable x, we can calculate the moments of the probability density for x: $\langle x \rangle, \langle x^2 \rangle, \ldots$ Then the average of an exponential of x can be expressed as an expansion in moments

$$\langle e^{ikx} \rangle = \sum_{n=0}^{\infty} \frac{(ik)^n}{n!} \langle x^n \rangle \tag{17.2.27}$$

An alternate way of expressing this expansion is in terms of the cumulants $g_n(x)$

$$\left\langle e^{\mathrm{i}kx} \right\rangle = \exp\left(\sum_{n=1}^{\infty} \frac{(\mathrm{i}k)^n}{n!} g_n(x) \right) \tag{17.2.28}$$

where the first few cumulants are:

$$g_1(x) = \langle x \rangle \qquad \text{mean} \tag{17.2.29}$$
$$g_2(x) = \left\langle x^2 \right\rangle - \langle x \rangle^2 \qquad \text{variance} \tag{17.2.30}$$
$$g_3(x) = \left\langle x^3 \right\rangle - 3 \langle x \rangle \left\langle x^2 \right\rangle + 2 \langle x \rangle^3 \qquad \text{skewness} \tag{17.2.31}$$

These cumulants are also readily generalized to multi-variate distributions:

$$g_1(x) = \langle x \rangle \tag{17.2.32}$$
$$g_2(x, y) = \langle xy \rangle - \langle x \rangle \langle y \rangle \tag{17.2.33}$$
$$g_3(x, y, z) = \langle xyz \rangle - (\langle x \rangle \langle yz \rangle + \langle y \rangle \langle zx \rangle + \langle z \rangle \langle xy \rangle) + 2 \langle x \rangle \langle y \rangle \langle z \rangle \tag{17.2.34}$$

An expansion in cumulants converges much more rapidly than an expansion in moments, particularly when you consider that x may be a time-dependent variable. Particularly useful is the observation that all cumulants with $n < 2$ vanish for Gaussian probability densities.

We obtain the cumulants above by expanding eq. (17.2.27) and (17.2.28) and comparing terms in powers of x. We start by postulating that, instead of expanding the exponential directly, we can instead expand the exponential argument in powers of an operator or variable H

$$F = \exp[g] = 1 + g + \frac{1}{2} g^2 + \cdots \tag{17.2.35}$$

$$g = g_1 H + \frac{1}{2} g_2 H^2 + \cdots \tag{17.2.36}$$

Inserting eq. (17.2.36) into eq. (17.2.35) and collecting terms in orders of H gives

$$\begin{aligned} F &= 1 + \left(g_1 H + \frac{1}{2} g_2 H^2 + \cdots \right) + \frac{1}{2} \left(g_1 H + \frac{1}{2} g_2 H^2 + \cdots \right)^2 + \cdots \\ &= 1 + g_1 H + \frac{1}{2} \left(g_2 + g_1^2 \right) H^2 + \cdots \end{aligned} \tag{17.2.37}$$

Now comparing this with the expansion of the exponential

$$\begin{aligned} F &= \exp[fH] \\ &= 1 + f_1 H + \frac{1}{2} f_2 H^2 + \cdots \end{aligned} \tag{17.2.38}$$

allows one to see that

$$\begin{aligned} g_1 &= f_1 \\ g_2 &= f_2 - f_1^2 \end{aligned} \tag{17.2.39}$$

The cumulant expansion can also be applied to time-correlations. For small fluctuations, the classical expansion is

$$\begin{aligned} F(t) &= \left\langle \exp\left[-\mathrm{i} \int_0^t dt\, \omega(t) \right] \right\rangle \\ &= \exp\left[-\mathrm{i} \int_0^t dt\, g_1(t) - \frac{1}{2} \int_0^t dt_2 \int_0^t dt_2\, g_2(t_1, t_2) - \frac{\mathrm{i}}{6} \int_0^t dt_3 \int_0^t dt_2 \int_0^t dt_2\, g_3(t_1, t_2, t_3) + \cdots \right] \end{aligned} \tag{17.2.40}$$

or for the case of time-ordered exponential operators:

$$\begin{aligned} F(t) &= \left\langle \exp_+\left[-\mathrm{i} \int_0^t dt\, \omega(t) \right] \right\rangle \\ &= \exp\left[-\mathrm{i} \int_0^t d\tau\, g_1(\tau) - \int_0^t d\tau_2 \int_0^{\tau_2} d\tau_1\, g_2(\tau_2, \tau_1) + \cdots \right] \end{aligned} \tag{17.2.41}$$

where the time-dependent cumulants are now

$$g_1(\tau) = \langle \omega(\tau) \rangle \tag{17.2.42}$$

$$\begin{aligned} g_2(\tau_2, \tau_1) &= \langle \omega(\tau_2)\, \omega(\tau_1) \rangle - \langle \omega(\tau_2) \rangle \langle \omega(\tau_1) \rangle \\ &= \langle \delta\omega(\tau_2)\, \delta\omega(\tau_1) \rangle \end{aligned} \tag{17.2.43}$$

For Gaussian statistics, all higher cumulants vanish.

References

(1) In many figures the width of the Gaussian distribution is labeled with the standard deviation (here Δ). This is meant to symbolize that Δ is the parameter that determines the width, and not that it is the line width. For Gaussian distributions, the full line width at half maximum amplitude (FWHM) is 2.35Δ.

(2) Anderson, P. W. A Mathematical Model for the Narrowing of Spectral Lines by Exchange or Motion. *Journal of the Physical Society of Japan* **1954**, *9* (3), 316-339. DOI: 10.1143/jpsj.9.316

(3) Kubo, R. A Stochastic Theory of Line-Shape and Relaxation. *Fluctuation, Relaxation and Resonance in Magnetic Systems*; Ter Haar, D., Ed.; Oliver and Boyd, 1962; pp 23-68.

This page titled 17.2: Gaussian-Stochastic Model for Spectral Diffusion is shared under a CC BY-NC-SA 4.0 license and was authored, remixed, and/or curated by Andrei Tokmakoff via source content that was edited to the style and standards of the LibreTexts platform.

17.3: The Energy Gap Hamiltonian

How can we describe the stochastic fluctuations of a quantum mechanical system? This is not immediately obvious, given that the quantum equations of motion are deterministic. We will find that there is a quantitative similarity between the Gaussian-stochastic and a quantum system interacting with a harmonic bath. As a starting point for describing quantum fluctuations, we will return to the Displaced Harmonic Oscillator model, but re-cast it in a way that mirrors the Gaussian-stochastic model. We refer to this as the Energy Gap Hamiltonian.

We previously described the DHO model in terms of the eigenstates of the material Hamiltonian H_0, and interpreted the dipole correlation function and resulting lineshape in terms of the overlap between two vibrational wave packets evolving on the ground and excited surfaces $|E\rangle$ and $|G\rangle$.

$$C_{\mu\mu}(t) = |\mu_{eg}|^2 \, e^{-\mathrm{i}(E_e - E_g)t/\hbar} \, \langle \varphi_g(t) \, | \varphi_e(t) \, \rangle \tag{17.3.1}$$

Expressed in a slightly different physical picture, we can also conceive of this process as the coupled harmonic nuclear motions modulating the electronic energy gap between electronic ground and excited states, $\omega_{eg}(t)$. We can imagine rewriting the same Hamiltonian in a form with a new physical picture that describes how the electronic energy gap varies as a function of the harmonic coordinate q. Motivated by calculating a time-dependent expectation value of the electronic energy gap, we define the energy gap Hamiltonian (EGH) as

$$H_{eg} = H_e - H_g \tag{17.3.2}$$

As before, the DHO Hamiltonian is

$$H_0 = |e\rangle \, E_e \, \langle e| + |g\rangle \, E_g \, \langle g| + H_e + H_g \tag{17.3.3}$$

where the ground and excited state vibrational Hamiltonians expressed in reduced units are

$$\begin{aligned} H_e &= \hbar\omega_0 \left(\underset{\sim}{p}^2 + (\underset{\sim}{q} - \underset{\sim}{d})^2 \right) \\ H_g &= \hbar\omega_0 \left(\underset{\sim}{p}^2 + \underset{\sim}{q}^2 \right) \end{aligned} \tag{17.3.4}$$

$$\underset{\sim}{p} = \hat{p} \, (2\hbar\omega_0 m)^{-1/2} \tag{17.3.5}$$

$$\underset{\sim}{q} = \hat{q} \, (m\omega_0/2\hbar)^{1/2} \tag{17.3.6}$$

$$\underset{\sim}{d} = d \, (m\omega_0/2\hbar)^{1/2} \tag{17.3.7}$$

Inserting eq. (17.3.2) allows us to re-write the DHO Hamiltonian in terms of the EGH:

$$H_0 = |e\rangle \, E_e \, \langle e| + |g\rangle \, E_g \, \langle g| + H_{eg} + 2H_g \tag{17.3.8}$$

If we evaluate eq. (17.3.2), we find the Hamiltonian describes a linear coupling of the electronic system to q:

$$\begin{aligned} H_{eg} &= -2\hbar\omega_0 \underset{\sim}{d} \underset{\sim}{q} + \hbar\omega_0 \underset{\sim}{d}^2 \\ &= -m\omega_0^2 dq + \lambda \end{aligned} \tag{17.3.9}$$

The slope of H_{eg} versus q is proportional to the oscillator displacement and describes the coupling strength between the electronic and vibrational degrees of freedom, $c = m\omega_0^2 d$. The average value, or expectation value, of the energy gap Hamiltonian is $\langle H_{eg} \rangle = \lambda$.

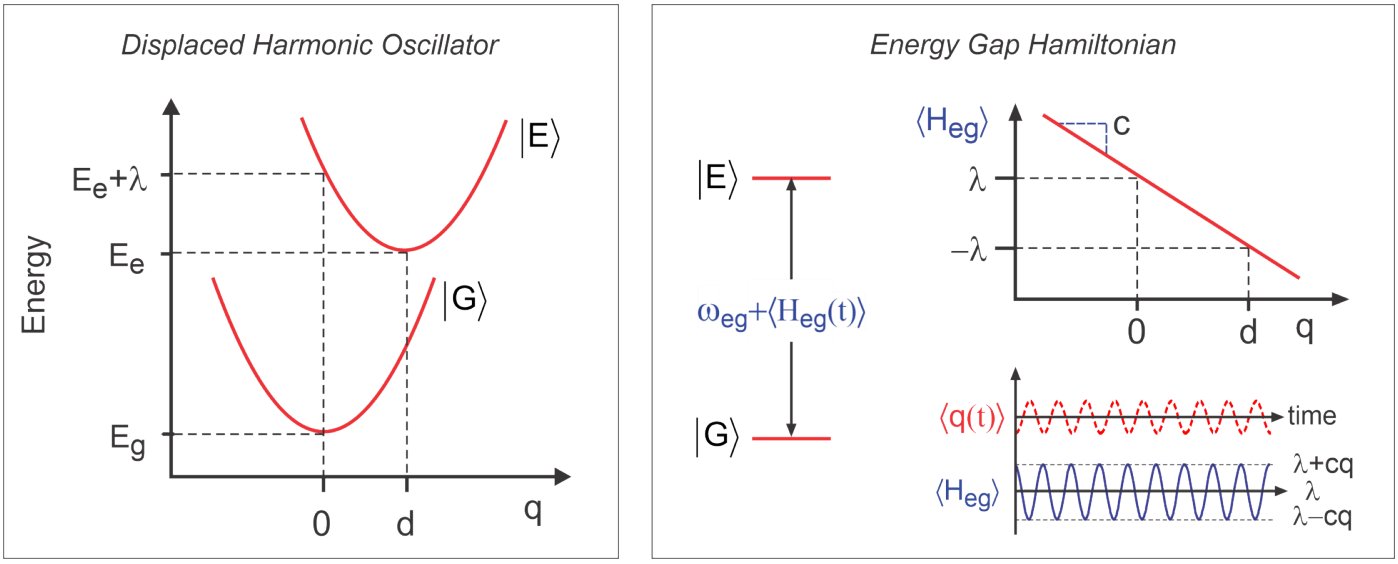


Figure 17.3.1: Illustration of the relationship between the displaced harmonic oscillator and the electronic energy gap Hamiltonians. The energy gap Hamiltonian is time-dependent and the time-dependent behavior of the harmonic nuclear coordinate map onto the time-dependence of the electronic energy gap.

To obtain the absorption lineshape from the dipole correlation function

$$C_{\mu\mu}(t) = |\mu_{eg}|^2 \, e^{-i\omega_{eg}t} F(t) \tag{17.3.10}$$

we must evaluate the dephasing function.

$$F(t) = \left\langle e^{iH_g t} e^{-iH_e t} \right\rangle = \left\langle U_g^\dagger U_e \right\rangle \tag{17.3.11}$$

For the new picture, we wish to express the dephasing function in terms of the time dependence of the energy gap H_{eg}. That is, if $F(t) = \langle U_{eg} \rangle$, then what is U_{eg}, the time-propagator for the energy gap Hamiltonian? The transformation of the time-propagator from the DHO Hamiltonian to the EGH is similar to our derivation of the interaction picture. Noting the mapping of our current problem to the Hamiltonian used for the interaction picture

$$H_e = H_g + H_{eg} \quad \Longleftrightarrow \quad H = H_0 + V \tag{17.3.12}$$

we see that we can represent the time dependence of the electronic energy gap H_{eg} using

$$\begin{aligned} e^{-iH_e t/\hbar} &= e^{-iH_g t/\hbar} \exp_+ \left[\frac{-i}{\hbar} \int_0^t d\tau \, H_{eg}(\tau) \right] \\ U_e &= U_g U_{eg} \end{aligned} \tag{17.3.13}$$

Where the time-dependence of the EGH is expressed in terms of H_g:

$$\begin{aligned} H_{eg}(t) &= e^{iH_g t/\hbar} H_{eg} e^{-iH_g t/\hbar} \\ &= U_g^\dagger H_{eg} U_g \end{aligned} \tag{17.3.14}$$

Thus the time dependence of the EGH reflects how the electronic energy gap is modulated by its interactions with the harmonic oscillator.

Transformation of time-propagators

More generally and setting $\hbar = 1$, if we have a time-dependent operator of the form

$$e^{iH_A t} A e^{-iH_B t} \tag{17.3.15}$$

we can also express the dynamics through the difference Hamiltonian $H_{BA} = H_B - H_A$

$$Ae^{-\mathrm{i}(H_B-H_A)t} = Ae^{-\mathrm{i}H_{BA}t} \tag{17.3.16}$$

using a commonly performed unitary transformation. If we write

$$H_B = H_A + H_{BA} \tag{17.3.17}$$

we can apply the same procedure we used for partitioning the dynamics in the interaction picture to write

$$e^{-\mathrm{i}H_Bt} = e^{-\mathrm{i}H_At}\exp_+\left[-\frac{\mathrm{i}}{\hbar}\int_0^t d\tau\, H_{BA}(\tau)\right] \tag{17.3.18}$$

where

$$H_{BA}(\tau) = e^{\mathrm{i}H_At}H_{BA}e^{-\mathrm{i}H_At} \tag{17.3.19}$$

Then, we can also write:

$$e^{\mathrm{i}H_At}e^{-\mathrm{i}H_Bt} = \exp_+\left[-\frac{\mathrm{i}}{\hbar}\int_0^t d\tau\, H_{BA}(\tau)\right] \tag{17.3.20}$$

Equation (17.3.13) immediately implies that the dephasing function is

$$F(t) = \left\langle e^{\mathrm{i}H_gt/\hbar}e^{-\mathrm{i}H_et/\hbar}\right\rangle = \left\langle \exp_+\left[\frac{-\mathrm{i}}{\hbar}\int_0^t d\tau H_{eg}\left(\tau\right)\right]\right\rangle \tag{17.3.21}$$

It is interesting to note that the quantum dephasing function appears in the same form as in our earlier classical derivation of the Gaussian-stochastic model, although here the time-dependence of the transition frequency is simple, undamped harmonic oscillations.

In the case of Gaussian statistics, as we would expect from small fluctuations about an average energy gap, the second-order cumulant expansion allows the dephasing function to be written in terms of the first and second cumulants, $g_1(\tau)$ and $g_2(\tau_2,\tau_1)$:

$$\begin{aligned} F(t) =& \exp\left[\frac{-i}{\hbar}\int_0^t d\tau\left\langle H_{eg}(\tau)\right\rangle\right. \\ &\left. + \left(\frac{-i}{\hbar}\right)^2\int_0^t d\tau_2\int_0^{\tau_2} d\tau_1\left[\left\langle H_{eg}\left(\tau_2\right)H_{eg}\left(\tau_1\right)\right\rangle - \left\langle H_{eg}\left(\tau_2\right)\right\rangle\left\langle H_{eg}\left(\tau_1\right)\right\rangle\right]\right] \end{aligned} \tag{17.3.22}$$

Note that the cumulant expansion here involves a time-ordered expansion. The first cumulant term depends on the expectation value of H_{eg}, which is the reorganization energy:

$$\left\langle H_{eg}\right\rangle = \hbar\omega_0\underset{\sim}{d}^2 = \lambda \tag{17.3.23}$$

and therefore $g_1(\tau) = -\mathrm{i}\lambda t/\hbar$.

The second cumulant in (17.3.22) involves a double integral over the energy gap correlation function, which describes the time-dependent changes of the electronic transition frequency relative to its average value. Since $\left\langle H_{eg}\right\rangle$ is independent of time, we can write this as

$$C_{eg}\left(\tau_2,\tau_1\right) = \frac{1}{\hbar^2}\left[\left\langle H_{eg}\left(\tau_2\right)H_{eg}\left(\tau_1\right)\right\rangle - \left\langle H_{eg}\right\rangle^2\right] = \frac{1}{\hbar^2}\left\langle \delta H_{eg}\left(\tau_2\right)\delta H_{eg}\left(\tau_1\right)\right\rangle \tag{17.3.24}$$

where

$$\begin{aligned} \delta H_{eg}(t) &= H_{eg}(t) - \left\langle H_{eg}\right\rangle \\ &= -m\omega_0^2 d\hat{q}(t) \end{aligned} \tag{17.3.25}$$

To make a direct connection with the Gaussian-stochastic model, we can define the time-dependent transition frequency as

$$\delta\hat{\omega}_{eg} \equiv \frac{\delta H_{eg}}{\hbar} \tag{17.3.26}$$

The carat is retained over the $\delta\omega_{eg}$ to remind us that this is an operator. Then the energy gap correlation function is written

$$C_{eg}\left(\tau_2,\tau_1\right)=\left\langle\delta\hat{\omega}_{eg}\left(\tau_2\right)\delta\hat{\omega}_{eg}\left(\tau_1\right)\right\rangle \tag{17.3.27}$$

Note that the zero-time value of C_{eg} gives the variance in the distribution of transition frequencies sampled by the system, $C_{eg}\left(0\right)=\left\langle\delta\hat{\omega}_e g^2\right\rangle$, which is equivalent to Δ^2 in the Gaussian-stochastic model.

We now arrive at an expression for the dephasing function:

$$F(t)=e^{-\mathrm{i}\lambda t/\hbar-g_2(t)} \tag{17.3.28}$$

$$g_2(t)=\int_0^t d\tau_2\int_0^{\tau_2}d\tau_1\,C_{eg}\left(\tau_2,\tau_1\right) \tag{17.3.29}$$

and the dipole correlation function can be expressed as

$$C_{\mu\mu}(t)=\left|\mu_{eg}\right|^2 e^{-\mathrm{i}(E_e-E_g+\lambda)t/\hbar}e^{-g_2(t)} \tag{17.3.30}$$

This is the correlation function expression that determines the absorption lineshape for a time-dependent energy gap.

Let's now evaluate the energy gap correlation function for the case of coupling to a single harmonic mode. Making use of eq. (17.3.25), we can see that the energy gap correlation function is given by

$$\begin{aligned}C_{eg}\left(\tau_2,\tau_1\right)&=\sum_n p_n\langle n|\delta\hat{\omega}_{eg}\left(\tau_2\right)\delta\hat{\omega}_{eg}\left(\tau_1\right)|n\rangle\\&=\frac{1}{\hbar^2}\sum_n p_n\langle n|e^{\mathrm{i}H_g(\tau_2-\tau_1)/\hbar}\delta H_{eg}e^{-iH_g(\tau_2-\tau_1)/\hbar}\delta H_{eg}|n\rangle\\&=\frac{m\omega_0^3\underset{\sim}{d}^2}{\hbar}\langle q(t)q(0)\rangle\end{aligned} \tag{17.3.31}$$

Here we have substituted $t=(\tau_2-\tau_1)$. Using the bath oscillator correlation function

$$C_{qq}(t)=\langle q(t)q(0)\rangle=\frac{\hbar}{2m\omega_0}\left[\left(\bar{n}+1\right)e^{-\mathrm{i}\omega_0 t}+\bar{n}e^{\mathrm{i}\omega_0 t}\right] \tag{17.3.32}$$

we find

$$C_{eg}(t)=\omega_0^2 S\left[\left(\bar{n}+1\right)e^{-\mathrm{i}\omega_0 t}+\bar{n}e^{\mathrm{i}\omega_0 t}\right] \tag{17.3.33}$$

As before, $S=d^2\left(m\omega_0/2\hbar\right)$ is the Huang-Rhys factor, $\bar{n}=\left(e^{\beta\hbar\omega_0}-1\right)^{-1}$ is the thermally averaged occupation number for the oscillator, and $\beta=1/k_BT$. The energy gap correlation function is a complex function, which can be separated into real and imaginary parts

$$C_{eg}(t)=C'_{eg}+\mathrm{i}C''_{eg} \tag{17.3.34}$$

$$\begin{aligned}C'_{eg}(t)&=\omega_0^2 S\coth\left(\beta\hbar\omega/2\right)\cos\left(\omega_0 t\right)\\C''_{eg}(t)&=\omega_0^2 S\sin\left(\omega_0 t\right)\end{aligned} \tag{17.3.35}$$

using the relation

$$2\bar{n}(\omega)+1=\coth\left(\beta\hbar\omega/2\right) \tag{17.3.36}$$

and $\coth(x)=(e^x+e^{-x})/(e^x-e^{-x})$. Here we see that the real part of the energy gap correlation function is temperature dependent, whereas the imaginary part is not.

To discuss the temperature dependence of $C_{eg}\left(t\right)$, it is helpful to look at the high and low temperature limits of the $\coth$ function (Figure 17.3.2). We can simplify our notation by defining the reduced inverse temperature variable

$$\underset{\sim}{\beta}=\frac{\beta\hbar\omega_0}{2}=\frac{\hbar\omega_0}{2k_BT} \tag{17.3.37}$$

which sets the temperature scale relative to the frequency of the harmonic oscillator. Then we find the limiting behavior to be

$$\begin{aligned} \lim_{\underset{\sim}{\beta}\to\infty} \coth(\underset{\sim}{\beta}) &= 1 \qquad (T \to 0) \\ \lim_{\underset{\sim}{\beta}\to 0} \coth(\underset{\sim}{\beta}) &\approx \underset{\sim}{\beta}^{-1} \qquad (\text{for } 2k_B T \gg \hbar\omega_0) \end{aligned} \tag{17.3.38}$$

At the low temperature limit, $\coth(\beta) \to 1$ and $\bar{n} \to 0$. The magnitudes of the real and imaginary components of $\tilde{C}_{eg}(t)$ are the same, and the energy gap correlation function is modulated as $\omega_0^2 S \exp(-i\omega_0 t)$. In the high temperature limit, $\coth(\beta)$ grows as $2k_B T/\hbar\omega_0$, so that the magnitude of the real component of $\tilde{C}_{eg}(t)$ grows linearly with temperature and dominates the imaginary part ($C'_{eg} \gg C''_{eg}$). In this limit, effectively, the energy gap correlation function $C_{eg}(t)$ becomes real and even in time.

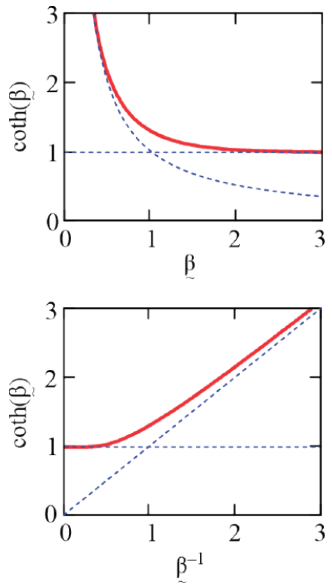


Figure 17.3.2: Behavior of $\coth(\underset{\sim}{\beta})$ function as a function of inverse temperature $\underset{\sim}{\beta}$ and temperature $\underset{\sim}{\beta}^{-1}$. Dashed lines illustrate limiting behavior for small and large $\underset{\sim}{\beta}$.

Next, we can evaluate the lineshape function using eq. (17.3.29):

$$g_2(t) = -S\left[(\bar{n}+1)\left(e^{-i\omega_0 t}-1\right) + \bar{n}\left(e^{i\omega_0 t}-1\right)\right] - iS\omega_0 t \tag{17.3.39}$$

$$= -S\left[\coth(\underset{\sim}{\beta})\left(1-\cos\omega_0 t\right) + \left(\sin\omega_0 t - \omega_0 t\right)\right] \tag{17.3.40}$$

▶ **Derivation**

$$\begin{aligned} g_2(t) &= \int_0^t d\tau_2 \int_0^{\tau_2} d\tau_1\, C_{eg}(\tau_2-\tau_1) \\ &= \int_0^t d\tau_2 \int_0^{\tau_2} d\tau_1\, \omega_0^2 S\left((\bar{n}+1)\, e^{-i\omega_0(\tau_2-\tau_1)} + \bar{n}\, e^{i\omega_0(\tau_2-\tau_1)}\right) \\ &= \omega_0^2 S \int_0^t d\tau_2 \left(\frac{(\bar{n}+1)}{-i\omega_0} e^{-i\omega_0\tau_2}\left(e^{i\omega_0\tau_2}-1\right) + \frac{\bar{n}}{i\omega_0} e^{i\omega_0\tau_2}\left(e^{i\omega_0\tau_2}-1\right)\right) \\ &= \omega_0^2 S \int_0^t d\tau_2 \left(\frac{(\bar{n}+1)}{i\omega_0}\left(e^{-i\omega_0\tau_2}-1\right) + \frac{\bar{n}}{-i\omega_0}\left(e^{i\omega_0\tau_2}-1\right)\right) \\ &= \omega_0^2 S \left(\frac{(\bar{n}+1)}{-i\omega_0}\left(\frac{e^{-i\omega_0 t}-1}{-i\omega_0} - t\right) + \frac{\bar{n}}{i\omega_0}\left(\frac{e^{i\omega_0 t}-1}{i\omega_0} - t\right)\right) \\ &= -S\left((\bar{n}+1)\left(e^{-i\omega_0 t}-1+i\omega_0 t\right) + \bar{n}\left(e^{i\omega_0 t}-1-i\omega_0 t\right)\right) \\ &= -S\left[(\bar{n}+1)\left(e^{-i\omega_0 t}-1\right) + \bar{n}\left(e^{i\omega_0 t}-1\right)\right] - iS\omega_0 t \end{aligned}$$

Now we can separate the real and imaginary parts by substituting $e^{i\omega_0 t} = \cos\omega_0 t + i\sin\omega_0 t$

$$
\begin{aligned}
g_2(t) &= -S\left((2\bar{n}+1)\left(\cos\omega_0 t - 1\right) + \mathrm{i}\left(-\sin\omega_0 t + \omega_0 t\right)\right) \\
&= S\left(\underbrace{\coth\left(\frac{\beta\hbar\omega_0}{2}\right)\left(1-\cos\omega_0 t\right)}_{g'} + \mathrm{i}\left(\underbrace{\sin\omega_0 t}_{g''} - \omega_0 t\right)\right) \\
&= g'(t) + \mathrm{i}g''(t) - \mathrm{i}S\omega_0 t \\
&= g'(t) + \mathrm{i}g''(t) - \underbrace{\mathrm{i}\lambda t/\hbar}_{-g_1}
\end{aligned}
$$

The leading term in eq. (17.3.39) will result in a vibrational progression on the absorption spectrum that we also found in the DHO model, the second term leads to hot bands, and the final term includes the reorganization energy ($\lambda = S\hbar\omega_0$). Noting eq. (17.3.28), we see that this final factor will cancel with the reorganization energy obtained from the first cumulant, so we will redefine the lineshape function such that term disappears

$$
F(t) = e^{-g(t)} \qquad\qquad g(t) = \lambda t/\hbar + g_2(t) \tag{17.3.41}
$$

Then the lineshape function for a single mode is

$$
g(t) = -S\left[(\bar{n}+1)\left(e^{-\mathrm{i}\omega_0 t} - 1\right) + \bar{n}\left(e^{\mathrm{i}\omega_0 t} - 1\right)\right] \tag{17.3.42}
$$

or in terms of its real and imaginary parts

$$
g(t) = g' + \mathrm{i}g'' \tag{17.3.43}
$$

$$
\begin{aligned}
-g'(t) &= S\coth(\underset{\sim}{\beta})\left(1-\cos\omega_0 t\right) \\
-g''(t) &= S\sin\omega_0 t
\end{aligned} \tag{17.3.44}
$$

Like $C_{eg}(t)$, in the high temperature limit $g' \gg g''$. Because these enter the dipole correlation function as exponential arguments, the imaginary part of $g(t)$ will reflect the bath-induced energy shift of the electronic transition gap and vibronic structure, and the real part will reflect damping, and therefore the broadening of the lineshape.

$$
C_{\mu\mu}(t) = \left|\mu_{eg}\right|^2 e^{-\mathrm{i}(\omega_{eg}t - g''(t))} e^{-g'(t)} \tag{17.3.45}
$$

Now, we see that the dephasing function is given by

$$
F(t) = \exp\left[S\left((\bar{n}+1)\left(e^{-\mathrm{i}\omega_0 t} - 1\right) + \bar{n}\left(e^{\mathrm{i}\omega_0 t} - 1\right)\right)\right] \tag{17.3.46}
$$

$$
= \exp[S\coth(\underset{\sim}{\beta})(1-\cos\omega t) + \mathrm{i}\sin\omega t)] \tag{17.3.47}
$$

Let's confirm that we get the same result as with our original DHO model, when we take the low temperature limit. Setting $\bar{n} \to 0$ we see that eq. (17.3.46) reduces to our original result

$$
F(t) = \exp\left[S\left(e^{-\mathrm{i}\omega_0 t} - 1\right)\right] \qquad\qquad (T=0) \tag{17.3.48}
$$

Since $g' \gg g''$ in the high temperature limit, we can focus on the real term. To simplify the notation, we define the temperature-weighted Huang-Rhys factor $\underset{\sim}{S} = S\beta^{-1} = S(2k_B T/\hbar\omega_0)$. Then from eq. (17.3.38) we obtain

$$
\begin{aligned}
F(t) &= e^{\underset{\sim}{S}} \exp\left[\underset{\sim}{S}\cos\left(\omega_0 t\right)\right] \\
&= \sum_{j=0}^{\infty} \frac{e^{\underset{\sim}{S}}\underset{\sim}{S}^j}{j!}\cos^j\left(\omega_0 t\right)
\end{aligned} \tag{17.3.49}
$$

This has a series of oscillations at harmonics of the vibrational frequency ω_0, which leads to an absorption spectrum that contains a series of sidebands equally spaced by ω_0 and symmetrically spread on either side of ω_{eg}. The amplitudes of these peaks are scaled by the traditional Franck-Condon factors as well as the temperature. The envelope of the lineshape can be obtained by applying the short time expansion of $e^{-\mathrm{i}\omega_0 t}$ in eq. (17.3.39) and calculating the absorption lineshape from the resulting dipole correlation function, which results in

$$
\sigma_{\mathrm{abs}}(\omega) = \left|\mu_{eg}\right|^2 \sqrt{\frac{\pi}{\Delta^2}} \exp\left[\frac{-\left(\omega - \omega_{eg} - S\omega_0\right)^2}{2\Delta^2}\right] \tag{17.3.50}
$$

As we observed with the DHO, the resonance is centered at $\omega = \omega_{eg} + S\omega_0$, where $S\hbar\omega_0 = \lambda$. We also see that the linewidth is described by Δ, which grows as the square root of temperature:

$$\Delta^2 = \omega_0^2 \underset{\sim}{S} = \omega_0^2 S \frac{2k_B T}{\hbar\omega_0} \tag{17.3.51}$$

Note that Δ^2 reflects the variance in the frequency fluctuations $\langle \delta\omega_{eg}^2 \rangle$ and is comprised of two terms, $\omega_0^2 S$ which sets the scale for the interactions of the harmonic mode with the electronic transition at \(0 \, \text{K}\), and a thermal factor that broadens with growing temperature as the expectation value for the mean square displacement of the oscillator grows. Note also that Δ^2 corresponds to the zero-time value of the energy gap correlation function, $C_{eg}(0)$, in eq. (17.3.33).

Spectral representation of the energy gap correlation function

For a complicated spectrum of vibrational motions composed of many modes, representing the nuclear motions in terms of a spectrum rather than a beat pattern is often easier. It turns out that calculations are often easier performed in the frequency domain. Since time- and frequency-domain representations are complementary, we can also express the frequency correlation function in terms of its spectrum.

To start, we define a Fourier transform pair that relates the time and frequency domain representations:

$$C_{eg}(\omega) = \int_{-\infty}^{+\infty} e^{\mathrm{i}\omega t} C_{eg}(t)\, dt \tag{17.3.52}$$

$$C_{eg}(t) = \frac{1}{2\pi} \int_{-\infty}^{+\infty} e^{-\mathrm{i}\omega t} C_{eg}(\omega)\, d\omega \tag{17.3.53}$$

Since the energy gap correlation function has the property $C_{eg}(-t) = C_{eg}^*(t)$, it also follows from (17.3.52) that the energy gap fluctuation spectrum is entirely real:

$$C_{eg}(\omega) = 2\mathrm{Re} \int_0^{\infty} e^{\mathrm{i}\omega t} C_{eg}(t)\, dt \tag{17.3.54}$$

or

$$C_{eg}(\omega) = C'_{eg}(\omega) + C''_{eg}(\omega) \tag{17.3.55}$$

Here $C'_{eg}(\omega)$ and $C''_{eg}(\omega)$ are the Fourier transforms of the real and imaginary components of $C_{eg}(t)$, respectively. Note the lack of an i in this equation. $C'_{eg}(\omega)$ and $C''_{eg}(\omega)$ are even and odd in frequency. Thus while $C_{eg}(\omega)$ is entirely real valued, it is asymmetric about $\omega = 0$ and spectrally represents both real and imaginary features of the energy gap correlation function.

With these definitions in hand, we can rewrite the energy gap correlation function (eq. 17.3.33) for the spectrum created by coupling to a single harmonic mode of frequency ω_α:

$$C_{eg}(\omega_\alpha) = \omega_\alpha^2 S(\omega_\alpha) \left[(\bar{n}_\alpha + 1)\, \delta(\omega - \omega_\alpha) + \bar{n}_\alpha \delta(\omega + \omega_\alpha) \right] \tag{17.3.56}$$

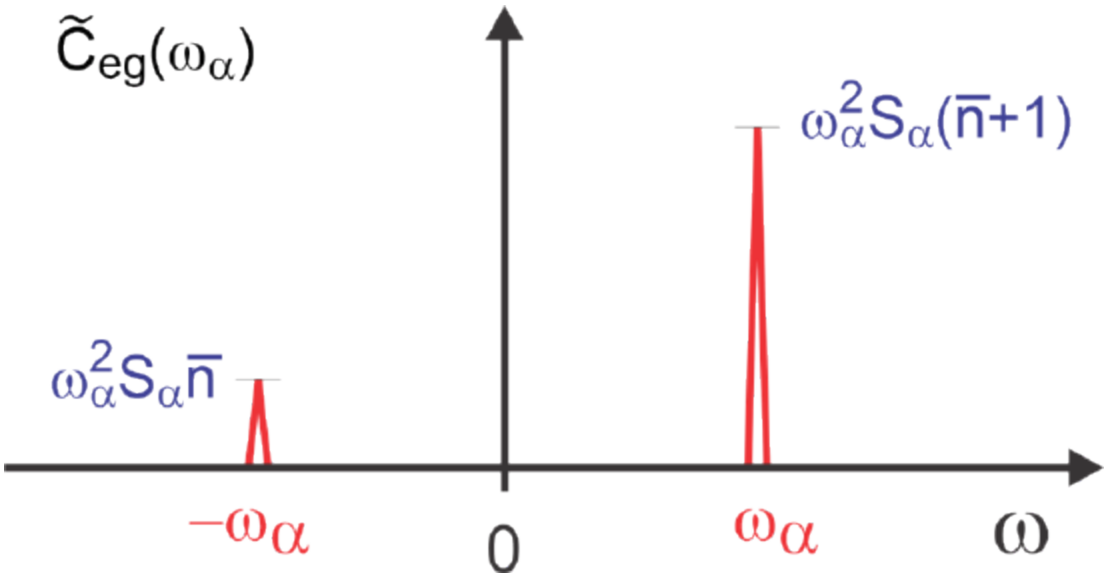


Figure 17.3.3: Illustration of single mode spectrum of the energy gap correlation function.

This is a spectrum that characterizes how bath vibrational modes of a frequency ω_α and thermal occupation together modify the observed energy of the system. The first and second terms in (17.3.56) describe upward and downward energy shifts of the system as a result of their interactions with the environment, respectively. Coupling to a vibration most often leads to an upshift of the energy gap transition energy, since additional energy from the environment (λ) is needed for electronic excitation. However, as with hot bands, the bath may already have thermal energy available to transfer to the system, which results in a down-shift in the energy gap. The net balance of upward and downward shifts averaged over the bath follows the detailed balance expression

$$C_{eg}\left(-\omega\right) = e^{-\beta\hbar\omega} C_{eg}(\omega) \tag{17.3.57}$$

The balance of rates tends toward equivalence with increasing temperature.

We can also separate the real and imaginary components of the energy gap spectrum

$$C'_{eg}\left(\omega_\alpha\right) = \omega_\alpha^2 S\left(\omega_\alpha\right) \coth\left(\beta\hbar\omega_\alpha/2\right) \left[\delta\left(\omega-\omega_\alpha\right) + \delta\left(\omega+\omega_\alpha\right)\right] \tag{17.3.58}$$

$$C''_{eg}\left(\omega_\alpha\right) = \omega_\alpha^2 S\left(\omega_\alpha\right) \left[\delta\left(\omega-\omega_\alpha\right) + \delta\left(\omega+\omega_\alpha\right)\right] \tag{17.3.59}$$

These representations illustrate that the even and odd parts in the spectral representation are not independent, but can be related to one another through:

$$C'_{eg}\left(\omega_\alpha\right) = \coth\left(\beta\hbar\omega_\alpha/2\right) C''_{eg}\left(\omega_\alpha\right) \tag{17.3.60}$$

$$C_{eg}\left(\omega_\alpha\right) = \left(1+\coth\left(\beta\hbar\omega_\alpha/2\right)\right) C''_{eg}\left(\omega_\alpha\right) \tag{17.3.61}$$

That is, given either the real or imaginary part of the energy gap correlation spectrum, we can predict the other part. This relationship is one manifestation of the fluctuation-dissipation theorem.

Due to being temperature independent, $\tilde{C}''_{eg}\left(\omega_\alpha\right)$ is the commonly used representation. One can obtain the energy gap correlation function from $\tilde{C}''_{eg}\left(\omega_\alpha\right)$ using

$$C_{eg}(t) = \frac{1}{2\pi}\int_{-\infty}^{\infty} d\omega_\alpha\, C''_{eg}\left(\omega_\alpha\right)\left[\coth\left(\beta\hbar\omega/2\right)\cos\left(\omega_\alpha t\right) + \mathrm{i}\sin\left(\omega_\alpha t\right)\right] \tag{17.3.62}$$

and the lineshape function from

$$g(t) = \int_0^\infty d\omega\, \frac{C''_{eg}(\omega)}{\pi\omega^2}\left[\coth\left(\frac{\beta\hbar\omega}{2}\right)\left(1-\cos\omega t\right) + \mathrm{i}\sin\omega t\right] \tag{17.3.63}$$

This page titled 17.3: The Energy Gap Hamiltonian is shared under a CC BY-NC-SA 4.0 license and was authored, remixed, and/or curated by Andrei Tokmakoff via source content that was edited to the style and standards of the LibreTexts platform.

17.4: Spectral Density for Condensed Phase Spectroscopy

Collective motions in condensed matter

How do we use the energy gap Hamiltonian to deal with condensed phases? For condensed phase problems, the system coordinates that we observe in an experiment are embedded within a continuum of nuclear motions, and the EGH can be generalized to treat a continuum of harmonic motions. Whether in an ordered crystalline lattice or in a disordered medium such as a liquid, polymer, or complex fluid, the motions of atoms and molecules cannot occur independently of their environment. The medium is dense, and one cannot move one molecule without moving others. As a result, the behavior of the system is governed by collective dynamics that can involve the various complex motions of many constituent molecules or atoms. These motions may vary from as small as femtosecond and picosecond scale fluctuations in local configurations to the wavelength-long collective motion of entire domains of molecules, which can occur over many decades of time—from picoseconds to nanoseconds, and longer. In solids, these motions can be described as phonons. However, the collective motions of liquids are more difficult to describe as they involve highly dynamic configurational fluctuations and collective structural rearrangements.

Experimental study of these nuclear collective motions has always been complex, particularly in soft and disordered matter. For crystalline matter, inelastic neutron scattering and x-ray scattering measurements have provided direct insight into the phonon dispersion curves and phonon densities of state. For soft matter, both these methods and spectroscopy have played important roles.

Dielectric relaxation spectroscopy, light scattering, and neutron scattering can directly measure spectra associated with these motions in the frequency domain. Dielectric relaxation spectroscopy (DS) measures the frequency-dependent complex permittivity of a sample as a function of the frequency of an alternating electric field, most often in the 10^{8}–10^{12} Hz frequency range. The DS spectrum characterizes the collective molecular motions caused by molecular charge reorganization when adapting to a changing field direction. Thus DS is most sensitive to the reorientation of dipoles within the sample. Light scattering, low-frequency Raman scattering, and time-resolved optical Kerr effect spectroscopy all measure the frequency-dependent motions that influence the polarizability of the sample in the same frequency range. Inelastic neutron scattering (NS) can be used to obtain the dynamic structure factor, a representation of the time- and length-scale of collective nuclear motions of the sample. Each spectroscopy observes the spectrum of motions as filtered through the experiment's ability to observe them. That is, they reveal a unique a spectral density that reflects the density of states for collective motions scaled by a frequency-dependent coupling of the observable to motions. Figure 17.4.1 illustrates the results of these experiments on liquid water.

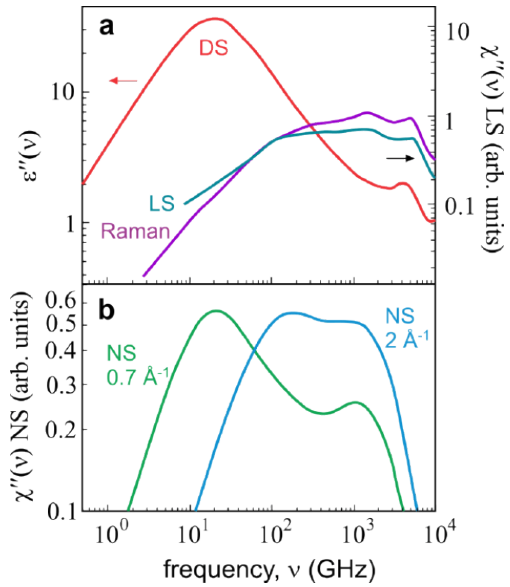


Figure 17.4.1: Low frequency spectra of intermolecular motions in liquid H_2O at 298 K obtained from (a) dielectric relaxation spectroscopy (DS), light scattering (LS), and Raman spectroscopy (Raman), and (b) neutron scattering (NS) at two momentum transfer vectors $Q = 0.7$ Å^{-1} and 2 Å^{-1}. Adapted from DOI:10.1103/PhysRevLett.117.185501

Ultrafast spectroscopy has also played an important role in describing intermolecular motions, although indirectly, by monitoring the ways in which vibrational and collective dynamics influence optical spectroscopy. In a similar manner to the direct techniques, ultrafast spectroscopy can be used to characterize a spectral density associated with the influence that the environment has on the electronic transition frequency and absorption spectrum, with the advantage that it directly tracks the collective dynamics of the medium in time.

Given the diversity of methods used to understand collective dynamics and fluctuations in condensed matter, it is valuable to have a strategy for analyzing a variety of different methods with the same framework. What is common to all methods is the density of states $W(\omega)$, a frequency domain representation of the dynamics that indicates the amplitude of nuclear motions present within a given frequency. Our strategy, which follows the formalism popularized by Mukamel and is outlined in Figure 17.4.2, starts with (1) a density of states $W(\omega)$ which may be experimentally deduced or obtained from molecular dynamics simulations, and (2) a frequency-dependent coupling factor $S(\omega)$ that describes how sensitive a particular experiment is to a certain dynamical process. These are the inputs that determine the spectral density $\rho(\omega)$, which is used to compute experimental observables. In our case the frequency-domain spectral density $\rho(\omega)$ is used to compute a time-domain frequency correlation function, a lineshape function, and a dipole correlation function that can be Fourier transformed to obtain an absorption spectrum.

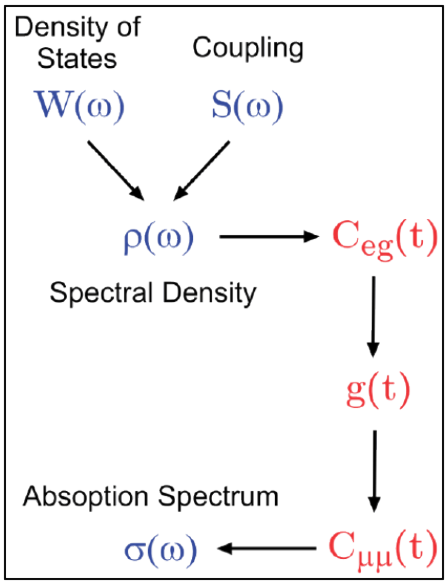


Figure 17.4.2: Scheme to calculate experimental observables in the time-domain (red) given a frequency-domain spectral density as input.

EGH using a spectral density

The EGH is readily generalized to the case of a continuous distribution harmonic oscillators of varying mode frequency and coupling strength, if we statistically characterize the density of states and the strength of the interaction between the system and this bath. For a discrete set of normal modes, the dephasing function is a product of dephasing functions for each normal mode. Therefore the lineshape function is obtained from a sum of contributions from the modes:

$$g(t) = \sum_{\alpha} g(t, \omega_\alpha) \tag{17.4.1}$$

Here $g(t, \omega_\alpha)$ refers to the time-dependence of the lineshape function for a single harmonic mode of frequency ω_α, given by eqs. (17.3.43) and (17.3.44). For a continuum, we treat the modes as continuous and indistinguishable, so the sums in the equations above can be replaced by integrals over a continuous distribution that is characterized by a density of states $W(\omega)$ and a smoothly varying frequency dependent coupling constant $S(\omega)$. For instance, eq. (17.4.1) becomes

$$\begin{aligned} g(t) &= \int_{-\infty}^{\infty} d\omega_\alpha W(\omega_\alpha) g\left(t, \omega_\alpha\right) \\ &= \int_{-\infty}^{\infty} d\omega_\alpha W(\omega_\alpha) S(\omega_\alpha) \left[\coth\left(\frac{\beta\hbar\omega_\alpha}{2}\right)\left(1-\cos\omega_\alpha t\right) + \mathrm{i}\sin\omega_\alpha t\right] \end{aligned} \tag{17.4.2}$$

Coupling to a continuum leads to dephasing, which results from interaction with a continuum of modes of varying frequency. This

will be characterized by damping of the energy gap frequency correlation function $C_{eg}(t)$

$$C_{eg}(t) = \int_{-\infty}^{\infty} d\omega_\alpha \, C_{eg}\left(t, \omega_\alpha\right) W(\omega_\alpha) \tag{17.4.3}$$

Here $C_{eg}\left(t, \omega_\alpha\right)$ refers to the energy gap frequency correlation function for a single harmonic mode with a mean frequency ω_α, given in eq. (17.3.31). This expresses the modulation of the energy gap in the time domain, but for our purposes it is easier to express the continuous distribution of coupled bath modes in the frequency domain:

$$\begin{aligned} C_{eg}(\omega) &= \int_{-\infty}^{\infty} d\omega_\alpha \, W(\omega_\alpha) C_{eg}(\omega_\alpha) \\ &= \int_{-\infty}^{\infty} d\omega_\alpha \, \omega_\alpha^2 W(\omega_\alpha) S(\omega_\alpha) \left[\left(\bar{n}_\alpha + 1\right) \delta\left(\omega - \omega_\alpha\right) + \bar{n}_\alpha \delta\left(\omega + \omega_\alpha\right)\right] \end{aligned} \tag{17.4.4}$$

The integral of a single harmonic mode spectrum over a continuous density of states provides a coupling-weighted density of states that reflects the action spectrum for the system-bath interaction.

Comparing eqs. (17.4.2) and (17.4.4) with eqs. (17.3.62) and (17.3.63) suggests that we can represent the coupling-weighted density of states in these equations as a spectral density $\rho(\omega)$, which is defined as

$$\begin{aligned} \rho(\omega) &\equiv \frac{\tilde{C}_{eg}''(\omega)}{\pi \omega^2} \\ &= \frac{1}{\pi} W(\omega) S(\omega) \end{aligned} \tag{17.4.5}$$

Note $\rho(\omega)$ is real, defined only for positive frequencies, and has units of inverse angular frequency. A number of important quantities can now be computed directly from $\rho(\omega)$. The reorganization energy can be obtained from the first moment of the spectral density

$$\lambda = \hbar \int_0^{\infty} d\omega \, \omega \rho(\omega) \tag{17.4.6}$$

From eqs. (17.3.29) and (17.4.4) we obtain the energy gap correlation function and lineshape function in terms of the spectral density as

$$C_{eg}(t) = \int_0^{\infty} d\omega \, \omega^2 \rho(\omega) \left[\coth\left(\frac{\beta\hbar\omega}{2}\right) \cos\left(\omega t\right) + \mathrm{i} \sin\left(\omega t\right)\right] \tag{17.4.7}$$

$$g(t) = \int_0^{\infty} d\omega \, \rho(\omega) \left[\coth\left(\frac{\beta\hbar\omega}{2}\right) \left(1 - \cos\omega t\right) + \mathrm{i} \sin\omega t\right] \tag{17.4.8}$$

In these expressions, the real part will dominate at high temperature, as expected for a classical system. Additionally, we can quantify the overall magnitude of the fluctuations of the bath, i.e. the variance in $\delta\omega_{eg}$, using the zero-time value of $C_{eg}(t)$,

$$\Delta^2 = C_{eg}(0) = \int_0^{\infty} d\omega \, \omega^2 \rho(\omega) \coth\left(\frac{\beta\hbar\omega}{2}\right) \tag{17.4.9}$$

Equations (17.4.6) to (17.4.9) are general expressions written in terms of an arbitrary spectral distribution that encodes the time scale and amplitude of energy gap fluctuations. Given a spectral density, you can calculate various spectroscopic observables and other time-dependent processes in a fluctuating environment.

Now, let's evaluate the behavior of the lineshape function and absorption lineshape for different forms of the spectral density. We will be motivated by the functional form of the density of states and spectral densities observed for random or noisy processes in phonons or condensed phase intermolecular motions. How do these functions behave? There are no firm rules here. Since the density of states vanishes at $\omega = 0$, we expect densities of states at the lowest frequencies to grow as a power of frequency, for instance ω^2 for a Debye density of states. However, the density of states must remain finite and integrable, so one expects to reach a cutoff frequency above which the density of states or spectral density will decrease to zero. Depending on the process of interest, spectral densities for stochastic processes can scale as $\rho(\omega) \sim \omega^{-n}$, where $n = 0$, 1, or 2.

One common form of the spectral density that follows the expected behavior is

$$\rho(\omega) = A\frac{1}{\omega_c}\left(\frac{\omega}{\omega_c}\right)^s e^{-\omega/\omega_c} \tag{17.4.10}$$

The parameter s sets the scaling of how the spectral density grows with ω at low frequency, and ω_c is a cut-off frequency that sets an exponential rate of drop-off at high frequencies. A is a unitless normalization constant that depends on s and ω_c, and the units of ρ are inverse angular frequency. These spectral densities, examples of which are shown as a function of s in Figure 17.4.3, have the desired property of being an odd function in ω and integrable over ω. The case $s = 1$ is known as the Ohmic spectral density, whereas $s > 1$ is super-ohmic and $s < 1$ is sub-ohmic.

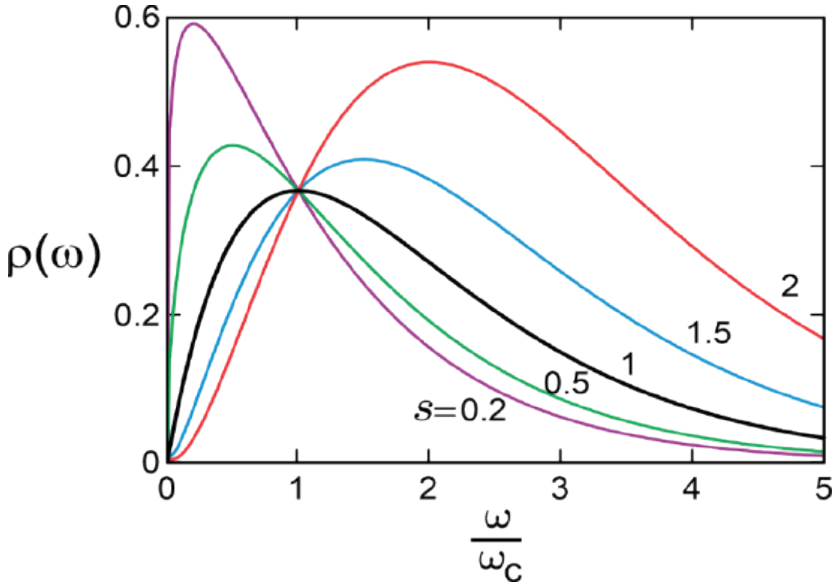


Figure 17.4.3: Spectral density function given in eq. (17.4.10) illustrating the growth as $(\omega/\omega_c)^s$ for different values of the scaling factor s.

Let's examine the spectroscopy associated with an Ohmic spectral density. Inserting the Ohmic case of eq. (17.4.10) into eq. (17.4.6) leads us to find that the constant $A = \lambda\pi/2\hbar\omega_c$. We can rewrite the spectral density (using the reorganization energy λ) as

$$\rho(\omega) = \frac{\pi}{2}\frac{\lambda}{\hbar\omega_c}\frac{\omega}{\omega_c^2}e^{-\omega/\omega_c} \tag{17.4.11}$$

From $\rho(\omega)$ and a given value of λ, we can calculate spectroscopic observables by numerically integrating the equations above. However, it is helpful to look at the analytical solutions to these equation components in the high temperature limit $(k_BT \gg \hbar\omega_c)$ to understand what they represent.

The mean square amplitude of bath fluctuations $\langle\Delta^2\rangle$ obtained from eq. (17.4.9) is

$$\begin{aligned}\Delta^2 &= \pi\omega_c^2\left(\frac{\lambda}{\hbar\omega_c}\right)\left(\frac{2k_BT}{\hbar\omega_c}\right)\\ &= \left(\frac{2\pi\lambda k_BT}{\hbar^2}\right)\end{aligned} \tag{17.4.12}$$

This has the same form as eq. (17.3.51), but it is written in a form that emphasizes two primary contributions to the amplitude, each shown in parentheses. The first is proportional to the reorganization energy, i.e. the coupling between the system and harmonic bath, but scaled relative to the cutoff frequency, ω_c. The second factor is related to the thermal occupation of the harmonic bath modes at the cutoff frequency $(2k_BT/\hbar\omega_c \approx 2\bar{n}(\omega_c) + 1)$, which varies with temperature.

Also in the high temperature limit, the energy gap correlation function for the harmonic bath is

$$C'_{eg}(t) = \Delta^2\frac{1 - 3t^2\omega_c^2}{(1 + t^2\omega_c^2)^3} \tag{17.4.13}$$

and the lineshape function obtained from eq. (17.4.8) is

$$g'(t) = \frac{1}{2}\Delta^2 \left(\frac{t^2\omega_c^2}{1+t^2\omega_c^2} \right) \tag{17.4.14}$$

The dephasing function $F(t) = e^{-g'(t)}$ decays in a Gaussian manner ($F(t) \sim e^{-t^2}$) for short times ($t\omega_c \ll 1$) with a rate given by Δ^2. For long times, $F(t)$ decays to a constant offset given by the exponential of this factor. We also see that the cutoff frequency sets the timescale for switching between the short and long-time behavior, i.e. the correlation time for dephasing is essentially the inverse of the cutoff frequency $\tau_c \approx \omega_c^{-1}$.

Examples of the spectroscopy that arises from an Ohmic spectral density are illustrated in Figure 17.4.4. A cutoff frequency of $\omega_c = 40\ \text{cm}^{-1}$ is chosen to reflect what one would expect for the dynamics of a molecular liquid or solution. The reorganization energy is chosen to be $\lambda = 25\ \text{cm}^{-1}$ to emphasize temperature-dependent changes, although this is a small number that is closer in line with vibrational than electronic spectroscopy. With increasing temperature, the corresponding absorption lineshapes move from sharply peaked to a Gaussian with linewidths that scale with temperature as $\sqrt{T}$.

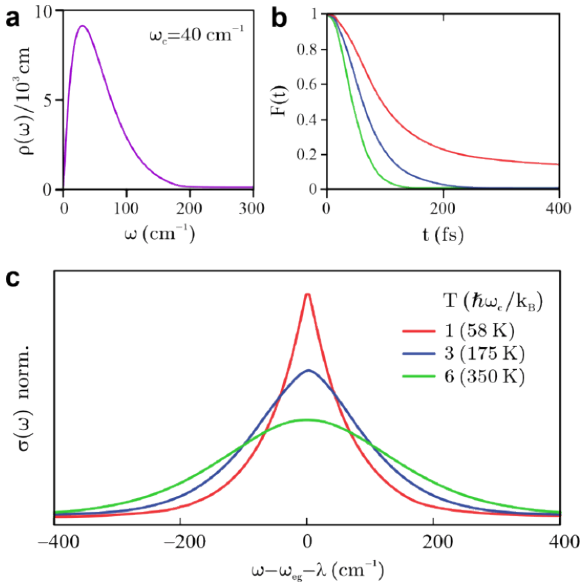


Figure 17.4.4: Example of the temperature-dependent dephasing functions and absorption spectra for an electronic transition coupled to an ohmic spectrum with $\omega_c = 40\ \text{cm}^{-1}$ and $A = 1$. Temperature is expressed in integer multiples of $\hbar\omega_c/k_B$.

This overall behavior is reminiscent of what we observed for the Gaussian-stochastic model. The correspondence can be made precisely in the high temperature limit by using a Lorentzian spectral density centered at $\omega = 0$, with a corresponding exponentially decaying energy gap correlation function. To keep the proper definition of λ, we define:

$$\rho(\omega) = \frac{\lambda}{\pi\hbar\omega}\frac{2\Lambda}{\omega^2+\Lambda^2} \tag{17.4.15}$$

where Λ is the spectral density linewidth. The corresponding modulation amplitude from eq. (17.4.9) is

$$\Delta^2 = \lambda\frac{2\pi k_B T}{\hbar^2} \tag{17.4.16}$$

and the corresponding energy gap correlation function is

$$C'_{eg}(t) = \Delta^2 \exp(-\Lambda t) \tag{17.4.17}$$

The lineshape function is

$$g'(t) = \frac{\Delta^2}{\Lambda^2}\left[\exp(-\Lambda t) + \Lambda t - 1\right] \tag{17.4.18}$$

This is the same expression as the Gaussian-stochastic model, with the correlation time given by $\tau_c = \Lambda^{-1}$. Strikingly, the interaction of an electronic transition with a harmonic bath, when characterized by a Lorentzian spectral density, results in an absorption spectrum that is the same as that predicted for a stochastically modulated energy gap. This is another manifestation

of how interactions of quantum systems with continua lead to irreversible relaxation processes. For completeness, the complex energy gap correlation function and lineshape functions are given by

$$C_{eg}(t) = \Delta^2 \exp\left(-\Lambda t\right)\left[\coth(\beta\hbar\Lambda/2) - \mathrm{i}\right] \tag{17.4.19}$$

$$g(t) = \frac{\Delta^2}{\Lambda^2}\left[\exp\left(-\Lambda t\right) + \Lambda t - 1\right]\left[\coth(\beta\hbar\Lambda/2) - \mathrm{i}\right] \tag{17.4.20}$$

We can look further at the correspondence of the Gaussian-stochastic model and EGH. As we originally indicated, a system's dynamics lies on a continuously varying scale between the fast and slow modulation limits, which can be quantified through the factor

$$\kappa = \Delta \cdot \tau_c = \frac{\sqrt{2\pi\lambda k_B T}}{\hbar\Lambda} \tag{17.4.21}$$

This expression indicates that the contributions of the reorganization energy and temperature to the numerator must be weighed relative to the width of the spectral density when determining the type of line broadening present. If we consider systems with broad spectral densities and the corresponding fast correlation times, such that $\Lambda \gg \omega$, the spectral density derived from eq. (17.4.15) decays as ω^{-1}:

$$\rho(\omega) = \frac{2\lambda}{\pi\Lambda\hbar\omega} \tag{17.4.22}$$

For the lineshape function we find

$$g'(t) = \Gamma t \tag{17.4.23}$$

with the homogeneous dephasing rate given by

$$\Gamma = \frac{2\pi\lambda k_B T}{\Lambda\hbar^2} \tag{17.4.24}$$

This is the expected result for the fast modulation limit in the Gaussian-stochastic model in which the homogeneous dephasing rate is $\Gamma = \Delta^2\tau_c$.

Example: Temperature-dependent absorption spectrum of a polycyclic aromatic

Let's consider an example: the electronic absorption spectrum of a polycyclic aromatic chromophore embedded in a polymer matrix and how it varies as a function of temperature. For this example, parameters are for the eight-ring polycyclic terrylene in polyethylene. The parameters are drawn from a low temperature ($1.8\ \mathrm{K}$) study of a number of single molecule fluorophores. The zero-phonon line (pure electronic transition) is at $\omega_{eg} = 17400\ \mathrm{cm}^{-1}$. For the spectral density, there are contributions from the Franck-Condon active molecular vibration and from the polymer environment. We select the four vibrational modes of the ring system with the largest dimensionless displacements and calculate their Huang-Rhys factors:

$\omega_i(\mathrm{cm}^{-1})$	S_i
1562	0.054
1272	0.274
536	0.026
243	0.14

Resonance Raman spectra can also be used effectively to determine Huang Rhys factors for specific vibrations. The contribution of each vibration to the spectral density is then determined from $\rho_{\mathrm{vib}}(\omega) = \Sigma_i \frac{1}{\pi} S_i W\left(\omega - \omega_i\right)$, though to simplify the computation and visualization, the density of states of a particular vibration was set to be a Lorentzian lineshape with a width of $5\ \mathrm{cm}^{-1}$ instead of a delta function. To mimic the collective motions of the polymer matrix we use a phonon spectral density $\rho_{\mathrm{ph}}(\omega)$ of the form in eq. (17.4.10) with an ω^2 rise at low frequency and an exponential high frequency tail ($s = 2$), assigning a cutoff frequency of $\omega_c = 40\ \mathrm{cm}^{-1}$ and a phonon reorganization energy of $\lambda_{\mathrm{ph}} = 100\ \mathrm{cm}^{-1}$. The total spectral density is then the sum $\rho = \rho_{\mathrm{vib}} + \rho_{\mathrm{ph}}$, which

is illustrated in Figure 17.4.5a.

The temperature dependence of the lineshape function is calculated for $T = 10$, 100, and 300 K from eq. (17.4.8), the corresponding $F(t)$ is determined from $\exp(-g(t))$, and the absorption lineshape $\sigma(\omega)$ is obtained from Fourier transforming the resulting dipole correlation function. These are plotted in Figure 17.4.5b, c and d, respectively. At the lowest temperature, the harmonic bath is not thermally occupied, which can be judged by comparing it with the effective temperature associated with the bath cutoff frequency ($T_{\text{eff}} = \hbar\omega_c/k_B = 58$ K). The real part of $g(t)$ has high frequency oscillations from the vibrations, superimposed over a slower rise to a baseline that grows with temperature, reflecting a growing thermal occupation of the harmonic bath. For $g(t)$, $F(t)$, and $\sigma(\omega)$, the changing thermal occupation of the phonon density of states dominates the changing dynamics. Spectrally, we observe that the sharp vibrational progressions seen at low temperatures become washed out by the bath at high temperatures. The vibronic structure from the dominant 1272 cm^{-1} mode remains, but it is significantly broadened.

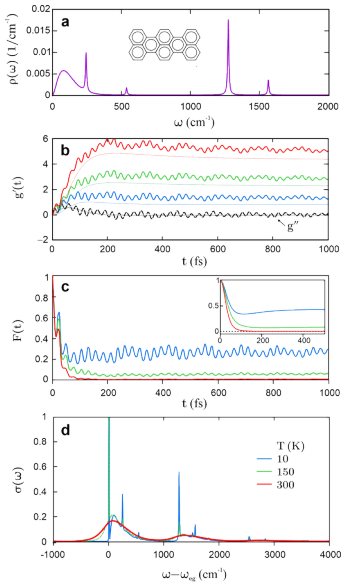


Figure 17.4.5: Example of the temperature-dependent vibronic dynamics and absorption spectrum predicted from the spectral density $\rho(\omega)$ shown in (a). (b) The real part of the lineshape function $g'(t)$ varies with temperature, whereas the imaginary part $g''(t)$ shown in black is constant. The thin smooth lines illustrate the behavior of $g(t)$ when only the phonon spectral density is included in the calculation. Color coding of the temperature for all panels are shown in (d). (c) Dephasing functions corresponding to the same lineshape functions. Calculations with only the phonon spectral density is shown in the inset. (d) Absorption spectra for the three temperatures.

This page titled 17.4: Spectral Density for Condensed Phase Spectroscopy is shared under a CC BY-NC-SA 4.0 license and was authored, remixed, and/or curated by Andrei Tokmakoff via source content that was edited to the style and standards of the LibreTexts platform.

17.5: The Harmonic Bath's Relation to the Langevin Equation

Why does coupling to a harmonic bath result in the same behavior as the classical stochastic equations for fluctuations? Why does coupling to a continuum of bath states derived from deterministic equations of motion have the same physical manifestation as interactions with a system whose perturbations are only predictable in a statistical sense? The answer lies in the lack of knowledge of the state of all of the particles present. When we stepped from describing the influence of nuclear motions on a quantum observable by summing over discrete modes to integrating over a continuum of indistinguishable modes and coupling constants, we washed away information on specific coordinates. In such systems, observing a subset of particles within an unpredictable bath, motions will appear to have stochastic character even if the underlying dynamics of each particle are deterministic—much like trying to predict weather.

In this section we will look more carefully at the equivalence of these pictures. The first step is to describe the classical approach to a fluctuating environment using the Langevin equation. The second is to show how behavior is recovered for a quantum harmonic bath in the framework of the Brownian oscillator Hamiltonian.

Langevin Equation

Let's go back to describing the electronic absorption spectrum from a classical perspective. It's quite common to think that the electronic transition of interest is coupled to a particular nuclear coordinate Q, which we will call a *local coordinate*. This local coordinate could be an intramolecular vibrational mode, the rattling of the molecule within a solvent shell, a lattice vibration, or other dynamic molecular interactions that influence the electronic transition frequency. If the electronic transition is dependent on one or more of these local coordinates, describing Q allows us to describe the spectroscopy. However, in condensed matter this local mode inevitably has further degrees of freedom that it may be interacting with that are more distant or collective in nature. The local mode is one of a continuum of other motions, and therefore Q experiences a fluctuating environment.

The classical description of the stochastic fluctuations experienced by Q is commonly formulated with a Langevin equation. In essence, this takes the driven oscillator problem we have used before and adds a fluctuating force acting on a particle. In the case of a particle that is confined in a harmonic potential, the equation is

$$m\ddot{Q}(t) + m\omega_0^2 Q^2 + m\gamma\dot{Q} = f_R(t) \tag{17.5.1}$$

As before, the left-hand side represents the acceleration, local restoring force, and damping force on the harmonic oscillator. The local mode is influenced by $f_R(t)$, a random fluctuating force exerted by the surroundings on Q. Under steady-state conditions, it stands to reason that the random force acting on Q is the origin of the damping. The environment acts on Q with stochastic perturbations that add and remove kinetic energy, and this ultimately leads to dissipation of any excess energy. Therefore, the Langevin equation is modelled as a Gaussian stationary process. We take $f_R(t)$ to have a time-averaged value of zero,

$$\langle f_R(t) \rangle = 0 \tag{17.5.2}$$

and obey the classical fluctuation-dissipation theorem, which relates the damping constant to the correlation function for the fluctuating forces.

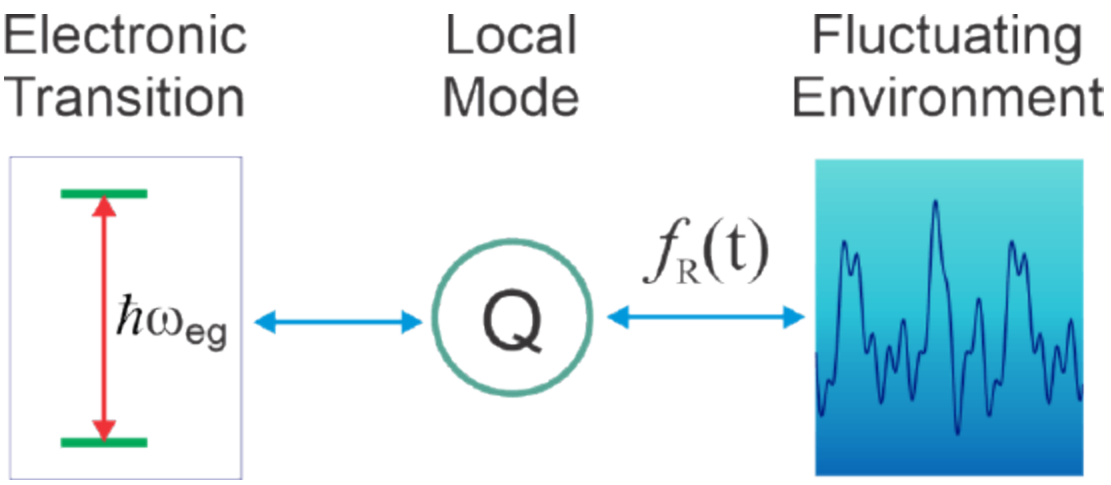


Figure 17.5.1: Diagram illustrating the semiclassical approach to describing the electronic spectroscopy of an electronic energy gap modulated by a stochastic oscillator.

$$\gamma = \frac{1}{2mk_BT}\int_{-\infty}^{\infty}\langle f_R(t) f_R(0)\rangle \tag{17.5.3}$$

Thus γ describes the friction that the fluctuations exert on the motions of Q. We will pay particular attention to the Markovian case

$$\langle f_R(t) f_R(0)\rangle = 2m\gamma k_BT\delta(t) \tag{17.5.4}$$

which indicates that the fluctuations immediately lose all correlation on the time scale of the evolution of Q.

The Langevin equation can be used to describe the correlation function for the time dependence of Q. For the Markovian case, eq. (17.5.1) leads to

$$C_{QQ}(t) = \frac{k_BT}{m\omega_0^2}\left(\cos\zeta t + \frac{\gamma}{2\zeta}\sin\zeta t\right)e^{-\gamma t/2} \tag{17.5.5}$$

where the reduced frequency $\zeta = \sqrt{\omega_0^2 - \gamma^2/4}$. The frequency domain expression, obtained by Fourier transformation, is

$$\tilde{C}_{QQ}(\omega) = \frac{\gamma k_BT}{m\pi}\frac{1}{\left(\omega_0^2 - \omega^2\right)^2 + \omega^2\gamma^2} \tag{17.5.6}$$

Remembering that the absorption lineshape was ultimately determined by the quantum mechanical dynamics of the coupled harmonic vibrations, one can imagine an analogous classical description of the spectroscopy of a molecule that experiences interactions with a fluctuating environment. In essence, this is what we did when discussing the Gaussian stochastic model of the lineshape.

A more general description of the position of a particle subject to a fluctuating force is the Generalized Langevin Equation. The GLE accounts for the possibility that the damping may be time-dependent and carry memory of earlier configurations of the system:(1)

$$m\ddot{Q}(t) + m\omega_0^2Q^2 + m\int_0^t d\tau\,\gamma(t-\tau)\,\dot{Q}(\tau) = f_R(t) \tag{17.5.7}$$

The memory kernel, $\gamma(t-\tau)$, is the correlation function in eq. (17.5.3). The force due to friction on Q depends on the history of the system through τ, the time preceding t, and the relaxation of $\gamma(t-\tau)$. The classical fluctuation-dissipation relationship relates the magnitude of the fluctuating forces on the system coordinate to the damping

$$\langle f_R(t) f_R(\tau)\rangle = 2mk_BT\gamma(t-\tau) \tag{17.5.8}$$

As expected, for the case that $\gamma(t-\tau) = \gamma\delta(t-\tau)$, the GLE reduces to the Markovian case, eq. (17.5.4).

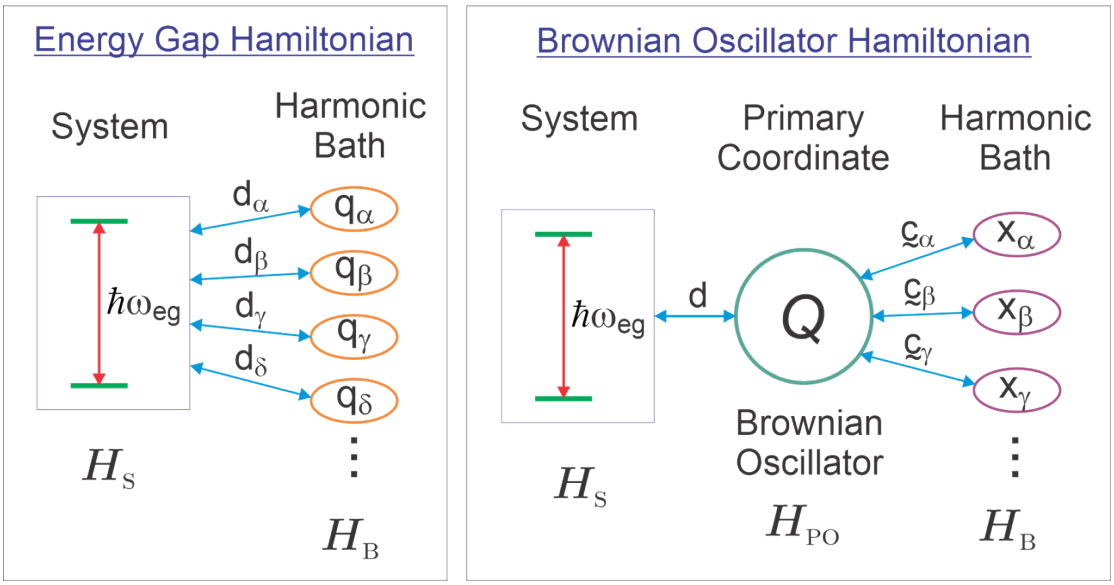


Figure 17.5.2: Schematic of the differences of bath interactions in the Energy Gap Hamiltonian and the Brownian Oscillator Hamiltonian.

To demonstrate that the classical dynamics of the particle described under the GLE are related to the quantum mechanical dynamics for a particle interacting with a harmonic bath, we will outline the derivation of a quantum mechanical analog of the classical GLE. The first key conceptual step, illustrated in Figure 17.5.2, is to recognize that the description of the absorption lineshape from the Energy Gap Hamiltonian is equivalent to the one that is derived from an electronic transition that is modulated through its interaction with one local mode, which in turn interacts with a harmonic bath. The bath for the EGH was a sum or integral over a continuum of independent harmonic (normal) modes, here written in reduced coordinates:

$$H_B = \sum_{\alpha=1}^{N} \hbar\omega_\alpha \left(\underset{\sim}{p}_\alpha^2 + \underset{\sim}{q}_\alpha^2\right) \tag{17.5.9}$$

However, with a harmonic Hamiltonian one can transform to a set of N coupled harmonic coordinates in any way we choose with the appropriate transformation. Specifically, we want to transform from a set of N delocalized normal modes to a frame of reference that includes one local mode Q and $(N-1)$ other linearly coupled normal modes, x_i. This essentially is a process of extracting Q out of the bath continuum. This transformation is expressed through the matrix S, which diagonalizes the local mode Hamiltonian as $\boldsymbol{q} = \boldsymbol{S}^{-1}\boldsymbol{x}$. With this transformation from q_α to Q and x_i, we can write the bath Hamiltonian in eq. (17.5.9) as the interaction of our local mode Q with the transformed harmonic bath through linear coupling coefficients C_i that depend on the normal mode transformation.

$$H_B = \hbar\Omega_0 \left(\underset{\sim}{P}^2 + \underset{\sim}{Q}^2\right) + \sum_{i=1}^{N-1} \hbar\omega_i \left(\underset{\sim}{p}_i^2 + \underset{\sim}{x}_i^2\right) - \underset{\sim}{Q}\sum_i C_i \underset{\sim}{x}_i \tag{17.5.10}$$

To do this we need to derive an expression for the time-evolution of the system under the influence of the harmonic bath.

This conceptual picture underlies the quantum mechanical analog to the classical GLE. Now, let's construct such a Hamiltonian from the beginning, writing it as one primary harmonic mode interacting through a linear coupling to a harmonic bath.

$$H_{BO} = H_{PO}(P,Q) + H_B(p_\alpha, q_\alpha) + V(Q, q_\alpha) \tag{17.5.11}$$

The Hamiltonian for the primary oscillator is

$$H_{PO} = \hbar\Omega_0 \left(\underset{\sim}{P}^2 + \underset{\sim}{Q}^2\right) \tag{17.5.12}$$

It describes a mode with reduced mass M and frequency Ω_0, whereas m_α, ω_α, p_α and q_α are bath variables. The Hamiltonian for the bath and its interaction with the primary oscillator can be written as a sum of contributions from many independent displaced harmonic oscillators(2)

$$H_B + V = \sum_\alpha \hbar\omega_\alpha \left(\underset{\sim}{p}_\alpha^2 + \left(\underset{\sim}{q}_\alpha - \underset{\sim}{c}_\alpha \underset{\sim}{Q}\right)^2\right) \tag{17.5.13}$$

where the coordinates and momenta are written in reduced form

$$\begin{aligned} \underset{\sim}{q}_\alpha &= q_\alpha \sqrt{\frac{m_\alpha \omega_\alpha}{2\hbar}} \\ \underset{\sim}{p}_\alpha &= \frac{p_\alpha}{\sqrt{2\hbar m_\alpha \omega_\alpha}} \end{aligned} \tag{17.5.14}$$

Also, the reduced coupling of the α^{th} bath oscillator to the primary oscillator is

$$\underset{\sim}{c}_\alpha = \frac{c_\alpha}{\omega_\alpha \sqrt{m_\alpha \omega_\alpha M \Omega_0}} \tag{17.5.15}$$

We will refer to this as the Brownian oscillator Hamiltonian, although it is also known as the spin-boson model or Caldeira-Leggett model.(3) Equation (17.5.13) shows that each of the bath oscillators is displaced with respect to the primary oscillator by an amount dependent on their mutual coupling. Expanding eq. (17.5.13) and collecting terms, we find that we can separate terms as in the harmonic bath model

$$H_B = \sum_\alpha \hbar \omega_\alpha \left(\underset{\sim}{p}_\alpha^2 + \underset{\sim}{q}_\alpha^2 \right) \tag{17.5.16}$$

$$V = -2 \sum_\alpha \hbar \omega_\alpha \underset{\sim}{d}_\alpha \underset{\sim}{q}_\alpha + \lambda_B \tag{17.5.17}$$

The reorganization energy due to the bath oscillators is

$$\lambda_B = \sum_\alpha \hbar \omega_\alpha \underset{\sim}{d}_\alpha^2 \tag{17.5.18}$$

and the unitless bath oscillator displacement is

$$\underset{\sim}{d}_\alpha = \underset{\sim}{Q} \underset{\sim}{c}_\alpha \tag{17.5.19}$$

Finally, to show that it looks like eq. (17.5.10), we can regroup the total Hamiltonian as

$$H_{BO} = \hbar \bar{\Omega}_0 \left(\underset{\sim}{P}^2 + \underset{\sim}{Q}^2 \right) + \sum_\alpha \hbar \omega_\alpha \left(\underset{\sim}{p}_\alpha^2 + \underset{\sim}{q}_\alpha^2 \right) - 2 \underset{\sim}{Q} \sum_\alpha \hbar \omega_\alpha \underset{\sim}{c}_\alpha \underset{\sim}{q}_\alpha \tag{17.5.20}$$

where the renormalized frequency of the primary oscillator is

$$\bar{\Omega}_0^2 = \Omega_0^2 + \Omega_0 \sum_\alpha \omega_\alpha \underset{\sim}{c}_\alpha^2 \tag{17.5.21}$$

To demonstrate the equivalence of the dynamics under the Brownian oscillator Hamiltonian and the GLE, one can derive an equation of motion for the primary oscillator coupled to the harmonic bath, using the Heisenberg equation of motion to describe the time-dependence of the raising and lowering operators for the system and bath. The resulting equation of motion for the primary oscillator can be written in a form that is isomorphic to the classical GLE,

$$\dot{P}(t) + M\Omega^2 Q(t) + M \int_0^t dt' \gamma(t - t') \dot{Q}(t') = f_R(t) \tag{17.5.22}$$

To make this connection we have defined the memory kernel and force from the bath acting on the primary oscillator as

$$\begin{aligned} \gamma(t) &= 2\bar{\Omega} \textstyle\sum_\alpha \omega_\alpha \underset{\sim}{c}_\alpha^2 \cos(\omega_\alpha t) \\ &= \frac{1}{M} \textstyle\sum_\alpha \frac{c_\alpha^2}{m_\alpha \omega_\alpha^2} \cos \omega_\alpha t \end{aligned} \tag{17.5.23}$$

$$f_R(t) = \sum_\alpha c_\alpha \left[q_\alpha(0) \cos \omega_\alpha t + \frac{p_\alpha(0)}{m_\alpha \omega_\alpha} \sin \omega_\alpha t \right] \tag{17.5.24}$$

Although these relationships are written as a sum, these expressions generalize readily to a spectral density for coupling of the primary oscillator and the bath:

$$\gamma(\omega) = \frac{\pi}{2} \sum_{\alpha} \frac{c_{\alpha}^2}{m_{\alpha}\omega_{\alpha}^2} \delta(\omega - \omega_{\alpha}) \tag{17.5.25}$$

This demonstrates that the quantum harmonic bath acts a dissipative environment, with the friction on the system coordinate given by eq. (17.5.23). What we have shown here is an outline of the reasoning, but detailed discussion of these relationships can be found elsewhere.(4)(5)(6) The picture that emerges from this description it that the many modes of a harmonic bath together exert forces that cause the primary oscillator to behave in a stochastic manner, which is ultimately reflected in the absorption lineshape.

References

(1) Nitzan, A. *Chemical dynamics in condensed phases: Relaxation, transfer and reactions in condensed molecular systems*; Oxford University Press, 2006. DOI: 10.1093/oso/9780198529798.001.0001

(2) Mukamel, S. *Principles of Nonlinear Optical Spectroscopy*; Oxford University Press, 1995.

(3) Caldeira, A. O.; Leggett, A. J. Quantum tunnelling in a dissipative system. *Annals of Physics* **1983**, *149* (2), 374-456. DOI: 10.1016/0003-4916(83)90202-6

(4) Weiss, U. *Quantum Dissipative Systems*, 3rd ed.; World Scientific, 2008.

(5) Leggett, A. J.; Chakravarty, S.; Dorsey, A. T.; Fisher, M. P. A.; Garg, A.; Zwerger, W. Dynamics of the dissipative two-state system. *Reviews of Modern Physics* **1987**, *59* (1), 1-85. DOI: 10.1103/RevModPhys.59.1

(6) Yan, Y.; Xu, R. Quantum mechanics of dissipative systems. *Annual Review of Physical Chemistry* **2005**, *56*, 187-219. DOI: 10.1146/annurev.physchem.55.091602.094425

This page titled 17.5: The Harmonic Bath's Relation to the Langevin Equation is shared under a CC BY-NC-SA 4.0 license and was authored, remixed, and/or curated by Andrei Tokmakoff via source content that was edited to the style and standards of the LibreTexts platform.

17.6: Readings

General Readings

1. Fleming, G. R.; Cho, M. Chromophore-Solvent Dynamics. *Annual Review of Physical Chemistry* **1996**, *47*, 109-134. DOI: 10.1146/annurev.physchem.47.1.109
2. McHale, J. L. *Molecular Spectroscopy*, 1 st ed.; Prentice-Hall, 1999.
3. Mukamel, S. *Principles of Nonlinear Optical Spectroscopy*; Oxford University Press, 1995.
4. Nitzan, A. *Chemical dynamics in condensed phases: Relaxation, transfer and reactions in condensed molecular systems*; Oxford University Press, 2006. DOI: 10.1093/oso/9780198529798.001.0001
5. Weiss, U. *Quantum Dissipative Systems*, 3rd ed.; World Scientific, 2008.

Gaussian-Stochastic Model for Spectral Diffusion

1. Kubo, R. A Stochastic Theory of Line-Shape and Relaxation. *Fluctuation, Relaxation and Resonance in Magnetic Systems*; Ter Haar, D., Ed.; Oliver and Boyd, 1962; pp 23-68.
2. Kubo, R.; Tomita, K. A General Theory of Magnetic Resonance Absorption. *Journal of the Physical Society of Japan* **1954**, *9* (6), 888-919. DOI: 10.1143/JPSJ.9.888
3. McHale, J. L. *Molecular Spectroscopy*, 1st ed.; Prentice-Hall, 1999.
4. Mukamel, S. *Principles of Nonlinear Optical Spectroscopy*; Oxford University Press, 1995.
5. Schatz, G. C.; Ratner, M. A. *Quantum Mechanics in Chemistry*; Dover Publications, 2002; sec 7.4 and sec 7.5.
6. Andrews, D. L. A unified theory of radiative and radiationless molecular energy transfer. *Chemical Physics* **1989**, *135* (2), 195-201. DOI: 10.1016/0301-0104(89)87019-3
7. Anderson, P. W. A Mathematical Model for the Narrowing of Spectral Lines by Exchange or Motion. *Journal of the Physical Society of Japan* **1954**, *9* (3), 316-339. DOI: 10.1143/jpsj.9.316
8. Wang, C. H. *Spectroscopy of Condensed Media: Dynamics of Molecular Interactions*; Academic Press, 1985. DOI: 10.1016/B978-0-12-734780-6.X5001-8

Spectral Density for Condensed Phase Spectroscopy

1. Mukamel, S. *Principles of Nonlinear Optical Spectroscopy*; Oxford University Press, 1995; ch 7 and ch 8.

This page titled 17.6: Readings is shared under a CC BY-NC-SA 4.0 license and was authored, remixed, and/or curated by Andrei Tokmakoff via source content that was edited to the style and standards of the LibreTexts platform.

18: QUANTUM RELAXATION PROCESSES

18.1: Vibrational Relaxation
18.2: Golden Rule Vibrational Relaxation Rates
18.3: Multiquantum relaxation of polyatomic molecules
18.4: Redfield Theory and Master Equation
18.5: Readings

This page titled 18: Quantum Relaxation Processes is shared under a CC BY-NC-SA 4.0 license and was authored, remixed, and/or curated by Andrei Tokmakoff via source content that was edited to the style and standards of the LibreTexts platform.

18.1: Vibrational Relaxation

Here we want to address how excess energy deposited into a molecular vibration undergoes irreversible energy relaxation as a result of interactions with other intra- and intermolecular degrees of freedom. Why is this process important? It is the fundamental process by which nonequilibrium states thermalize. As chemists, this plays a particularly important role in chemical reactions, where efficient vibrational relaxation of an activated species is important to stabilizing the product (P) and not allowing it to re-cross to the reactant well (R), as illustrated in Figure 18.1.1.

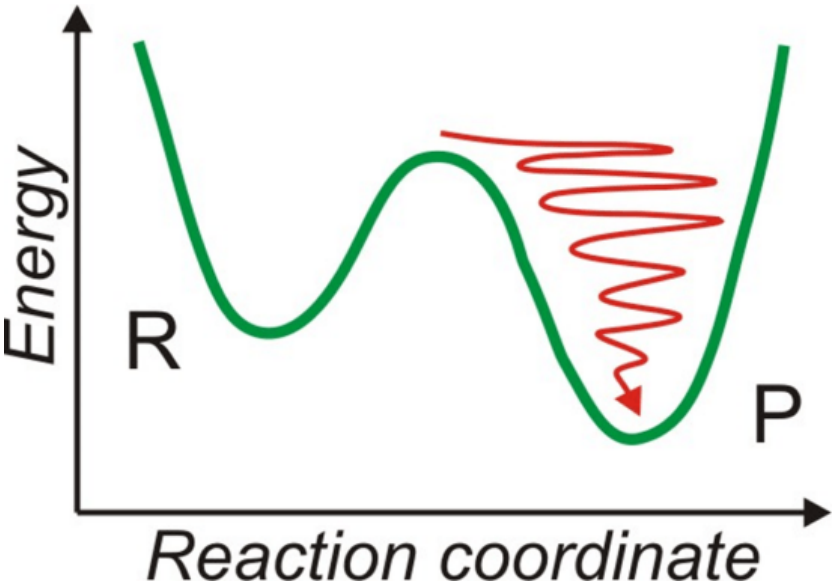


Figure 18.1.1: Illustration of vibrational energy dissipation during an activated chemical transformation from reactants (R) to products (P).

Further, the rare activation event for chemical reactions is similar to the reverse of this process. Although the specific processes we are describing are vibrational couplings and relaxation, the mathematical formalism for describing electronic population relaxation both through electron–phonon coupling and through spin–lattice relaxation is very similar to this presentation. Although the specific processes we are describing are vibrational couplings and relaxation, the mathematical formalism for describing electronic population relaxation both through electron–phonon coupling and through spin–lattice relaxation is very similar to this presentation.

For an isolated molecule with few vibrational coordinates, an excited vibrational state must relax by interacting with the remaining internal vibrations or the rotational and translational degrees of freedom. If a lot of energy must be dissipated in a single step, radiative relaxation may be more likely. In the condensed phase, relaxation is usually mediated by the interactions with the environment—for instance, the solvent or lattice. The solvent or lattice forms a continuum of intermolecular motions that can absorb the energy of the vibrational relaxation. Quantum mechanically, this means that vibrational relaxation (the annihilation of a vibrational quantum) leads to excitation of solvent or lattice motion (creation of an intermolecular vibration that increases the occupation of higher lying states).

For polyatomic molecules, it is common to think of energy relaxation from high lying vibrational states $(k_B T \ll \hbar\omega_0)$ in terms of cascaded redistribution of energy through coupled modes of the molecule and its surroundings leading finally to thermal equilibrium, as shown in Figure 18.1.2. We seek ways of describing these highly non-equilibrium relaxation processes in quantum systems.

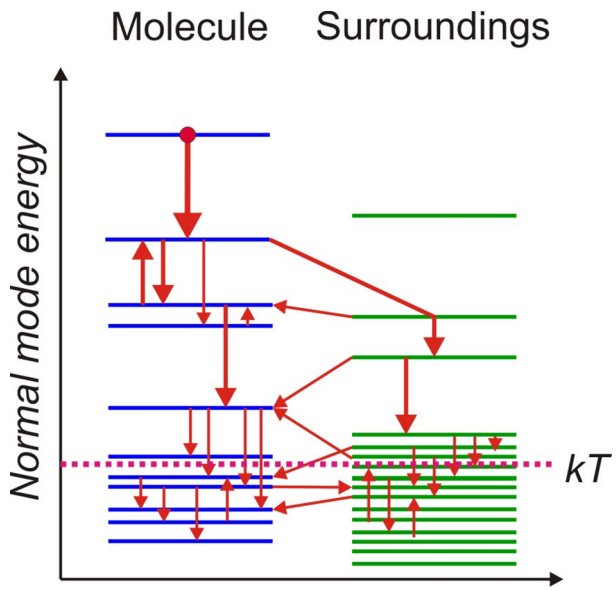


Figure 18.1.2: Illustration of cascaded energy flow that follows the dissipation of energy initially deposited in a single high frequency molecular vibration.

Classically, vibrational relaxation reflects the surroundings exerting a friction on the vibrational coordinate, which damps its amplitude and heats the sample. We have seen that a Langevin equation for an oscillator experiencing a fluctuating force $f(t)$ describes such a process:

$$\ddot{Q}(t) + \omega_0^2 Q^2 - \gamma \dot{Q} = \frac{f(t)}{m} \tag{18.1.1}$$

This equation assigns a phenomenological damping rate γ to the vibrational relaxation we wish to describe. However, we know in the long-time limit, the system must thermalize and the dissipation of energy is related to the fluctuations of the environment through the classical fluctuation-dissipation relationship. Specifically,

$$\langle f(t) f(0) \rangle = 2m\gamma k_B T \delta(t) \tag{18.1.2}$$

More generally, classical descriptions relate the vibrational relaxation rates to the correlation function for the fluctuating forces acting on the excited coordinate.

In these classical pictures, efficient relaxation requires a matching of frequencies between the vibrational period of the excited oscillator and the spectrum of fluctuation of the environment. Since these fluctuations are dominated by motions that are of the energy scale of $k_B T$, such models do not work effectively for high frequency vibrations, whose with frequency $\omega \gg k_B T/\hbar$. We would like to develop a quantum model that allows for these processes and to understand the correspondence between these classical pictures and quantum relaxation.

This page titled 18.1: Vibrational Relaxation is shared under a CC BY-NC-SA 4.0 license and was authored, remixed, and/or curated by Andrei Tokmakoff via source content that was edited to the style and standards of the LibreTexts platform.

18.2: Golden Rule Vibrational Relaxation Rates

Let's treat the problem of a vibrational system H_S that relaxes through weak coupling V with a continuum of bath states H_B using perturbation theory. The eigenstates of H_S are $|a\rangle$ and those of H_B are $|\alpha\rangle$. Although our earlier perturbative treatment did not satisfy energy conservation, here we can take care of it by explicitly treating the bath states.

$$H = H_0 + V \tag{18.2.1}$$

$$H_0 = H_S + H_B \tag{18.2.2}$$

$$H_S = |a\rangle E_a \langle a| + |b\rangle E_b \langle b| \tag{18.2.3}$$

$$H_B = \sum_\alpha |\alpha\rangle E_\alpha \langle \alpha| \tag{18.2.4}$$

$$H_0 |a\alpha\rangle = (E_a + E_\alpha)\,|a\alpha\rangle \tag{18.2.5}$$

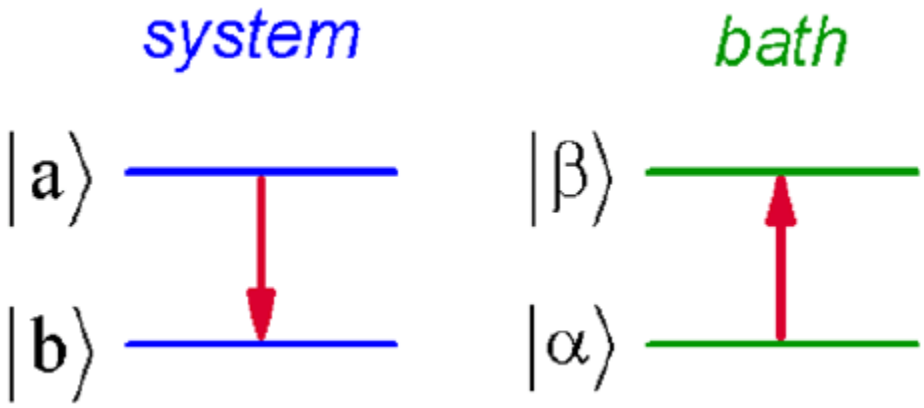


Figure 18.2.1: Illustration of the net energy conservation in the system and bath during vibrational relaxation of the system.

We will describe transitions from an initial state $|i\rangle = |a\alpha\rangle$ with energy $E_a + E_\alpha$ to a final state $|f\rangle = |b\beta\rangle$ with energy $E_b + E_\beta$. Since we expect energy conservation to hold, this undoubtedly requires that a change in the system states will require an equal and opposite change of energy in the bath. Initially, we take $p_a = 1$ and $p_b = 0$. If the interaction potential is V, Fermi's Golden Rule says the transition from $|i\rangle$ to $|f\rangle$ is given by

$$\begin{aligned} k_{fi} &= \frac{2\pi}{\hbar} \sum_{i,f} p_i \left|\langle i|V|f\rangle\right|^2 \delta\left(E_f - E_i\right) \\ &= \frac{2\pi}{\hbar} \sum_{a,\alpha,b,\beta} p_{a,\alpha} \left|\langle a\alpha|V|b\beta\rangle\right|^2 \delta\left((E_b + E_\beta) - (E_a + E_\alpha)\right) \\ &= \frac{1}{\hbar^2} \int_{-\infty}^{+\infty} dt \sum_{a,\alpha,b,\beta} p_{a,\alpha} \langle a\alpha|V|b\beta\rangle\langle b\beta|V|a\alpha\rangle \exp\left[-\mathrm{i}\left((E_b - E_a) + (E_\beta - E_\alpha)\right) t/\hbar\right] \end{aligned} \tag{18.2.6}$$

Equation (18.2.8) is just a restatement of the time domain version of (18.2.6).

$$k_{fi} = \frac{1}{\hbar^2} \int_{-\infty}^{+\infty} dt\, \langle V(t) V(0)\rangle \tag{18.2.7}$$

$$V(t) = e^{\mathrm{i}H_0 t} V e^{-\mathrm{i}H_0 t} \tag{18.2.8}$$

Now, the matrix element involves both evaluation in both the system and bath states, but if we write this in terms of a matrix element in the system coordinate $V_{ab} = \langle a|V|b\rangle$:

$$\langle a\alpha|V|b\beta\rangle = \langle \alpha\,|V_{ab}|\,\beta\rangle \tag{18.2.9}$$

Then we can write the rate as

$$
\begin{aligned}
k_{ba} &= \frac{1}{\hbar^2}\int_{-\infty}^{+\infty} dt \sum_{\alpha,\beta} p_\alpha \left\langle \alpha \left| e^{+\mathrm{i}E_\alpha t} V_{ab} e^{-\mathrm{i}E_\beta t} \right| \beta \right\rangle \left\langle \beta \left| V_{ba} \right| \alpha \right\rangle e^{-\mathrm{i}\omega_{ba}t} \\
&= \frac{1}{\hbar^2}\int_{-\infty}^{+\infty} dt \left\langle V_{ab}(t) V_{ba}(0) \right\rangle_B e^{-\mathrm{i}\omega_{aa}t}
\end{aligned} \tag{18.2.10}
$$

$$
V_{ab}(t) = e^{\mathrm{i}H_B t}\, V_{ab} e^{-\mathrm{i}H_B t} \tag{18.2.11}
$$

Equation (18.2.12) says that the relaxation rate is determined by a correlation function

$$
C_{ba}(t) = \langle V_{ab}(t) V_{ba}(0) \rangle \tag{18.2.12}
$$

which describes the time-dependent changes to the coupling between b and a. The time dependence of the interaction arises from the interaction with the bath; hence its time evolution under H_B. The subscript $\langle \cdots \rangle_B$ means an equilibrium thermal average over the bath states

$$
\langle \cdots \rangle_B = \sum_\alpha p_\alpha \langle \alpha | \cdots | \alpha \rangle \tag{18.2.13}
$$

Note also that eq. (18.2.12) is similar but not quite a Fourier transform. This expression says that the relaxation rate is given by the Fourier transform of the correlation function for the fluctuating coupling evaluated at the energy gap between the initial and final states. Alternatively, we could think of the rate in terms of a vibrational coupling spectral density, and the rate is given by its magnitude at the system energy gap ω_{ba}.

$$
k_{ba} = \frac{1}{\hbar^2} \tilde{C}_{ba}\left(\omega_{ab}\right) \tag{18.2.14}
$$

where the spectral representation $\tilde{C}_{ba}(\omega_{ab})$ is defined as the Fourier transform of $C_{ba}(t)$.

Vibration coupled to a harmonic bath

To evaluate these expressions, let's begin by considering the specific case of a system vibration coupled to a harmonic bath, which we will describe using a spectral density. Imagine that we prepare the system in an excited vibrational state, $|1\rangle$, and we want to describe relaxation to the ground state $|0\rangle$.(1)

$$
H_S = \hbar\omega_0 \left(\underset{\sim}{P}^2 + \underset{\sim}{Q}^2 \right) \tag{18.2.15}
$$

$$
H_B = \sum_\alpha \hbar\omega_\alpha \left(\underset{\sim}{p}_\alpha^2 + \underset{\sim}{q}_\alpha^2 \right) = \sum_\alpha \hbar\omega_\alpha \left(a_\alpha^\dagger a_\alpha + \frac{1}{2} \right) \tag{18.2.16}
$$

We will take the system-bath interaction to be linear in the bath coordinates:

$$
V = H_{SB} = \sum_\alpha c_\alpha \underset{\sim}{Q} \underset{\sim}{\alpha}_\alpha \tag{18.2.17}
$$

Here c_α is a coupling constant which describes the strength of the interaction between the system and bath mode α. Note that this form suggests that the system vibration is a local mode interacting with a set of normal vibrations of the bath.

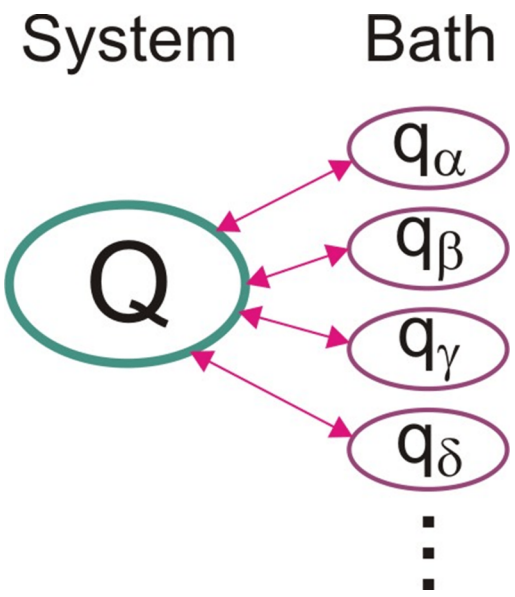


Figure 18.2.2: Illustration of the system coordinate Q coupled bilinearly to a bath of harmonic modes, q_i.

For the case of single quantum relaxation from $|a\rangle = |1\rangle$ to $b = |0\rangle$, we can write the coupling matrix element as

$$V_{ba} = \langle b|V|a\rangle = \sum_{\alpha} \xi_{\alpha} \left(a_{\alpha}^{\dagger} + a_{\alpha}\right) \tag{18.2.18}$$

where ξ is a generalized coupling constant that depends explicitly on the the matrix element $\langle b|Q|a\rangle$:

$$\xi_{\alpha} = c_{\alpha} \frac{\sqrt{m_{Q} m_{q} \omega_{0} \omega_{\alpha}}}{2\hbar} \langle b|Q|a\rangle \tag{18.2.19}$$

Evaluating eq. (18.2.14) is now much the same as problems we've had previously:

$$\begin{aligned} \langle V_{ab}(t) V_{ba}(0)\rangle_{B} &= \left\langle e^{\mathrm{i}H_{B}t}\ V_{ab}\ e^{-\mathrm{i}H_{B}t}\ V_{ba}\right\rangle_{B} \\ &= \sum_{\alpha} \xi_{\alpha}^{2} \left[(\bar{n}_{\alpha}+1)\, e^{-\mathrm{i}\omega_{\alpha}t} + \bar{n}_{\alpha} e^{+\mathrm{i}\omega_{\alpha}t}\right] \end{aligned} \tag{18.2.20}$$

here $\bar{n}_{\alpha} = \left(e^{\beta\hbar\omega_{\alpha}} - 1\right)^{-1}$ is the thermally averaged occupation number of the bath mode at ω_{α} In evaluating this we take advantage of relationships we have used before

$$\begin{aligned} e^{iH_{B}t} a_{\alpha} e^{-\mathrm{i}H_{B}t} &= a_{\alpha} e^{-\mathrm{i}\omega_{\alpha}t} \\ e^{\mathrm{i}H_{B}t} a_{\alpha}^{\dagger} e^{-\mathrm{i}H_{B}t} &= a_{\alpha}^{\dagger} e^{+i\omega_{\alpha}t} \end{aligned} \tag{18.2.21}$$

$$\begin{aligned} \left\langle a_{\alpha} a_{\alpha}^{\dagger}\right\rangle &= \bar{n}_{\alpha} + 1 \\ \left\langle a_{\alpha}^{\dagger} a_{\alpha}\right\rangle &= \bar{n}_{\alpha} \end{aligned} \tag{18.2.22}$$

So, now by Fourier transforming (18.2.22) we have the rate as

$$k_{ba} = \frac{1}{\hbar^{2}} \sum_{\alpha} \xi_{\alpha}^{2} \left[\underbrace{(\bar{n}_{\alpha}+1)\, \delta\left(\omega_{ba} + \omega_{\alpha}\right)}_{\text{downward}} + \underbrace{\bar{n}_{\alpha} \delta\left(\omega_{ba} - \omega_{\alpha}\right)}_{\text{upward}} \right] \tag{18.2.23}$$

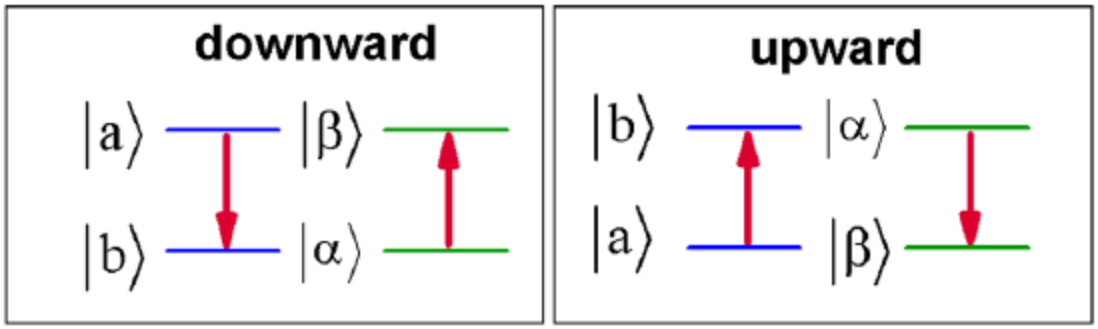


Figure 18.2.3: Diagram of the net rate of energy relaxation as a sum of contributions from the upward and downward transition rates.

This expression describes two relaxation processes which depend on temperature. The first "downward" process obeys $-\omega_{ba} = \omega_a$ and becomes the dominant term as $T \to 0$ K. This implies that $E_a > E_b$ and that a loss of energy in the system is balanced by an equal rise in energy of the bath. That is $|\beta\rangle = |\alpha + 1\rangle$. The second "upward" term is only allowed for elevated temperatures in which thermal energy remains in the bath states. It describes relaxation of the system by transfer to a higher energy state $E_b > E_a$, with a concerted decrease of the energy of the bath ($|\beta\rangle = |\alpha - 1\rangle$). Naturally, this process vanishes if there is no thermal energy in the bath.(2)

To more accurately model the relaxation due to a continuum of modes, we can replace the explicit sum over bath states with an integral over a density of bath states W

$$k_{ba} = \frac{1}{\hbar^2} \int d\omega_\alpha \, W(\omega_\alpha) \; \xi_\alpha^2(\omega_\alpha) \left[(\bar{n}(\omega_\alpha) + 1) \, \delta(\omega_{ba} + \omega_\alpha) \; + \; \bar{n}(\omega_\alpha) \; \delta(\omega_{ba} - \omega_\alpha) \right] \tag{18.2.24}$$

We can also define a spectral density, which is the vibrational coupling-weighted density of states:

$$\rho_{ba}(\omega_\alpha) \equiv W(\omega_\alpha) \, \xi_\alpha^2(\omega_\alpha) \tag{18.2.25}$$

Then the relaxation rate is:

$$\begin{aligned} k_{ba} &= \frac{1}{\hbar^2} \int d\omega_\alpha \, W(\omega_\alpha) \xi_\alpha^2(\omega_\alpha) \left[(\bar{n}(\omega_\alpha) + 1) \delta \left(\omega_{ba} + \omega_\alpha \right) + \bar{n}(\omega_\alpha) \; \delta \left(\omega_{ba} - \omega_\alpha \right) \right] \\ &= \frac{1}{\hbar^2} \left[(\bar{n}(\omega_{ba}) + 1) \, \rho_{ba}(\omega_{ab}) + \bar{n}(\omega_{ba}) \; \rho_{ba}(-\omega_{ab}) \right] \end{aligned} \tag{18.2.26}$$

We see that the Fourier transform of the fluctuating coupling correlation function in eq. (18.2.22) is equivalent to the coupling-weighted density of states, ρ_{ba}, which we evaluate at ω_{ba} or $-\omega_{ba}$ depending on whether we are looking at upward or downward transitions. Note that $\bar{n}$ still refers to the occupation number for the bath, although it is evaluated at the energy splitting between the initial and final system states, $\bar{n}(\omega_{ba})$. Equation (18.2.27) is a full quantum expression, and obeys detailed balance between the upward and downward rates of transition between two states:

$$k_{ba} = \exp\left(-\beta \hbar \omega_{ab}\right) k_{ab} \tag{18.2.27}$$

From our description of the two level system in a harmonic bath, we see that high frequency relaxation ($k_B T \ll \hbar\omega_0$) only proceeds with energy from the system going into a mode of the bath at the same frequency, but at lower frequencies ($k_B T \approx \hbar\omega_0$) that energy can flow both from the system into the bath and also from the bath back into the system. When the vibration has energies that are thermally populated in the bath, we return to the classical picture of a vibration in a fluctuating environment, in which the environment can both increase and dissipate the energy of the vibration.

Note that, in a cascaded relaxation scheme like that shown in figure (18.1.1), as the excess energy of the system approaches $k_B T$, the fraction of transitions that raise the system energy increases. Also note, the bi-linear coupling in eq. (18.2.19)—used again in our treatment of quantum fluctuations—can be associated with both changes in the bath's energy (relaxation) and shifts in its frequency (dephasing).

References

(1) Note that we are using an equilibrium property, the coupling correlation function, to describe a nonequilibrium process, the relaxation of an excited state. Underlying the validity of the expressions are the principles of linear response. In practice this also implies a time scale separation between the equilibration of the bath and the relaxation of the system state. The bath correlation function should work fine if it has rapidly equilibrated, even though the system may not have. An instance where this would work well is electronic spectroscopy, where relaxation and thermalization in the excited state occurs on picosecond time scales, whereas the electronic population relaxation is on nanosecond time scales.

(2) There is an exact analogy between this problem and the interaction of matter with a quantum radiation field. The interaction potential is instead a quantum vector potential and the bath is the photon field of different electromagnetic modes. Equation (18.2.25) describes has two terms that describe emission and absorption processes. The leading term describes the possibility of spontaneous emission, where a material system can relax in the absence of light by emitting a photon at the same frequency.

This page titled 18.2: Golden Rule Vibrational Relaxation Rates is shared under a CC BY-NC-SA 4.0 license and was authored, remixed, and/or curated by Andrei Tokmakoff via source content that was edited to the style and standards of the LibreTexts platform.

18.3: Multiquantum relaxation of polyatomic molecules

(1)Vibrational relaxation of polyatomic molecules in solids or in solution involves anharmonic coupling of energy between internal vibrations of the molecule, also called IVR (internal vibrational energy redistribution). Mechanical interactions between multiple modes of vibration of the molecule act to rapidly scramble energy deposited into one vibrational coordinate and lead to cascaded energy flow toward equilibrium.

For this problem, the bilinear coupling above doesn't capture the proper relaxation process. Instead, we can express the molecular potential energy in terms of well-defined normal modes of vibration for the system and the bath, and these interact weakly through small anharmonic terms in the potential. Then we can extend the perturbative approach above to include the effect of multiple accepting vibrations of the system or bath. For a set of system- and bath coordinates, the combined potential energy for the system (V_S) and the system-bath interaction (V_{SB}) can be expanded as

$$V_S + V_{SB} = \frac{1}{2}\sum_a \frac{\partial^2 V}{\partial Q_a^2} Q_a^2 + \frac{1}{6}\sum_{a,\alpha,\beta} \frac{\partial^3 V}{\partial Q_a \partial q_\alpha \partial q_\beta} Q_a q_\alpha q_\beta + \frac{1}{6}\sum_{a,b,\alpha} \frac{\partial^3 V}{\partial Q_a \partial Q_b \partial q_\alpha} Q_a Q_b q_\alpha \cdots \tag{18.3.1}$$

Focusing explicitly on the first cubic expansion term, for one system oscillator:

$$V_S + V_{SB} = \frac{1}{2} m\Omega^2 \underset{\sim}{Q}^2 + V^{(3)} \underset{\sim}{q_\alpha} \underset{\sim}{q_\beta} \tag{18.3.2}$$

Here, the system-bath interaction potential describes the case for a cubic anharmonic coupling that involves one vibration of the system Q interacting weakly with two vibrations of the bath, q_α and q_β, so that $\hbar\Omega \gg V^{(3)}$. Energy deposited in the system vibration will dissipate to these two vibrations of the bath in a three-quantum process. Higher-order expansion terms would describe interactions involving four or more quanta.

Working specifically with the cubic example, we can use the harmonic bath model to calculate the rate of energy relaxation. This picture is applicable if a vibrational mode of frequency Ω relaxes by transferring its energy to another vibration close in energy (ω_α), with the energy difference ω_β being accounted for by a continuum of intermolecular motions. For this case, one can show:

$$k_{ba} = \frac{1}{\hbar^2}\left[\left(\bar{n}(\omega_\alpha)+1\right)\left(\bar{n}(\omega_\beta)+1\right)\rho_{ba}(\omega_{ab}) + \left(\bar{n}(\omega_\alpha)+1\right)\bar{n}(\omega_\beta)\,\rho_{ba}(\omega_{ab})\right] \tag{18.3.3}$$

where $\rho(\omega) \equiv W(\omega)\left(V^{(3)}(\omega)\right)^2$. Here we have taken the frequencies of the initial vibration Ω and accepting mode ω_α to be much greater than the bath mode ω_β. The two terms in equation (18.3.3) describe two possible relaxation pathways, shown in Figure 18.3.1. In the first, annihilation of a quantum of frequency Ω leads to the creation of two quanta, one each of ω_α and ω_β . The second term describes the dissipation of a vibration through coupling to a higher energy vibration, with the excess energy being absorbed from the bath—annihilation of a quantum of Ω leads to the creation of one quantum of ω_α and the annihilation of one quantum of ω_β. Naturally, this latter pathway is only allowed when there is adequate thermal energy present in the bath.

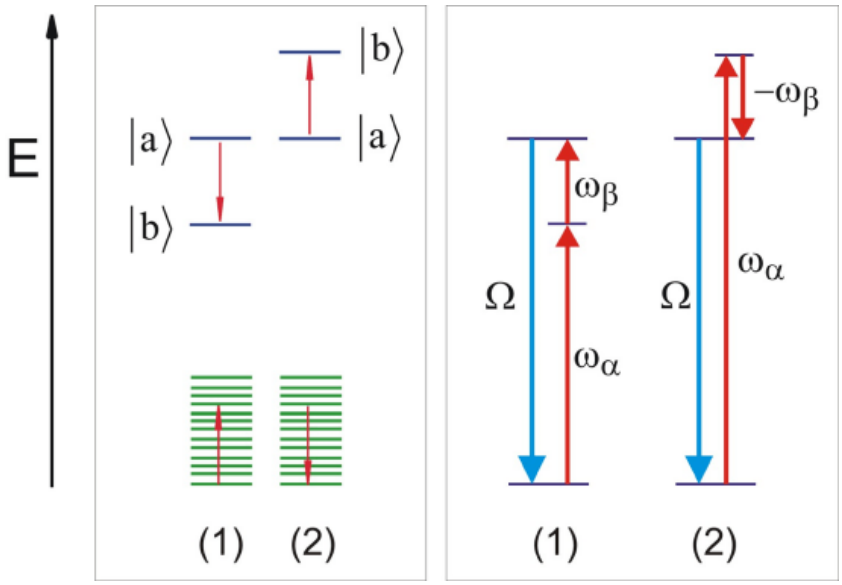


Figure 18.3.1

Rate calculations using classical vibrational relaxation

In general, we would like a practical way to calculate relaxation rates, and calculating quantum correlation functions is not practical. How do we use classical calculations for the bath, for instance drawing on a classical molecular dynamics simulation? Is there a way to get a quantum mechanical rate?

The first problem is that the quantum correlation function is complex $C^*_{ab}(t) = C_{ab}(-t)$ and the classical correlation function is real and even $C_{\rm Cl}(t) = C_{\rm Cl}(-t)$. To connect these two correlation functions, one can derive a quantum correction factor that allows one to predict the quantum correlation function based on the classical one. This is based on the assumption that at high temperature it should be possible to substitute the classical correlation function with the real part of the quantum correlation function

$$C_{\rm Cl}(t) \Rightarrow C'_{ba}(t) \tag{18.3.4}$$

To make this adjustment we start with the frequency domain expression derived from the detailed balance expression $\tilde{C}(-\omega) = e^{-\beta\hbar\omega}\tilde{C}(\omega)$

$$\tilde{C}(\omega) = \frac{2}{1+\exp(-\beta\hbar\omega)}\tilde{C}'(\omega) \tag{18.3.5}$$

Here, $\tilde{C}'(\omega)$ is defined as the Fourier transform of the real part of the quantum correlation function. So the vibrational relaxation rate is

$$k_{ba} = \frac{4}{\hbar^2\left(1+\exp\left(-\hbar\omega_{ba}/kT\right)\right)}\int_0^\infty dt\, e^{-{\rm i}\omega_{ba}t}\,{\rm Re}\left[\langle V_{ab}(t)V_{ba}(0)\rangle\right] \tag{18.3.6}$$

Now we will assume that one can replace a classical calculation of the correlation function here, as in eq. (18.3.4). The leading term out front can be considered a "quantum correction factor" that accounts for the detailed balance of rates encoded in the quantum spectral density.

In practice, a classical calculation might be done with molecular dynamics simulations. Here one has an explicit characterization of the intermolecular forces that would act to damp the excited vibrational mode. One can calculate the system-bath interactions by expanding the vibrational potential of the system in the bath coordinates

$$\begin{aligned} V_S + V_{SB} &= V_0 + \sum_\alpha \frac{\partial V^\alpha}{\partial Q}Q + \sum_\alpha \frac{\partial^2 V^\alpha}{\partial Q^2}Q^2 + \cdots \\ &= V_0 + FQ + GQ^2 + \cdots \end{aligned} \tag{18.3.7}$$

Here V^α represents the potential of an interaction of one solvent coordinate acting on the excited vibrational system coordinate Q. The second term in this expansion FQ depends linearly on the system 0 and bath α coordinates, and we can use variation in

this parameter to calculate the correlation function for the fluctuating interaction potential. Note that F is the *force* that molecules exert on Q! Thus, the relevant classical correlation function for vibrational relaxation is a force correlation function

$$C_{\mathrm{Cl}}(t) = \langle F(t)F(0)\rangle \tag{18.3.8}$$

$$k_{\mathrm{Cl}} = \frac{1}{k_B T}\int_0^\infty dt \cos\omega_{ba} t \langle F(t)F(0)\rangle \tag{18.3.9}$$

References

(1) Kenkre, V. M.; Tokmakoff, A.; Fayer, M. D. Theory of vibrational relaxation of polyatomic molecules in liquids. *Journal of Chemical Physics* **1994**, *101* (12), 10618-10629. DOI: 10.1063/1.467876

This page titled 18.3: Multiquantum relaxation of polyatomic molecules is shared under a CC BY-NC-SA 4.0 license and was authored, remixed, and/or curated by LibreTexts.

18.4: Redfield Theory and Master Equation

Next, we will more generally formulate a quantum mechanical picture of the coherent and incoherent relaxation processes that result from the interaction between a prepared system and its environment. This description will apply to the case where we separate the degrees of freedom in our problem into a system and a bath that interact. We have limited information about the bath's degrees of freedom. As a statistical mixture, we only have knowledge of the probability of occupying states of the bath and not of the phase relationships required to describe a deterministic quantum system. For such problems, the density matrix is the natural tool.

Our approach to this problem starts with the same Hamiltonian as in Section 18.2, equations (18.2.1) and (18.2.2). The system degrees of freedom that we are most interested in are governed by H_S, and we observe the system through measurements of a system operator, A. The remaining degrees of freedom constitute a bath which interacts with the system. Again, the eigenstates of H_S are denoted $|a\rangle$ and those of H_B are $|\alpha\rangle$. Since we will not be making observations of the state of the bath, we perform a partial trace over the bath degrees of freedom, i.e. a sum over diagonal elements in α, to obtain the reduced density matrix, σ.

$$\sigma = \mathrm{Tr}_B(\rho) \tag{18.4.1}$$

Where $Tr_B(\cdots) = \sum_\alpha \langle\alpha|\cdots|\alpha\rangle$. We will use σ to describe the expectation value of A using

$$\begin{aligned}\langle A\rangle &= \mathrm{Tr}[\rho(t)A] \\ &= \mathrm{Tr}[\sigma(t)A] \\ &= \sum_{a,b}\sigma_{ab}(t)A_{ba}\end{aligned} \tag{18.4.2}$$

Where the elements of the reduced density matrix are

$$\sigma_{ab} = \sum_\alpha \langle a\alpha|\rho|b\alpha\rangle = \mathrm{Tr}_B\,\rho_{ab} \tag{18.4.3}$$

Note, that since $\mathrm{Tr}(A\times B) = \mathrm{Tr}A\,\mathrm{Tr}B$ for direct product states, all we need to do is describe time evolution of σ to understand the time dependence to A.

We work in the interaction picture to treat the time evolution of the reduced density matrix. Drawing on our earlier discussion of the density matrix, we integrate the equation of motion in the interaction picture

$$\dot\rho_I = -\frac{\mathrm{i}}{\hbar}\left[V_I(t),\rho_I(t)\right] \tag{18.4.4}$$

to obtain

$$\rho_I(t) = \rho_I(0) - \frac{\mathrm{i}}{\hbar}\int_0^t d\tau\left[V_I(\tau),\rho_I(\tau)\right] \tag{18.4.5}$$

Remember that the density matrix in the interaction picture is

$$\rho_I(t) = U_0^\dagger\,\rho(t)\,U_0 = e^{\mathrm{i}(H_S+H_B)t/\hbar}\,\rho(t)\,e^{-i(H_S+H_B)t/\hbar} \tag{18.4.6}$$

and similarly

$$V_I(t) = U_0^\dagger\,V\,U_0 = e^{\mathrm{i}(H_S+H_B)t/\hbar}\,V(t)\,e^{-i(H_S+H_B)t/\hbar} \tag{18.4.7}$$

Substituting equation (18.4.5) into (18.4.4) we have

$$\dot\rho_I(t) = -\frac{\mathrm{i}}{\hbar}\left[V_I(t),\rho_I\left(t_0\right)\right] - \frac{1}{\hbar^2}\int_0^t dt'\left[V_I(t),\left[V_I\left(t'\right),\rho_I\left(t'\right)\right]\right] \tag{18.4.8}$$

Now taking a trace over the bath states

$$\dot{\sigma}_I(t) = -\frac{\mathrm{i}}{\hbar}\mathrm{Tr}_B\left[V_I(t), \rho_I\left(t_0\right)\right] - \frac{1}{\hbar^2}\int_0^t dt'\,\mathrm{Tr}_B\left[V_I(t), \left[V_I\left(t'\right), \rho_I\left(t'\right)\right]\right] \tag{18.4.9}$$

If we assume that (1) the interaction between the system and bath is small enough that the system does not alter the bath and (2) that the bath remains at thermal equilibrium, then

$$\rho_I(t) \approx \sigma_I(t)\rho_{\mathrm{eq}}^B \tag{18.4.10}$$

$$\rho_{\mathrm{eq}}^B = \frac{e^{-\beta H_B}}{Z} \tag{18.4.11}$$

Then we obtain a second-order equation of motion for σ_I:

$$\dot{\sigma}_I(t) = -\frac{\mathrm{i}}{\hbar}\mathrm{Tr}_B\left[V_I(t), \sigma_I(0)\rho_{\mathrm{eq}}^B\right] - \frac{1}{\hbar^2}\int_0^t dt'\,\mathrm{Tr}_B\left[V_I(t), \left[V_I\left(t'\right), \sigma_I\left(t'\right)\rho_{\mathrm{eq}}^B\right]\right] \tag{18.4.12}$$

The last term involves an integral over a correlation function for a fluctuating interaction potential. This looks similar to a linear response function, and it is also the same form as the relaxation rates from Fermi's Golden Rule that we just discussed.

The first term in eq. (18.4.12) involves a thermal average over the interaction potential, $\langle V\rangle_R = \mathrm{Tr}_B\left[V\rho_{\mathrm{eq}}^B\right]$. If this average value is zero, which would be the case for an off-diagonal form of V, we can drop the first term in the equation of motion for σ_I. If it is not zero, it is possible to redefine the Hamiltonian such that $H_0 \to H_0 + \langle V\rangle_B$ and $V(t) \to V(t) - \langle V\rangle_B$, which recasts it in a form where $\langle V\rangle_B \to 0$ and the first term can be neglected.

Now let's evaluate the equation of motion for the case where the system-bath interaction can be written as a product of operators in the system ($\hat{A}$) and bath ($\hat{\beta}$):

$$H_{SB} = V = \hat{A}\hat{\beta} \tag{18.4.13}$$

This is equivalent to the bilinear coupling form that was used in our prior description of dephasing and population relaxation. There we took the interaction to be linearly proportional to the system and bath coordinate(s): $V = cQq$. The time evolution in the two variables is separable and given by

$$\begin{aligned}\hat{A}(t) &= U_S^\dagger \hat{A}\left(t_0\right) U_S \\ \hat{\beta}(t) &= U_B^\dagger \hat{\beta}\left(t_0\right) U_B\end{aligned} \tag{18.4.14}$$

where $U_S = e^{-\mathrm{i}H_S t/\hbar}$ and $U_B = e^{-\mathrm{i}H_B t/\hbar}$. The equation of motion for σ_I becomes

$$\begin{aligned}\dot{\sigma}_I(t) = \frac{1}{\hbar^2}\int_0^t dt' &\Big[\hat{A}(t)\hat{A}(t')\sigma(t') - \hat{A}(t')\sigma(t')\hat{A}(t)\Big]\,\mathrm{Tr}_B\left(\hat{\beta}(t)\hat{\beta}(t')\rho_{\mathrm{eq}}^B\right) \\ &-\Big[\hat{A}(t)\sigma(t')\hat{A}(t') - \sigma(t')\hat{A}(t')\hat{A}(t)\Big]\,\mathrm{Tr}_B\left(\hat{\beta}(t')\hat{\beta}(t)\rho_{\mathrm{eq}}^B\right)\end{aligned} \tag{18.4.15}$$

Here the history of the evolution of $\hat{A}$ depends on the time dependence of the bath variables coupled to the system. The time dependence of the bath enters as a bath correlation function

$$\begin{aligned}C_{\beta\beta}\left(t-t'\right) &= \mathrm{Tr}_B\left(\hat{\beta}(t)\hat{\beta}(t')\rho_{\mathrm{eq}}^B\right) \\ &= \left\langle\hat{\beta}(t)\hat{\beta}(t')\right\rangle_B \\ &= \left\langle\hat{\beta}\left(t-t'\right)\hat{\beta}(0)\right\rangle_B\end{aligned} \tag{18.4.16}$$

The bath correlation function can be evaluated using the methods that we have used in the Energy Gap Hamiltonian and Brownian Oscillator Models. Switching integration variables to the time interval prior to observation

$$\tau = t - t' \tag{18.4.17}$$

we obtain

$$\dot{\sigma}_I(t) = -\frac{1}{\hbar^2}\sum_{\alpha,\beta}\int_0^t d\tau\Big[\hat{A}(t),\hat{A}(t-\tau)\sigma_I(t-\tau)\Big]\,C_{\beta\beta}(\tau) - \Big[\hat{A}(t),\sigma_I(t-\tau)\hat{A}(t-\tau)\Big]\,C^*_{\beta\beta}(\tau) \tag{18.4.18}$$

Here we have made use of $C^*_{\beta\beta}(\tau) = C_{\beta\beta}(-\tau)$. For the case that the system-bath interaction results from interactions with many bath coordinates

$$V = \sum_\alpha \hat{A}\hat{\beta}_\alpha \tag{18.4.19}$$

then eq. (18.4.18) becomes

$$\dot{\sigma}_I(t) = -\frac{1}{\hbar^2}\sum_{\alpha,\beta}\int_0^t d\tau\Big[\hat{A}(t),\hat{A}(t-\tau)\sigma_I(t-\tau)\Big]\,C_{\alpha\beta}(\tau) - \Big[\hat{A}(t),\sigma_I(t-\tau)\hat{A}(t-\tau)\Big]\,C^*_{\alpha\beta}(\tau) \tag{18.4.20}$$

with the bath correlation function

$$C_{\alpha\beta}(\tau) = \left\langle \hat{\beta}_\alpha(\tau)\hat{\beta}_\beta(0)\right\rangle_B \tag{18.4.21}$$

Equation (18.4.18) or (18.4.20) indicates that the rates of exchange of amplitude between the system states carries memory of the bath's influence on the system. That is, $\sigma_I(t)$ is dependent on $\sigma_I(t-\tau)$. If we make the Markov approximation-for which the dynamics of the bath are much faster than the evolution of the system and the system has no memory of its past—in eq. (18.4.15) we make the substitution

$$\sigma(t') = \sigma(t')\,\delta(t-t') \Rightarrow \sigma(t) \tag{18.4.22}$$

or equivalently in eq. (18.4.18) we set

$$\sigma_I(t-\tau) \Rightarrow \sigma_I(t) \tag{18.4.23}$$

For the subsequent work, we use this approximation. Similarly, the presence of a time scale separation between a slow system and a fast bath allows us to change the upper integration limit in eq. (18.4.18) from t to ∞.

Redfield Equation

To describe the exchange of amplitude between system states induced by the bath, we will want to evaluate the matrix elements of the reduced density matrix in the system eigenstates (a, b, c, d). To begin, we use eq. (18.4.18) to write the time-dependent matrix elements as

$$\dot{\sigma}^I_{ab}(t) = -\sum_{c,d}\frac{1}{\hbar^2}\int_0^\infty d\tau\Big[\hat{A}_{ac}(t)\hat{A}_{cd}(t-\tau)\sigma^I_{cb}(t) - \hat{A}_{ac}(t-\tau)\sigma^I_{cd}(t)\hat{A}_{cb}(t)\Big]\,C_{\beta\beta}(\tau) - \Big[\hat{A}_{ac}(t)\sigma^I_{cd}(t)\hat{A}_{cb}(t-\tau) - \sigma^I_{ac}(t)\hat{A}_{cd}(t-\tau)\hat{A}_{cb}(t)\Big]\,C^*_{\beta\beta}(\tau) \tag{18.4.24}$$

Now, let's convert the time-dependence from expression in terms of the interaction picture into a Schrodinger representation, using

$$\begin{aligned}\left\langle a\left|\hat{A}(t)\right|b\right\rangle &= e^{i\omega_{ab}t}A_{ab}\\ \left\langle a\left|\sigma^I\right|b\right\rangle &= e^{i\omega_{ab}t}\sigma_{ab}\\ \dot{\sigma}^I_{ab} &= \frac{\partial}{\partial t}\left\langle a\left|\sigma^I\right|b\right\rangle\end{aligned} \tag{18.4.25}$$

To see how this turns out, consider the first term in eq. (18.4.24):

$$\dot{\sigma}^I_{ab}(t) = -\sum_{c,d}\frac{1}{\hbar^2}\int_0^\infty d\tau\,\hat{A}_{ac}(t)\hat{A}_{cd}(t-\tau)\sigma^I_{cb}(t)C_{\beta\beta}(\tau) \tag{18.4.26}$$

Returning to the Schrödinger picture we find

$$\dot{\sigma}_{ab}(t)e^{\mathrm{i}\omega_{ab}\tau}+\mathrm{i}\omega_{ab}e^{\mathrm{i}\omega_{ab}\tau}\sigma_{ab}=-\sum_{c,d}\frac{1}{\hbar^2}\hat{A}_{ac}\,\hat{A}_{cd}\,\sigma_{db}(t)\,e^{\mathrm{i}\omega_{ac}t+\mathrm{i}\omega_{cd}t+\mathrm{i}\omega_{\omega}t}\int_0^{\infty}d\tau\,e^{-\mathrm{i}\omega_{ca}\tau}C_{\beta\beta}(\tau) \tag{18.4.27}$$

Defining the Fourier-Laplace transform of the bath correlation function:

$$\tilde{C}_{\beta\beta}(\omega)=\int_0^{\infty}d\tau\,e^{\mathrm{i}\omega\tau}C_{\beta\beta}(\tau) \tag{18.4.28}$$

We have

$$\dot{\sigma}_{ab}(t)=-\mathrm{i}\omega_{ab}\sigma_{ab}-\sum_{c,d}\frac{1}{\hbar^2}\hat{A}_{ac}\hat{A}_{cd}\sigma_{cb}(t)\tilde{C}_{\beta\beta}\left(\omega_{dc}\right) \tag{18.4.29}$$

Here the spectral representation of the bath correlation function is being evaluated at the energy gap between system states ω_{dc}. So the evolution of coherences and populations in the system states is governed by their interactions with other system states, governed by the matrix elements, and this is modified depending on the fluctuations of the bath at different system state energy gaps. In this manner, eq. (18.4.24) becomes

$$\begin{aligned}\dot{\sigma}_{ab}(t)=&-\mathrm{i}\omega_{ab}\sigma_{ab}(t)-\frac{1}{\hbar^2}\sum_{c,d}\Big[\hat{A}_{ac}\hat{A}_{cd}\sigma_{cb}(t)\tilde{C}_{\beta\beta}\left(\omega_{cc}\right)-\hat{A}_{ac}\hat{A}_{db}\sigma_{cd}(t)\tilde{C}_{\beta\beta}\left(\omega_{ca}\right) &(18.4.30)\\ &-\hat{A}_{ac}\hat{A}_{cb}\sigma_{cd}(t)\tilde{C}^{*}_{\beta\beta}\left(-\omega_{cb}\right)+\hat{A}_{cd}\hat{A}_{cb}\sigma_{ac}(t)\tilde{C}^{*}_{\beta\beta}\left(-\omega_{cd}\right)\Big]\\ =&-\mathrm{i}\omega_{ab}\sigma_{ab}(t)-\sum_{c,d}\left[\Gamma^{+}_{ac,cd}\sigma_{db}(t)-\Gamma^{-}_{ac,db}\sigma_{cd}(t)-\Gamma^{+}_{ac,db}\sigma_{cd}(t)+\Gamma^{-}_{cd,db}\sigma_{ac}(t)\right] &(18.4.31)\end{aligned}$$

We see that the off-diagonal reduced density matrix elements—the coherences—oscillate with at a frequency given by the energy splitting between the states, but the amplitude of these states are modified, rising and falling at rates given by the constants $\Gamma^{\pm}_{ab,cd}$. The rate constants are defined through:

$$\Gamma^{+}_{ab,cd}=\frac{1}{\hbar^2}A_{ab}A_{cd}\;\tilde{C}_{\beta\beta}(\omega_{dc}) \tag{18.4.32}$$

$$\Gamma^{-}_{ab,cd}=\frac{1}{\hbar^2}A_{ab}A_{cd}\;\tilde{C}_{\beta\beta}(\omega_{ba}) \tag{18.4.33}$$

The coupled differential equations in eq. (18.4.31) express the relaxation dynamics of the system states almost entirely in terms of the system Hamiltonian. The influence of the bath only enters through the bath correlation function.

The common alternate way of writing eq. (18.4.31) is in terms of the relaxation super-operator, $\mathcal{R}$

$$\dot{\sigma}_{ab}(t)=-\mathrm{i}\omega_{ab}\sigma_{ab}-\sum_{c,d}\mathcal{R}_{ab,cd}\,\sigma_{cd}(t) \tag{18.4.34}$$

or in the interaction picture

$$\dot{\sigma}^{I}_{ab}(t)=\sum_{c,d}\sigma^{I}_{cd}(t)\,\mathcal{R}_{ab,cd}\;e^{\mathrm{i}(E_a-E_b-E_c+E_d)t/\hbar} \tag{18.4.35}$$

Equation (18.4.34), the reduced density matrix equation of motion for a Markovian bath, is known as the Redfield equation. It describes the irreversible and oscillatory components of the amplitude in the $|a\rangle\langle b|$ coherence as features resulting from dissipation to the bath and feeding from other states. $\mathcal{R}$ describes the rates of change of the diagonal and off-diagonal elements of σ_I and is expressed as:

$$\mathcal{R}_{ab,cd}=\delta_{db}\sum_{k}\left[\Gamma^{+}_{ak,kc}-\Gamma^{+}_{db,ad}-\Gamma^{-}_{db,ad}\right]+\delta_{ac}\sum_{k}\Gamma^{-}_{dk,kb} \tag{18.4.36}$$

where k refers to a system state.

The derivation described above can be performed without assuming a form to the system-bath interaction potential as we did in eq. (18.4.13). If so, one can write the relaxation operator in terms of a correlation function for the system-bath interaction

$$\Gamma^{+}_{ab,cd} = \frac{1}{\hbar^2}\int_0^\infty d\tau \left\langle V_{ab}(\tau)V_{cd}(0)\right\rangle_B e^{-\mathrm{i}\omega_{cd}\tau} \tag{18.4.37}$$

$$\Gamma^{-}_{ab,cd} = \frac{1}{\hbar^2}\int_0^\infty d\tau \left\langle V_{ab}(0)V_{cd}(\tau)\right\rangle_B e^{-\mathrm{i}\omega_{ab}\tau} \tag{18.4.38}$$

The tetradic notation for the Redfield relaxation operator accounts for all possible dynamic evolution processes within a multistate system. In particular we identify four classes of relaxation processes, depending on the number of states involved:

- aa, aa: Population Relaxation
  - Rate of loss of the population in a
- ab, ab: Coherence Relaxation or Dephasing
  - Damping of the coherence ab
- aa, bb: Population Transfer
  - Rate of transfer of population from state b to state a
- ab, cd: Coherence Transfer
  - Rate at which amplitude in an oscillating superposition between two states (c and d) couples to form oscillating amplitude between two other states (a and b)

The origin and meaning of these terms will be discussed below.

Secular Approximation

From eq. (18.4.35) we note that the largest changes in matrix elements of result from a resonance condition:

$$\begin{gathered}\exp\left[\mathrm{i}\left(E_a - E_b - E_c + E_d\right)t/\hbar\right] \approx 1 \\ E_a - E_b - E_c + E_d \approx 0\end{gathered} \tag{18.4.39}$$

which is satisfied for three possible cases:

$$\begin{aligned} a = c \;;\; b = d &\Longrightarrow \quad \mathcal{R}_{ab,ab} \\ a = b \;;\; c = d &\Longrightarrow \quad \mathcal{R}_{aa,cc} \\ a = b = c = d &\Longrightarrow \quad \mathcal{R}_{aa,aa} \end{aligned} \tag{18.4.40}$$

In evaluating relaxation rates, often only these *secular* terms are retained. Whether this approximation is valid must be considered on a case-by-case basis and depends on the nature of the system eigenvalues and the bath correlation function.

Population Relaxation and the Master Equation

To understand the information in the relaxation operator and the classification of relaxation processes, let's first consider the relaxation of the diagonal elements of the reduced density matrix. Using the secular approximation,

$$\dot{\sigma}_{aa}(t) = -\sum_b \mathcal{R}_{aa,bb}\,\sigma_{bb}(t) \tag{18.4.41}$$

Considering first the case that $a \neq b$, eq. (18.4.40) gives the relaxation operator as

$$\mathcal{R}_{aa,bb} = -\Gamma^{+}_{ba,ab} - \Gamma^{-}_{ba,ab} \tag{18.4.42}$$

Recognizing that Γ^{+} and Γ^{-} are Hermitian conjugates,

$$\begin{aligned}\mathcal{R}_{aa,bb} &= -\frac{1}{\hbar^2}\left|A_{ab}\right|^2 \int_0^\infty d\tau\, C_{\beta\beta}(\tau)\, e^{-\mathrm{i}\omega_{ba}\tau} \;+\; c.c. \\ &= -\frac{1}{\hbar^2}\int_0^\infty d\tau \left\langle V_{ba}(\tau)V_{ab}(0)\right\rangle_B e^{-\mathrm{i}\omega_{ab}\tau} \;+\; c.c.\end{aligned} \tag{18.4.43}$$

So $\mathcal{R}_{aa,bb}$ is a real valued quantity. However, since $\langle V_{ba}(\tau)V_{ab}(0)\rangle = \langle V_{ba}(0)V_{ab}(-\tau)\rangle$,

$$\mathcal{R}_{aa,bb} = -\frac{1}{\hbar^2}\int_{-\infty}^{+\infty} dt \left\langle V_{ba}(\tau)V_{ab}(0)\right\rangle_B e^{\mathrm{i}\omega_{ba}\tau} \tag{18.4.44}$$

So we see that the relaxation tensor results in the same rate of population relaxation between states a and b as we previously derived from Fermi's Golden rule:

$$\mathcal{R}_{aa,bb} = -w_{ab} \qquad (a \neq b) \tag{18.4.45}$$

For the case that $a = b$, eq. (18.4.40) gives the relaxation operator as

$$\begin{aligned} \mathcal{R}_{aa,aa} &= -\left(\Gamma^{+}_{aa,aa} + \Gamma^{-}_{aa,aa}\right) + \sum_{k} \left(\Gamma^{+}_{ak,ka} + \Gamma^{-}_{ak,ka}\right) \\ &= \sum_{k \neq a} \left(\Gamma^{+}_{ak,ka} + \Gamma^{-}_{ak,ka}\right) \end{aligned} \tag{18.4.46}$$

The relaxation accounts for the dissipation induced by bath interactions with all states of the system (last term), but with the influence of self-relaxation (first term) removed. The net result is that we are left with the net rate of relaxation from a to all other system states ($a \neq k$)

$$\mathcal{R}_{aa,aa} = \sum_{k \neq a} w_{ka} \tag{18.4.47}$$

This term $\mathcal{R}_{aa,aa}$ is also referred to as the inverse of T_1, the population lifetime of the a state.

The combination of these observations shows that the diagonal elements of the reduced density matrix follow a master equation that describes the net gain and loss of population in a particular state

$$\dot{\sigma}_{aa}(t) = \sum_{b \neq a} w_{ab}\sigma_{bb}(t) - \sum_{k \neq a} w_{ka}\sigma_{aa}(t) \tag{18.4.48}$$

Coherence Relaxation

Now let's consider the relaxation of the off-diagonal elements of the reduced density matrix. It is instructive to limit ourselves at first to one term in the relaxation operator, so that we write the equation of motion as

$$\dot{\sigma}_{ab}\,(t) = -\mathrm{i}\omega_{ab}\sigma_{ab}(t) - \mathcal{R}_{ab,ab}\,\sigma_{ab}(t) + \cdots \tag{18.4.49}$$

The relaxation operator gives

$$\begin{aligned} \mathcal{R}_{ab,ab} &= -\left(\Gamma^{+}_{aa,bb} + \Gamma^{-}_{aa,bb}\right) + \sum_{k} \left(\Gamma^{+}_{ak,ka} + \Gamma^{-}_{bk,kb}\right) \\ &= -\left(\Gamma^{+}_{aa,bb} + \Gamma^{-}_{aa,bb} - \Gamma^{+}_{aa,aa} - \Gamma^{-}_{bb,bb}\right) + \left(\sum_{k \neq a} \Gamma^{+}_{ak,ka} + \sum_{k \neq b} \Gamma^{-}_{bk,kb}\right) \end{aligned} \tag{18.4.50}$$

In the second step, we have separated the sum into two terms, one involving relaxation constants for the two coherent states, and the second involving all other states. The latter term looks very similar to the relaxation rates in eq. (18.4.46). In fact, if we factor out the imaginary parts of these terms and add them as a correction to the frequency in eq. (18.4.49), $\omega_{ab} \rightarrow (\omega_{ab} + \mathrm{Im}[\text{term 2}])$, then the remaining expression is directly related to the population lifetimes of the a and b states:

$$\begin{aligned} \mathrm{Re}\left(\sum_{k \neq a} \Gamma^{+}_{ak,ka} + \sum_{k \neq b} \Gamma^{-}_{bk,kb}\right) &= \frac{1}{2}\sum_{k \neq b} w_{kb} - \frac{1}{2}\sum_{k \neq a} w_{ka} \\ &= \frac{1}{2}\left(\frac{1}{T_{1,a}} + \frac{1}{T_{1,b}}\right) \end{aligned} \tag{18.4.51}$$

This term accounts for the decay of the coherence as a sum of the rates of relaxation of the a and b states.

The meaning of the first term on the right hand side of eq. (18.4.51) is a little less obvious. If we write out the four contributing relaxation factors explicitly using the system-bath correlation functions in eqs. (18.4.37) and (18.4.38), the real part can be written as

$$\begin{aligned}\mathrm{Re}\left(\Gamma^{+}_{aa,bb}+\Gamma^{-}_{aa,bb}-\Gamma^{+}_{aa,aa}-\Gamma^{-}_{bb,bb}\right) &= \int_0^\infty d\tau \left\langle \left[V_{bb}(\tau)-V_{aa}(\tau)\right]\left[V_{bb}(0)-V_{aa}(0)\right]\right\rangle_B \\ &\equiv \int_0^\infty d\tau \left\langle \Delta V(\tau)\Delta V(0)\right\rangle_B\end{aligned} \tag{18.4.52}$$

In essence, this term involves an integral over a correlation function that describes variations in the a-b energy gap, which varies as a result of its interactions with the bath. So this term, in essence, accounts for the fluctuations of the energy gap that we previously treated with stochastic models. Of course, in the current case, we have made a Markovian bath assumption, so the fluctuations are treated as rapid and only assigned an interaction strength Γ which is related to the linewidth. In an identical manner to the fast modulation limit of the stochastic model we see that the relaxation rate is related to the square of the amplitude of modulation, multiplied by the correlation time for the bath:

$$\int_0^\infty d\tau \left\langle \Delta V(\tau)\Delta V(0)\right\rangle_B = \left\langle \Delta V^2\right\rangle \tau_c \equiv \Gamma \tag{18.4.53}$$

As earlier this is how the pure dephasing contribution to the Lorentzian lineshape is defined. It is also assigned a time scale $T_2^* = \Gamma^{-1}$.

To summarize, we see that the relaxation of coherences has contributions from pure-dephasing and from the lifetime of the states involved. Explicitly, the equation of motion in eq. (18.4.49) can be re-written

$$\dot{\sigma}_{ab}(t) = -\mathrm{i}\underset{\sim}{\omega}_{ab}\,\sigma_{ab}(t) - \frac{1}{T_2}\sigma_{ab}(t) \tag{18.4.54}$$

where the dephasing time is

$$\frac{1}{T_2} = \frac{1}{T_2^*} + \frac{1}{2}\left(\frac{1}{T_{1,a}}+\frac{1}{T_{1,b}}\right) \tag{18.4.55}$$

and the frequency has been corrected as a result interactions with the bath with the (small) imaginary contributions to to $\mathcal{R}_{ab,ab}$:

$$\underset{\sim}{\omega}_{ab} = \omega_{ab} + \mathrm{Im}\left[\mathcal{R}_{ab,ab}\right] \tag{18.4.56}$$

This page titled 18.4: Redfield Theory and Master Equation is shared under a CC BY-NC-SA 4.0 license and was authored, remixed, and/or curated by LibreTexts.

18.5: Readings

Multiquantum relaxation of polyatomic molecules

1. Egorov, S. A.; Berne, B. J. Vibrational energy relaxation in the condensed phases: Quantum vs classical bath for multiphonon processes. *Journal of Chemical Physics* **1997**, *107* (16), 6050-6061. DOI: 10.1063/1.474273
2. Kenkre, V. M.; Tokmakoff, A.; Fayer, M. D. Theory of vibrational relaxation of polyatomic molecules in liquids. *Journal of Chemical Physics* **1994**, *101* (12), 10618-10629. DOI: 10.1063/1.467876
3. Nitzan, A. *Chemical dynamics in condensed phases: Relaxation, transfer and reactions in condensed molecular systems*; Oxford University Press, 2006; ch 11. DOI: 10.1093/oso/9780198529798.001.0001
4. Oxtoby, D. W. Vibrational Population Relaxation in Liquids. *Advances in Chemical Physics: Photoselective Chemistry. Part 2, Volume 47*; Jortner, J., Levine, R. D., Rice, S. A., Eds.; Vol. 2; 1981; pp 487-519. DOI: 10.1002/9780470142660.ch14
5. Skinner, J. L. Semiclassical approximations to golden rule rate constants. *Journal of Chemical Physics* **1997**, *107* (20), 8717-8718. DOI: 10.1063/1.474998
6. Slichter, C. P. *Principles of Magnetic Resonance, with Examples from Solid State Physics*; Harper & Row, 1963.

Reduced Density Matrix Description of Relaxation

1. Blum, K. *Density Matrix Theory and Applications*; Plenum Press, 1981.
2. Nitzan, A. *Chemical dynamics in condensed phases: Relaxation, transfer and reactions in condensed molecular systems*; Oxford University Press, 2006; ch 10. DOI: 10.1093/oso/9780198529798.001.0001
3. Pollard, W. T.; Friesner, R. A. Solution of the Redfield equation for the dissipative quantum dynamics of multilevel systems. *Journal of Chemical Physics* **1994**, *100* (7), 5054-5065. DOI: 10.1063/1.467222
4. Slichter, C. P. *Principles of Magnetic Resonance, with Examples from Solid State Physics*; Harper & Row, 1963.

This page titled 18.5: Readings is shared under a license and was authored, remixed, and/or curated by LibreTexts.

19: ENERGY AND CHARGE TRANSFER

19.1: Intermolecular Electronic Interactions
19.2: Resonance Energy Transfer and Transition Dipole Coupling
19.3: Förster Resonance Energy Transfer
19.4: Marcus Theory for Electron Transfer
19.5: Readings

This page titled 19: Energy and Charge Transfer is shared under a CC BY-NC-SA 4.0 license and was authored, remixed, and/or curated by Andrei Tokmakoff via source content that was edited to the style and standards of the LibreTexts platform.

19.1: Intermolecular Electronic Interactions

In this chapter, we will describe the intermolecular transport of an electron or electronic excitation energy from a donor molecule to an acceptor molecule. These are among the most important fundamental processes in chemistry, since they underlie every chemical reaction, most energy transduction process, and numerous material functions that we seek to technologically exploit. As a result, there is a rich history and extensive literature dedicated to this field. The objective here is to provide a fundamental description of the most important and most common concepts in electronic energy and charge transport from a time-dependent perspective in a transparent and hopefully simple manner.

How do we go about describing such problems? Generally, the system of interest will consist of a donor molecule and an acceptor molecule, and we will have to specify the initial and final state of the joint system. We also will need to specify an intermolecular electronic interaction potential that gives rise to the process of interest. Thus, it will not surprise you that we will formulate the description of these processes in terms of a familiar Hamiltonian

$$H = H_0 + V \tag{19.1.1}$$

in which H_0 describes the electronic states of the donor and acceptor, as well as any vibrational states they are coupled to, and V is the electronic coupling. There are many questions that arise at the outset: What types of intermolecular interactions give rise to the transport process? Is the coupling V strong or weak? Should we describe the electronic states in a diabatic or adiabatic basis? How do nuclear degrees of freedom influence the electronic couplings? For weak couplings, we can describe the rate of transport of electrons and electronic excitation with perturbation theory, drawing on Fermi's Golden Rule. This approach underlies common descriptions of electronic energy transport and non-adiabatic electron transfer. We will discuss this regime, concentrating on the influence of the vibrational motions that electronic transport and excitation are coupled to. However, the electronic couplings can also be strong, in which case the resulting states become delocalized. We will discuss this limit in the context of excitons that arise in molecular aggregates.

To begin, it is useful to catalog a number of electronic interactions of interest, involving the transfer of an electron or electronic energy from a donor molecule D to an acceptor molecule A. We can use schematic HOMO/LUMO occupancy diagrams to illustrate the change of electronic configuration between the initial and final states of the system, emphasizing the close relationship between the various transport processes. These diagrams also serve as a reminder not to forget the electronic spin state of the initial and final states, although this will not play a crucial role in the specific examples exampled here. Additionally, we need to remember that these diagrams only indicate change between the initial and final state and are not meant to imply a dynamical mechanism.

(a) Resonance energy transfer (RET)

RET refers to the nonradiative transfer of an electronic excitation from D to A:

$$D^* + A \rightarrow D + A^* \tag{19.1.2}$$

It arises from a Coulomb interaction that is operative at long range, i.e., distances large compared to molecular dimensions, and requires electronic resonance between electronic energy gaps of D and A. Theodor Förster developed the first practical expressions describing this effect, hence it is commonly referred to as FRET (Förster Resonance Energy Transfer).

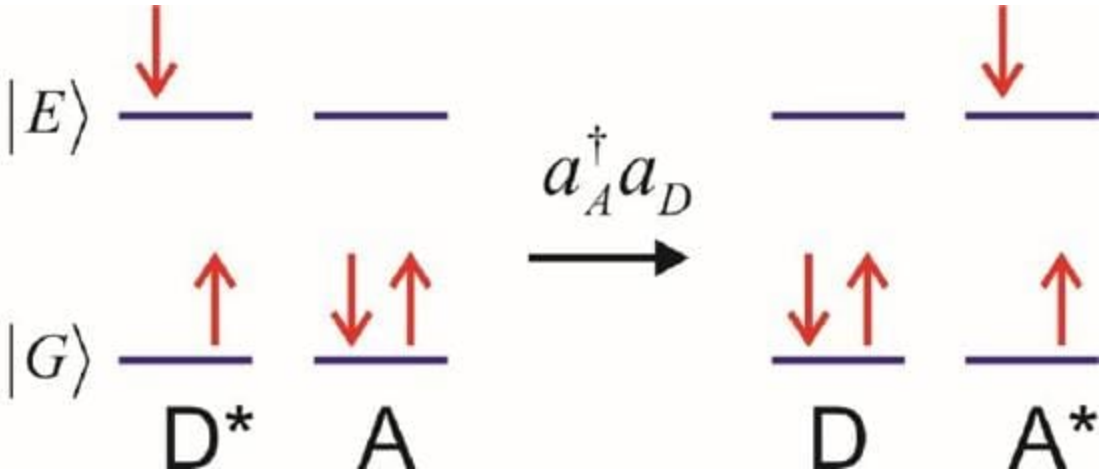


Figure 19.1.1

(b) Electron transfer (ET)

Transfer of electronic charge between donor and acceptor molecules is most commonly described in the framework of Marcus theory for nonadiabatic electron transfer. The interaction mechanism requires wavefunction overlap. There is no change in net spin.

Ground state ET:



Figure 19.1.2

Excited state ET:

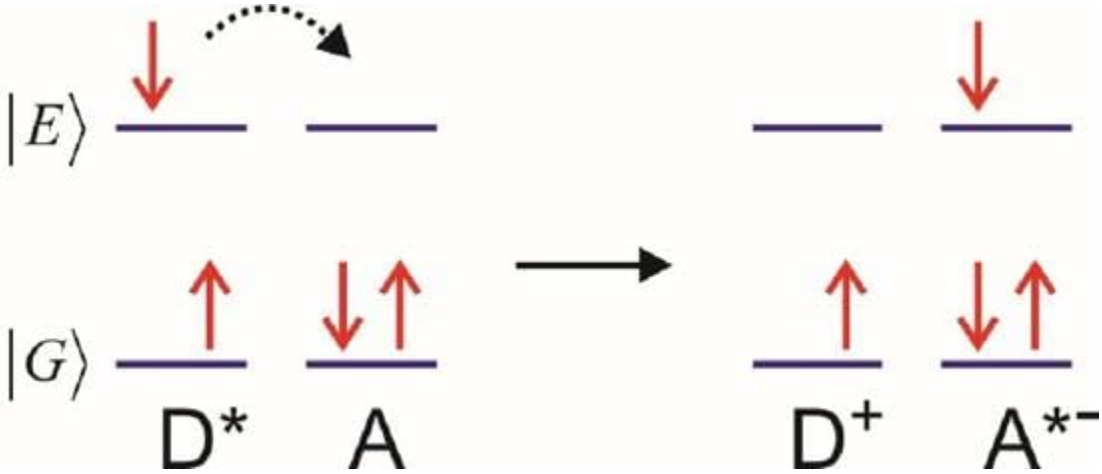


Figure 19.1.3

Hole transfer:

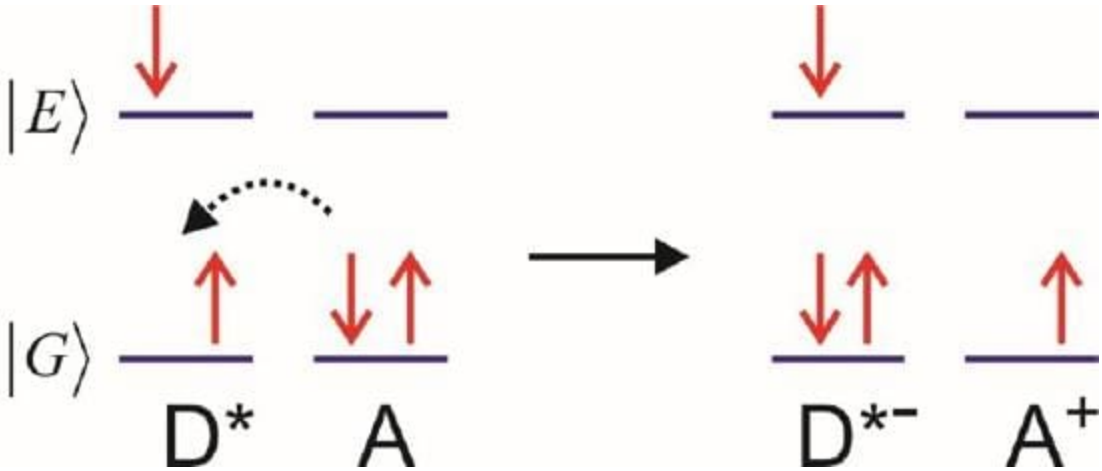


Figure 19.1.4

(c) Electron-exchange energy transfer

Electron-exchange energy transfer involves the transport of electronic excitation energy through the concerted exchange of electrons between the ground and excited states of acceptor and donor. This kind of interaction is often called Dexter transfer. These transfers require wavefunction overlap and are operative with singlet or triplet states.

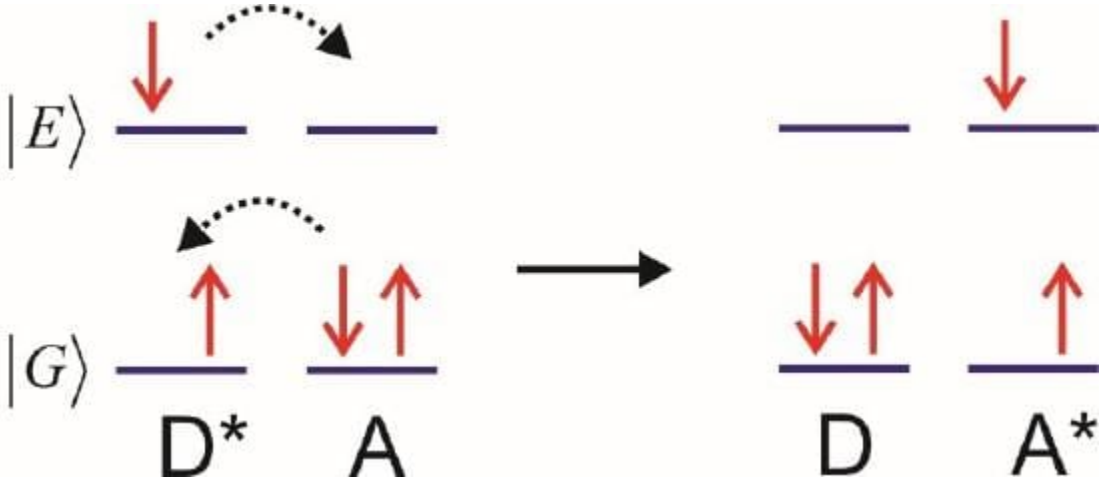


Figure 19.1.5

(d) Singlet fission

Singlet fission refers to splitting of a singlet electronic excitation to create of two excited triplet states, whereas the reverse process is singlet-triplet annihiliation.

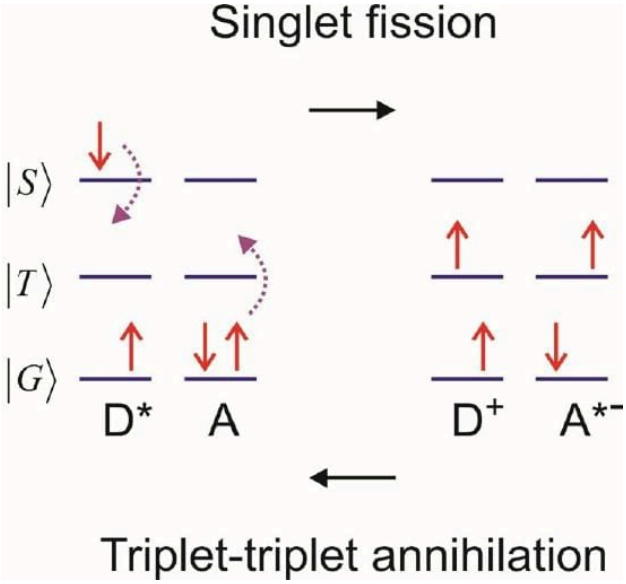


Figure 19.1.6

Note, that this is by no means a comprehensive list of electronic interactions, but it is meant to catalog the most common intermolecular electronic charge transport processes. Of these we will look carefully into the first two processes. There are also additional intramolecular electronic relaxation processes involving two electronic states which we are not addressing, such as internal conversion and intersystem crossing.

This page titled 19.1: Intermolecular Electronic Interactions is shared under a CC BY-NC-SA 4.0 license and was authored, remixed, and/or curated by Andrei Tokmakoff via source content that was edited to the style and standards of the LibreTexts platform.

19.2: Resonance Energy Transfer and Transition Dipole Coupling

Resonance energy transfer is a short-range energy transport process in which the motion of charges within a donor generates a field that induces the motion of charges in an acceptor. Classically, it is described as a dipole-dipole interaction, in which the donor's oscillating dipole moment produces an oscillating field that drives the acceptor dipole into motion. As we described with the driven oscillator problem in Section 6.2, energy is transferred to the acceptor dipole most efficiently when its natural frequency matches that of the donor's. Quantum mechanically, the interaction is described as the coupling of two transition dipole moments.

At its heart, resonance energy transfer originates from Coulomb interactions between the charges on the donor and acceptor:

$$V = \sum_{i,j} \frac{z_i^D z_j^A}{\left| r_i^D - r_j^A \right|} \tag{19.2.1}$$

Here the sum is over the charges (z) of all electrons and nuclei in the donor (i) and acceptor (j). As is, this is challenging to work with, but when the donor and acceptor are well separated, we can recast this formula as a dipole–dipole interaction. We define a frame of reference for the donor and acceptor molecule and assume that the distance between molecules is large. Then we can reduce the charge distributions within those molecules to a point dipole moment, as illustrated in Figure 19.2.1:

$$\begin{aligned} \boldsymbol{\mu}^D &= \sum_i z_i^D \left(\mathbf{r}_i^D - \mathbf{r}_0^D \right) \\ \boldsymbol{\mu}^A &= \sum_j z_j^A \left(\mathbf{r}_J^A - \mathbf{r}_0^A \right) \end{aligned} \tag{19.2.2}$$

The interaction between donor and acceptor takes the form of an interaction between point dipoles:

$$V = \frac{3 \left(\boldsymbol{\mu}_A \cdot \hat{r} \right) \left(\boldsymbol{\mu}_D \cdot \hat{r} \right) - \boldsymbol{\mu}_A \cdot \boldsymbol{\mu}_D}{r^3} \tag{19.2.3}$$

where $r = \left| \mathbf{r}_0^D - \mathbf{r}_0^A \right|$ is the distance between donor and acceptor dipoles and $\hat{r}$ is a unit vector that marks the direction between them. Note the short range $1/r^3$ distance dependence.

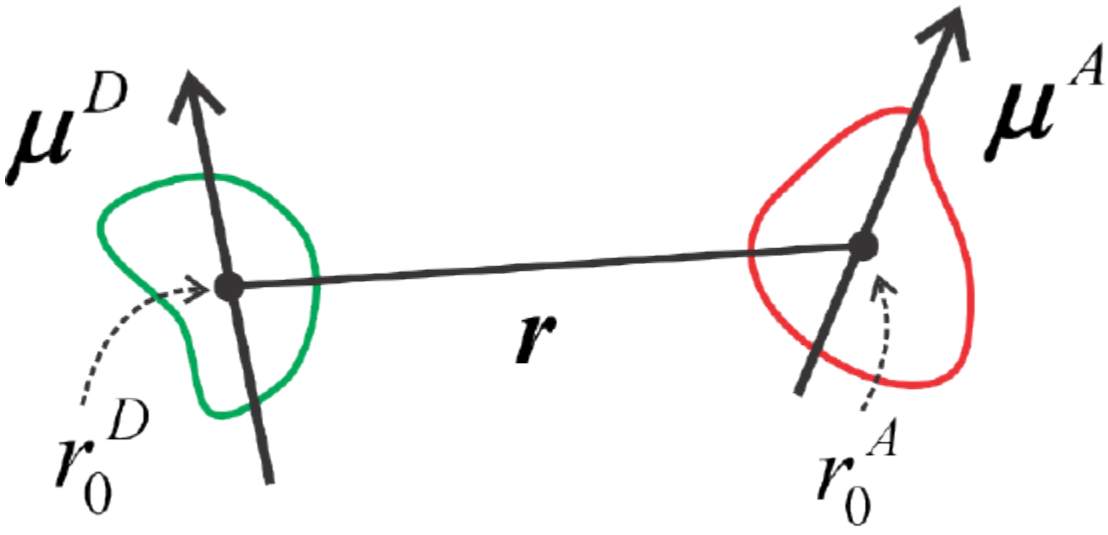


Figure 19.2.1: Illustration of donor-acceptor interactions reduced to an interaction between point dipoles. The charge distributions of the donor and acceptor molecules, encompassed in the green and red lines, are separated by a large distance compared to their spatial dimensions.

We can see from eq. (19.2.3) that the interaction depends on the magnitude, separation, and orientation of the donor and acceptor dipoles. When these properties are fixed and independent, it is convenient to separate the distance and orientation variables. For

the dipole operator, we separate its magnitude and orientation as

$$\boldsymbol{\mu}_A = \hat{u}_A \mu_A \tag{19.2.4}$$

This allows eq. (19.2.3) to be written as

$$V = \mu_A \mu_D \frac{\kappa}{r^3} \tag{19.2.5}$$

where all of the orientational factors are now in the term κ:

$$\kappa = 3\left(\hat{u}_A \cdot \hat{r}\right)\left(\hat{u}_D \cdot \hat{r}\right) - \hat{u}_A \cdot \hat{u}_D \tag{19.2.6}$$

This function carries a value of 2 for a head-to-tail alignment, -1 for head-to-head alignment, and 0 for perpendicular dipoles. Figure 19.2.2 illustrates the case of two parallel dipoles, showing how it varies as a function of the angle between the dipole and the vector defining their separation. This illustrates the importance of orientational variables in resonance energy transfer, since it can change the magnitude and sign of the coupling, or even eliminate what might otherwise be a strong interaction.

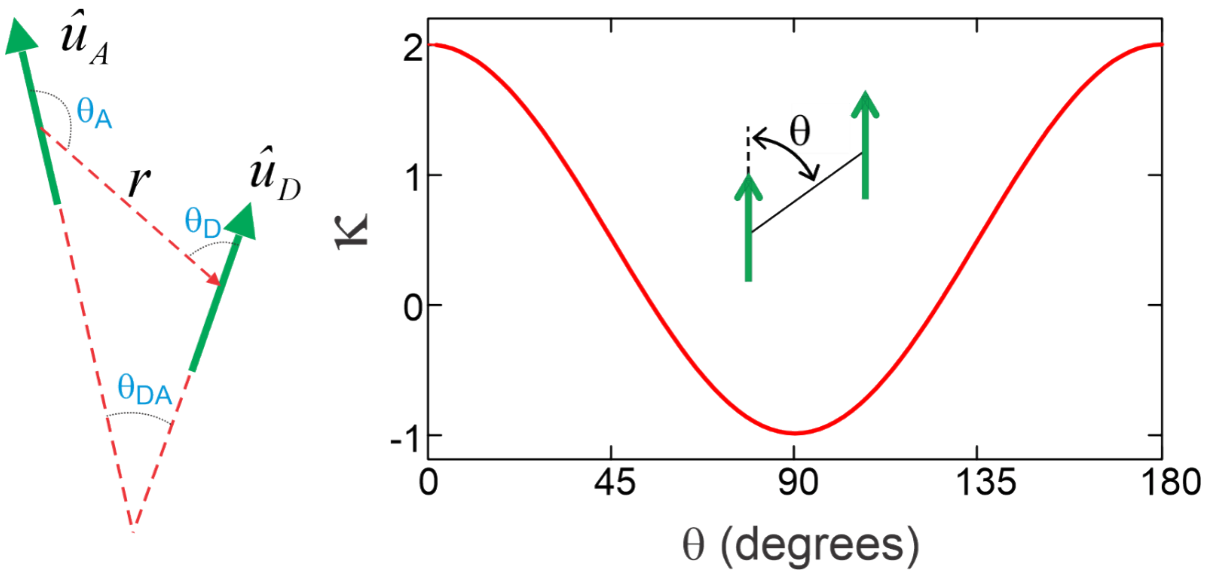


Figure 19.2.2: (Left) Definition of the orientational variables governing the dipole-dipole interaction $\kappa = 3\cos\theta_A \cos\theta_D - \cos\theta_{DA}$. (Right) Dependence of the orientational factor κ on the angle between two parallel dipoles ($\theta = \theta_A = \pi - \theta_D;\ \theta_{DA} = 0$).

As written, the dipole-dipole interaction described by eq. (19.2.3) is time-independent and applies to interactions among all molecular dipoles in condensed matter. Resonance energy transfer refers to the time-dependent consequence of this dipole-dipole coupling, when the initial state of the system is an oscillating donor dipole moment prepared by an external excitation. Now the time-dependent dipole acts as the source of an electromagnetic field that acts on acceptor dipoles. Equation (19.2.3) is still operable for time-dependent dipole interactions, as long as we remain in the electromagnetic near field. This means that the donor and acceptor dipoles are separated by $r \ll c/\Omega$, where Ω is the frequency of the oscillating donor dipole. As before, we also require that r is large compared to the dimensions of the donor and acceptor molecules. This description works well for the case of electronic energy transfer in which one works with separations on the order of a few nanometers.

At donor-acceptor separations beyond the near field, the dipole-dipole interaction disappears due to its $1/r^3$ distance dependence. As we saw when discussing dipole radiation, in the far-field limit the donor acts as a source of electromagnetic radiation with a slower $1/r$ drop in its fieldstrength. This radiation can be absorbed by an acceptor, but this process is classified as radiative energy transfer. As we will see, the rates of energy transfer depend on the square of the coupling; thus, resonance energy transfer scales with $1/r^6$, versus the $1/r^2$ scaling of radiative energy transfer. As a result, radiative energy transfer is a relatively inefficient effect that is only operative over distances longer than the wavelength of the radiation (hundreds of nanometers), while resonance energy transfer is the dominant effect on molecular scales (single nanometers).

Quantum mechanically, the resonant dipole-dipole interaction can be described in the same way, with the dipole operator replacing classical dipole moment. If the energy transfer process is described by

$$D^* + A \rightarrow D + A^* \tag{19.2.7}$$

One can specify the initial state of the joint donor-acceptor system as $|D^*, A\rangle$ and the final state as $|D, A^*\rangle$. The donor-acceptor interaction is computed from

$$\begin{aligned} V_{A,D} &= \langle A^* D| \, V \, |D^* A\rangle \\ &= \frac{\kappa}{r^3} \, \langle A^* D| \, \mu_A \mu_D \, |D^* A\rangle \end{aligned} \tag{19.2.8}$$

When the dipole operators of the donor and acceptor commute, this can be written as a product of donor and acceptor transition dipole moments:

$$V_{A,D} = \frac{\kappa}{r^3} \, \langle A^*| \, \mu_A \, |A\rangle \, \langle D| \, \mu_D \, |D^*\rangle \tag{19.2.9}$$

This is known as transition dipole coupling (TDC).

While our focus here is on electronic energy transfer, transition dipole coupling is also used to describe resonance energy transfer between vibrational transition dipoles in condensed phase spectroscopy, although the range of validity of this model is more limited. Electronic transition dipole moments are typically 1–2 orders of magnitude larger than vibrational transition dipoles, and therefore electronic TDCs are effective on substantially longer distance scales than vibrational TDCs: nanometers versus Ångstroms. In the vibrational case, the dipole-dipole approximation of the donor and acceptor charges made in eq. (19.2.2) often cannot be justified because the short distance between the two molecules is on the same scale as the charge distributions moving in the vibration, and more detailed descriptions of the Coulombic interaction in eq. (19.2.1) are needed.

This page titled 19.2: Resonance Energy Transfer and Transition Dipole Coupling is shared under a CC BY-NC-SA 4.0 license and was authored, remixed, and/or curated by Andrei Tokmakoff via source content that was edited to the style and standards of the LibreTexts platform.

19.3: Förster Resonance Energy Transfer

Förster resonance energy transfer (FRET) refers to the resonance energy transfer of an electronic excitation from a donor molecule to an acceptor molecule. Named for Förster's widely accessible theory,(1)(2) this description uses transition dipole coupling to describe the rate of transfer when the oscillations of an optically driven electronic transition on the donor are resonant with an electronic energy gap of the acceptor. The expressions Förster obtained for the energy transfer rate describe the resonance conditions in terms of readily obtained donor emission and acceptor absorption spectra, making them very useful for interpreting experiments, and the sharp $1/r^6$ dependence on distance is often used to spectroscopically characterize the proximity of donor and acceptor. Because fluorescent donors are both a practical and theoretical requirement, FRET is sometimes considered the acronym for "fluorescence resonance energy transfer," but this association can lead to confusion. It is important to remember that the energy transfer mechanism is a near-field non-radiative process, even if fluorescence plays an important role in the experiment.

Our objective here is to describe the molecular factors that govern w_{ET} in the limit of weak coupling, where a Golden Rule description is relevant. Our system will be described by the joint state of the donor and acceptor, which includes the electronic ground and excited states of both donor and acceptor molecules (D, D^*, A, and A^*). Although there are four possible electronic configurations of the joint system, for our purposes, we will only need to consider the two electronic configurations that play a role in the resonance transfer: the initial state $|D^*A\rangle$ and the final state $|DA^*\rangle$. We will make use of the displaced harmonic oscillator model, and thus each ket specifies the electronic state (e or g) and vibrational state (n) of the donor and acceptor. For instance:

$$|D^*A\rangle = |e_D n_D; g_A n_A\rangle \tag{19.3.1}$$

Working with the DHO approach, the Hamiltonian of the donor-acceptor system is:

$$\begin{aligned} H_0 =& |D^*\rangle\, H_E^D\, \langle D^*| + |D\rangle\, H_G^D\, \langle D| \\ &+ |A^*\rangle\, H_E^A\, \langle A^*| + |A\rangle\, H_G^A\, \langle A| \end{aligned} \tag{19.3.2}$$

Each of these terms is defined as previously in Chapter 16, with both electronic energy and dependence on a displaced nuclear coordinate. The donor and acceptor electronic energy gaps each depend on independent nuclear coordinates q_D and q_A, and their excited states have different displacements d_D and d_A. To illustrate how these various factors define each term each term in eq. (19.3.2), we use the donor excited state H_E^D as an example. This state is defined with both E_e^D, the electronic energy of the donor excited state, and H_e^D, the dependence of the total energy on the displacement of the donor coordinate:

$$H_E^D = |e_D\rangle\, E_e^D\, \langle e_D| + H_e^D \tag{19.3.3}$$

$$H_e^D = \hbar\omega_D \left(\underset{\sim}{p}_D^2 + \left(\underset{\sim}{q}_D - \underset{\sim}{d}_D \right)^2 \right) \tag{19.3.4}$$

For this Hamiltonian, the donor reorganization energy, Huang-Rhys factor, and electronic excited state displacement are related by

$$\lambda_D = \hbar\omega_D S_D = \tfrac{1}{2} m\omega_D^2 d_D^2 \tag{19.3.5}$$

and the electronic energy difference is given by

$$\omega_{eg}^D = \left(E_e^D - E_g^D \right)/\hbar \tag{19.3.6}$$

Similar expressions hold for the acceptor: $\lambda_A = \hbar\omega_A S_A = \tfrac{1}{2} m\omega_A^2 d_A^2$ and $\omega_{eg}^A = \left(E_e^A - E_g^A \right)/\hbar$.

The four electronic states (D, D^*, A, and A^*) are pictured in Figure 19.3.1. Figure 19.3.1 also identifies the sequence of absorption, resonance energy transfer, and fluorescence events that occur in a FRET experiment. These processes occur at different frequencies, as governed by the electron-nuclear coupling, and the donor and acceptor absorption and fluorescence lineshapes are pictured in Figure 19.3.2.

The sequence of events in a FRET experiment are as follows. (1) Absorption of light by the donor from its ground state ($q_D = 0$) is followed by rapid vibrational relaxation that dissipates the reorganization energy of the donor λ_D in the excited state over the course of picoseconds. (2) This leaves the donor in an electronic coherence that oscillates at the energy gap Ω_{D^*}, corresponding

to the excited donor at $q_D = d_D$. The time scale for FRET is typically nanoseconds, so this picosecond preparation process is typically much faster than the transfer phase. (3) For energy transfer to occur, there must be resonance between the Ω_{D^*} frequency oscillation of the excited donor coherence at $q_D = d_D$ and the electronic energy gap Ω_A of the acceptor in the ground state configuration $q_A = 0$. (4) Following the energy transfer to the acceptor, there is vibrational relaxation by an amount λ_A. Then the acceptor emits fluorescence that is spectrally red-shifted from the donor fluorescence.

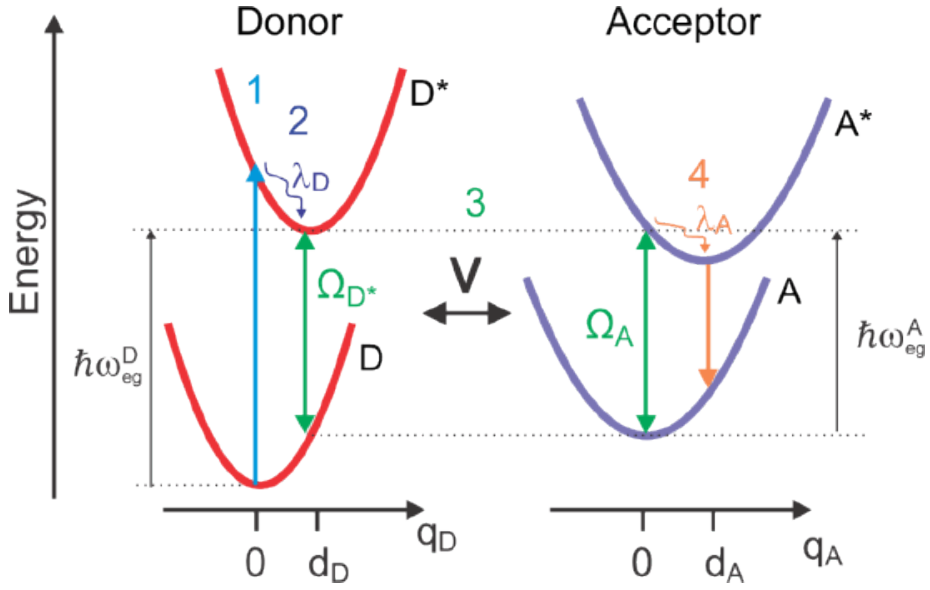


Figure 19.3.1: Ground and excited states potential energy surfaces of the the donor and acceptor molecules and the sequence of interactions in the FRET process. (1) Initial electronic excitation of the donor, (2) vibrational relaxation results in a lower donor energy gap Ω_{D^*}, (3) resonance between the donor and acceptor energy gaps leads to energy transfer to the acceptor, and (4) the electronic excitation of the acceptor relaxes and is emitted as red-shifted fluorescence.

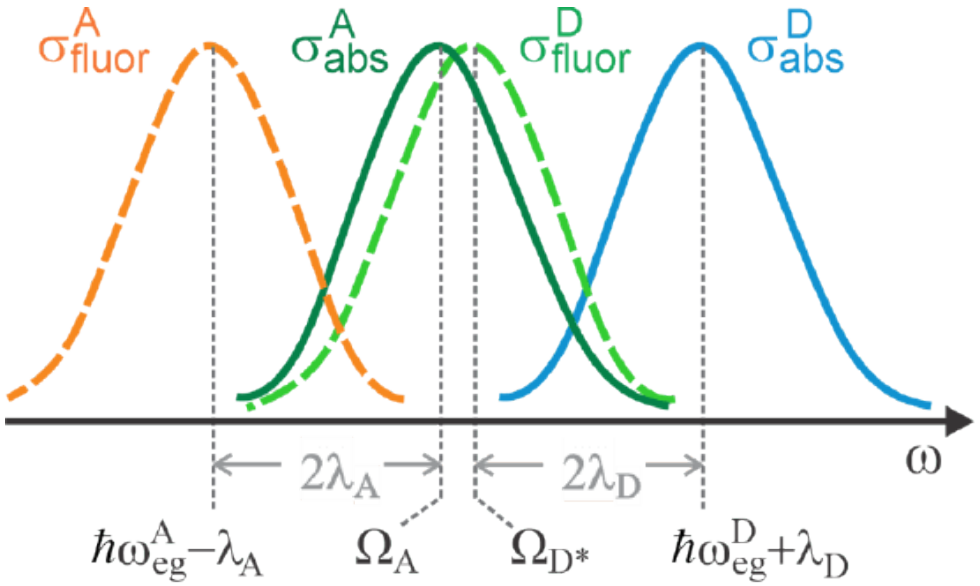


Figure 19.3.2: Illustration of the absorption and fluorescence lineshapes σ of the donor and acceptor. The frequency axis is labeled by the mean electronic energy gap for the four processes.

We will describe step (3), using the Golden Rule to calculate the rate of energy transfer between the initial state $|D^*A\rangle$ and the final state $|A^*D\rangle$. For this purpose, it is helpful to define the vertical energy gaps for the donor and acceptor in the initial state, Ω_{D^*} and Ω_A, shown in Figure 19.3.1. Within the DHO framework, these can be expressed as

$$\begin{aligned} \Omega_{D^*} &= \omega_{eg}^D - \lambda_D/\hbar \qquad (q_D = d_D) \\ \Omega_A &= \omega_{eg}^A + \lambda_A/\hbar \qquad (q_A = 0) \end{aligned} \tag{19.3.7}$$

The maximum transfer rate will be observed when $\Omega_{D^*} \approx \Omega_A$, which naturally results in the language of resonance in the energy

transfer process. However, there is a risk that one might begin to interpret this as a static phenomenon. As our discussion of fluctuations illustrated, the same formalism can be recast as a fluctuating energy gap, whose dynamics are characterized by a spectral density or energy gap correlation function. In this picture the electronic energy gaps of the donor in its excited state and the acceptor in its ground state both exhibit time dependent fluctuations due to the nuclear dynamics, and energy transfer proceeds efficiently when degeneracies occur between Ω_{D^*} and Ω_A (Figure 19.3.3).

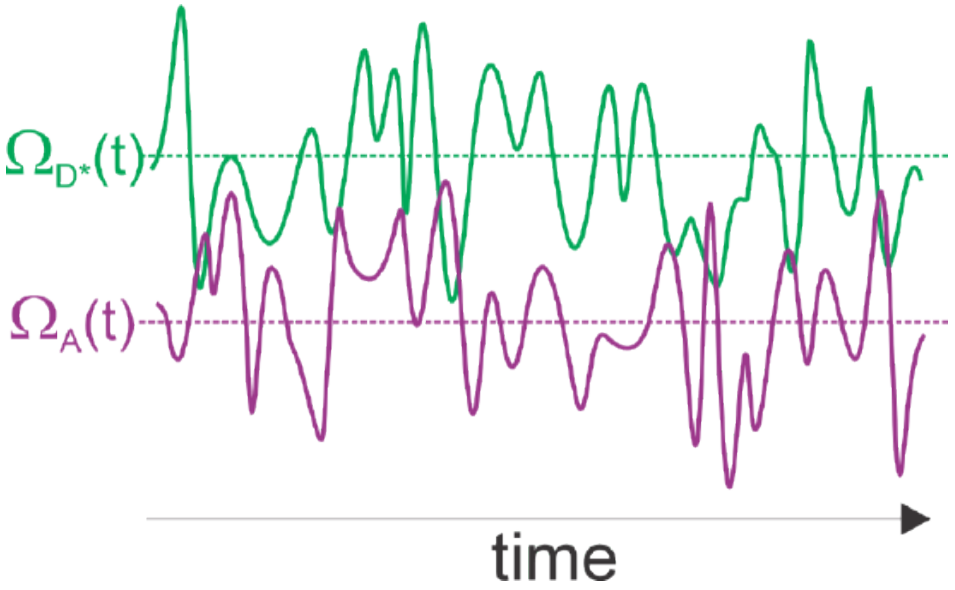


Figure 19.3.3: Time-dependent fluctuations in the energy gaps for a donor and acceptor in a condensed phase environment.

Since the donor and acceptor are weakly coupled, we can write our Hamiltonian for this problem in a form that can be solved by perturbation theory ($H = H_0 + V$). For the interaction between donor and acceptor we use the dipole-dipole coupling expression from eq. (19.2.05)

$$V = \boldsymbol{\mu}_A \boldsymbol{\mu}_D \frac{\kappa}{r^3} \tag{19.3.8}$$

where $\boldsymbol{\mu}_D$ and $\boldsymbol{\mu}_A$ are the dipole operators and κ contains the dipole orientational factors

$$\kappa = 3\left(\hat{u}_A \cdot \hat{r}\right)\left(\hat{u}_D \cdot \hat{r}\right) - \hat{u}_A \cdot \hat{u}_D \tag{19.3.9}$$

Note, this separation implies that the orientation of the dipoles is independent of their positions relative to one another—an assumption that regularly comes into question. The dipole operators here only act on the electronic states of one molecule (the donor or acceptor) and are independent of the nuclear configuration (the Condon approximation). We can express the dipole operators in terms of the matrix elements that couple the ground and excited electronic states for the donor and acceptor as

$$\mu_A = |A\rangle\, \mu_{AA^*}\, \langle A^*| + |A^*\rangle\, \mu_{A^*A}\, \langle A| \tag{19.3.10}$$

$$\mu_D = |D\rangle\, \mu_{DD^*}\, \langle D^*| + |D^*\rangle\, \mu_{D^*D}\, \langle D| \tag{19.3.11}$$

We can obtain the rates of energy transfer by using the Golden Rule in the form of a correlation function in the interaction picture Hamiltonian:

$$w_{k\ell} = \frac{1}{\hbar^2} \int_{-\infty}^{+\infty} dt\, \langle V_I(t) V_I(0) \rangle \tag{19.3.12}$$

where $V_I(t) = e^{\mathrm{i}H_0 t/\hbar} V e^{-\mathrm{i}H_0 t/\hbar}$. Note that this is not a Fourier transform since we are applying the expression for a constant perturbation. The correlation function is evaluated as an average over an equilibrium system, even though we are initially in the excited donor state. This is reasonable for the case that there is a clear time scale separation between the picosecond vibrational relaxation following the initial excitation of the donor and the time scale (inverse rate) of the energy transfer process. Given the initial state $|D^*A\rangle$, on substituting eq. (19.3.8) in eq. (19.3.12) we find

$$w_{\mathrm{ET}} = \frac{1}{\hbar^2} \int_{-\infty}^{+\infty} dt \frac{\langle \kappa^2 \rangle}{r^6} \langle D^*A|\, \mu_D(t)\mu_A(t)\mu_D(0)\mu_A(0)\, |D^*A\rangle \tag{19.3.13}$$

Here the donor and acceptor dipole operators in the interaction picture are

$$\begin{aligned}\mu_D(t) &= e^{\mathrm{i}(H_E^D+H_G^D)t/\hbar}\ \mu_D\ e^{-\mathrm{i}(H_E^D+H_G^D)/\hbar} \\ \mu_A(t) &= e^{\mathrm{i}(H_G^A+H_G^E)t/\hbar}\ \mu_A\ e^{-\mathrm{i}(H_G^A+H_G^E)t/\hbar}\end{aligned} \tag{19.3.14}$$

Note the sharp $1/r^6$ distance dependence, which arises from squaring the transition dipole coupling.

In writing eq. (19.3.13) we have also neglected the rotational motion of the dipoles. Even if we have already separated the magnitude and orientation of the dipole moments, if they reorient on the timescale of energy transfer, we should calculate an orientation average as a correlation function:

$$\left\langle \kappa^2 \right\rangle = \langle \kappa(t)\kappa(0) \rangle \tag{19.3.15}$$

Here the thermal average is over the direction of excited donors at time zero and the orientation of acceptors are time t. This factor is more readily evaluated if the orientation of the donor is initially isotropically distributed and the acceptor rapidly reorients to also become isotropically distributed regardless of its initial configurations. Then we orientationally average over all possible donor and acceptor orientation to obtain $\left\langle \kappa^2 \right\rangle = 2/3$. The description of $\left\langle \kappa^2 \right\rangle$ under various static and dynamics conditions are the subject of an extensive literature, as is the correlation of κ with r.

Since the dipole operators act only on $|A\rangle$ or $|D^*\rangle$ and the Hamiltonians for D and A commute, we can separate the correlation function in eq. (19.3.13) into a product of two correlation functions for the donor and acceptor states.

$$\begin{aligned}w_{\mathrm{ET}} &= \frac{1}{\hbar^2}\int_{-\infty}^{+\infty} dt\, \frac{\left\langle \kappa^2 \right\rangle}{r^6} \left\langle D^* \right| \mu_D(t)\mu_D(0) \left| D^* \right\rangle \left\langle A \right| \mu_A(t)\mu_A(0) \left| A \right\rangle \\ &= \frac{1}{\hbar^2}\int_{-\infty}^{+\infty} dt\, \frac{\left\langle \kappa^2 \right\rangle}{r^6} C_{D^*D^*}(t) C_{AA}(t)\end{aligned} \tag{19.3.16}$$

This is an overlap integral between the dipole correlation functions for the dynamics of the donor in the excited state and the acceptor in its ground state. Remember that these are the same correlation functions that we used in describing donor emission (fluorescence) and acceptor absorption in our discussion of the DHO model.

Remembering that $|D^*\rangle$ represents the electronic and nuclear configuration $|e_D n_D\rangle$, we can use the displaced harmonic oscillator Hamiltonian or energy gap Hamiltonian to evaluate the correlation functions. Let's examine the integral in eq. (19.3.16), for the case of the Gaussian lineshapes we obtained in Section 16.1 from the short time approximation of the DHO correlation function (applying $\exp(\pm \mathrm{i}\omega_0 t) \approx 1 \pm \mathrm{i}\omega_0 t - \omega_0^2 t^2/2$). The donor emission and acceptor absorption correlation functions are

$$\begin{aligned}C_{D^*D^*}(t) &= |\mu_{DD^*}|^2 \exp\left(\mathrm{i}\omega_{eg}^D t + \mathrm{i}S_D\omega_D t - \frac{1}{2}S_D\omega_D^2 t^2\right) \\ &= |\mu_{DD^*}|^2 \exp\left(\mathrm{i}\omega_{D^*} t - \frac{1}{2\hbar}\lambda_D\omega_D t^2\right)\end{aligned} \tag{19.3.17}$$

$$\begin{aligned}C_{AA}(t) &= |\mu_{AA^*}|^2 \exp\left(-\mathrm{i}\omega_{eg}^A t - \mathrm{i}S_A\omega_A t - \frac{1}{2}S_A\omega_A^2 t^2\right) \\ &= |\mu_{AA^*}|^2 \exp\left(-\mathrm{i}\omega_A t - \frac{1}{2\hbar}\lambda_A\omega_A t^2\right)\end{aligned} \tag{19.3.18}$$

Evaluating the integral, we find

$$w_{\mathrm{ET}} = \frac{\kappa^2 |\mu_{DD^*}|^2 |\mu_{AA^*}|^2}{\hbar^2 r^6}\sqrt{\frac{2\pi\hbar}{\lambda_D\omega_D + \lambda_A\omega_A}}\exp\left\{-\frac{(\Omega_{D^*} - \Omega_A)^2}{2\hbar(\lambda_D\omega_D + \lambda_A\omega_A)}\right\} \tag{19.3.19}$$

We observe that the peak efficiency occurs when the energy gaps for the donor excited state and acceptor ground state are matched $\Omega_{D^*} = \Omega_A$, but that energy transfer can still remain effective within a range of frequencies governed by the donor and acceptor reorganization energy $\sigma = \sqrt{\lambda_A\hbar\omega_A + \lambda_D\hbar\omega_D}$.

Overlap Integral

In practice, the overlap integrals are commonly evaluated in the frequency domain. The dipole correlation functions can be expressed in terms of the inverse Fourier transforms of a fluorescence or absorption lineshape:

$$C_{D^*D^*}(t) = \frac{1}{2\pi}\int_{-\infty}^{+\infty} d\omega\, e^{-i\omega t}\sigma^{D}_{\text{fluor}}(\omega) \tag{19.3.20}$$

$$C_{AA}(t) = \frac{1}{2\pi}\int_{-\infty}^{+\infty} d\omega\, e^{-i\omega t}\sigma^{A}_{\text{abs}}(\omega) \tag{19.3.21}$$

We then make use of Parsival's Theorem, which states that if a Fourier transform pair is defined for two functions, the integral over a product of those functions is equal whether evaluated in the time or frequency domain:

$$\int_{-\infty}^{\infty} f_1(t) f_2^*(t)\, dt = \frac{1}{2\pi}\int_{-\infty}^{\infty} \tilde{f}_1(\omega)\tilde{f}_2^*(\omega)\, d\omega \tag{19.3.22}$$

This allows us to express the energy transfer rate as a spectral overlap integral J_{DA} between the donor fluorescence and acceptor absorption spectra:

$$w_{\text{ET}} = \frac{\langle\kappa^2\rangle}{2\pi\hbar^2 r^6}\left|\mu_{DD^*}\right|^2\left|\mu_{AA^*}\right|^2 J_{DA} \tag{19.3.23}$$

$$J_{DA} = \int_{-\infty}^{+\infty} d\omega\, \underset{\sim}{\sigma}^{A}_{\text{abs}}(\omega)\underset{\sim}{\sigma}^{D}_{\text{fluor}}(\omega) \tag{19.3.24}$$

Here we have factored out the transition dipole matrix elements and written the overlap integral in terms of $\underset{\sim}{\sigma}$, the unit area normalized lineshape: $\underset{\sim}{\sigma} = \sigma/\left|\mu\right|^2$. From eq. (19.3.23) we see that the energy transfer rate scales as r^{-6}, depends on the strengths of the electronic transitions for donor and acceptor molecules, and requires overlap between the donor fluorescence and acceptor absorption spectra.

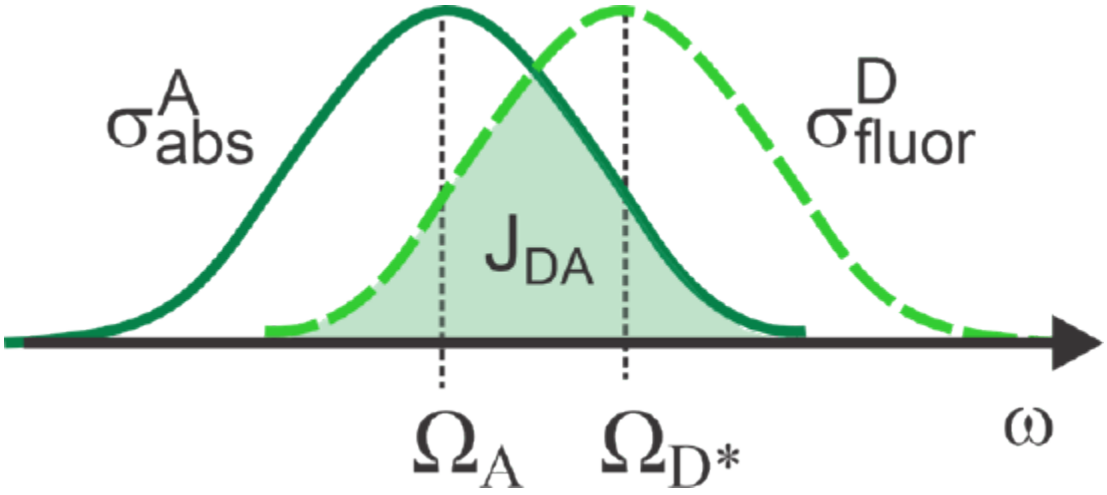


Figure 19.3.4: Variables describing the donor emission and acceptor absorption lineshapes in calculating the spectral overlap integral.

As illustrated in Figure 19.3.4, the overlap integral is a measure of how well matched in frequency the donor emission and acceptor absorption transitions are. Unlike the delta-function expression, this is a smoothly varying metric of how close to resonance and how efficient the dipole-dipole coupling is. To illustrate the resonance condition, let's calculate the overlap integral using the Gaussian lineshapes we obtain from equations (19.3.17) and (19.3.18):

$$\underset{\sim}{\sigma}^{D}_{\text{fluor}}(\omega) = \sqrt{\frac{2\pi\hbar}{\lambda_D\omega_D}}\exp\left(-\frac{\left(\hbar\omega-\hbar\Omega_{D^*}\right)^2}{2\lambda_D\hbar\omega_D}\right) \tag{19.3.25}$$

$$\underset{\sim}{\sigma}^{A}_{\text{abs}}(\omega) = \sqrt{\frac{2\pi\hbar}{\lambda_A\omega_A}}\exp\left(-\frac{\left(\hbar\omega-\hbar\Omega_{A}\right)^2}{2\lambda_A\hbar\omega_A}\right) \tag{19.3.26}$$

From which we obtain

$$J_{DA} = (2\pi)^{\frac{3}{2}}\sqrt{\frac{\hbar}{\omega_A\lambda_A+\omega_D\lambda_D}}\exp\left(-\frac{\left(\Omega_{D^*}-\Omega_A\right)^2}{2\hbar\left(\omega_A\lambda_A+\omega_D\lambda_D\right)}\right) \tag{19.3.27}$$

and the energy transfer rate in eq. (19.3.19). Again, the exponential argument is maximized when the peak absorption frequency for the acceptor in the ground state Ω_A matches the emission frequency for the donor in the excited state Ω_{D^*}, and the effective frequency range over which energy transfer remains efficient is governed by the linewidths of absorption and emission spectra $\sigma_A = \sqrt{\lambda_A \hbar \omega_A}$ and $\sigma_D = \sqrt{\lambda_D \hbar \omega_D}$.

Critical transfer distance

The significant impact of Förster's theory was that he was able to recast eq. (19.3.19) into a form that could be related to readily accessible experimental measurements and provide a clear manner of predicting the distance over which FRET is efficient. To simplify the prefactors in eq. (19.3.19), he related $|\mu_{AA^*}|^2$ to the molar extinction coefficient for acceptor absorption, and he related $|\mu_{DD^*}|^2$ to the donor radiative lifetime in the absence of the acceptor, τ_D, (another experimental observable) using the Einstein A coefficient. The latter assumption oversimplifies the photophysics of dye molecules, but this assumption allows one to express the rate of energy transfer in a simple form, wrapping the spectral overlap integral and proportionality factors into the critical transfer distance R_0:

$$w_{\mathrm{ET}} = \frac{1}{\tau_D}\left(\frac{R_0}{r}\right)^6 \tag{19.3.28}$$

We note that the energy transfer rate carries a rapidly dropping $1/r^6$ distance dependence, and that R_0 marks the distance at which the rate of energy transfer equals the rate of donor fluorescence $w_{\mathrm{fl}} = \tau_D^{-1}$. Thus, at a separation of R_0 a donor excitation has equal likelihood of relaxing through fluorescence or energy transfer. Including all of the proportionality factors, such as the $(4\pi\varepsilon_0)^{-1}$ we left out of eq. (19.3.8), and accounting for the nonradiative relaxation of the donor, the practical definition which allows one to calculate R_0 readily from experimental data is

$$R_0^6 = \frac{9000\ln(10)\phi_D\left\langle\kappa^2\right\rangle}{128\pi^5 n^4 N_A}\int_0^\infty d\bar{\nu}\,\frac{\underset{\sim}{\sigma}^D_{\mathrm{fluor}}(\bar{\nu})\;\varepsilon_A(\bar{\nu})}{\bar{\nu}^4} \tag{19.3.29}$$

$\bar{\nu}$ represents units of frequency in cm^{-1}. The fluorescence spectrum $\underset{\sim}{\sigma}^D_{\mathrm{fluor}}$ must be normalized to unit area, so that $\underset{\sim}{\sigma}^D_{\mathrm{fluor}}(\bar{\nu})$ is expressed in cm (inverse wavenumbers). The absorption spectrum $\varepsilon_A(\bar{\nu})$ must be expressed in molar decadic extinction coefficient units $\mathrm{liter/mol\cdot cm}$. n is the index of refraction of the solvent, N_A is Avagadro's number, and ϕ_D is the donor fluorescence quantum yield.

FRET efficiency

While there are different ways of performing them, FRET experiments generally measure the efficiency of transfer from donor to acceptor, rather than the rate itself. That is, given an electronically excited donor molecule, what is the probability that this excitation will transfer to the acceptor rather than relaxing through other donor fluorescence or other non-radiative processes? The energy transfer efficiency can be expressed in terms of the underlying rates of energy transfer w_{ET}, the donor fluorescence radiative emission rate w_{fl}, and non-radiative donor relaxation processes w_{nr} as

$$\eta = \frac{w_{\mathrm{ET}}}{w_{\mathrm{ET}} + w_{\mathrm{fl}} + w_{\mathrm{nr}}} \tag{19.3.30}$$

This equation can be re-written in different forms. In the absence of the acceptor τ_D, the donor fluorescence lifetime reflects the radiative (fluorescence) and non-radiative donor relaxation rates, therefore:

$$\tau_D^{-1} = w_{\mathrm{fl}} + w_{\mathrm{nr}} \tag{19.3.31}$$

Equation (19.3.31) can be used with eq. (19.3.28) to express the distance dependence of the transfer efficiency as

$$\eta(r) = \frac{1}{1+\left(\frac{r}{R_0}\right)^6} \tag{19.3.32}$$

This function, pictured in Figure 19.3.5, shows that R_0 marks the point of 50% FRET efficiency and that the donor-acceptor separation beyond which FRET becomes inefficient (typically a few nanometers for bright dye molecules). Small changes in distance near R_0 lead to large changes in FRET efficiency, and therefore η can be used as an effective proximity sensor to determine if acceptors lie closer than R_0. Within a range of approximately $\pm 30\%$ of R_0 there is a clean correlation between η and

r, which is the reason that FRET is often called a spectroscopic ruler; however, note that η is completely insensitive to distance above and below this range.

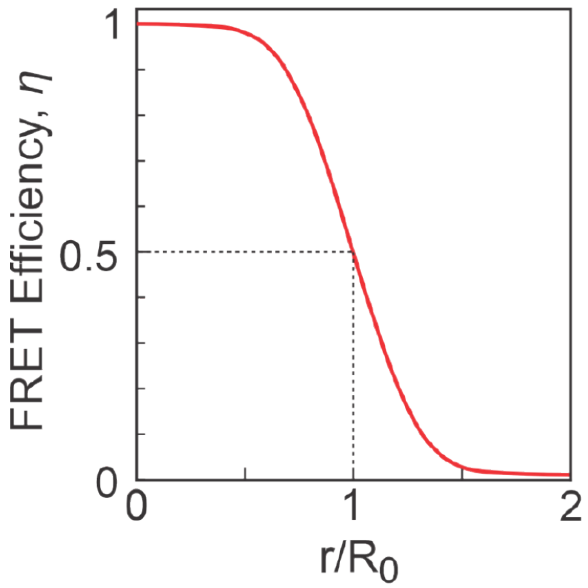


Figure 19.3.5: FRET efficiency as a function of donor-acceptor separation

To experimentally measure the FRET efficiency, one approach it to compare the donor fluorescence lifetime in the absence and presence of the acceptor. Since the fluorescence lifetime reflects the relaxation of the initial excited donor population through all relaxation channels, in the presence of the acceptor it is given by

$$\tau_{DA}^{-1} = w_{\mathrm{ET}} + w_{\mathrm{fl}} + w_{\mathrm{nr}} \tag{19.3.33}$$

Inserting this and eq. (19.3.31) into eq. (19.3.30) allows us to express the FRET efficiency as

$$\eta = 1 - \frac{\tau_{DA}}{\tau_D} \tag{19.3.34}$$

Thus, the efficiency of energy transfer reflects the fractional decrease of the donor fluorescence lifetime due to the acceptor.

Since the rate of donor fluorescence emission is proportional to fluorescence intensity in steady state measurements, η can likewise be measured by the change in fluorescence intensity on adding the acceptor. With continuous excitation, the intensity of emitted donor fluorescence is proportional to the rate of excitation k_{ex} and the rate of fluorescence emission, w_{fl}. The donor fluorescence intensities without and with the acceptor present are given by

$$I_D \propto \frac{w_{\mathrm{fl}}}{w_{\mathrm{fl}} + w_{\mathrm{nr}}} k_{\mathrm{ex}} \qquad I_{DA} = \frac{w_{\mathrm{fl}}}{w_{\mathrm{ET}} + w_{\mathrm{fl}} + w_{\mathrm{nr}}} k_{\mathrm{ex}} \tag{19.3.35}$$

Using these expressions, we can show that the energy transfer efficiency is related to the fractional change of intensity upon introducing the acceptor:

$$\eta_{\mathrm{ET}} = 1 - \frac{I_{DA}}{I_D} \tag{19.3.36}$$

Changes in FRET efficiency can also be measured by observing anticorrelated changes in donor and acceptor intensity, I_{DA} and I_A, for instance by measuring the fraction of the intensity emitted by donor and acceptor: $\phi_{DA} = I_{DA}/\left(I_{DA} + I_A\right)$ and $\phi_A = I_A/\left(I_{DA} + I_A\right)$, or by $\phi_A - \phi_{AD}$. This is a practical experimental strategy for observing changes in η; however, measurements involving acceptor fluorescence cannot be related to the FRET efficiency in any simple way, since they also depend on the acceptor's photophysical properties.(3)(4)(5)

References

(1) Förster, T. Zwischenmolekulare Energiewanderung und Fluoreszenz. *Annalen der Physik* **1948**, *437* (1-2), 55-75. DOI: 10.1002/andp.19484370105

(2) Förster, T. Transfer mechanisms of electronic excitation. *Discussions of the Faraday Society* **1959**, *27*, 7-17, 10.1039/DF9592700007. DOI: 10.1039/DF9592700007

(3) Andrews, D. L. A unified theory of radiative and radiationless molecular energy transfer. *Chemical Physics* **1989**, *135* (2), 195-201. DOI: 10.1016/0301-0104(89)87019-3

(4) Lakowicz, J. R. *Principles of Fluorescence Spectroscopy*, 3rd ed.; Springer, 2006. DOI: 10.1007/978-0-387-46312-4

(5) Scholes, G. D. Long-range resonance energy transfer in molecular systems. *Annual Review of Physical Chemistry* **2003**, *54*, 57-87. DOI: 10.1146/annurev.physchem.54.011002.103746

This page titled 19.3: Förster Resonance Energy Transfer is shared under a CC BY-NC-SA 4.0 license and was authored, remixed, and/or curated by Andrei Tokmakoff via source content that was edited to the style and standards of the LibreTexts platform.

19.4: Marcus Theory for Electron Transfer

The displaced harmonic oscillator (DHO) formalism and the Energy Gap Hamiltonian have been used extensively to describe charge transport reactions, such as electron and proton transfer. Here we describe the rates of electron transfer (ET) between weakly coupled donor and acceptor states when the potential energy depends on a nuclear coordinate, i.e., nonadiabatic electron transfer. These results reflect the findings of Marcus' theory of electron transfer.

We can represent the problem as calculation of the transfer or reaction rate for the transfer of an electron from a donor to an acceptor

$$D + A \rightarrow D^{+} + A^{-} \tag{19.4.1}$$

This reaction is mediated by a nuclear coordinate q. This need not be, and generally isn't, a simple vibrational coordinate. For electron transfer in solution, we most commonly consider electron transfer to progress along a solvent rearrangement coordinate, in which the solvent reorganizes its configuration so that dipoles or charges help to stabilize the extra negative charge at the acceptor site. This type of *collective* coordinate is illustrated in Figure 19.4.1. It's important to recognize that the solvent dipoles are not responding to the electron hopping to the acceptor. Rather, the electron motion and natural fluctuations in the solvent are coupled, and the electron transfer is enabled by natural fluctuations in solvent configuration. The external reorganization of the medium along the electron transfer coordinate is referred to as "outer shell" electron transfer, whereas the response of internal vibrational modes that change with ET is called "inner shell". The influence of collective solvent rearrangements or intramolecular vibrations can be captured with the use of an electronic transition coupled to a harmonic bath.

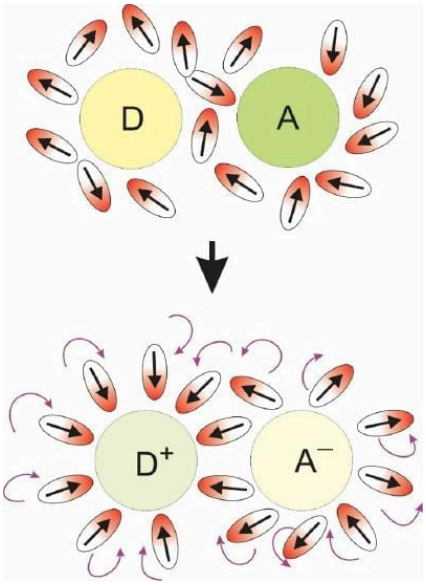


Figure 19.4.1: Illustration of a solvation coordinate in which the reorganization of donor dipoles stabilizes the new charge separated configuration.

Normally we associate the rates of electron transfer with the free energy along the electron transfer coordinate. Processes such as the ones pictured in Figure 19.4.1, with electrons hopping back and forth between particles, are conceptually represented through diabatic energy surfaces (Figure 19.4.2). These diabatic states are mixed in the crossing region by electronic coupling J, resulting in transfer. From this adiabatic surface, the rate of transfer for the forward reaction is related to the flux across the barrier. From classical transition state theory, we can associate the rate with the free energy barrier using $k_f = A \exp\left(-\Delta G^{\dagger}/k_B T\right)$. Quantum mechanically, if the coupling is weak, we can describe the rates of transfer between donor and acceptor in the diabatic basis with the Golden Rule.

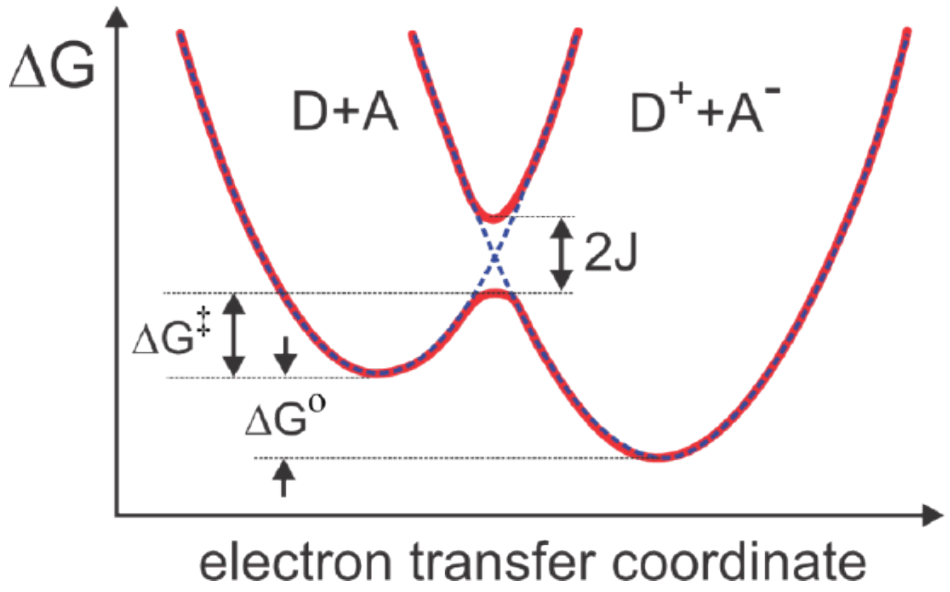


Figure 19.4.2: Adiabatic free energy surfaces describing states for the electron on the donor or acceptor along the electron transfer coordinate.

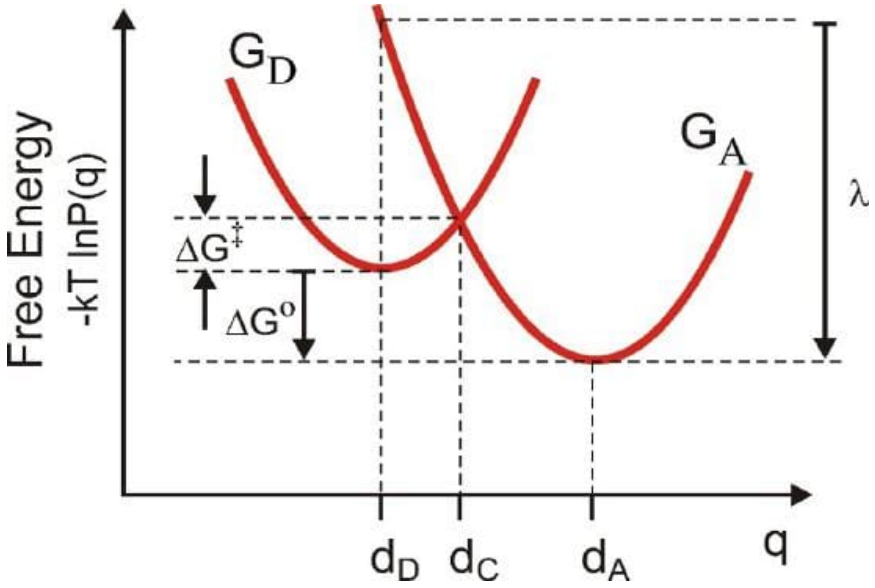


Figure 19.4.3: Model for nonadiabatic description of electron transfer using the displaced harmonic oscillator.

To begin, we consider a simple classical derivation of the free-energy barrier and the rate of electron transfer from donor to acceptor states for the case of weakly coupled diabatic states (Figure 19.4.3). First, we assume that the free energy or potential of mean force for the initial and final state, $G(q) = -k_B T \ln P(q)$, is well represented by two parabolas with different displacements along the same nuclear coordinate, q:

$$\begin{aligned} G_D(q) &= \frac{1}{2} m\omega_0^2 (q - d_D)^2 \\ G_A(q) &= \frac{1}{2} m\omega_0^2 (q - d_A)^2 + \Delta G^\circ \end{aligned} \tag{19.4.2}$$

Here ΔG° is the standard free energy change for the transfer of an electron from the donor to the acceptor. It is also helpful to define the reorganization energy λ, the energy that would need to be dissipated on the acceptor surface if the electron were abruptly shifted from the donor to the acceptor at $q = d_D$,

$$\begin{aligned} \lambda &= G_A(d_D) - G_A(d_A) \\ &= \frac{1}{2} m\omega_0^2 (d_D - d_A)^2 \end{aligned} \tag{19.4.3}$$

Note, this is the same as the energy needed to displace the donor state from its equilibrium position d_D to d_A, the nuclear configuration that is most stable for the acceptor state.

To find the barrier height $\Delta G^{\ddagger}$, we first find the point d_C where the two parabolas cross: $G_D(d_C) = G_A(d_C)$. Using eq. (19.4.2) and solving for d_C gives

$$\begin{aligned} d_C &= \frac{\Delta G^{\circ}}{m\omega_0^2}\left(\frac{1}{d_A - d_D}\right) + \frac{d_A + d_D}{2} \\ &= \frac{\Delta G^{\circ}}{2\lambda}\left(d_A - d_D\right) + \frac{d_A + d_D}{2} \end{aligned} \tag{19.4.4}$$

Then, the free energy barrier for electron transfer $\Delta G^{\ddagger}$. in the perturbative limit can be calculated as the free energy difference between the donor at d_C relative to equilibrium (d_D):

$$\begin{aligned} \Delta G^{\ddagger} &= G_D\left(d_C\right) - G_D\left(d_D\right) \\ &= \frac{1}{2} m\omega_0^2 \left(d_C - d_D\right)^2 \\ &= \frac{1}{4\lambda}\left[\Delta G^{\circ} + \lambda\right]^2 \end{aligned} \tag{19.4.5}$$

We see that the magnitude of the barrier is governed by the sum of the standard free energy change and the reorganization energy. The reorganization energy characterizes the energy needed to reorganize the surroundings to stabilize the electron on the acceptor and is always positive, so a larger reorganization energy results in a higher barrier. Inserting this expression for the barrier into the Arrhenius expression, the rate constant for electron transfer via activated barrier crossing is

$$k_{\mathrm{ET}} = A \exp\left[\frac{-\left(\Delta G^{\circ} + \lambda\right)^2}{4\lambda k_B T}\right] \tag{19.4.6}$$

This curve has qualitatively reproduced observations of a maximum electron transfer rate under the conditions $-\Delta G^{\circ} = \lambda$, which occurs when the acceptor and donor parabolas crosse at the donor minimum.

We expect that we can more accurately describe nonadiabatic electron transfer using the DHO or Energy Gap Hamiltonian, which will include the possibility of tunneling through the barrier when donor and acceptor nuclear wavefunctions overlap. We will write the electron transfer rate in terms of two potential energy surfaces, $|D\rangle = |d, n_d\rangle$ and $|A\rangle = |a, n_a\rangle$, which describe the vibronic potential where the electron is either on the donor or acceptor. We recognize that when we calculate thermally averaged transfer rates that this is equivalent to describing the diabatic free energy surfaces. The DHO Hamiltonian is

$$H = H_0 + V \tag{19.4.7}$$

$$H_0 = |a\rangle E_A \langle a| + |d\rangle E_D \langle d| + H_A(q) + H_D(q) \tag{19.4.8}$$

These are represented by harmonic potentials, displaced from one another vertically in energy by

$$\Delta E = E_A - E_D \tag{19.4.9}$$

and horizontally along the reaction coordinate q

$$\begin{aligned} H_D &= \hbar\omega_0\left(\underset{\sim}{p}^2 + (\underset{\sim}{q} - \underset{\sim}{d}_D)^2\right) \\ H_A &= \hbar\omega_0\left(\underset{\sim}{p}^2 + (\underset{\sim}{q} - \underset{\sim}{d}_A)^2\right) \end{aligned} \tag{19.4.10}$$

Unlike our description of FRET, the donor and acceptor surfaces are each a function of the same nuclear coordinate, and we have set the frequency of these oscillators equal for simplicity.

The electronic interaction between the donor and acceptor surfaces is assigned a coupling J_{AD}

$$V = J_{AD}\left[|d\rangle \langle a| + |a\rangle \langle d|\right] \tag{19.4.11}$$

Similar to the Condon approximation, this equation implies that the magnitude of the matrix element for electron transfer does not depend on the nuclear coordinate. That statement does not mean that nuclear motion doesn't influence the electron transfer rate—the Franck-Condon factors that govern the overlap of nuclear wavefunctions along the coordinate q are still included in the DHO formalism, such that a smaller separation between donor and acceptor leads to more efficient transfer. Typically, this

electronic coupling is expected to drop off exponentially with the separation between donor and acceptor orbitals,

$$J(R_{AD}) = J_{AD} \exp\left(-\beta_E R_{AD}\right) \tag{19.4.12}$$

where β_E is the parameter governing the distance dependence of the overlap integral and $R_A - R_D$ is the separation between donor and acceptor molecules. We will see that our description effectively captures a similar exponential dependence in terms of the nuclear displacement along the reaction coordinate.

Marcus evaluated the perturbation theory expression for the transfer rate by calculating Franck-Condon factors for the overlap of donor and acceptor surfaces, in a manner similar to our treatment of the DHO electronic absorption spectrum. Using this strategy, we can proceed to calculate the rates of electron transfer using the Golden Rule expression for the transfer of amplitude from state ℓ to state k

$$w_{k\ell} = \frac{1}{\hbar^2} \int_{-\infty}^{+\infty} dt \, \langle V_I(t) V_I(0) \rangle \tag{19.4.13}$$

Using $V_I(t) = e^{\mathrm{i}H_0 t/\hbar} V e^{-\mathrm{i}H_0 t/\hbar}$, we can write the electron transfer rate as

$$w_{\mathrm{ET}} = \frac{|J|^2}{\hbar^2} \int_{-\infty}^{+\infty} dt \, e^{-\mathrm{i}\Delta E t/\hbar} F(t) \tag{19.4.14}$$

where $F(t)$ now describes the time-dependent overlap between donor and acceptor nuclear wavepackets

$$F(t) = \left\langle e^{\mathrm{i}H_d t/\hbar} e^{-\mathrm{i}H_a t/\hbar} \right\rangle \tag{19.4.15}$$

Alternatively, we can cast this in the form of the Energy Gap Hamiltonian, using the spectral density of a harmonic bath or correlation function to specify the nuclear dynamics. This carries with it a dynamical interpretation of the electron transfer process that is more in line with the outer-sphere electron transfer pictured in Figure 19.4.1. The donor and acceptor states have time-dependent, fluctuating energies as a result of their interaction with the environment. Occasionally, the energies of the donor and acceptor states coincide, such that the energy gap between them is zero. At this point transfer becomes efficient. By integrating over the correlation function for these energy gap fluctuations, we characterize the statistics for barrier crossing, and therefore forward electron transfer.

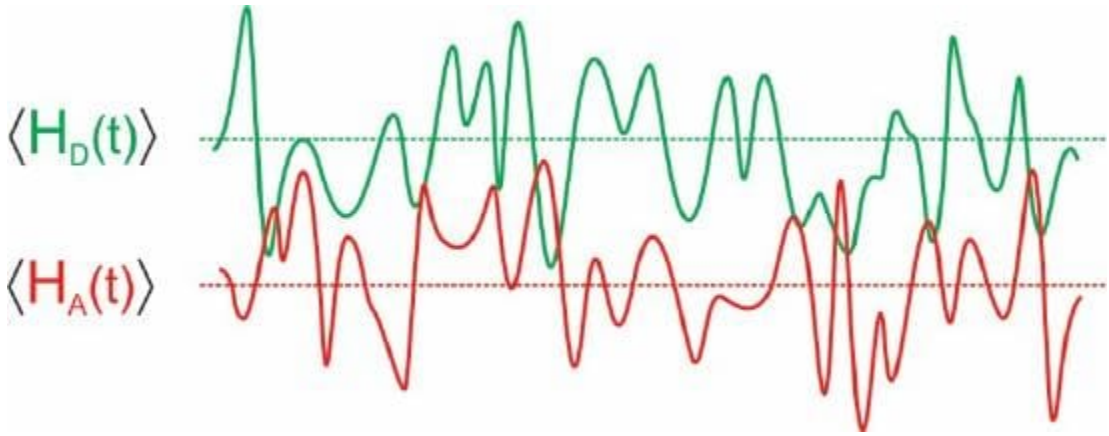


Figure 19.4.4: Visualization of how fluctuating nuclear motions in the electron transfer coordinate modulate the energy gap between donor and acceptor states energy leading to curve crossings where electron transfer becomes efficient. The number of crossings is exaggerated for the illustration—degeneracies are typically a rare event.

To develop this, we follow the same process as before. We define a donor-acceptor energy gap Hamiltonian as

$$H_{AD} = H_A - H_D \tag{19.4.16}$$

and the reorganization energy as

$$\lambda = \langle H_{AD} \rangle \tag{19.4.17}$$

The energy gap dephasing function is expressed in terms of the energy gap Hamiltonian as

$$F(t) = \left\langle \exp_+ \left[-\frac{\mathrm{i}}{\hbar} \int_0^t dt' H_{AD}(t') \right] \right\rangle \tag{19.4.18}$$

$$H_{AD}(t) = e^{\mathrm{i}H_D t/\hbar} H_{AD} e^{-\mathrm{i}H_D t/\hbar} \tag{19.4.19}$$

These expressions and application of the cumulant expansion to eq. (19.4.18) allow us to express the transfer rate in terms of a lineshape function and energy gap correlation function

$$F(t) = \exp\left[-\frac{\mathrm{i}}{\hbar} \langle H_{AD} \rangle t - g(t) \right] \tag{19.4.20}$$

$$g(t) = \int_0^t d\tau_2 \int_0^{\tau_2} d\tau_1 \, C_{AD}(\tau_2 - \tau_1) \tag{19.4.21}$$

$$C_{AD}(t) = \frac{1}{\hbar^2} \langle \delta H_{AD}(t) \delta H_{AD}(0) \rangle \tag{19.4.22}$$

The lineshape function can also be written as a sum of many coupled nuclear coordinates, q_α. This expression is commonly applied to the vibronic (inner shell) contributions to the transfer rate:

$$\begin{aligned} g(t) &= -\sum_\alpha \left(\underset{\sim}{d}_\alpha^A - \underset{\sim}{d}_\alpha^D \right)^2 \left[(\bar{n}_\alpha + 1)\left(e^{-\mathrm{i}\omega_\alpha t} - 1 + \mathrm{i}\omega_0 t \right) + \bar{n}_\alpha \left(e^{\mathrm{i}\omega_\alpha t} - 1 - \mathrm{i}\omega_0 t \right) \right] \\ &= -\sum_\alpha \left(\underset{\sim}{d}_\alpha^A - \underset{\sim}{d}_\alpha^D \right)^2 \left[\coth(\beta\hbar\omega_\alpha/2)(\cos\omega_\alpha t - 1) - \mathrm{i}(\sin\omega_\alpha t - \omega_\alpha t) \right] \end{aligned} \tag{19.4.23}$$

Substituting the expression for a single harmonic mode into the Golden Rule rate expression eq. (19.4.13) gives

$$\begin{aligned} w_{\mathrm{ET}} &= \frac{|J_{AD}|^2}{\hbar^2} \int_{-\infty}^{+\infty} dt \, e^{-\mathrm{i}\Delta E t/\hbar - g(t)} \\ &= \frac{|J_{AD}|^2}{\hbar^2} \int_{-\infty}^{+\infty} dt \, e^{-\mathrm{i}(\Delta E + \lambda)t/\hbar} \exp\left[S_{AD} \left(\coth(\beta\hbar\omega_0/2)(\cos\omega_0 t - 1) - \mathrm{i}\sin\omega_0 t \right) \right] \end{aligned} \tag{19.4.24}$$

where

$$S_{AD} = \left(\underset{\sim}{d}_A - \underset{\sim}{d}_D \right)^2 \tag{19.4.25}$$

and

$$\lambda = \hbar\omega_0 S_{AD} \tag{19.4.26}$$

This expression is very similar to the one that we evaluated for the absorption lineshape of the Displaced Harmonic Oscillator model.

To get a feeling for the dependence of w_{ET} on q, we can look at the classical limit $\hbar\omega \ll k_B T$. This corresponds to the case where one is describing a low frequency “solvent mode” or “outer sphere” effect on the electron transfer. Now, we neglect the imaginary part of $g(t)$ and take the limit :

$$w_{\mathrm{ET}} = \frac{|J_{AD}|^2}{\hbar^2} \int_{-\infty}^{+\infty} dt \, e^{-\mathrm{i}(\Delta E + \lambda)t} \exp\left(-\left(\frac{2 S_{AD} k_B T}{\hbar\omega_0} \right)(1 - \cos\omega_0 t) \right) \tag{19.4.27}$$

The high-temperature limit also means the low frequency limit for ω_0. This means that we can expand $\cos\omega_0 t \approx 1 - (\omega_0 t)^2/2$ and find

$$w_{\mathrm{ET}} = \frac{|J_{AD}|^2}{\hbar} \sqrt{\frac{\pi}{\lambda k_B T}} \exp\left[\frac{-(\Delta E + \lambda)^2}{4\lambda k_B T} \right] \tag{19.4.28}$$

For a thermally averaged rate, it is reasonable to associate the average electronic energy gap with the standard free energy of reaction, $\Delta E \to \Delta G^\circ$. Therefore, this expression is equivalent to the classical Marcus’s result for the electron transfer rate, eq. (19.4.6), where the pre-exponential A is

$$A = \sqrt{\frac{\pi}{\lambda k_B T}} \frac{|J_{AD}|^2}{\hbar} \tag{19.4.29}$$

Equation (19.4.28) has a nonlinear dependence of the electron transfer rate on the driving force of the forward transfer, i.e., the reaction free energy. As illustrated in Figure 19.4.5, it predicts that the ET rate will increase as the driving force for the reaction ($-\Delta G^\circ$) increases, until a maximum rate is reached for $-\Delta G^\circ = \lambda$, where the donor and acceptor surfaces cross at the bottom of the donor parabola ($q = d_D$). The rate then decreases. This decrease of w_{ET} with increasing $-\Delta G^\circ$ is known as the "inverted regime." The inverted behavior means that extra vibrational excitation is needed to reach the curve crossing—now at $q < d_D$—as the acceptor well is lowered further. An example of the high temperature behavior for varying degrees of coupling to a low frequency solvent mode is shown in Figure 19.4.6.

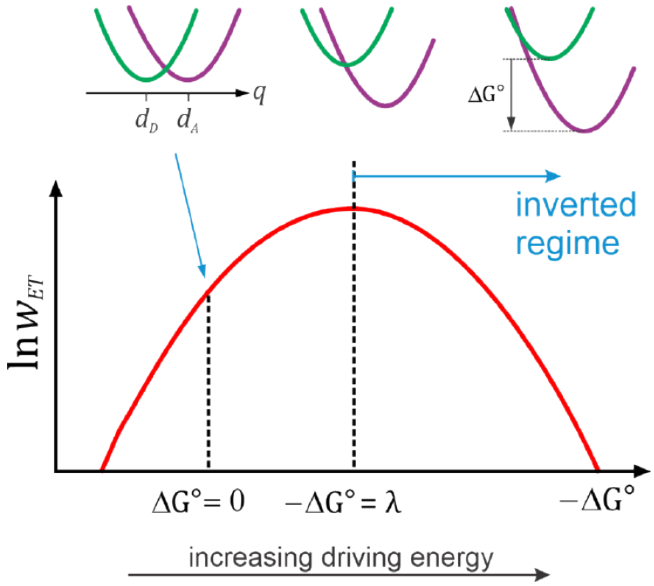


Figure 19.4.5: Illustration of the parabolic dependence of $\ln w$ on the thermodynamic driving force ΔG°, showing that rates decrease once $-\Delta G^\circ$ exceeds λ (the inverted regime), along with the corresponding changes to the donor and acceptor free energy surfaces.

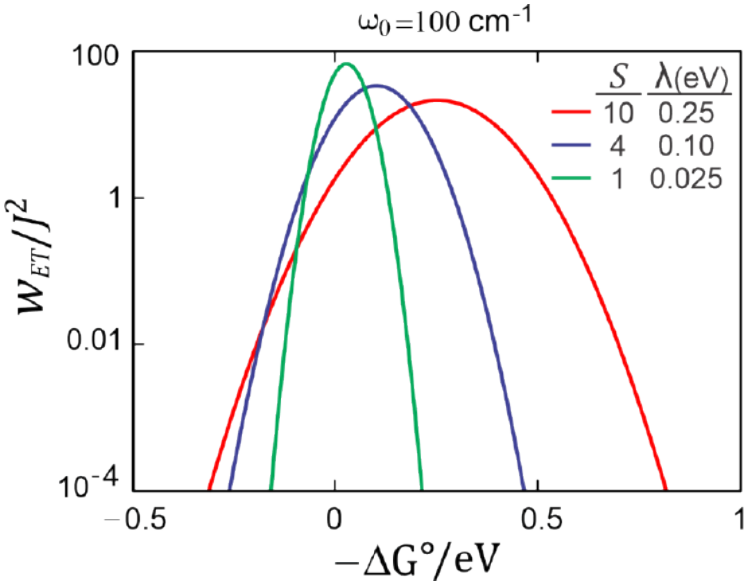


Figure 19.4.6: Rates of electron transfer as a function of ΔG° for different couplings to a $100\ \mathrm{cm}^{-1}$ mode at $T = 300\ \mathrm{K}$.

Particularly in intramolecular electron transfer, it is common that one wants to separately account for a high frequency intramolecular vibration (inner sphere ET) that is not within the classical limit applied to the low frequency, classical solvent response. If an additional high frequency mode (ω_0) and a lineshape function in the form eq. (19.4.24) are added to the low frequency mode, the rate expression becomes(1)

$$w_{\mathrm{ET}} = \frac{|J|^2}{\hbar}\sqrt{\frac{\pi}{\lambda_0 kT}}\sum_{j=0}^{\infty}\left(\frac{e^{-S}}{j!}S^j\right)\exp\left[\frac{-\left(\Delta G^\circ + \lambda_0 + j\hbar\omega_0\right)^2}{4\lambda_0 kT}\right] \tag{19.4.30}$$

Here, λ_0 is the solvation reorganization energy and S is the Huang-Rhys factor for the high-frequency mode. For this case, the same inverted regime exists, although the symmetric Gaussian dependence of w_{ET} on ΔG° no longer exists. The asymmetry here exists because the Franck-Condon factors that govern tunneling differ between the inverted regime and the normal regime, with a narrower barrier in the inverted regime. Examples of the rates obtained with eq. (19.4.30) are plotted in Figure 19.4.7.

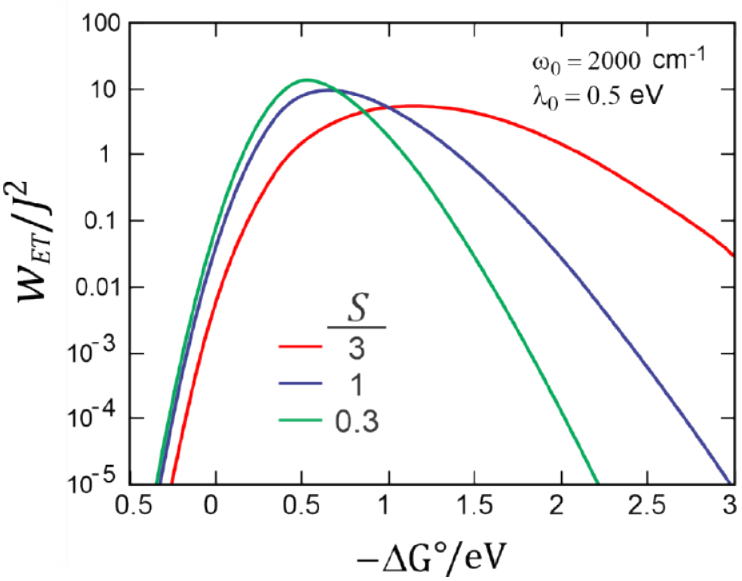


Figure 19.4.7: Rates of electron transfer as a function of ΔG° for different couplings to a $100\ \mathrm{cm}^{-1}$ mode at $T = 300\ \mathrm{K}$.

As with electronic spectroscopy, a more general and effective way of accounting for the nuclear motions that mediate the electron transfer process is to describe the coupling weighted density of states as a spectral density ρ. Then solvent and vibrational contributions of arbitrary form can be incorporated into the transfer event by applying a harmonic bath coupling model using the lineshape function

$$g(t) = \int_0^\infty d\omega\,\rho(\omega)\left[\coth\left(\frac{\beta\hbar\omega}{2}\right)(1-\cos\omega t) + \mathrm{i}\,(\sin\omega t - \omega t)\right] \tag{19.4.31}$$

References

(1) Jortner, J. The temperature dependent activation energy for electron transfer between biological molecules. *Journal of Chemical Physics* **1976**, *64* (12), 4860-4867. DOI: 10.1063/1.432142

This page titled 19.4: Marcus Theory for Electron Transfer is shared under a CC BY-NC-SA 4.0 license and was authored, remixed, and/or curated by Andrei Tokmakoff via source content that was edited to the style and standards of the LibreTexts platform.

19.5: Readings

Förster Resonance Energy Transfer

1. Andrews, D. L. A unified theory of radiative and radiationless molecular energy transfer. *Chemical Physics* **1989**, *135* (2), 195-201. DOI: 10.1016/0301-0104(89)87019-3
2. Lakowicz, J. R. *Principles of Fluorescence Spectroscopy*, 3rd ed.; Springer, 2006. DOI: 10.1007/978-0-387-46312-4
3. Scholes, G. D. Long-range resonance energy transfer in molecular systems. *Annual Review of Physical Chemistry* **2003**, *54*, 57-87. DOI: 10.1146/annurev.physchem.54.011002.103746

Marcus Theory for Electron Transfer

1. Barbara, P. F.; Meyer, T. J.; Ratner, M. A. Contemporary issues in electron transfer research. *Journal of Chemical Physics* **1996**, *100* (31), 13148-13168. DOI: 10.1021/jp9605663
2. Georgievskii, Y.; Hsu, C.-P.; Marcus, R. A. Linear response in theory of electron transfer reactions as an alternative to the molecular harmonic oscillator model. *Journal of Chemical Physics* **1999**, *110* (11), 5307-5317. DOI: 10.1063/1.478425
3. Jortner, J. The temperature dependent activation energy for electron transfer between biological molecules. *Journal of Chemical Physics* **1976**, *64* (12), 4860-4867. DOI: 10.1063/1.432142
4. Marcus, R. A.; Sutin, N. Electron transfers in chemistry and biology. *Biochimica et Biophysica Acta (BBA) - Reviews on Bioenergetics* **1985**, *811* (3), 265-322. DOI: 10.1016/0304-4173(85)90014-X
5. Nitzan, A. *Chemical dynamics in condensed phases: Relaxation, transfer and reactions in condensed molecular systems*; Oxford University Press, 2006. DOI: 10.1093/oso/9780198529798.001.0001
6. Schatz, G. C.; Ratner, M. A. *Quantum Mechanics in Chemistry*; Dover Publications, 2002.

This page titled 19.5: Readings is shared under a CC BY-NC-SA 4.0 license and was authored, remixed, and/or curated by LibreTexts.

20: EXCITONS

20.1: What are excitons?
20.2: Frenkel excitons in molecular aggregates
20.3: Absorption spectrum of a dimer
20.4: Absorption spectra of J aggregates
20.5: Frenkel exciton transport
20.6: Tight-binding model
20.7: Readings

This page titled 20: Excitons is shared under a CC BY-NC-SA 4.0 license and was authored, remixed, and/or curated by Andrei Tokmakoff via source content that was edited to the style and standards of the LibreTexts platform.

20.1: What are excitons?

The term “exciton” is used to describe the delocalized electronic excited states of semiconductors, molecular solids, and chromophore aggregates. These systems are typically made up of a periodic lattice of coupled atomic or molecular orbitals, resulting in electronic eigenstates that are spread across the structure. However, excitons also exist in disordered matter involving two or more interacting chromophores. As you might imagine, excitons play a critical role in describing electron and electronic energy transport within materials—both molecular and atomic solids—as well as the interactions of these materials with light and their novel optical properties.

Since the term has been applied by different communities to diverse types of matter with widely varying electronic properties, there can be confusion about how we should use the term “exciton.” As a result, we distinguish between Frenkel excitons and Wannier-Mott excitons. In the context of semiconductor physics, the electronic states are highly delocalized and described through their band structure, and the electron-hole pairs created through electronic excitation across the band gap are referred to as Wannier-Mott excitons: the excited electron found in the conduction band and the “hole” or electron vacancy that is left in the valence band. The quasiparticle language (“-ons”) is invoked because we describe the properties and transport of these paired electrons and holes as single particles with an effective mass, even though the underlying excitation can involve the electronic states of numerous atoms. The electron-hole pairs are bound by a Coulomb attraction, but the binding energy is low enough that one can dissociate the exciton for the purpose of macroscopic charge transport.

A second class of excitons are Frenkel excitons. This term refers to electronic excitations in molecular solids and chromophore aggregates. In such systems, the interaction of one molecule with its neighbor is often well described through weak transition dipole coupling or other coulombic interactions. Although band structure may arise in chromophore aggregates with little energetic disorder, it is more common that disorder keeps the excitation localized to one or two molecules, far fewer than excitons in semiconductors. Frenkel excitons are often used to describe the transport of electronic excitation energy rather than charge transport.

So, why do we use the same word for these different types of electronic excitations? One reason is that the Frenkel exciton Hamiltonian and the tight binding Hamiltonian commonly used to describe both Frenkel and Wannier-Mott excitons have an identical general form, even though the underlying constituents and couplings they describe are very different. The other reason is that we can apply the electron-hole language to the molecular context, even though, for Frenkel excitons, the electron in the LUMO and hole in the HOMO are localized to the same molecule. In materials with stronger intermolecular couplings, the exciton takes on charge transfer character such that the electron and hole can reside on different molecules. Strongly bound excitons have a binding energy of $1\ \mathrm{eV}$ or greater, which can be compared to the weak $1\text{–}100\ \mathrm{meV}$ binding energy of Wannier-Mott excitons in inorganic semiconductors, such as GaAs and CdSe.

This chapter will focus on describing the Frenkel excitons typically found in molecular condensed matter, describe the band structure that can occur in chromophore aggregates, and illustrate the consequences for the optical spectroscopy of those aggregates and electronic energy transfer within them. For contrast and completeness, the final section provides an introduction into the tight-binding model of Wannier-Mott excitons, providing enough information to see how different parameterization of the same Hamiltonian can provide a description of electronic states in very different types of matter.

This page titled 20.1: What are excitons? is shared under a CC BY-NC-SA 4.0 license and was authored, remixed, and/or curated by Andrei Tokmakoff via source content that was edited to the style and standards of the LibreTexts platform.

20.2: Frenkel excitons in molecular aggregates

Frenkel excitons are responsible for electronic energy transport in organic chromophore aggregates, photosynthetic light harvesting complexes, and organic photovoltaic devices. The transport is characterized either as a diffusive process of exciton hopping via transition dipole interactions or, if electronic interactions are strong enough, as coherent wavepackets. In plants, algae and photosynthetic bacteria, light harvesting takes place within complexes of numerous spatially organized and energetically matched chromophores such as bacterochlorophylls or phycobilins. Exciton transport is used to describe the how the excitation energy from light absorption is funneled through these chromophores to a reaction center where charge separation occurs. In molecular aggregates and organic semiconductors, Frenkel excitons are used to describe the optical absorption spectrum, energy transport, and light emission from these materials. These properties play an important role in the design of organic solar cells and OLEDs.

To investigate Frenkel excitons, we will investigate a model for a linear aggregate of N identical molecules periodically arranged along x by a lattice spacing α. The length of the chain is $L = \alpha N$. The molecules are indexed with integer values (n) between 0 and $N-1$. (Figure 20.2.1). Each molecule has a transition dipole moment μ, which makes an angle β with the axis of the chain (x). Each molecule is described by a two-level electronic system with a ground state $|g\rangle$ and excited state $|e\rangle$, and electronic excitation moves an electron from the ground state of one molecule to an unoccupied orbital of the same molecule.

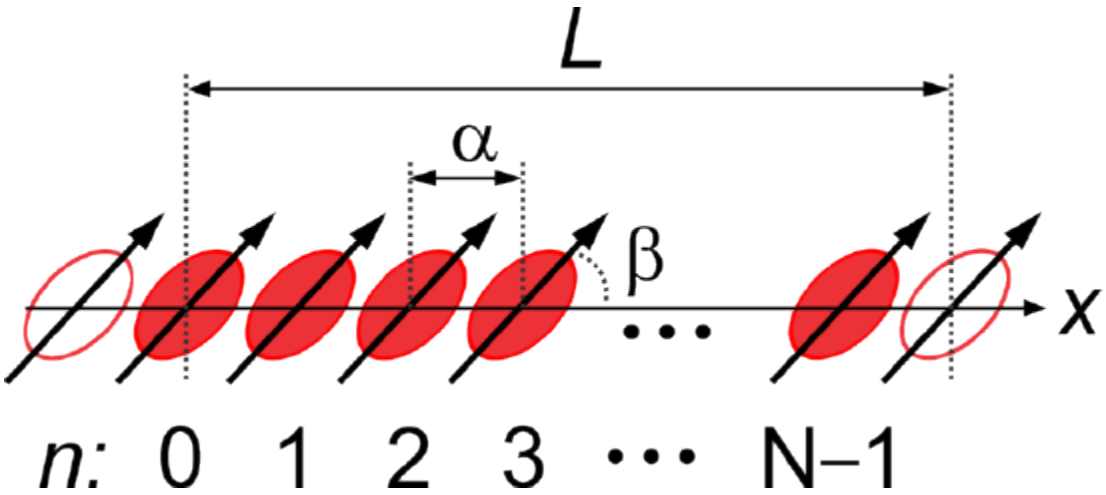


Figure 20.2.1: Illustration of the variables describing the linear chain of coupled chromophores equally spaced by α along x.

In the absence of interactions, we can specify the state of the system $|\psi\rangle$ by identifying whether each molecule is in the excited or ground state. If the state of molecule n within the chain is φ_n, which can take on values of g or e, then the state of the system is given by the product state

$$|\psi\rangle = |\varphi_0, \varphi_1, \varphi_2 \cdots \varphi_n \cdots \varphi_{N-1}\rangle \tag{20.2.1}$$

This representation is referred to as the *site basis*, since it is expressed in terms of the site of each molecule in the chain. For simplicity we write the ground state of the system as

$$|G\rangle = |g, g, g \ldots, g\rangle \tag{20.2.2}$$

If we excite one molecule within the aggregate, we have a singly excited (one-exciton) state in which the n^{th} molecule is excited, so that

$$|\psi\rangle = |g, g, g, \ldots, e, \ldots, g\rangle \equiv |n\rangle \tag{20.2.3}$$

For shorthand, we identify this product state as $|n\rangle$. For our model, the singly excited state is assigned a site energy ε_0 corresponding to the electronic energy gap.

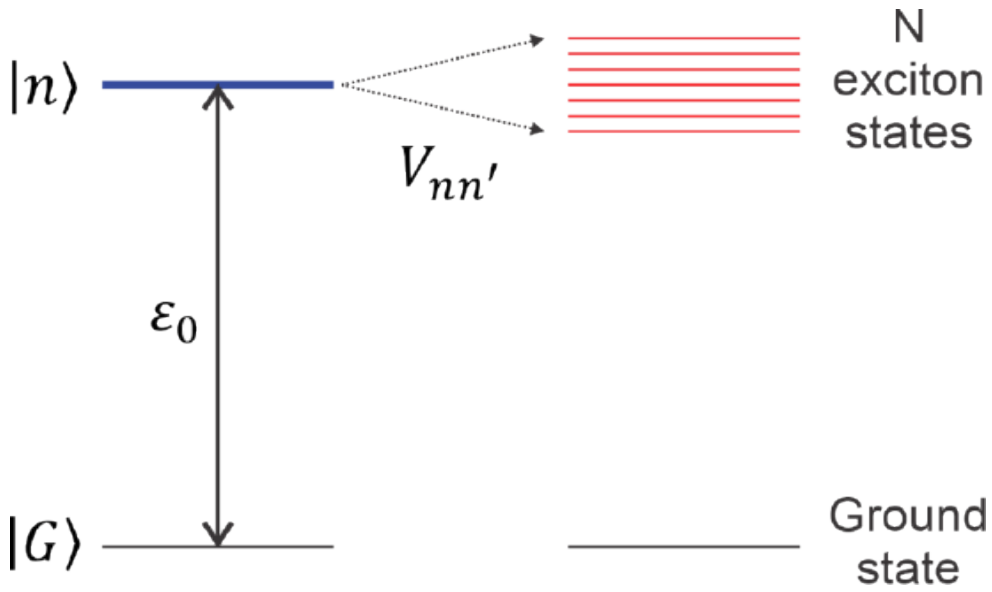


Figure 20.2.2: Energy level diagram for the N degenerate sites with excited state enegy ε_0, and the resulting exciton band that is split due to coupling.

In the absence of coupling, the singly excited states are N-fold degenerate, corresponding to a single excitation at any of the N sites. When coupling between molecules is introduced, the mixing of these degenerate states leads to exciton states (Figure 20.2.2). The coupling between molecule n and molecule n' is given by the matrix element $V_{nn'}$. We will assume that a molecule interacts only with its two nearest neighbors, and that each pairwise interaction has a magnitude J:

$$V_{nn'} = J\delta_{n,n'\pm 1} \tag{20.2.4}$$

We will also assume that V takes the form of a transition dipole interaction. The coupling strength J is given by $J = \kappa\mu^2/\alpha^3$, where μ is the electronic transition dipole moment, and κ is the orientational factor we described before. κ dictates that when the transition dipole angle $\beta < 54.7\,°$, the sign of the coupling is negative ($J < 0$). This arises from an offset stack of chromophores or head-to-tail arrangement, which is known as a J-aggregate (after Edwin Jelley). In contrast when $\beta > 54.7\,°$ then $J > 0$, and the system is known as an H-aggregate (Figure 20.2.3).

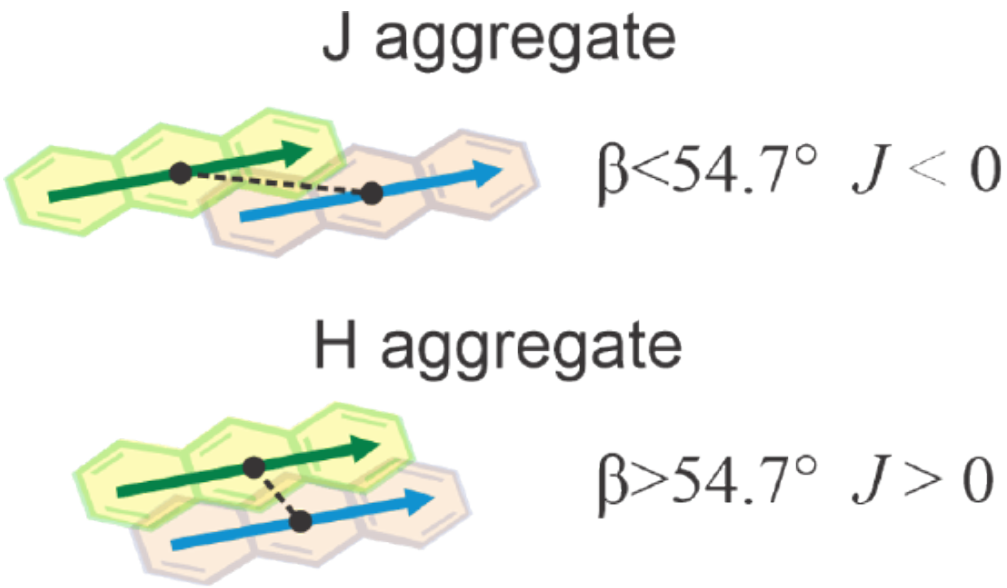


Figure 20.2.3: J- and H-aggregates differ in the configuration of transition dipole moments in the aggregate, which determines the sign of the coupling.

With these definitions, we can write the Frenkel exciton Hamiltonian for the aggregate in terms of a system Hamiltonian H_0 that reflects the possibility of an electronic excitation at each site H_S and the couplings between sites V

$$\begin{aligned} H_0 &= H_S + V \\ &= \varepsilon_0 \sum_{n=1}^{N} |n\rangle \langle n| + J \sum_{n',\, n=0}^{N-1} |n'\rangle \langle n| \, \delta_{n,n'\pm 1} \end{aligned} \tag{20.2.5}$$

The Hamiltonian takes the form of an $N \times N$ tri-diagonal matrix, and the exciton states are the eigenstates of this Hamiltonian. Written in second quantization, this Hamiltonian is

$$H_0 = \varepsilon_0 \sum_n a_n^\dagger a_n + J \sum_{n \neq n'} a_{n'}^\dagger a_n \tag{20.2.6}$$

where $a_n^\dagger$ and a_n are the Pauli creation and annihilation operators for fermions.

To determine the exciton states, we look for solutions in the form of an expansion in the site basis wavefunctions:

$$|\psi(x)\rangle = \sum_{n=0}^{N-1} c_n(x) \, |\varphi_n(x - x_n)\rangle \tag{20.2.7}$$

This expression indicates that the wavefunction of an excited molecule at each site is the same; only its participation in an exciton wavefunction. Thus, the expansion coefficients c_n carry a position dependence along x, and the molecular wavefunction for molecule n is centered at $x_n = n\alpha$.

To determine the expansion coefficients, we will start by applying periodic boundary conditions, meaning that all molecules (including the ends of the chain) are coupled to their two nearest neighbors. This approximation is reasonable for long chains, and it effectively means we are describing the states of an N-molecule aggregate within an infinite chain. In terms of the Hamiltonian eq. (20.2.5), this means that we allow n' to take on the values -1 to N, or, in its matrix form, we also add elements that couple the first and last member of the chain: $J_{0,N-1} = J_{N-1,0} = J$.

Rather than diagonalizing the Hamiltonian, we can take advantage of its translational symmetry to obtain the eigenstates. The symmetry of the Hamiltonian is such that it is unchanged by any integral number of translations along the chain. That is, the results are unchanged for any summation in eqs. (20.2.5) and (20.2.7) over N consecutive integers. Similarly, the molecular wavefunction at any site is unchanged by such a translation. Written in terms of a displacement operator $D = e^{\mathrm{i}p_x \alpha/\hbar}$ that shifts the molecular wavefunction by one lattice constant α, the eigenstates are

$$|\varphi\,(x + n\alpha)\rangle = D^n \, |\varphi(x)\rangle \tag{20.2.8}$$

Thus, when the eigenstates are displaced by a lattice constant, they will vary only by a phase shift.

$$|\psi(x + \alpha)\rangle = e^{\mathrm{i}k\alpha} \, |\psi(x)\rangle \tag{20.2.9}$$

Here k, the wavevector or reciprocal lattice vector, is a real quantity. Thus the expansion coefficients in eq. (20.2.7) will only vary between sites by a spatially varying phase factor, and their amplitude will reflect an excitation spread equally among the N sites. This observation is known as Bloch's theorem, which states that the eigenstates of a periodic potential $u(x)$ will be a product of a spatially varying phase factor and the periodic function, u:

$$|\psi(x)\rangle = e^{\mathrm{i}kx} u(x) \tag{20.2.10}$$

Now let's investigate k. If the linear chain has N molecules, the eigenstates must remain unchanged when undergoing a translation by the length of the chain $L = \alpha N$:

$$|\psi(x_n + L)\rangle = |\psi(x_n)\rangle \tag{20.2.11}$$

Therefore, we see that our wavefunctions must satisfy $e^{\mathrm{i}kL} = 1$, or(1)

$$Nk\alpha = 2\pi m \tag{20.2.12}$$

where k is the wavenumber, and m is an index that labels the exciton eigenstates of an N molecule chain. Since there are N sites on the chain, unique solutions to eq. (20.2.12) require that m can only take on N consecutive integer values, for a total of N exciton eigenstates. From eq. (20.2.12), we can express the wavenumber as

$$k_m = \frac{2\pi}{\alpha} \frac{m}{N} \tag{20.2.13}$$

We see that for an N site lattice, m takes on the N consecutive integer values such that k_m varies over a 2π range of angles. Like the site index n, there is no unique choice of m. By convention, k_m is chosen such that

$$-\frac{\pi}{\alpha} < k_m \leqslant \frac{\pi}{\alpha} \tag{20.2.14}$$

Then the corresponding values of m are integers from $-(N-1)/2$ to $(N-1)/2$ if there are an odd number of lattice sites or $-(N-2)/2$ to $N/2$ for an even number of sites. For example, a 20-molecule chain would have $m = -9, -8, \ldots 9, 10$.

These findings lead to the general form for the exciton eigenstates

$$|k_m\rangle = \frac{1}{\sqrt{N}} \sum_{n=0}^{N-1} e^{ink_m\alpha} |n\rangle \tag{20.2.15}$$

The factor of $N^{-1/2}$ assures proper normalization of the wavefunction. Comparing eqs. (20.2.15) and (20.2.7), we see that the expansion coefficients for the n^{th} site of the m^{th} eigenstate is

$$c_{m,n} = \frac{1}{\sqrt{N}} e^{ink_m\alpha} = \frac{1}{\sqrt{N}} e^{2\pi imn/N} \tag{20.2.16}$$

These coefficients have fixed amplitude and vary only by phase, which can be quantified through:

$$\phi_{m,n} = \frac{2\pi mn}{N} \tag{20.2.17}$$

Thus, the exciton eigenstates are plane-waves, and eq. (20.2.16) gives the matrix elements for the transformation from the site basis to the exciton basis. From eq. (20.2.16), we see that for state $|k_0\rangle$, with $m = 0$, the phase angle is the same for all sites. In other words, the transition dipoles of the chain will oscillate in-phase, adding constructively for all sites. For the case that $k_m = \pi/\alpha$, each site is out-of-phase with its nearest neighbors. In Figure 20.2.4, we show an example of how the expansion coefficients and phase of the site wavefunctions vary as a function of exciton state for a 12-molecule aggregate.

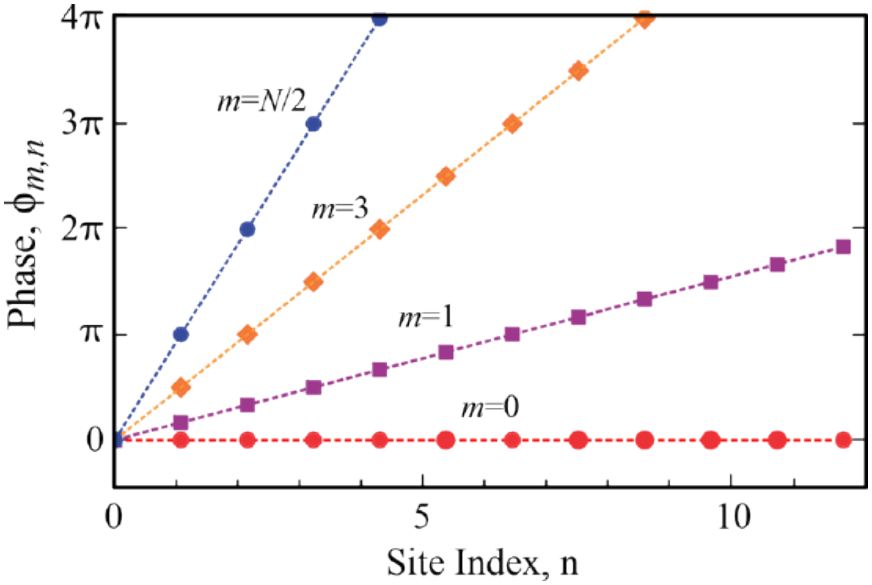


Figure 20.2.4: Phase $\phi_{m,n}$ for the $m = 0, 1, 3$ and 6 exciton states of an $N = 12$ molecule aggregate. For $m = 0$ all sites are in phase, whereas for $m = N/2 = 6$, all sites are out of phase with their neighbors

Finally, let's solve for the exciton energy eigenvalues by calculating the expectation value of the Hamiltonian operator, eq. (20.2.5)

$$E(k_m) = \langle m| H_0 |m\rangle \tag{20.2.18}$$

From the two terms in H_0, we calculate two contributions to the energy:

$$\langle m|\, H_S\, |m\rangle = \frac{1}{N}\sum_{n=0}^{N-1}\varepsilon_0 = \varepsilon_0 \tag{20.2.19}$$

$$\begin{aligned}\langle m|\, V\, |m\rangle &= \frac{1}{N}\sum_{n=0}^{N-1}\left\{e^{\mathrm{i}k_m\alpha}\,\langle n-1|\, V\, |n\rangle + e^{-\mathrm{i}k_m\alpha}\,\langle n+1|\, V\, |n\rangle\right\} \\ &= 2J\cos(k_m\alpha)\end{aligned} \tag{20.2.20}$$

So that the total energy of the m^{th} exciton state is

$$E(k_m) = \varepsilon_0 + 2J\cos(k_m\alpha) \tag{20.2.21}$$

We predict that the band of exciton states varies in energy between $\varepsilon_0 - 2J$ and $\varepsilon_0 + 2J$. If we take J as negative, as is expected for the case of J-aggregates, then $k = 0$ is at the bottom of the band, as illustrated in Figure 20.2.5 for an $N = 12$ aggregate. For this even-numbered case, there are single states at the band extrema, $m = 0$ at the bottom of the band and $m = 6$ at the top, and pairs of degenerate $\pm m$ states in between. The density of states—the number of states per energy interval—is greatest at the band extrema and least in the center of the band. For the case of H-aggregates, in which the coupling is positive ($J > 0$), the dispersion relationship and energy ordering is inverted, with the $m = 0$ ($k = 0$) state at the top of the band and $m = 6$ ($k = \pi/a$) at the bottom.

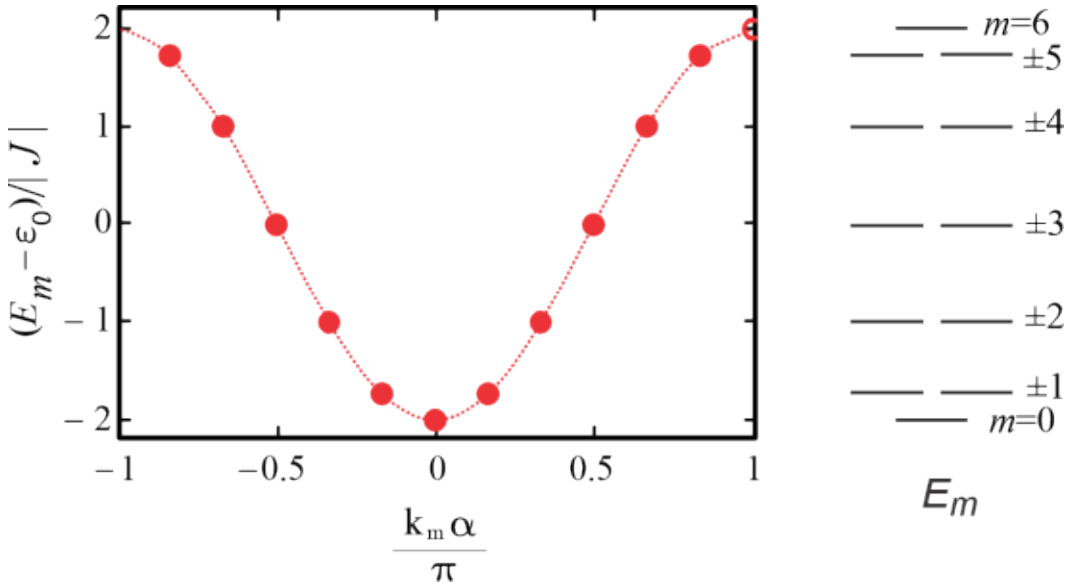


Figure 20.2.5: Dispersion relation (left) and corresponding energy level structure (right) for a J-aggregate ($J < 0$) with $N = 12$. The points indicate the energy and wavevector of the 12 exciton states. The dashed line represents the dispersion relationship in the limit $N \to \infty$.

One assumption of our model is that only the Coulombic coupling between nearest neighbors is taken into account. If longer-range couplings between sites are also included, many of the qualitative observations remain unchanged; however, the exciton energies are modified. Including long-range interactions has the effect of shifting the exciton band asymmetrically about ε_0, such that the bottom of the band is at $E(k_0) = \varepsilon_0 + 2.4J$ with $J < 0$, and the top of the band is at $E(k_N) = \varepsilon_0 - 1.8J$.

The finite size of typical molecular aggregates means that periodic boundary conditions may not be appropriate to our calculations, and in fact removing this condition has effects on the exciton states and energies. Under these open boundary conditions, the molecules at the end of the chain are only coupled to their one nearest neighbor. In this case, it is helpful to label the sites from $n = 1, 2 \ldots N$, and the exciton states $m = 1, 2 \ldots N$. Under those conditions, one can solve for the eigenstates using use the boundary condition that $\psi = 0$ at sites 0 and $N + 1$. The change in boundary conditions gives *sine* solutions for the exciton wavefunctions

$$|k_m\rangle = \sqrt{\frac{2}{N+1}}\sum_{n=1}^{N}\sin\left(\frac{\pi m n}{N+1}\right)|n\rangle \tag{20.2.22}$$

and the exciton energies are

$$E_m = \varepsilon_0 + 2J\cos\left(\frac{\pi m}{N+1}\right) \qquad m = 1, 2 \ldots N \tag{20.2.23}$$

These expressions can also be written in terms of the wavenumber $k_m = \pi m/\alpha\,(N+1)$. Note that the exciton states in eq. (20.2.22) take on the form of particle-in-a-box eigenstates, where the m^{th} state has $(m-1)$ nodes. Equation (20.2.22) also expresses a transformation from the site basis to the exciton (eigen) basis where the transformation matrix elements are

$$T_{mn} = \sqrt{\frac{2}{N+1}}\sin\left(\frac{\pi mn}{N+1}\right) \tag{20.2.24}$$

Extending the Frenkel exciton model to properly account for three-dimensions can rapidly become complex depending on how anisotropic the system is in terms of structure and interactions, and the types of intermolecular couplings that need to be accounted for. We can take one step in this direction by considering a simple cubic lattice of molecules, where the lattice constant α, nearest neighbor couplings J, site energy ε_0, and chain length $L = N\alpha$ are all uniform in $x, y,$ and z, and no couplings exist between the three dimensions. We still only consider the one-exciton states in which a single excitation exists across the whole lattice, so we need to index the location of that excitation site with $|n_x, n_y, n_z\rangle$. The exciton states take on the same form

$$|\mathbf{k_m}\rangle = \frac{1}{\sqrt{N^3}}\sum_{n_x,n_y,n_z} e^{\mathrm{i}(k_x n_x\alpha + k_y n_y\alpha + k_z n_z\alpha)}\,|n_x, n_y, n_z\rangle \tag{20.2.25}$$

where the summation is taken over n_j, $j = \{x, y, z\}$, and n_j runs from 0 to $N-1$ in each axis. Here the exciton state $|\mathbf{k}_m\rangle$ is defined through three independent wavenumbers k_j with $j = \{x, y, z\}$, which are indexed through m_j:

$$k_j = \frac{2\pi m_j}{N\alpha} \qquad j = \{x, y, z\} \tag{20.2.26}$$

For open boundary conditions, the eigenstates are written as products of sines instead, just as

expected for the 3D particle in a box. The corresponding energies are

$$E\left(\mathbf{k}_m\right) = \varepsilon_0 + 2J\left[\cos\left(k_x\alpha\right) + \cos\left(k_y\alpha\right) + \cos\left(k_z\alpha\right)\right] \tag{20.2.27}$$

Here we see that the overall bandwidth for a large N is $12J$, varying from $\varepsilon_0 + 6J$ and $\varepsilon_0 - 6J$, reflecting the value of k_j at the band extrema, and the bandstructure is a 3D surface rather than a line.

References

(1) Patterson, J. D.; Bailey, B. C. *Solid-State Physics: Introduction to the Theory*, 3rd ed.; Springer, 2018. DOI: 10.1007/978-3-319-75322-5

This page titled 20.2: Frenkel excitons in molecular aggregates is shared under a CC BY-NC-SA 4.0 license and was authored, remixed, and/or curated by Andrei Tokmakoff via source content that was edited to the style and standards of the LibreTexts platform.

20.3: Absorption spectrum of a dimer

The absorption spectra of Frenkel excitons show unique spectral features that reflect the properties of the coupled system and its interaction with the environment. To describe the spectroscopy of an array of many coupled chromophores, it is first instructive to work through the spectroscopy of a pair of coupled molecules. In essence, we are describing the absorption spectrum of the coupled two-level system that we have used on several occasions before. We consider a pair of molecules (1 and 2), which each have an electronic energy gap between their ground and excited states ($|e\rangle$ and $|g\rangle$) of ε_0 and a transition dipole moment $\boldsymbol{\mu}$. The transition dipole moments have the same magnitude but are oriented with an angle 2θ between them.

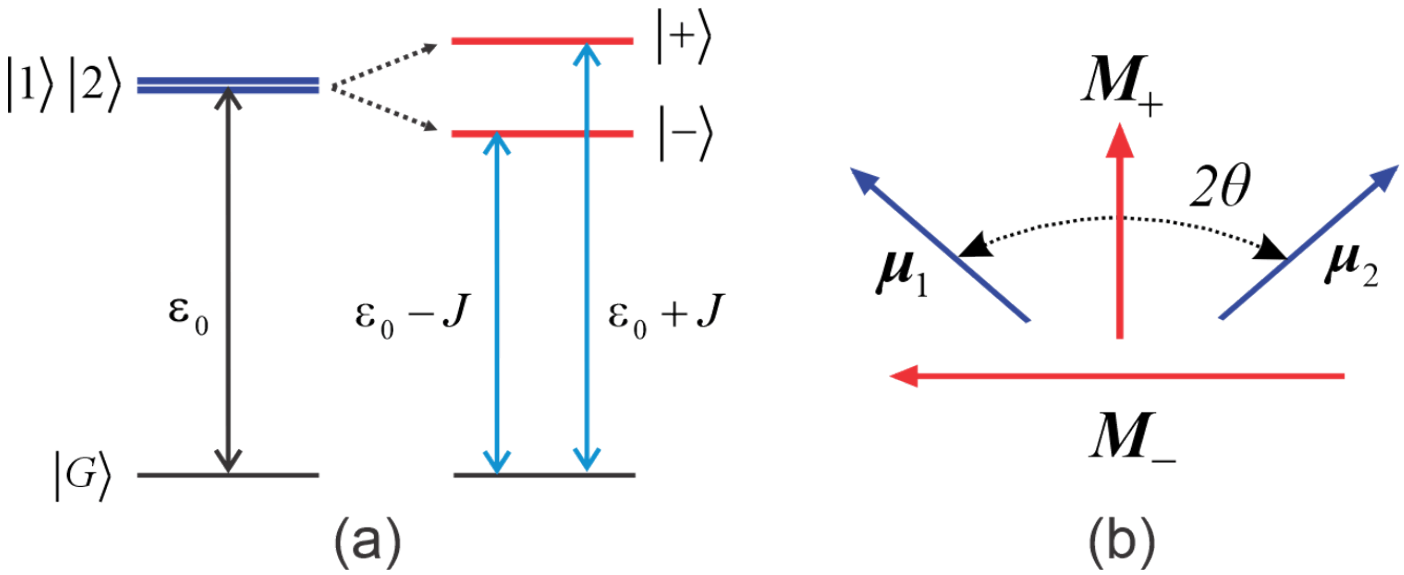


Figure $20.3.1$: Spectroscopy of the coupled dimer. (a) The two degenerate sites (1 and 2) have an excited state energy ε_0 relative to the ground state, and coupling splits to form two exciton states $|+\rangle$ and $|-\rangle$. (b) The transition dipole moments for the sites are μ_1 and μ_2 with an angle 2θ between them. Once coupled, the exciton transition dipole moments are M_+ and M_-.

The excited states as $|1\rangle$ and $|2\rangle$ are coupled through a transition dipole interaction

$$V = J\left(|2\rangle\langle 1| + |1\rangle\langle 2|\right) \tag{20.3.1}$$

so the Hamiltonian for the molecular excited states is given by the degenerate two-level system:

$$H = \begin{pmatrix} \varepsilon_0 & J \\ J & \varepsilon_0 \end{pmatrix} \tag{20.3.2}$$

From our studies of the coupled two-state system, we know that when the coupling between states is much larger than the energy splitting between the uncoupled states ($|\epsilon_1 - \epsilon_2| \ll 2V$), as it is in this degenerate exciton case, then the resulting eigenstates $|\pm\rangle$ are symmetric and antisymmetric combinations of the two, whose energy eigenvalues are split by $2J$. The eigenvalues are

$$E_\pm = \varepsilon_0 \pm J \tag{20.3.3}$$

and the eigenstates are

$$|\pm\rangle = \frac{1}{\sqrt{2}}\left(|1\rangle \pm |2\rangle\right) \tag{20.3.4}$$

The exciton states are equally mixed combinations of the two sites. We know this example well, but we can also see how these states emerge from the exciton eigenstates described in the previous section by eq. (20.2.15). Setting $N = 2$, we see that $m = 0$ or 1 and $k_m = 0$ or π/α. Substituting these values gives us the expected symmetric and antisymmetric eigenstates:

$$
\begin{aligned}
|k_0\rangle &= \frac{1}{\sqrt{2}} \sum_{n=0}^{1} e^{in\cdot 0} |n\rangle = \frac{1}{\sqrt{2}} (|0\rangle + |1\rangle) \qquad (k = 0) \\
|k_1\rangle &= \frac{1}{\sqrt{2}} \sum_{n=0}^{1} e^{in\pi} |n\rangle = \frac{1}{\sqrt{2}} (|0\rangle - |1\rangle) \qquad (k = \pi/\alpha)
\end{aligned} \tag{20.3.5}
$$

You might wonder why the splitting between the two exciton energies $E_+ - E_-$ is $2J$, when eq. (20.2.21) led us to expect a $4J$ difference between the top and bottom of the band. The key distinction here lies in the boundary conditions. If one applied the periodic boundary conditions used in (20.2.21), the coupling would be double counted, leading to a splitting of $4J$.

The dipole operator for the dimer is given by the sum of each site's dipoles

$$\mathbf{M} = \boldsymbol{\mu}_1 + \boldsymbol{\mu}_2 \tag{20.3.6}$$

So we can calculate the transition dipole matrix elements for excitations from the ground $|G\rangle$ to exciton states $|\pm\rangle$ using

$$\mathbf{M}_\pm = \langle \pm | \mathbf{M} | G \rangle = \frac{1}{\sqrt{2}} (\boldsymbol{\mu}_1 \pm \boldsymbol{\mu}_2) \tag{20.3.7}$$

$\mathbf{M}_+$ and $\mathbf{M}_-$ are oriented perpendicular to each other in the molecular frame. If we confine the molecular dipoles to be within a plane, with an angle 2θ between them, then the amplitude of $\mathbf{M}_+$ and $\mathbf{M}_-$ is given by

$$
\begin{aligned}
M_+ &= 2\mu \cos\theta \\
M_- &= 2\mu \sin\theta
\end{aligned} \tag{20.3.8}
$$

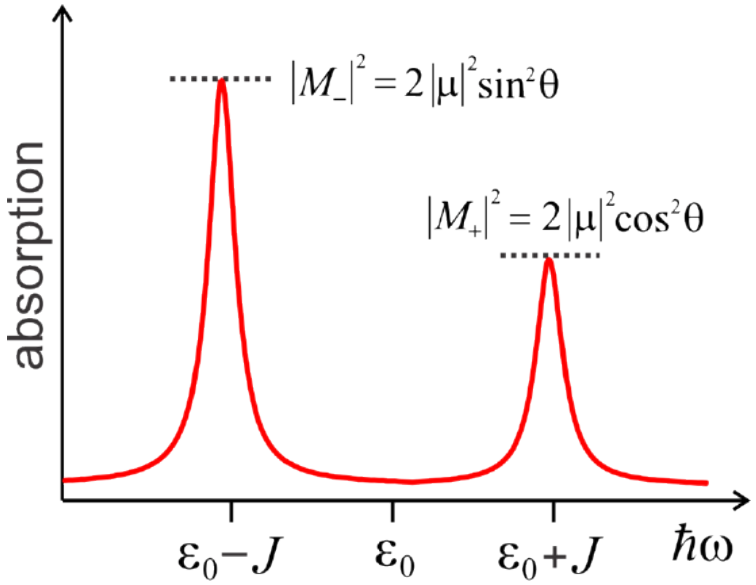


Figure 20.3.2: Absorption spectrum of the dimer excitons for the case $J > 0$, showing how the relative intensity of the two bands depends on the relative orientation of the two site transition dipoles.

We now have all the information to describe the absorption spectrum of the dimer (Figure 20.3.2). There are two transitions from the ground state and the $|\pm\rangle$ exciton states. These are resonant at $\hbar\omega = \varepsilon_0 \pm J$ and have an amplitude $|M_\pm|^2$. The $2J$ splitting between the peaks is referred to as the Davydov splitting. The relative amplitude of the peaks allows one to infer the angle between the molecular transition dipoles. When $\theta = 0\,^\circ$ or $90\,^\circ$, all amplitude appears in one transition with magnitude $2\,|\mu|^2$, while the other transition is dark. Of course, the angle between dipoles also affects the strength and sign of the coupling and therefore influences the Davydov splitting and the identity of the lower exciton transition. For the case of co-planar dipoles that are parallel with each other, as in the H and J-aggregates, the energy splitting between bands is given by

$$\Delta E = E_+ - E_- = \frac{2\,|\mu|^2}{r^3} \left(1 - 3\cos^2\theta\right) \tag{20.3.9}$$

The shift of the exciton bands of the dimer is illustrated in Figure 20.3.3.

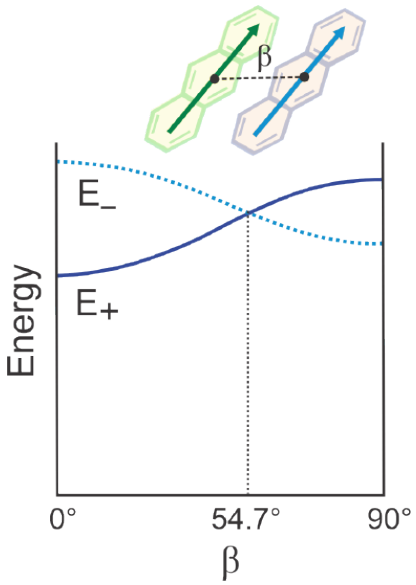


Figure 20.3.3: The shift in energy of the E_+ and E_- dimer exciton bands as a function of the angle β between parallel transition dipoles.

This page titled 20.3: Absorption spectrum of a dimer is shared under a CC BY-NC-SA 4.0 license and was authored, remixed, and/or curated by Andrei Tokmakoff via source content that was edited to the style and standards of the LibreTexts platform.

20.4: Absorption spectra of J aggregates

Let's now extend our analysis to look at the absorption spectra of Frenkel excitons in the linear aggregates discussed in Section 20.2. For this we need to evaluate the exciton transition dipole matrix elements

$$\mathbf{M}_{mG} = \langle k_m | \, \mathbf{M} \, | G \rangle \tag{20.4.1}$$

The dipole operator for the chain is a sum of the dipole operators for each site:

$$\mathbf{M} = \sum_{n=0}^{N-1} \boldsymbol{\mu}_n \tag{20.4.2}$$

substituting this into eq. (20.2.15) gives the exciton transition dipole moment as a sum over the site transition dipoles, weighted by a phase factor on each site:

$$\mathbf{M}_{mG} = \frac{1}{\sqrt{N}} \sum_{n=0}^{N-1} e^{ink_m\alpha} \langle n | \, \boldsymbol{\mu}_n \, | G \rangle \tag{20.4.3}$$

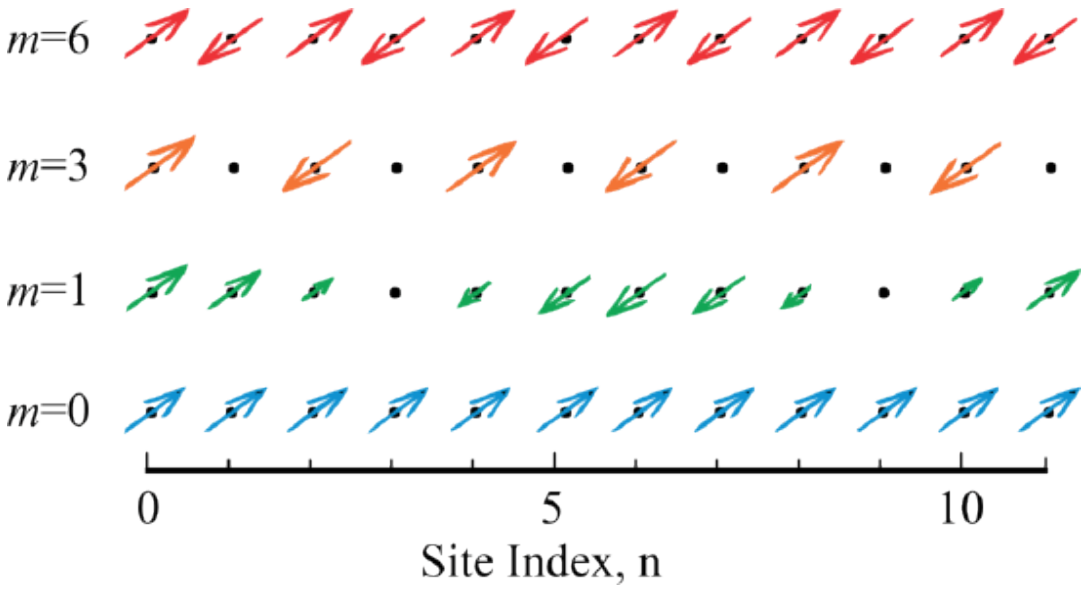


Figure 20.4.1: Illustration of the phase relationship between the site transition dipole moments for four exciton states, illustrating that the vector sum is zero for all but the $k_m = 0$ state.

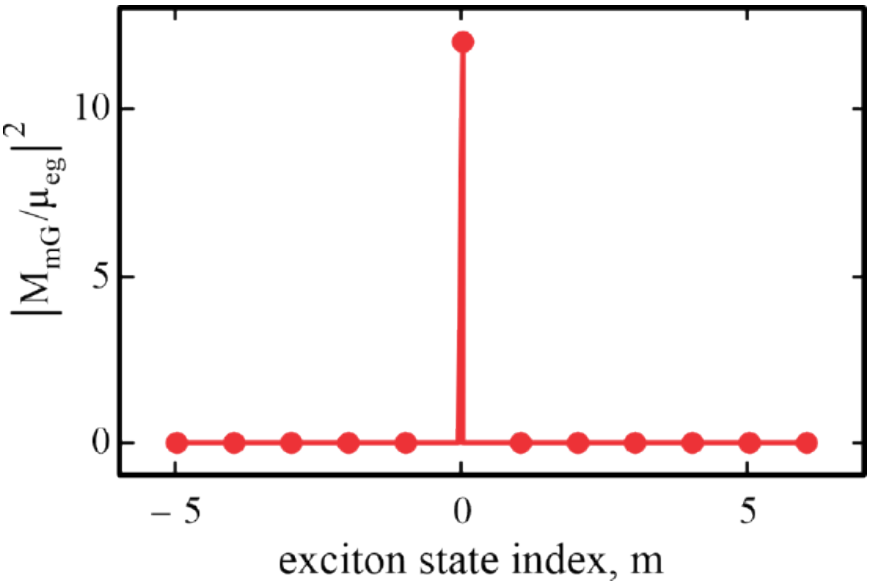


Figure 20.4.2: The transition dipole matrix elements for the exciton states of a $N = 12$ J-aggregate.

We observe that the phase of each transition dipole for site n in the chain matches the site's phase relationship within the corresponding k_m exciton state. From a time-dependent perspective, all of the site transition dipoles have the same amplitude but are oscillating with different phases that may constructively or destructively interfere, influencing the ability of the exciton to absorb light. Figure 20.4.1 shows an illustration of the phase relationships between dipoles in a chain with $N = 12$. For the current case, in which all of the dipoles are parallel to one another, transitions from the ground state to the $k_m = 0$ state will carry all of the oscillator strength (Figure 20.4.2). This follows directly from eq. (20.4.3). Recognizing that the magnitude and direction of each individual transition moment is the same, $\langle n| \boldsymbol{\mu}_n |G\rangle = \boldsymbol{\mu}_{eg}$, we obtain

$$M_{mG} = \sqrt{N}\boldsymbol{\mu}_{eg} \sum_{n=0}^{N-1} e^{\mathrm{i}nk_m\alpha} = \sqrt{N}\boldsymbol{\mu}_{eg} \frac{e^{\mathrm{i}Nk_m\alpha} - 1}{e^{\mathrm{i}k_m\alpha} - 1} \tag{20.4.4}$$

$$|M_{mG}|^2 = N\boldsymbol{\mu}_{eg} \frac{\sin^2(\pi m)}{\sin^2(\pi m/N)} \tag{20.4.5}$$

Since $k_m = 2\pi m/\alpha N$ and m is an integer, the last term is 0 unless $m = 0$.

We are now in a position to plot the absorption spectrum for the aggregate, summing over eigenstates and assuming a Lorentzian lineshape for the system:

$$\sigma(\omega) = \sum_m |M_m|^2 \frac{\Gamma^2}{(\hbar\omega - E(k_m)) + \Gamma^2} \tag{20.4.6}$$

For a 12-oscillator chain with negative coupling, the spectrum is plotted in Figure 20.4.3. We have one peak corresponding to the k_0 mode that is peaked at $\hbar\omega = \varepsilon_0 - 2J$ and carries the oscillator strength of all 12 dipoles. With knowledge of the absorption peak for the monomer at ε_0 and the absorption frequency of the aggregate, one can determine J.

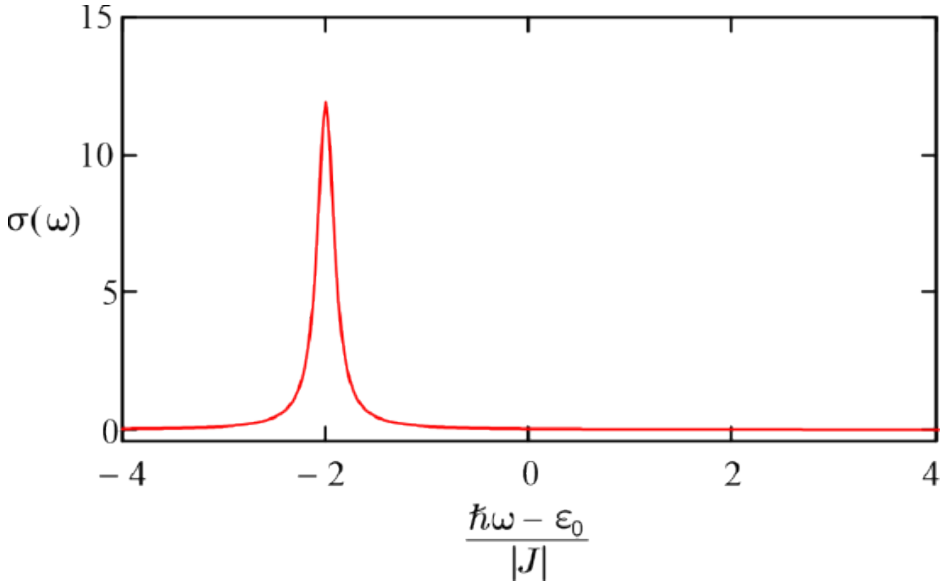


Figure 20.4.3: Absorption spectrum for $N = 12$ aggregate with periodic boundary conditions and $J < 0$. We assume a Lorentzian lineshape with $\Gamma = 0.1J$.

Observing only a single peak due to exact destructive interference between the site transition dipoles in all but one exciton state is a consequence of imposing periodic boundary conditions. Open boundary conditions loosen these selection rules. If you calculate the exciton transition dipole moments using the exciton states in eq. (20.2.22), the transition dipole moments are found to be:

$$|\mathbf{M}_{mG}|^2 = \boldsymbol{\mu}^2 \left(\frac{1-(-1)^m}{2}\right)^2 \frac{2}{N+1}\cot^2\left(\frac{\pi m}{2\,(N+1)}\right) \qquad m = 1, 2, \ldots N) \tag{20.4.7}$$

The leading term indicates that even values of m result in no absorption, but odd m transitions contribute to some extent. In Figure 20.4.4 we can observe this behavior for J-aggregates of varying size, showing that minor transitions to $m = 3$ and 5 bands are observed in addition to the dominant $m = 1$ transition, for which all oscillators are in phase. At large values of N, the $m = 1$ transition carries 81% of the oscillator strength, with approximately 9% in the transition to the $m = 3$ state.

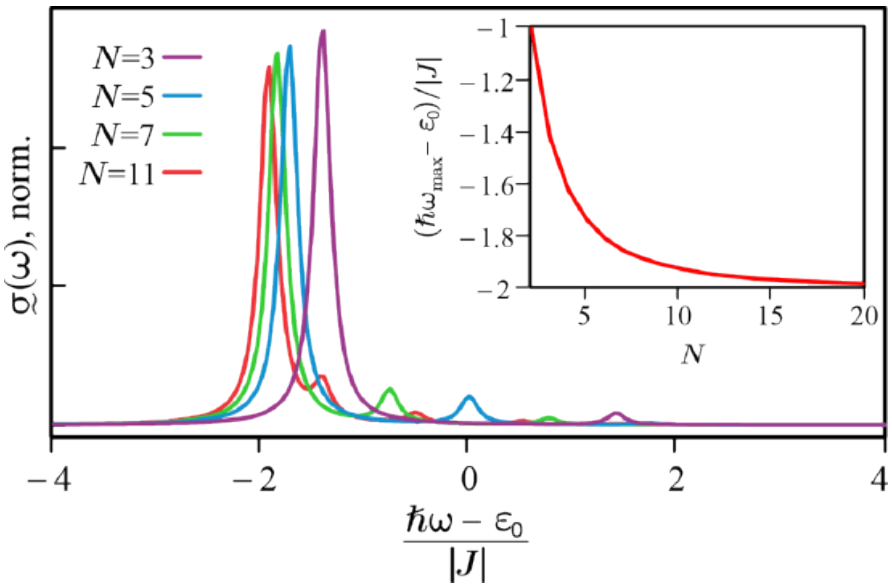


Figure 20.4.4: Area normalized absorption spectra for J aggregates ($J < 0$) of varying size (N) showing the main transition to the $m = 1$ state and minor peaks for $m = 3$ and $m = 5$. The inset shows how the absorption maximum shifts asymptotically with N to $\epsilon_0 - 2J$.

In Figure 20.4.4 we also observe that the transition frequency to the $m = 1$ band red-shifts with increasing aggregate size, only asymptotically reaching a frequency of $\epsilon_0 - 2J$ once $N > 20$. Thus, the shift of the aggregate's $m = 1$ transition relative to the

monomer is influenced both by the size of the aggregate and the coupling J.

Disorder and Exchange Narrowing

The Frenkel exciton model is idealized in the sense that all sites are taken to have identical energies. In reality, we expect that thermal fluctuations and local variations in the environment of different sites will result in site energy variations, and that slight irregularities of the packing or organization of the chain will lead to differences in the couplings between chromophores. These origins of energetic disorder complicate the modeling of real chromophore aggregates, however there are simper ways of assessing what happens. If all molecules within the chain do not have same site energy, then we can model this effect as Gaussian random disorder. The energy of a given site is then assigned a shift relative to the average value:

$$\varepsilon_n = \varepsilon_0 + \delta\varepsilon_n \tag{20.4.8}$$

We add the disorder as an extra term to the Frenkel exciton Hamiltonian, eq. (20.2.5), to account for this variation.

$$H_0 = H_S + H_{\text{dis}} + V \tag{20.4.9}$$

$$H_{\text{dis}} = \sum_n \delta\varepsilon_n \left|n\right\rangle \left\langle n\right| \tag{20.4.10}$$

What one finds is that disorder has the effect of shifting and mixing the homogeneous exciton states. The correction to the exciton energies due to disorder is given by

$$\delta E(k_m) = \left\langle k_m \left| H_{\text{dis}} \right| k_m \right\rangle = \frac{2}{N+1} \sum_n \sin^2\left(\frac{\pi m n}{N+1}\right) \delta\varepsilon_n \tag{20.4.11}$$

When we now statistically average over a Gaussian random distribution of $\delta\varepsilon_n$ with a standard deviation Δ, we find that the resulting exciton energies are also Gaussian random variables, with a standard deviation of $\Delta\sqrt{3/2\,(N+1)}$. So, the delocalization of the eigenstates has the effect of averaging the disorder over approximately N sites, which subsequently narrows the distribution of energies by a factor of approximately $\sqrt{N+1}$. This resulting narrowing of the absorption lineshape with delocalization is called exchange narrowing. This depends on the distribution of site energies being relatively small: $\Delta \ll 3\pi \left|J\right| / N^{3/2}$.

This page titled 20.4: Absorption spectra of J aggregates is shared under a CC BY-NC-SA 4.0 license and was authored, remixed, and/or curated by Andrei Tokmakoff via source content that was edited to the style and standards of the LibreTexts platform.

20.5: Frenkel exciton transport

The Frenkel exciton model provides a mechanism for describing excitation energy transport in chains of identical electronic chromophores. If an excitation is initialized at site $|n_i\rangle$, the subsequent time evolution is determined by the superposition of the chain's eigenstates at that location

$$\begin{aligned} |n_i\rangle &= \sum_{m=1}^{N} b_{m,i} \, |k_m\rangle \\ b_{m,i} &= \sqrt{\frac{2}{N+1}} \sin\left(\frac{\pi m n_i}{N+1}\right) \end{aligned} \tag{20.5.1}$$

We can then calculate the probability of the excitation being at a final site n_f, $P_{n_f}(t) = |c_{n_f}(t)|^2$, from the amplitude at the final site at time t:

$$c_{n_f}(t) = \langle n_f | \, U(t) \, |n_i\rangle = \frac{2}{N+1} \sum_{m=1}^{N} \sin\left(\frac{\pi m n_i}{N+1}\right) \sin\left(\frac{\pi m n_f}{N+1}\right) e^{-\mathrm{i}E_k t/\hbar} \tag{20.5.2}$$

Here $U = e^{-\mathrm{i}H_0 t/\hbar}$ is the usual time-propagator. We see that this oscillates in a complex manner with time, reflecting the initial exciton superposition state.

However, this expression isn't particularly useful, because it doesn't describe traditional motion of a particle along a chain, and the question that we posed and answered wouldn't occur in reality. Why? Because even if the initial and final states are designated at the ends of the chain ($n_i = 1, n_f = N$), the exciton states are delocalized over all sites. That is, since the exciton states in eq. (20.5.1) involve the whole chain, even the act of preparing the initial state at one end of the chain involves creating a superposition of eigenstates that carry well-defined phase relationships between all sites. In this wave—rather than particle—formulation, there isn't a real meaning to the concept of being at a site. Nonetheless, there is a lot of interest in realizing this type of coherent energy transport. For instance, a more realistic design of directional transport, one can imagine coupling energetically distinct donor and acceptor molecules to the ends of the chain.

Without digging into this topic in detail, we can make some predictions about how fast the excitation can move along a chain by calculating the group velocity of an exciton wavepacket using:

$$v_{\mathrm{gr}}(k) = \frac{1}{\hbar}\frac{dE}{dk} \tag{20.5.3}$$

For the Frenkel Hamiltonian eq. (20.2.23) we obtain

$$v_{\mathrm{gr}}(k) = -\frac{2J\alpha}{\hbar}\sin(k\alpha) \tag{20.5.4}$$

This indicates that the speed at which an electronic excitation can move in the lattice is governed by the coupling between sites. The group velocity depends strongly on k, and the maximum group velocity occurs at $k = \pi/2$:

$$v_{\max} = \frac{2Ja}{\hbar} \tag{20.5.5}$$

This maximal velocity sets the fastest possible ballistic propagation down the chain. We can estimate the minimum time it takes for an exciton to cross a chain of N chromophores as

$$t_{\min} = \frac{L}{v_{\max}} = \frac{N\hbar}{2J} \tag{20.5.6}$$

Let's evaluate these variables using some characteristic parameter values. If the lattice spacing is $\alpha = 0.5$ nm and the coupling is $J = 100$ cm^{-1}, then the maximum phase velocity $v_{\max} = 1.9 \times 10^4$ m/s, and the time it takes to travel down a $N = 12$ or 6 nm chain is 320 fs. Note that the scaling in eq. (20.5.6) is linear with chain length, reflecting ballistic quantum transport reminiscent of a particle or wave traveling at fixed speed: $x = vt$. Excitation transfer in this manner is known as the coherent transport regime, which relies on maintaining well-defined phase relationships between the wavefunctions on each site.

In realistic settings, environmental fluctuations such as vibrations or solvent motions induce dephasing, which dynamically alters the phase relationships between chain sites. This has the effect of localizing the excitation to one or two sites within the chain and disrupts coherent transport down the chain. With increasing dynamic or static disorder, the transport process transitions from ballistic (wave-like) to diffusive, with excitations hopping from one chromophore to an adjacent site. In this “strong dephasing” or Forster/Dexter regime, energy transfer is governed by uncorrelated transfer of excitations between sites with no memory (phase-relationship) of where the excitation was previously. If each site is assigned a dephasing rate Γ that describes the loss of coherence, one can derive an effective hopping rate

$$k_{\text{eff}} = \frac{J^2}{\hbar^2 \Gamma} \tag{20.5.7}$$

by solving the Liouville equation for the population difference between adjacent sites. Then one can describe energy flow through the chain in terms of rate equations for the energy transport between adjacent sites:

$$\frac{dp_n}{dt} = k_{\text{eff}} \left[p_{n-1} - 2p_n + p_{n+1} \right] \tag{20.5.8}$$

In this limit, excitation propagates diffusively through the chain, and the it takes for the excitation to reach the end of the chain is

$$t_{\text{diff}} \approx \frac{N^2}{2k_{\text{eff}}} \tag{20.5.9}$$

Note that the transport time scale is now quadratic in the chain length, as expected for diffusive (random walk) transport, where $\langle x^2 \rangle = \mathscr{D}t$ and $\mathscr{D}$ is a diffusion constant. The scaling behavior for transport time with distance is the essential discriminator of the transport mechanism. In coherent (ballistic) transport the transport time t is proportional to distance, $t \sim N$, whereas diffusive transport scales with the square of distance, $t \sim N^2$.

In his original work, Forster derived an expression for the diffusion constant of the electronic energy transfer ($\mathscr{D}_{\text{EET}}$) on a lattice of chromophores through FRET. By summing the single-pair rate $k_0(r) = R_0^6/r^6\tau_0$ over the distribution of sites on the lattice, he found

$$\mathscr{D}_{\text{EET}} = \frac{\eta}{\tau_0} R_0^6 C^{4/3} \tag{20.5.10}$$

where τ_0 is the radiative lifetime, C is the number density of chromophores, and η is a dimensionless constant between 2 and 3 that depends on the type of lattice. This expression overpredicts the actual diffusion constant in systems with disorder, and it generally over-estimates the effective energy transfer rate, likely due to other nonradiative relaxation processes that ensue. However, even small variations in the assumptions of how chromophores are distributed can have qualitative impacts on the scaling with C and R_0. Over the decades since, the theory of exciton diffusion has been extended greatly to include different descriptions of the Coulombic coupling, multiple competing transfer and relaxation processes, and many other experimental observables, such as the excitation survival probability.

Example: Exciton Diffusion in Solution

Calculate the average rate of energy transfer and the exciton diffusion constant in a homogeneous solution of chromophores with a concentration (number density) C, using the single donor-acceptor rate $k_0(r) = R_0^6/r^6\tau_0$.

We will assume that an orientationally averaged value of $\kappa^2 = 2/3$ has been included in R_0, and the positions of acceptors have a uniform angular distribution. Then, for acceptors characterized by a radial distribution function $g(r)$, the effective rate of transfer in solution is

$$k_{\text{eff}} = \int dr\, 4\pi r^2 C g(r) k_0(r) \tag{20.5.11}$$

For a uniform distribution of acceptors, $g(r) = 1$ once one is beyond the radius of the molecule, a. In practice, a lower limit of 0 would diverge in the integral, but acceptors can’t be in the same position as donors anyway. We deal with this by setting $g(r) = 0$ for $r < a$—the hard sphere radial distribution function. This gives us

$$k_{\text{eff}} = \int_a^\infty dr\, 4\pi r^2 C k_0(r) = \left(\frac{4\pi}{3}\right)\frac{CR_0^6}{\tau_0 a^3} \tag{20.5.12}$$

For the diffusion constant, we want to calculate rate of change in the mean square displacement of the exciton. In three-dimensions, $dr^2/dt = 6\mathscr{D}_{\text{EET}}$. We can obtain this by averaging the rate of energy transfer over the distribution of the acceptor distances: $6\mathscr{D} = \sum_j k\left(r_j\right) r_j^2$ or as an integral

$$\mathscr{D}_{\text{EET}} = \frac{1}{6}\int_0^\infty 4\pi\rho g(r) r^2 k(r) r^2\, dr = \left(\frac{2\pi}{3}\right)\frac{CR_0^6}{\tau_0 a} \tag{20.5.13}$$

This describes how the electronic excitation will radially diffuse from one site, however, this process doesn't continue indefinitely. Ultimately, the exciton will relax due to radiative and non-radiative processes. From the diffusion constant, we can estimate the exciton diffusion length, L_{EET}, the root-mean-squared distance over which the exciton diffuses over the fluorescence lifetime, τ_0:

$$L_{\text{EET}} = \sqrt{6\mathscr{D}_{\text{EET}}\tau_0} = \sqrt{\frac{4\pi C}{a}} R_0^3 \tag{20.5.14}$$

Now let's make some predictions for excitation energy transport in a dilute solution of a bright fluorescent chromophore. We choose a critical transfer distance of $R_0 = 5\ \text{nm}$, which we would obtain by calculating the Forster overlap integral between the chromophores absorption and emission spectrum. Let's also choose a radius of $a = 0.5\text{nm}$ from the approximate size of a bright dye molecules, and a fluorescence lifetime of $\tau_0 = 5\ \text{ns}$. Then let's look at the energy diffusion parameters for a solution with $C = 1\text{mM}$ concentration. We calculate the effective rate of energy transfer as $k_{\text{eff}} = 69\ \text{ns}^{-1}$, the exciton diffusion constant as $\mathscr{D} = 8.7 \times 10^{-5}\ \text{cm}^2\text{s}^{-1}$, and the exciton diffusion length as $L_{\text{EET}} = 16\ \text{nm}$. In practice, these numbers far exceed what one observes in experiment, reflecting limitations to the assumptions of the model, particularly by neglecting the role of disorder and competing relaxation processes.

This page titled 20.5: Frenkel exciton transport is shared under a CC BY-NC-SA 4.0 license and was authored, remixed, and/or curated by LibreTexts.

20.6: Tight-binding model

The principles we have discussed for Frenkel exciton states in molecular aggregates bear significant resemblance to the Tight-Binding model used for Wannier-Mott exciton states. In the Tight Binding (TB) model, the band structure in semiconductors arises from the same form of the Hamiltonian in eq. (20.2.5).(1) However, the electronic states and couplings involved are different, and the model is concerned both with the excited states of the conduction band and the hole in the valence band. This means that the electronic and optical properties of interest for these classes of exciton vary considerably. From the chemist's perspective, the TB model is a Hückel model for the solid in which the band structure arises from electronic couplings that mix either HOMO or LUMO atomic orbitals within the lattice. The exciton states are linear combinations of atomic orbitals (LCAO). The term "tight binding" might throw you off because it's a bit different than our usual language, where interactions between degenerate states are always described as the strong-coupling limit. The term "tight binding" refers to the localization of the initial sites on atomic or molecular sites, and it is typically applied as a contrast to the free electron model for electron motion in materials.

Let's look a bit more into the way the model is applied. We'll simplify this by just considering a linear chain of atomic orbitals instead of a 3D solid, although we are interested in the $N \to \infty$ limit. In its simplest representation, the coupling between adjacent atoms is taken to be proportional to the one-electron resonance (or hopping) integral:(2)(3)

$$H_{n,n'} = \int \phi_n^* H_0 \phi_{n'} \, d^3r \qquad (n \neq n') \tag{20.6.1}$$

If we account only for interactions between orbitals on pairs of adjacent atoms (φ_A and φ_B), the matrix element $H_{AB} = \langle \varphi_A | H_0 | \varphi_B \rangle$ can be computed from the Hamiltonian for a single electron that resides at a distance R_A and R_B from the two nuclei:

$$H_0 = -\left(\frac{\hbar^2}{2m}\right)\nabla^2 - \frac{Z_A e^2}{|r - R_A|} - \frac{Z_B e^2}{|r - R_B|} \tag{20.6.2}$$

In the solid-state physics, the nearest-neighbor interaction H_{AB} is called the hopping integral and commonly written as the constant T or t. However, it corresponds to the same coupling constant J that we used in the Frenkel exciton model, and so we express the interaction terms in our exciton Hamiltonian as

$$H_{n,n'} = J\delta_{n,n'\pm 1} \tag{20.6.3}$$

We also assign a constant site energy ε_0 to each orbital in the chain. Combining the site energies and couplings leads to the TB Hamiltonian which is the same as the Frenkel exciton Hamiltonian in eq. (20.2.6):

$$H_0 = \varepsilon_0 \sum_n a_n^\dagger a_n + J \sum_{\substack{n, \\ n'=n\pm 1}} a_{n'}^\dagger a_n \tag{20.6.4}$$

We build the exciton states as linear combinations of atomic orbitals $|\varphi_n\rangle$ using the Bloch theorem:

$$|\psi_k\rangle = \sum_n e^{ikn\alpha} |\varphi_n\rangle \tag{20.6.5}$$

Again, α is the lattice parameter (the spacing between atoms), and k is the wavevector. We previously indexed the wavevector of a finite aggregate with integers, but now the solid is an extended system in which the states are essentially continuous. As a result, we consider k a continuous variable over the range $-\pi/\alpha < k \leq \pi/\alpha$. Substitution of eq. (20.6.4) into the Schrödinger equation $H|\psi_k\rangle = E|\psi_k\rangle$ leads to the dispersion relationship of the exciton energies:

$$E(k) = \varepsilon_0 + 2J\cos k\alpha \tag{20.6.6}$$

This is the same expression as seen in eq. (20.2.21), a bandwidth of $4J$ and a continuous variation in energy as a function of k, pictured by the line in Figure 20.2.5. In this simple model, the interaction between sites results in $J < 0$ causing $k = 0$ to lie at the bottom of the band, but it is possible for the sign of J to be positive, which places $k = 0$ at the top of the band.

The dispersion relationship contains important dynamical information on exciton transport—for instance, the group velocity $v_{\text{gr}} = \hbar^{-1} dE/dk$, as described in eq. (20.5.4). It is often described in relationship to the dispersion relation for a free electron E_{free}

$= \hbar^2 k^2 / 2m_e$, which shows a parabolic relation between E and k. One observes similar behavior for the exciton band in the limit of $k \approx 0$. We can see this by expanding the cosine in eq. (20.6.6) as $1 - (k\alpha)^2$ to find $E(k) = (\varepsilon_0 + 2J) - 2J\alpha^2 k^2$. To connect the form of the expression for a free electron to the exciton quasiparticle, we can define an effective mass for the electron, m^*, using

$$\frac{1}{m^*} = \frac{1}{\hbar^2} \frac{d^2 E}{dk^2}\bigg|_{k=0} \tag{20.6.7}$$

Applying this to the linear chain TB model, eq. (20.6.6), gives

$$m^* = -\frac{\hbar^2}{2J\alpha^2} \tag{20.6.8}$$

and the dispersion relationship in the parabolic approximation is

$$E(k) - E(0) = \frac{\hbar^2 k^2}{2m^*} \tag{20.6.9}$$

The effective mass becomes the metric that describes how tightly bound the electron is. Smaller site couplings J results in higher effective masses m^*. These "heavier" electrons are more tightly bound to their site and therefore less mobile. We discuss this more just below. Notice also that the curvature of the band at $k = 0$ and the effective mass are negative when $J > 0$. This provides motivation for recasting the properties of an electron vacancy in the valence band as a positively charged hole that has a positive effective mass.

Equation (20.6.6) also illustrates that the density of states in energy as a function of k varies nonlinearly as before, with the densest distribution of states near the band extrema. We can characterize the density of states with the relation

$$\rho(k) = \frac{\partial k}{\partial E} \tag{20.6.10}$$

We can evaluate this by solving eq. (20.6.6) for k

$$k = \frac{1}{\alpha} \mathrm{acos}\left(\frac{E(k) - \varepsilon_0}{2J} \right) \tag{20.6.11}$$

which gives

$$\rho(k) = -\frac{1}{\alpha} \frac{1}{\sqrt{4J^2 - (E(k) - \varepsilon_0)^2}} \tag{20.6.12}$$

At the band edges, $k = 0, \pm\pi/2$, the energy splitting $|E(k) - \varepsilon_0|$ approaches $|2J|$ and the density of states diverges.

The calculation above is illustrative of how we can develop an exciton model to describe the exciton states, their energies and band structure, and gain information on the fundamental properties that shape their bulk electrical transport properties. However, these results are applicable only for 1D chains under the assumptions of the model. The behavior is qualitatively different for excitons in three dimensions, with the density of states exhibiting a smooth broad maximum at band center and dropping to zero at the band edges. Examination of these features in any detail is best left for solid state physics textbooks, such as those listed in the readings. However, one important general observation that we can end with is that the density of states in 1, 2, or 3 dimensions will scale with the energy of the states as $E^{-1/2}$, E, and $E^{1/2}$, respectively. The energy scaling behavior of these density-of-states in turn influences the form of the spectral densities that we use to calculate the influence of band-structure on the dynamics of these electronic excitations.

To put some of these ideas on a concrete footing, let's discuss how this model helps understand the band structure of the II-VI semiconductor cadmium selenide. Although the Cd and Se orbitals hybridize, to an approximation, the valence band is formed from the Se $4p$ orbitals and the conduction band is formed from the Cd $5s$ orbitals. The net transfer of two electrons from Cd to Se results in a valence band that is fully occupied whereas the conduction band is empty. We will describe this through the TB model using interactions between Cd and Se atomic orbitals. To be sure, describing CdSe's band structure is far more involved than a one-dimensional chain of simple s and p orbitals, and there are additional important factors—such as spin—that we have not addressed. Nonetheless, several aspects of the calculation are the same as needed for a real solid, and we can draw several important insights.

The starting point is the coupling between atoms. The Cd $5s$ and Se $4p$ energies are far enough apart, that their hybridization is

small, and the dominant atomic interactions in the lattice are between the same type of nearest neighbor atoms, as assumed in the TB model. To calculate the coupling, we compute the resonance integral for adjacent orbitals. Taking the atoms to be along the z-axis, the matrix elements for the $\mathrm{Cd}\ 5s$ orbitals are

$$\langle 5s(0)\,|H_0|\,5s(\alpha_{\mathrm{Cd}})\rangle = J_{\mathrm{Cd}} \tag{20.6.13}$$

and the integrals for the $\mathrm{Se}\ 4p$ orbitals involved include one for the p_z (p_σ) orbitals and two for the p_x and p_y orbitals (p_π)

$$\langle 4p_z(0)\,|H_0|\,p_z(\alpha_{\mathrm{Se}})\rangle = J_{\mathrm{Se},\sigma} \tag{20.6.14}$$

$$\langle 4p_\pi(0)\,|H_0|\,p_\pi(\alpha_{\mathrm{Se}})\rangle = J_{\mathrm{Se},\pi} \tag{20.6.15}$$

These are the most important terms to include.

Let's think for a moment about what the sign of these integrals will be. The overlap between $\mathrm{Cd}\ 5s$ orbitals and the favorable Coulomb interaction means the interaction favors bonding and lowers the energy of the system, i.e. $J_{\mathrm{Cd}} < 0$. A calculation of the integral results in a coupling value of $J_{\mathrm{Cd}} \approx -0.54\ \mathrm{eV}$ for Cd atoms that are spaced by $\alpha_{\mathrm{Cd}} = 4.30\ \text{Å}$, as they are in the wurtzite structure of CdSe. On the other hand, for the $\mathrm{Se}\ 4p$ orbitals, while the p_π integrals have favorable overlap and $J_{\mathrm{Se},\pi} < 0$, the p_σ integral involves overlap between two orbitals of opposite sign, therefore $J_{\mathrm{Se},\sigma} > 0$. This results in two offsetting interactions, one of which stabilizes the interaction, and the other that destabilizes it. Within a wurtzite lattice, where $\alpha_{\mathrm{Se}} = 4.35\ \text{Å}$, the integrals result in $J_{\mathrm{Se},\pi} \approx -0.33\ \mathrm{eV}$ and $J_{\mathrm{Se},\sigma} \approx 1.31\ \mathrm{eV}$, leading to a net coupling $J_{\mathrm{Se}} = J_{\mathrm{Se},\sigma} + 2J_{\mathrm{Se},\pi} \approx +0.65\ \mathrm{eV}$. The p_σ integral dominates the interaction. As a result the nearest neighbor integrals result in a positive J for the $\mathrm{Se}\ p$ interactions but a negative J for the $\mathrm{Cd}\ 5s$ band. While these calculations oversimplify the real properties of the 3D solid, they do capture the main factors that govern the interactions and the sign of the couplings.

What does this mean for the band structure? Similarly to the observations for Frenkel excitons, this means that we expect the $k = 0$ states to be at the bottom of the band for the $\mathrm{Cd}\ 5s$ conduction band and at the top of the $\mathrm{Se}\ 4p$ valence band. However, beyond this argument based on the nearest-neighbor interactions, we can qualitatively rationalize this simply in terms of the phase of complex orbitals at each site within an exciton eigenstate. For $5s$ orbitals, we expect the lowest energy state to be that in which all orbitals of the chain are in-phase, corresponding to $k = 0$. For higher values of k, the increasing nodes in the chain raise the energy of the band, culminating with $k = \pi/\alpha$ at the top of the band, where all adjacent orbitals are out of phase with each other (Figure 20.6.1). The scenario is reversed for the $\mathrm{Se}\ 4p$ band, because the nearest-neighbor interactions are dominated by the $4p_z$ orbitals, which have a node at the Se nucleus. In this case, the most energetically favorable interactions for the exciton arises at $k = \pi/\alpha$ when nearest neighbor orbitals are out of phase, resulting in maximal constructive overlap.

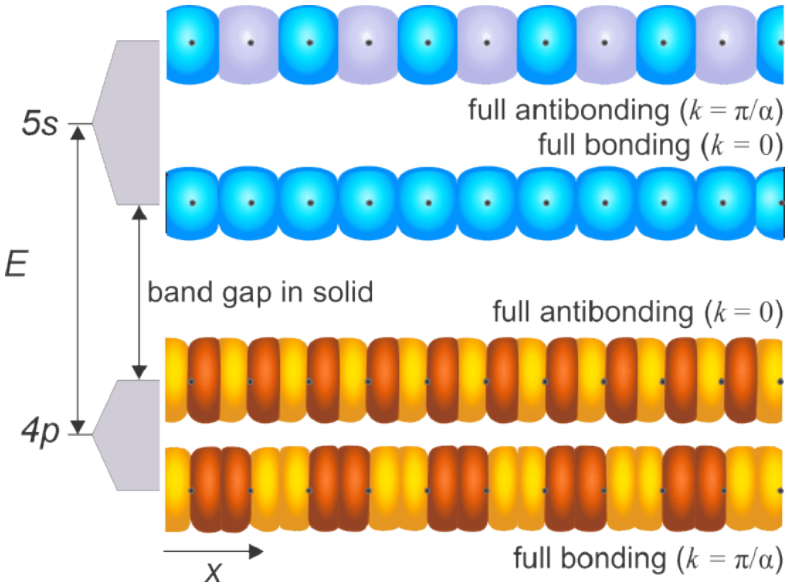


Figure 20.6.1: Illustration of valence and conduction bands in CdSe formed by linear combinations of $4p$ and $5s$ orbitals. Adapted from Simons, *Advanced Theoretical Chemistry*.(2)

Optical excitation of an electron across this band gap results in an electron-hole pair that can evolve in time and space, but not entirely independently. To properly describe the electron-hole correlations in a Hamiltonian requires separate one-electron hopping integrals for the valence and conduction band interactions, as well as two-electron Coulomb and exchange integrals over

for the configuration of particle and hole, in addition to spin for the electron-hole pair. Since the dominant interaction between electron and hole is the Coulomb attraction, we can take a step forward in describing the exciton properties by focusing on this effect. The Wannier model discards the lattice entirely, describing the electron-hole pair as two particles of opposite charge bound by a Coulomb interaction. This results in a Hamiltonian that is effectively the same as for a hydrogen atom, except that we use the two effective masses, and the Coulomb interaction is treated as screened by the remaining electrons and nuclei through an effective dielectric constant for the medium, ε:

$$H_0 = -\frac{\hbar^2}{2\mu^*}\nabla^2 - \frac{e^2}{4\pi\varepsilon_0\varepsilon r} \tag{20.6.16}$$

Here r is the distance between the electron and hole, and μ^* is the reduced mass of the electron and hole

$$\mu^* = \frac{m_e^* m_h^*}{m_e^* + m_h^*} = \frac{\hbar^2}{2\alpha^2\left(|J_e| + |J_h|\right)} \tag{20.6.17}$$

Within this model, it is possible to compute the binding energy for the electron-hole pair. This is the energy needed to separate the exciton into a noninteracting electron and hole, and is computed much like the ionization energy of hydrogen atom in its $n = 1$ state:

$$E_b = -\frac{\mu^* e^4}{2\hbar^2\left(4\pi\varepsilon_0\varepsilon\right)^2} = \frac{\mu^*}{\varepsilon^2 m_e} R_y \tag{20.6.18}$$

R_y refers to Rydbergs $(13.6\ \mathrm{eV})$. Also, like a hydrogen atom, one can calculate the exciton radius by describing the average separation of the electron and hole (analogous to the Bohr radius a_0)

$$R_{\mathrm{ex}} = \frac{4\pi\varepsilon_0\varepsilon\hbar^2}{\mu^* e^2} = \frac{\mu^*}{\varepsilon m_e} a_0 \tag{20.6.19}$$

We can see that the dielectric constant is the proportionality constant between the binding energy in Rydbergs and the exciton radius in a_0 $(53\ \mathrm{pm})$: $R_{\mathrm{ex}}/a_0 = \varepsilon E_b/R_y$.

Let's use the Wannier model to calculate the binding energy for CdSe in its wurtzite structure. There one finds that the effective mass of the electron and hole are $m_e^* = 0.13 m_e$ and $m_h^* = 0.45 m_e$, resulting in a reduced exciton mass of $\mu^* = 0.10 m_e$. For the dielectric constant, the screening of an exciton by the electrons of the medium is obtained from the high-frequency dielectric constant $\varepsilon_\infty = 6$, but if we want to include the effect of the nuclear motion in screening, we would use the static dielectric constant of 9.5. The latter results in values that are relatively close to experiment. The exciton binding energy is then calculated as $E_b = 15\ \mathrm{meV}$ and the exciton radius is $R_{\mathrm{ex}} = 5.0\ \mathrm{nm}$. The exciton radius is an order of magnitude larger than the lattice parameter α, indicating that the exciton is delocalized over thousands of Cd and Se atoms. The binding energy is less than thermal energy at room temperature $k_B T = 26\ \mathrm{meV}$, indicating that electrons and holes can spontaneously separate, and these free electron-hole pairs will be responsible for the optical properties and conductivity of the solid.

References

(1) The exciton Hamiltonian site energy ε_0 corresponds to the coulomb integral α of Hückel theory, and the coupling J corresponds to the resonance integral β.

(2) Simons, J. Bands of Orbitals in Solids. *Advanced Theoretical Chemistry*; LibreTexts, 2021; p 11573.

(3) Simons, J. Hückel or Tight Binding Theory. *Advanced Theoretical Chemistry*; LibreTexts, 2021; p 17181.

This page titled 20.6: Tight-binding model is shared under a CC BY-NC-SA 4.0 license and was authored, remixed, and/or curated by Andrei Tokmakoff via source content that was edited to the style and standards of the LibreTexts platform.

20.7: Readings

Frenkel excitons in molecular aggregates

1. Agranovič, V. M. *Excitations in Organic Solids*; Oxford University Press, 2008. DOI: 10.1093/acprof:oso/9780199234417.001.0001
2. Davydov, A. S. *Theory of Molecular Excitons*; Springer, 2013. DOI: 10.1007/978-1-4899-5169-4
3. Knoester, J. Optical Properties of Molecular Aggregates. *Organic Nanostructures: Science and Applications*; Agranovič, V. M., La Rocca, G. C., Eds.; Proceedings of the International School of Physics "Enrico Fermi", IOS Press, 2002; pp 149-186. DOI: 10.3254/978-1-61499-005-5-149

Absorption Spectrum of a Dimer

1. Kasha, M.; Rawls, H. R.; El-Bayoumi, M. A. The exciton model in molecular spectroscopy. *Pure and Applied Chemistry* **1965**, *11* (3-4), 371-392. DOI: 10.1351/pac196511030037

Good entry material for Frenkel excitons

1. The presentation on molecular excitons closely mirrors that of:
   - Knoester, J. Optical Properties of Molecular Aggregates. *Organic Nanostructures: Science and Applications*; Agranovič, V. M., La Rocca, G. C., Eds.; Proceedings of the International School of Physics "Enrico Fermi", IOS Press, 2002; pp 149-186. DOI: 10.3254/978-1-61499-005-5-149
2. A nice review paper that covers the basics of Frenkel excitons in many types of molecular aggregates, the role of disorder, and electronic energy transport at the level of this chapter.
   - Jansen, T. L. C.; Günther, L. M.; Knoester, J.; Köhler, J. Electronically excited states in cylindrical molecular aggregates: Exciton delocalization, dynamics, and optical response. *Chemical Physics Reviews* **2024**, *5* (4), 041305. DOI: 10.1063/5.0225327

Excellent Resources on excitons from a chemists perspective

1. Accessible textbook that covers numerous topics in electronic structure and excitation transport in molecular systems.
   - Bittner, E. R. *Quantum dynamics: applications in biological and materials systems*; CRC Press, 2010. DOI: 10.1201/b15835
2. Comprehensive text on the theory of electronic energy transfer with a detailed theoretical presentation.
   - May, V.; Kühn, O. *Charge and Energy Transfer Dynamics in Molecular Systems*; Wiley-VCH Verlag, 2011. DOI: 10.1002/9783527633791

Wannier-Mott excitons and electronic band structure

1. The classic text on solid state physics that handles everything.
   - Ashcroft, N. W.; Mermin, N. D. *Solid State Physics*; Harcourt, 1976.
2. Excellent introductory text
   - Singleton, J. *Band Theory and Electronic Properties of Solids*; Oxford University Press, 2001. DOI: 10.1093/oso/9780198506454.001.0001

This page titled 20.7: Readings is shared under a CC BY-NC-SA 4.0 license and was authored, remixed, and/or curated by Andrei Tokmakoff via source content that was edited to the style and standards of the LibreTexts platform.

21: APPENDICES

21.1: Math and Physics Reference Material

21.1.1: Atomic Units

21.1.2: Dirac Delta Function

21.1.3: Gaussian Integrals and Error Function

21.2: Quantum Mechanics- Extra Topics

21.2.1: Numerically Solving the Schrödinger Equation

21.2.2: Separation of Subsystems

21.2.3: Morse Oscillator

This page titled 21: Appendices is shared under a CC BY-NC-SA 4.0 license and was authored, remixed, and/or curated by Andrei Tokmakoff via source content that was edited to the style and standards of the LibreTexts platform.

21.1: MATH AND PHYSICS REFERENCE MATERIAL

21.1.1: Atomic Units
21.1.2: Dirac Delta Function
21.1.3: Gaussian Integrals and Error Function

This page titled 21.1: Math and Physics Reference Material is shared under a CC BY-NC-SA 4.0 license and was authored, remixed, and/or curated by LibreTexts.

21.1.1: Atomic Units

Setting $\hbar = 1 = e = m_e$

	Atomic Units (AU)	Equivalent SI Units
Charge (elementary charge)	e	$1.602 \times 10^{-19}\text{C}$
Length (Bohr radius)	a_0	$5.2918 \times 10^{-11}\ \text{m}$
Mass (mass of an electron)	m_e	$9.109 \times 10^{-31}\ \text{kg}$
Electric dipole moment	$M = ea_0$	$8.478 \times 10^{-18}\ \text{C} \cdot \text{m} = 2.542\ \text{D}$
Energy (Hartrees)	$E_h = \frac{\hbar^2}{m_e a_0^2}$	$4.360 \times 10^{-18}\ \text{J} = 27.21\ \text{eV}$
Electric Field	$\frac{E_h}{ea_0}$	$5.142 \times 10^{11}\ \text{V} \cdot \text{m}^{-1} = 51.42\ \text{V} \cdot \text{A}^{-1}$
Force	$F = \frac{E_h}{a_0}$	$8.239 \times 10^{-8}\ \text{N}$
Momentum	$\frac{\hbar}{a_0}$	$1.993 \times 10^{-24}\ \text{kg} \cdot \text{m} \cdot \text{s}^{-1}$
Permittivity	$4\pi\epsilon_0 = \frac{e^2}{a_0 E_h}$	$1.1126 \times 10^{-10}\ \text{F} \cdot \text{m}^{-1}$

This page titled 21.1.1: Atomic Units is shared under a CC BY-NC-SA 4.0 license and was authored, remixed, and/or curated by Andrei Tokmakoff via source content that was edited to the style and standards of the LibreTexts platform.

21.1.2: Dirac Delta Function

We define the Dirac delta function $\delta(x)$ as a function that has the value zero for all points except when the argument x is zero. There it takes on a value of one:

$$\delta(x) = \begin{cases} 0 & x \neq 0 \\ 1 & x = 0 \end{cases} \tag{21.1.2.1}$$

Integrating over the delta function gives a value of one.

$$\int_{-\infty}^{+\infty} \delta(x-a)\, dx = 1 \tag{21.1.2.2}$$

Therefore the delta function is often used to represent the completeness of a continuous basis set. We can use the delta function to pick out the value of a function for a specific value a using the convolution integral

$$\int_{-\infty}^{+\infty} \delta(x-a) f(x)\, dx = f(a) \tag{21.1.2.3}$$

The delta function is the derivative of the unit step function Θ :

$$\delta(x) = \frac{d}{dx}\Theta(x) \tag{21.1.2.4}$$

$$\Theta(x) = \begin{cases} 0 & x < 0 \\ 1 & x \geq 0 \end{cases} \tag{21.1.2.5}$$

The Dirac delta function can be represented in terms of the zero-width limit of continuous functions that are peaked at $x = 0$ and drop to zero in the limits $x = \pm\infty$:

$$\delta(x) = \lim_{a\to\infty} \frac{2\sin^2 \frac{1}{2}ax}{\pi a x^2} \tag{21.1.2.6}$$

$$\delta(x) = \lim_{a\to\infty} \frac{\sin ax}{\pi x} \tag{21.1.2.7}$$

$$\delta(x) = \lim_{a\to 0} \operatorname{Im}\left[\frac{1}{\pi[x - \mathrm{i}a]}\right] \tag{21.1.2.8}$$

$$\delta(x) = \lim_{a\to 0} \frac{a}{\pi\left[x^2 + a^2\right]} \tag{21.1.2.9}$$

$$\delta(x) = \lim_{a\to 0} \frac{1-\cos ax}{\pi a x^2} \tag{21.1.2.10}$$

$$\delta(x) = \lim_{a\to\infty} \sqrt{\frac{a}{\pi}} e^{-ax^2} \tag{21.1.2.11}$$

The delta function is also be expressed through a Fourier transform as

$$\delta(x) = \frac{1}{2\pi} \int_{-\infty}^{+\infty} e^{\mathrm{i}kx}\, dk \tag{21.1.2.12}$$

Other useful identities for the delta function:

$$\delta(ax) = \frac{1}{|a|}\delta(x) \tag{21.1.2.13}$$

$$x\frac{d}{dx}\delta(x) = -\delta(x) \tag{21.1.2.14}$$

$$\delta(-x) = \delta(x) \tag{21.1.2.15}$$

$$x\delta(x) = 0 \tag{21.1.2.16}$$

$$\delta\left(x^2 - a^2\right) = \frac{1}{2}a^{-1}\{\delta(x-a) + \delta(x+a)\} \tag{21.1.2.17}$$

$$\int \delta(a-x)\delta(x-b)\,dx = \delta(a-b) \tag{21.1.2.18}$$

$$f(x)\delta(x-a) = f(a)\delta(x-a) \tag{21.1.2.19}$$

In three dimensions, we can write the delta function in terms of three separable degrees of freedom. In Cartesian variables

$$\delta(\boldsymbol{r}) = \delta(x)\delta(y)\delta(z) \tag{21.1.2.20}$$

In spherical coordinates (r, θ, ϕ)

$$\delta\left(\mathbf{r} - \mathbf{r}_0\right) = \frac{1}{r^2\sin\theta}\delta\left(r - r_0\right)\delta\left(\theta - \theta_0\right)\delta\left(\phi - \phi_0\right) \tag{21.1.2.21}$$

and the angular component can be expressed in spherical harmonics as:

$$\frac{1}{\sin\theta}\delta\left(\theta - \theta_0\right)\delta\left(\phi - \phi_0\right) = \sum_{\ell=1}^{\infty}\sum_{m=-\ell}^{\ell} Y_{\ell,m}^{*}(\theta,\phi)Y_{\ell,m}\left(\theta_0,\phi_0\right) \tag{21.1.2.22}$$

$$\int_0^{\pi} d\theta \int_0^{2\pi} d\phi\delta\left(\theta - \theta_0\right)\delta\left(\phi - \phi_0\right) = 1 \tag{21.1.2.23}$$

The Dirac delta function should be distinguished from the Kronecker delta function, which is a function of two integers, i and j, such that

$$\delta_{ij} = \begin{cases} 0 & i \neq j \\ 1 & i = j \end{cases} \tag{21.1.2.24}$$

The Kronecker delta is equivalent to the identity matrix $\mathbf{I}$.

This page titled 21.1.2: Dirac Delta Function is shared under a CC BY-NC-SA 4.0 license and was authored, remixed, and/or curated by Andrei Tokmakoff via source content that was edited to the style and standards of the LibreTexts platform.

21.1.3: Gaussian Integrals and Error Function

Gaussian Distribution

The Gaussian or Normal distribution function in one dimension is

$$P(x) = \frac{1}{\sqrt{2\pi\sigma^2}} \exp \frac{(x - x_0)^2}{2\sigma^2} \tag{21.1.3.1}$$

where x_0 is the mean value of the distribution, σ is the standard deviation, and $\sigma^2 = \langle x^2 \rangle - \langle x \rangle^2$ is the variance of the distribution.

Gaussian integrals

The general strategy with solving Gaussian definite integrals is to complete the square in exponential argument to recast it as a simpler integral. To illustrate, let's integrate the product of a Gaussian and a complex exponential of the form

$$I = \int_{-\infty}^{+\infty} dt\, e^{-\alpha t^2} e^{\mathrm{i}\omega t - \gamma t} \tag{21.1.3.2}$$

where α is a real positive number. Assigning $\beta = \mathrm{i}\omega - \gamma$, we can add $-\beta^2/4\alpha$ to the exponential argument, we can write it as

$$I = e^{\beta^2/4\alpha} \int_{-\infty}^{+\infty} dt\, \exp\left(-\alpha\left(t - \frac{\beta}{2\alpha}\right)^2\right) \tag{21.1.3.3}$$

The simpler Gaussian integral here is $\sqrt{\pi\,/\,\alpha}$, so

$$I = \sqrt{\frac{\pi}{\alpha}} e^{\beta^2/4\alpha} \tag{21.1.3.4}$$

Table of Gaussian integrals

$$\int_{-\infty}^{+\infty} dt\, \mathrm{e}^{-\alpha t^2} = \sqrt{\frac{\pi}{\alpha}} \tag{21.1.3.5}$$

$$\int_{0}^{+\infty} dt\, \mathrm{e}^{-\alpha t^2} = \frac{1}{2}\sqrt{\frac{\pi}{\alpha}} \tag{21.1.3.6}$$

$$\int_{0}^{\infty} dt\, t\, \mathrm{e}^{-\alpha t^2} = \frac{1}{2\alpha} \tag{21.1.3.7}$$

$$\int_{-\infty}^{+\infty} dt\, t^2 \mathrm{e}^{-\alpha t^2} = \sqrt{\frac{\pi}{4\alpha^3}} d \int_{-\infty} dt\, t^2 \mathrm{e}^{-\alpha t^2} = -\frac{d}{d\alpha}\int_{-\infty}^{+\infty} dt\, \mathrm{e}^{-\alpha t^2} \tag{21.1.3.8}$$

$$\int_{-\infty}^{+\infty} dy \int_{-\infty}^{+\infty} dx \mathrm{e}^{-(ax^2+2bxy+cy^2)} = \frac{\pi}{\sqrt{ac}-b^2} \tag{21.1.3.9}$$

$$\int_{0}^{\infty} dt\, t^{2n} \mathrm{e}^{-\alpha t^2} = \frac{1\cdot 3\cdot \ldots (2n-1)}{2^{n+1}a^n}\sqrt{\frac{\pi}{\alpha}} \qquad (n = 0, 1, 2 \ldots) \tag{21.1.3.10}$$

$$\int_{0}^{+\infty} dt\, t^{2n+1} \mathrm{e}^{-\alpha t^2} = \frac{n!}{2a^{n+1}} \qquad (n = 0, 1, 2 \ldots) \tag{21.1.3.11}$$

$$\int_{-\infty}^{\infty} dt\, t^{2n+1} \mathrm{e}^{-\alpha t^2} = 0 \qquad (n = 0, 1, 2 \ldots) \tag{21.1.3.12}$$

$$\int_{-\infty}^{+\infty} \exp^{-(at^2+bt+c)} = \sqrt{\frac{\pi}{a}} \exp\left[\frac{b^2}{4a} - c\right] \tag{21.1.3.13}$$

$$\int_{-\infty}^{+\infty} dt\, \exp\left(-\alpha\left(t - \frac{\mathrm{i}x}{2\alpha}\right)^2\right) = \int_{-\infty}^{+\infty} dt \mathrm{e}^{-\alpha t^2 + \mathrm{i}xt + x^2/4\alpha} = \sqrt{\frac{\pi}{\alpha}} \tag{21.1.3.14}$$

$$\int_{-\infty}^{+\infty} \exp\left(-\beta \mathrm{x}^2\right) \cos\left(\mathrm{bx}\right)\, \mathrm{dx} = \sqrt{\frac{\pi}{\beta}} \exp\left(-\frac{\mathrm{b}^2}{4}\beta\right) \tag{21.1.3.15}$$

$$\int_{-\infty}^{+\infty} dy \int_{-\infty}^{+\infty} dx\, \mathrm{e}^{-(ax^2+2bxy+cy^2)} = \frac{\pi}{\sqrt{ac-b^2}} \tag{21.1.3.16}$$

Error Function

The error function, $\mathrm{erf}(z)$, is a complex sigmoidal step function that appears in integrals over Gaussian distributions and Gaussian convolutions. If is defined through a definite integral over a Gaussian function as

$$\mathrm{erf}(z) = \frac{2}{\sqrt{\pi}} \int_0^z e^{-t^2} dt \tag{21.1.3.17}$$

The complementary error function, $\mathrm{erfc}(z)$, is

$$\mathrm{erfc}(z) \equiv \frac{2}{\sqrt{\pi}} \int_z^\infty e^{-t^2} dt \tag{21.1.3.18}$$

and $\mathrm{erfc}(x) = 1 - \mathrm{erf}(x)$.

The imaginary error function is defined as

$$\mathrm{erfi}(z) \equiv -\mathrm{i}\,\mathrm{erf}(\mathrm{i}z) = \frac{2}{\sqrt{\pi}} \int_0^z e^{t^2} dt \tag{21.1.3.19}$$

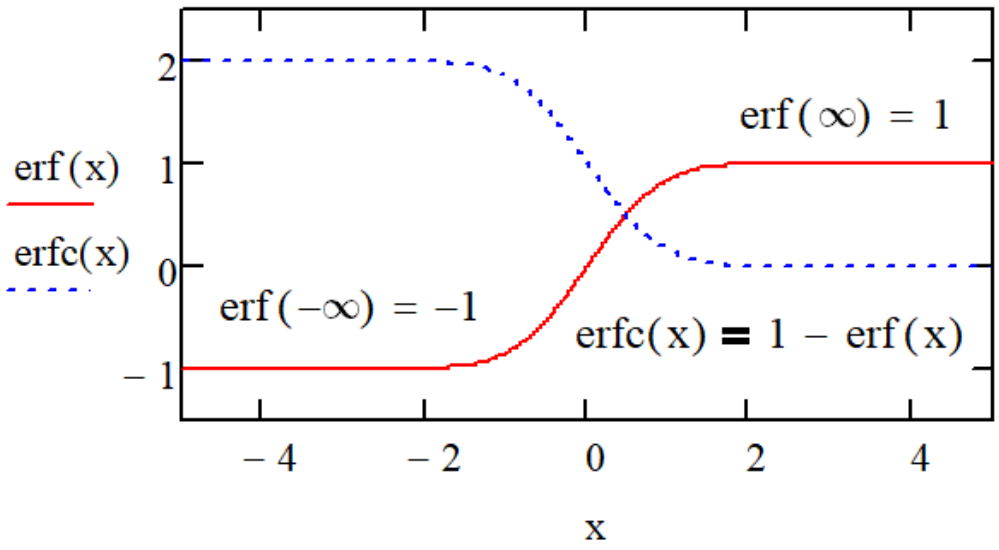


Figure 1. (CC- by Andrei Tokmakoff)

Error Function Identities

$$\operatorname{erf}(-z) = -\operatorname{erf}(z) \tag{21.1.3.20}$$

$$\frac{2}{\sqrt{\pi}}\int_a^b dz\, \mathrm{e}^{-\alpha z^2} = \operatorname{erf}(b) - \operatorname{erf}(a) \tag{21.1.3.21}$$

$$\operatorname{erf}(z^*) = (\operatorname{erf}(z))^* \tag{21.1.3.22}$$

$$\frac{d}{dx}\operatorname{erf}(z) = \sqrt{\frac{4}{\pi}}\mathrm{e}^{-z^2} \tag{21.1.3.23}$$

$$\operatorname{erf}(z) = \sqrt{\frac{4}{\pi}}\sum_{n=0}^{\infty}\frac{(-1)^n z^{2n+1}}{n!(2n+1)} \tag{21.1.3.24}$$

Gaussian integrals involving the error function

$$\int e^{-a^2z^2+bz}\, dz = \frac{\sqrt{\pi}}{2a}\exp\left(\frac{b^2}{4a^2}\right)\operatorname{erf}\left(az - \frac{b}{2a}\right) \tag{21.1.3.25}$$

$$\int_0^\infty e^{-a^2x^2+bx}\, dx = \frac{\sqrt{\pi}}{2a}\exp\left(\frac{b^2}{4a^2}\right)\left[1 + \operatorname{erf}\left(\frac{b}{2a}\right)\right] \tag{21.1.3.26}$$

$$\int dt\, \mathrm{e}^{-(at^2+2bt+c)} = \frac{1}{2}\sqrt{\frac{\pi}{a}}\exp\left(\frac{b^2-ac}{a}\right)\operatorname{erf}\left(\sqrt{a}t + \frac{b}{\sqrt{a}}\right) \tag{21.1.3.27}$$

$$\int_0^\infty dt\, \mathrm{e}^{-(at^2+2bt+c)} = \frac{1}{2}\sqrt{\frac{\pi}{a}}\exp\left(\frac{b^2-ac}{a}\right)\operatorname{erfc}\left(\frac{b}{\sqrt{a}}\right) \tag{21.1.3.28}$$

$$\int_{-\infty}^\infty dt\, \mathrm{e}^{-(at^2+2bt)} = \sqrt{\frac{\pi}{a}}\mathrm{e}^{\frac{-b^2}{a}} \tag{21.1.3.29}$$

$$\int_0^\infty dt\, \mathrm{e}^{-(at^2+2bt)} = \frac{1}{2}\sqrt{\frac{\pi}{a}}\mathrm{e}^{b^2/a}\operatorname{erfc}\left(\frac{b}{\sqrt{a}}\right) \tag{21.1.3.30}$$

$$\int_0^x dt\, \mathrm{e}^{-\alpha t^2} = \sqrt{\frac{\pi}{4\alpha}}\operatorname{erf}\left(\frac{x}{\sqrt{\alpha}}\right) \tag{21.1.3.31}$$

$$\int_0^x dt\, t^2\mathrm{e}^{-\alpha t^2} = \frac{2}{\sqrt{\pi}}x\mathrm{e}^{-\alpha x^2} + \sqrt{\frac{\pi}{4\alpha^3}}\operatorname{erf}\left(\frac{x}{\sqrt{\alpha}}\right) \tag{21.1.3.32}$$

Error function integrals

$$\int \operatorname{erf}(az)\,dz = z\operatorname{erf}(az) + \frac{1}{a\sqrt{\pi}}\exp\left(-a^2z^2\right) \tag{21.1.3.33}$$

$$\int \operatorname{erfc}(az)\,dz = z\operatorname{erfc}(az) - \frac{1}{a\sqrt{\pi}}\exp\left(-a^2z^2\right) \tag{21.1.3.34}$$

$$\int \operatorname{erf}(az)e^{bz}\,dz = \frac{1}{b}e^{bz}\operatorname{erf}(az) - \frac{1}{b}\exp\left(\frac{b^2}{4a^2}\right)\operatorname{erf}\left(az - \frac{b}{2a}\right) \tag{21.1.3.35}$$

$$\int_0^\infty \operatorname{erf}(ax)e^{-bx}\,dx = \frac{1}{b}\exp\left(\frac{b^2}{4a^2}\right)\operatorname{erfc}\left(\frac{b}{2a}\right) \qquad \left(\operatorname{Re}(b) > 0, |\arg a| < \frac{\pi}{4}\right) \tag{21.1.3.36}$$

$$\int_0^\infty e^{-at}\operatorname{erf}\sqrt{bt}\,dt = \frac{1}{a}\sqrt{\frac{b}{a+b}} \qquad (\operatorname{Re}(a+b) > 0) \tag{21.1.3.37}$$

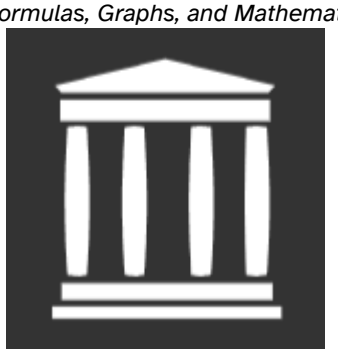
$$\int_0^\infty e^{-at}\operatorname{erfc}\sqrt{\frac{b}{t}}\,dt = \frac{1}{a}e^{-2\sqrt{ab}} \qquad (\operatorname{Re}(a) > 0, \operatorname{Re}(b) > 0) \tag{21.1.3.38}$$

$$\int_0^\infty dt\,\mathrm{e}^{-at^2}\operatorname{erf}(bx) = \sqrt{\frac{1}{a\pi}}\operatorname{atan}\frac{1}{a} \tag{21.1.3.39}$$

$$\int_0^\infty dt\,\frac{\mathrm{e}^{-at^2}}{t^2+b^2} = \frac{1}{2}\frac{\pi}{b}\mathrm{e}^{ab^2}\operatorname{erfc}(\sqrt{a}b) \tag{21.1.3.40}$$

References

(1) *Handbook of Mathematical Functions with Formulas, Graphs, and Mathematical Tables*, 7th ed.; Abramowitz, M., Stegun, I. A., Eds.; National Bureau of Standards, 1968.



This page titled 21.1.3: Gaussian Integrals and Error Function is shared under a CC BY-NC-SA 4.0 license and was authored, remixed, and/or curated by Andrei Tokmakoff via source content that was edited to the style and standards of the LibreTexts platform.

21.2: QUANTUM MECHANICS- EXTRA TOPICS

21.2.1: Numerically Solving the Schrödinger Equation
21.2.2: Separation of Subsystems
21.2.3: Morse Oscillator

This page titled 21.2: Quantum Mechanics- Extra Topics is shared under a CC BY-NC-SA 4.0 license and was authored, remixed, and/or curated by LibreTexts.

21.2.1: Numerically Solving the Schrödinger Equation

Often the bound potentials that we encounter are complex and the time-independent Schrödinger equation will need to be evaluated numerically. There are two common numerical methods for solving for the eigenvalues and eigenfunctions of a potential. Both methods require truncating and discretizing a region of space that is normally spanned by an infinite dimensional Hilbert space. The Numerov method is a finite difference method that calculates the shape of the wavefunction by integrating step-by-step across along a grid. The DVR method makes use of a transformation between a finite discrete basis and the finite grid that spans the region of interest.

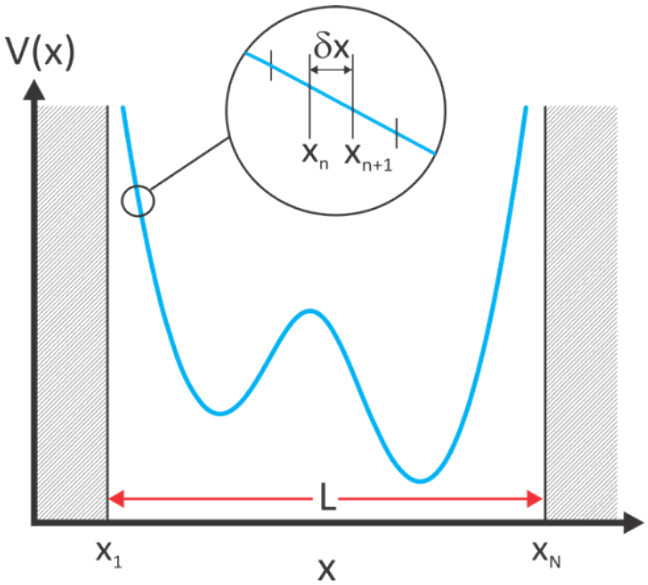


Figure 1. Selection and discretization of a space bounding the region for which the TISE will be solved numerically. A space of length L is discretized into N points separated by a spacing δx over which the potential varies slowly.

The Numerov Method(1)

A one-dimensional Schrodinger equation for a particle in a potential can be numerically solved on a grid that discretizes the position variable using a finite difference method. The TISE is

$$[T + V(x)]\psi(x) = E\psi(x)$$

with $T = -\frac{\hbar^2}{2m}\frac{\partial^2}{\partial x^2}$, which we can write as

$$\psi''(x) = -k^2(x)\psi(x) \tag{21.2.1.1}$$

where $k^2(x) = \frac{2m}{\hbar^2}[E - V(x)]$.

If we discretize the variable x, choosing a grid spacing δx over which V varies slowly, we can use a three-point finite difference to approximate the second derivative:

$$f_i'' \approx \frac{1}{\delta x^2}\left(f\left(x_{i+1}\right) - 2f\left(x_i\right) + f\left(x_{i-1}\right)\right) \tag{21.2.1.2}$$

The discretized Schrodinger equation can then be written in the form

$$\psi\left(x_{i+1}\right) - 2\psi\left(x_i\right) + \psi\left(x_{i-1}\right) = -k^2\left(x_i\right)\psi\left(x_i\right) \tag{21.2.1.3}$$

Using the equation for $\psi\left(x_{i+1}\right)$, one can iteratively solve for the eigenfunction. In practice, we discretize over a range of space

such that the highest and lowest values lie in a region where the potential is very high or forbidden. Splitting the space into N points, chose the first two values $\psi(x_1) = 0$ and $\psi(x_2)$ to be a small positive or negative number, guess E, and propagate iteratively to $\psi(x_N)$. A comparison of the wavefunctions obtained by propagating from x_1 to x_N with that obtained propagating from x_N to x_1 tells us how good our guess of E was.

The Numerov Method improves on eq. (3) by taking account for the fourth derivative of the wavefunction $\Psi^{(4)}$, leading to errors on the order $O(\delta x^6)$. Equation (2) becomes

$$f_i'' \approx \frac{1}{\delta x^2}\left(f(x_{i+1}) - 2f(x_i) + f(x_{i-1})\right) - \frac{\delta x^2}{12} f_i^{(4)}$$

By differentiating eq. (1) we know $\psi^{(4)}(x) = -\left(k^2(x)\psi(x)\right)''$, and the discretized Schrödinger equation becomes

$$\psi''(x_i) = \frac{1}{\delta x^2}\left(\psi(x_{i+1}) - 2\psi(x_i) + \psi(x_{i-1})\right) + \frac{1}{12}\left(k^2(x_{i+1})\psi(x_{i+1}) - 2k^2(x_{i+1})\psi(x_i) + k^2(x_{i+1})\psi(x_{i-1})\right)$$

This equation leads to the iterative solution for the wavefunction

$$\psi(x_{i+1}) = \left(1 - \frac{\delta x^2}{12}k^2(x_{i+1})\right)^{-1}\left(\psi(x_i)\left(2 + \frac{10\delta x^2}{12}k^2(x_i)\right) - \psi(x_{i-1})\left(1 - \frac{\delta x^2}{12}k^2(x_{i-1})\right)\right)$$

Discrete Variable Representation(2)

Numerical solutions to the wavefunctions of a bound potential in the position representation require truncating and discretizing a region of space normally spanned by an infinite dimensional Hilbert space. The DVR approach uses a real space basis set whose eigenstates $\varphi_i(x)$ we know and that span the space of interest—for instance harmonic oscillator wavefunctions—to express the eigenstates of a Hamiltonian in a grid basis θ_j that is meant to approximate the real space continuous basis $\delta(x)$. The two basis sets, which we term the eigenbasis (φ) and grid basis (θ), will be connected through a unitary transformation

$$\Phi^\dagger \varphi(x) = \theta(x) \qquad \Phi\theta(x) = \varphi(x)$$

For N discrete points in the grid basis, there will be N eigenvectors in the eigenbasis, allowing the properties of projection and completeness will hold in both bases. Wavefunctions can be obtained by constructing the Hamiltonian in the eigenbasis, $H = T(\hat{p}) + V(\hat{x})$, transforming to the DVR basis, $H^{DVR} = \Phi H \Phi^\dagger$, and diagonalizing.

Here we will discuss a version of DVR in which the grid basis is set up to mirror the continuous $|x\rangle$ eigenbasis. We begin by choosing the range of x that contain the bound states of interest and discretizing these into N points (x_i) equally spaced by δx. We assume that the DVR basis functions $\theta_j(x_i)$ resemble the infinite dimensional position basis

$$\theta_j(x_i) = \sqrt{\Delta x}\delta_{ij}$$

Our truncation is enabled using a projection operator in the reduced space

$$P_N = \sum_{i=1}^{N} |\theta_i\rangle\langle\theta_i| \approx 1$$

which is valid for appropriately high N. The complete Hamiltonian can be expressed in the DVR basis $H^{DVR} = T^{DVR} + V^{DVR}$. For the potential energy, since $\{\theta_i\}$ is localized with $\langle\theta_i \mid \theta_j\rangle = \delta_{ij}$, we make the DVR approximation, which casts V^{DVR} into a diagonal form that is equal to the potential energy evaluated at the grid point:

$$V_{ij}^{\mathrm{DVR}} = \langle\theta_i|V(\hat{x})|\theta_j\rangle \approx V(x_i)\,\delta_{ij} \tag{21.2.1.4}$$

This comes from approximating the transformation as $\Phi V(\hat{x})\Phi^\dagger \approx V\left(\Phi\hat{x}\Phi^\dagger\right)$.

For the kinetic energy matrix elements $\langle\theta_i|T(\hat{p})|\theta_j\rangle$, we need to evaluate second derivatives between different grid points. Fortunately, Colbert and Miller have simplified this process by finding an analytical form for the T^{DVR} matrix for a uniformly gridded box with a grid spacing of Δx.(3)

$$T_{ij}^{\mathrm{DVR}} = \frac{\hbar^2(-1)^{i-j}}{2m\Delta x^2} \begin{Bmatrix} \pi^2/3 & i=j \\ 2/(i-j)^2 & i \neq j \end{Bmatrix} \tag{21.2.1.5}$$

This comes from a Fourier expansion in a uniformly gridded box. Naturally this looks oscillatory in x at period of δx. Expression becomes exact in the limit of $N \to \infty$ or $\Delta x \to 0$.

The numerical routine becomes simple and efficient. We construct a Hamiltonian filling with matrix elements whose potential and kinetic energy contributions are given by eq. (21.2.1.4) and eq. (21.2.1.5). Then we diagonalize H^{DVR}, from which we obtain N eigenvalues and the N corresponding eigenfunctions.

References

(1) Levine, I. N. *Quantum Chemistry*, 5th ed.; Prentice-Hall, 2000.

(2) Light, J. C.; Carrington, T. Discrete-Variable Representations and their Utilization. *Advances in Chemical Physics Volume 114*; Prigogine, I., Rice, S. A., Eds.; Advances in chemical physics, John Wiley & Sons, Inc., 2000; pp 263-310. DOI: 10.1002/9780470141731.ch4

(3) Colbert, D. T.; Miller, W. H. A novel discrete variable representation for quantum mechanical reactive scattering via the S-matrix Kohn method. *Journal of Chemical Physics* **1992**, *96* (3), 1982-1991. DOI: 10.1063/1.462100

This page titled 21.2.1: Numerically Solving the Schrödinger Equation is shared under a CC BY-NC-SA 4.0 license and was authored, remixed, and/or curated by Andrei Tokmakoff via source content that was edited to the style and standards of the LibreTexts platform.

21.2.2: Separation of Subsystems

Separability and Product States

While single particles are rarely of interest in chemical applications, molecular wavefunctions are another extreme involving thousands of electrons and nuclei. In such complex systems, how do we identify which particles matter and which have little bearing on our problem? We must be able to identify ways of concentrating on the subset of interest, whether this is an isolated polyatomic molecule or a small molecule interacting with a complex solvent environment. Separation of the Hamiltonian into these subsets is the underpinning of all strategies.

To start, consider the example of a Hamiltonian that can be written as a sum of two contributions:

$$\hat{H} = \hat{H}_1 + \hat{H}_2 \tag{21.2.2.1}$$

These subsystems refer to completely separable degrees of freedom, with no interactions between them. This example is rarely encountered, but it could refer to cases where interactions are negligible, such as the case of two isolated molecules. If so we can find solutions to the timeindependent Schrödinger equation (TISE) for each subsystem: $H_1 \left|\psi_{1,n}\right\rangle = E_{1,n} \left|\psi_{1,n}\right\rangle$ and $H_2 \left|\psi_{2,m}\right\rangle = E_{2,m} \left|\psi_{2,m}\right\rangle$ where n and m are the indices labeling the eigenstates and energy eigenvalues of the 1 and 2 subsystems, respectively. Since they are independent, with the operators only acting in their space, the wavefunction of the joint system Ψ can be represented in terms of product states of the eigenstates of the two sub-systems: $\left|\Psi_{n,m}\right\rangle = \left|\psi_{1,n}\right\rangle \left|\psi_{2,m}\right\rangle$, and the energy of the full system is simply additive in the two subsystems

$$H|\Psi\rangle = (H_1 + H_2) \left|\psi_1\psi_2\right\rangle = (E_1 + E_2) \left|\psi_1\psi_2\right\rangle \tag{21.2.2.2}$$

Furthermore, the full wavefunction can be expressed as an expansion in the product basis:

$$|\Psi\rangle = \sum_{n,m} c_n c_m \left|\psi_{1,n}\psi_{2,m}\right\rangle \tag{21.2.2.3}$$

This reasoning extends to as many separable degrees of freedom in which the Hamiltonians can be expressed as a sum of independent terms. We will commonly specify the state of the multiparticle or multistate system using the quantum numbers for the subsystems: $|\psi\rangle = |n_0, n_1, n_2 \cdots\rangle$. In its matrix form, we write the Hamiltonian in eq. (21.2.2.3) in a block diagonal form in which the individual contributions H_i form one of the blocks, and the ket wavefunction $|\psi\rangle$ is a tensor product of the column vectors $|\psi_i\rangle$

As one might expect, this form of the Hamiltonian serves to dramatically simplify solutions to the Schrödinger equation. This form occurred above in the description of the $3\mathrm{D}$ particle in a box and the spherically symmetric potential in which we separated the radial Hamiltonian from the full Hamiltonian. Even when not strictly possible, approximations that allow us to cast the problem in this form are cornerstones of much of molecular quantum mechanics, for instance in the adiabatic approximation, which uses a time-scale separation to partition the problem by fast and slow degrees of freedom. Such strategies are often used for describing molecular quantum states in terms of product states in the electronic, nuclear, rotational, and spin degrees of freedom, where electron-nuclear, ro-vibrational, and spin-orbit couplings are treated perturbatively.

Interacting systems

Naturally, a non-interacting universe is uninteresting if not unphysical, and Hamiltonians cannot typically be fully decoupled. Let's reexamine our two-subsystem example, but now allowing them to interact through a potential

$$\hat{H}' = \hat{H}_1 + \hat{H}_2 + \hat{V}_{1,2} \tag{21.2.2.4}$$

This form indicated that the two systems can influence the energy of each other but not exchange particles, as one might expect of intermolecular interactions. The product states that we determined in the absence of interactions ($\hat{V}_{1,2} \to 0$) are not eigenstates of the new Hamiltonian H', as the eigenstates of H_1 become entangled with those of H_2. Nonetheless, the original product states still form a complete basis by which to express the new state of the system:

$$|\Psi'\rangle = \sum_{n,m} C_{n.m} |\psi_{1,n}\psi_{2,m}\rangle \tag{21.2.2.5}$$

However, $C_{n,m} \neq c_n c_m$, generally speaking. To the extent that the interaction is weak, the degree of mixing is small and the corrections to the energy eigenvalues and eigenstates can be made with perturbation theory. We will be more quantitative about what "weak" means soon.

To look at this further, consider the full TISE for the Hamiltonian in eq. (21.2.2.4) $H' |\Psi'\rangle = E_{\text{tot}} |\Psi'\rangle$ evaluated in the original orthonormal product state basis

$$\hat{H}' |\psi_1'\psi_2'\rangle = [E_1 + E_2 + E_{1,2}] |\psi_1'\psi_2'\rangle \tag{21.2.2.6}$$

Here ψ_i' are the new subsystem wavefunctions which we added a prime to in order to indicate a change of projection onto the original basis set $(C_{n,m})$, and $E_{1,2} = \left\langle \psi_1'\psi_2' \middle| \hat{V}_{1,2} \middle| \psi_1'\psi_2' \right\rangle$ is the energy change of the full system that results from turning on the interaction $\hat{V}_{1,2}$. If we operate from the left with the wavefunction for space 2, $\langle\psi_2'|$, we obtain

$$\left[H_1 + \left\langle \psi_2' \middle| \hat{V}_{1,2} \middle| \psi_2' \right\rangle \right] |\psi_1'\rangle = [E_1 + \delta E_1] |\psi_1'\rangle \tag{21.2.2.7}$$

δE_1 is the energy shift in system 1 due to the interaction with system 2. Notice in this process we have ended up with a TISE for system 1 with corrections due to its interaction with system 2. This correction is obtained by integrating the interaction potential over the full ψ_2 space. We have thus retained our explicit description of system 1 but have only retained information on the average influence of the particles and fields in system 2 in the interaction expectation value, and thus this is considered a mean-field approximation.

To summarize, we have made multiple approximations in this strategy but gained an important advantage. We do not allow exchange of particles between subsystems, which assures us that the product states remain a complete basis before and after the interaction, and the interactions must be weak $(E_1 \ll \delta E_1)$ so that the two subsystems to not become significantly entangled. The key advantage is that we have found a strategy to study the structure, interactions, and dynamics of a molecule or other quantum system interacting with its environment, which in principle assume arbitrary complexity. Approximations that allow us to cast the problem in this form are important in many aspects of molecular quantum mechanics, and they form the basis for perturbation theory.

This page titled 21.2.2: Separation of Subsystems is shared under a CC BY-NC-SA 4.0 license and was authored, remixed, and/or curated by Andrei Tokmakoff via source content that was edited to the style and standards of the LibreTexts platform.

21.2.3: Morse Oscillator

The Morse oscillator is a model for a particle in a one-dimensional anharmonic potential energy surface with a dissociative limit at infinite displacement.(1) It is commonly used for describing the spectroscopy of diatomic molecules and anharmonic vibrational dynamics, and most of its properties can be expressed through analytical expressions.(2) The Morse potential is

$$V(x) = D_e \left[1 - e^{-\alpha x}\right]^2 \tag{21.2.3.1}$$

where $x = (r - r_0)$. D_e sets the depth of the energy minimum at $r = r_0$ relative to the dissociation limit as $r \to \infty$, and α sets the curvature of the potential. If we expand V in powers of x

$$V(x) \approx \frac{1}{2}\kappa x^2 + \frac{1}{6}gx^3 + \frac{1}{24}hx^4 + \cdots \tag{21.2.3.2}$$

we find that the harmonic, cubic, and quartic expansion coefficients are $\kappa = 2D_e\alpha^2, g = -6D_e\alpha^3$ and $h = 14D_e\alpha^4$.

The Morse oscillator Hamiltonian for a diatomic molecule of reduced mass m_R bound by this potential is

$$H = \frac{p^2}{2m_R} + V(x) \tag{21.2.3.3}$$

and has the eigenvalues

$$E_n = \hbar\omega_0 \left[\left(n + \frac{1}{2}\right) - x_e \left(n + \frac{1}{2}\right)^2\right] \qquad n = 0, 1, 2, 3 \ldots \tag{21.2.3.4}$$

Here $\omega_0 = \sqrt{2D_e\alpha^2/m_R}$ is the fundamental frequency and $x_e = \hbar\omega_0/4D_e$ is the anharmonic constant. Similar to the harmonic oscillator, the frequency $\omega_0 = \sqrt{\kappa/m_R}$. The anharmonic constant x_e is commonly seen in the spectroscopy expression for the anharmonic vibrational energy levels

$$G(v) = \omega_e \left(v + \frac{1}{2}\right) - \omega_e x_e \left(v + \frac{1}{2}\right)^2 + \omega_e y_e \left(v + \frac{1}{2}\right)^3 + \cdots \tag{21.2.3.5}$$

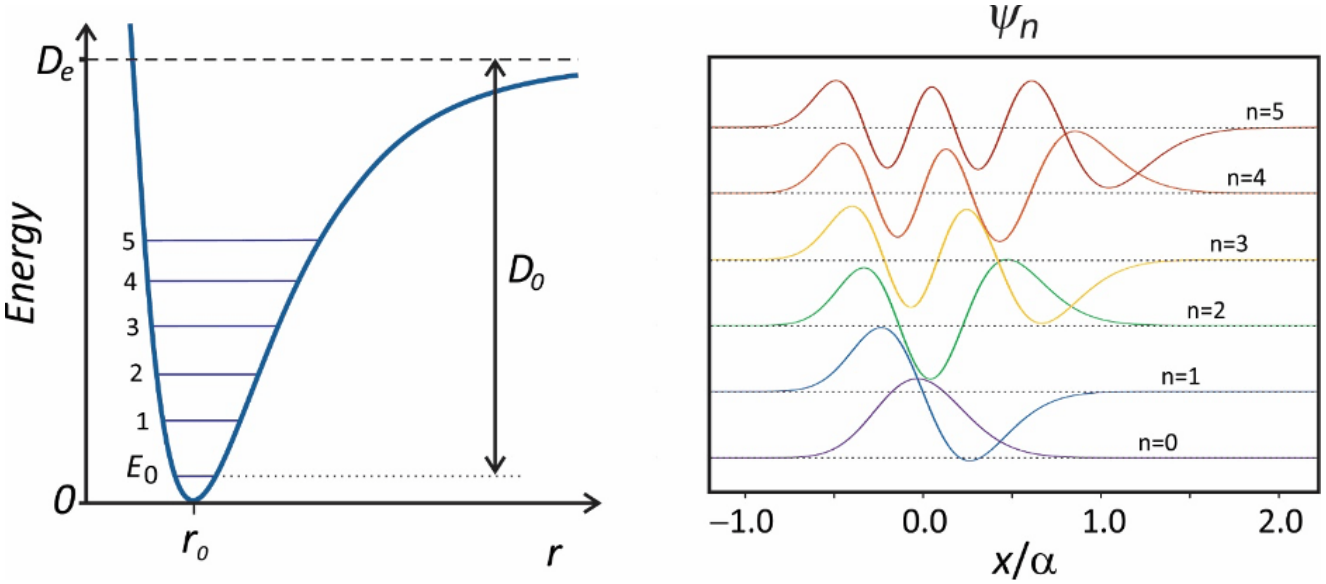
From eq. (21.2.3.4), the ground state (or zero-point) energy is

$$E_0 = \frac{1}{2}\hbar\omega_0 \left(1 - \frac{1}{2}x_e\right) \tag{21.2.3.6}$$

So the dissociation energy for the Morse potential is given by $D_0 = D_e - E_0$. The transition energies are

$$E_n - E_m = \hbar\omega_0(n - m)\left[1 - x_e\left(n + m + \frac{1}{2}\right)\right] \tag{21.2.3.7}$$

The proper harmonic expressions are obtained from the corresponding Morse oscillator expressions by setting $D_e \to \infty$ or $x_e \to 0$.



21.2.3.1: Shape of the Morse potential illustrating the first six energy eigenvalues.

21.2.3.2: First six eigenfunctions of the Morse oscillator potential.

The wavefunctions for the Morse oscillator can also be expressed analytically in terms of associated Laguerre polynomials $\mathcal{L}_n^b(z)$: (3)

$$\psi_n = N_n e^{-z/2} z^{b/2} \mathcal{L}_n^b(z) \tag{21.2.3.8}$$

where $N_n = [\alpha \cdot b \cdot n!/\Gamma(k-n)]^{1/2}, z = k\exp[-\alpha x], b = k - 2n - 1$, and $k = 4D_e/\hbar\omega_0$. These expressions and those for matrix elements in x, x^2, $\mathrm{e}^{-\alpha x}$, and $x\mathrm{e}^{-\alpha x}$ have been given by Vasan and Cross.(4)

References

(1) Morse, P. M. Diatomic Molecules According to the Wave Mechanics. II. Vibrational Levels. *Physical Review* **1929**, *34*, 57-64. DOI: 10.1103/PhysRev.34.57

(2) Lefebvre-Brion, H. l. n.; Field, R. W. *The spectra and dynamics of diatomic molecules*, 2nd ed.; Elsevier Academic Press, 2004. DOI: 10.1016/B978-0-12-441455-6.X5000-8

(3) Gallas, J. A. C. Some matrix elements for Morse oscillators. *Physical Review A* **1980**, *21* (6), 1829-1834. DOI: 10.1103/PhysRevA.21.1829

(4) Vasan, V. S.; Cross, R. J. Matrix elements for Morse oscillators. *Journal of Chemical Physics* **1983**, *78* (6), 3869-3871. DOI: 10.1063/1.445164

This page titled 21.2.3: Morse Oscillator is shared under a CC BY-NC-SA 4.0 license and was authored, remixed, and/or curated by Andrei Tokmakoff via source content that was edited to the style and standards of the LibreTexts platform.

Notation and variables used

On Notation

$\mathbf{X}$	Bold roman text indicates a vector.
$\tilde{X}$	Tilde above variable refers to a complex function, typically a Fourier or Laplace transform variable
$\underset{\sim}{X}$	Tilde under variable refers to a reduced variable
$\dot{X}, \ddot{X}$	A dot over a variable indicates a time derivative. Two dots indicates a second time derivative.
X', X''	When applied to a complex function, variables with a prime or double-prime symbol correspond to the real or imaginary parts, respectively. They are also used to represent derivatives with respect to position.
$\bar{X}$	Bar over variable indicates average value, usually time-average, or in the context of molecular spectroscopy it refers to the cm^{-1} units convention
$\hat{X}$	A circumflex over variable labels it as a quantum mechanical operator
$\hat{\varepsilon}$	A circumflex over an epsilon $\hat{\varepsilon}$ represents a unit vector
$[\hat{X}, \hat{Y}]$	The commutator of the operators $\hat{X}$ and $\hat{Y}$
$[\hat{X}, \hat{Y}]_+$	The anticommutator of the operators $\hat{X}$ and $\hat{Y}$
$\exp_{\pm}[...]$	Positive or negative time-ordered exponential operator

Variables used in the book

$\hat{A}$	A quantum mechanical operator
$\hat{A}^\dagger$	Hermitian adjoint (conjugate transpose) of operator $\hat{A}$
$\hat{A}_H$	Operator in the Heisenberg picture
$\hat{A}_I$	Operator in the interaction picture
A_0	Amplitude of the vector potential of an electromagnetic field
$\mathcal{A}$	Electromagnetic vector potential
$\hat{a}$	Lowering operator for bosons
$\hat{a}^\dagger$	Raising operator for bosons
α	absorption coefficient or polarizability
α and β	Index variables for bath states, or the spin states: $\alpha = \vert +\rangle =$ up, $\beta = \vert -\rangle =$ down
β	Phase shift or $1/k_B T$
B	Rotational constant or Einstein coefficient
$\mathcal{B}$	Magnetic field
$\hat{b}$	Unit vector for the polarization direction of the magnetic field
b_m	Complex amplitude of eigenstate m expressed in interaction picture
c	Speed of light in a vacuum
C	Correlation function
C_{AA}	Time-correlation function in the internal variable or operator A

c_n	(Complex, time-varying) amplitude of eigenstate in superposition state
d	Nuclear displacement
$\mathscr{D}$	Diffusion Coefficient
$\hat{D}$	Displacement operator
δ	Dirac delta function
δ_{ij}	Kronecker delta. $\delta_{ij} = 1$ if $i = j$ and 0 otherwise.
$\hat{\varepsilon}$	Unit vector (typically for polarization of an electromagnetic field) use $\hat{\varepsilon}_x, \hat{\varepsilon}_y, \hat{\varepsilon}_z$
ε_n	An energy eigenvalue
ϵ	Molar decadic extinction coefficient ($L\ mol^{-1}\ cm^{-1}$)
E	Energy
$\mathcal{E}$	Electric field
E_n	An energy eigenvalue
f, F	Force
F	Dephasing function
$\mathcal{F}[...]$	Fourier transform
$\mathcal{F}^{-1}[\cdots]$	Inverse Fourier transform
φ	Scalar potential or eigenfunction
g	Lineshape function or radial distribution function
$\hat{G}$	Time-propagation superoperator
γ, Γ	Exponential damping rate, or HWHM linewidth of a Lorentzian
H	Hamiltonian Operator
H_0	Zero-order Hamiltonian or Time-independent part of Hamiltonian
$\mathcal{H}_n(x)$	Hermite polynomials
h	Planck's constant, $6.62606957 \times 10^{-34}\ \mathrm{J\ s}\ (\mathrm{m^2\ kg\ s^{-1}})$
$\hbar$	Reduced Planck's constant, $h/2\pi, 1.054571726 \times 10^{-34}\ \mathrm{J\cdot\ s}\ (\mathrm{m^2\ kg\ s^{-1}})$
$\mathbf{I}, \mathbb{I}$	Identity matrix, $I_{ij} = \delta_{ij}$
i	$\sqrt{-1}$
i	Typically used as an index variable for a matrix or summation
j	Typically used as an index variable for a matrix or summation
J	Rotational angular momentum, transverse current density, or coupling constant
k	Index variable, typically for wavevector
$\boldsymbol{k}$	Wavevector
$\hat{k}$	Unit vector along the wavevector
k_B	Boltzmann's constant
κ	Harmonic oscillator force constant
$\lvert k\rangle$	A specific eigenstate, typically a final (target) state in a time-dependent problem
$\lvert \ell\rangle$	A specific eigenstate, typically the initial state in a time-dependent problem
$\mathcal{L}$	Laplace transformation or Laguerre polynomial

L	Orbital angular momentum operator, Lagrangian transformation, or path length
λ	A parameter (number) or wavelength
m	Mass. Occasionally the dipole operator.
m_r, μ_r	Reduced mass
$\boldsymbol{\mu}$	Dipole operator
$\boldsymbol{\mu}_0$	Permanent dipole moment. μ_0 is also the magnetic vacuum permeability 1.25664\times\10^{-6} T\,m\,A^{-1}.
$\boldsymbol{\mu}'$	Dipole derivative with respect to a vibrational coordinate: $\boldsymbol{\mu}' = \partial\boldsymbol{\mu}/\ \partial q\vert_{q=q_0}$
$\mu_{k\ell}$	Transition dipole matrix element
μ^*	Reduced mass of an electron-hole pair
ν	Frequency in s^{-1}
$\bar{\nu}$	Frequency in cm^{-1}
n	Vibrational quantum number or eigenstate index
$\bar{n}$	Thermally averaged occupation number for Bosons
$\vert n\rangle$	The n^{th} eigenstate (eigenket) of complete basis set
$\hat{p}$	momentum operator
p, P	Probability density or probability of occupying a quantum state
$\mathcal{P}$	Power or parity
$\mathbb{P}$	Principle part
$q, \hat{q}$	Nuclear coordinate. In the context of system-bath problems, it refers to the operators of the bath Hamiltonian.
$Q, \hat{Q}$	Nuclear coordinate or normal mode, typically an operator of the system Hamiltonian
ρ	Density matrix
ρ_{eq}	Equilibrium density matrix
ρ_0	Initial state of the density matrix in a time-dependent problem
$\rho_I^{(n)}$	The n^{th}-order perturbation theory expansion of the density matrix
r	Distance between two points
$\mathbf{r}$	vector indicating the separation and orientation between two points
$\mathbf{R}$	Center of mass or bond length
R	Response function
$\mathcal{R}$	Redfield relaxation tensor or radial integral
S	Huang-Rhys factor ($\underset{\sim}{d}^2$ reduced harmonic oscillator displacement squared), the Poynting vector, or the step response function
σ	Absorption cross-section, reduced density matrix, polarization index, or standard deviation
t, τ	Time. t is used for time points; τ is used for time-intervals
T	Kinetic energy
Θ	Heaviside unit step function
U	Time evolution operator or propagator
$\mathcal{U}$	Potential energy
U_0	Time evolution operator under H_0

U_I	Time evolution operator in the interaction picture. Evolution under $V_I(\tau)$
v	Velocity
$\hat{V}$	Potential Energy Operator
$V(t)$	Time-dependent potential
$V_I(\tau)$	Time-dependent potential in the interaction picture
$V_{k\ell}$	Matrix element in the potential
w	Transition rate in s^{-1}
$w_{k\ell}$	Transition rate from initial state $\|\ell\rangle$ to final state $\|k\rangle$
$\bar{w}_{nk}$	Transition rate from state $\|k\rangle$ to a continuum of states $\|n\rangle$
W	Density of states
ω	An angular frequency or energy expressed as $E/\hbar$
ω_0	Fundamental frequency of a harmonic oscillator
$\omega_{k\ell}$	Bohr frequency. Frequency splitting between state $\|k\rangle$ and state $\|\ell\rangle$, $\omega_{k\ell} = (E_k - E_\ell)/\hbar = -\omega_{\ell k}$
Ω, Ω_R	Rabi Frequency
x, X	Position operator. When used for vibrational displacement, it is typically used to distinguish from a separate set of coordinates q, Q, for instance between local and normal modes.
Y	Spherical harmonics
z, z_i	Charge. One of many charges.
Z	Partition function or atomic number
χ	Susceptibility
Ω_0	Reduced frequency for damped harmonic oscillator $\Omega_0 = \sqrt{\omega_0^2 - \gamma^2}$
ϕ	Phase of oscillation
Φ	Nuclear part of Born-Oppenheimer wavefunction
Ψ	The total time-dependent wavefunction in the position representation
$\|\psi\rangle$	The wavefunction or state of the system. A column vector of expansion coefficients.
$\langle\psi\|$	Hermitian conjugate of wavefunction. A row vector: complex conjugate transpose
$\|\psi\rangle_H$	Heisenberg picture wavefunctions
$\|\psi_S\rangle$	Schrödinger picture wavefunctions
ξ	Coupling constant

This page titled Notation and variables used is shared under a CC BY-NC-SA 4.0 license and was authored, remixed, and/or curated by LibreTexts.

INDEX

A

absorbance
7.6: Absorption Cross Section

Absorption
14.3: The Response Function and Energy Absorption
16.1: The Displaced Harmonic Oscillator Model

absorption spectrum
15.1: Absorption Spectra from Time-Correlation Functions

Adiabatic process
5.1: Adiabatic Processes

Adiabatic states
5.3: Nonadiabatic Coupling
5.4: Diabatic and Adiabatic States
5.5: Landau–Zener Transition Probability

angular momentum
1.6: Angular Momentum

anharmonicity
18.3: Multiquantum relaxation of polyatomic molecules
21.2.3: Morse Oscillator
3.6: Time-Dependent Perturbation Theory

Antisymmetrized correlation function
13.4: Quantum Time-Correlation Functions
14.4: Quantum Linear Response Functions

Atomic spectroscopy
10.2: Selection Rules in the Electric Dipole Approximation

Atomic units
21.1.1: Atomic Units

B

Boltzmann distribution
12.3: Equilibrium Systems

Brownian oscillator model
17.5: The Harmonic Bath's Relation to the Langevin Equation

C

Causality
14.1: Classical Linear Response Theory
2.4: Equation of Motion for the Time-Evolution Operator

CdSe
20.6: Tight-binding model

Chemical exchange
17.2: Gaussian-Stochastic Model for Spectral Diffusion

Chirped pulse
3.3: Transitions Induced by a Time-Dependent Potential

Coherence
2.1: Dynamics with a Time-Independent Hamiltonian

Coherence transfer
18.4: Redfield Theory and Master Equation

Commutators
1.3: Dirac Notation and Matrix Mechanics

Completing the square
21.1.3: Gaussian Integrals and Error Function

Constant perturbation
3.7: The Golden Rule

Continuous basis set
4.1: Position and Momentum Representation

Continuum, coupling to
11.1: Introduction

Correlation coefficient
12.2: Statistics of Ensembles

Correlation function, Rotational
13.2: Examples of Classical Time-Correlation Functions

Correlation function, Velocity
13.2: Examples of Classical Time-Correlation Functions

Correlation Function, Vibrational
13.2: Examples of Classical Time-Correlation Functions

Correlation functions
13.1: Classical Time-Correlation Functions
13.2: Examples of Classical Time-Correlation Functions

correlation time
13.1: Classical Time-Correlation Functions
17.2: Gaussian-Stochastic Model for Spectral Diffusion

coupling
2.3: Two-Level System

Creation and annihilation operators
1.5: Raising and Lowering Operators

Cumulant expansion
17.2: Gaussian-Stochastic Model for Spectral Diffusion

D

Debye (unit)
10.1: The Molecular Transition Dipole Moment

Decoherence
12.1: Concepts for Condensed Matter

Delta function
21.1.2: Dirac Delta Function

density matrix
12.5: The Density Matrix
18.4: Redfield Theory and Master Equation

Density of states
17.4: Spectral Density for Condensed Phase Spectroscopy

Dephasing
12.1: Concepts for Condensed Matter
15.4: Line Broadening Mechanisms
17.1: Line-broadening, dephasing, and spectral diffusion
18.4: Redfield Theory and Master Equation

Dephasing function
17.2: Gaussian-Stochastic Model for Spectral Diffusion

Detailed balance
13.4: Quantum Time-Correlation Functions
13.5: Transition Rates from Time Correlation Functions
14.6: Relaxation of a Prepared State
17.3: The Energy Gap Hamiltonian

Dexter transfer
19.1: Intermolecular Electronic Interactions

Diabatic states
5.4: Diabatic and Adiabatic States
5.5: Landau–Zener Transition Probability

diatomic molecules
10.2: Selection Rules in the Electric Dipole Approximation

Dielectric relaxation
17.4: Spectral Density for Condensed Phase Spectroscopy

Dipole autocorrelation function
15.1: Absorption Spectra from Time-Correlation Functions

Dipole operator
10.1: The Molecular Transition Dipole Moment
15.2: Describing Diverse Spectroscopies with the Dipole Correlation Function

Dirac Notation
1.3: Dirac Notation and Matrix Mechanics

Discrete variable representation
21.2.1: Numerically Solving the Schrödinger Equation

disorder
20.4: Absorption spectra of J aggregates

Dispersion
4.3: Free-Particle Wavepacket

Displaced harmonic oscillator
16.1: The Displaced Harmonic Oscillator Model
17.3: The Energy Gap Hamiltonian

Displacement operator
1.7: Exponential Operators
10.3: Molecular Electronic Spectroscopy and Franck Condon Factors
16.1: The Displaced Harmonic Oscillator Model

Dissipation
12.1: Concepts for Condensed Matter

Driven harmonic oscillator
6.2: Absorption by a Driven Oscillator
6.3: Complex formulation of the driven dipole oscillator

DVR
21.2.1: Numerically Solving the Schrödinger Equation

Dyson expansion
2.5: Dynamics with a Time-Dependent Hamiltonian

E

Effective mass
20.6: Tight-binding model

Ehrenfest's principle
2.6: Schrödinger and Heisenberg Representations

Eigenfunction
1.2: Describing a System Quantum Mechanically

eigenvalues
1.2: Describing a System Quantum Mechanically

Einstein A coefficient
11.3: Spontaneous Emission
9.4: Light-Matter Interactions and Spontaneous Emission

Einstein B coefficient
7.6: Absorption Cross Section

Electric dipole approximation
7.4: Electric Dipole Hamiltonian

Electric dipole Hamiltonian
7.4: Electric Dipole Hamiltonian

Electric dipole transitions
15.2: Describing Diverse Spectroscopies with the Dipole Correlation Function

Electric quadrupole transitions
10.2: Selection Rules in the Electric Dipole Approximation

Electrical anharmonicity
10.2: Selection Rules in the Electric Dipole Approximation
16.3: Semiclassical Approximation to the Dipole Correlation Function

Electromagnetic energy density
9.4: Light-Matter Interactions and Spontaneous Emission

electromagnetic field
7.2: Electromagnetic Plane Waves
9.3: Electromagnetic field

electromagnetic waves
7.8: Appendix- Electromagnetic Fields and Potentials

electron transfer
19.1: Intermolecular Electronic Interactions
19.4: Marcus Theory for Electron Transfer

Electron transfer, rate
19.4: Marcus Theory for Electron Transfer

Ensemble averaging
12.2: Statistics of Ensembles

erf
21.1.3: Gaussian Integrals and Error Function

erfc
21.1.3: Gaussian Integrals and Error Function

Ergodic systems
13.1: Classical Time-Correlation Functions

Error function
21.1.3: Gaussian Integrals and Error Function

Exciton diffusion
20.5: Frenkel exciton transport

Exciton transport
20.5: Frenkel exciton transport

Excitons
20.1: What are excitons?

Exponential decay
11.2: Coupling to a continuum
11.4: Relaxation and Line-broadening

Exponential operators
1.7: Exponential Operators

F

Fermi's Golden Rule
13.5: Transition Rates from Time Correlation Functions
3.7: The Golden Rule

field:pchem
2: The Schrödinger Equation and Time-Propagator

Fluctuations
12.1: Concepts for Condensed Matter

fluorescence
16.1: The Displaced Harmonic Oscillator Model

Fock states
9.3: Electromagnetic field

Förster Resonance Energy Transfer
19.1: Intermolecular Electronic Interactions
19.3: Förster Resonance Energy Transfer

Frenkel excitons
20.1: What are excitons?
20.2: Frenkel excitons in molecular aggregates

FRET
19.3: Förster Resonance Energy Transfer

FWHM
17.2: Gaussian-Stochastic Model for Spectral Diffusion

G

Gaussian distribution
21.1.3: Gaussian Integrals and Error Function

Gaussian integrals
21.1.3: Gaussian Integrals and Error Function

Gaussian lineshape
17.2: Gaussian-Stochastic Model for Spectral Diffusion

Golden rule
13.5: Transition Rates from Time Correlation Functions
18.2: Golden Rule Vibrational Relaxation Rates

Group velocity
20.5: Frenkel exciton transport
4.3: Free-Particle Wavepacket

H

H aggregates
20.2: Frenkel excitons in molecular aggregates

Hamiltonian, Brownian oscillator
17.5: The Harmonic Bath's Relation to the Langevin Equation

Hamiltonian, Electric dipole
7.4: Electric Dipole Hamiltonian

Hamiltonian, Energy gap
17.3: The Energy Gap Hamiltonian
17.5: The Harmonic Bath's Relation to the Langevin Equation

Hamiltonian, Molecular
5.2: Born–Oppenheimer Approximation

Harmonic bath
16.2: Coupling to a Harmonic Bath
17.5: The Harmonic Bath's Relation to the Langevin Equation
18.2: Golden Rule Vibrational Relaxation Rates

harmonic oscillator
1.4: Basic Quantum Models
13.2: Examples of Classical Time-Correlation Functions
13.4: Quantum Time-Correlation Functions
14.2: Example- Response of a damped harmonic oscillator
14.7: Example- Response of an abruptly shifted oscillator
2.6: Schrödinger and Heisenberg Representations
6.2: Absorption by a Driven Oscillator

Harmonic oscillator, correlation function
15.3: Vibrational and Rotational Spectroscopy

Harmonic perturbation
3.7: The Golden Rule

Heisenberg equation
2.6: Schrödinger and Heisenberg Representations

Heisenberg representation
2.6: Schrödinger and Heisenberg Representations

Hermite polynomials
1.4: Basic Quantum Models

Hermitian conjugate
1.3: Dirac Notation and Matrix Mechanics

Hilbert space
1.2: Describing a System Quantum Mechanically

Homogeneous broadening
15.4: Line Broadening Mechanisms
17.1: Line-broadening, dephasing, and spectral diffusion

Hopping integral
20.6: Tight-binding model

Hückel theory
20.6: Tight-binding model

Hydrogen atom
1.6: Angular Momentum
10.2: Selection Rules in the Electric Dipole Approximation

I

Impulse response
14.1: Classical Linear Response Theory
14.6: Relaxation of a Prepared State

Inhomogeneous broadening
15.4: Line Broadening Mechanisms
17.1: Line-broadening, dephasing, and spectral diffusion

Inner product
1.3: Dirac Notation and Matrix Mechanics

Intensity
7.2: Electromagnetic Plane Waves

Intensity, peak
7.7: Quantitative Examples of Light-Matter Interactions

interaction picture
3.5: The Interaction Picture

Inverted regime
19.4: Marcus Theory for Electron Transfer

Irreversible relaxation
11.1: Introduction
11.4: Relaxation and Line-broadening
14.6: Relaxation of a Prepared State

IVR
18.3: Multiquantum relaxation of polyatomic molecules

J

J aggregates
20.2: Frenkel excitons in molecular aggregates
20.4: Absorption spectra of J aggregates

K

Kubo lineshape
17.2: Gaussian-Stochastic Model for Spectral Diffusion

Kubo model
17.2: Gaussian-Stochastic Model for Spectral Diffusion

L

Lamb shift
11.3: Spontaneous Emission

Langevin equation
17.5: The Harmonic Bath's Relation to the Langevin Equation
18.1: Vibrational Relaxation

LCAO
20.6: Tight-binding model

Lineshape function
17.3: The Energy Gap Hamiltonian
17.4: Spectral Density for Condensed Phase Spectroscopy

Linewidth
15.4: Line Broadening Mechanisms

Lorentz force
7.3: Classical Light-Matter Interactions

Lorentzian lineshape
11.4: Relaxation and Line-broadening
17.2: Gaussian-Stochastic Model for Spectral Diffusion
6.2: Absorption by a Driven Oscillator
6.3: Complex formulation of the driven dipole oscillator

M

Magnetic dipole transitions
10.2: Selection Rules in the Electric Dipole Approximation

Magnus expansion
12.6: Time-Dependence of the Density Matrix

Marcus Theory
19.4: Marcus Theory for Electron Transfer

Master equation
18.4: Redfield Theory and Master Equation

Maxwell's equations
7.8: Appendix- Electromagnetic Fields and Potentials

Memory kernel
17.5: The Harmonic Bath's Relation to the Langevin Equation

Mixed states
12.1: Concepts for Condensed Matter
12.4: Mixed States

Molar extinction coefficient
7.6: Absorption Cross Section
7.7: Quantitative Examples of Light-Matter Interactions

Moments of a distribution
12.2: Statistics of Ensembles

Morse oscillator
21.2.3: Morse Oscillator

Motional narrowing
17.1: Line-broadening, dephasing, and spectral diffusion
17.2: Gaussian-Stochastic Model for Spectral Diffusion

N

Nonadiabatic coupling
5.4: Diabatic and Adiabatic States

Numerov method
21.2.1: Numerically Solving the Schrödinger Equation

O

Ohmic spectral density
17.4: Spectral Density for Condensed Phase Spectroscopy

operators
1.2: Describing a System Quantum Mechanically
1.3: Dirac Notation and Matrix Mechanics

Orientational Relaxation
15.4: Line Broadening Mechanisms

Overlap integral
19.3: Förster Resonance Energy Transfer

P

Parseval's theorem
13.6: Appendix- Weiner-Khinchin Theorem and the Power Spectrum

Pauli matrices
2.3: Two-Level System

perturbation theory
3.6: Time-Dependent Perturbation Theory

Phase velocity
4.3: Free-Particle Wavepacket

photon
11.3: Spontaneous Emission
9.2: Hamiltonian for quantized electromagnetic field
9.3: Electromagnetic field
9.5: Coherent States

pi pulse
7.7: Quantitative Examples of Light-Matter Interactions

Plane waves
1.4: Basic Quantum Models
7.2: Electromagnetic Plane Waves
7.8: Appendix- Electromagnetic Fields and Potentials

Poisson distribution
10.3: Molecular Electronic Spectroscopy and Franck Condon Factors
9.5: Coherent States

Polarizability
6.5: Polarizability

Population relaxation
18.1: Vibrational Relaxation
18.4: Redfield Theory and Master Equation

Power spectrum
13.6: Appendix- Weiner-Khinchin Theorem and the Power Spectrum

Poynting vector
7.2: Electromagnetic Plane Waves

Principal part
11.2: Coupling to a continuum

probability density
1.2: Describing a System Quantum Mechanically

Pure state
12.1: Concepts for Condensed Matter

Q

Quantum correction factor
18.3: Multiquantum relaxation of polyatomic molecules

R

Rabi frequency
2.3: Two-Level System
3.4: Resonant Driving of a Two-Level System
7.7: Quantitative Examples of Light-Matter Interactions

radiative lifetime
19.3: Förster Resonance Energy Transfer

Raising and lowering operators
1.5: Raising and Lowering Operators

Raman spectroscopy
15.3: Vibrational and Rotational Spectroscopy

Rate processes
3.7: The Golden Rule

Redfield theory
18.4: Redfield Theory and Master Equation

Reorganization energy
17.3: The Energy Gap Hamiltonian
17.4: Spectral Density for Condensed Phase Spectroscopy
19.4: Marcus Theory for Electron Transfer

resonance energy transfer
19.1: Intermolecular Electronic Interactions
19.2: Resonance Energy Transfer and Transition Dipole Coupling

response function
14.1: Classical Linear Response Theory
14.4: Quantum Linear Response Functions
6.4: Response of an Impulsively Driven Oscillator

Response function, Nonlinear
14.5: Nonlinear response functions

rigid rotor
1.6: Angular Momentum
15.3: Vibrational and Rotational Spectroscopy

Rigid rotor, selection rules
15.3: Vibrational and Rotational Spectroscopy

rotation
13.2: Examples of Classical Time-Correlation Functions

Rotational correlation function
15.3: Vibrational and Rotational Spectroscopy

rotational spectroscopy
15.3: Vibrational and Rotational Spectroscopy

S

Scalar potential
7.8: Appendix- Electromagnetic Fields and Potentials

Schrödinger picture
2.6: Schrödinger and Heisenberg Representations

Secular approximation
18.4: Redfield Theory and Master Equation
3.4: Resonant Driving of a Two-Level System

selection rules
10.1: The Molecular Transition Dipole Moment
10.2: Selection Rules in the Electric Dipole Approximation
10.4: Appendix - Rotational Transition Matrix Elements

Singlet fission
19.1: Intermolecular Electronic Interactions

Spectral density
13.4: Quantum Time-Correlation Functions
16.2: Coupling to a Harmonic Bath
17.3: The Energy Gap Hamiltonian
17.4: Spectral Density for Condensed Phase Spectroscopy
17.5: The Harmonic Bath's Relation to the Langevin Equation

spectral diffusion
17.1: Line-broadening, dephasing, and spectral diffusion

spherical harmonics
1.6: Angular Momentum

spin
1.6: Angular Momentum
Split operator approximation
3.2: Integrating the TDSE Directly
Spontaneous emission
11.3: Spontaneous Emission
9.4: Light-Matter Interactions and Spontaneous Emission
Stationary processes
14.1: Classical Linear Response Theory
Stationary states
2.1: Dynamics with a Time-Independent Hamiltonian
Step response
14.6: Relaxation of a Prepared State
Stochastic processes
17.1: Line-broadening, dephasing, and spectral diffusion
Superposition states
2.1: Dynamics with a Time-Independent Hamiltonian
Susceptibility
14.1: Classical Linear Response Theory
14.6: Relaxation of a Prepared State
Symmetrized correlation function
13.4: Quantum Time-Correlation Functions
14.6: Relaxation of a Prepared State

T

Tight Binding Theory
20.6: Tight-binding model
Transition dipole coupling
19.2: Resonance Energy Transfer and Transition Dipole Coupling
Transition dipole moment
10.1: The Molecular Transition Dipole Moment
10.2: Selection Rules in the Electric Dipole Approximation
10.4: Appendix - Rotational Transition Matrix Elements
7.5: The Dipole Operator and Transition Dipole Matrix Elements
Transition dipole moment, exciton
20.4: Absorption spectra of J aggregates
Tunnel ionization
7.7: Quantitative Examples of Light-Matter Interactions

U

Unitary transformation
1.3: Dirac Notation and Matrix Mechanics

V

Vector calculus
7.8: Appendix- Electromagnetic Fields and Potentials
Vector potential
7.2: Electromagnetic Plane Waves
7.8: Appendix- Electromagnetic Fields and Potentials
9.2: Hamiltonian for quantized electromagnetic field
Velocity autocorrelation function
13.2: Examples of Classical Time-Correlation Functions
Vibrational relaxation
18.1: Vibrational Relaxation
18.3: Multiquantum relaxation of polyatomic molecules
Vibronic progression
16.1: The Displaced Harmonic Oscillator Model

W

Wave equations
7.8: Appendix- Electromagnetic Fields and Potentials
Wavepacket
16.1: The Displaced Harmonic Oscillator Model
4.2: Free-Particle Eigenstates
5.5: Landau–Zener Transition Probability
White noise
13.6: Appendix- Weiner-Khinchin Theorem and the Power Spectrum

This page titled Index is shared under a CC BY-NC-SA 4.0 license and was authored, remixed, and/or curated by Andrei Tokmakoff via source content that was edited to the style and standards of the LibreTexts platform.

GLOSSARY

C

Canonical transformation | A transformation in which the phase space variables Q and P are transformed to new phase space variables q and p but the canonical equations of motion (Hamilton's) are preserved.

Coupling | An interaction between particles, fields, or quantum states. Typically refers to a term in a Hamiltonian that describes the influence of one particle or molecular quantity on another. Potential couplings describe the potential energy as a function of the time-dependent position of two or more particles or fields, whereas kinetic couplings depend on their momenta. Coupling is also used to refers to off-diagonal terms or matrix elements in a matrix Hamiltonian. Coupling to an external potential, for instance in perturbation theory, typically only accounts for the influence of the external interactions on the system of interest rather that the mutual effect of two particles on each other.

D

Damping | The time-dependent decrease in the amplitude of an oscillating system due to dissipation, friction, or a viscous force.

Degrees of freedom | Independent variables describing the position and momenta of particles. While a particle is described by six canonical variables, i.e. the x, y, z components of the position and momentum at a certain time point, we refer to this as three degrees of freedom or a three dimensional problem.

Dissipation | The irreversible flow of energy out of a system into its surroundings. This typically refers to the flow of energy in the form of heat, and can be used in the context of an equilibrium, steady-state or non-equilibrium process.

E

Exciton | An electron-hole pair that results from electronic excitation.

F

Field | A physical quantity that is assigned to a position in space. A field can be static or time-dependent. It can be a scalar field with only one value at each point or it can be a vector field which assigns a vector to each point. An example of a time-dependent vector field is velocity.

FWHM | Stands for *Full Width at Half Maximum*. This is the standard general metric for the width of a lineshape. The frequency width is measured between the 50% amplitude points between the peak and baseline. For a Gaussian lineshape the FWHM $= 2.35\sigma$.

G

Gauge transformation | A transformation of the vector and scalar electromagnetic potentials that leaves the observable electric and magnetic fields unchanged. See Section 7.8.

P

Polaron | Electronic excitation of a lattice in which the atoms around the excitation are polarized, and the deformation propagates in time. A large polaron is one in which the polarization is over a region much larger than the lattice spacing, whereas a small polaron extends over a region approximately equal to the lattice spacing.

Q

Quasiparticle | Delocalized quantum excitations spanning many particles whose behavior can be described like a single particle: photons, phonons, excitons, plasmons, holes.

R

Relaxation | The return of population in a non-equilibrium system to its equilibrium distribution.

U

Unitary transformation | A transformation that results in a different representation of the wavefunction, but the state of the system is unchanged.

This page titled Glossary is shared under a CC BY-NC-SA 4.0 license and was authored, remixed, and/or curated by Andrei Tokmakoff via source content that was edited to the style and standards of the LibreTexts platform.

DETAILED LICENSING

Overview

Title: Time-Dependent Quantum Mechanics and Spectroscopy 2025e (Tokmakoff)

Webpages: 166

Applicable Restrictions: Noncommercial

All licenses found:

- CC BY-NC-SA 4.0: 97% (161 pages)
- Undeclared: 3% (5 pages)

By Page

- Time-Dependent Quantum Mechanics and Spectroscopy 2025e (Tokmakoff) - *CC BY-NC-SA 4.0*
  - Front Matter - *CC BY-NC-SA 4.0*
    - Title Page - *CC BY-NC-SA 4.0*
    - Info Page - *CC BY-NC-SA 4.0*
    - Table of Contents - *Undeclared*
    - Licensing - *CC BY-NC-SA 4.0*
    - Preface - *CC BY-NC-SA 4.0*
  - 1: Overview of Time-Independent Quantum Mechanics - *CC BY-NC-SA 4.0*
    - 1.1: Introduction - *CC BY-NC-SA 4.0*
    - 1.2: Describing a System Quantum Mechanically - *CC BY-NC-SA 4.0*
    - 1.3: Dirac Notation and Matrix Mechanics - *CC BY-NC-SA 4.0*
    - 1.4: Basic Quantum Models - *CC BY-NC-SA 4.0*
    - 1.5: Raising and Lowering Operators - *CC BY-NC-SA 4.0*
    - 1.6: Angular Momentum - *CC BY-NC-SA 4.0*
    - 1.7: Exponential Operators - *CC BY-NC-SA 4.0*
    - 1.8: Readings - *CC BY-NC-SA 4.0*
  - 2: The Schrödinger Equation and Time-Propagator - *CC BY-NC-SA 4.0*
    - 2.1: Dynamics with a Time-Independent Hamiltonian - *CC BY-NC-SA 4.0*
    - 2.2: Time-Evolution Operator - *CC BY-NC-SA 4.0*
    - 2.3: Two-Level System - *CC BY-NC-SA 4.0*
    - 2.4: Equation of Motion for the Time-Evolution Operator - *CC BY-NC-SA 4.0*
    - 2.5: Dynamics with a Time-Dependent Hamiltonian - *CC BY-NC-SA 4.0*
    - 2.6: Schrödinger and Heisenberg Representations - *CC BY-NC-SA 4.0*
    - 2.7: Readings - *CC BY-NC-SA 4.0*
  - 3: Solving the Time-Dependent Schrödinger Equation - *CC BY-NC-SA 4.0*
    - 3.1: Introduction - *CC BY-NC-SA 4.0*
    - 3.2: Integrating the TDSE Directly - *CC BY-NC-SA 4.0*
    - 3.3: Transitions Induced by a Time-Dependent Potential - *CC BY-NC-SA 4.0*
    - 3.4: Resonant Driving of a Two-Level System - *CC BY-NC-SA 4.0*
    - 3.5: The Interaction Picture - *CC BY-NC-SA 4.0*
    - 3.6: Time-Dependent Perturbation Theory - *CC BY-NC-SA 4.0*
    - 3.7: The Golden Rule - *CC BY-NC-SA 4.0*
    - 3.8: Readings - *CC BY-NC-SA 4.0*
  - 4: Wavepacket Dynamics - *CC BY-NC-SA 4.0*
    - 4.1: Position and Momentum Representation - *CC BY-NC-SA 4.0*
    - 4.2: Free-Particle Eigenstates - *CC BY-NC-SA 4.0*
    - 4.3: Free-Particle Wavepacket - *CC BY-NC-SA 4.0*
    - 4.4: Readings - *CC BY-NC-SA 4.0*
  - 5: Adiabatic Approximation - *CC BY-NC-SA 4.0*
    - 5.1: Adiabatic Processes - *CC BY-NC-SA 4.0*
    - 5.2: Born–Oppenheimer Approximation - *CC BY-NC-SA 4.0*
    - 5.3: Nonadiabatic Coupling - *CC BY-NC-SA 4.0*
    - 5.4: Diabatic and Adiabatic States - *CC BY-NC-SA 4.0*
    - 5.5: Landau–Zener Transition Probability - *CC BY-NC-SA 4.0*
    - 5.6: Adiabaticity criterion - *CC BY-NC-SA 4.0*
    - 5.7: Readings - *CC BY-NC-SA 4.0*
  - 6: Classical Description of Spectroscopy - *CC BY-NC-SA 4.0*
    - 6.1: Introduction - *CC BY-NC-SA 4.0*
    - 6.2: Absorption by a Driven Oscillator - *CC BY-NC-SA 4.0*
    - 6.3: Complex formulation of the driven dipole oscillator - *CC BY-NC-SA 4.0*
    - 6.4: Response of an Impulsively Driven

Oscillator - *CC BY-NC-SA 4.0*
- 6.5: Polarizability - *CC BY-NC-SA 4.0*
- 6.6: Appendix- Laplace Transform Solution for the Driven Damped Oscillator - *CC BY-NC-SA 4.0*
- 6.7: Readings - *CC BY-NC-SA 4.0*

◦ 7: Interaction of Light and Matter - *CC BY-NC-SA 4.0*
- 7.1: Introduction - *CC BY-NC-SA 4.0*
- 7.2: Electromagnetic Plane Waves - *CC BY-NC-SA 4.0*
- 7.3: Classical Light–Matter Interactions - *CC BY-NC-SA 4.0*
- 7.4: Electric Dipole Hamiltonian - *CC BY-NC-SA 4.0*
- 7.5: The Dipole Operator and Transition Dipole Matrix Elements - *CC BY-NC-SA 4.0*
- 7.6: Absorption Cross Section - *CC BY-NC-SA 4.0*
- 7.7: Quantitative Examples of Light-Matter Interactions - *CC BY-NC-SA 4.0*
- 7.8: Appendix- Electromagnetic Fields and Potentials - *CC BY-NC-SA 4.0*
- 7.9: Appendix- Magnetic Dipole and Electric Quadrupole Transitions - *CC BY-NC-SA 4.0*
- 7.10: Readings - *CC BY-NC-SA 4.0*

◦ 8: Emission of Radiation - *CC BY-NC-SA 4.0*
- 8.1: Classical rate of light emission - *CC BY-NC-SA 4.0*
- 8.2: Radiation from an Oscillating Dipole - *CC BY-NC-SA 4.0*
- 8.3: Appendix- Wave equation with a source - *CC BY-NC-SA 4.0*
- 8.4: Readings - *CC BY-NC-SA 4.0*

◦ 9: Quantum Electromagnetic Field - *CC BY-NC-SA 4.0*
- 9.1: Introduction - *CC BY-NC-SA 4.0*
- 9.2: Hamiltonian for quantized electromagnetic field - *CC BY-NC-SA 4.0*
- 9.3: Electromagnetic field - *CC BY-NC-SA 4.0*
- 9.4: Light-Matter Interactions and Spontaneous Emission - *CC BY-NC-SA 4.0*
- 9.5: Coherent States - *CC BY-NC-SA 4.0*
- 9.6: Readings - *CC BY-NC-SA 4.0*

◦ 10: Transition Dipole Moment and Selection Rules - *CC BY-NC-SA 4.0*
- 10.1: The Molecular Transition Dipole Moment - *CC BY-NC-SA 4.0*
- 10.2: Selection Rules in the Electric Dipole Approximation - *CC BY-NC-SA 4.0*
- 10.3: Molecular Electronic Spectroscopy and Franck Condon Factors - *CC BY-NC-SA 4.0*
- 10.4: Appendix - Rotational Transition Matrix Elements - *CC BY-NC-SA 4.0*
- 10.5: Readings - *Undeclared*

◦ 11: Irreversible Relaxation - *CC BY-NC-SA 4.0*
- 11.1: Introduction - *CC BY-NC-SA 4.0*
- 11.2: Coupling to a continuum - *CC BY-NC-SA 4.0*
- 11.3: Spontaneous Emission - *CC BY-NC-SA 4.0*
- 11.4: Relaxation and Line-broadening - *CC BY-NC-SA 4.0*
- 11.5: Readings - *Undeclared*

◦ 12: Quantum Statistical Mechanics For Condensed Matter - *CC BY-NC-SA 4.0*
- 12.1: Concepts for Condensed Matter - *CC BY-NC-SA 4.0*
- 12.2: Statistics of Ensembles - *CC BY-NC-SA 4.0*
- 12.3: Equilibrium Systems - *CC BY-NC-SA 4.0*
- 12.4: Mixed States - *CC BY-NC-SA 4.0*
- 12.5: The Density Matrix - *CC BY-NC-SA 4.0*
- 12.6: Time-Dependence of the Density Matrix - *CC BY-NC-SA 4.0*
- 12.7: Readings - *Undeclared*

◦ 13: Correlation Functions - *CC BY-NC-SA 4.0*
- 13.1: Classical Time-Correlation Functions - *CC BY-NC-SA 4.0*
- 13.2: Examples of Classical Time-Correlation Functions - *CC BY-NC-SA 4.0*
- 13.3: Calculating the Correlation Function from a Discrete Trajectory - *CC BY-NC-SA 4.0*
- 13.4: Quantum Time-Correlation Functions - *CC BY-NC-SA 4.0*
- 13.5: Transition Rates from Time Correlation Functions - *CC BY-NC-SA 4.0*
- 13.6: Appendix- Weiner-Khinchin Theorem and the Power Spectrum - *CC BY-NC-SA 4.0*
- 13.7: Readings - *CC BY-NC-SA 4.0*

◦ 14: Linear Response Theory - *CC BY-NC-SA 4.0*
- 14.1: Classical Linear Response Theory - *CC BY-NC-SA 4.0*
- 14.2: Example- Response of a damped harmonic oscillator - *CC BY-NC-SA 4.0*
- 14.3: The Response Function and Energy Absorption - *CC BY-NC-SA 4.0*
- 14.4: Quantum Linear Response Functions - *CC BY-NC-SA 4.0*
- 14.5: Nonlinear response functions - *CC BY-NC-SA 4.0*
- 14.6: Relaxation of a Prepared State - *CC BY-NC-SA 4.0*
- 14.7: Example- Response of an abruptly shifted oscillator - *CC BY-NC-SA 4.0*
- 14.8: Readings - *CC BY-NC-SA 4.0*

◦ 15: Time-Domain Spectroscopy - *CC BY-NC-SA 4.0*
- 15.1: Absorption Spectra from Time-Correlation Functions - *CC BY-NC-SA 4.0*
- 15.2: Describing Diverse Spectroscopies with the Dipole Correlation Function - *CC BY-NC-SA 4.0*
- 15.3: Vibrational and Rotational Spectroscopy - *CC BY-NC-SA 4.0*
- 15.4: Line Broadening Mechanisms - *CC BY-NC-SA 4.0*
- 15.5: Readings - *CC BY-NC-SA 4.0*

- 16: Coupling of Electronic and Nuclear Motion - *CC BY-NC-SA 4.0*
  - 16.1: The Displaced Harmonic Oscillator Model - *CC BY-NC-SA 4.0*
  - 16.2: Coupling to a Harmonic Bath - *CC BY-NC-SA 4.0*
  - 16.3: Semiclassical Approximation to the Dipole Correlation Function - *CC BY-NC-SA 4.0*
  - 16.4: Readings - *CC BY-NC-SA 4.0*
- 17: Fluctuations and Dephasing - *CC BY-NC-SA 4.0*
  - 17.1: Line-broadening, dephasing, and spectral diffusion - *CC BY-NC-SA 4.0*
  - 17.2: Gaussian-Stochastic Model for Spectral Diffusion - *CC BY-NC-SA 4.0*
  - 17.3: The Energy Gap Hamiltonian - *CC BY-NC-SA 4.0*
  - 17.4: Spectral Density for Condensed Phase Spectroscopy - *CC BY-NC-SA 4.0*
  - 17.5: The Harmonic Bath's Relation to the Langevin Equation - *CC BY-NC-SA 4.0*
  - 17.6: Readings - *CC BY-NC-SA 4.0*
- 18: Quantum Relaxation Processes - *CC BY-NC-SA 4.0*
  - 18.1: Vibrational Relaxation - *CC BY-NC-SA 4.0*
  - 18.2: Golden Rule Vibrational Relaxation Rates - *CC BY-NC-SA 4.0*
  - 18.3: Multiquantum relaxation of polyatomic molecules - *CC BY-NC-SA 4.0*
  - 18.4: Redfield Theory and Master Equation - *CC BY-NC-SA 4.0*
  - 18.5: Readings - *Undeclared*
- 19: Energy and Charge Transfer - *CC BY-NC-SA 4.0*
  - 19.1: Intermolecular Electronic Interactions - *CC BY-NC-SA 4.0*
  - 19.2: Resonance Energy Transfer and Transition Dipole Coupling - *CC BY-NC-SA 4.0*
  - 19.3: Förster Resonance Energy Transfer - *CC BY-NC-SA 4.0*
  - 19.4: Marcus Theory for Electron Transfer - *CC BY-NC-SA 4.0*
  - 19.5: Readings - *CC BY-NC-SA 4.0*
- 20: Excitons - *CC BY-NC-SA 4.0*
  - 20.1: What are excitons? - *CC BY-NC-SA 4.0*
  - 20.2: Frenkel excitons in molecular aggregates - *CC BY-NC-SA 4.0*
  - 20.3: Absorption spectrum of a dimer - *CC BY-NC-SA 4.0*
  - 20.4: Absorption spectra of J aggregates - *CC BY-NC-SA 4.0*
  - 20.5: Frenkel exciton transport - *CC BY-NC-SA 4.0*
  - 20.6: Tight-binding model - *CC BY-NC-SA 4.0*
  - 20.7: Readings - *CC BY-NC-SA 4.0*
- 21: Appendices - *CC BY-NC-SA 4.0*
  - 21.1: Math and Physics Reference Material - *CC BY-NC-SA 4.0*
    - 21.1.1: Atomic Units - *CC BY-NC-SA 4.0*
    - 21.1.2: Dirac Delta Function - *CC BY-NC-SA 4.0*
    - 21.1.3: Gaussian Integrals and Error Function - *CC BY-NC-SA 4.0*
  - 21.2: Quantum Mechanics- Extra Topics - *CC BY-NC-SA 4.0*
    - 21.2.1: Numerically Solving the Schrödinger Equation - *CC BY-NC-SA 4.0*
    - 21.2.2: Separation of Subsystems - *CC BY-NC-SA 4.0*
    - 21.2.3: Morse Oscillator - *CC BY-NC-SA 4.0*
- Back Matter - *CC BY-NC-SA 4.0*
  - Notation and variables used - *CC BY-NC-SA 4.0*
  - Index - *CC BY-NC-SA 4.0*
  - Glossary - *CC BY-NC-SA 4.0*
  - Detailed Licensing - *CC BY-NC-SA 4.0*

This page titled Time-Dependent Quantum Mechanics and Spectroscopy 2025e (Tokmakoff) is shared under a CC BY-NC-SA 4.0 license and was authored, remixed, and/or curated by Andrei Tokmakoff via source content that was edited to the style and standards of the LibreTexts platform.